NASA-CR-171820

COLUMBIA: THE FIRST FIVE FLIGHTS

ENTRY HEATING DATA SERIES

VOLUME 1

AN OVERVIEW

By S. D. Williams

November 1984

(NASA-CR-171820) COLUMBIA: THE FIRST 5 FLIGHTS ENTRY HEATING DATA SERIES. VOLUME 1: AN OVERVIEW (Lockheed Engineering and Management) 483 p HC A21/MF A01 CSCL 22A N85-15777

Unclas
G3/16 13163

Prepared under Contract No. NAS 9-15800
Lockheed Engineering and Management Services Co., Inc.

for

NATIONAL AERONAUTICS AND SPACE ADMINISTRATION
Johnson Space Center
Houston, Texas

ACKNOWLEDGMENTS

I would like to take this opportunity to acknowledge several individuals without whose support, guidance, and assistance this series of archival documents would never have been published. First I would like to thank my very close colleague at NASA/JSC, Dr. D. M. Curry, LESS Subsystem Manager. Without his support, consultation, and guidance over the last decade the software leading to this analysis capability would never have been developed. Next, I would like to thank Ms. D. B. Lee, Aerothermal Subsystem Manager, also at NASA/JSC, for working very closely with me in establishing the formats contained in this series of documents. In addition to her continuous encouragement, her knowledge of the wind tunnel test data proved invaluable. I would also like to thank Mr. J. E. Colovin of Lockheed and Mr. S. M. Derry of NASA/JSC for their aid in running the MINIVER program and providing the reference heating data/parameters for each trajectory used in this analysis. Special thanks go to Dr. R. C. Ried, Special Assistant to the Director, NASA/JSC. It was due to his recommendation that this series of reports be developed for reference purposes. We spent many long hours in discussions and analyzing these data. Dr. W. D. Goodrich also spent many hours in consultation with me and his recommendations were largely instrumental in determining the format for the data presented in Vol. I.

S. D. W.

PREFACE

This series of documents was prepared over a two year time frame. During this time several flight data tapes were lost and were remade to permit the necessary analysis. This reinforced the need to archive the data in a more permanent form available to investigators. It is hoped that this data presented in terms of aerodynamic parameters will prove more beneficial to investigators than time history plots of the raw temperature.

NOMENCLATURE

α	Angle of Attack
b/2	Spanwise distance measured from plane of symmetry, 468.3 in.
BET	Best Estimated Trajectory
c	Local wing chord length, 414.6 in. for 50% semi-span, 248.1 in for 80% semi-span
Cp	Specific Heat
DFI	Development Flight Instrumentation
δ_{BF}	Body Flag deflection
δ_E	Elevon deflection
E/I	Entry Interface
FRSI	Flexible Reusable Surface Insulation
H_T	Total enthalpy
h	Film heat transfer coefficient
HRSI	High-temperature Reusable Surface Insulation
JSC	Johnson Space Center
L	Orbiter longitudinal length, 1285 in.
Lp	OMS Pod longitudinal length, 258.5 in.
LRSI	Low-temperature Reusable Surface Insulation
M_∞	Free stream Mach number
OEX	Orbiter Experiment
OMS	Orbital Maneuvering System
PSIA	Pounds per square inch, absolute
q_{conv}	Convective heat rate
RCC	Reinforced carbon-carbon
Re_{NS}	Normal shock Reynolds number based on orbiter characteristic length
Re_∞	Free stream Reynolds number based on orbiter characteristic length
STS	Space Transportation System
TAEM	Terminal Area Energy Management
T_{surf}	Surface Temperature
TPS	Thermal Protection System
X	Longitudinal Length

X/C	Normalized longitudial length from wing leading edge along a semi-span
X/L	Normalized longitudinal length from orbiter nose.
X/Lp	Normalized longitudinal length from OMS pod forward face
Y	distance in inches measured from plane of symmetry
Y/b/2	non-dimensional spanwise distance measured from plane of symmetry
Z	Horizontal distance

Subscripts

∞	Free Stream
NS	Normal Shock

INTRODUCTION

The Space Shuttle Orbiter represents the current approach in the design and development of hypersonic entry vehicles. This frontier effort can be characterized as placing a balanced emphasis on ground characterization testing, greater reliance on analytical based software for predictions, and experimental/analytical methodology development for subsystem verification.

Since the flowfields and resultant surface heating for a vehicle with the complex geometry of the Orbiter was not well understood a series of ground tests were conducted to aid in obtaining better understanding of the flow phenomena. Ground tests were conducted in wind tunnels to gain insight into the sensitivity of surface heating to angle of attack and Reynolds number. It was deduced that adequate characterizations could be derived for the hypersonic entry environment by using existing facilities with data taken at Mach 8.

Over 2,000 development flight instruments (DFI) were installed on the first flight Orbiter, Columbia, with the majority of the DFI flight data recorded during ascent and entry. Additional real-time instrumentation was used to continuously monitor the thermal subsystems during each flight. Successful completion of the first five flights of the Space Shuttle Orbiter provided data from thermocouples, pressure transducers, and radiometers to appraise aerothermodynamic/TPS performance during entry.

The entry heating data presented in this report include select measurement locations from the available flight data which are compared with data from similar locations obtained from wind tunnel tests. These data are presented in terms of the dynamic flow field parameters of interest to the aerothermodynamist, namely, angle of attack, Mach number, and Reynolds number. The objective is not only to archive the flight data, but to aid the analyst in bridging the gap between wind tunnel and flight testing, and to provide insight into the relative sensitivity of surface heating to these parameters.

DISCUSSION

The key to the development of a multi-mission, low cost, weight effective Orbital thermal protection system (TPS) was the development of unique reusable materials which could withstand the high temperature environment and also be integrated into a system design which could provide adequate insulation for the structure and internal systems. The Orbiter TPS consists of four different material configurations; coated reinforced carbon-carbon (RCC) for nose and wing leading edge areas where entry temperatures exceed 2300°F, high-temperature reusable surface insulation (HRSI) for temperatures between 1200°F and 2300°F, low-temperature reusable surface insulation (LRSI) between 700°F and 1200°F, and flexible reusable surface insulation (FRSI) for areas with surface temperatures not exceeding 700°F.

Successful completion of the initial five flights of Columbia have provided data from radiometers, thermocouples, and pressure transducers to appraise the aerothermodynamic envirnoment and TPS performance. The majority of the DFI were dedicated to various subsystems to support the analysis and certification requirements for subsequent flights. The location and identification of these instruments can be found in Ref. 1.

The surface heating rates presented in this volume are based on the thermal analysis of temperature measurements via the JSC NONLIN/INVERSE computer program, Ref. 2. These analyses consisted of calculated surface temperature and heating rate using embedded thermocouple temperature data. With the use of variable thermal properties (as functions of temperature and pressure) the effects of radiation loss and internal conduction is accounted for in the computation of both surface heating and in-depth thermal response.

The thermal analysis performed for each location and flight was initiated at either entry interface (E/I) or at the commencement of recorded data and terminated at 2500 seconds after E/I or the cessation of data recording, which ever occurred first. The time step size for all analysis was 5 seconds. Flight data were sampled at one second intervals and smoothed to five second intervals to be consistent with analysis requirements. For reference purposes, the critical mission times (E/I, TAEM, and touch down) for each flight are provided in Table I. The TPS configuration and material thickness were obtained either from Ref. 3 or from undocumented personal communications with thermal analyst at NASA/JSC and Rockwell International, Downey, California. Baseline thermophysical properties were used for all materials and can be found in Ref. 4. All heating rates were calculated with a view factor of 1. The surface emissivity on the lower windward surface was assumed to be 0.85 while on the lee side the emissivity was assumed to be 0.80.

The TPS performance analysis was influenced by the local pressures used. The sensitivity of the pressure transducers on the lower windward surface was sufficient to enable accurate calculation of the local surface conditions (heating and temperature) and in-depth thermal response. On the lee side, however, the full range (0-15 PSIA) pressure transducers did not accurately respond prior to approximately Mach 25 or $Re_{NS} = 7 \times 10^4$ due to the low level of surface pressure. Thus the analysis of the early response on the lee side is less accurate in a thermal sense. However from a practical viewpoint this insensitivity of the pressure sensors introduced an error of less than 5 to 10 percent on the surface heating and temperature. The greatest influence of pressure sensitivity is in the prediction of bondline structural thermal responses which is not the concern of this report.

On the lower centerline the data for the measurement at X/L=0.95 is not as accurate as for other locations. Most of the thermocouples used for surface heating and temperature calculations were 0.015 inches from the surface. In this location where there was a plug instrumented tile with thermocouples at different depths, the first in-depth thermocouple malfunctioned for all flights. The next in-depth thermocouple 0.30 inch from the surface, was used to calculate the surface heating and temperature. The use of data from this depth in combination with the data noise approaches the limits of the inverse program to calculate surface heating and temperature. Thus the data at this location appears to be more noisy and not as accurate as the data at other locations.

Values of angle of attack and the derived free stream Mach number were obtained from JSC/MPAD Best Estimated Trajectory (BET) data tapes for each flight. The corresponding values for normal shock Reynolds number (defined in Ref. 5), reference heating rate to a 1-foot sphere, reference film coefficient, and total enthalpy were obtained via the MINIVER computer program (Ref. 6).

The heating data presented are in terms of normalized film heat transfer coefficients using an approximate flight recovery enthalpy of 0.9 H_T. The deduced film heat transfer coefficient for flight data is given by:

$$h = q_{conv}/(0.9\ H_T - C_p\ T_{surf})$$

where q_{conv} is the convective heating rate from NONLIN/inverse, H_T is the total enthalpy from MINIVER, and the local surface enthalpy is calculated as:

$$C_p\ T_{surf} = 0.235\ T_{surf} + 9.786 \times 10^{-6}\ T^2_{surf} + 943.6/T_{surf} - 1.5$$

where T_{surf} is the surface temperature from NONLIN/INVERSE.

The objective of this analysis is to compare Orbiter heating rate data from flight with wind tunnel data at the same angles of attack and Reynolds number to establish whether the sensitivity of heating to these two parameters is similar for flight and wind tunnel conditions. It has been shown that normal shock Reynolds number (Ref. 5 and 7) can adequately be used to correlate wind tunnel data with flight data for entry vehicles such as the Apollo and Space Shuttle Orbiter. The advantage of using normal shock Reynolds number (Re_{NS}), as compared to freestream Reynolds number (Re_∞), is that the Re_{NS}, to a first order, accounts for the real gas effects. The scaling parameter (Re_{NS}/Re_∞), determined from the wind tunnel test environment at Mach 8, (Ref. 8-11) is 0.1121. Individual comparisons of flight and wind tunnel heat transfer coefficient data (0.9 H_T) vs. flight parameters (α, M_∞, Re_{NS}) have been previously reported (Ref. 12-16). As an aid to the reader the correlation between freestream and normal shock Reynolds numbers at wind tunnel conditions can be seen in Table II.

When observing the comparisons presented in this volume and Ref. 12-16 the analyst should exercise extreme care in extrapolating the wind tunnel data to flight and from this class of vehicles to other vehicle classes. The flow field characteristics (dynamics) that are present for wind tunnel conditions are significantly different from those existing at hypersonic flight conditions. The subscale models exposed to wind tunnel conditions are being monitored in an ideal gas environment. The wind tunnel, in order to achieve the supersonic velocities required for test purposes, operates at relatively low temperatures and enthalpies. At these test conditions the flow is chemically non-reacting and the flow energy is in either a translation (kinetic) or thermal state. During entry, however, the Orbiter TPS is subject to a chemically active environment. In comparison to wind tunnel conditions the flight conditions exhibit elevated temperatures and enthalpies which causes dissociation of molecules in the shock layer and the possible recombination of the atoms near the surface in the boundary layer. Therefore, the flow energy is now distributed in translational, thermal, and chemical states. Because the Orbiters TPS surface primary constituents are of moderate catalysis with respect to recombination the surface chemistry is relatively inert. Thus, the entry heating is primarily due to diffusions of thermal energy within the boundary layer. The thermal energy can, at times of peak heating, be relatively small compared to the energy within the translational and chemical states.

While the majority of the TPS surface has a moderate surface catalysis rate, the surface of several tiles were catalytically treated, as part of an Orbiter Experiment (OEX) to assess the effect of locally enhanced surface catalysis on local aeroheating. The location of these catalytic tiles on the lower surface centerline are indicated in Table III for each flight. In the X/L distributions the rise in heating due to the locally treated catalytic surface is shown as a discontinuity. This inferred jump in magnitude is based on a linear interpolation of the heating from the adjacent non-catalytic tiles, both forward and aft of the catalytic tile.

The heating rate distributions, especially on the lower windward surface, tend to demonstrate that the wind tunnel data are conservative relative to the heating experienced in flight. The data derived from the catalytic tiles illustrate the heating levels that could be anticipated using a more chemically active surface. Thus, any agreement between unscaled wind tunnel and flight data may be viewed as fortuitous because the wind tunnel tests did not simulate these chemical effects.

It should be stressed that this report is basically portraying experimental data only. That is, experimental data derived from wind tunnel tests and experimental data derived from flight. These comparisons permit the analyst to extrapolate, within limitations, from the heating at wind tunnel conditions to the aerothermodynamic heating that exists within the flight environment. Within this entry heating data series no attempt has been made to correlate flight data with analytical predictions. While this does limit, somewhat, the total understanding of the aerothermodynamic entry environment it is felt that this series will prove to be invaluable for future analysis. Other investigators, however, have attempted to provide insight into this entry envirnoment by correlating analytical methodologies with flight data. A partial list of such investigations can be found in Ref. 17-25.

A complete legend is provided on each plot that identifies the location for the heating rate distributions, wind tunnel test conditions, and flight data conditions. The wind tunnel data are presented as symbols which are identified by test, angle of attack, free stream Mach number, and normal shock Reynolds number. The flight data are presented by vector connected curves (solid and dashed) and are identified by flight, angle of attack, free stream Mach number, normal shock Reynolds number, and time in seconds after entry interface.

DATA RESULTS

The entry heating presented in this report is restricted to the lower surface centerline, lower wing surface 50% and 80% semi-spans, side fuselage (Z=400 trace), side Payload Bay Door (Z=440 trace), upper lee side centerline, and OMS pod (trace 3), see Figs. 1-4. The heating rate distributions are presented as h/h_{ref} vs. X/L on the lower and upper centerline and side (Z=400 and Z=440 traces), as h/h_{ref} vs. X/C on the lower wing 50% and 80% semi-spans, and h/h_{ref} vs. X/Lp on the OMS pod (trace 3). All wind tunnel data presented are for 0° body flap deflection, δ_{BF}, and elevon deflection, δ_E. All wind tunnel data are either taken at flight data measurement locations or by linear interpolation to the flight data measurement locations as explained in volumes 2-6 (Ref. 12-16).

The data presented in volumes 2-6 tend to represent the time-history data for each DFI analyzed. In contrast, the data in this volume are presented in terms of heating rate (h/h_{ref}) distributions, and provides a different perspective for viewing the same data. By examining heating rate distributions the analyst is more able to gain insight into the heating characteristics for this vehicle and is more able to develop and assess the sensitivity of the heating distributions to angle of attack and Reynolds number.

Complete flight data exists only for STS-2, STS-3 and STS-5. The entry heating data for STS-1 and STS-4 are available from 1065 seconds and 965 seconds after entry interface (400 K ft.), respectively. In volumes 2-6 the flight correlation parameters were given only during the times entry heating data were available. In this volume, however, the flight correlation parameters for each flight are provided for all entry times of interest. In addition to the time history and reference cross plots of α, M_∞, Re_{NS}, q_{ref}, and h_{ref} this volume provides time histories, and reference cross plots of H_T and Re_{NS}/Re_∞, as well as, time-history plots of the body flap and elevon deflections (right and left) δ_{BF}, δ_{E-RH}, and δ_{E-LH}. Plots of these correlation parameters are presented in Appendix A. As an aid to the reader, the page numbers for the specific correlation parameters can be found in Table IV.

The aerodynamic heating on the Orbiter is influenced by geometry, surface roughness, material catalysis, gas phase chemistry, angle of attack, Mach number, and Reynolds number. By selectively isolating each parameter the sensitivity of the heating can be assessed with respect to the other parameters. Geometry has remained unchanged since the same vehicle (OV-102) was used for the five DFI flights. The influence of surface roughness, and cataltysis can be isolated by comparing the heating variations within each flight and between flights. The sensitivities to gas phase chemistry and Mach number are difficult to assess because all the trajectories were so very similar. However, the trajectories were sufficiently different to provide insight into the sensitivities of heating as a function of angle of attack and Reynolds number for each flight and for all flights in composite.

Influence of Reynolds Number - Appendix B
Individual Flights - Constant Angle of Attack

A comparison of flight and wind tunnel heating rate data (h/h_{ref}) showing the influence of Re_{NS} at 40° angle of attack is presented in Appendix B. The page numbers for this data can be found in Table V. This comparison is presented for STS-2, STS-3, and STS-5 individually and covers the range $2 \times 10^4 \leq Re_{NS} \leq 8 \times 10^5$. This scans the Reynolds numbers range for approximately the order of magnitude Reynolds number range prior to wind tunnel data through the order of magnitude Reynolds number range that include wind tunnel test data.

The first 48 plots (16 per flight) present individual heating rate distributions along the lower windward centerline at each discrete Reynolds number. For comparison purposes the closest available wind tunnel data are also provided on these plots. In addition to showing the sensitivity to Reynolds numbers this data is provided as an aid to investigators in assessing the heating levels for the catalytic surfaces over the range of entry conditions. The following 42 plots (B49-B90) comparing flight and wind tunnel heating data are segregated into two Reynolds number ranges, $2 \times 10^4 \leq Re_{NS} \leq 9 \times 10^4$ and $1 \times 10^5 \leq Re_{NS} \leq 8 \times 10^5$, for each area under investigation.

The heating rate distribution on the lower centerline remained essentially unchanged with increasing Reynolds number for STS-2 and STS-3. For STS-5, however, the heating rate distribution exhibited a dependence on Reynolds number, increasing with increasing Reynolds number. The heating for all flight data indicates that the flow was laminar through the entire Reynolds number range when the vehicle was at 40° angle of attack. In contrast to the flight data the wind tunnel data exhibit a dependence on Reynolds number and go through transition from laminar to turbulent heating for $Re_{NS} > 4 \times 10^5$ aft of $X/L = 0.6$. This indicates the possible influence of tunnel noise on ground test data.

The influence of Body Flap deflection can be seen for all flight data. The order of magnitude decrease in heating on the aft end of the Orbiter ($0.9 \leq X/L \leq 1.0$) is an indication of separated flow. The flow reattaches on the Body Flap and causes the heating to increase by 1 to 1 1/2 orders of magnitude over the heating in the separated flow region, see Appendix A26-A30 for body flap deflections.

On the lower wing 50% semi-span ($Y/b/2 = 0.5$) the heating rate distribution for STS-2 and STS-3 remained essentially unchanged for the order of magnitude Reynolds number range prior to wind tunnel data ($2 \times 10^4 \leq Re_{NS} \leq 9 \times 10^4$), however, for STS-5 a dependence on Re_{NS} can be seen, see B59 and B60. For the order of magnitude Reynolds number range that contain the wind tunnel data there is an indication of turbulent flow around $X/C = 0.6$ for all flights although the flow was laminar at all other stations. The wind tunnel data indicated a dependence on Reynolds number and indicate turbulent heating for $Re_{NS} > 6 \times 10^5$ at all stations. The influence of elevon heating as a function of elevon deflection can be seen only for the higher Reynolds numbers. The elevon hinge line for the 50% semi-span was at $X/C = 0.76$.

On the lower wing 80% semi-span ($Y/b/2 = 0.8$) the heating rate distribution was essentially unchanged for all Reynolds numbers for STS-2. Only the data at the highest Reynolds numbers ($Re_{NS} > 6 \times 10^5$), indicate an increase in heating on the elevon trailing edge. For this semi-span the elevon hinge was at X/C = 0.71. The first two instruments behind the leading edge for STS-3 are suspiciously low and probably should not be used for analysis. The heating rate distribution for STS-3, neglecting these two instruments, is essentially the same as for STS-2 prior to the elevon hinge. The heating on the elevon illustrates the sensitivity of heating as a function of Reynolds number for a 3° elevon deflection on STS-3 that was not observed for the 1° deflection on STS-2.

As with the lower centerline and wing 50% semi-span, the heating on the 80% semi-span for STS-5 shows a dependence on Reynolds number on the decade prior to wind tunnel data. The heating distribution through the wind tunnel data range, however, remained unchanged on the wing with some dependence on the elevon heating levels as a function of the deflection angle. The wind tunnel heating data show a dependence on Reynolds number, increasing with increasing Reynolds number for $Re_{NS} > 5 \times 10^5$. The largest increase in heating was at X/C = 0.6 where the magnitude in heating increased approximately by a factor of 2. Transition in the wind tunnel occur only at the highest Reynolds number.

On the lower centerline the flight data tended to agree with the lower range wind tunnel data ($Re_{NS} \leq 3 \times 10^5$). On the lower wing 50% semi-span the flight data tend to agree with lower range wind tunnel data ($Re_{NS} \leq 4 \times 10^5$) forward of X/C = 0.6, with the 5×10^5 and 6×10^5 wind tunnel data at X/C = 0.6, and with the 5×10^5 wind tunnel data for X/C > 0.6. On the 80% semi-span the flight data were in close agreement with the lower range wind tunnel data ($Re_{NS} \leq 4 \times 10^5$). This represents a close correlation between flight and wind tunnel data for laminar flow conditions. In general, however, the wind tunnel data tend to be conservative relative to flight data. It is interesting to observe that the wind tunnel indicates a much earlier transition time (lower Reynolds number) than occurred in flight. This may, in part, be attributed to differences in enthalpy, model size, wind tunnel noise, and surface chemistry.

The side heating is more difficult to correlate since flow is more directly influenced by the upstream effects of the body curvature and wing leading edge. The flow on the lower surface tends to be characterized as either laminar or turbulent, whereas, the flow along the side is characterized more in terms of separation and reattachment or vortex flow during entry. Trendwise the wind tunnel data are conservative forward of X/L = 0.4 and tend to underestimate the flight data aft of X/L = 0.6, especially with increasing Reynolds number.

For the order of magnitude Reynolds number range prior to wind tunnel data the heating distributions along the Z=400 trace show an amazing similarity to the windward flight data; that is, relative insensitivity to Reynolds number for STS-2 and STS-3, and increase in heating with increase in Reynolds number for STS-5. In the decade containing wind tunnel data, however, both wind tunnel and flight data show a strong dependence on Reynolds number.

Although a lesser number of instruments were available on the side Payload Bay Door (Z=440 trace) the same observations tend to hold as for the Z=400 trace. The only difference is that the wind tunnel data tend to be a conservative estimate of the flight data forward of X/L = 0.6, and underestimates flight data aft of X/L = 0.6.

On the lee side upper centerline the wind tunnel data overestimate the flight data at all Reynolds numbers. On this surface the flow is complicated by the abrupt change in shuttle geometry due to the cabin (windshield and canopy). Both flight and wind tunnel data indicate strong reattachment on the canopy with an order of magnitude reduction in heating aft of the canopy along the Payload Bay doors. Only limited data are available for STS-2. However, all flight and wind tunnel data show a strong dependence on Reynolds number. Both wind tunnel and flight data show similar trends forward of X/L = 0.2. There is a wider variation in heating for flight data aft of X/L = 0.2 than would be implied from wind tunnel data.

A more complicated flow phenomenon exists on the OMS pod than for the other surface areas. The flow is directly influenced by the upstream effects of the body curvature and wing leading edge. The flow along the fuselage side and the wing upper surface contribute to the difficulty in describing the flow along this lee side surface. The heating rate distributions for all flight data are strongly dependent on Reynolds number. In general, the wind tunnel data did not predict the flight data on the OMS pod. While the wind tunnel data showed some dependence on Reynolds number it tended to underpredict flight data by a factor of 2 to 3.

The flight data in the low Reynolds number range presents an interesting problem. The data from STS-2 and STS-3 tend to be in agreement and show an insensitivity in the laminar heating as a function of Reynolds number. However, the heating data from STS-5 shows an influence on the level of heating that is directly dependent on Reynolds number. Between the flights for STS-4 and STS-5 the water proofing procedure was changed. This procedure was effective in preventing moisture penetration, but may have changed the surface characteristics for STS-5, i.e., the surface properties such as emissivity may have been degraded. In addition, at various locations on the vehicle tiles were replaced between flights. Thus at least two known factors may have influenced the heating on STS-5; possible surface property change, and possible surface roughness changes.

Influence of Reynolds Number - Appendix C
Composite Flights - Constant Angle of Attack

The heating rate distribution plots in Appendix B provide a measure of sensitivity for individual flight and wind tunnel data over two decades of Reynolds numbers for an angle of attack of 40°. An alternate assessment can be made by comparing the composite flight data to wind tunnel data. A comparison of the composite flight and wind tunnel heating distributions at wind tunnel Reynolds numbers conditions can be seen in Appendix C. In these plots both the 35° and 40° angle of attack wind tunnel data are provided for comparison purposes to the 40° angle of attack flight data. The page numbers for this data can be found in Table VI.

On the lower centerline the heating distribution for STS-5 is greater than that for STS-2 and STS-3, which are essentially in agreement, at each Reynolds number. The laminar wind tunnel heating data provides a conservative estimate of the STS-2 and STS-3 flight data, and are a close approximation of the STS-5 flight data. While the 40° angle of attack flight heating data remained laminar for all Reynolds numbers the wind tunnel data indicate turbulent heating for higher Reynolds numbers ($Re_{NS} > 4 \times 10^5$) on the aft position of the vehicle.

The heating distributions for STS-5 are greater than those for STS-2 and STS-3 on the wing 50% semi-span except at the two highest Reynolds numbers. The STS-2 and STS-3 heating data are in agreement at all Reynolds numbers and agree with the STS-5 data at the two highest Reynolds numbers. The wind tunnel data tend to provide a conservative estimate of the flight data for $1.050 \times 10^5 \leq Re_{NS} \leq 4.198 \times 10^5$. At $Re_{NS} = 5.248 \times 10^5$ the wind tunnel and STS-5 flight data were in close agreement. At higher Reynolds numbers the wind tunnel data indicated turbulent heating. With the exception of the first two measurements behind the leading edge on STS-3, the flight data were in agreement for all Reynolds numbers for the wing 80% semi-span. In general, flight and wind tunnel heating distributions were in close agreement until the wind tunnel became turbulent at $Re_{NS} = 7.767 \times 10^5$.

On the side fuselage Z = 400 trace the flight heating distribution data were in close agreement at all Reynolds numbers. The wind tunnel data provided a conservative estimate of flight data for $0.2 \leq X/L \leq 0.4$, were in reasonable agreement from 0.4 to 0.6, and tended to drastically underpredict the flight data for $X/L > 0.6$.

On the side Payload Bay Door (Z=440) the flight heating distributions tended to be more scattered. In general, the STS-5 data tended to be higher than STS-2 or STS-3. Both flight and wind tunnel data trends were consistent at all Reynolds numbers. Aft of $X/L = 0.6$ the wind tunnel data consistently underpredicted flight data. The wind tunnel data for the two forward stations tended to be a conservative estimate to flight data for all but the highest Reynolds number. For the two middle stations (X/L = 0.5 and 0.6) the comparison is more mixed. However, the wind tunnel data tended to agree with the data from at least one flight at X/L = 0.6.

As was mentioned previously, the wind tunnel heating data tended to be a conservative estimate for flight data at all Reynolds numbers on the upper centerline. In general, the heating distributions for flight data tend to be in close agreement. The greatest scatter in flight data was aft of the canopy, X/L > 0.2.

Comparison of heating distributions on the OMS pod is difficult to make due to the variation among the flights. At $Re_{NS} = 2.099 \times 10^5$, STS-3 and STS-5 tend to have similar heating distributions, and the STS-2 heating at X/Lp = 0.2 is much lower than both wind tunnel and data from STS-3 and STS-5. At $Re_{NS} = 4.198 \times 10^5$ the heating from STS-2 and STS-3 are similar and tend to approximate the 40° angle of attack wind tunnel data. The heating for STS-5 is 1 1/2 to 2 times greater than for STS-2 and STS-3 in the region where wind tunnel data exists and the flight data tend to be in agreement at X/Lp = 0.692. At $Re_{NS} = 6.297 \times 10^5$ the heating distributions for all flight data are similar with the STS-5 data greater than the STS-2 and STS-3 data which were in close agreement. The wind tunnel data underpredicted the flight data. At $Re_{NS} = 7.767 \times 10^5$ all flight data were in reasonable agreement while the wind tunnel data under predicted the flight data.

Influence of Angle of Attack - Appendix D
Individual Flights - Constant Reynolds Number

It is normally difficult to obtain a full matrix of heating data (h/h_{ref}) as a function of angle of attack and Reynolds number during flight similar to that which can be obtained from wind tunnel tests. During the development flights the majority of the heating data is for a 40° angle of attack. In order to obtain heating data at other angles of attack for low

Reynolds numbers push-over-pull-up (POPU) maneuvers were performed. These maneuvers were designed to provide an approximate ten degree variation in angle of attack over a short time span. This permits an assessment of the influence of angle of attack at essentially the same Reynolds number.

Comparisons of flight and wind tunnel heating rate data (h/h_{ref}) showing the influence of angle of attack for constant Reynolds numbers are presented in Appendix D. The page numbers for these data can be found in Table VII. These comparisons are presented for STS-2, STS-3, STS-4, and STS-5 individually, and covers $30° \leq \alpha \leq 45°$ in the laminar regime and $25° \leq \alpha \leq 35°$ in the turbulent regime for STS-4.

Heating rate distribution plots for STS-2 and STS-5 at 35°, 40°, and 45° angles of attack are compared to wind tunnel data for normal shock Reynolds numbers of 2×10^5 and 3×10^5, respectively. Comparisons between wind tunnel and STS-3 flight data are provided for 40° and 45° angles of attack at $Re_{NS} = 4 \times 10^5$. STS-4 data comparisons are presented for $\alpha = 30°$, 35°, and 40° at $Re_{NS} = 8 \times 10^5$, and for turbulent heating for $\alpha = 25°$, 30°, and 35° at $Re_{NS} = 2.5 \times 10^6$. The data for STS-3 are not from a POPU maneuver, but are derived from an unplanned angle of attack variation in the entry trajectory.

The plots shown in Appendix D show the relative sensitivity of heating to angle of attack. In general, the flight data are insensitive to angle of attack over this limited data range. For the lower Reynolds numbers the windward surface flight heating data remained laminar. It should be pointed out that on the lower centerline for STS-4 at the $\alpha = 33.8°$, $Re_{NS} = 8 \times 10^5$ flight condition the measurement data at $X/L = 0.95$ is questionable.

Influence of Angle of Attack - Appendix E
Composite Flights - Variable Reynolds Number

As opposed to the POPU maneuvers flight data for lower angles of attack occurred much later in time at high Reynolds numbers. In the previous sections comparisons at essentially the same angle of attack and Reynolds number could be made. For this section the only variable that is held constant is the angle of attack. The flight heating rate distributions are presented for the angle of attack that occurred latest in time. The wind tunnel data used for comparison with flight data are taken at the highest Reynolds number tested for the corresponding angle of attack.

The comparison of flight and wind tunnel heating rate data (h/h_{ref}) showing the influence of angle of attack for high Reynolds numbers are presented in Appendix E. The page numbers for this data can be found in Table VIII. This comparison is presented for all five flights at angles of attack from 40° down to 20° in 5° increments. In this series of plots the Reynolds numbers increase by an approximate factor of two for each 5° decrease in angle of attack. Although flight data were selected only on the basis of angle of attack, the Mach numbers and Reynolds numbers were fairly consistent between flights. The Mach number and Reynolds number range at each angle of attack were:

$$\alpha = 40°, \quad 11.5 \leq M_\infty \leq 13.5, \quad 7.1 \times 10^5 \leq Re_{NS} \leq 9.8 \times 10^5$$
$$\alpha = 35°, \quad 8.5 \leq M_\infty \leq 9.2, \quad 1.6 \times 10^6 \leq Re_{NS} \leq 1.8 \times 10^6$$
$$\alpha = 30°, \quad 6.9 \leq M_\infty \leq 7.7, \quad 2.5 \times 10^6 \leq Re_{NS} \leq 2.8 \times 10^6$$
$$\alpha = 25°, \quad 5.6 \leq M_\infty \leq 6.3, \quad 4.5 \times 10^6 \leq Re_{NS} \leq 5.4 \times 10^6$$
$$\alpha = 22.5°, \quad 5.0 \leq M_\infty \leq 5.6, \quad 6.4 \times 10^6 \leq Re_{NS} \leq 8.3 \times 10^6$$
$$\alpha = 20°, \quad 3.6 \leq M_\infty \leq 4.8, \quad 1.0 \times 10^7 \leq Re_{NS} \leq 1.5 \times 10^7$$

In general, excellent agreement can be seen between the wind tunnel and flight data for angles of attack of 40° and 35° on the windward attached flow surfaces. At the lower angles of attack, the flight Reynolds numbers are much higher than the highest wind tunnel Reynolds number tested. It is recommended that the reader exercise some degree of caution in comparing the 8.0 Mach, 7.7 x 10^5 normal shock Reynolds number wind tunnel data to the flight data. For instance, at 30° angle of attack the Reynolds number is approximately three and a half times greater at flight than at wind tunnel conditions.

Along the lower centerline the heating distribution at 40° angle of attack indicates that the laminar heating was consistent between flights. The data for STS-1 show the transition from laminar to turbulent heating aft of X/L = 0.4. At 35° angle of attack only STS-2 remained laminar; the other flight data were either in transition or turbulent. The flight data at 30° angle of attack were essentially turbulent, and were fully turbulent for angles of attack below 30°. Wind tunnel and flight data tend to be in agreement for both laminar and turbulent heating at all angles of attack except 25° and 20° where the wind tunnel data remained laminar and was an order of magnitude lower than the turbulent flight data.

Along the lower wing 50% semi-span the heating distribution at 40° angle of attack indicates that the laminar heating was consistent between flights. The wind tunnel data (in transition?) were approximately two times greater than the flight data. The 35° angle of attack data are extremely interesting; we have captured the instance where the heating for two flights (STS-4 and STS-5) were fully turbulent while the heating for the other three flights remained laminar. This difference between laminar and turbulent heating appears to illustrate the sensitivity of heating to Reynolds number for this angle of attack. The laminar wind tunnel data tends to agree with the laminar flight data. For angles of attack 30° and below the flight data were fully turbulent and approximately five times greater than the laminar wind tunnel data.

Along the lower wing 80% semi-span the heating distribution at 40° angle of attack indicates that the flight data were laminar (STS-1 and STS-3 may be attempting to trip) and varied slightly between flights. The wind tunnel data (in transition?) were slightly above the flight data. The 35° angle of attack flight data are interesting in that the data for STS-1 and STS-2 were laminar, fully turbulent for STS-4 and STS-5, and in transition from laminar to turbulent heating for STS-3 similar to the behavior on the windward centerline at this angle of attack. This variation illustrates the heating sensitivity to Reynolds numbers. The wind tunnel data tends to be consistent with the laminar flight data. The flight data for angles of attack of 30° and below are fully turbulent and in agreement at each angle of attack. The wind tunnel data lies below flight data for these lower angles of attack. The wind tunnel data appear to be in transition at 30° and 25° angles of attack, and laminar for 20° angle of attack.

Along the side fuselage Z=400 trace at 40° angle of attack the heating distributions for all flight and wind tunnel data were in agreement forward of X/L = 0.4. Aft of X/L = 0.4 the flight data shows some variation and lies above the wind tunnel data. At 35° angle of attack the flight data were fairly consistent between flights. The flight data tends to agree with wind tunnel data forward of X/L = 0.4 and lies above the wind tunnel data aft of X/L = 0.4. The flight data for 30° angle of attack was fairly consistent except for STS-4 forward of X/L = 0.4 which indicated attached flow. The wind tunnel data lie below the flight data especially aft of X/L 0.3. At 25° and 20° angles of attack the heating distributions for all flights were in agreement. The flight data at these lower angles of attack are probably an indication of attached flow and the wind tunnel data lie below the flight data.

Along the side Payload Bay door Z=440 trace at 40° angle of attack the heating distributions for the flight data have some variation between flights, but show a consistent trend. While the wind tunnel data are below the flight data, both wind tunnel and flight data follow the same trend through X/L=0.6. Aft of X/L=0.6 the wind tunnel data are an order of magnitude lower than flight data. At 35° angle of attack all flight data are in agreement and probably indicate attached flow. The flight data are apparently turbulent and approximately five times greater than the wind tunnel data except at X/L=0.8 where there is an order of magnitude variation between wind tunnel and flight. The flight Reynolds numbers are approximately twice the wind tunnel Reynolds numbers. For angles of attack of 30° and below the flight data are basically in agreement for all flights, and increase slightly with decreasing angle of attack. For these lower angles of attack the wind tunnel data are below the flight data and are at much lower Reynolds numbers.

Along the upper lee side centerline at 40° angle of attack the heating distribution from flight data are essentially in agreement, especially forward of X/L=0.3. The wind tunnel data are above the flight data. At 35° angle of attack the heating distributions for all flights are in excellent agreement except for $0.3 \leq X/L \leq 0.4$. In general, the wind tunnel and flight data are in agreement, except at X/L=0.17 where the flight data are not as strongly attached, and at X/L=0.4 where the flight data were lower than wind tunnel data. At 30° angle of attack the flight data are essentially in agreement. The flight data indicates the flow was more strongly attached at X/L=0.1 and more separated at X/L=0.6 than wind tunnel data. In general, the wind tunnel data tends to approximate the flight data. At 25° angle of attack the flight data are in close agreement. The wind tunnel data lie below the flight data except for the two forward stations and at X/L=0.7. The flight data were strongly attached forward of X/L=0.7. At 25° and 20° angles of attack the flight data were fairly consistent, and the wind tunnel data were lower than flight data. In reviewing these plots the reader should recall that no data exist for STS-1 and STS-2 for $0.3 \leq X/L \leq 0.5$. In general, there is remarkable repeatibility of the flight data in this separated flow region, and good agreement until $\alpha = 20°$ when the Reynolds numbers are drastically different.

The flow along the OMS Pod is more difficult to characterize in terms of the heating distributions than for other locations. This may be due in part to geometry and Reynolds number effects, as well as, other effects that are not easily identified. Better comparisons can be made at the lower angles of attack than at the higher angles of attack. For instance, at 22.5° and 25° angles of attack the heating distribution for both flight and wind tunnel are in close agreement, although some variation in heating exists between flights. At 30° angle of attack the flight data tend to be in agreement from flight to flight, but the heating rate X/Lp trend is the opposite of that shown for the wind tunnel data. The wind tunnel data lie below the flight data. At 35° angle of attack the general trend of both flight and wind tunnel data is similar. The greatest variation between flights occurs forward of X/Lp=0.3. Since the distributions for STS-4 and STS-5 tend to agree; and the heating for STS-1, STS-2, STS-3, and wind tunnel tend to agree this may be a surface roughness effect. At 40° angle of attack the heating distributions for STS-3 show no variation as a function of X/Lp and slight variation with X/Lp for STS-2 and STS-5. The heating data for STS-1 and STS-4 are inconsistent with other flight data. The wind tunnel data tend to lie below the data for the STS-2, STS-3, and STS-5.

CONCLUDING REMARKS

eating rate distributions from flight and wind tunnel data have been presented for the lower windward and upper lee side centerline, lower wing 50% and 80% semi-spans, side fuselage Z=400 trace, side Payload Bay Door Z=440 trace, and OMS Pod trace 3. These distributions are presented in terms of normalized film heat transfer coefficients as a function of angle-of-attack, and normal shock Reynolds number.

The surface heating rates and temperatures presented as film heat transfer coefficients are based on the thermal analysis of flight temperature measurements using the JSC NONLIN/INVERSE computer program.

The heating distributions were presented for Reynolds numbers and angles of attack scans for each location to show the sensitivity of heating to these parameters.

The heating rate distributions, especially on the lower windward surface, demonstrate that the use of wind tunnel data is good for predicting the design environment and generally agree with or overpredict the flight data. On some regions of the Orbiter, the wind tunnel data underpredicted the flight data; such as the aft region of the Payload Bay door and the front of the OMS pod.

The data presented in this volume are intended to provide an overview to the heating for the first five shuttle flights, and aid the analyst in bridging the gap between wind tunnel and flight testing. Volumes 2 through 6 contain detailed heating information for each instrument location. These volumes contain heating rate data (h/h_{ref}) presented in terms of angle of attack, Mach number, and normal shock Reynolds number. Time history plots of surface heating rates and temperatures are also presented in these volumes.

REFERENCES

1. Smith, J. A., STS-3 Structural and Aerodynamic Pressure and Aerothermodynamics and Thermal Protection System Measurement Locations, NASA/JSC 17889, January 15, 1982.

2. Williams, S. D. and Curry, D. M., An Analytical and Experimental Study Using a Single Embedded Thermocouple, J. Spacecraft and Rockets, Vol. 14, October 1977, pp. 632-637.

3. Space Shuttle Program Thermodynamic Design Data Book, SD73-SH-0226, Vol. 2C, Rockwell International, Downey, California, July 1977.

4. Space Shuttle Program Thermodynamic Design Data Book, Penetrations, Book II, SD73-SH-0226, Vol. 3D, Book 2, Rockwell International, Downey, California, March 1978.

5. Ried, R. C., Jr.; Goodrich, W. D.; Strouhal, G.; and Curry, D. M. : The Importance of Boundary Layer Transition to the Space Shuttle Design, Proceedings of the Boundary Layer Transition Workshop held Nov. 3-5, 1971. Aerospace Report No. TOR-0172 (S2816-16) -5, Dec. 20, 1971.

6. Hender, D. R., A Miniature Version of the JA70 Aerodynamic Heating Computer Program, H800 (MINIVER) MDC G0462, McDonnell Douglas Astronautics Company, Huntington Beach, CA, June 1970, Revised January 1972.

7. Williams, S. D., and Curry, D. M., An Assessment of the Space Shuttle Orbiter Thermal Environment Using Flight Data, AIAA Paper 83-1488, Presented at the AIAA 18th Thermophysics Conference, June 1-3, 1983, Montreal, Canada.

8. Martindale, W. R., Kaul, C. E., and Nutt, K. W., Test Results from the NASA/Rockwell International Space Shuttle Orbiter Heating Test (OH49B) conducted in the AEDC-VKF Tunnel B, AEDC-DR-74-73, Von Karman Gas Dynamics Facility, ARO, Inc., Arnold Engineering Development Center, Arnold Air Force Station, Tennessee, Sept. 5, 1974.

9. Martindale, W. R., Kaul, C. E., and Nutt, K.W., Test Results from the NASA/Rockwell International Space Shuttle Orbiter Heating Test (OH39B) conducted in the AEDC-VKF Tunnel B, AEDC-DR-75-17 Von Karman Gas Dynamics Facility, ARO, Inc., Arnold Engineering Development Center, Arnold Air Force Station, Tennessee, Feb. 28, 1975.

10. Knox, E. C., Thin-Skin Thermocouple Heat-Transfer Tests on a 0.0175-Scale 140C Shuttle Orbiter Conducted at Mach 8.0 in the AEDC-VKF Tunnel B, AEDC-DR-75-71, Von Karman Gas Dynamics Facility, ARO, Inc., Arnold Engineering Development Center, Arnold Air Force Station, Tennessee, July 30, 1975.

11. Hudson, D. G., and Nutt, K. W., Space Shuttle Orbital Maneuvering System POD Heating Test at Mach Number 8, AEDC-TSR-80-V2, Arnold Engineering Development Center, Arnold Air Force Station, Tennessee, January 1980.

12. Williams, S. D., Columbia: The First Five Flights Entry Heating Data Series, Vol. 2, The OMS Pod, NASA CR-171657, May 1983.

13. Williams, S. D., Columbia: The First Five Flights Entry Heating Data Series, Vol. 3, The Lower Windward Surface Centerline, NASA CR-171665, May 1983.

14. Williams, S. D., Columbia: The First Five Flights Entry Heating Data Series, Vol. 4, The Lower Windward Wing 50% and 80% Semi-Spans, NASA CR-171666, May 1983.

15. Williams, S. D., Columbia: The First Five Flights Entry Heating Data Series, Vol. 5, The Side Fuselage and Payload Bay Door, NASA CR-171732, January 1984.

16. Williams, S. D., Columbia: The First Five Flights Entry Heating Data Series, Vol. 6, The Upper Lee Side Surface Centerline, NASA CR-171795, July 1984.

17. Goodrich, W. D., Derry, S. M., and Bertin, J. J., Shuttle Orbiter Boundary Layer Transition at Flight and Wind Tunnel Conditions, NASA Conference Publication 2283-Part 2, Shuttle Performance: Lessons Learned, From the proceedings of a conference held at NASA Langley Research Center, Hampton, Virginia, March 8-10, 1983.

18. Shinn, J. L., Moss, J. N., and Simmonds, A. L. Viscous-Shock-Layer Heating Analysis for the Shuttle Windward Plane with Surface Finite Catalytic Recombination Rates, AIAA paper 82-0842, presented at AIAA/ASME 3rd Joint Thermophysics, Fluids, Plasma, and Heat Transfer Conference, June 7-11, 1982, St Louis, Missouri.

19. Scott, C. D. and Derry, S. M., Catalytic Recombination and The Space Shuttle Heating, AIAA paper 82-0841, presented at the AIAA/ASME 3rd Joint Thermophysics, Fluids, Plasma and Heat Transfer Conference, June 7-11, 1982, St. Louis, Missouri.

20. Scott, C. D., Effects of Nonequilibrium and Catalysis on Shuttle Heat Transfer, AIAA paper 83-1485, presented at AIAA 18th Thermophysics Conference, June 1-3, 1983, Montreal, Canada.

21. Lee, D. B. and Harthun, M. H., Aerothermodynamic Entry Environment of the Space Shuttle Orbiter, AIAA paper 82-0821, presented at AIAA/ASME 3rd Joint Thermophysics, Fluids, Plasma and Heat Transfer Conference, June 7-11, 1982, St. Louis, Missouri.

22. Throckmorton, D. A., and Hartung, L. C., Analysis of Entry Aerodynamic Heat Transfer Data for the Orbiter Wing Lower Surface, AIAA paper 84-0227, presented at the AIAA 22nd Aerospace Sciences Meeting, January 9-12, 1984, Reno, Nevada.

23. Hodge, J. K., and Audley, D. R., Aerothermodynamic Parameter Estimation from Space Shuttle Thermocouple Data During Transient Flight Test Maneuvers, AIAA paper 83-0482, presented at AIAA 21st Aerospace Sciences Meeting, January 10-13, 1983, Reno, Nevada.

24. Hamilton, H. H. II, Approximate Method of Predicting Heating on the Windward Side of Space Shuttle Orbiter and Comparisons with Flight Data, AIAA paper 82-0823, presented at AIAA/ASME 3rd Joint Thermophysics, Fluids, Plasma, and Heat Transfer Conference, June 7-11, 1982, St. Louis, Missouri.

25. Throckmorton, D. A., Influence of Radiant Energy Exchange on the Determination of Convective Heat Transfer Rates to Orbiter Lee Side Surfaces During Entry, AIAA paper 82-0824, presented at AIAA/ASME 3rd Joint Thermophysics Fluids, Plasma and Heat Transfer Conference, June 7-11, 1982, St. Louis, Missouri.

WINDWARD LOWER SURFACE

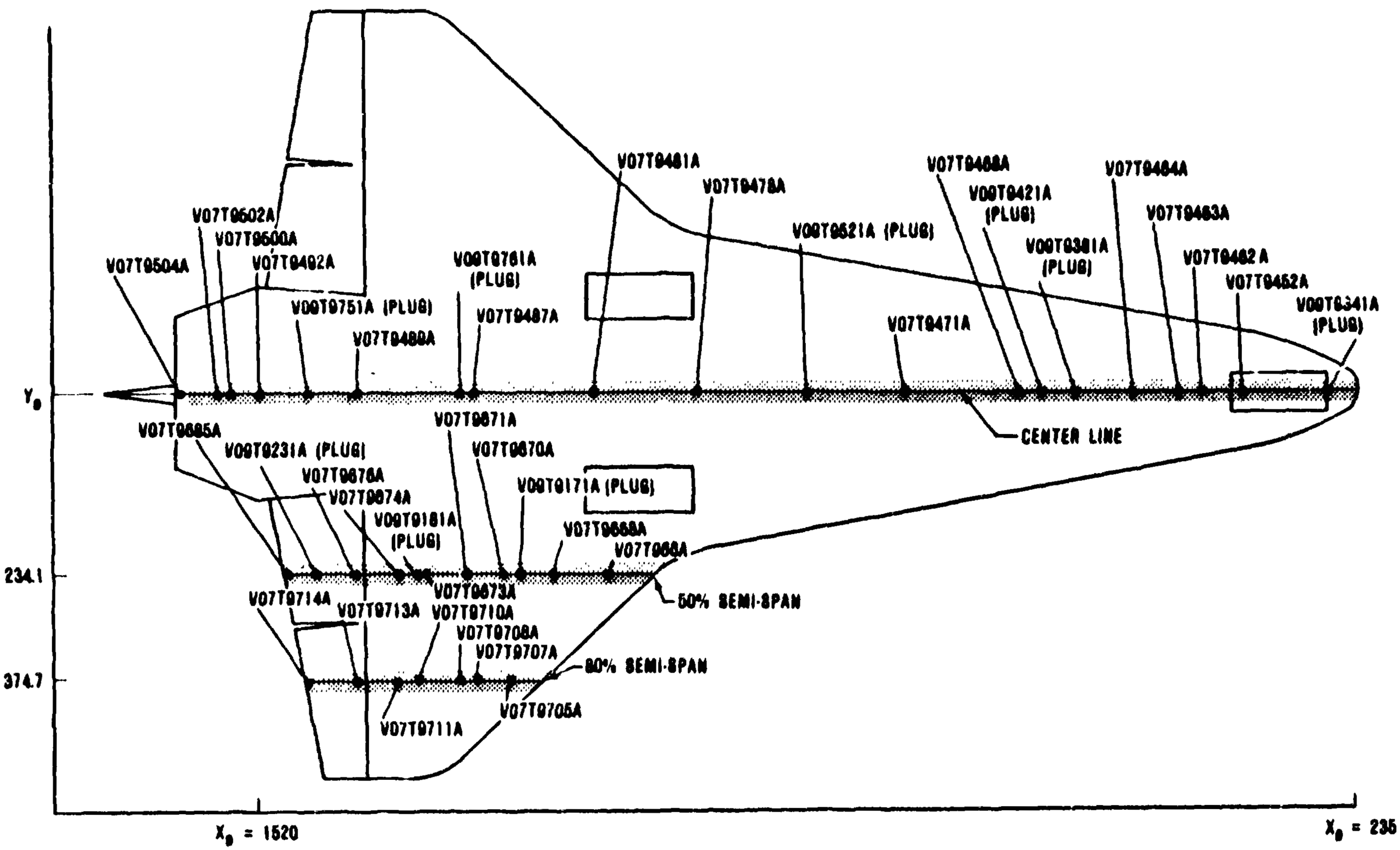

FIGURE 1.- LOCATION OF DFI LOWER SURFACE INSTRUMENTATION ON COLUMBIA (CENTERLINE AND WING 50% AND 80% SEMI-SPANS).

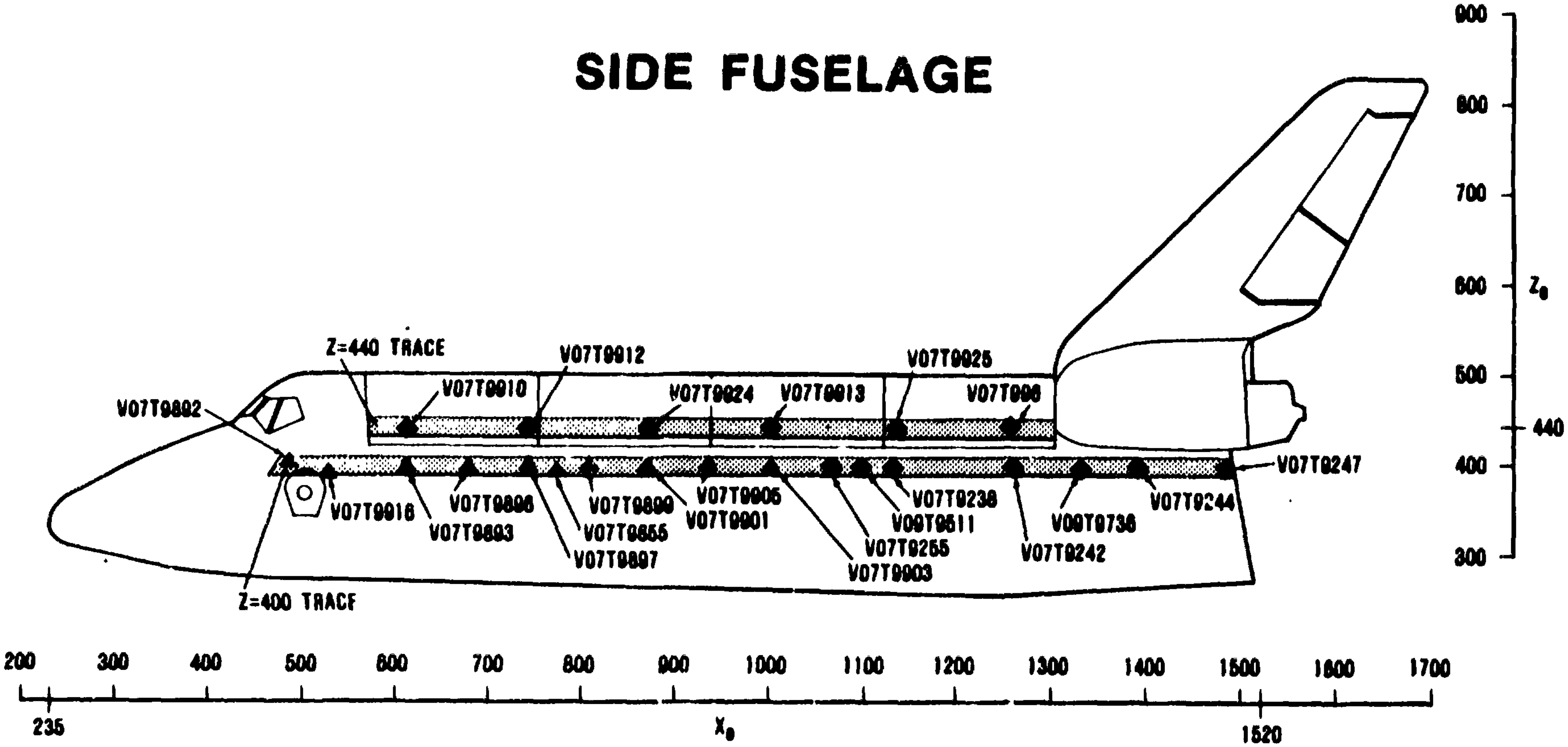

FIGURE 2.- LOCATION OF DFI INSTRUMENTATION ON THE FUSELAGE SIDE AND PAYLOAD BAY DOOR SIDE SURFACE.

LEE SIDE UPPER CENTERLINE

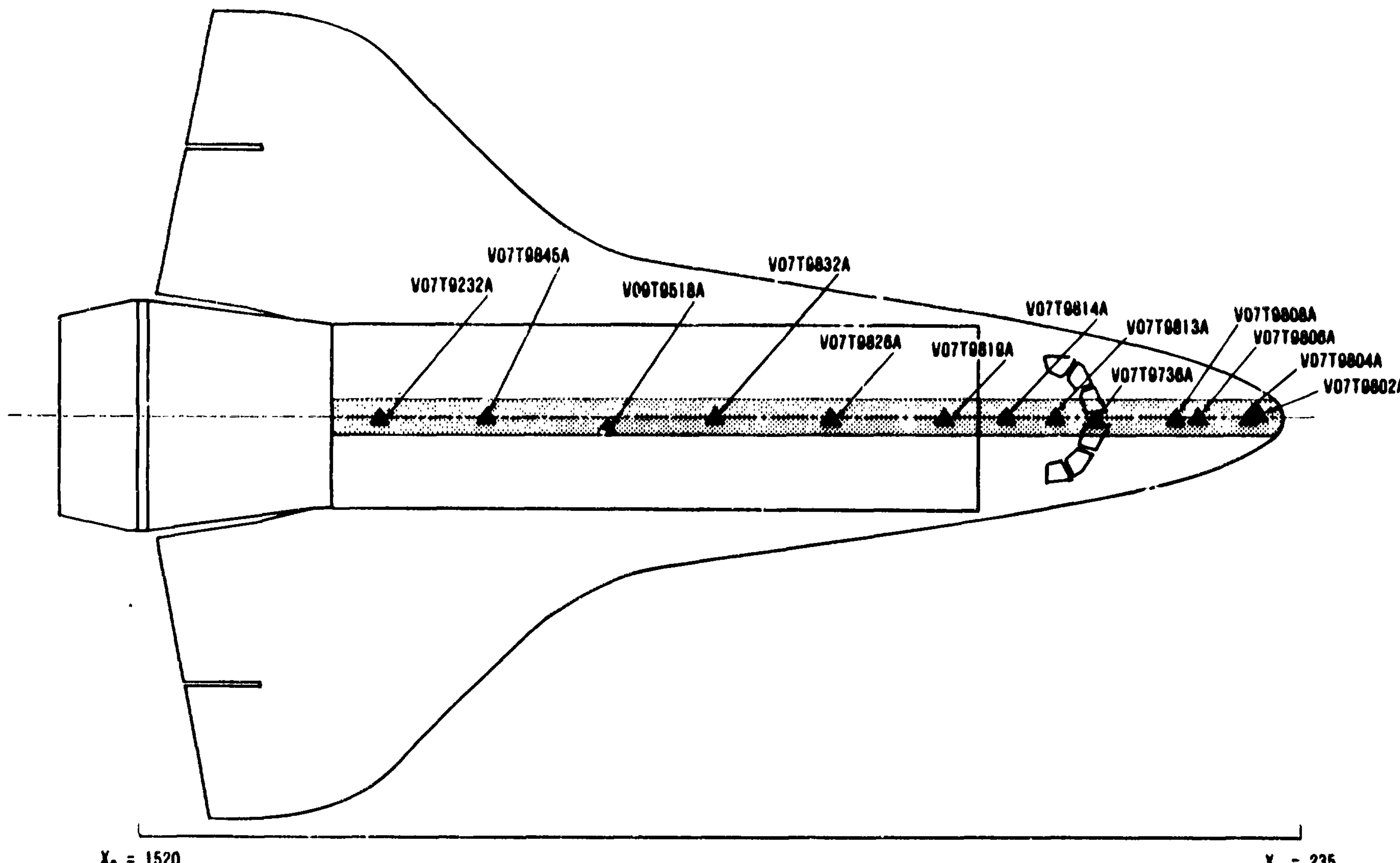

FIGURE 3.- LOCATION OF DFI LEE SIDE UPPER CENTERLINE INSTRUMENTATION ON COLUMBIA.

OMS POD - SIDE VIEW

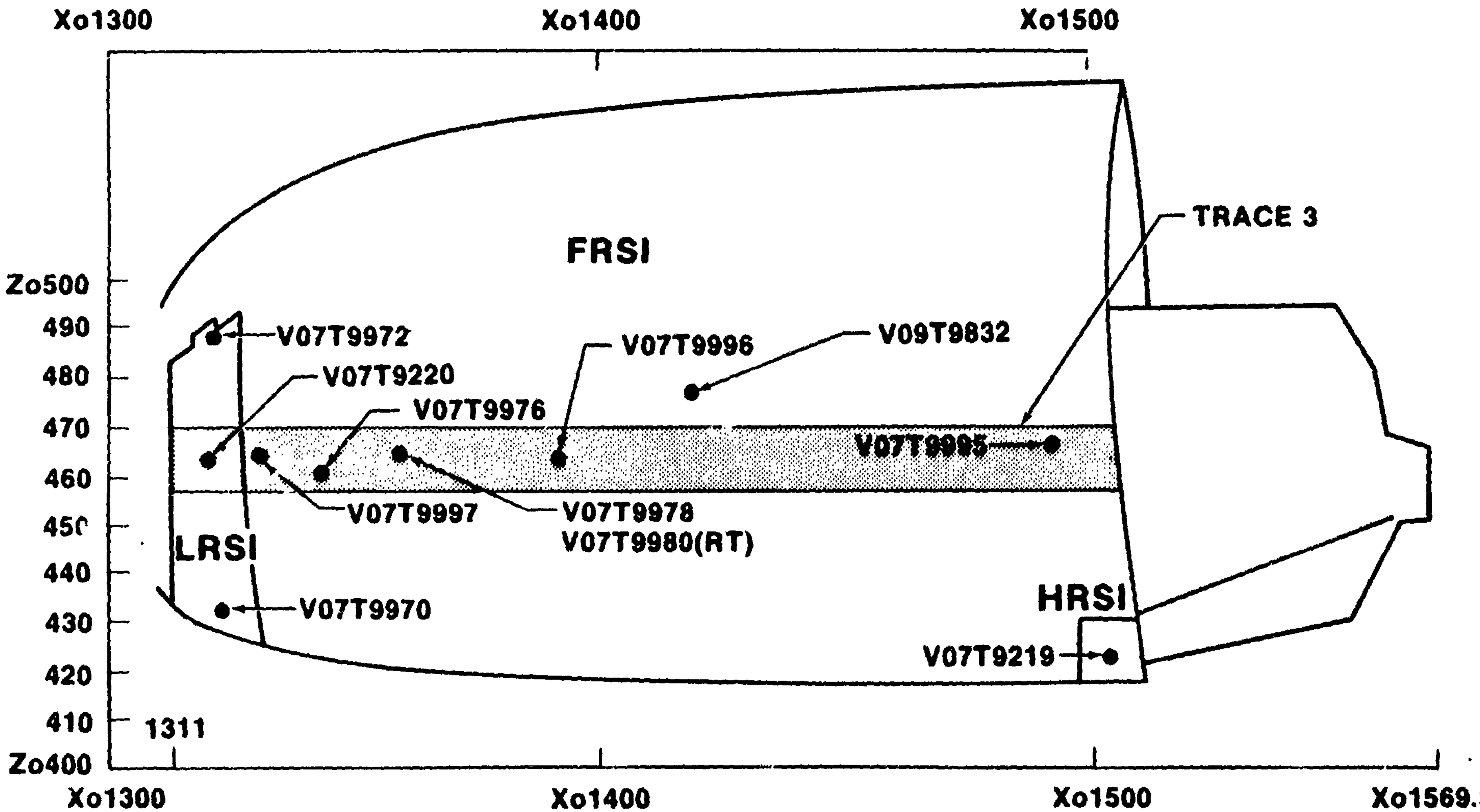

FIGURE 4A.- LOCATION OF DFI OMS POD (SIDE VIEW) INSTRUMENTATION ON COLUMBIA.

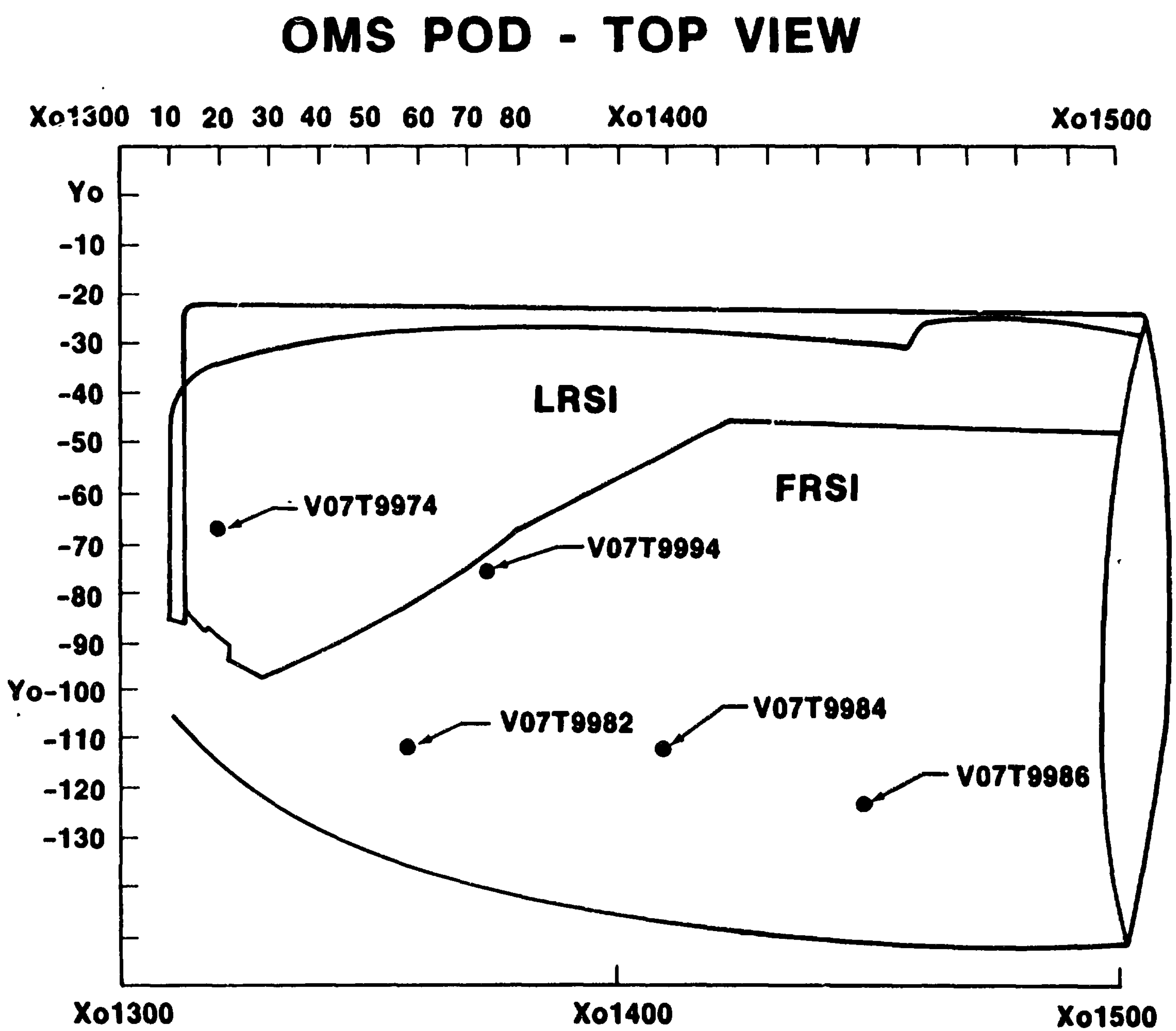

FIGURE 4B.- LOCATION OF DFI OMS POD (TOP VIEW) INSTRUMENTATION ON COLUMBIA.

TABLE I - Reference Greenwich Meridian Times for Flight Events

GMT Day:Hr:Min:Sec/GMT Seconds

Flight	Launch	SRBSEP SRB Separation	MECO Main Engine Cutoff	ENTRY	TAEM	TD TouchDown
STS-1	101:12:00:04.000 8856004.000	102:12:02:06.000 8856126.000	102:12:08:42.000 8856522.000	104:17:49:04.000 9049744.000	104:18:14:34.000 9051274.000	104:18:21:11.000 9051671.000
STS-2	316:15:09:59:815 27356999.815	316:15:12:09.900 27357129.900	316:15:18:38.000 27357518.000	318:20:50:36.000 27550236.000	318:21:16:30.000 27551790.000	318:21:23:11.000 27552191.000
STS-3	081.15:59:59:785 7055999.785	081:16:02:07.500 7056127.500	081:16:08:34.800 7056514.800	089:15:34:44.000 7745684.000	089:16:00:00.000 7747200.000	089:16:04:46.000 7747486.000
STS-4	178:14:59:59:793 15433199.793	178:15:02:08.793 15433328.793	178:15:08:32.509 15433712.509	185:15:40:23.000 16040423.000	185:16:03:20.000 16041800.000	185:16:09:39.900 16042179.900
STS-5	315:12:18:59.921 27260339.921	315:12:21:09.000 27260469.000	315:12:27:25.914 27260845.914	320:14:03:11.000 27698591.000	320:14:27:15.000 27700035.000	320:14:33:27.000 27700407.000

TABLE II

Correlation Between Free Stream and Normal Shock Reynolds Numbers at AEDC-B Wind Tunnel Conditions for 0.0175 Scale Orbiter ($L=0.0175 \times 107 = 1.8725$ ft)

Re_{∞}/ft $\times 10^6$	$Re_{\infty,L}$ $\times 10^6$	$Re_{NS,L}$ $\times 10^5$
0.50	0.936	1.050
1.00	1.873	2.099
1.50	2.809	3.149
2.00	3.745	4.198
2.50	4.681	5.248
3.00	5.618	6.297
3.50	6.554	7.347
3.70	6.928	7.767

NOTE: $Re_{NS}/Re_{\infty} = 0.1121$

TABLE III

Catalytic Tiles on the Lower Centerline By Flight

Mid	X/L	STS-1	STS-2	STS-3	STS-4	STS-5
Nose Cap	0.000					
V09T9341	0.026					
V07T9452	0.100				C	C
V07T9462	0.140					
V07T9463	0.160		C			C
V07T9464	0.200	1				C
V09T9381	0.260					
V09T9421	0.290		2			
V07T9468	0.300			C	C	C
V09T9471	0.400		C	C	C	C
V09T9521	0.500					
V07T9478	0.600					C
V07T9481	0.690					
V07T9487	0.800					
V09T9761	0.810					
V07T9489	0.900					
V09T9751	0.950					
V07T9492	0.990					
V07T9500	1.020					
V07T9502	1.030					
V07T9504	1.040					

[1] DATA TOO HIGH - IGNORE FOR STS-1

[2] DATA TOO HIGH - ANOMALY

[C] CATALYTIC SURFACE

TABLE IV

Page Numbers for Appendix A

Correlation Parameters

Flight Parameters		Page No. by Flight				
		STS-1	STS-2	STS-3	STS-4	STS-5
α	vs. t	1	2	3	4	5
M_∞	vs. t	6	7	8	9	10
H_T	vs. t	11	12	13	14	15
Re_{NS}	vs. t	16	17	18	19	20
Re_{NS}/Re_∞	vs. t	21	22	23	24	25
δ_{BF}	vs. t	26	27	28	29	30
δ_{E-RH}	vs. t	31	32	33	34	35
δ_{E-LH}	vs. t	36	37	38	39	40
q_{ref}	vs. t	41	42	43	44	45
h_{ref}	vs. t	46	47	48	49	50
α	vs. M_∞	51	52	53	54	55
α	vs. H_T	56	57	58	59	60
α	vs. Re_{NS}	61	62	63	64	65
α	vs. Re_{NS}/Re_∞	66	67	68	69	70
M_∞	vs. H_T	71	72	73	74	75
M_∞	vs. Re_{NS}	76	77	78	79	80
M_∞	vs. Re_{NS}/Re_∞	81	82	83	84	85
H_T	vs. Re_{NS}	86	87	88	89	90
H_T	vs. Re_{NS}/Re_∞	91	92	93	94	95
q_{ref}	vs. α	96	97	98	99	100
q_{ref}	vs. M_∞	101	102	103	104	105
q_{ref}	vs. Re_{NS}	106	107	108	109	110
h_{ref}	vs. α	111	112	113	114	115
h_{ref}	vs. M_∞	116	117	118	119	120
h_{ref}	vs. Re_{NS}	121	122	123	124	125

TABLE V
PAGE NUMBERS FOR APPENDIX B

Heating Rate Comparison - Influence of Re_{NS} (α= 40°)

Distribution - h/h_{ref} vs	$Re_{NS} \times 10^5$	Page No. by Flight		
		STS-2	STS-3	STS-5
X/L - Lower Centerline	0.2	1	17	33
	0.3	2	18	34
	0.4	3	19	35
	0.5	4	20	36
	0.6	5	21	37
	0.7	6	22	38
	0.8	7	23	39
	0.9	8	24	40
	1.0	9	25	41
	2.0	10	26	42
	3.0	11	27	43
	4.0	12	28	44
	5.0	13	29	45
	6.0	14	30	46
	7.0	15	31	47
	8.0	16	32	48
	0.2 - 0.9	49	51	53
	1.0 - 8.0	50	52	54
X/C - Lower Wing 50% Semi-Span	0.2 - 0.9	55	57	59
	1.0 - 8.0	56	58	60
X/C - Lower Wing 80% Semi-Span	0.2 - 0.9	61	63	65
	1.0 - 8.0	62	64	66
X/L - Side Fuselage (Z=400 Trace)	0.2 - 0.9	67	69	71
	1.0 - 8.0	68	70	72
X/L - Side Payload Bay Door (Z=440 Trace)	0.2 - 0.9	73	75	77
	1.0 - 8.0	74	76	78
X/L - Upper Centerline	0.2 - 0.9	79	81	83
	1.0 - 8.0	80	82	84
X/Lp - OMS Pod (Trace 3)	0.2 - 0.9	85	87	89
	1.0 - 8.0	86	88	90

TABLE VI

Page Numbers for Appendix C

Heating Rate Comparisons at Wind Tunnel Reynolds Numbers ($\alpha = 40°$)

Distribution - h/h_{ref} vs	Page No. by $Re_{NS} \times 10^5$							
	1.050	2.099	3.149	4.198	5.248	6.297	7.347	7.767
X/L - Lower Centerline	1	2	3	4	5	6		7
X/C - Lower Wing 50% Semi-Span	8	9	10	11	12	13		14
X/C - Lower Wing 80% Semi-Span	15	16	17	18	19	20		21
X/L - Side Fuselage (Z-400 Trace)	22	23	24	25	26	27	28	29
X/L - Side Payload Door (Z=440 Trace)	30	31	32	33	34	35	36	37
X/L - Upper Centerline	38	39	40	41	42	43		44
X/Lp - OMS Pod (Trace 3)		45		46		47		48

TABLE VII
PAGE NUMBERS FOR APPENDIX D

Heating Rate Comparison - Influence of Angle of Attack (Constant Re_{NS})

Distribution - h/h_{ref} vs	α	Re_{NS} $\times 10^5$	Page No. by Flight STS-2	STS-3	STS-4	STS-5
X/L Lower Centerline	35,40,45	2	1			
	35,40,45	3				2
	40,45	4		3		
	30,35,40	8			4	
	25,30,35	25			5	
X/C Lower Wing 50% Semi-Span	35,40,45	2	6			
	35,40,45	3				7
	40,45	4		8		
	30,35,40	8			9	
	25,30,35	25			10	
X/C Lower Wing 80% Semi-Span	35,40,45	2	11			
	35,40,45	3				12
	40,45	4		13		
	30,35,40	8			14	
	25,30,35	25			15	
X/L Side Fuselage (Z=400 Trace)	35,40,45	2	16			
	35,40,45	3				17
	40,45	4		18		
	30,35,40	8			19	
	25,30,35	25			20	
X/L Side Payload Bay Door (Z=440)	35,40,45	2	21			
	35,40,45	3				22
	40,45	4		23		
	30,35,40	8			24	
	25,30,35	25			25	

TABLE VII
PAGE NUMBERS FOR APPENDIX D (Continued)

Heating Rate Comparison - Influence of Angle of Attack (Constant Re_{NS})

Distribution - h/h_{ref} vs	α	Re_{NS} $\times 10^5$	Page No. by Flight			
			STS-2	STS-3	STS-4	STS-5
X/L Upper Centerline	35,40,45	2	26			
	35,40,45	3				27
	40,45	4		28		
	30,35,40	8			29	
	25,30,35	25			30	
X/LP OMS Pod (Trace 3)	35,40,45	2	31			
	35,40,45	3				32
	40,45	4		33		
	30,35,40	8			34	
	25,30,35	25			35	

TABLE VIII

PAGE NUMBERS FOR APPENDIX E

Heating Rate Comparisons - Influence of Angle of Attack (Variable Re_{NS})

Distribution - h/h_{ref}	Angle of Attack 40°	35°	30°	25°	22 1/2°	20°
X/L - Lower Centerline	1	2	3	4		5
X/C - Lower Wing 50% Semi-Span	6	7	8	9		10
X/C - Lower Wing 80% Semi-Span	11	12	13	14		15
X/L - Side Fuselage (Z=400 Trace)	16	17	18	19		20
X/L - Side Payload Bay Door (Z=440)	21	22	23	24		25
X/L - Upper Centerline	26	27	28	29		30
X/Lp - OMS Pod (Trace 3)	31	32	33	34	35	

APPENDIX A

CORRELATION PARAMETERS

STS-1 (107 FT LENGTH) FLIGHT PARAMETER COMPARISON

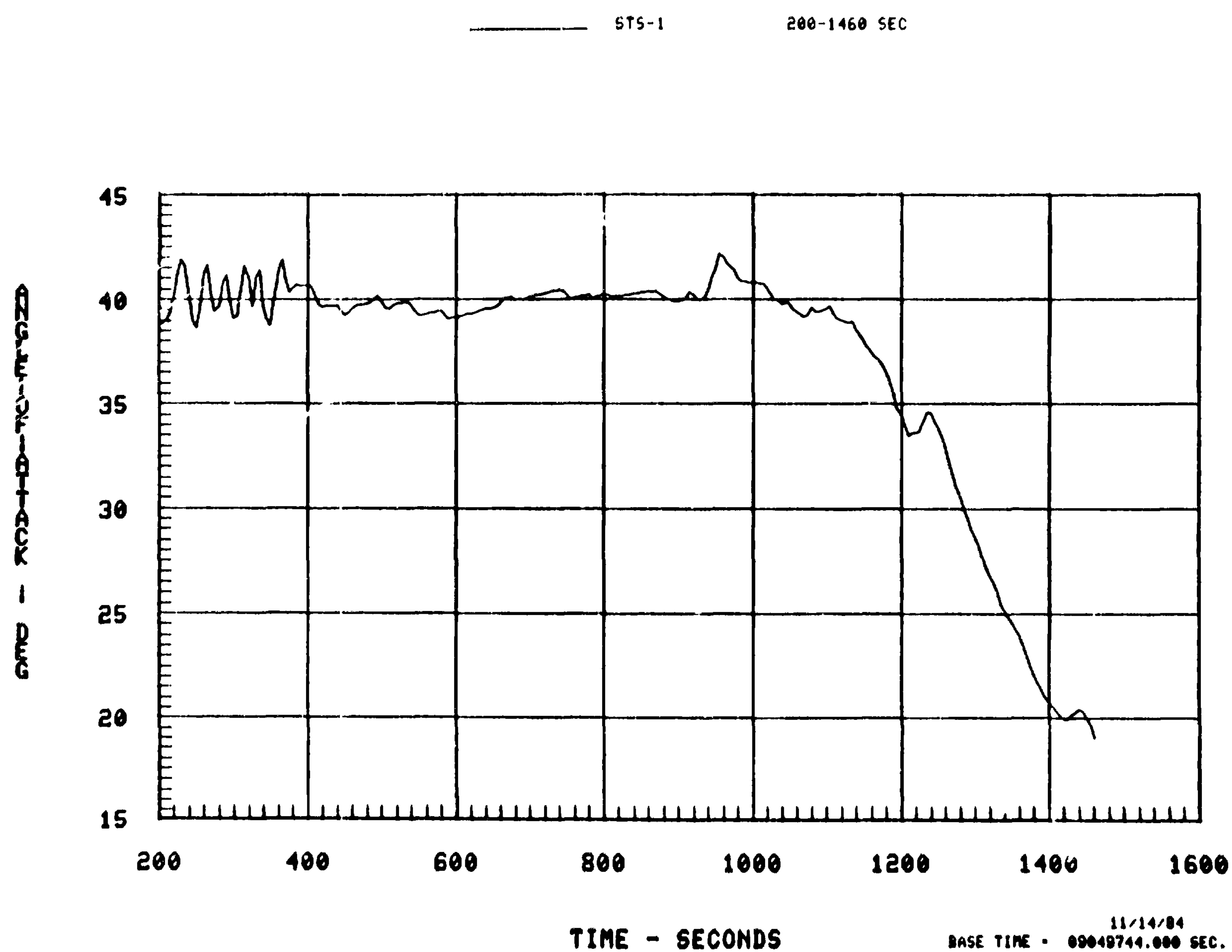

STS-2 (107 FT LENGTH) FLIGHT PARAMETER COMPARISON

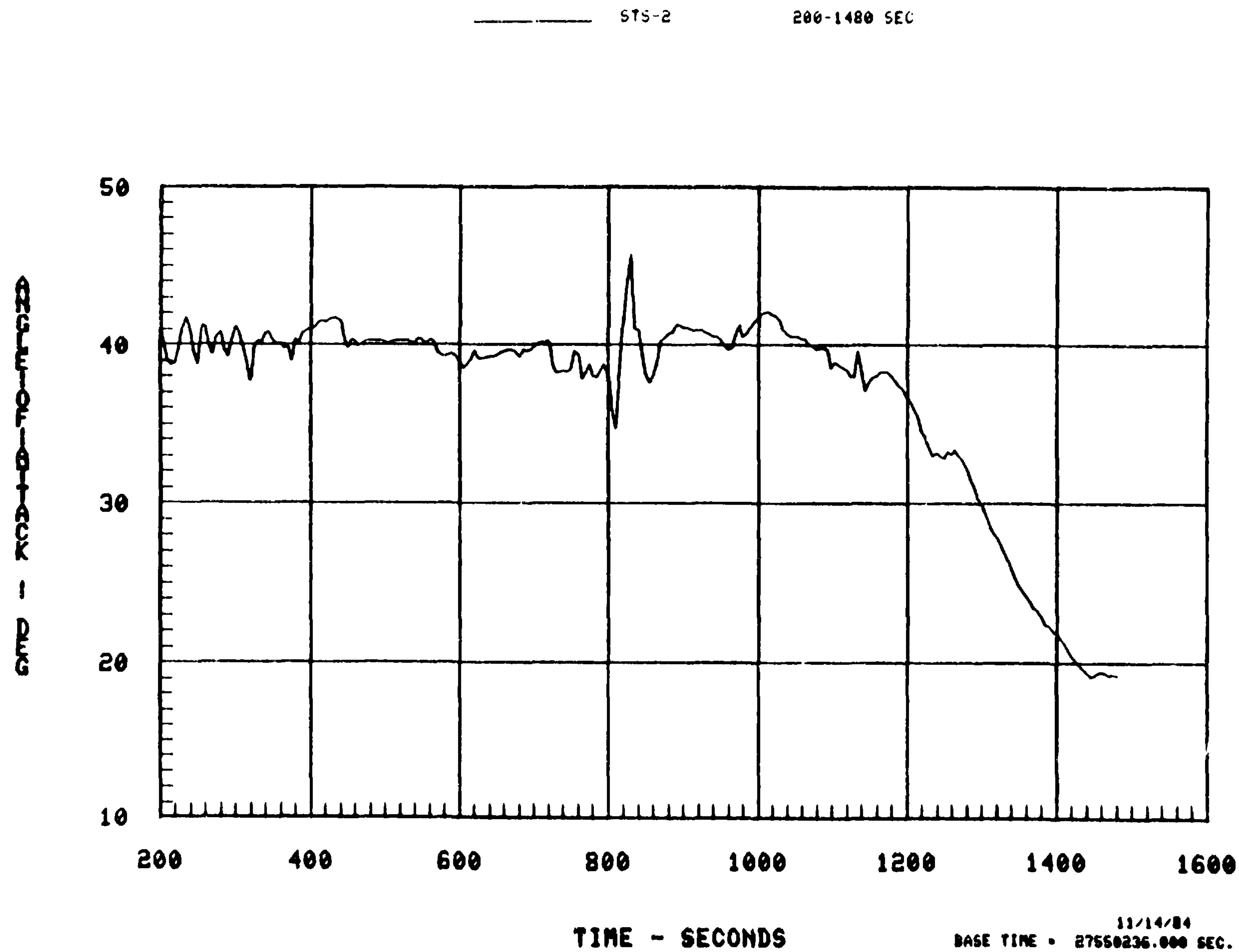

STS-3 (107 FT LENGTH) FLIGHT PARAMETER COMPARISON

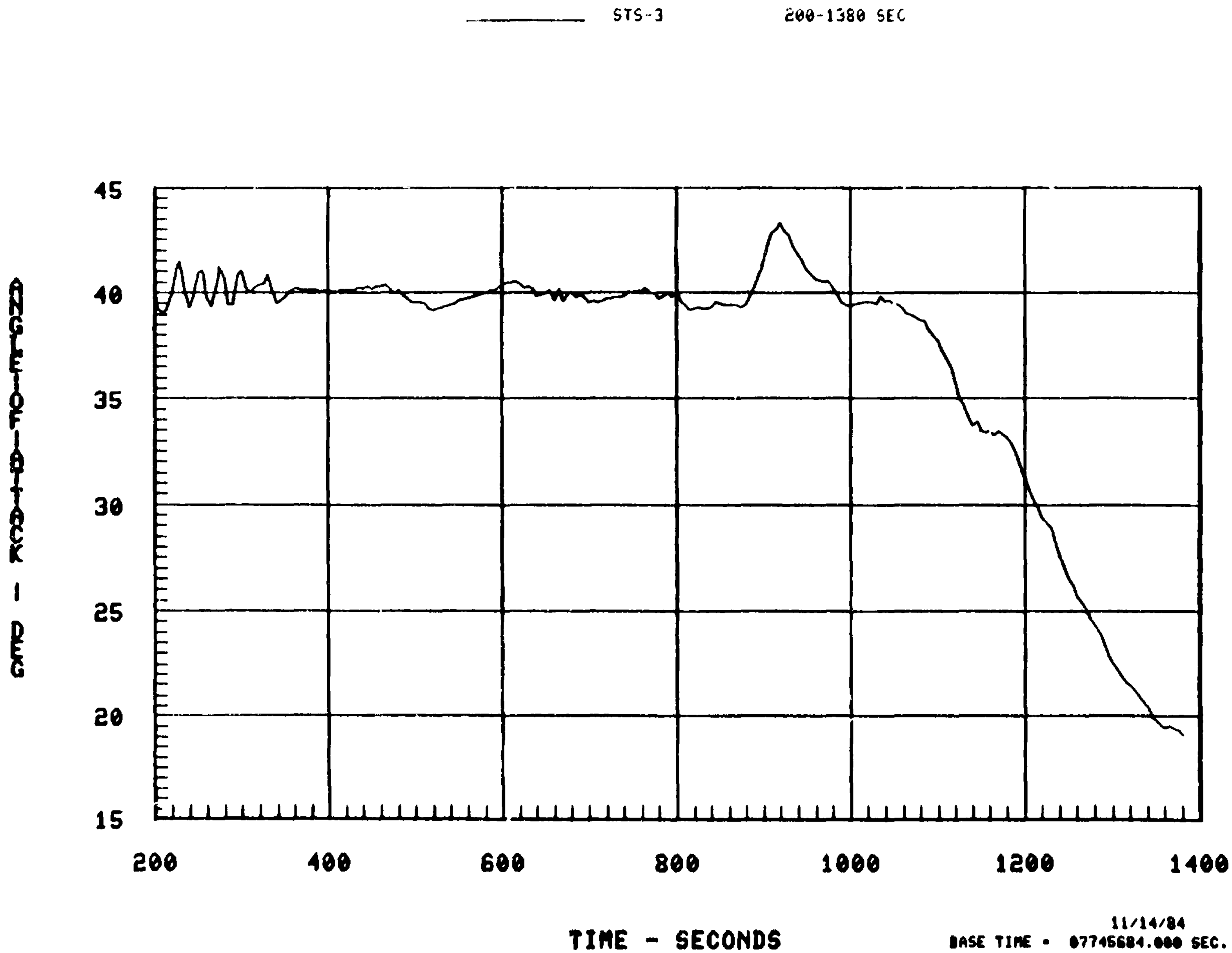

STS-4 (107 FT LENGTH) FLIGHT PARAMETER COMPARISON

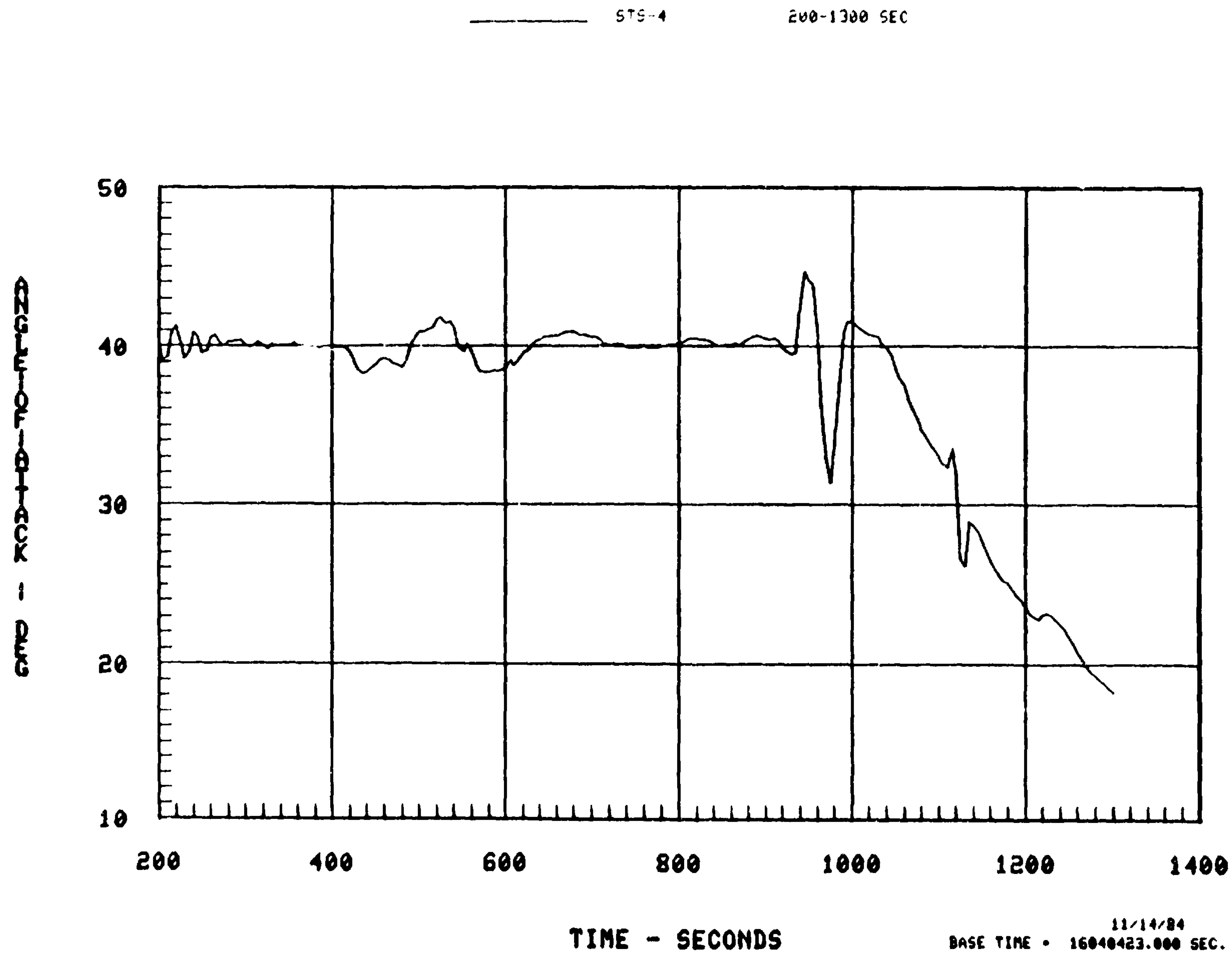

STS-5 (107 FT LENGTH) FLIGHT PARAMETER COMPARISON

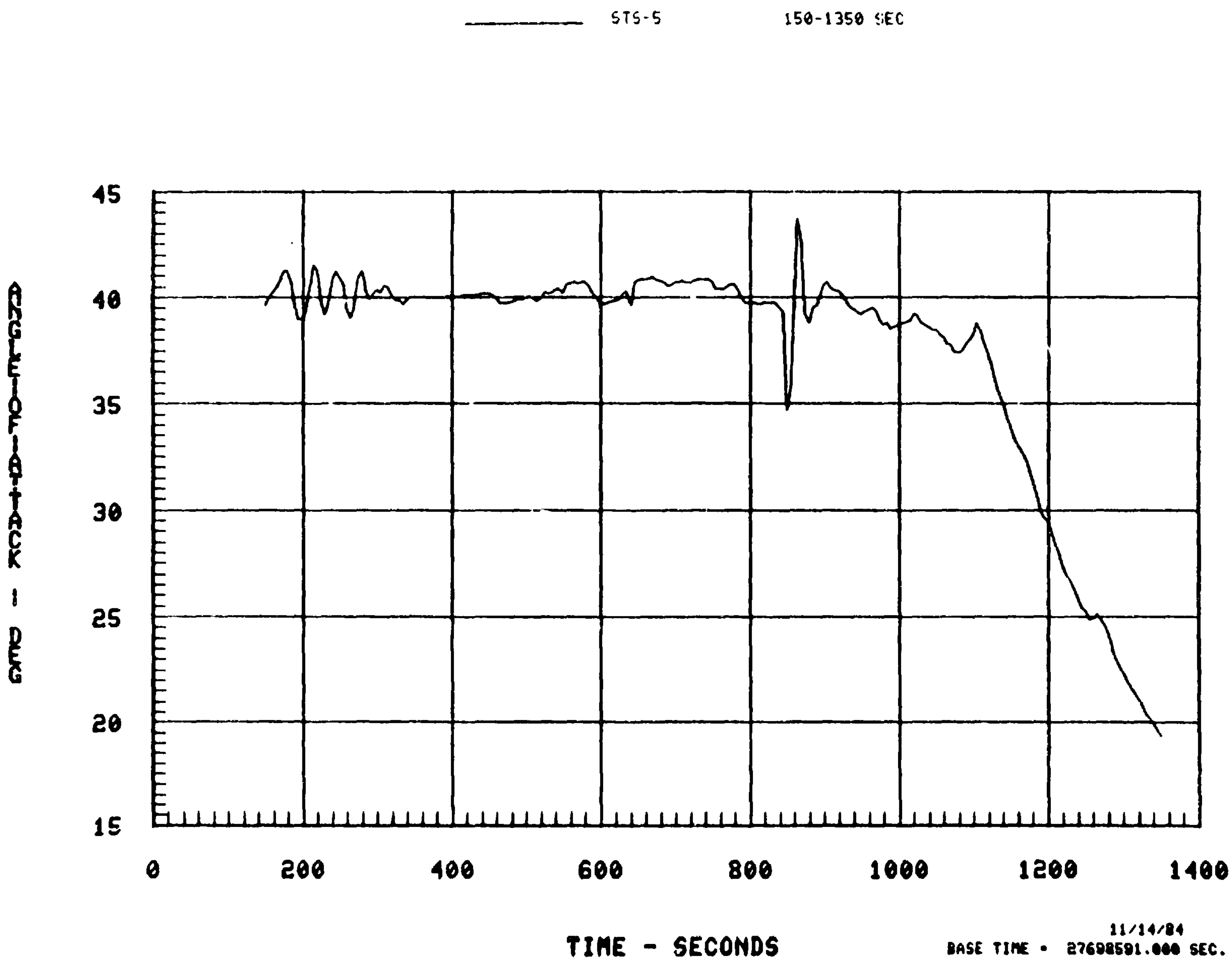

STS-1 (107 FT LENGTH) FLIGHT PARAMETER COMPARISON

———————— STS-1 200-1460 SEC

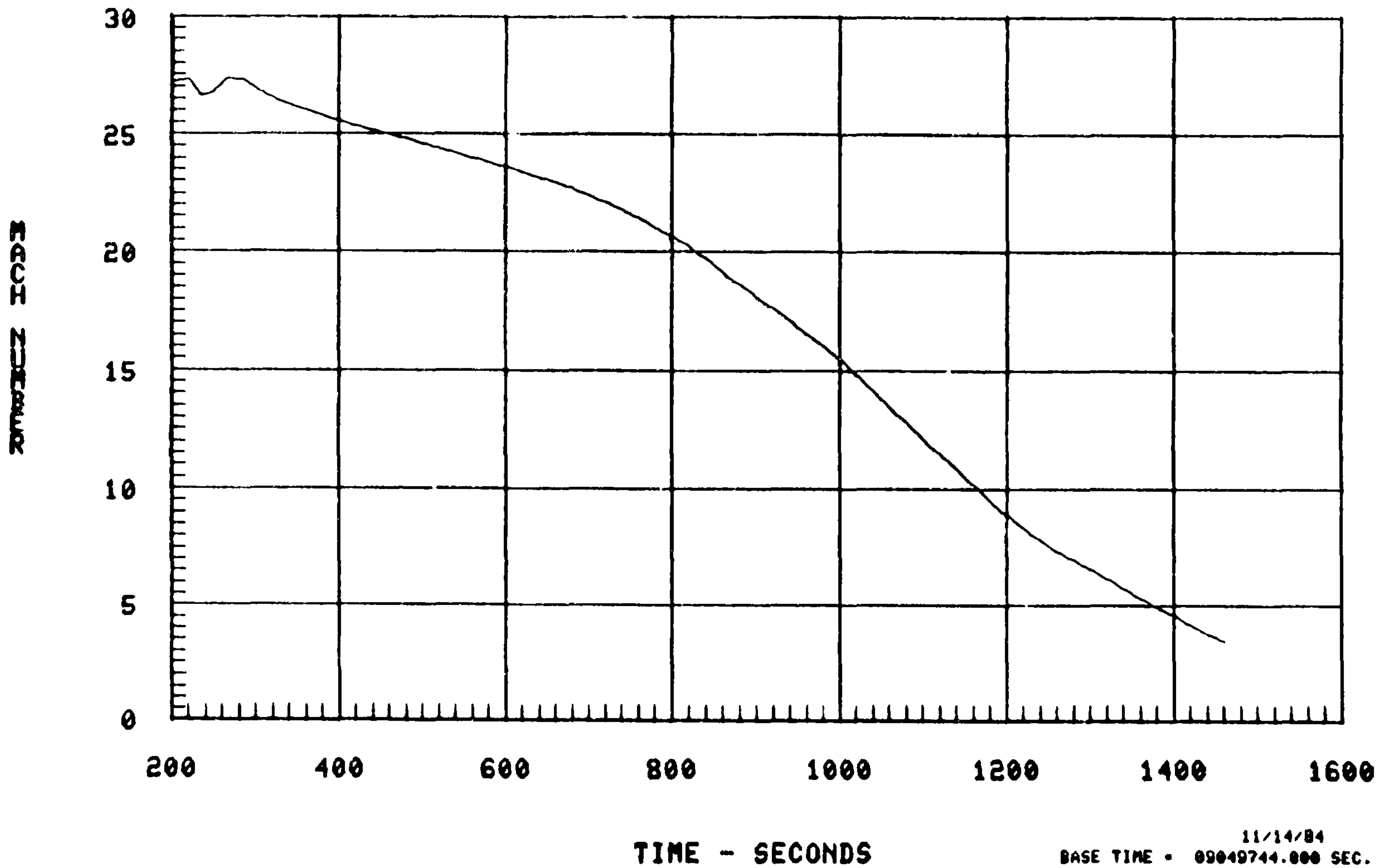

STS-2 (107 FT LENGTH) FLIGHT PARAMETER COMPARISON

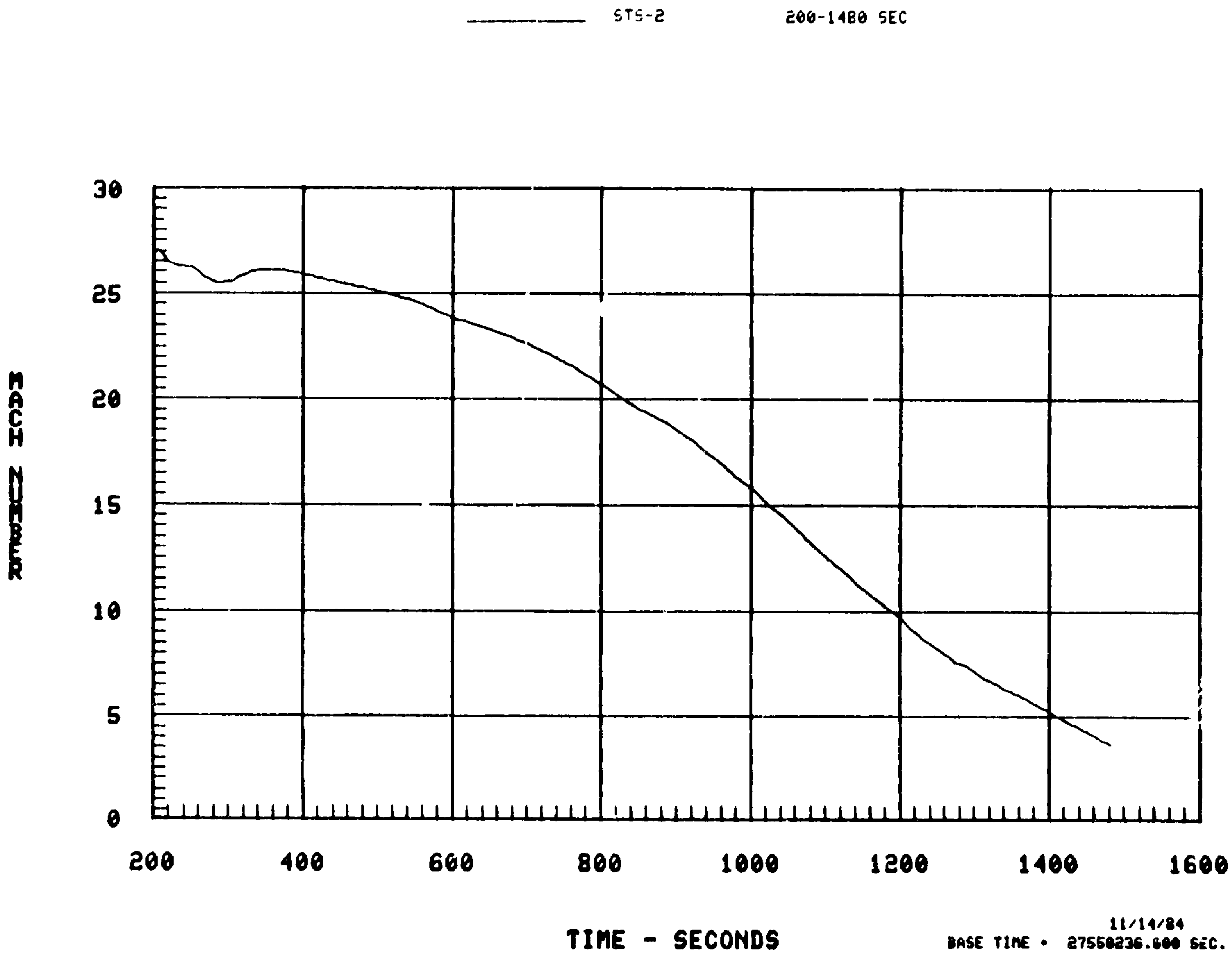

STS-3 (107 FT LENGTH) FLIGHT PARAMETER COMPARISON

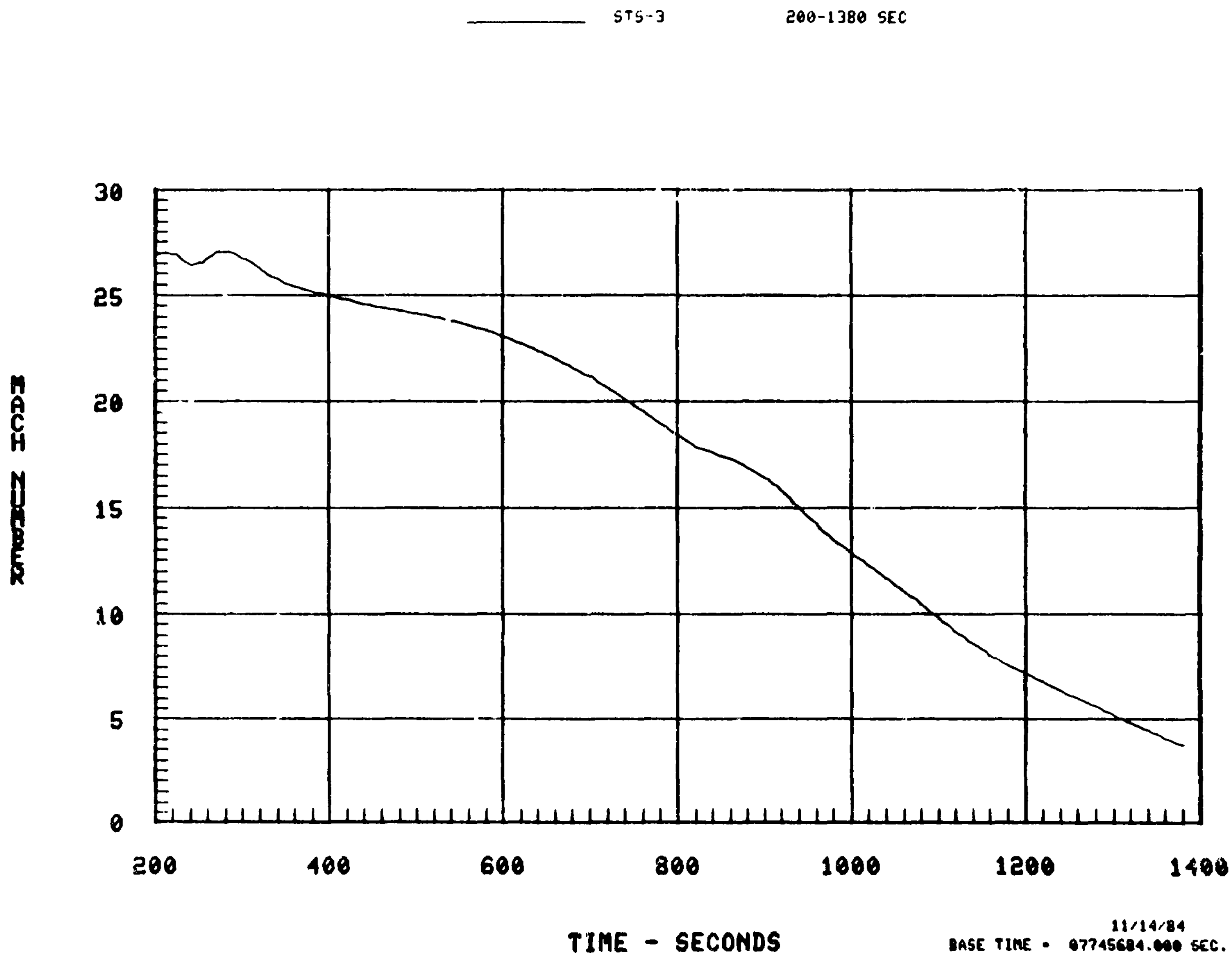

STS-4 (107 FT LENGTH) FLIGHT PARAMETER COMPARISON

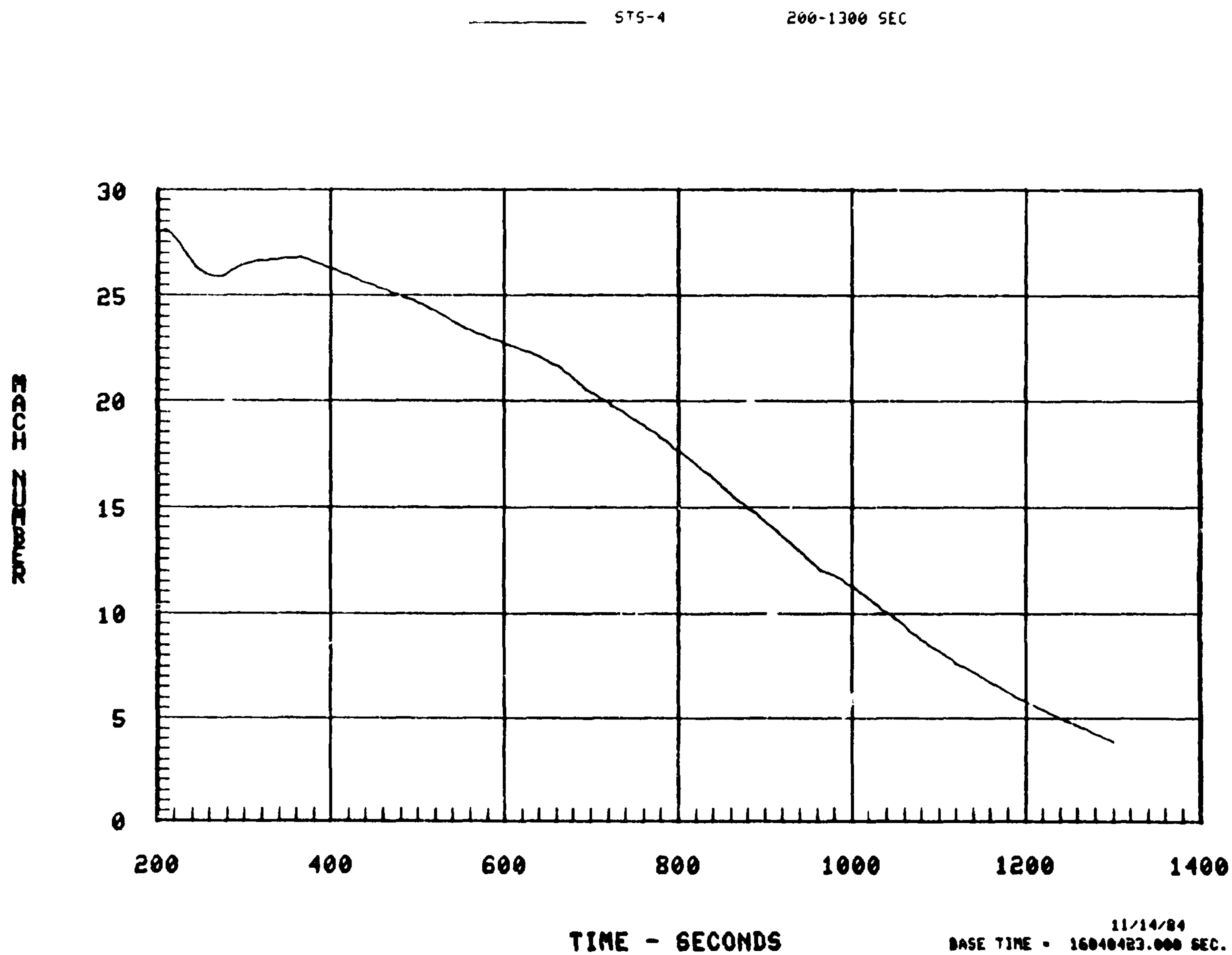

STS-5 (107 FT LENGTH) FLIGHT PARAMETER COMPARISON

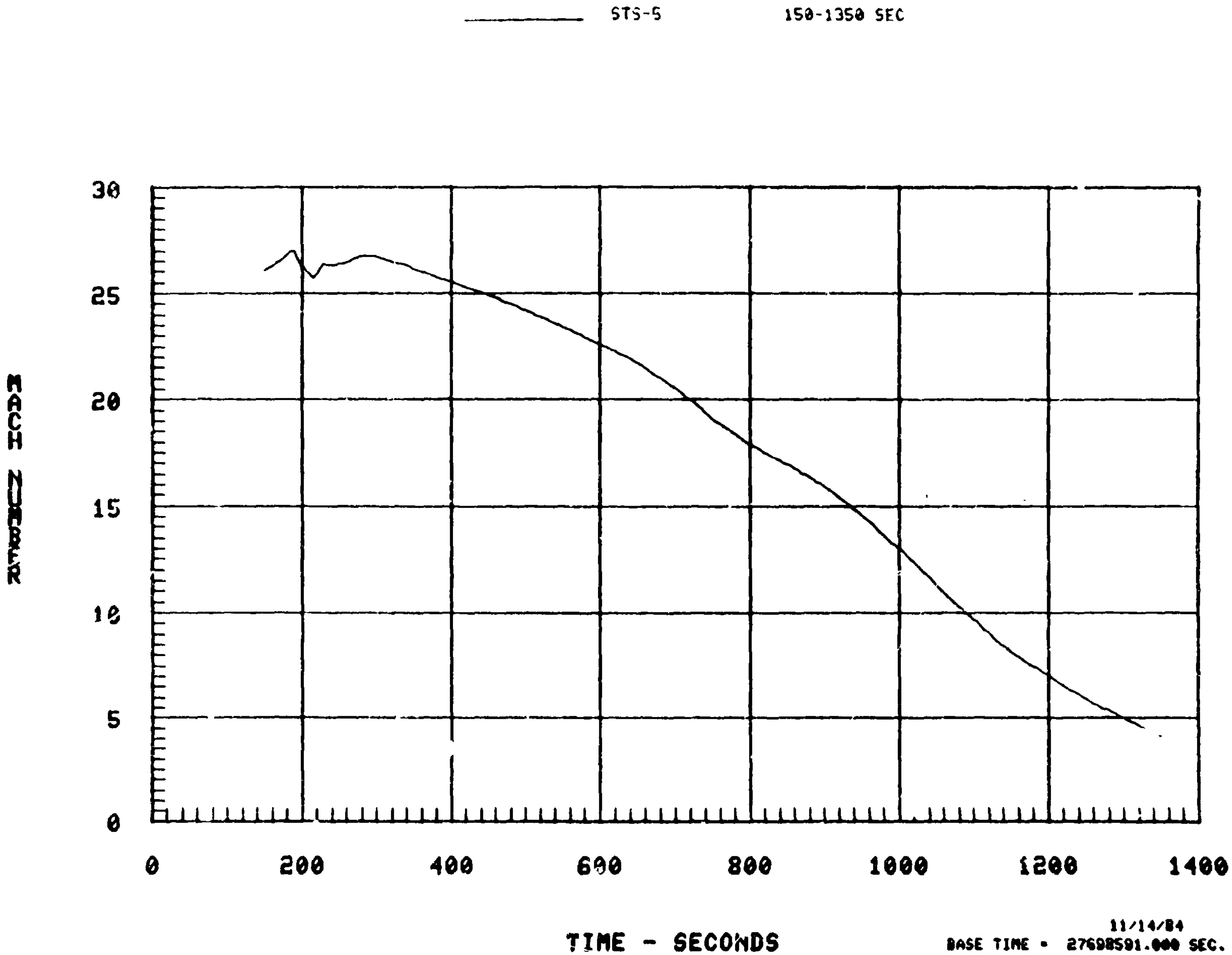

STS-1 (107 FT LENGTH) FLIGHT PARAMETER COMPARISON

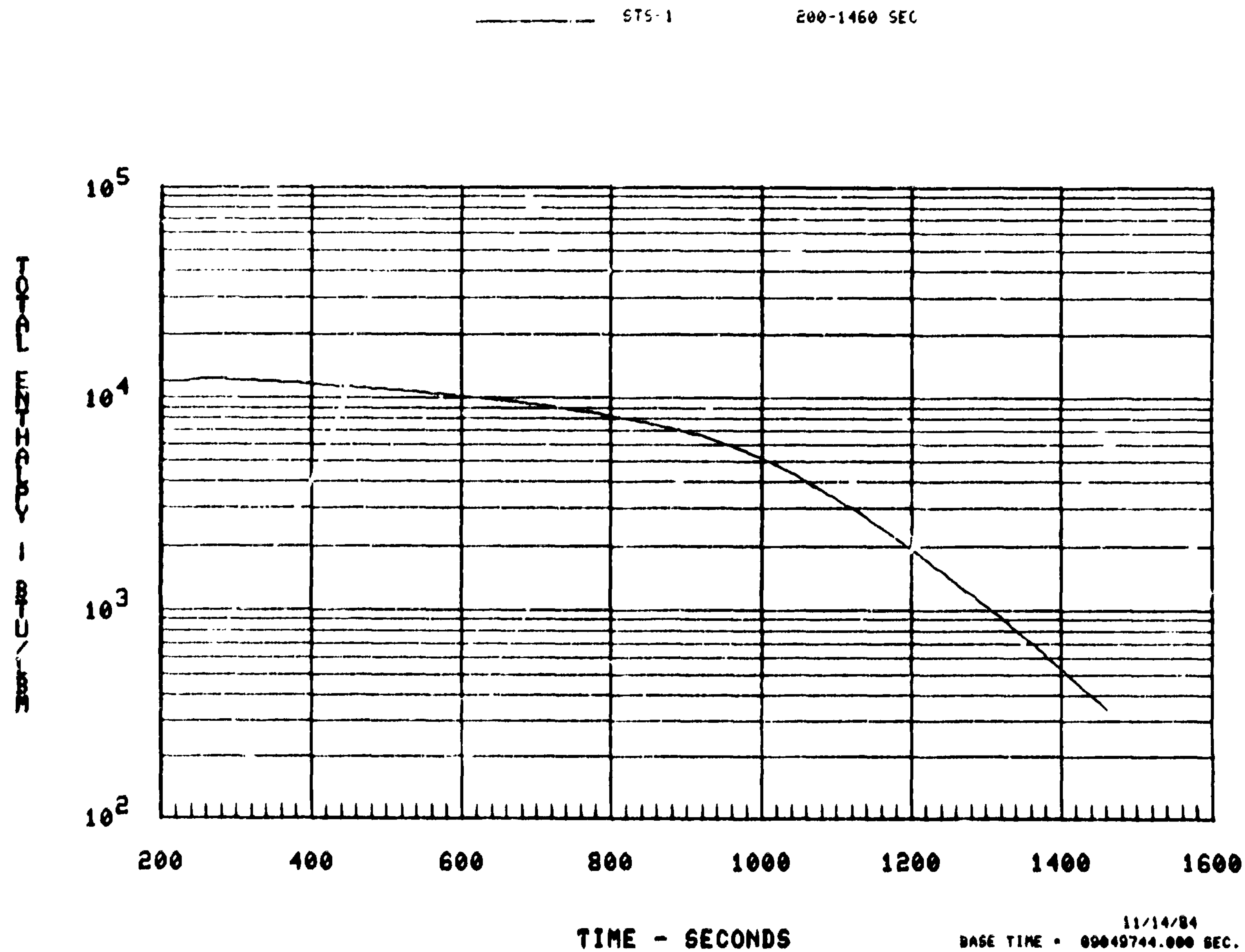

STS-2 (107 FT LENGTH) FLIGHT PARAMETER COMPARISON

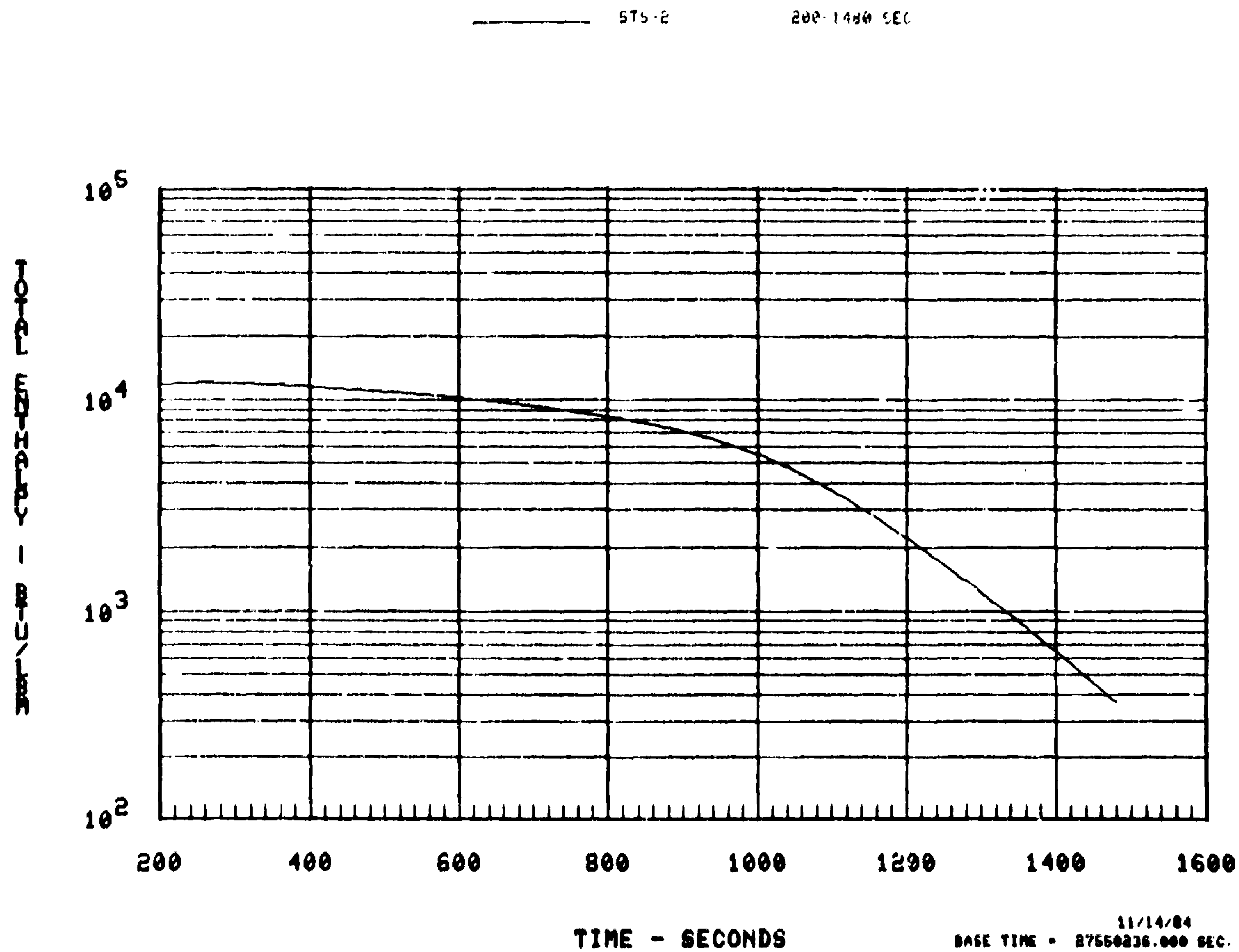

STS-3 (107 FT LENGTH) FLIGHT PARAMETER COMPARISON

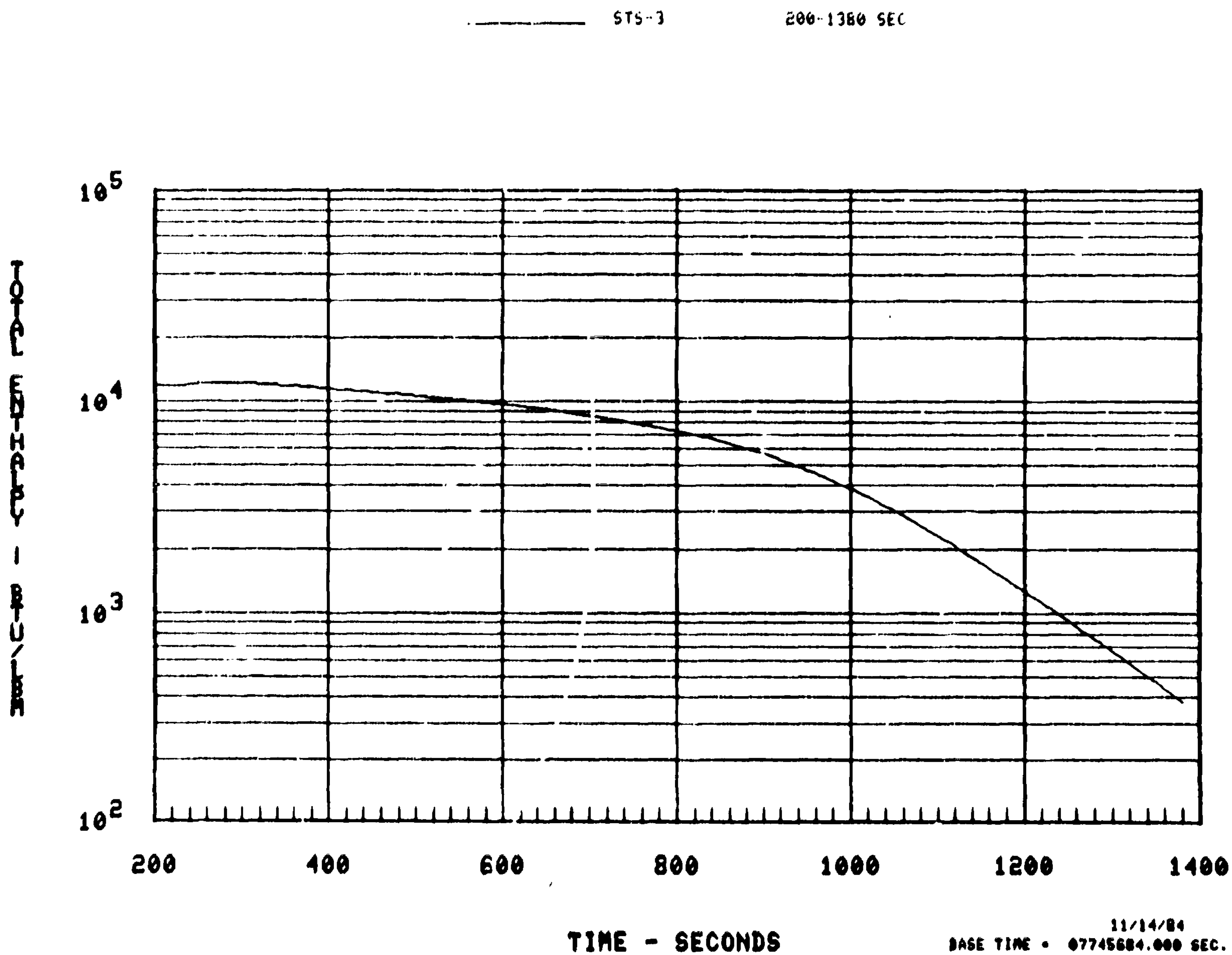

STS-4 (107 FT LENGTH) FLIGHT PARAMETER COMPARISON

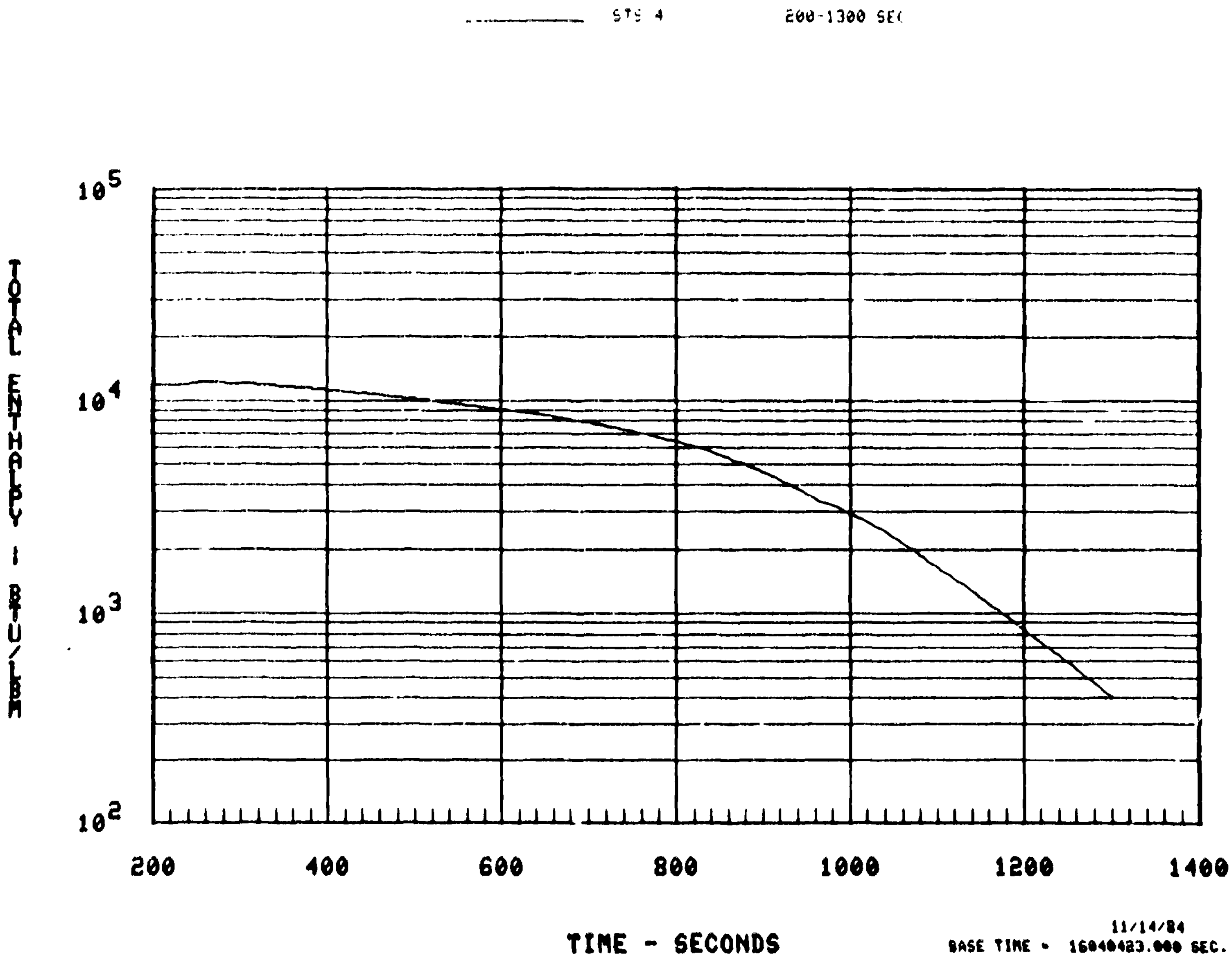

STS-5 (107 FT LENGTH) FLIGHT PARAMETER COMPARISON

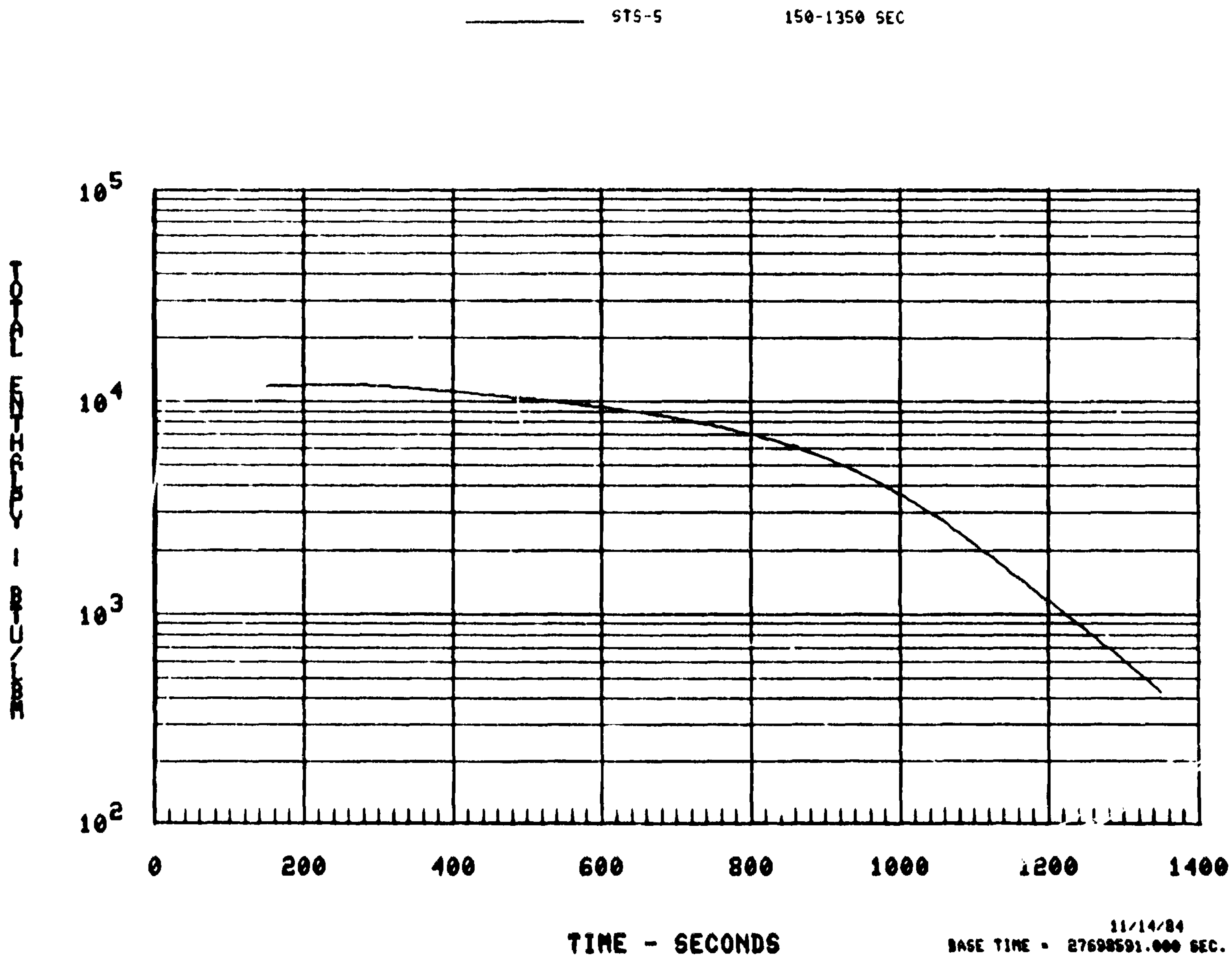

STS-1 (107 FT LENGTH) FLIGHT PARAMETER COMPARISON

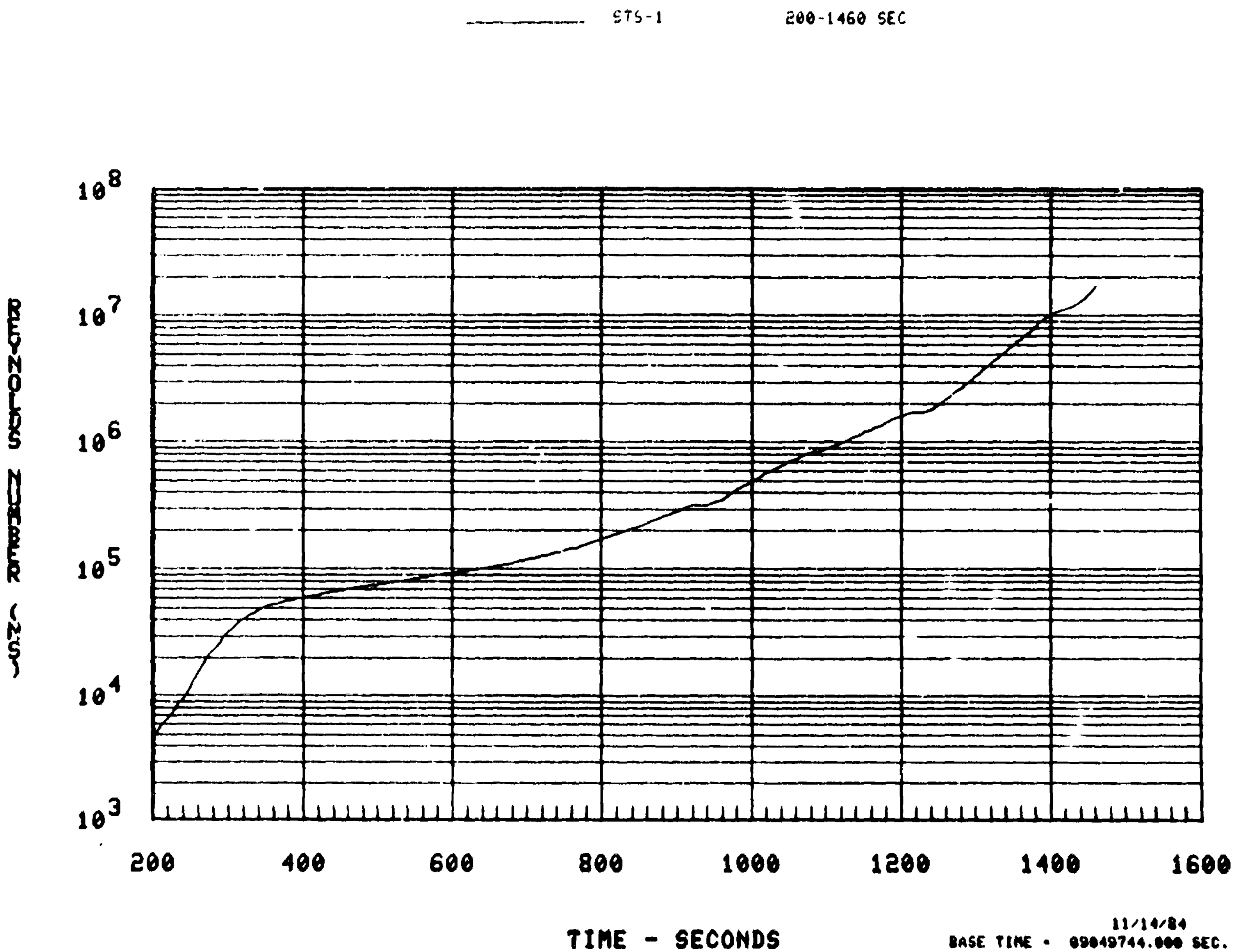

STS-2 (107 FT LENGTH) FLIGHT PARAMETER COMPARISON

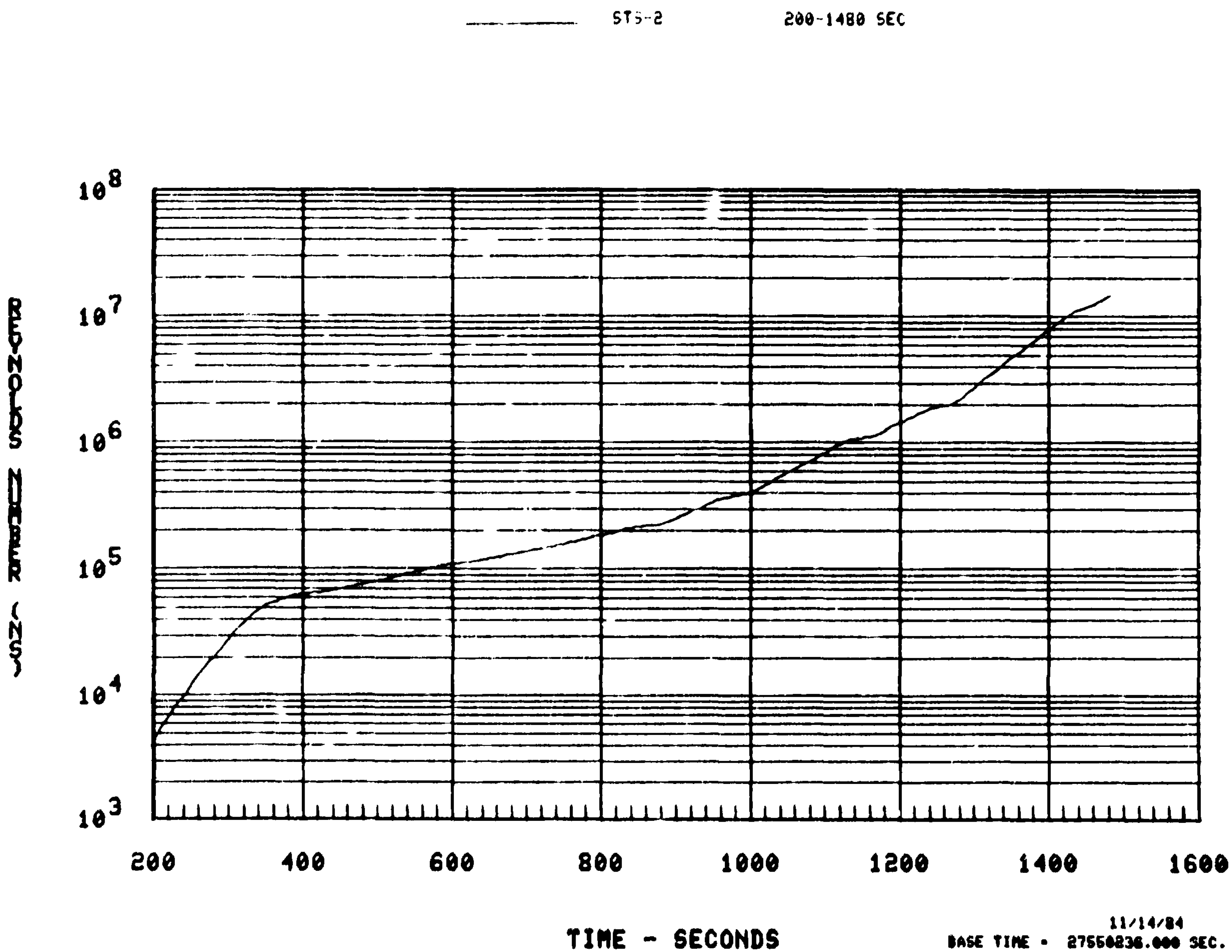

STS-3 (107 FT LENGTH) FLIGHT PARAMETER COMPARISON

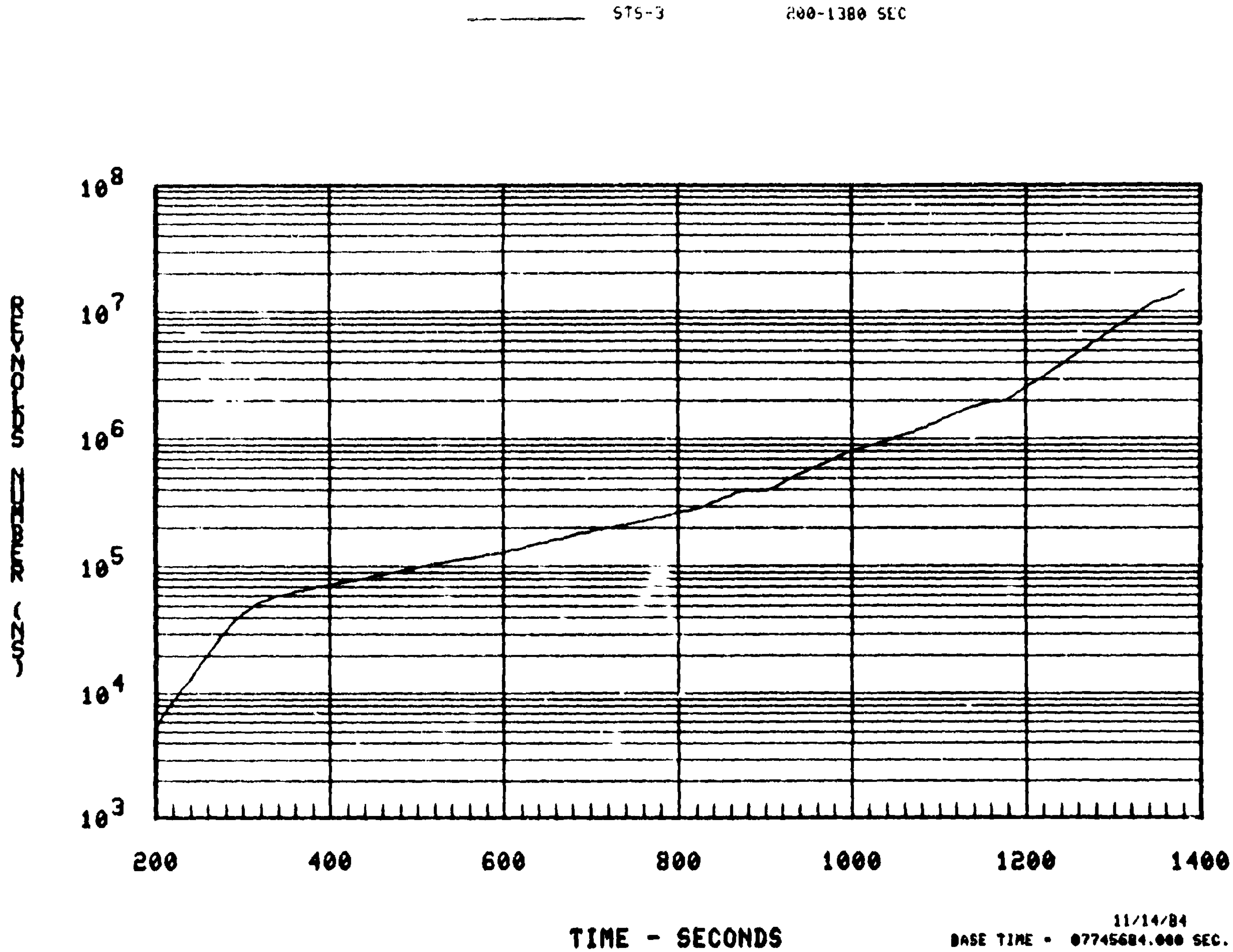

STS-4 (107 FT LENGTH) FLIGHT PARAMETER COMPARISON

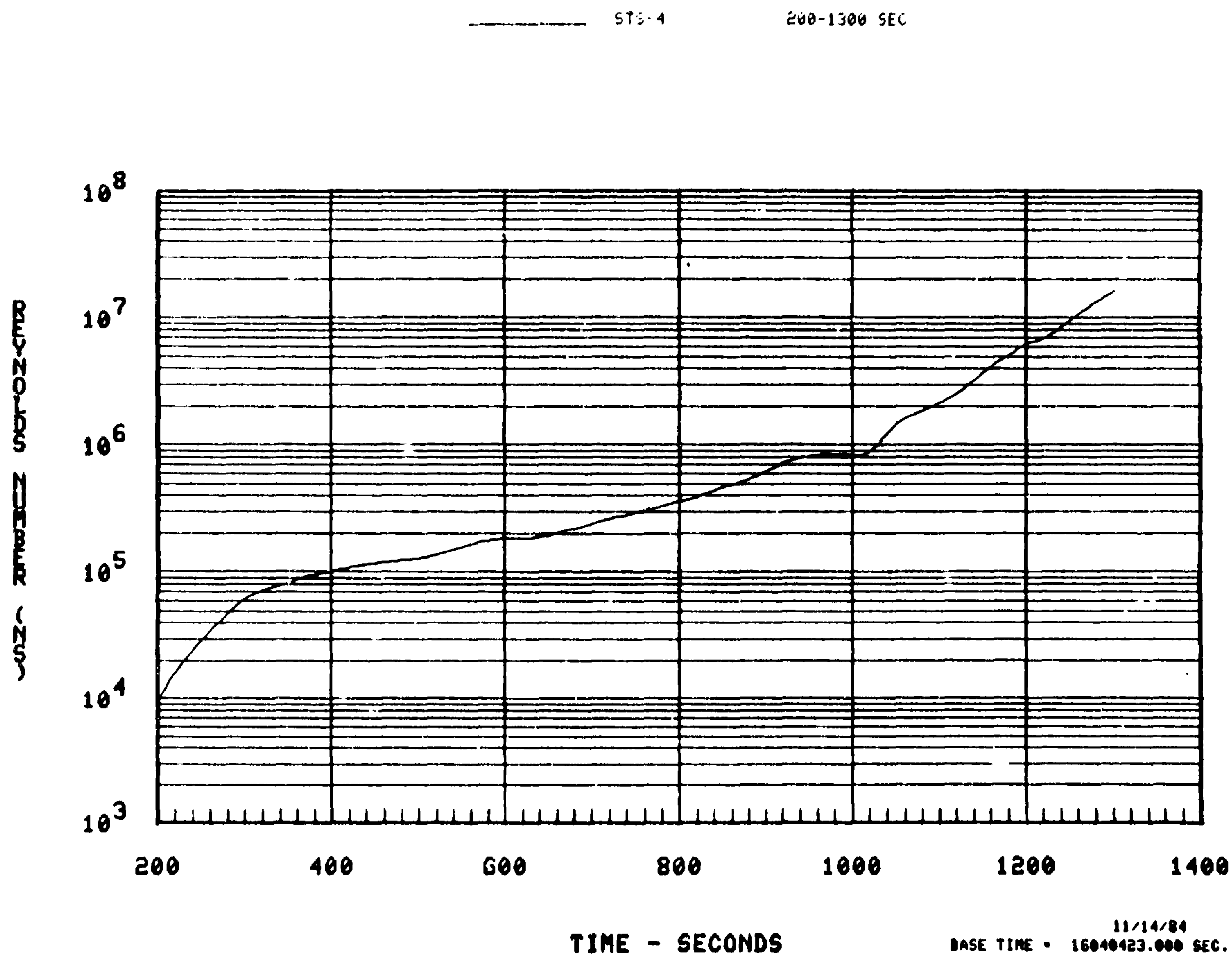

STS-5 (107 FT LENGTH) FLIGHT PARAMETER COMPARISON

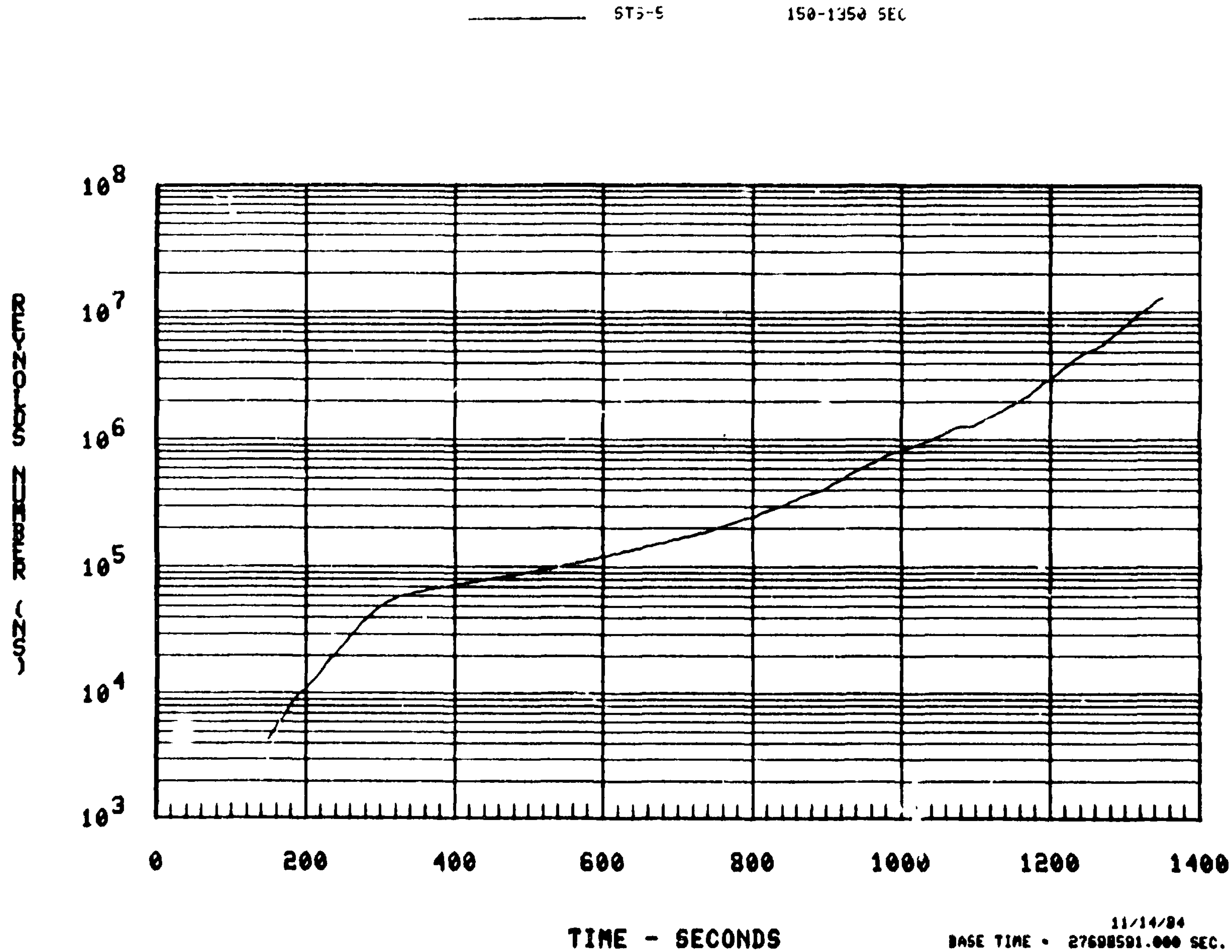

STS-1 (107 FT LENGTH) FLIGHT PARAMETER COMPARISON

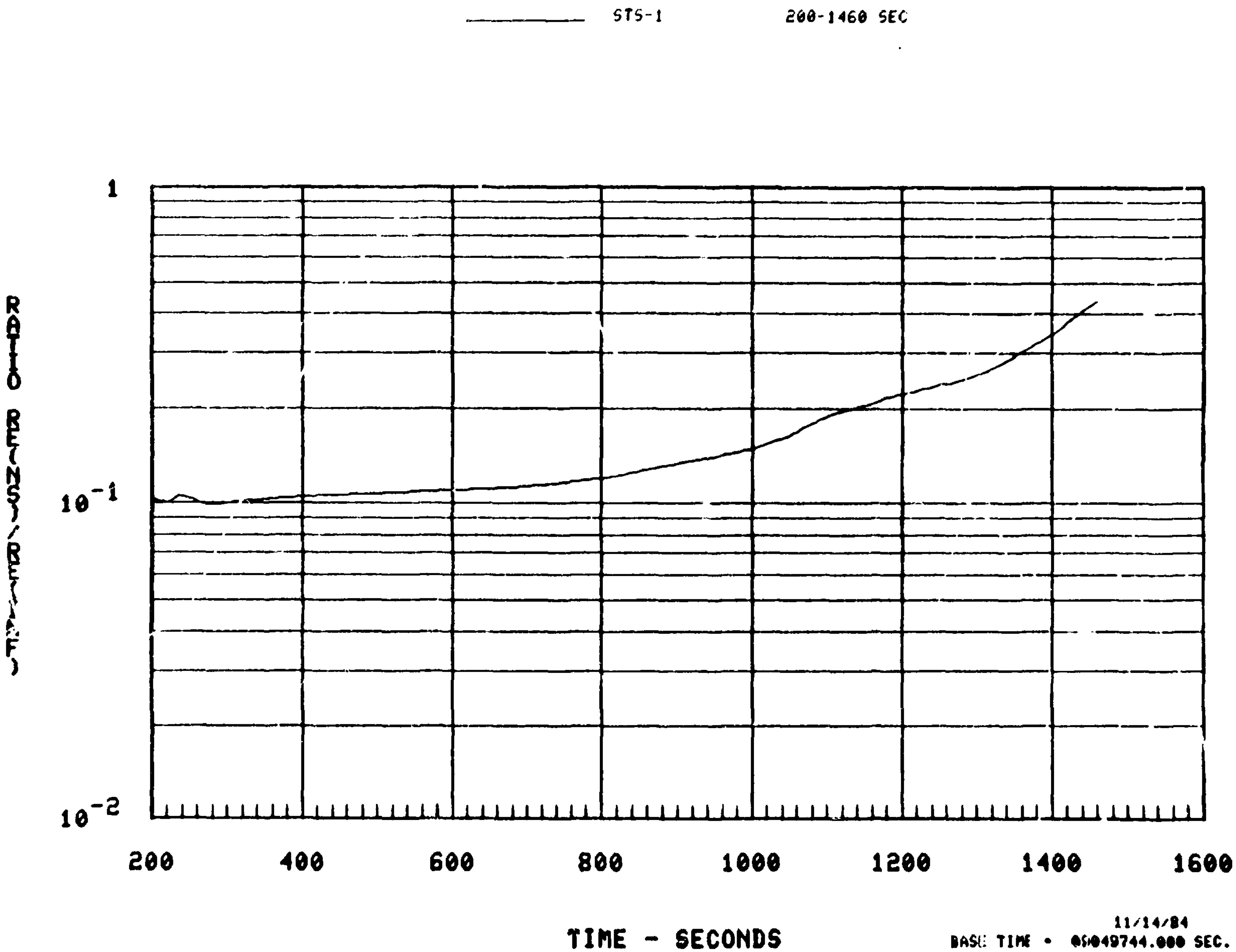

STS-2 (107 FT LENGTH) FL' .T PARAMETER COMPARISON

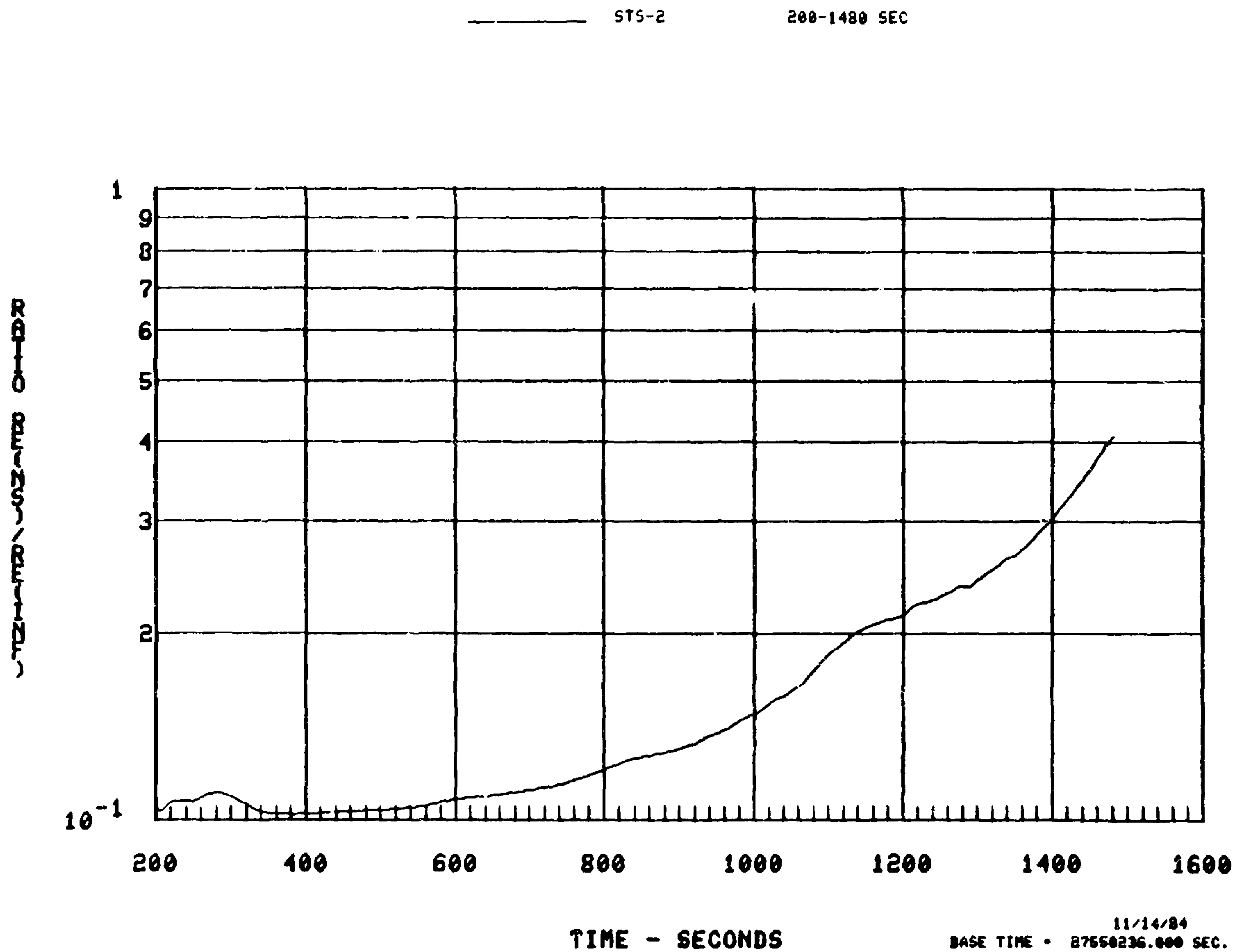

STS-3 (107 FT LENGTH) FLIGHT PARAMETER COMPARISON

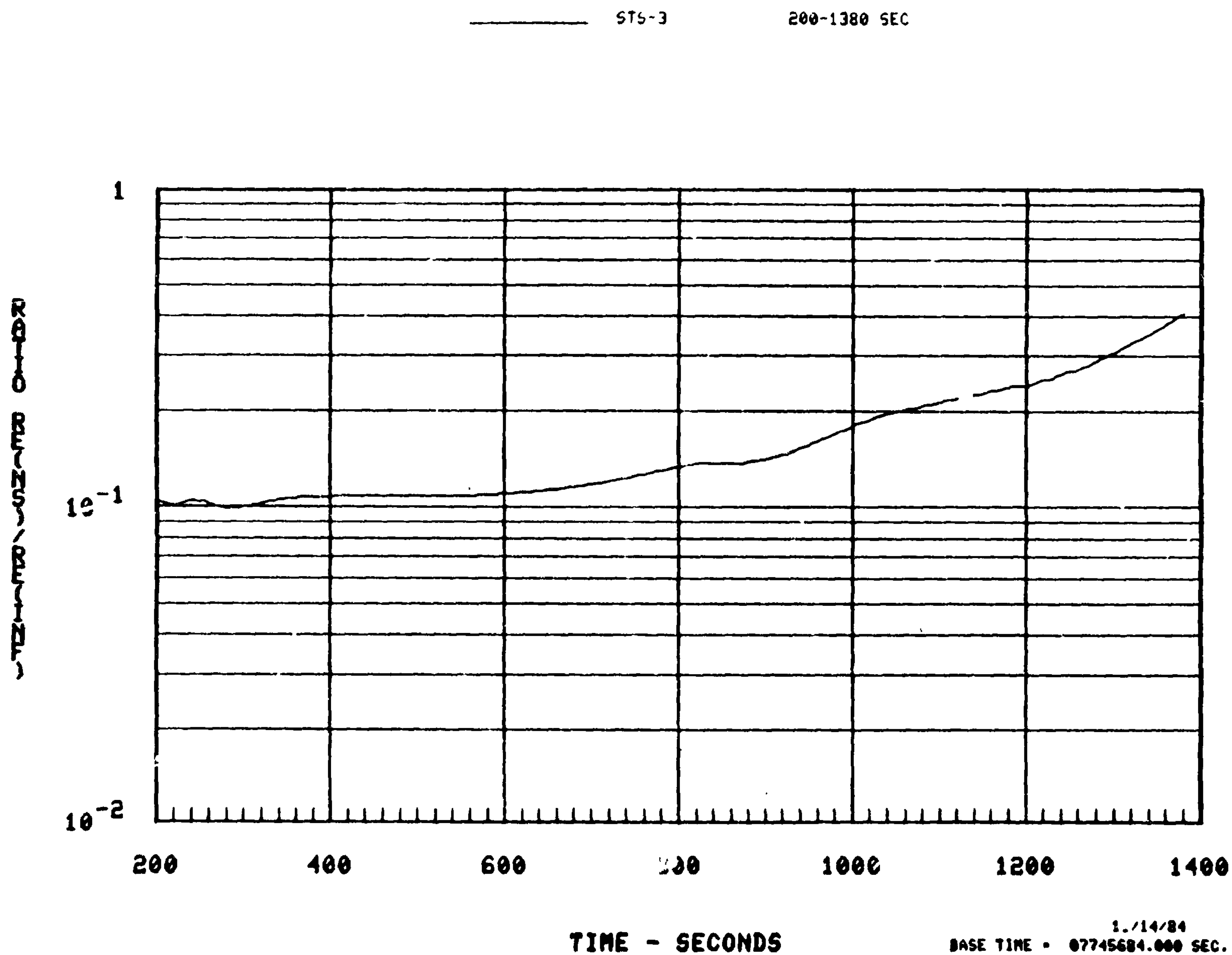

STS-4 (107 FT LENGTH) FLIGHT PARAMETER COMPARISON

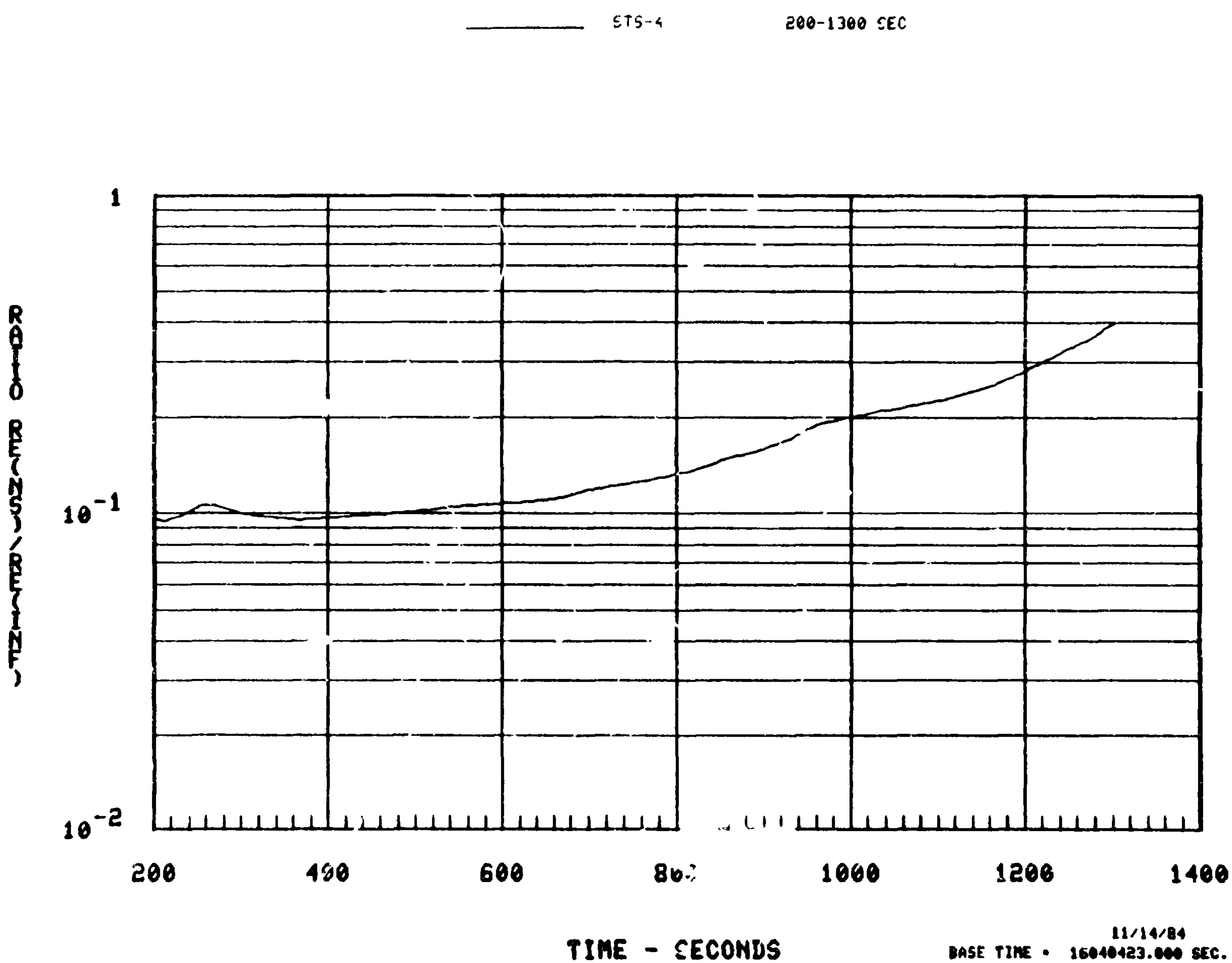

STS-5 (107 FT LENGTH) FLIGHT PARAMETER COMPARISON

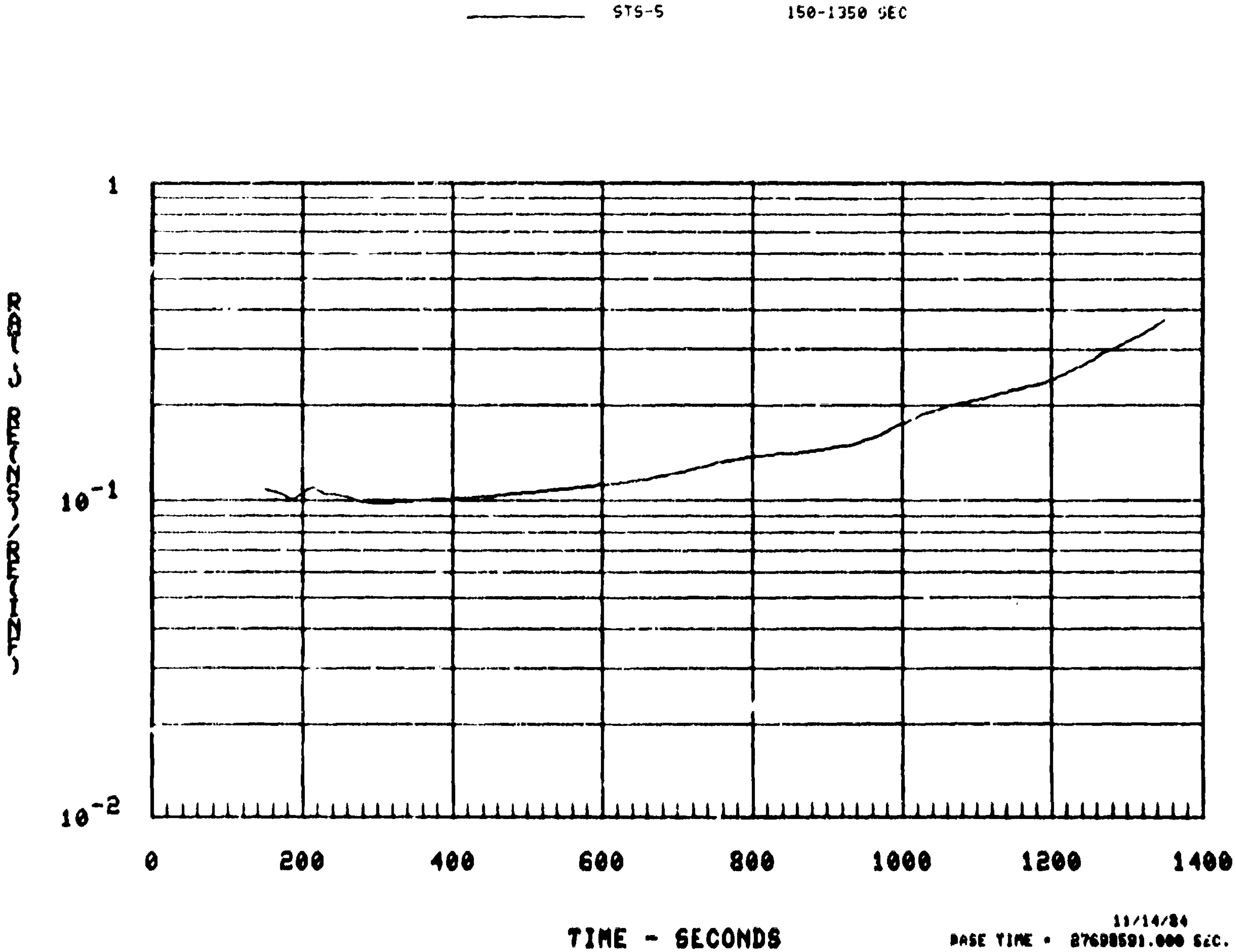

STS-1 V98U3005C BODY FLAP POS FEEDBACK

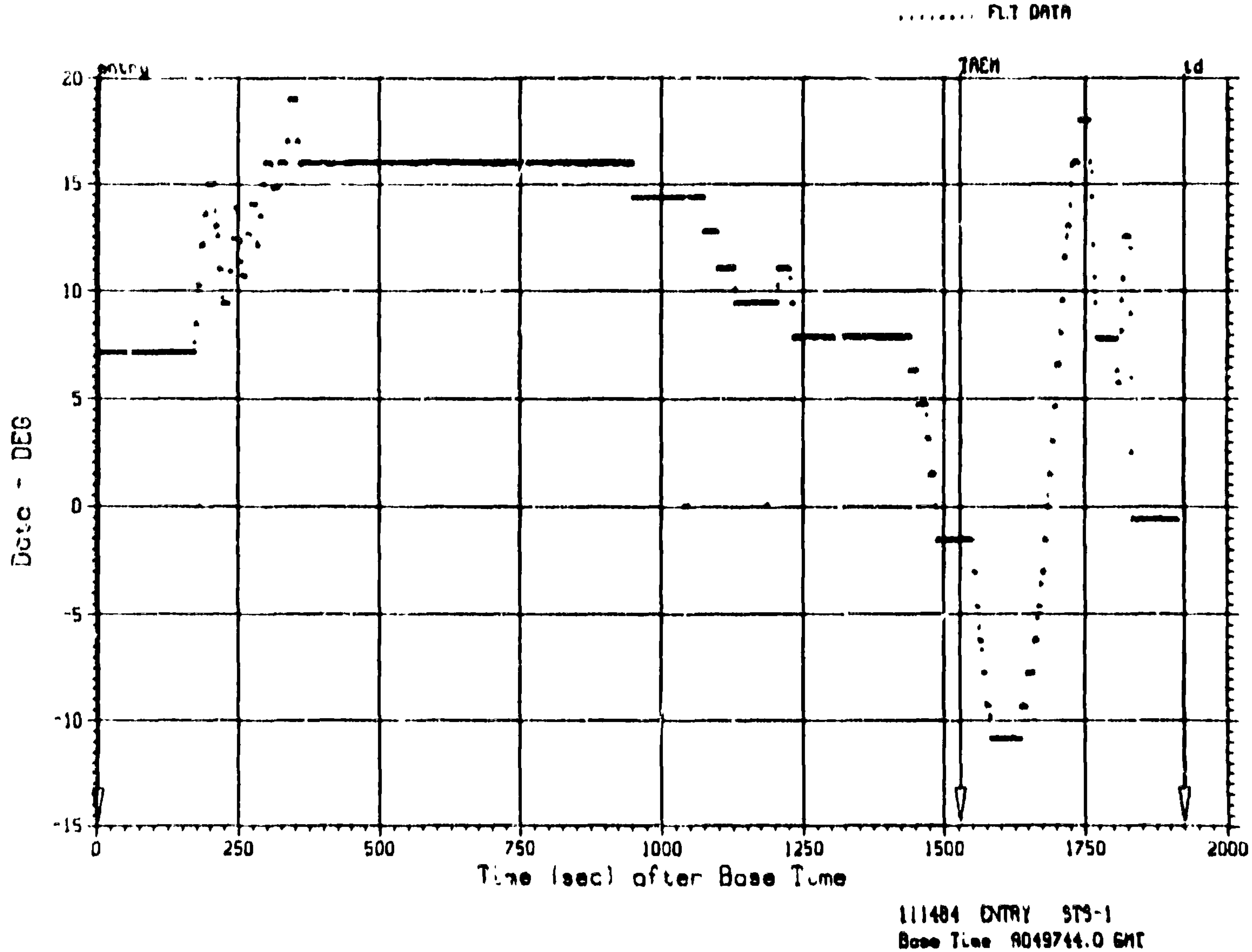

STS-2 V98U3005C BODY FLAP POS FEEDBACK

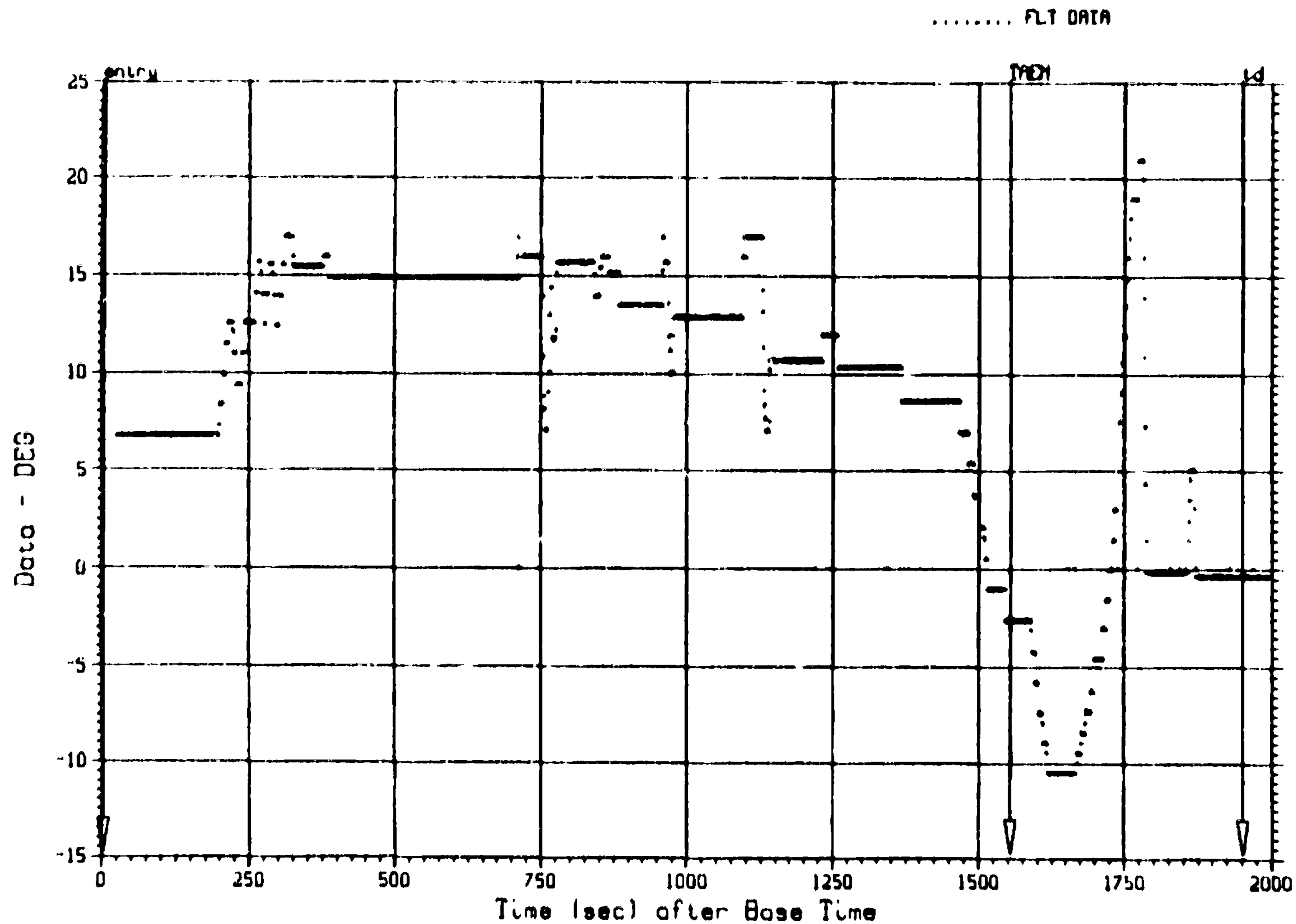

111484 ENTRY STS-2
Base Time 27[illegible]0236.0 GMT

STS 3

V98U3005C BODY FLAP POS FEEDBACK

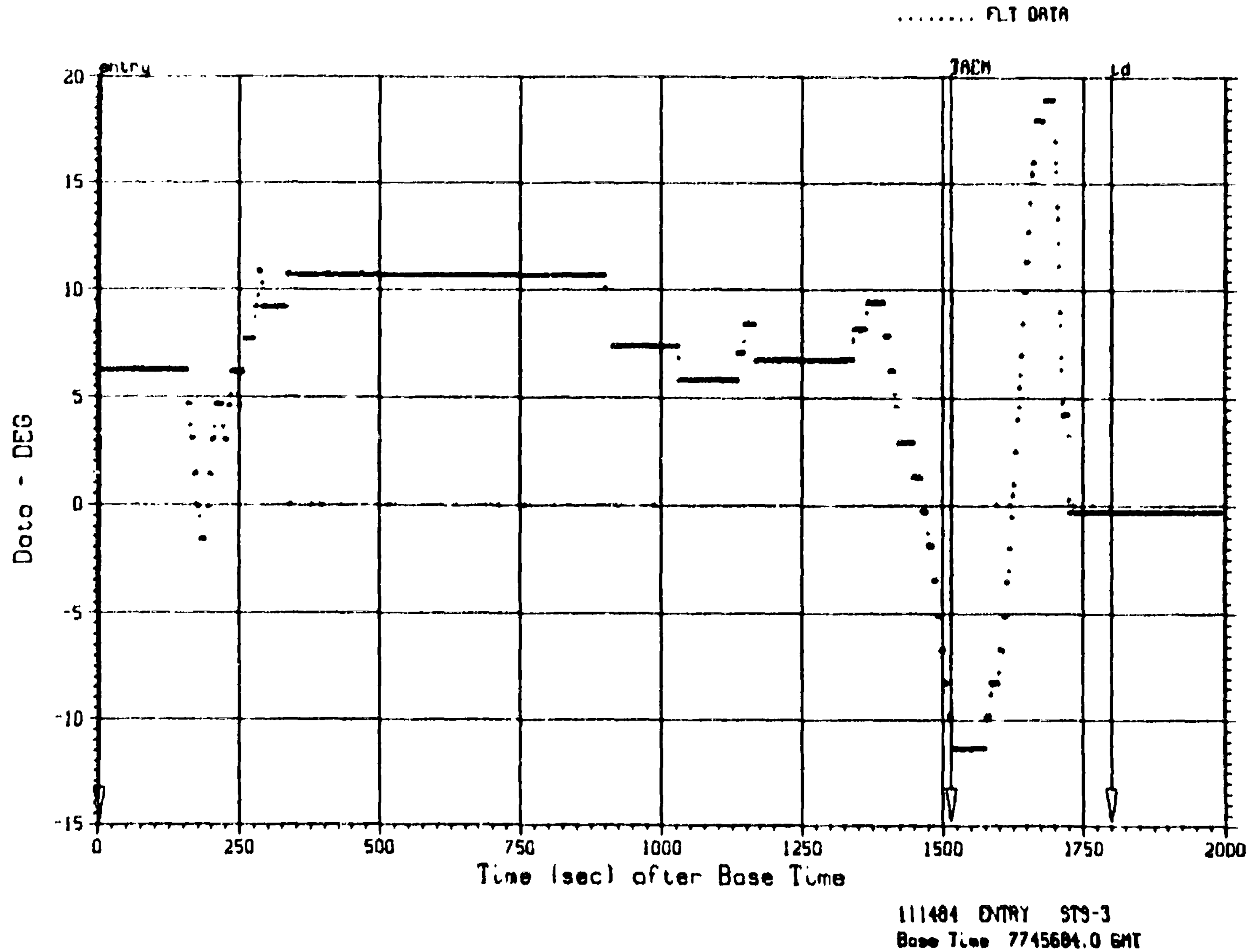

STS 4 V98U3005C BODY FLAP POS FEEDBACK

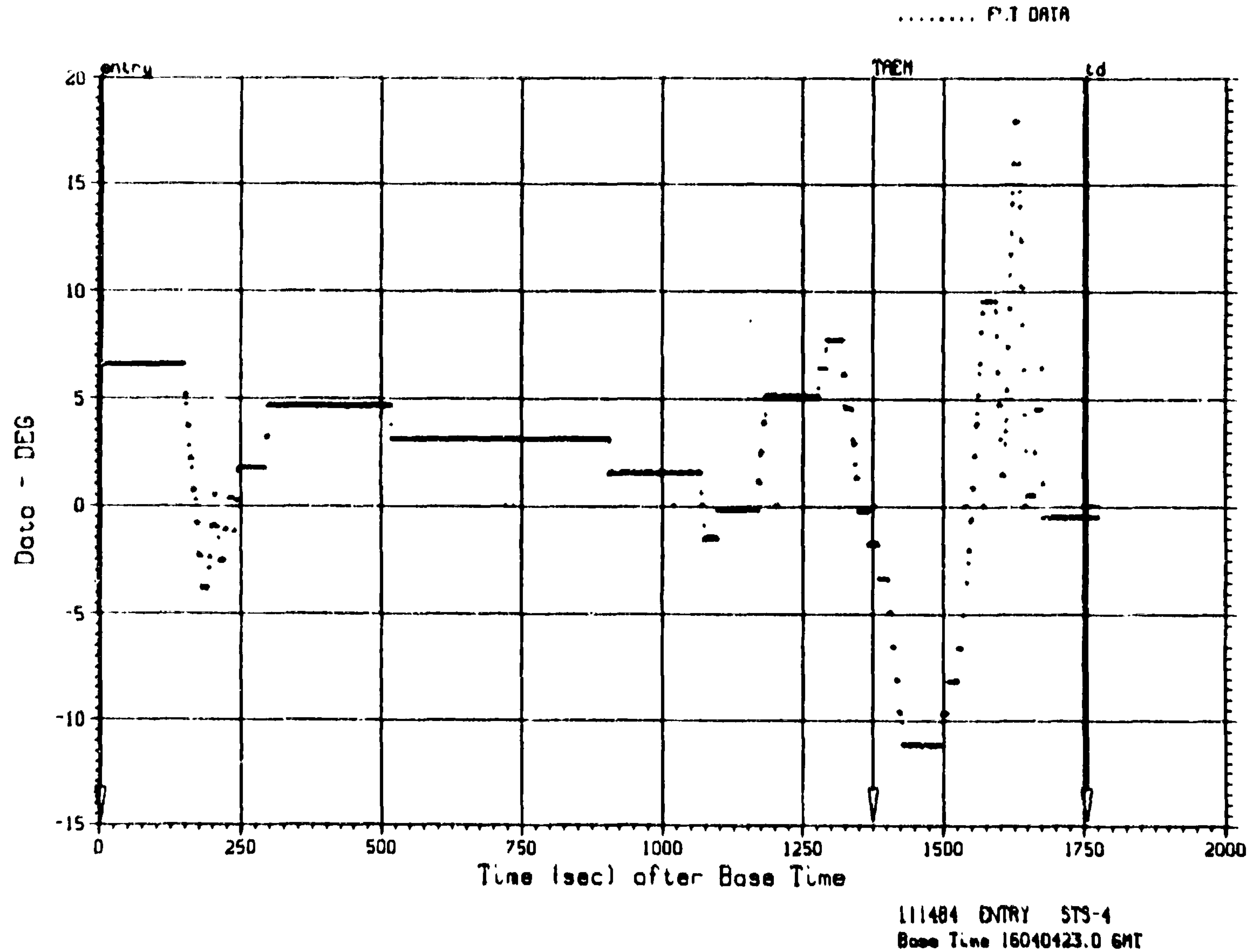

STS-5 V98U3005C BODY FLAP POS FEEDBACK

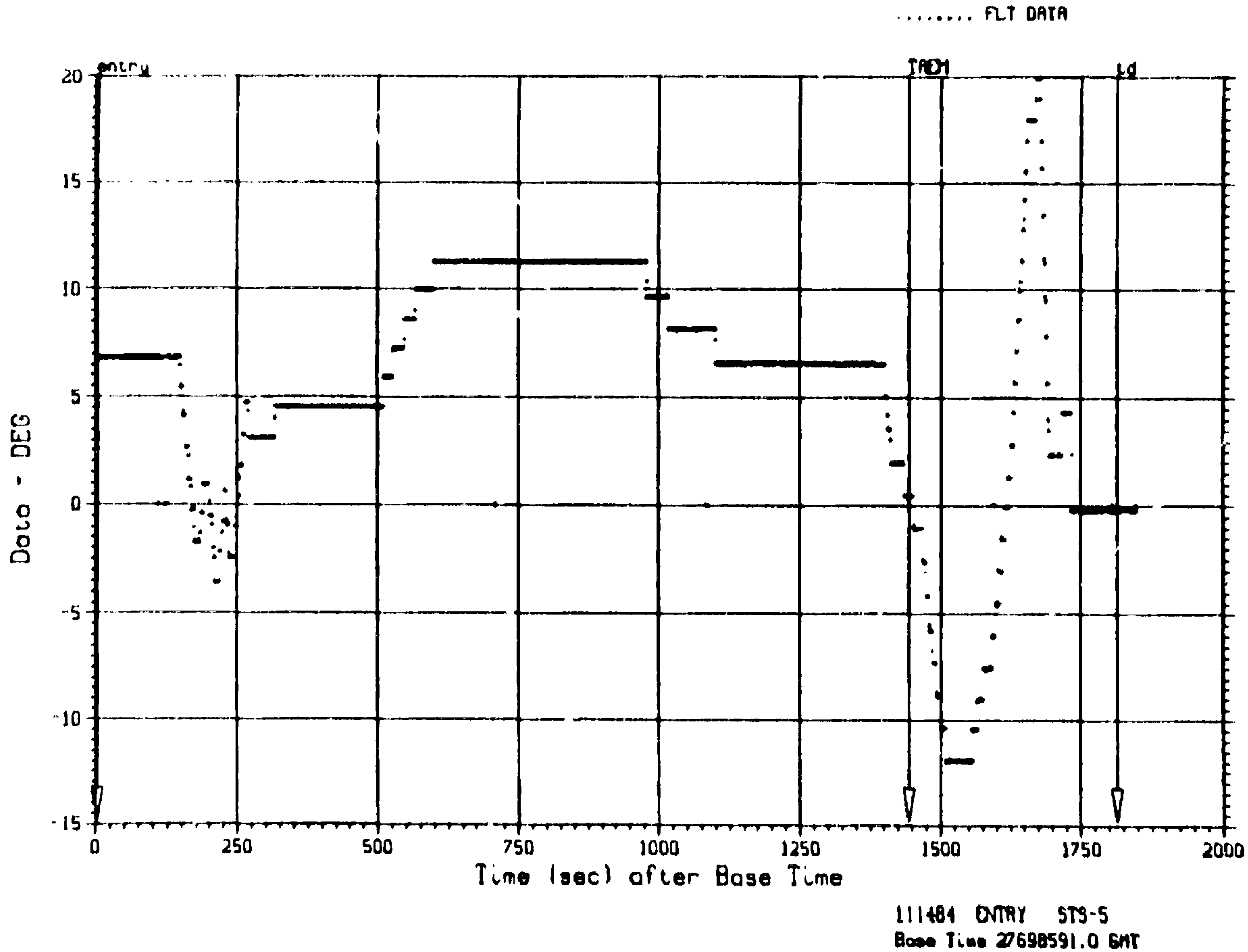

STS-1

V98H3478C RH ELEVON FEEDBACK

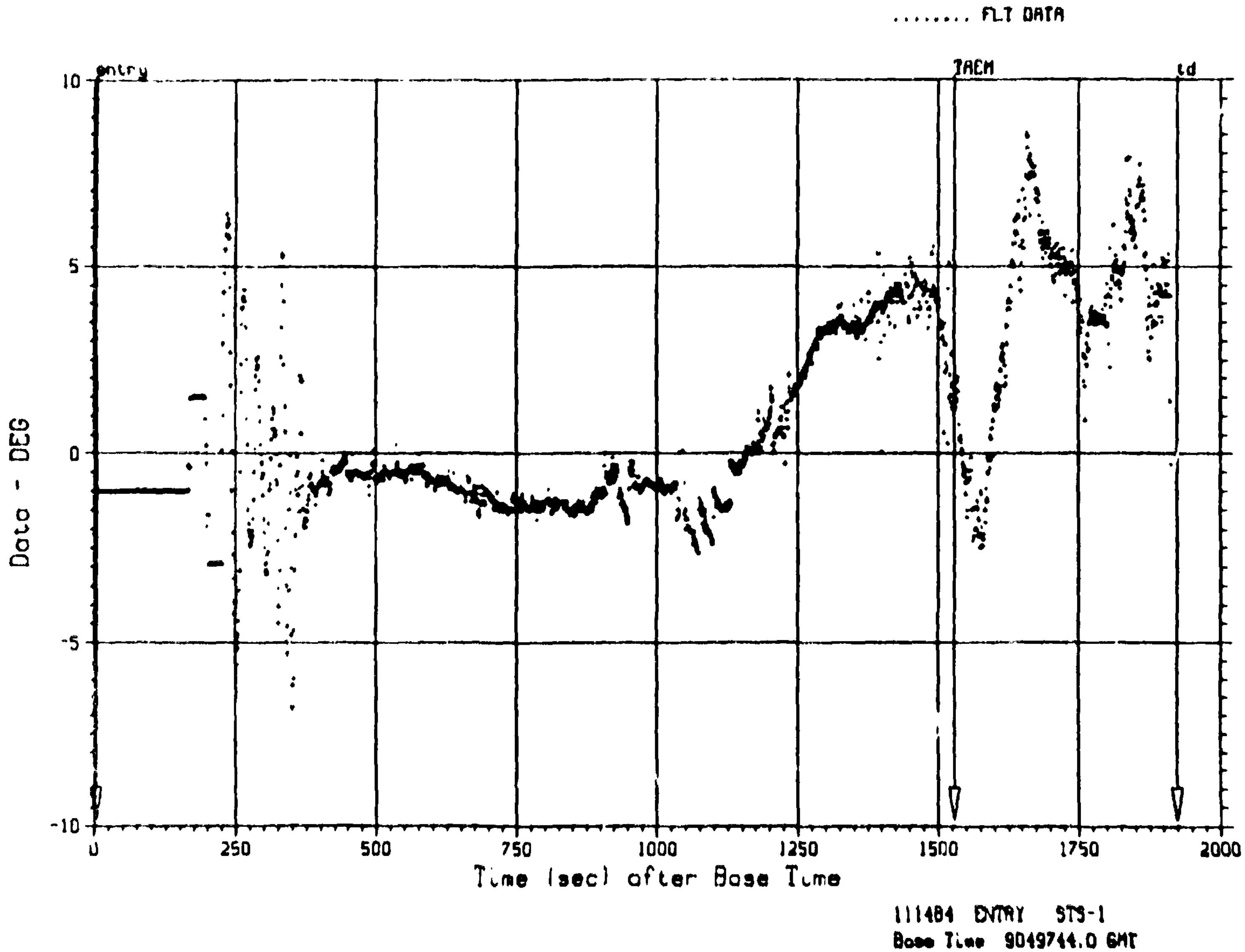

STS 2 V98H3478C RH ELEVON FEEDBACK

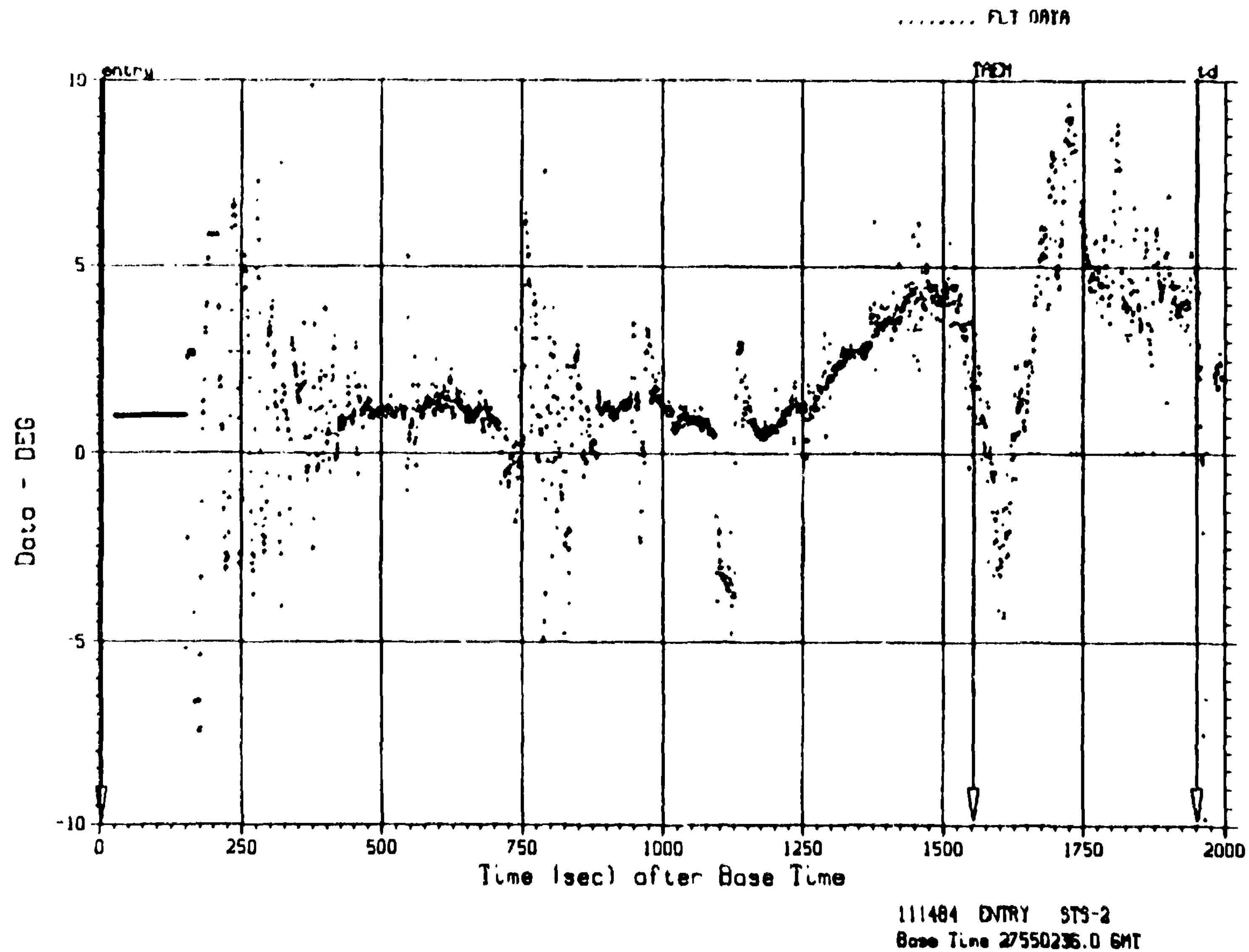

STS-3

V98H3478C RH ELEVON FEEDBACK

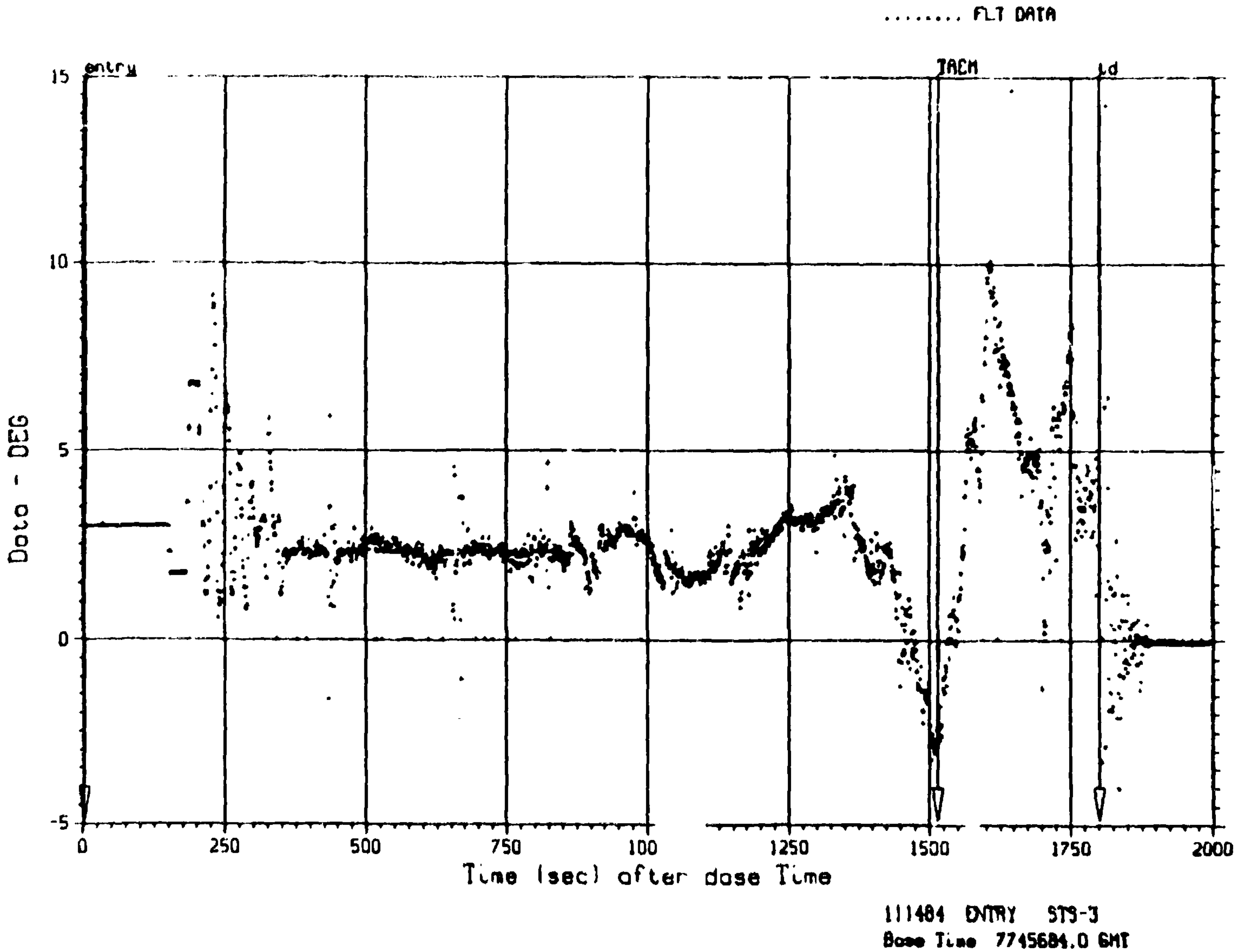

STS-4 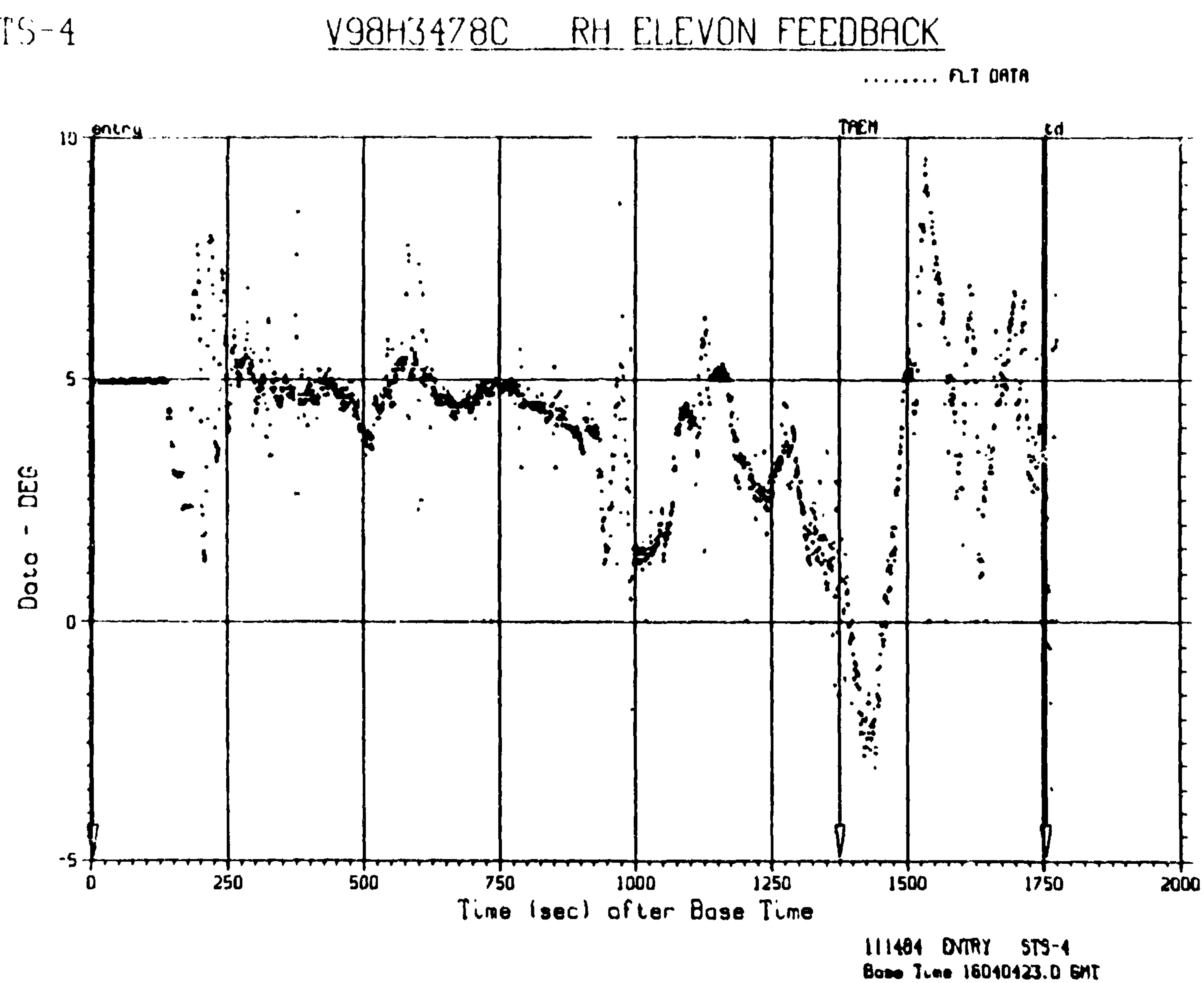
V98H3478C RH ELEVON FEEDBACK
.... FLT DATA
entry
TAEM
td
10
5
0
-5
Data - DEG
0
250
500
750
1000
1250
1500
1750
2000
Time (sec) after Base Time
111484 ENTRY STS-4
Base Time 16040423.0 GMT

STS-5

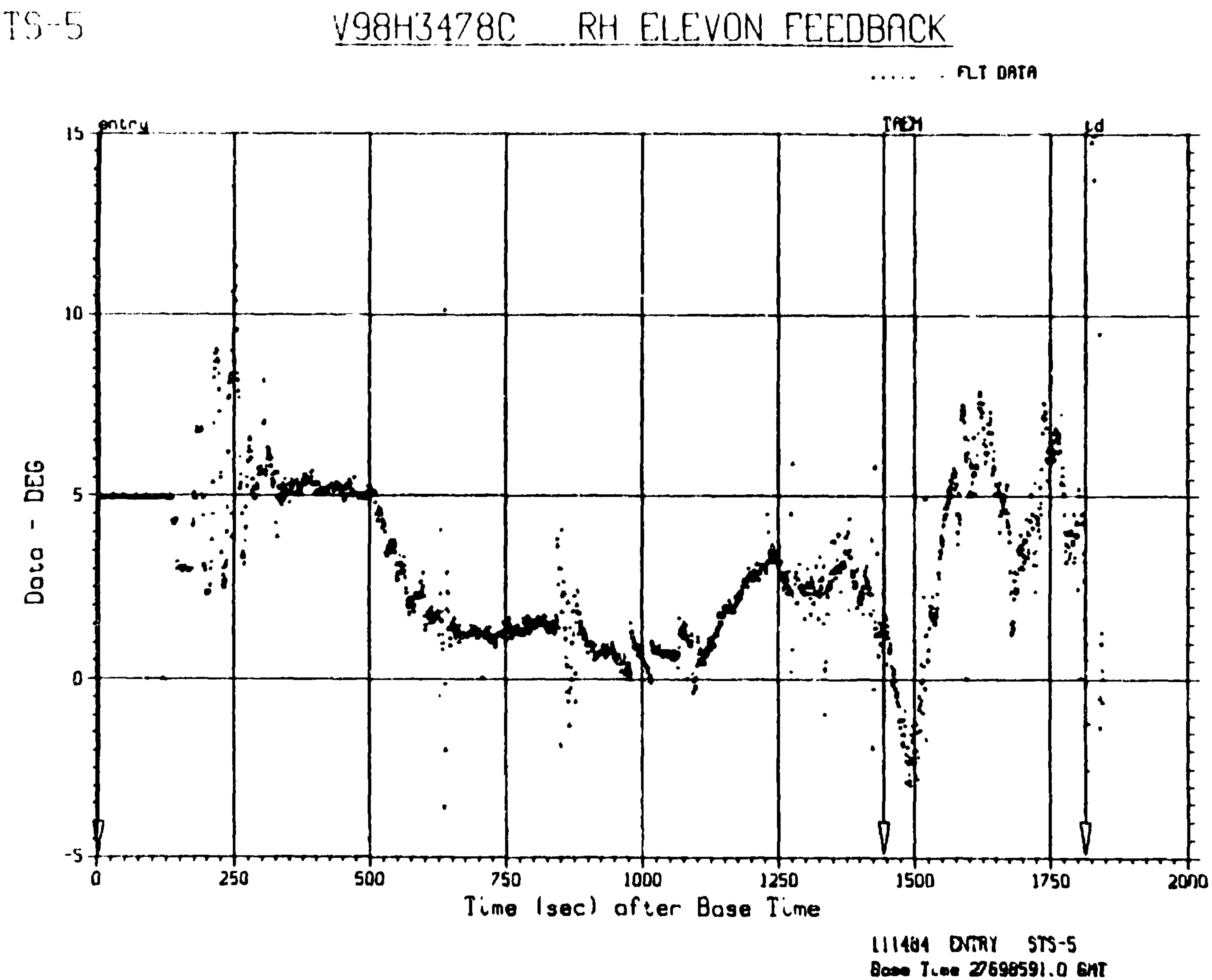

V98H3478C RH ELEVON FEEDBACK
FLT DATA
entry
TAEM
td
Data - DEG
15
10
5
0
-5
0
250
500
750
1000
1250
1500
1750
2000
Time (sec) after Base Time
111484 ENTRY STS-5
Base Time 27698591.0 GMT

STS-1

V98H3476C LH ELEVON FEEDBACK

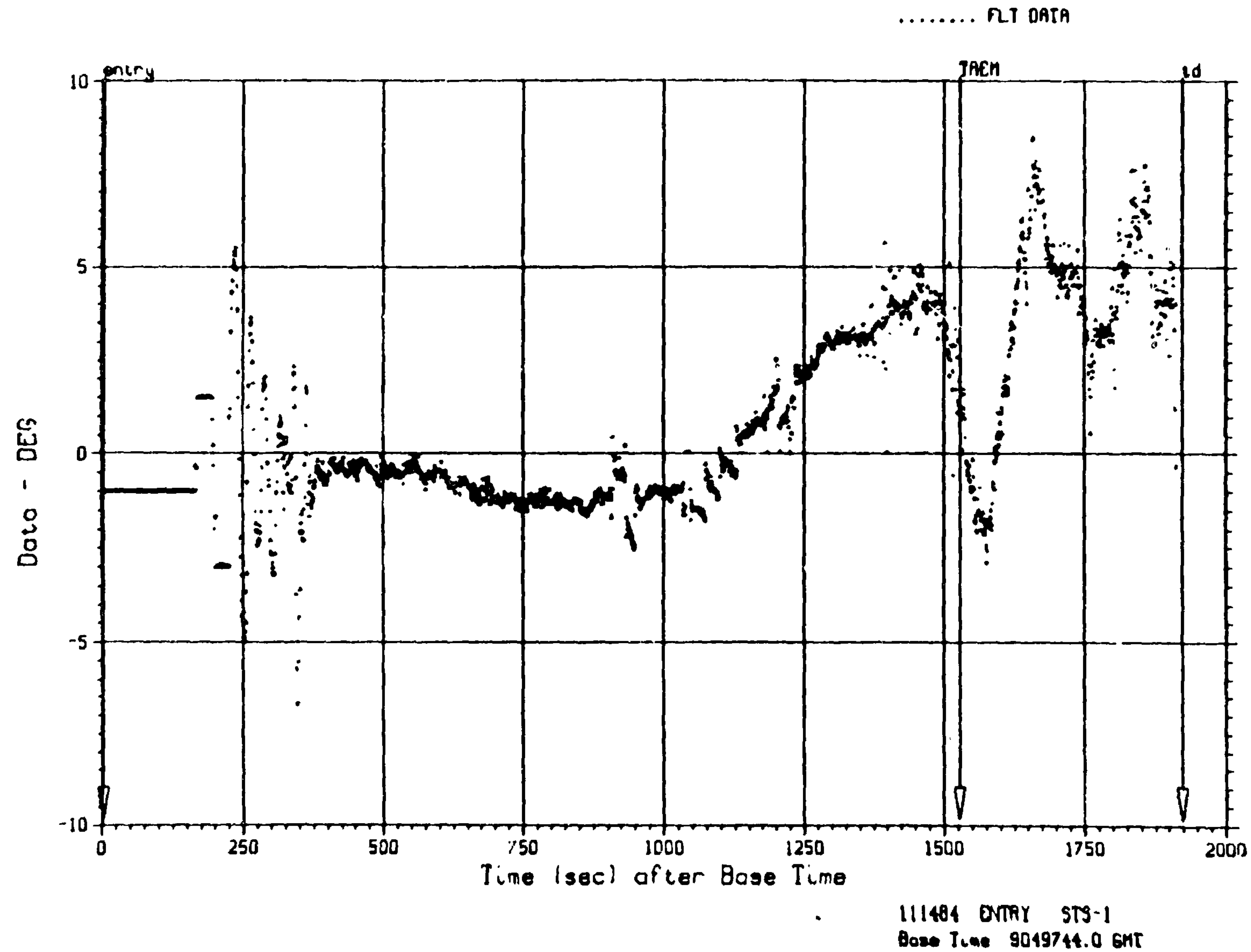

STS-2

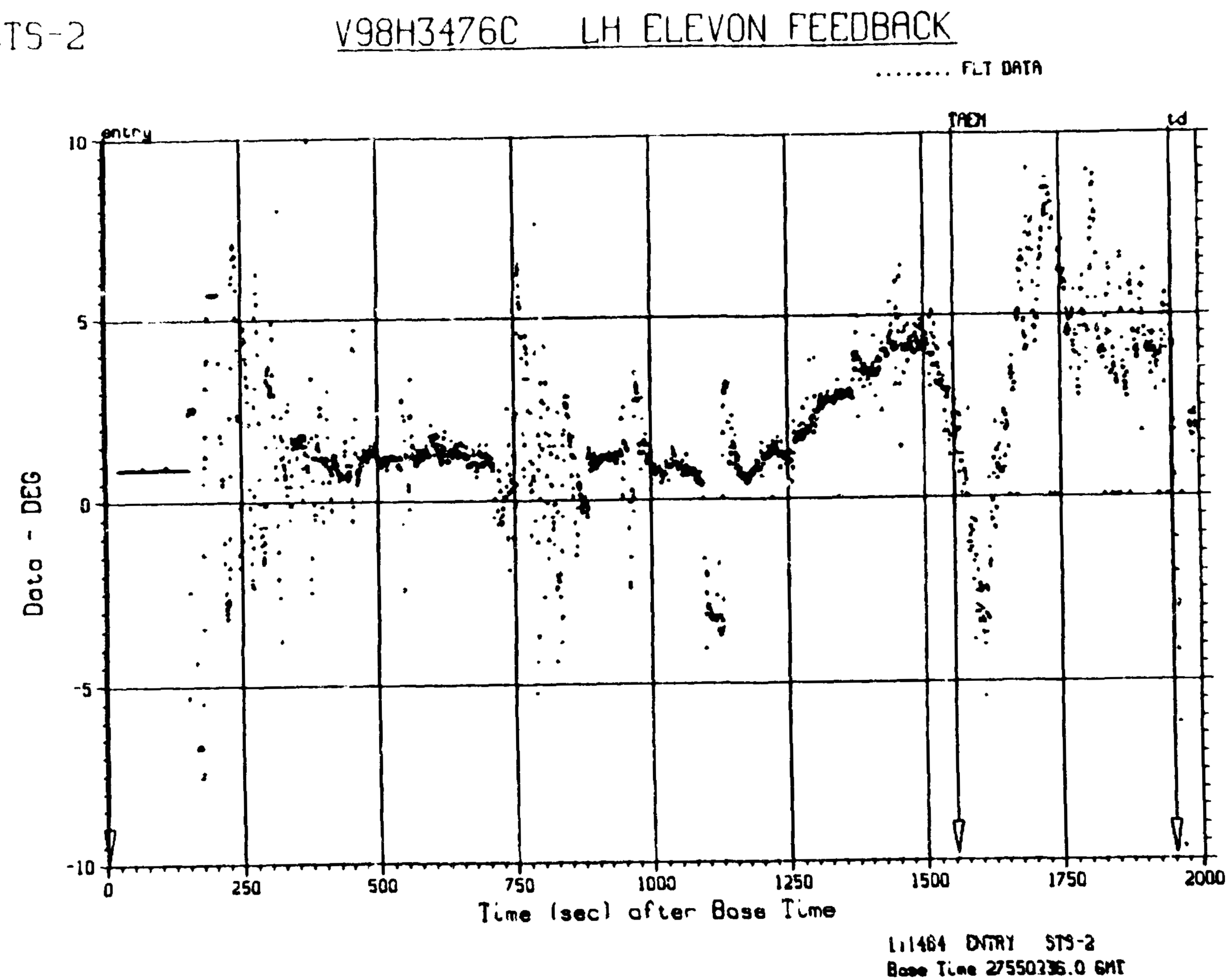
V98H3476C LH ELEVON FEEDBACK
.... FLT DATA
entry
TAEM
td
10
5
0
-5
-10
Data - DEG
0
250
500
750
1000
1250
1500
1750
2000
Time (sec) after Base Time
L11484 ENTRY STS-2
Base Time 27550336.0 GMT

STS-3

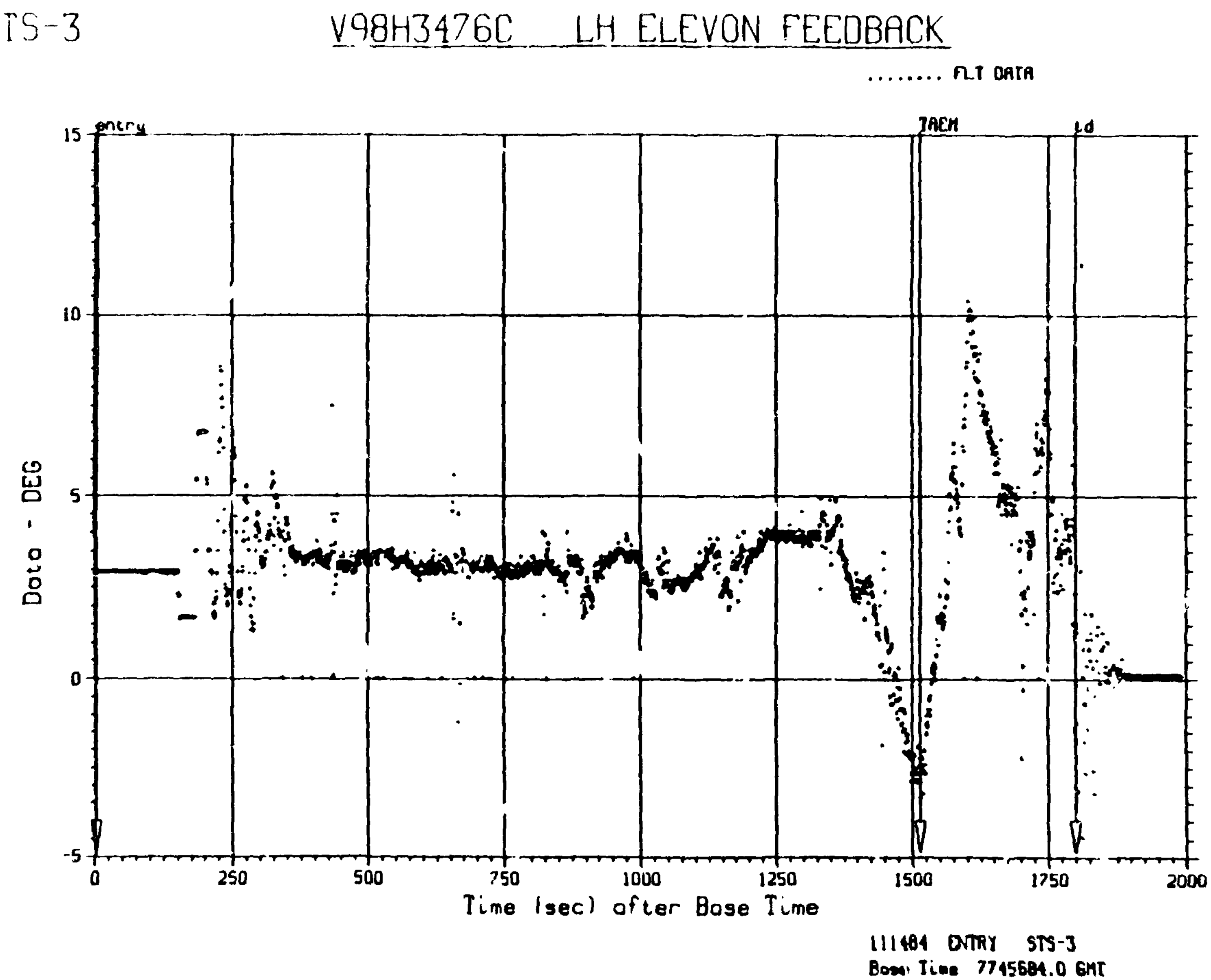

V98H3476C LH ELEVON FEEDBACK
.... FLT DATA
entry
7AEM
td
15
10
5
0
-5
0
250
500
750
1000
1250
1500
1750
2000
Data - DEG
Time (sec) after Base Time
111484 ENTRY STS-3
Base Time 7745684.0 GMT

STS-4 V98H3476C LH ELEVON FEEDBACK

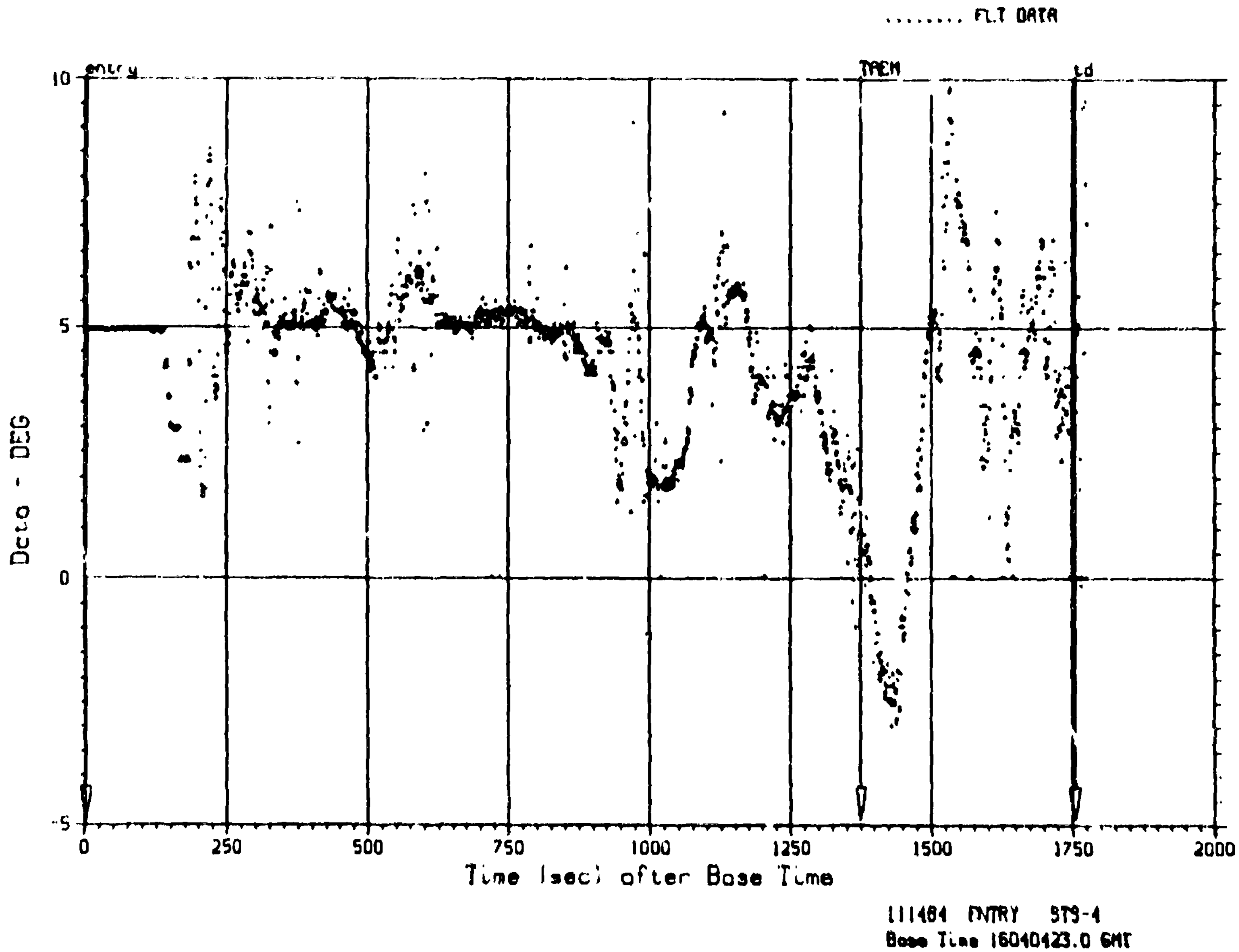

STS-5

V98H3476C LH ELEVON FEEDBACK

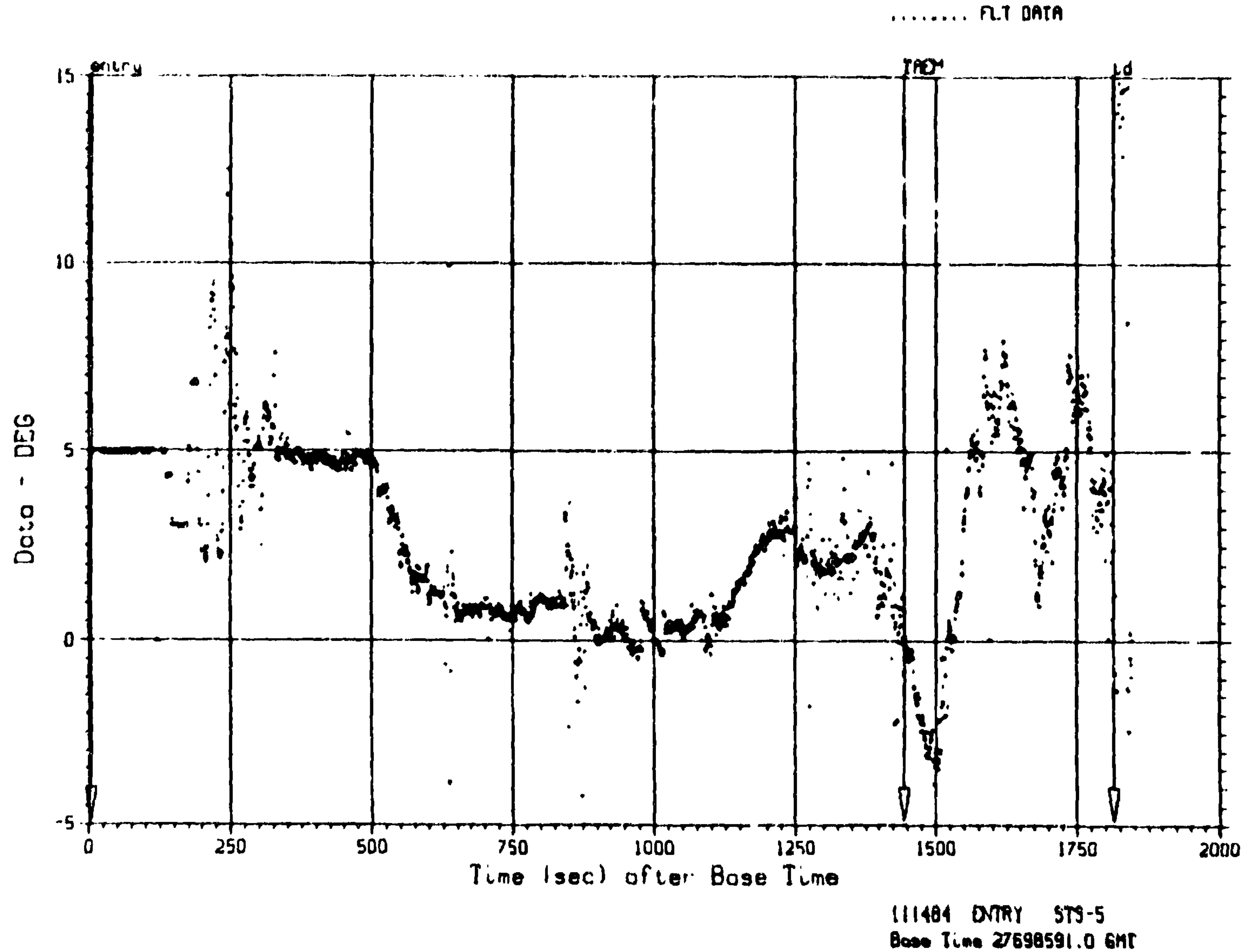

STS-1 (107 FT LENGTH) FLIGHT PARAMETER COMPARISON

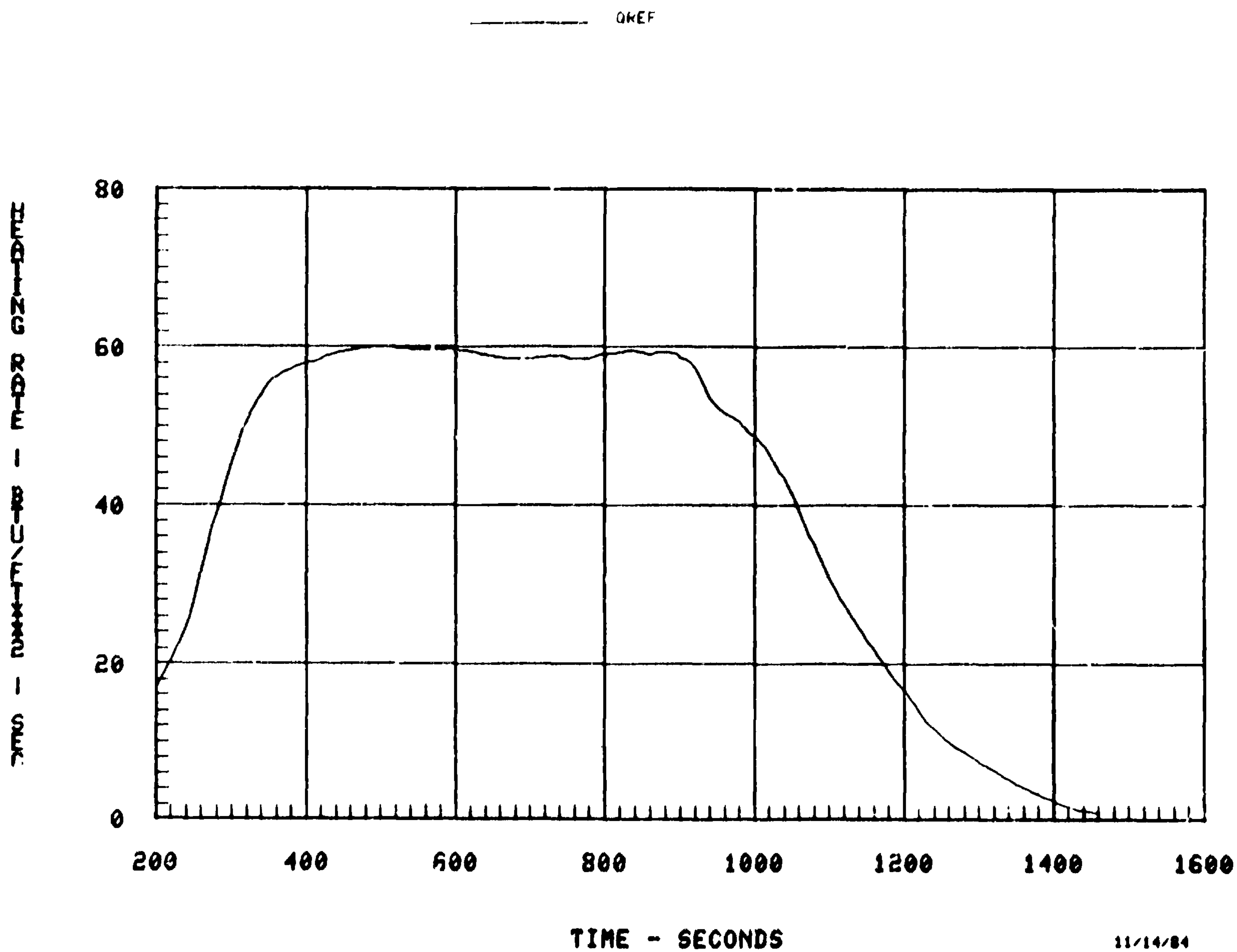

STS-2 (107 FT LENGTH) FLIGHT PARAMETER COMPARISON

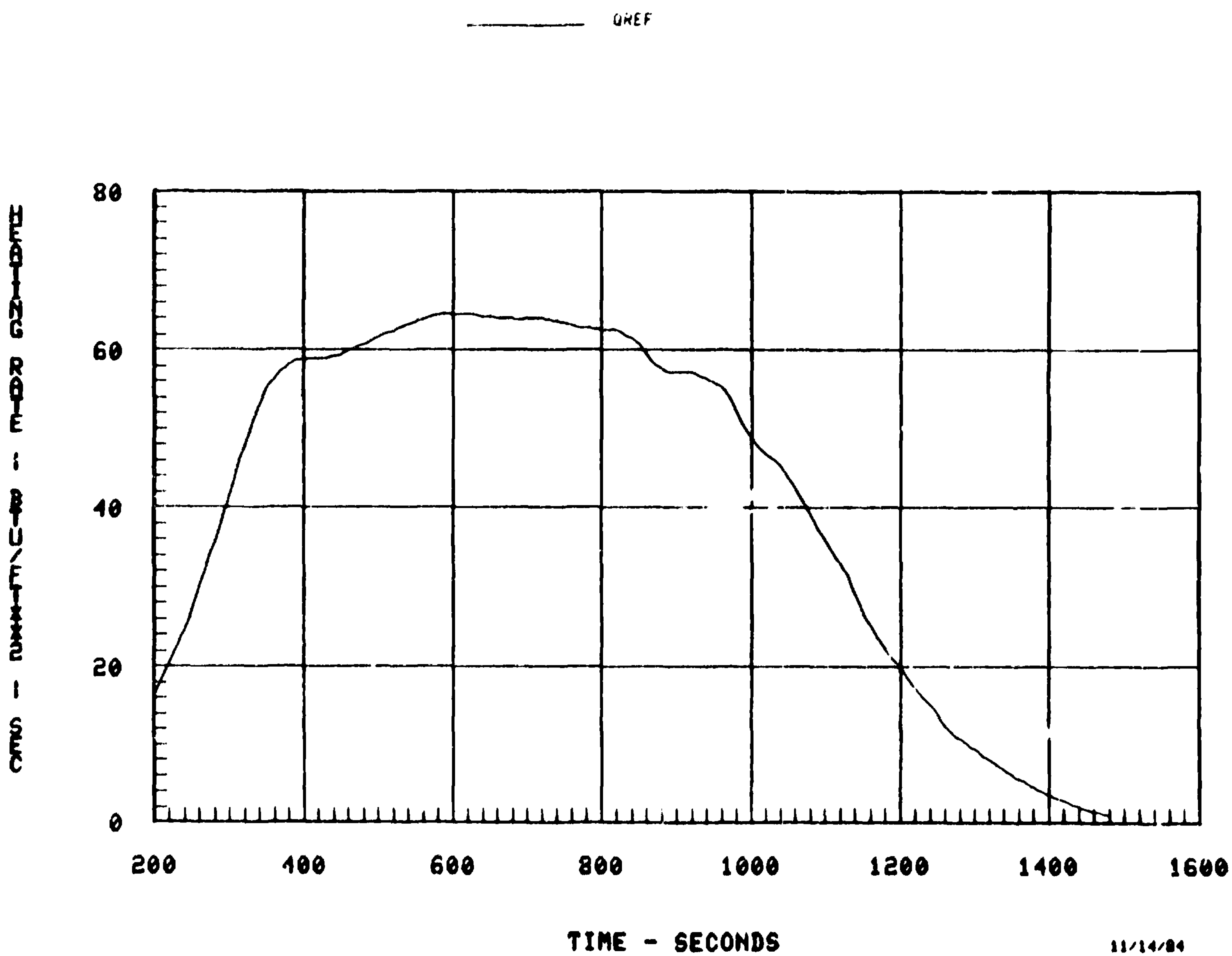

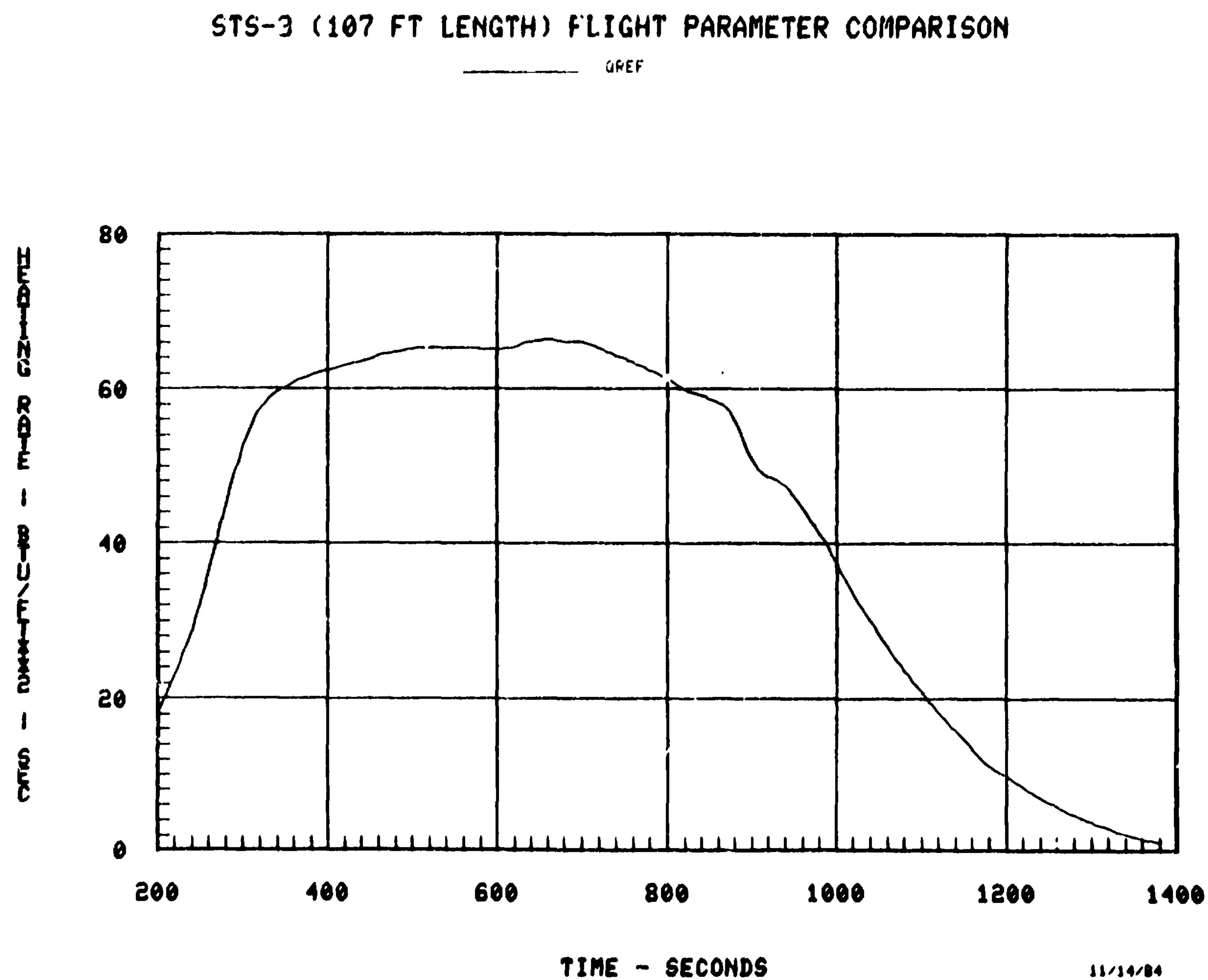

STS-3 (107 FT LENGTH) FLIGHT PARAMETER COMPARISON
QREF
HEATING RATE - BTU/FT**2 - SEC
80
60
40
20
0
200
400
600
800
1000
1200
1400
TIME - SECONDS
11/14/84

STS-4 (107 FT LENGTH) FLIGHT PARAMETER COMPARISON

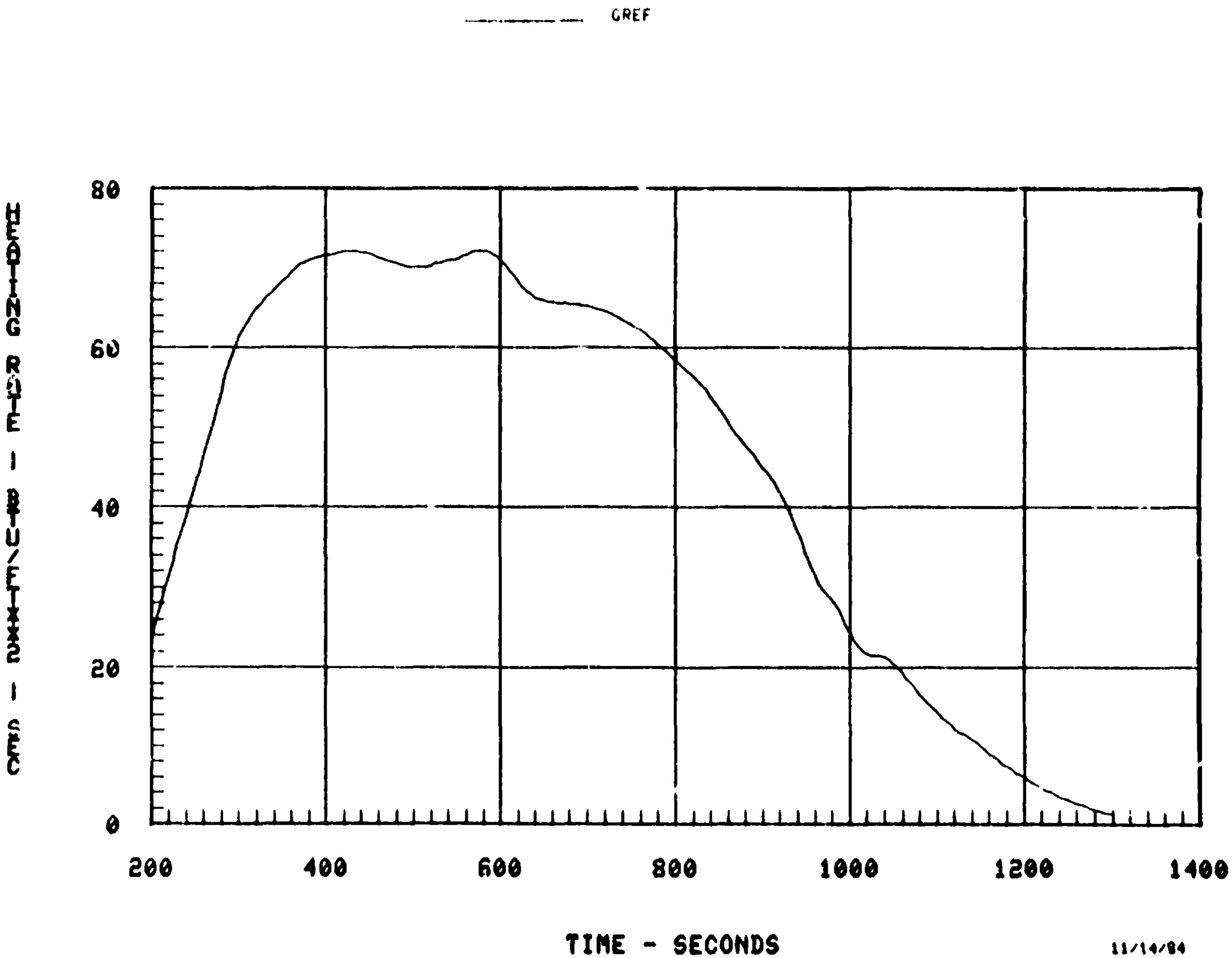

STS-5 (107 FT LENGTH) FLIGHT PARAMETER COMPARISON

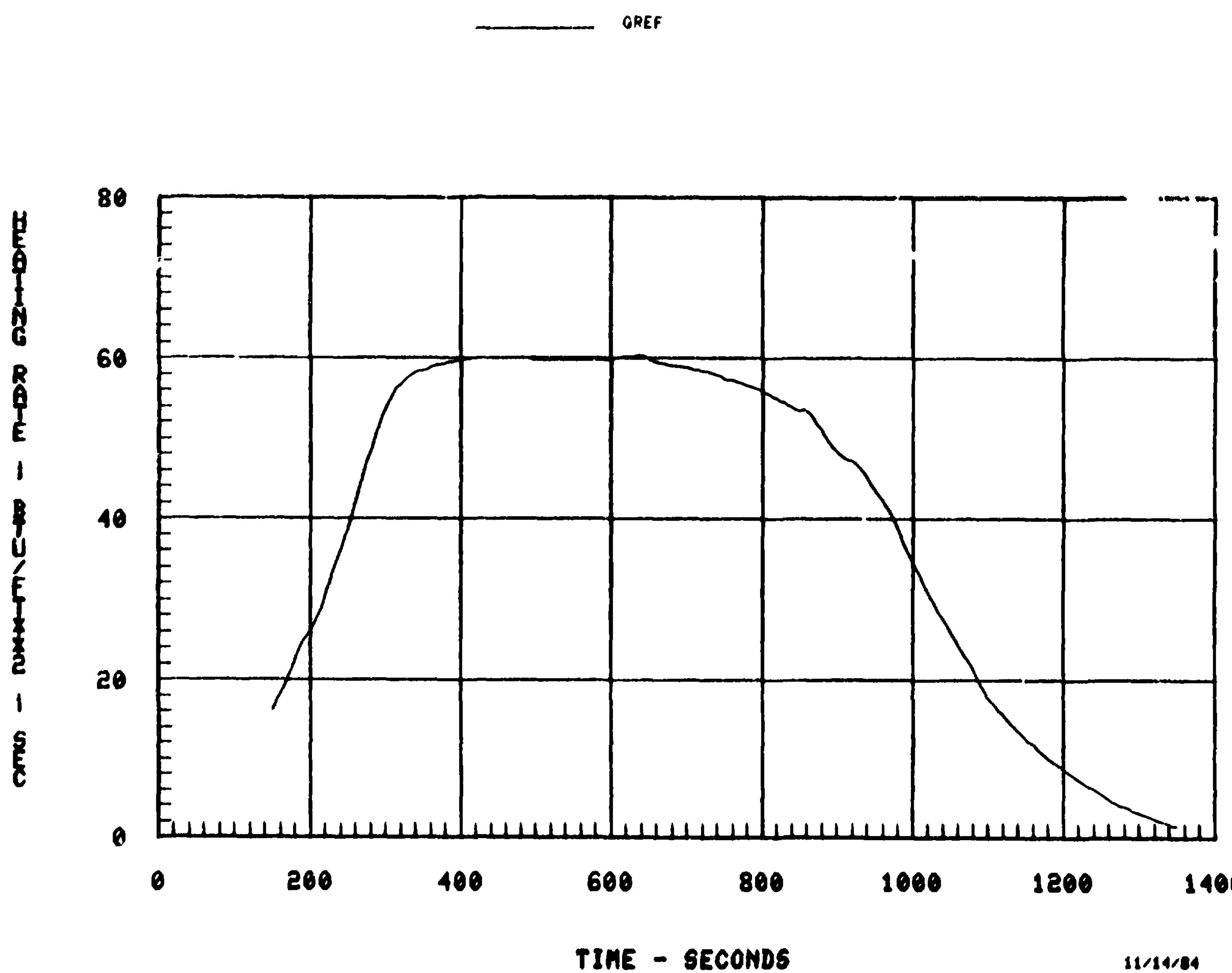

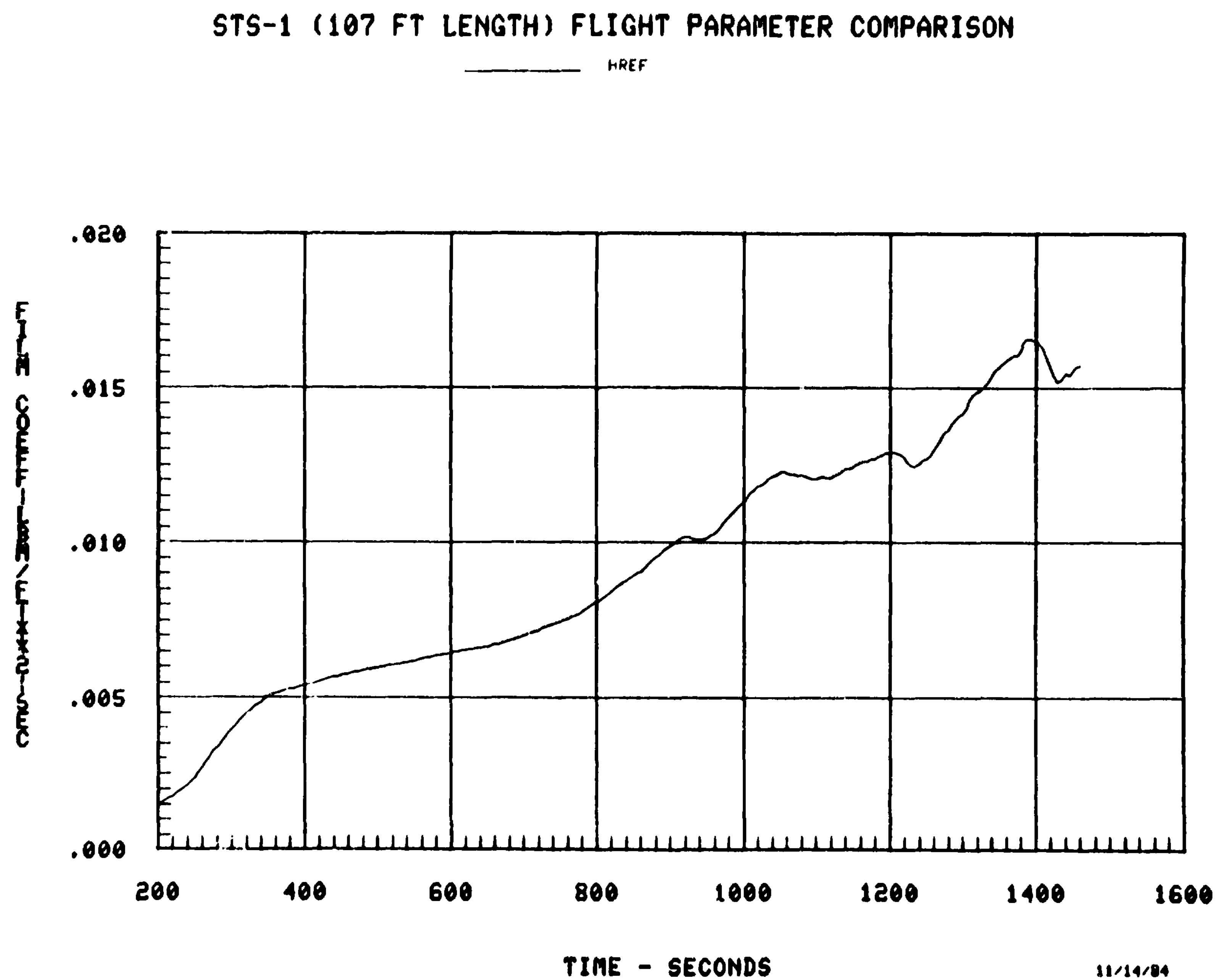
STS-1 (107 FT LENGTH) FLIGHT PARAMETER COMPARISON
HREF
FILM COEFF-LBM/FT**2-SEC
.020
.015
.010
.005
.000
200
400
600
800
1000
1200
1400
1600
TIME - SECONDS
11/14/84

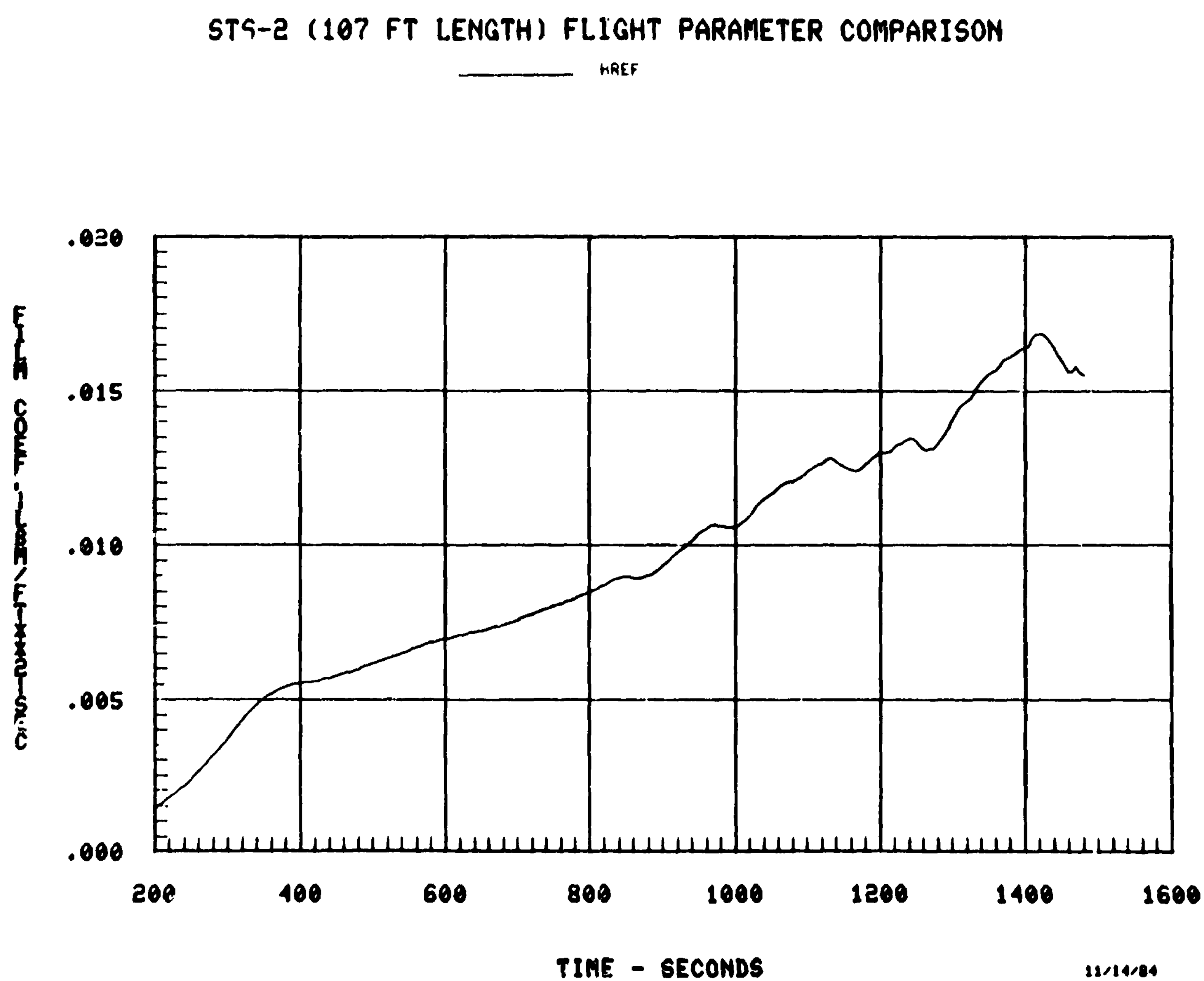
STS-2 (107 FT LENGTH) FLIGHT PARAMETER COMPARISON
HREF
FILM COEF.-LBM/FT**2-SEC
.020
.015
.010
.005
.000
200
400
600
800
1000
1200
1400
1600
TIME - SECONDS
11/14/84

STS-3 (107 FT LENGTH) FLIGHT PARAMETER COMPARISON

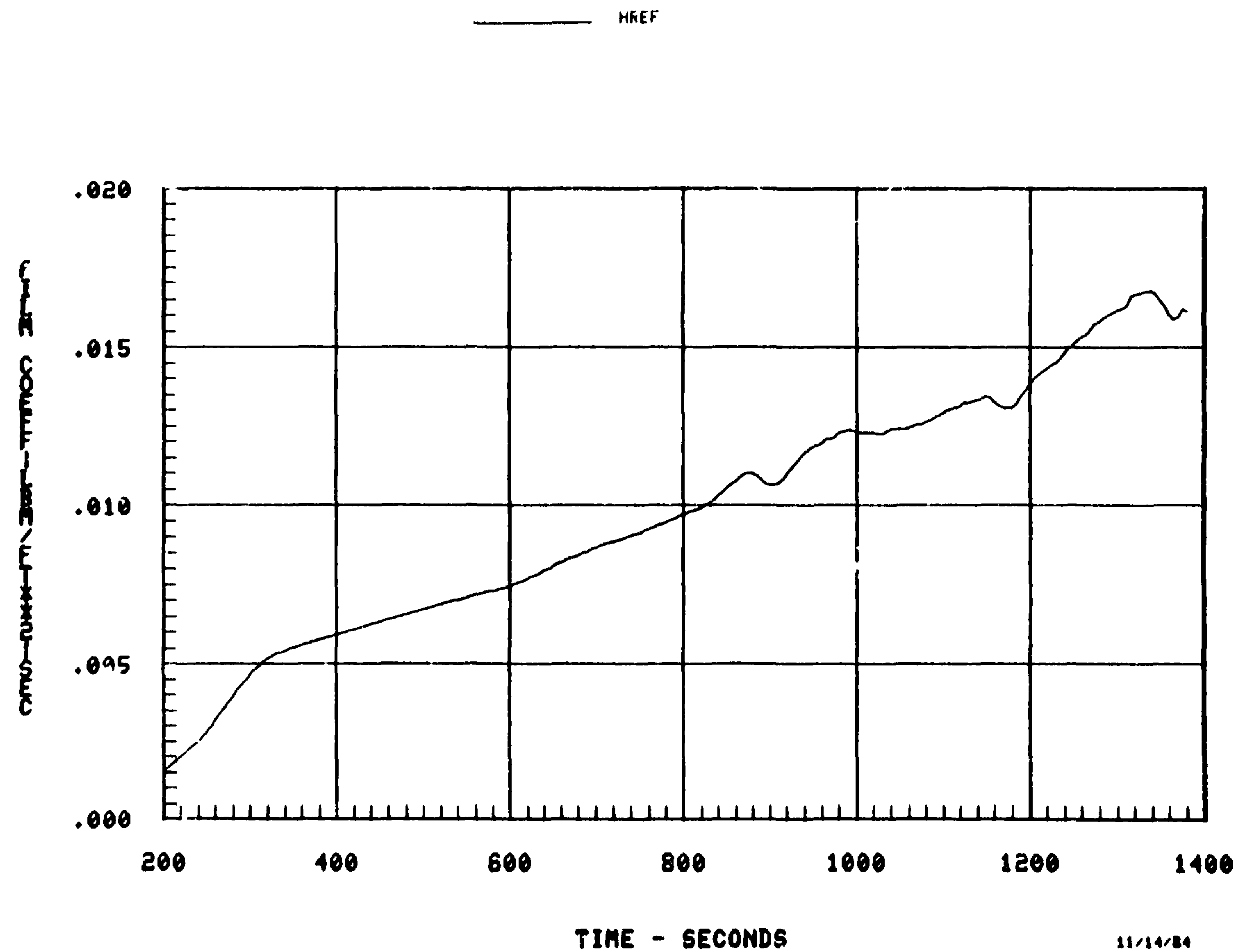

STS-4 (107 FT LENGTH) FLIGHT PARAMETER COMPARISON

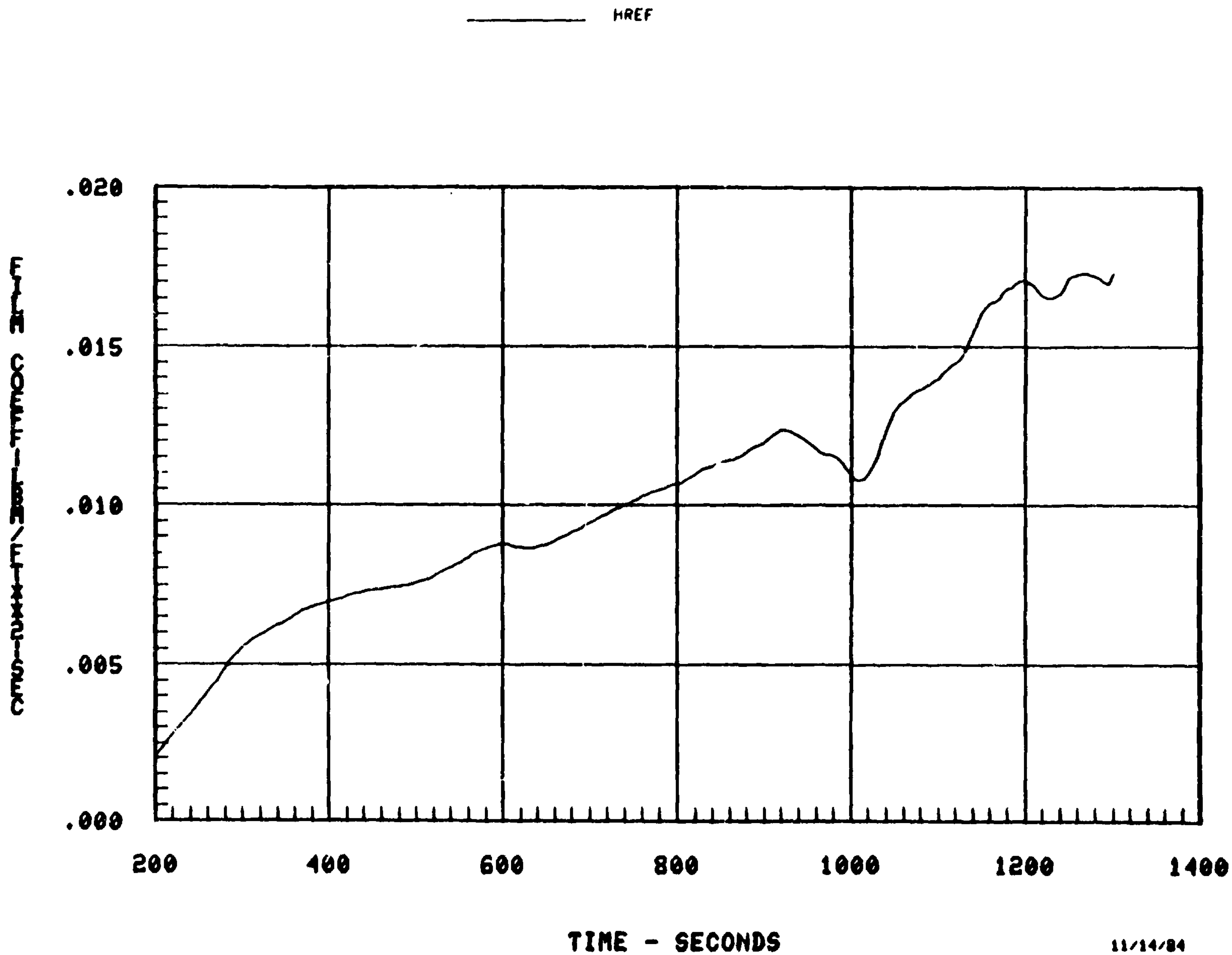

STS-5 (107 FT LENGTH) FLIGHT PARAMETER COMPARISON

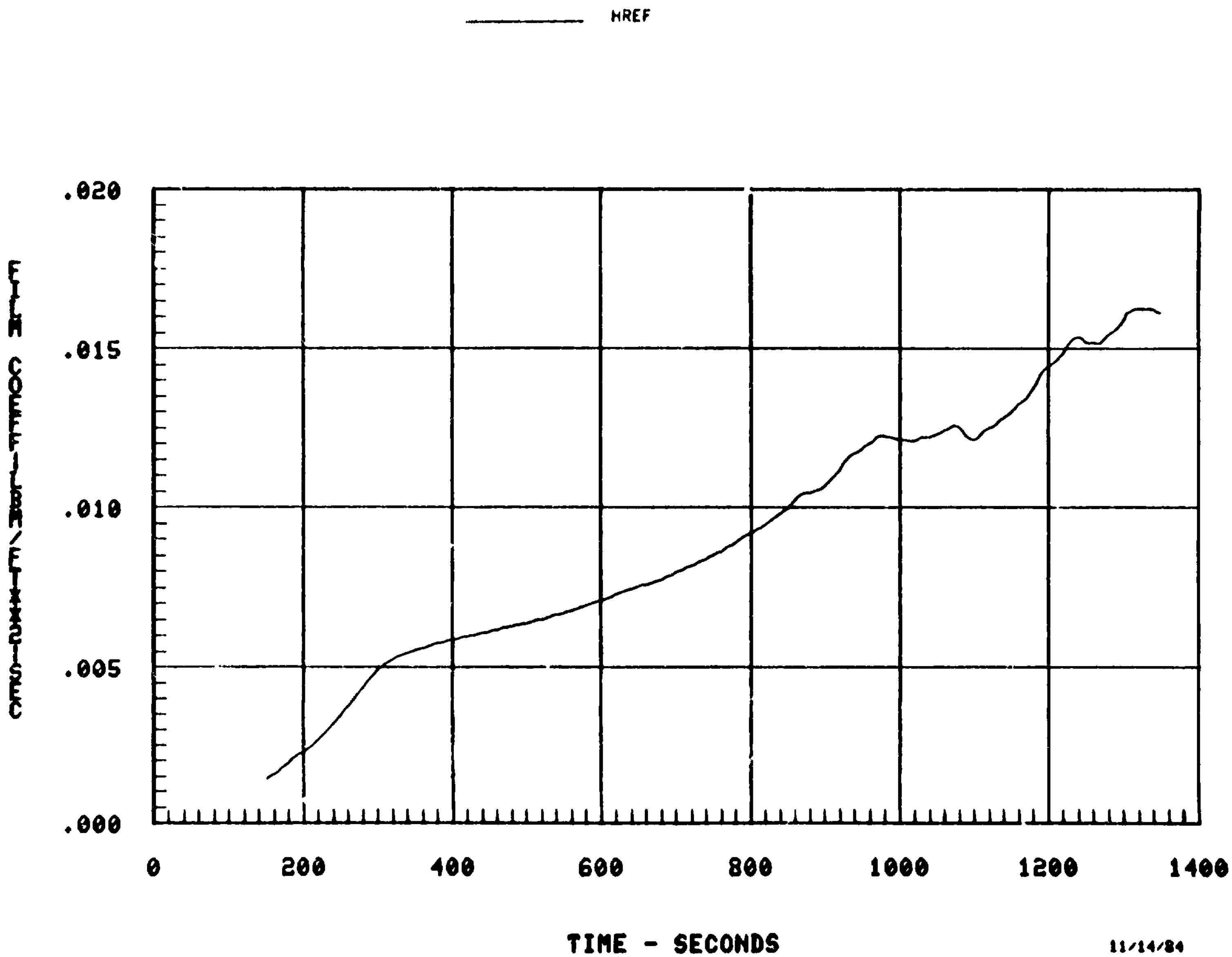

STS-1 (107 FT LENGTH) FLIGHT PARAMETER COMPARISON

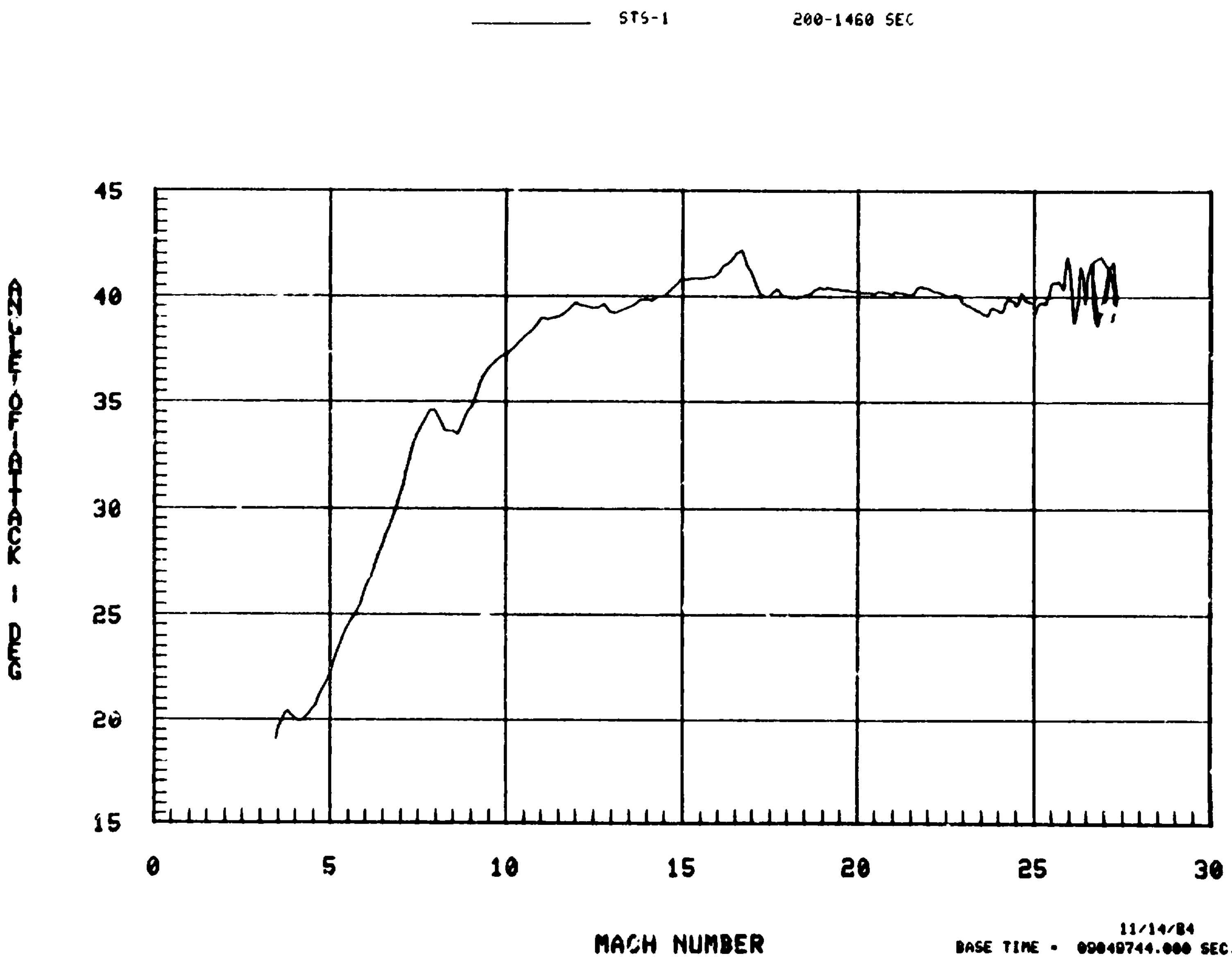

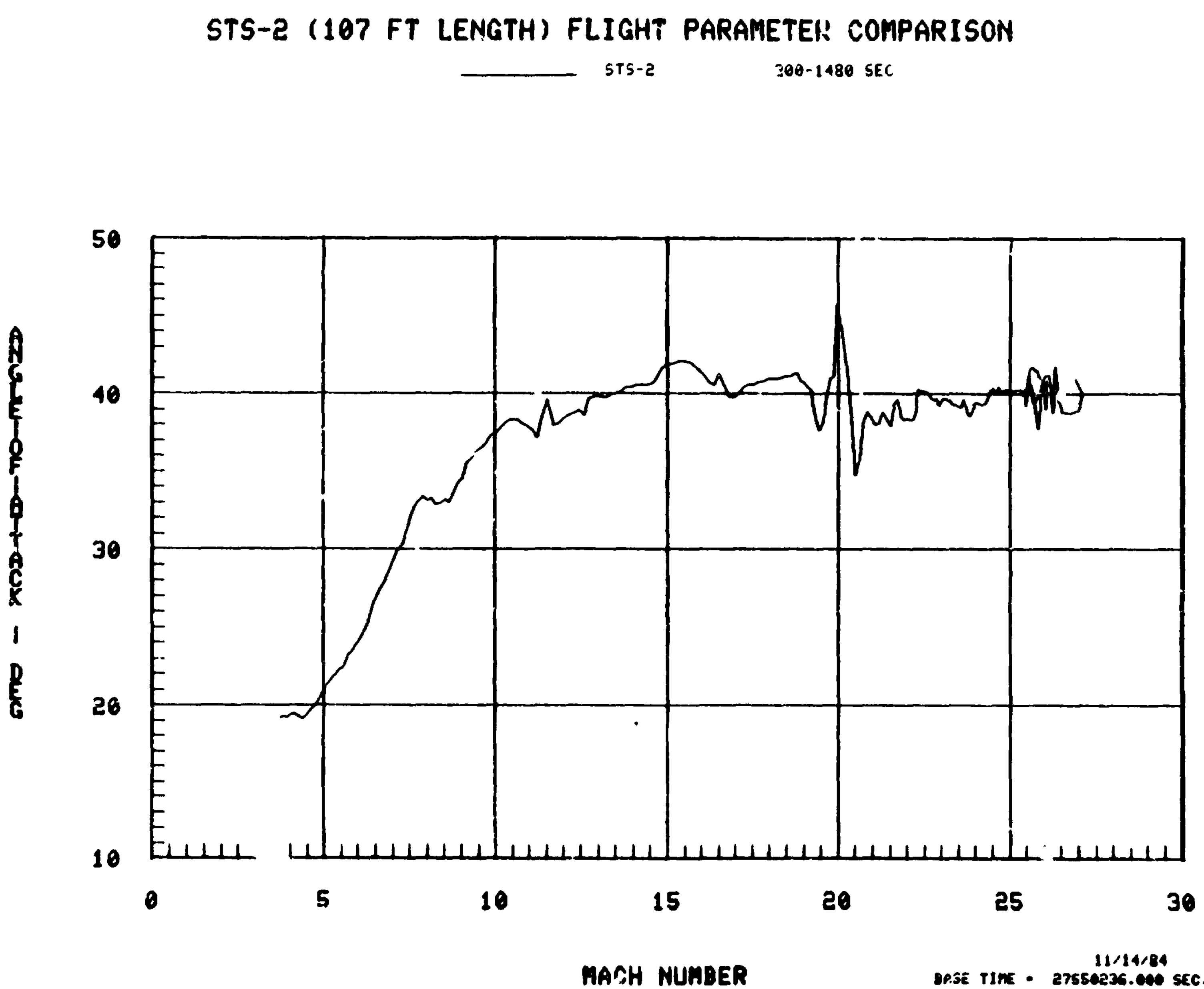
STS-2 (107 FT LENGTH) FLIGHT PARAMETER COMPARISON
STS-2
300-1480 SEC
ANGLE OF ATTACK - DEG
MACH NUMBER
50
40
30
20
10
0
5
10
15
20
25
30
11/14/84
BASE TIME = 275502360.000 SEC.

STS-3 (107 FT LENGTH) FLIGHT PARAMETER COMPARISON

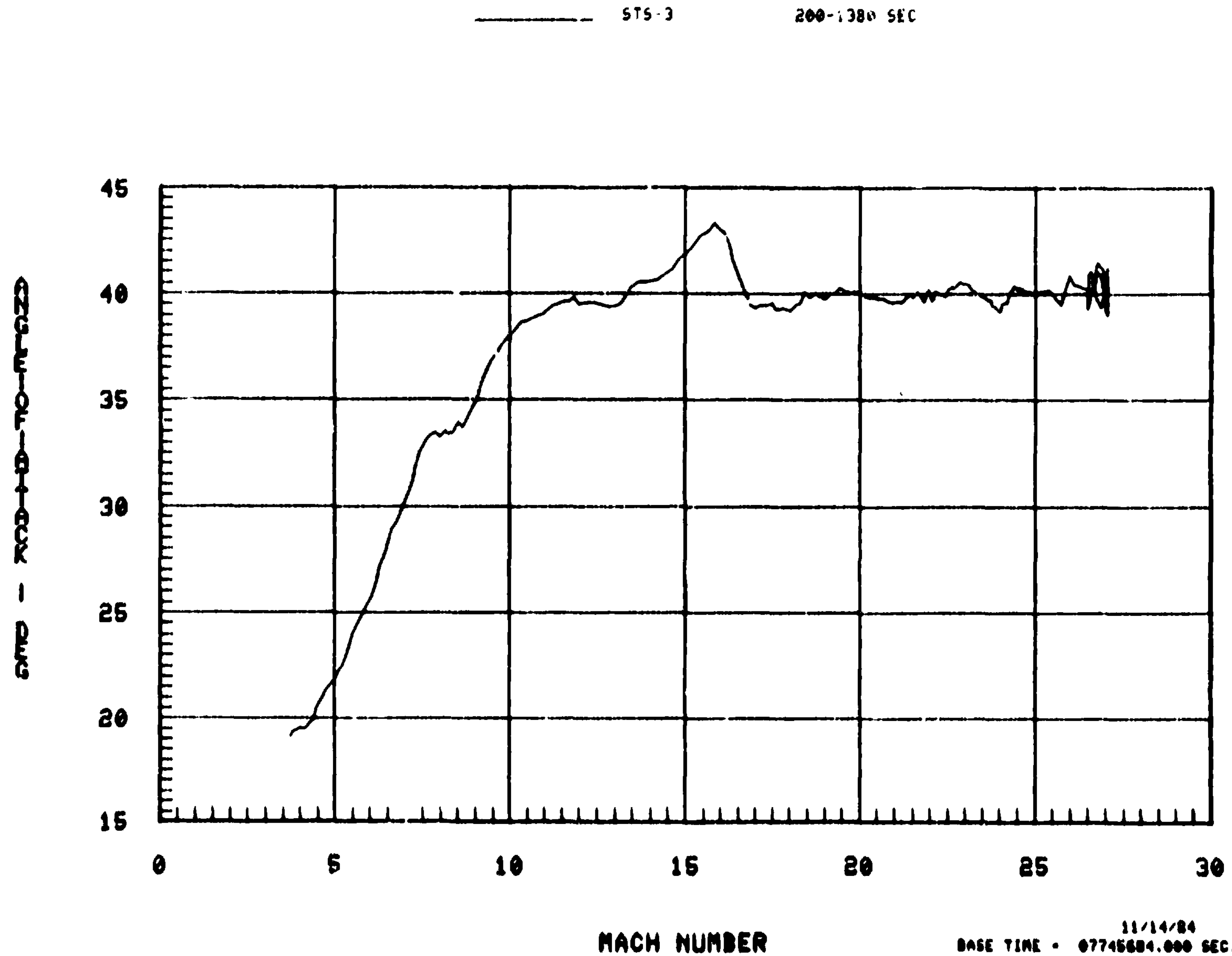

STS-4 (107 FT LENGTH) FLIGHT PARAMETER COMPARISON

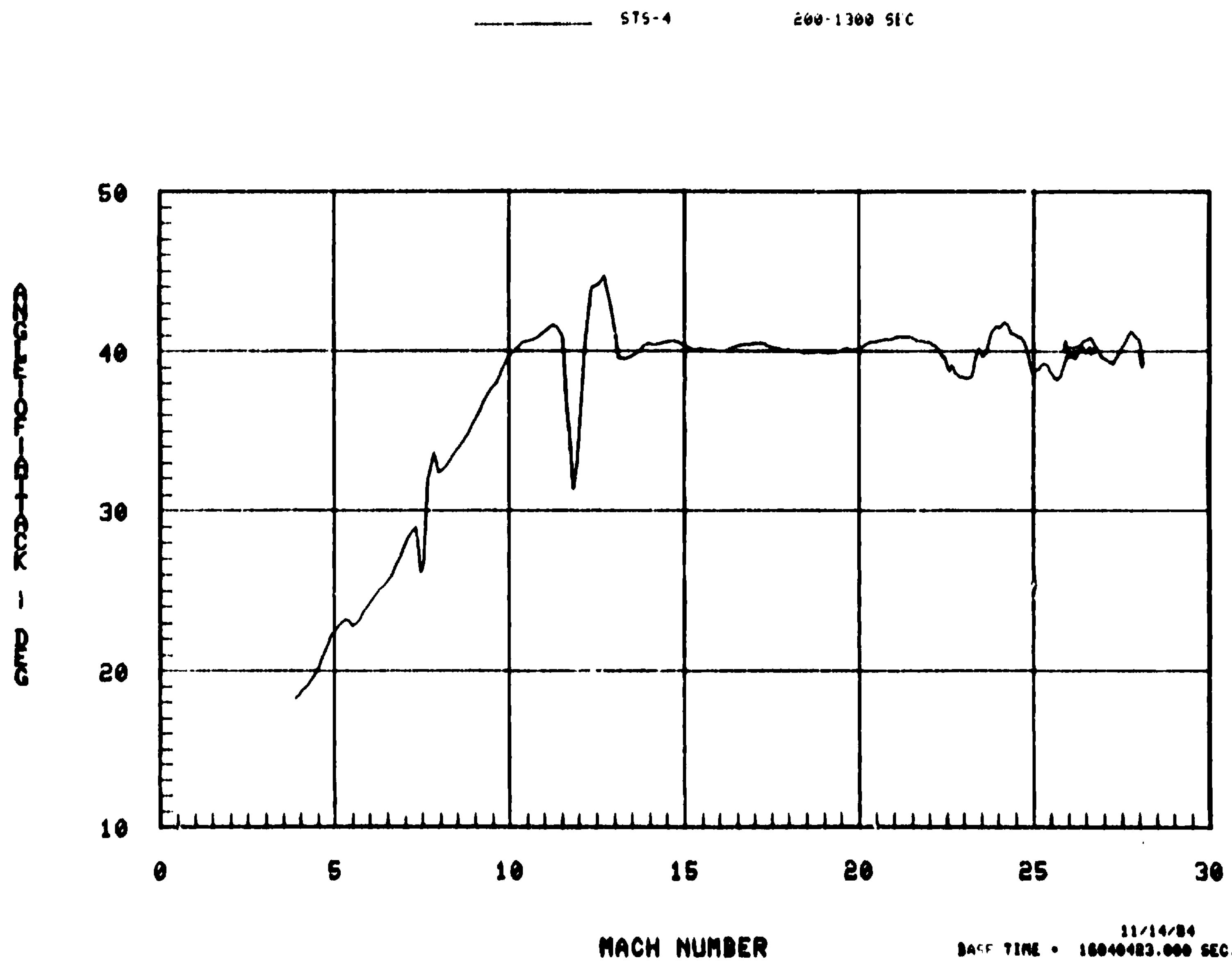

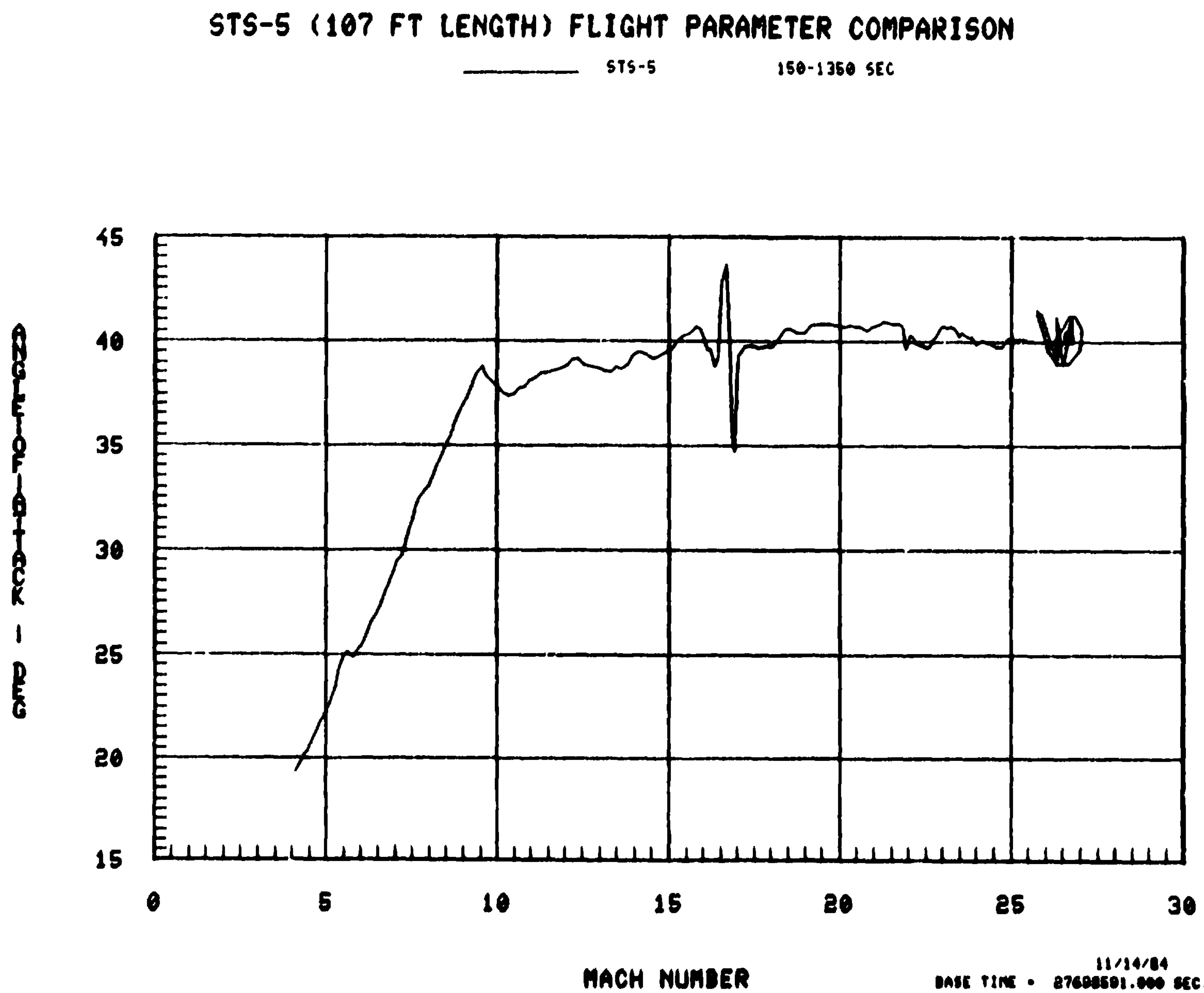
STS-5 (107 FT LENGTH) FLIGHT PARAMETER COMPARISON
STS-5
150-1350 SEC
ANGLE-OF-ATTACK - DEG
45
40
35
30
25
20
15
0
5
10
15
20
25
30
MACH NUMBER
11/14/84

STS-1 (107 FT LENGTH) FLIGHT PARAMETER COMPARISON

STS-1 200-1460 SEC

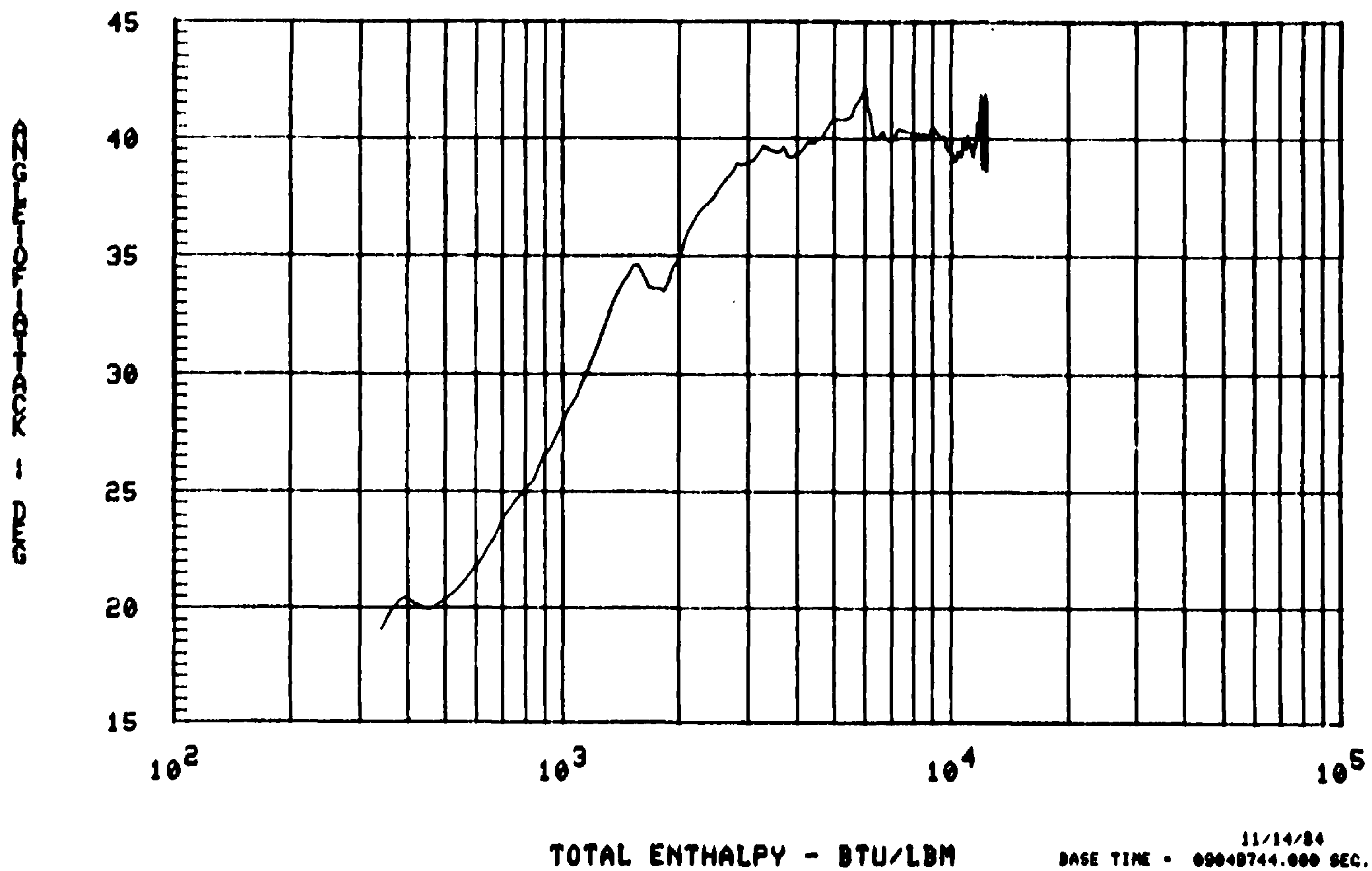

STS-2 (107 FT LENGTH) FLIGHT PARAMETER COMPARISON

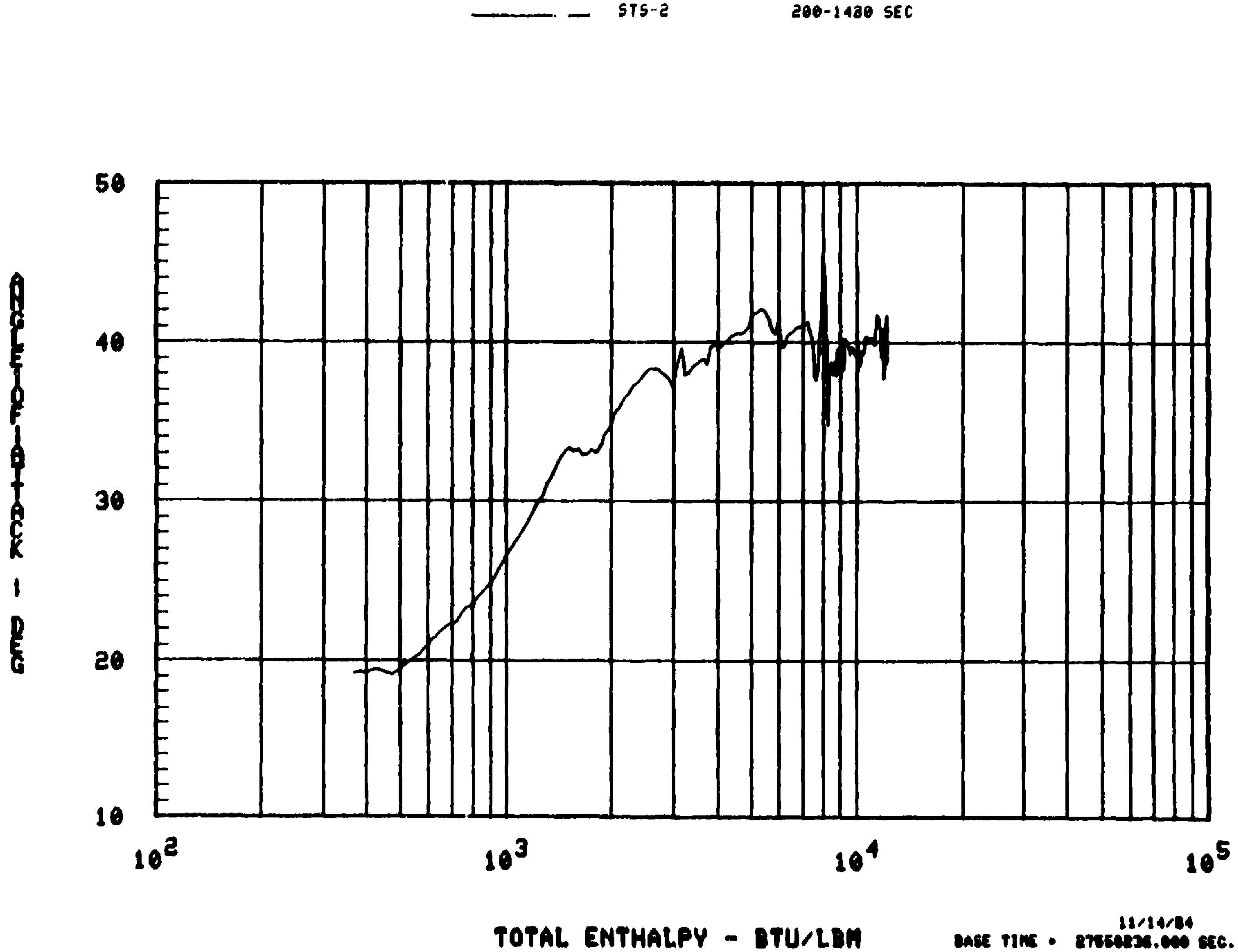

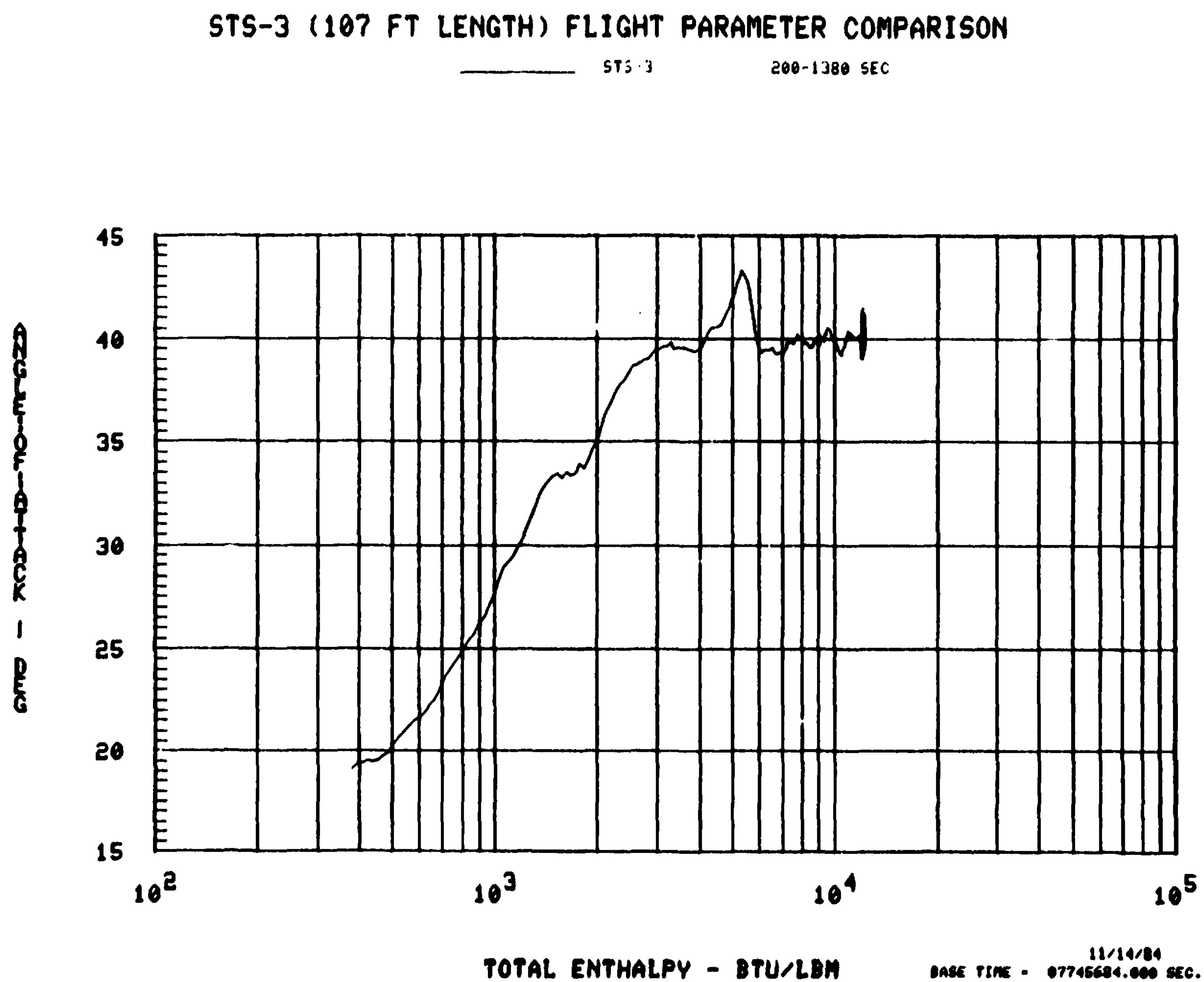
STS-3 (107 FT LENGTH) FLIGHT PARAMETER COMPARISON
STS-3
200-1380 SEC
45
40
35
30
25
20
15
ANGLE-OF-ATTACK - DEG
10^2
10^3
10^4
10^5
TOTAL ENTHALPY - BTU/LBM
11/14/84
BASE TIME - 07745684.000 SEC.

STS-4 (107 FT LENGTH) FLIGHT PARAMETER COMPARISON

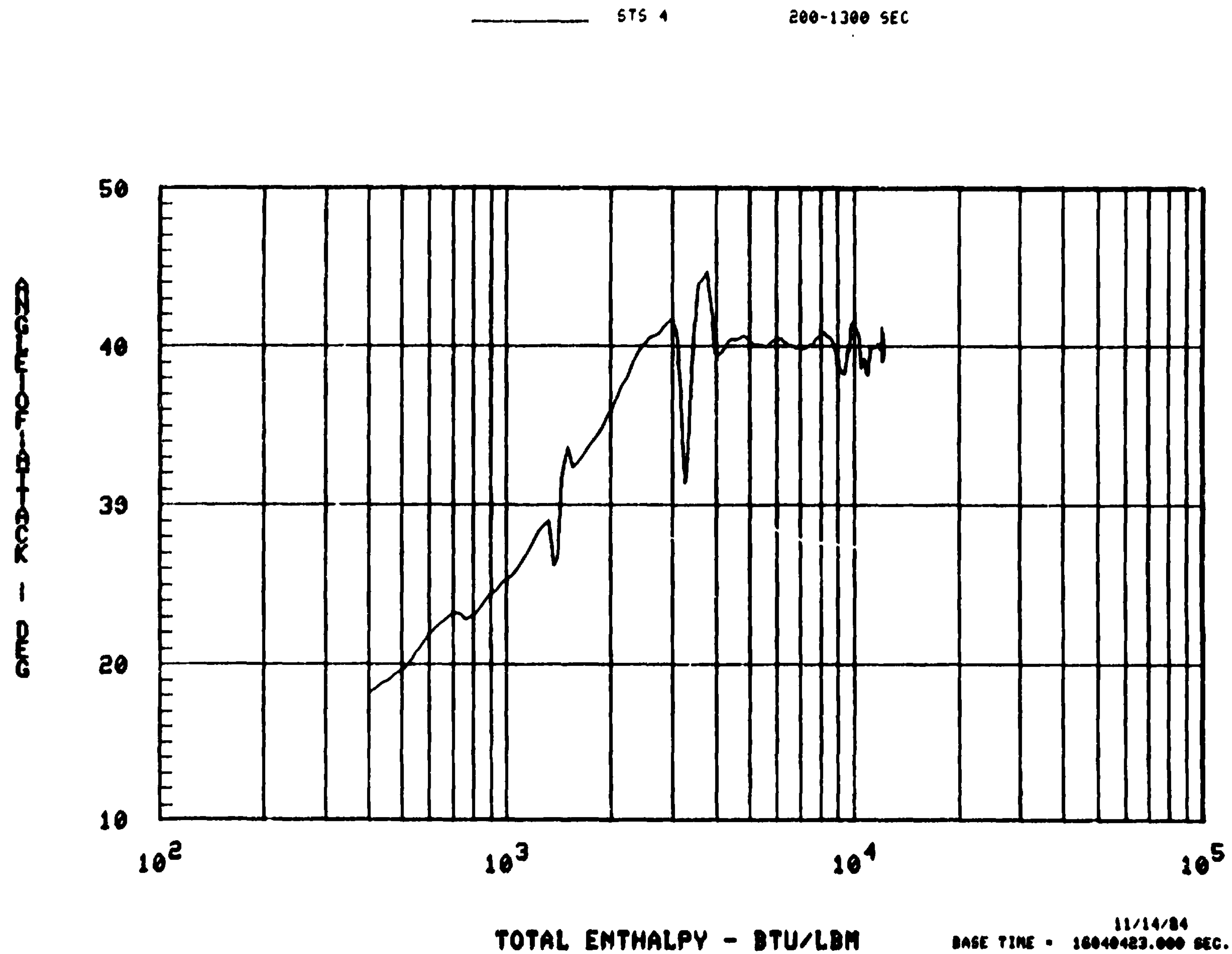

11/14/84
BASE TIME = 16040423.000 SEC.

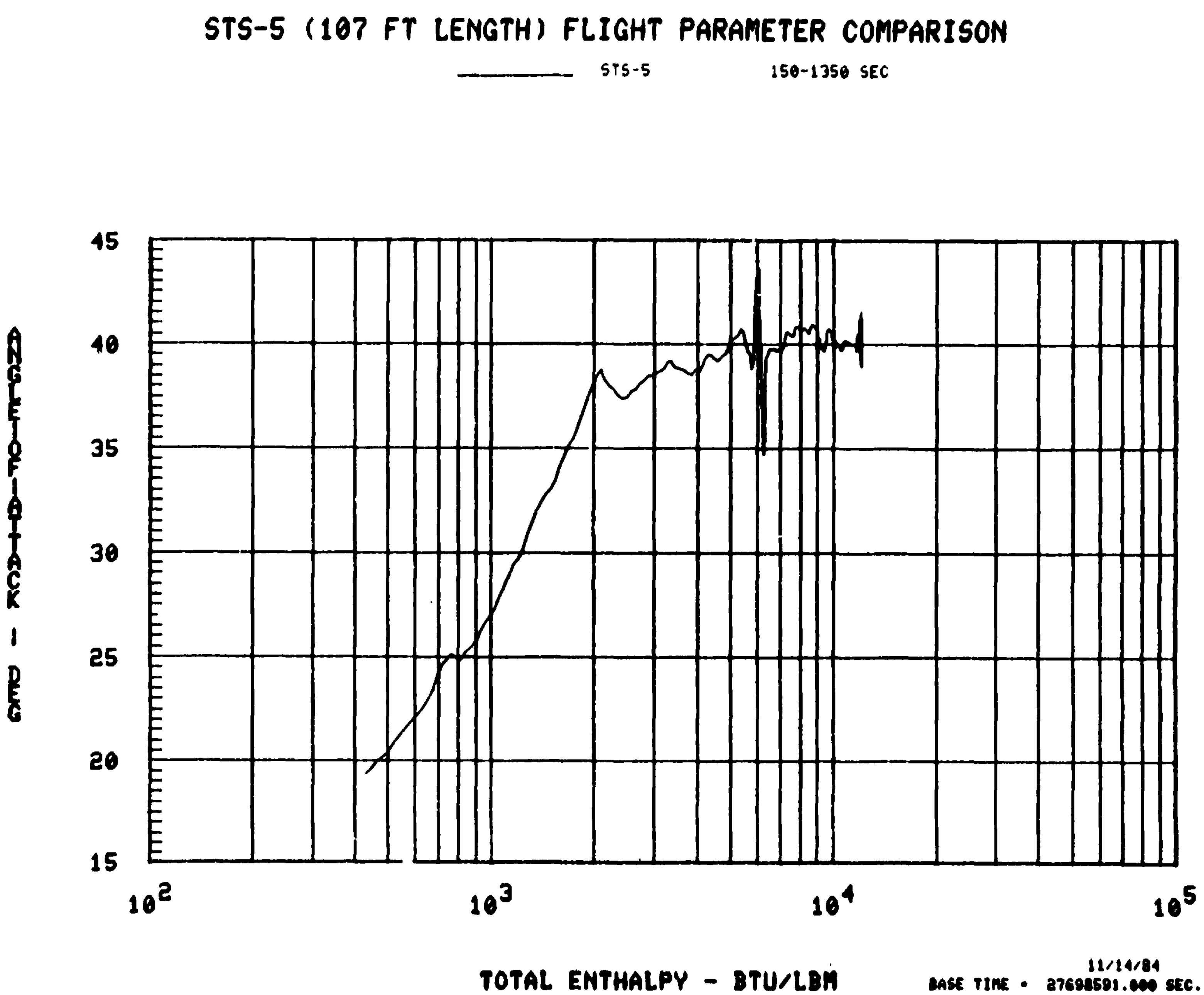
STS-5 (107 FT LENGTH) FLIGHT PARAMETER COMPARISON
STS-5
150-1350 SEC
ANGLE OF ATTACK - DEG
45
40
35
30
25
20
15
10^2
10^3
10^4
10^5
TOTAL ENTHALPY - BTU/LBM
11/14/84
BASE TIME • 27698591.000 SEC.

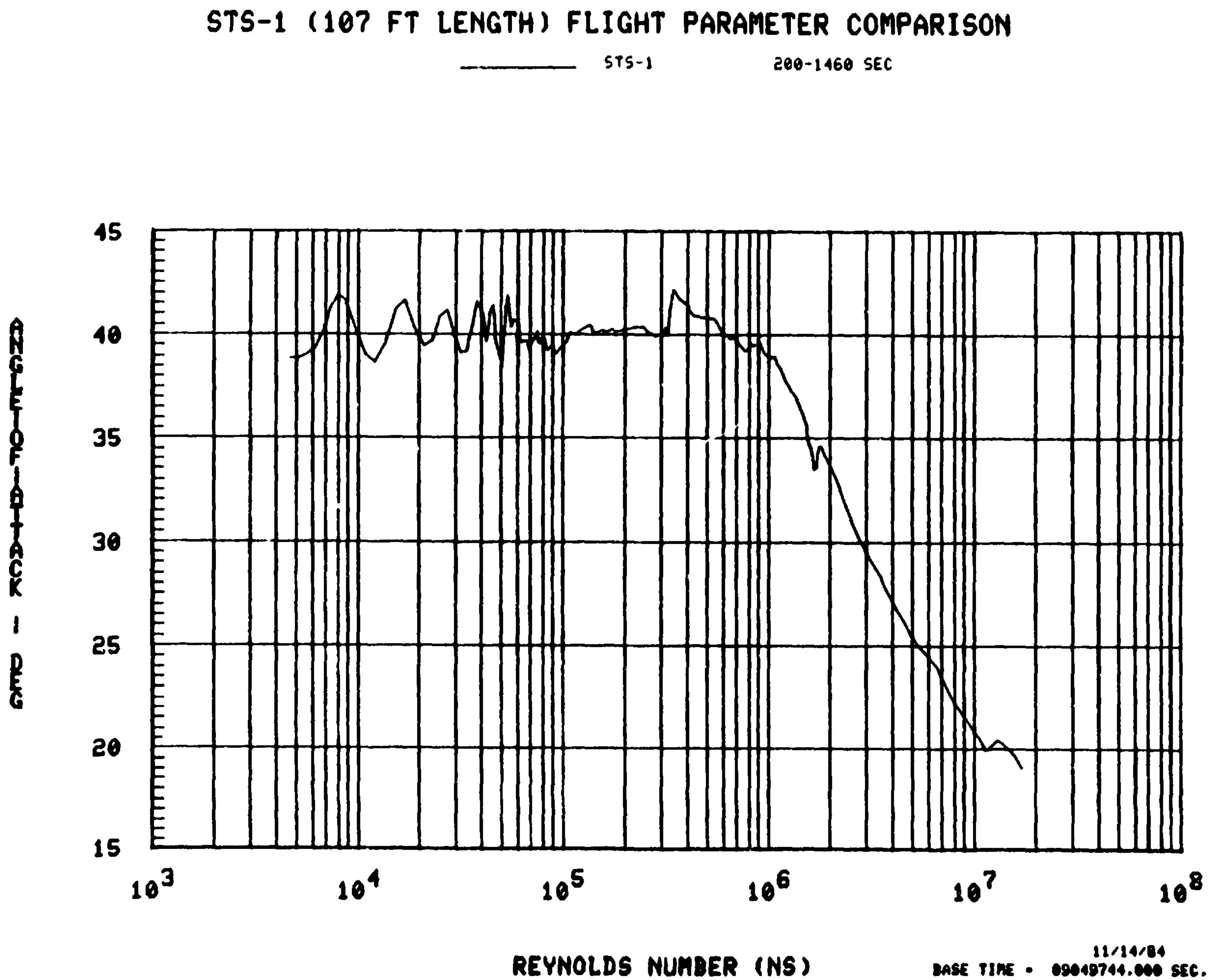
STS-1 (107 FT LENGTH) FLIGHT PARAMETER COMPARISON
STS-1 200-1460 SEC
ANGLE OF ATTACK - DEG
45
40
35
30
25
20
15
10^3
10^4
10^5
10^6
10^7
10^8
REYNOLDS NUMBER (NS)
11/14/84
BASE TIME = 09049744.000 SEC.

STS-2 (107 FT LENGTH) FLIGHT PARAMETER COMPARISON

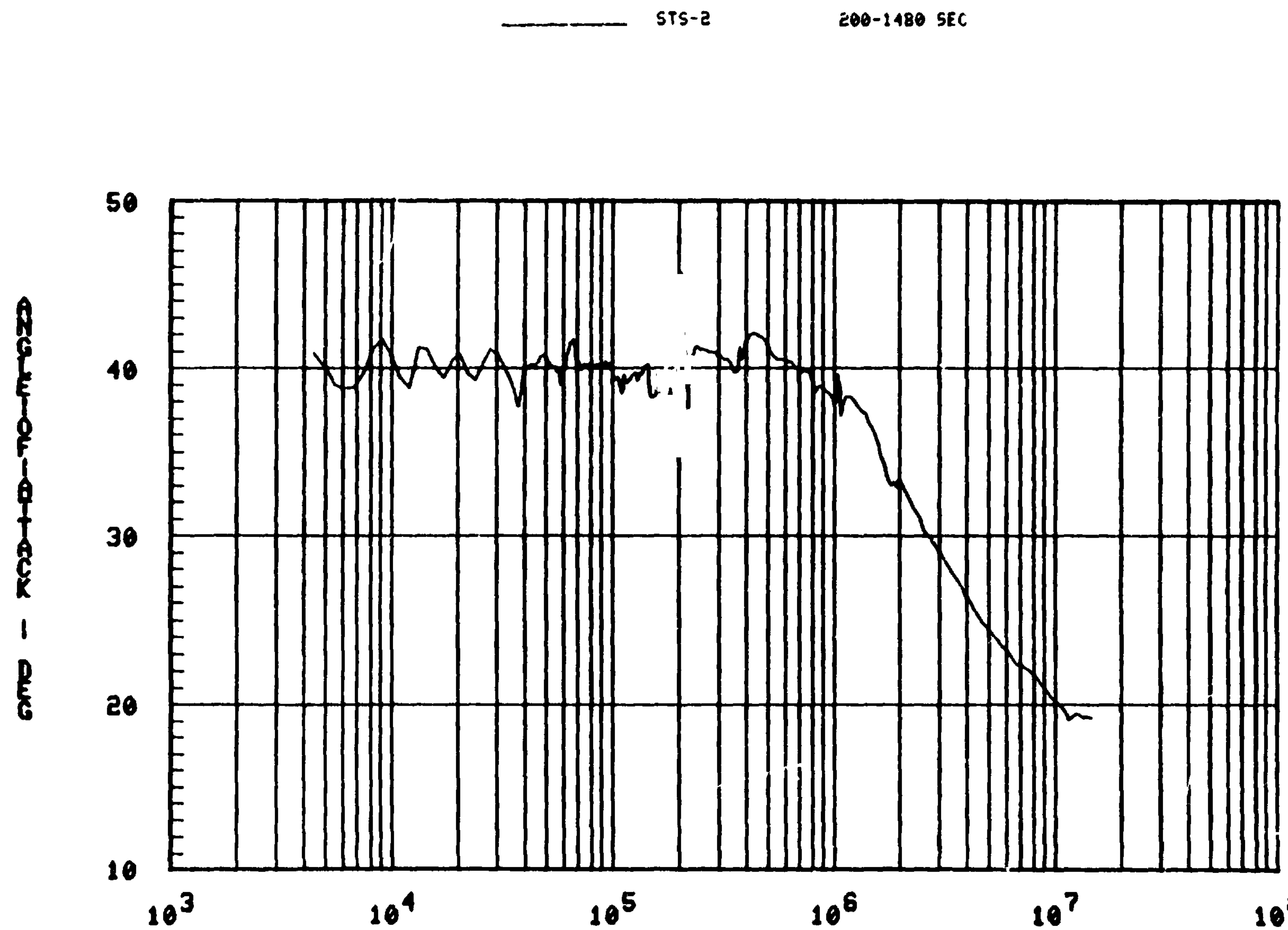

11/14/84
BASE TIME = 27550236.000 SEC.

STS-3 (107 FT LENGTH) FLIGHT PARAMETER COMPARISON

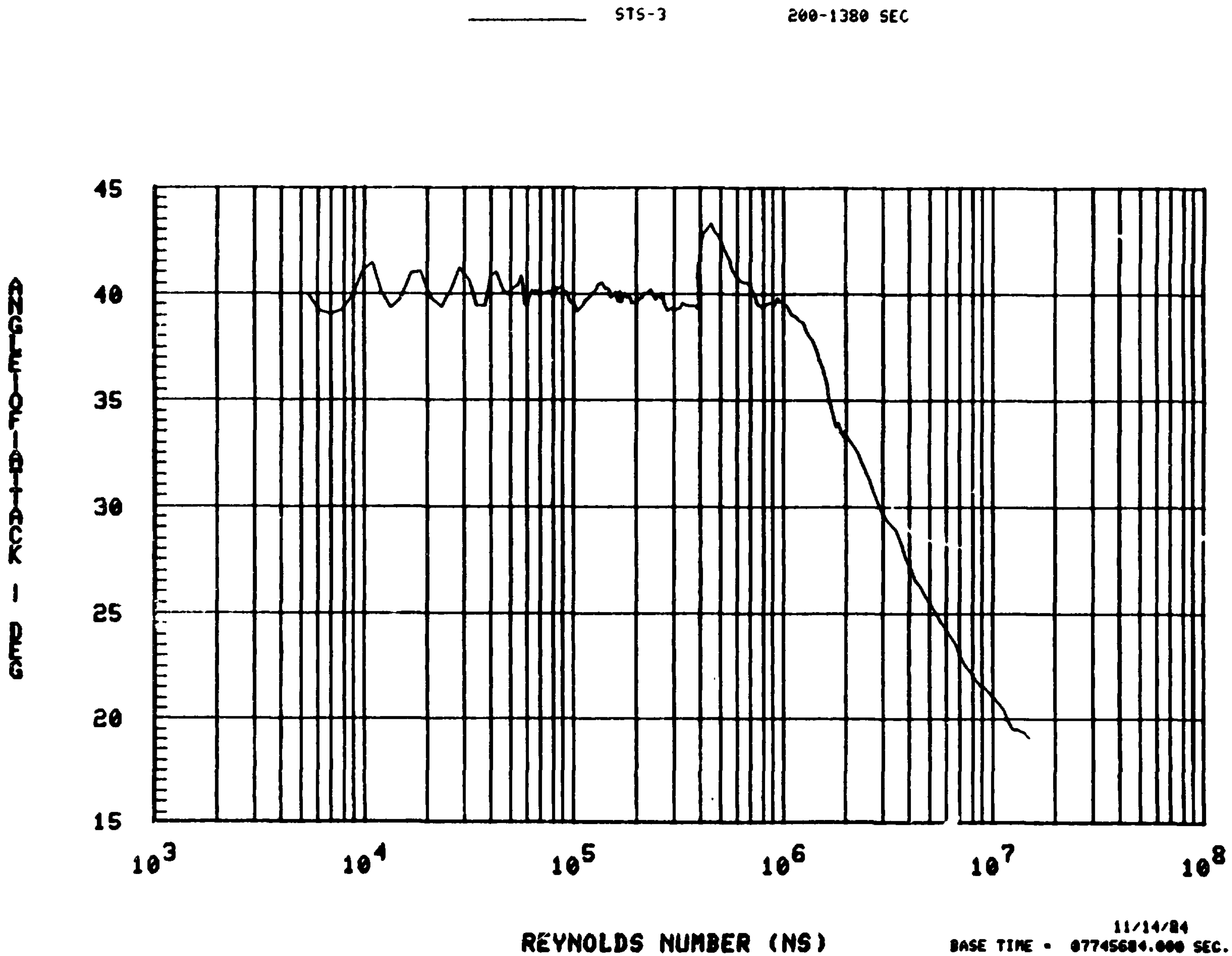

STS-4 (107 FT LENGTH) FLIGHT PARAMETER COMPARISON

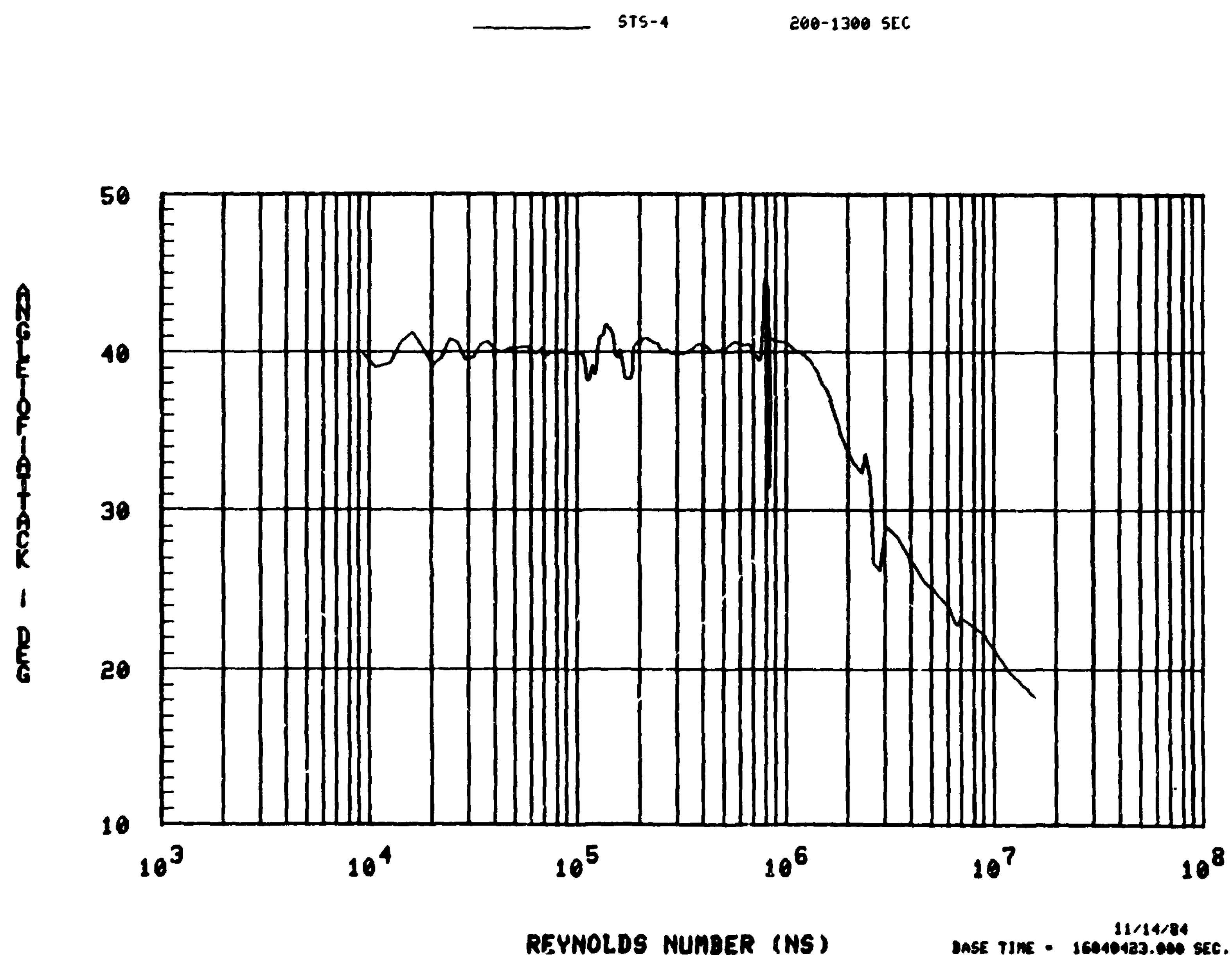

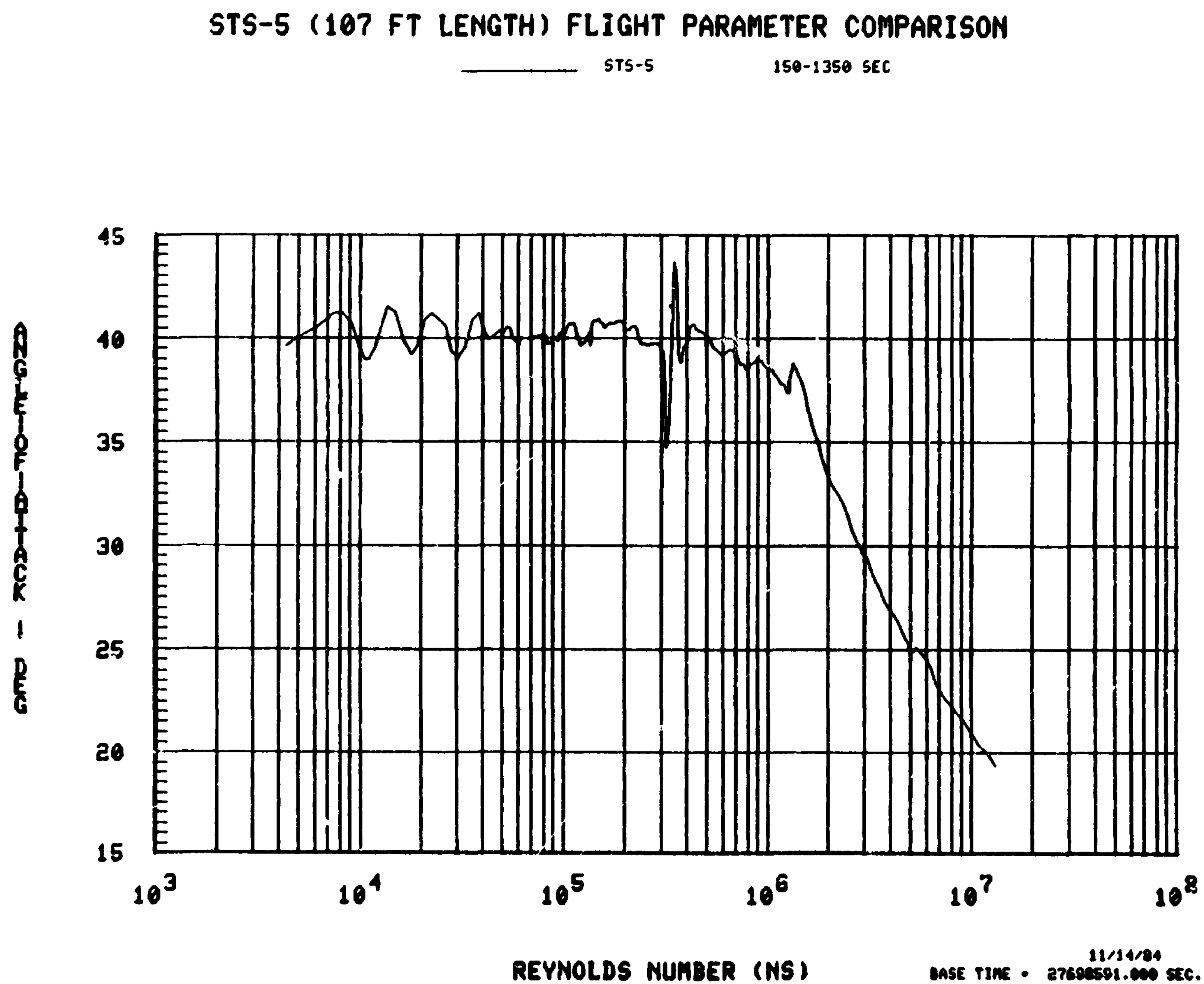
STS-5 (107 FT LENGTH) FLIGHT PARAMETER COMPARISON
STS-5
150-1350 SEC
ANGLE OF ATTACK - DEG
45
40
35
30
25
20
15
10^3
10^4
10^5
10^6
10^7
10^8
REYNOLDS NUMBER (NS)
11/14/84
BASE TIME = 27698591.000 SEC.

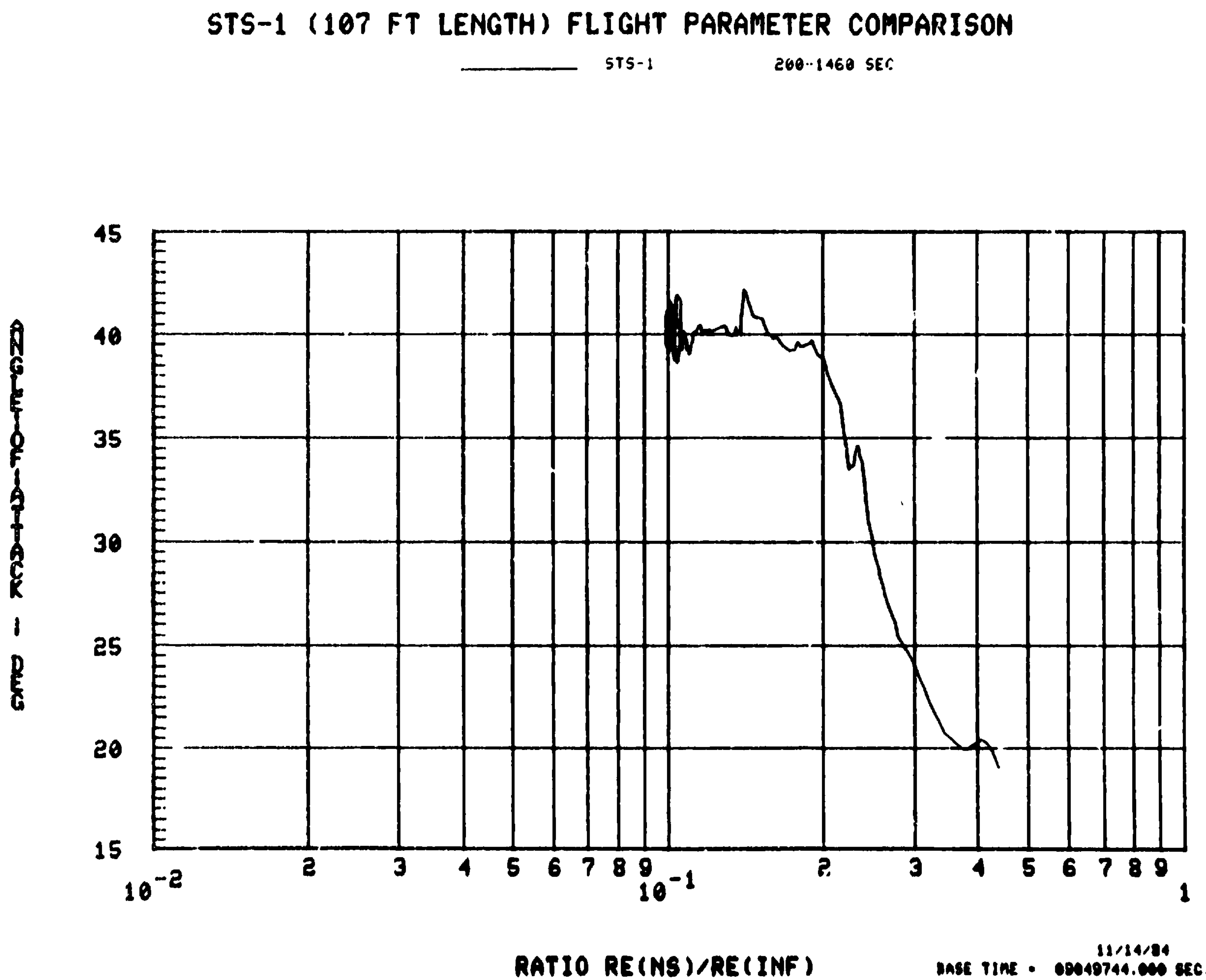
STS-1 (107 FT LENGTH) FLIGHT PARAMETER COMPARISON
STS-1
200-1460 SEC
ANGLE-OF-ATTACK - DEG
45
40
35
30
25
20
15
10^{-2}
2
3
4
5
6
7
8
9
10^{-1}
2
3
4
5
6
7
8
9
1
RATIO RE(NS)/RE(INF)
11/14/84
BASE TIME - 00049744.000 SEC.

STS-2 (107 FT LENGTH) FLIGHT PARAMETER COMPARISON

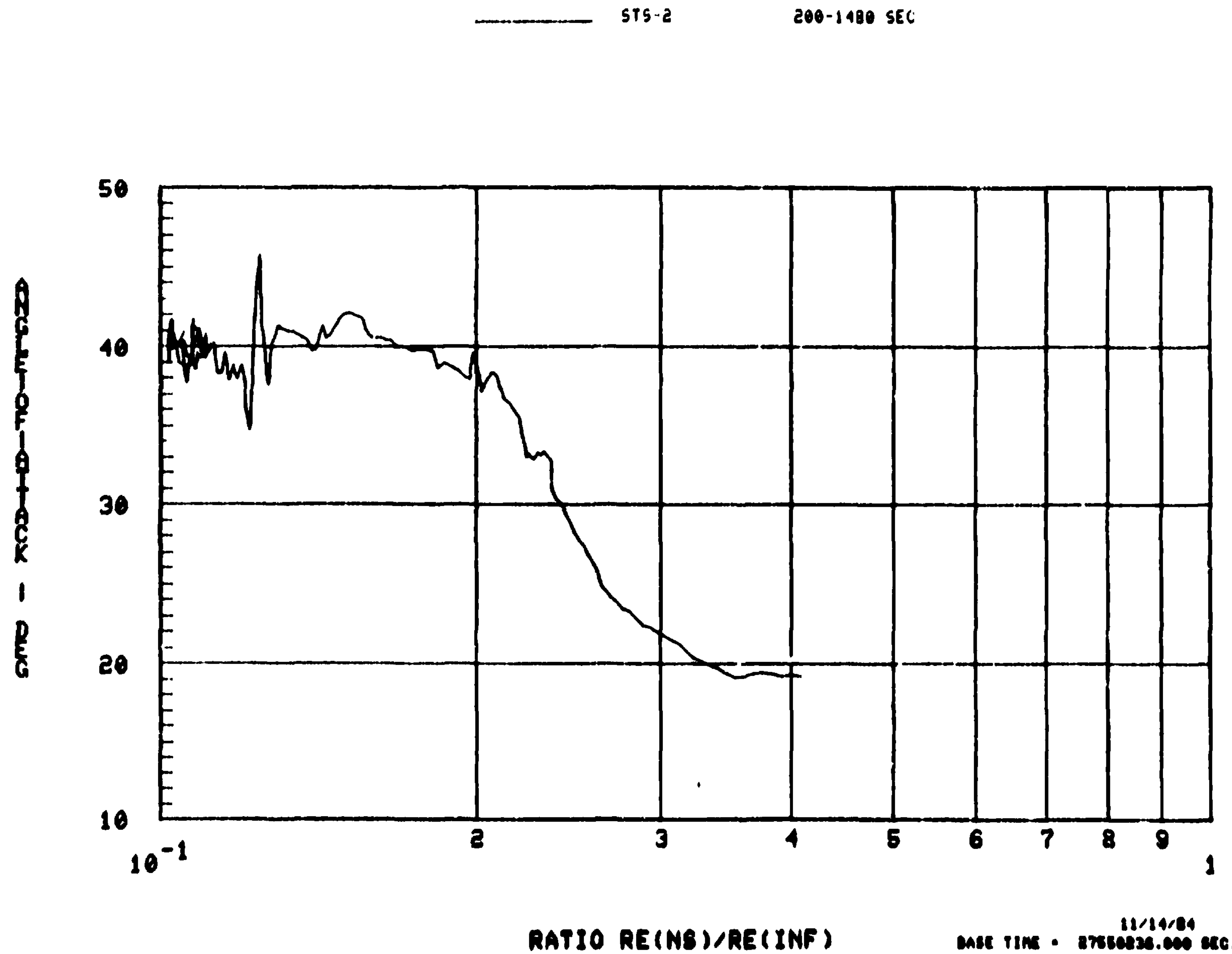

STS-3 (107 FT LENGTH) FLIGHT PARAMETER COMPARISON

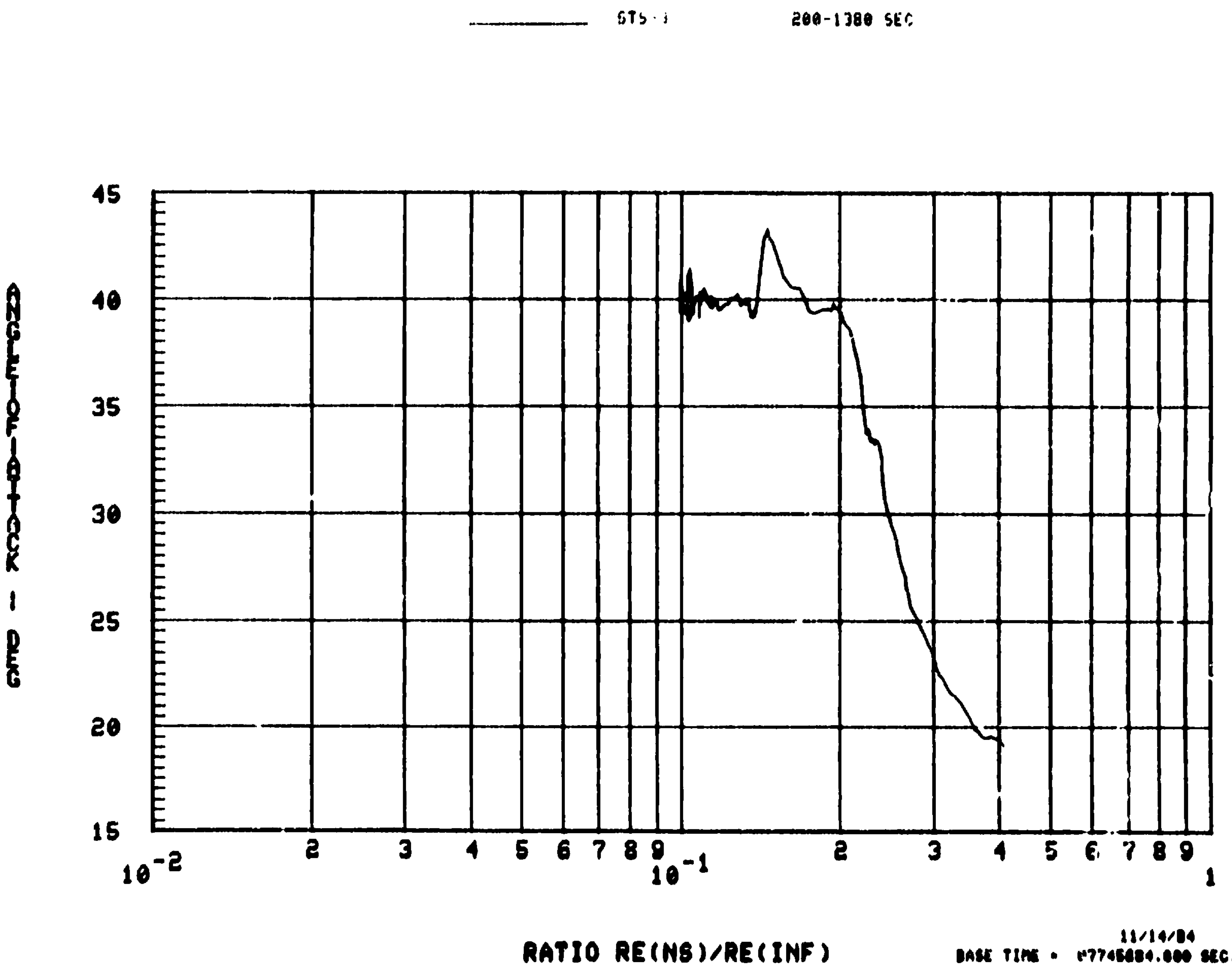

STS-4 (107 FT LENGTH) FLIGHT PARAMETER COMPARISON

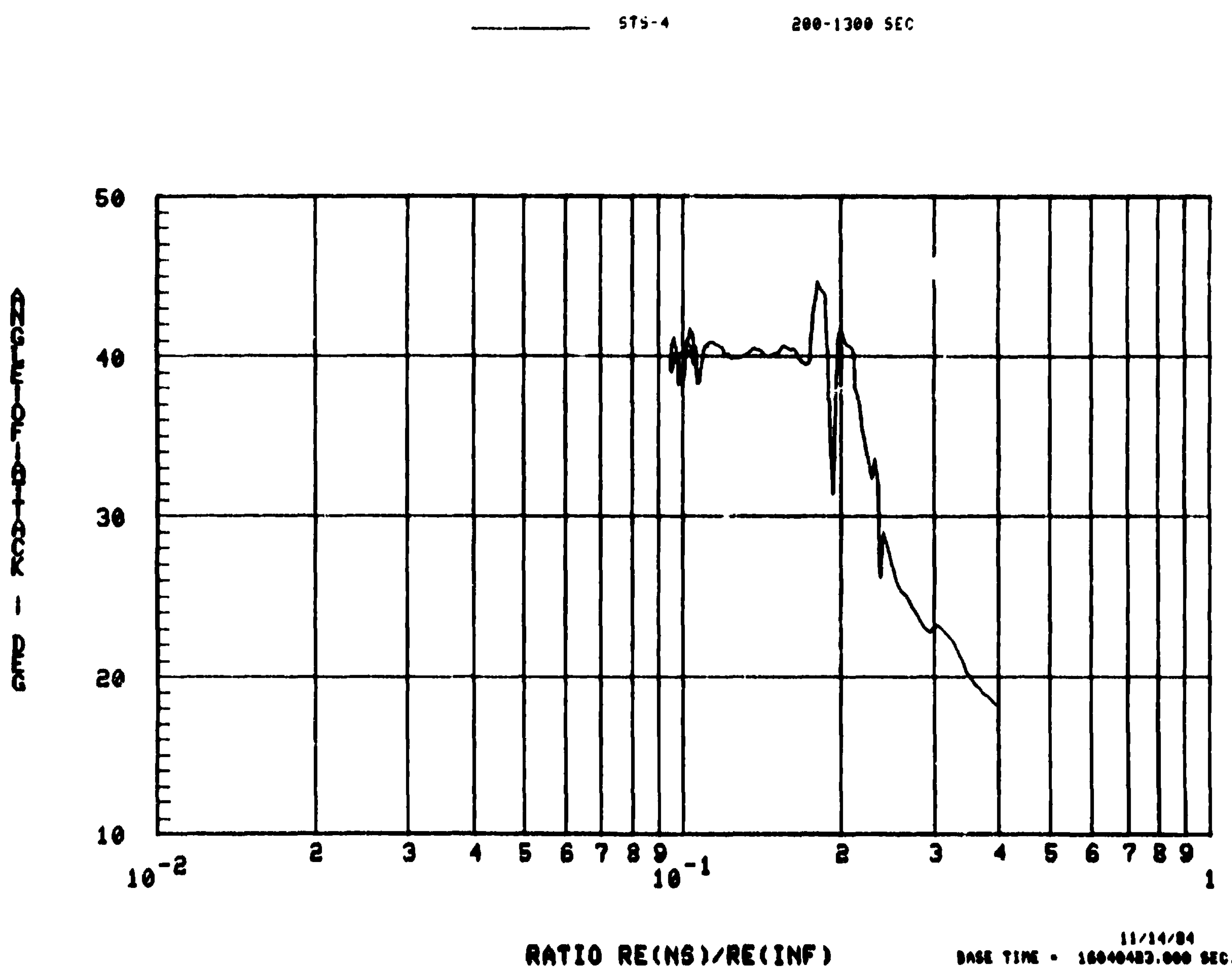

STS-5 (107 FT LENGTH) FLIGHT PARAMETER COMPARISON

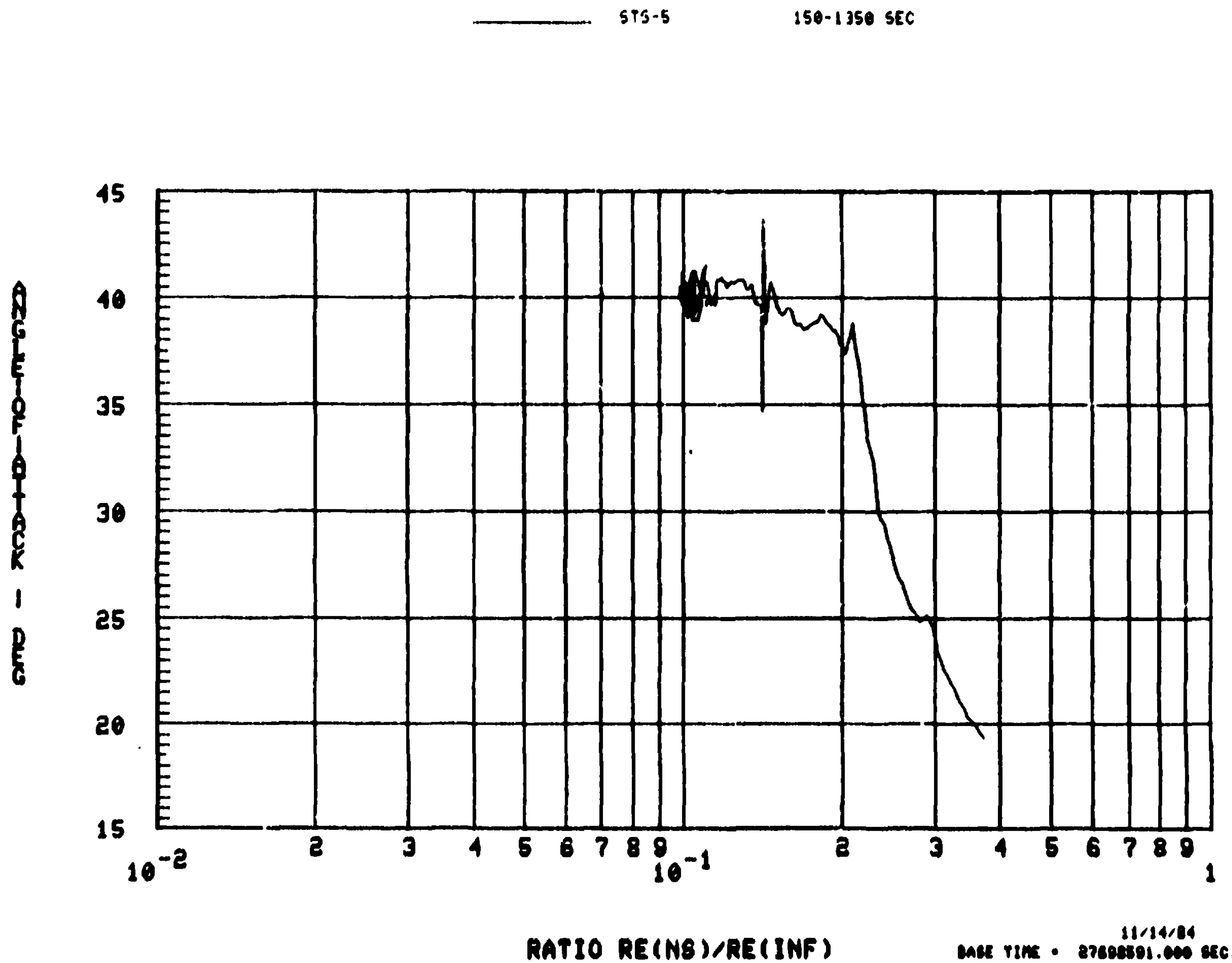

STS-1 (107 FT LENGTH) FLIGHT PARAMETER COMPARISON

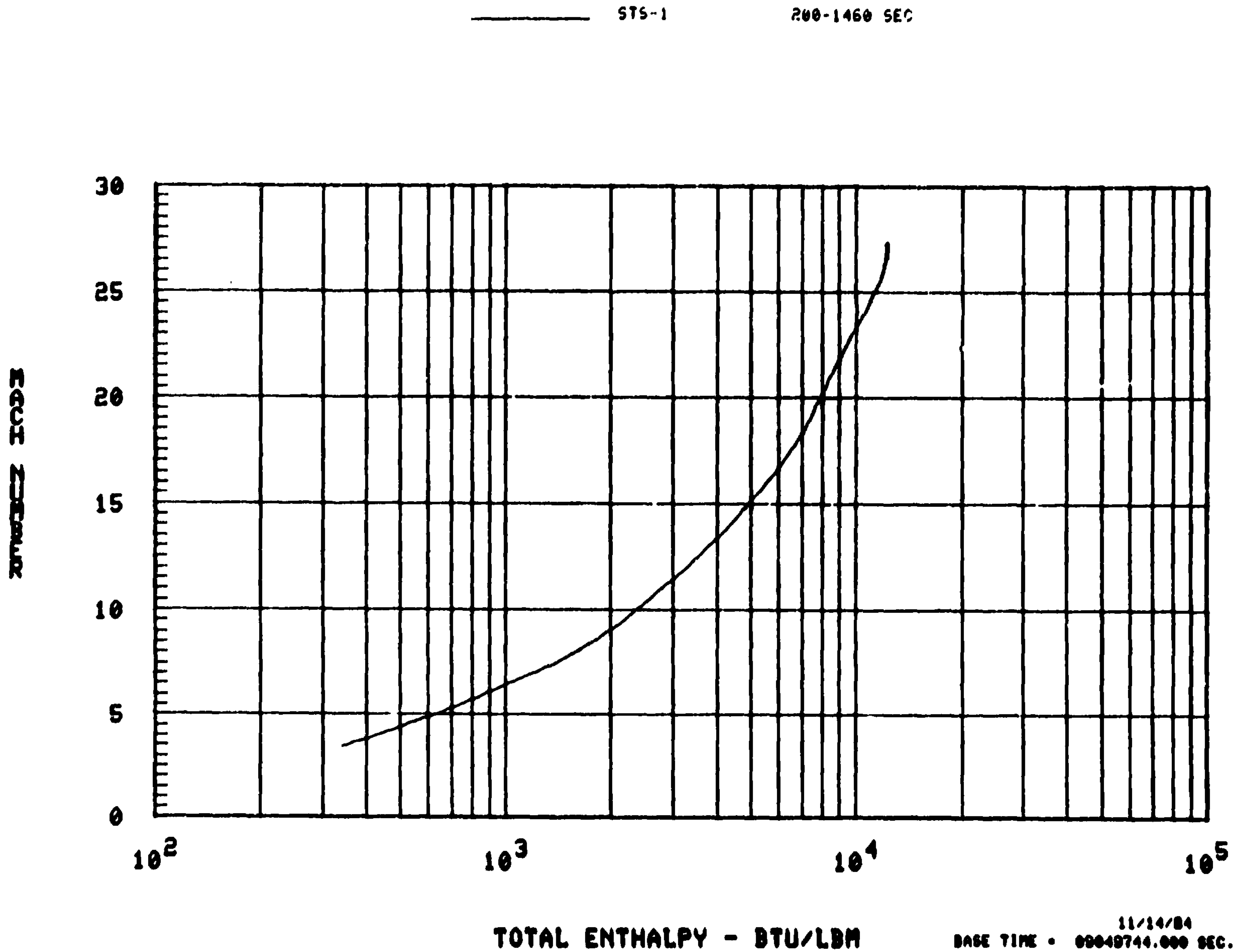

11/14/84
BASE TIME = 00040744.000 SEC.

STS-2 (107 FT LENGTH) FLIGHT PARAMETER COMPARISON

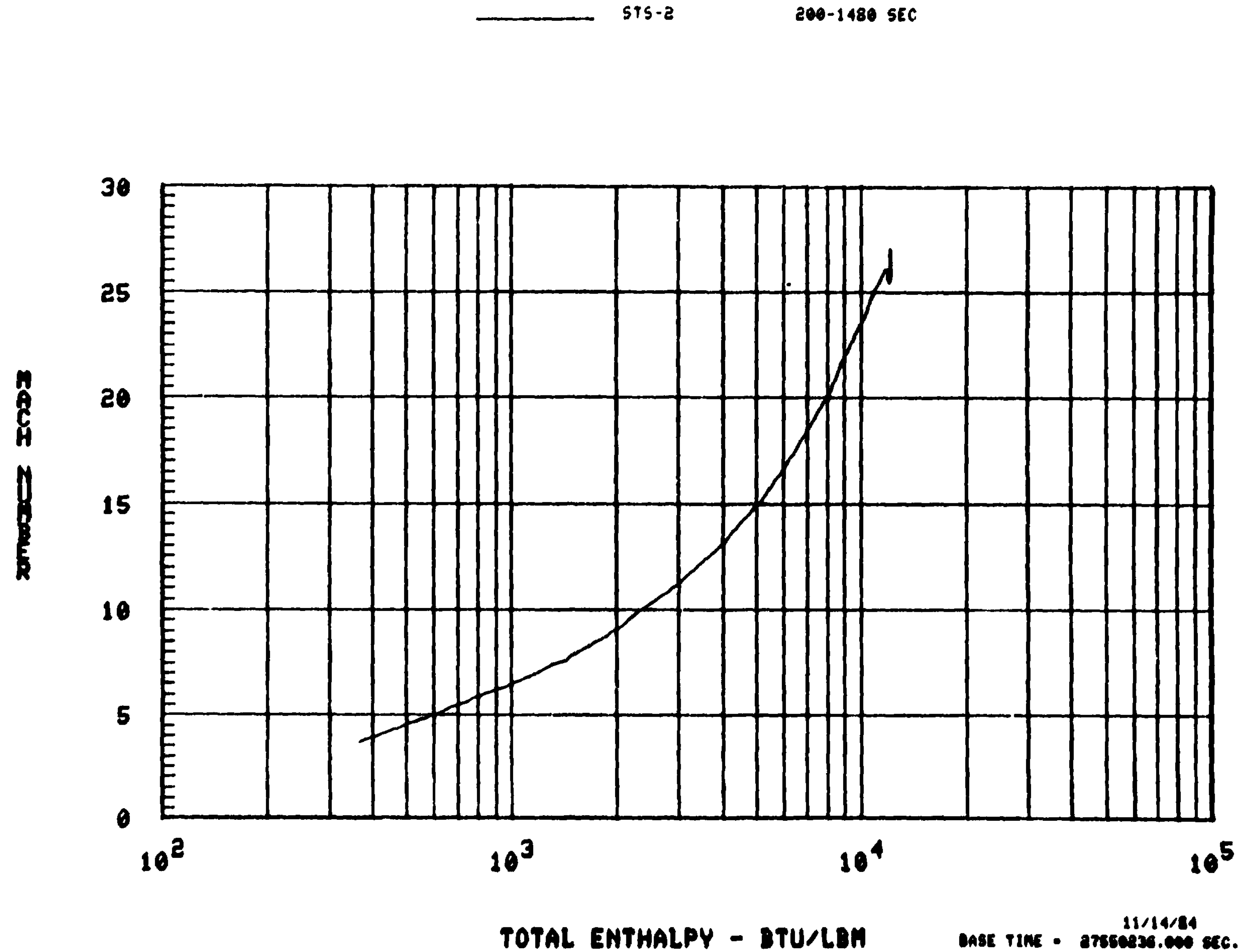

STS-3 (107 FT LENGTH) FLIGHT PARAMETER COMPARISON

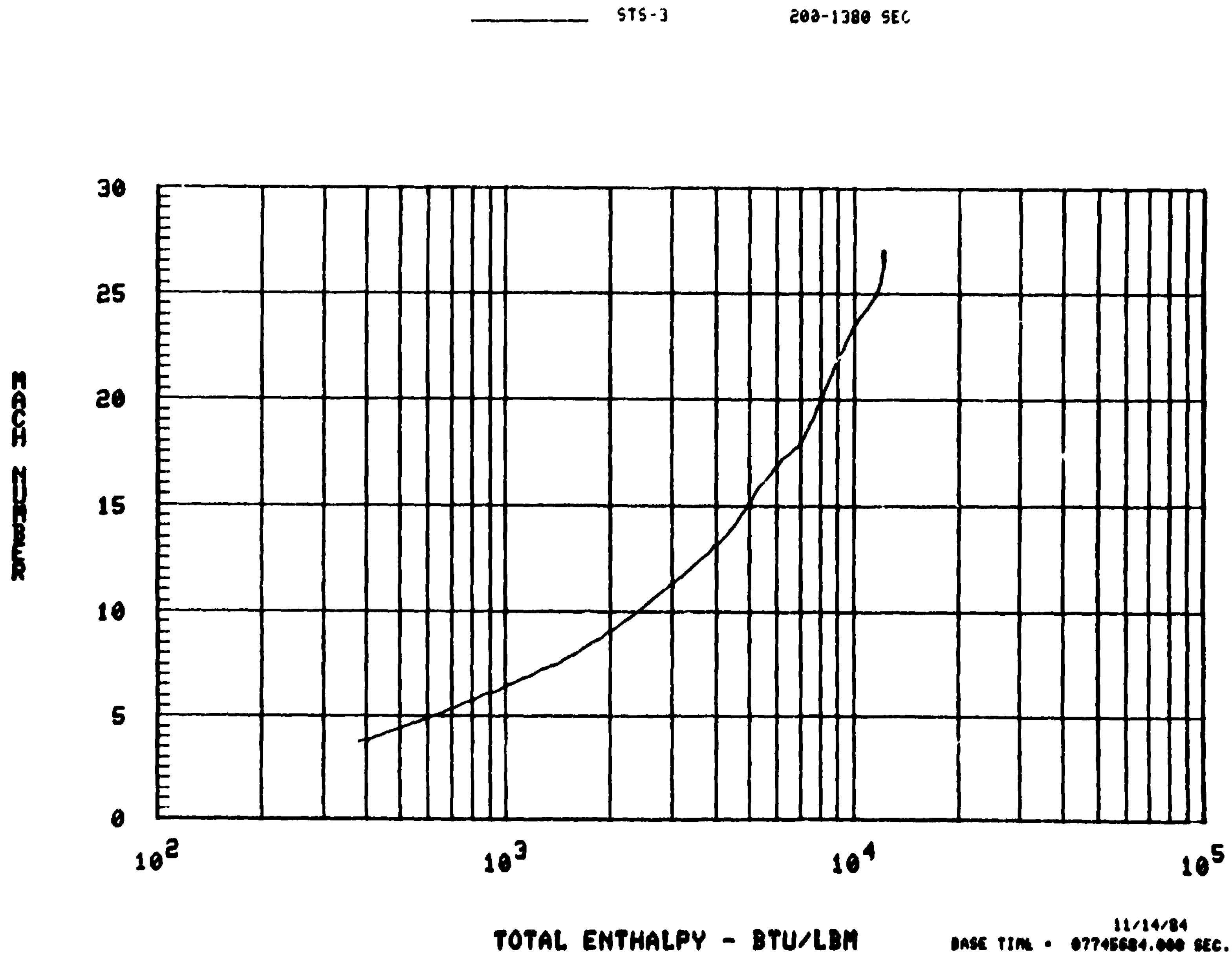

STS-4 (107 FT LENGTH) FLIGHT PARAMETER COMPARISON

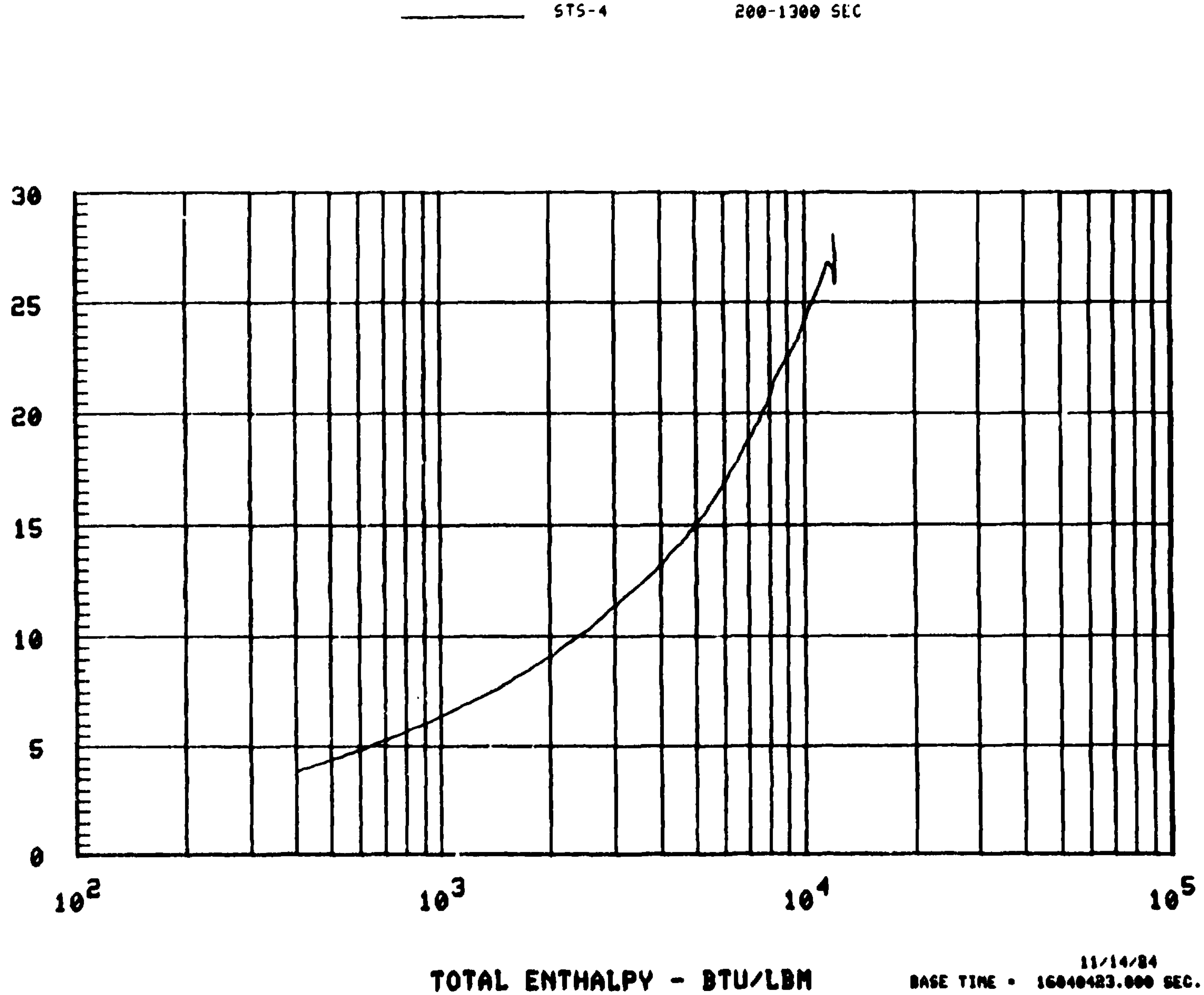

STS-5 (107 FT LENGTH) FLIGHT PARAMETER COMPARISON

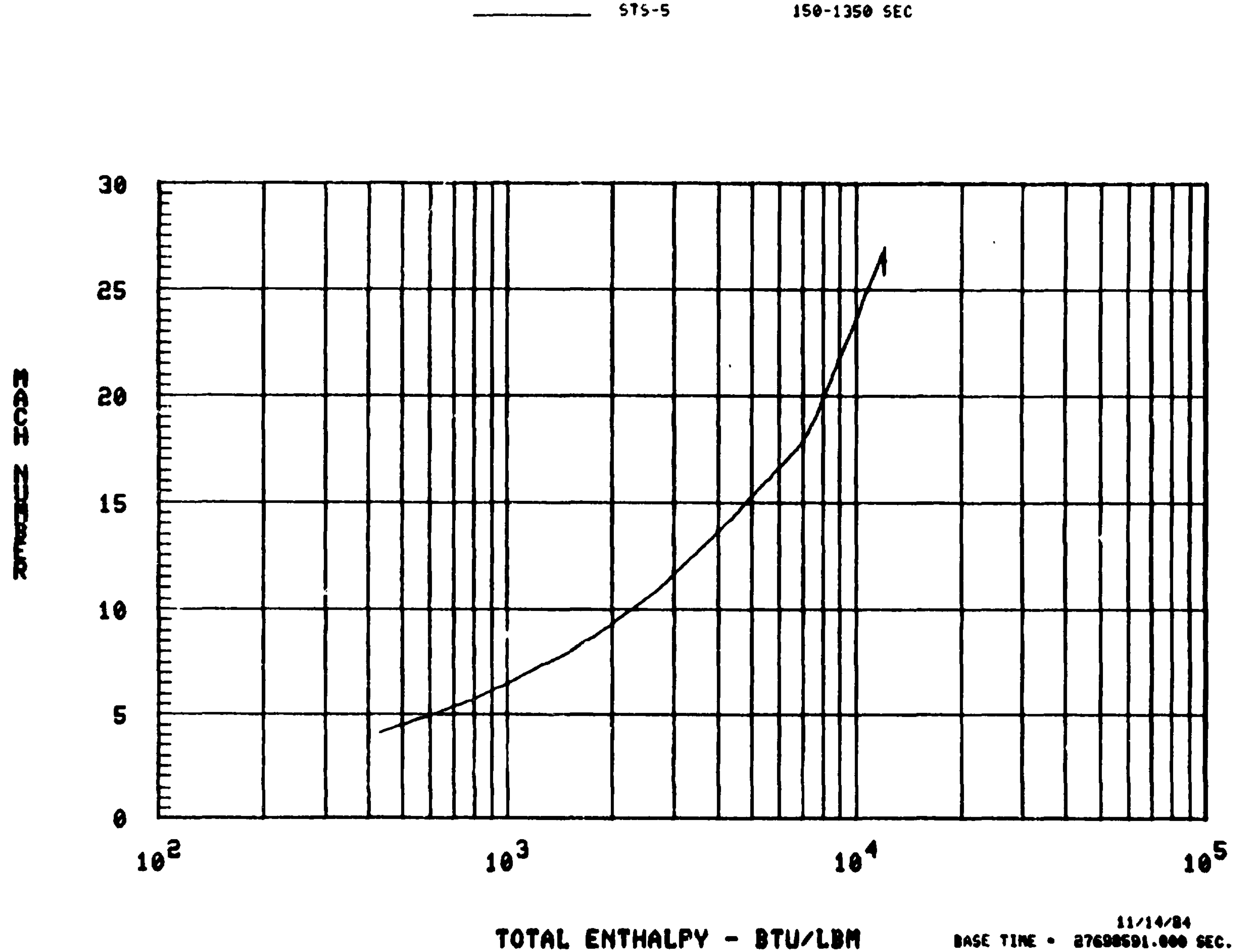

STS-1 (107 FT LENGTH) FLIGHT PARAMETER COMPARISON

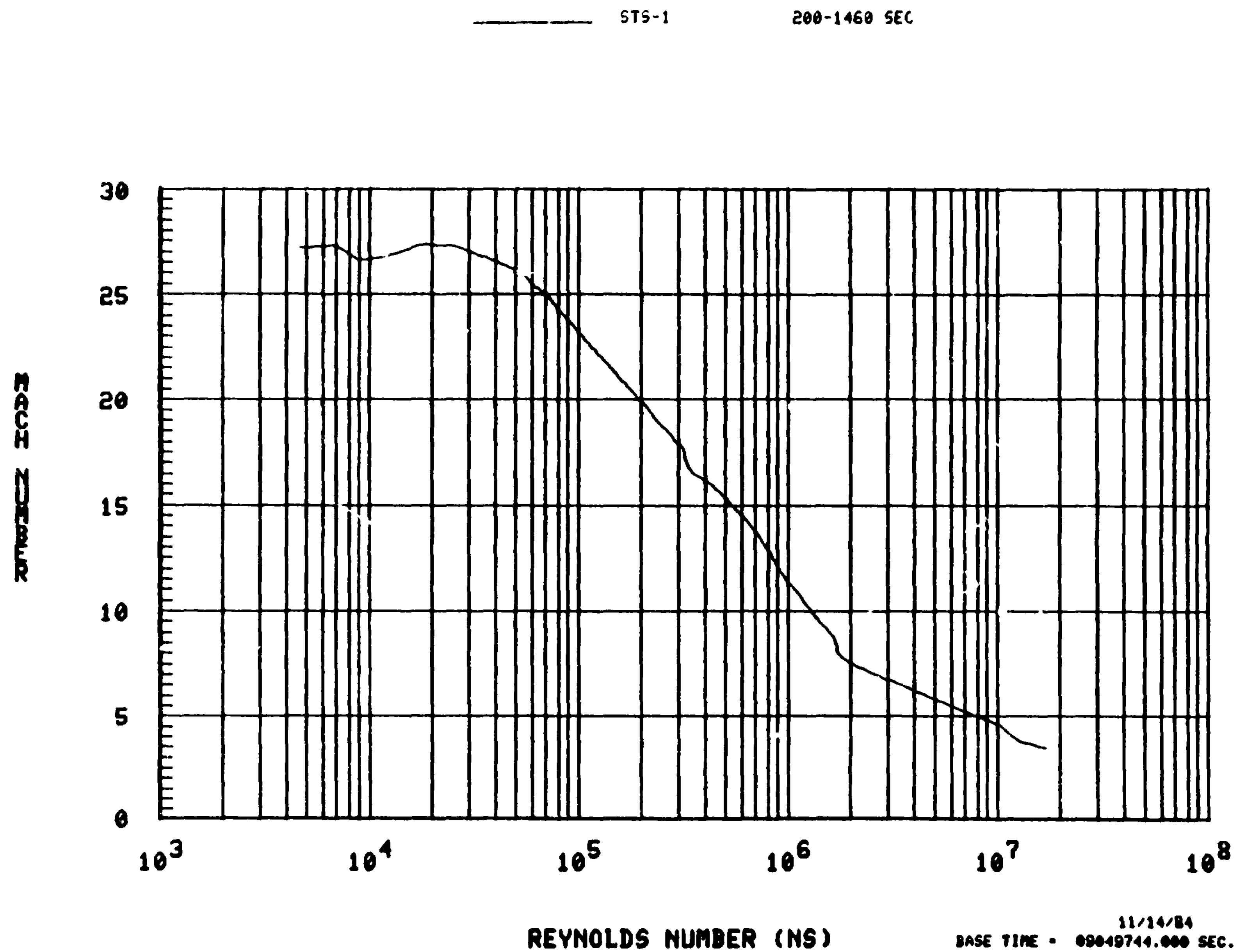

STS-2 (107 FT LENGTH) FLIGHT PARAMETER COMPARISON

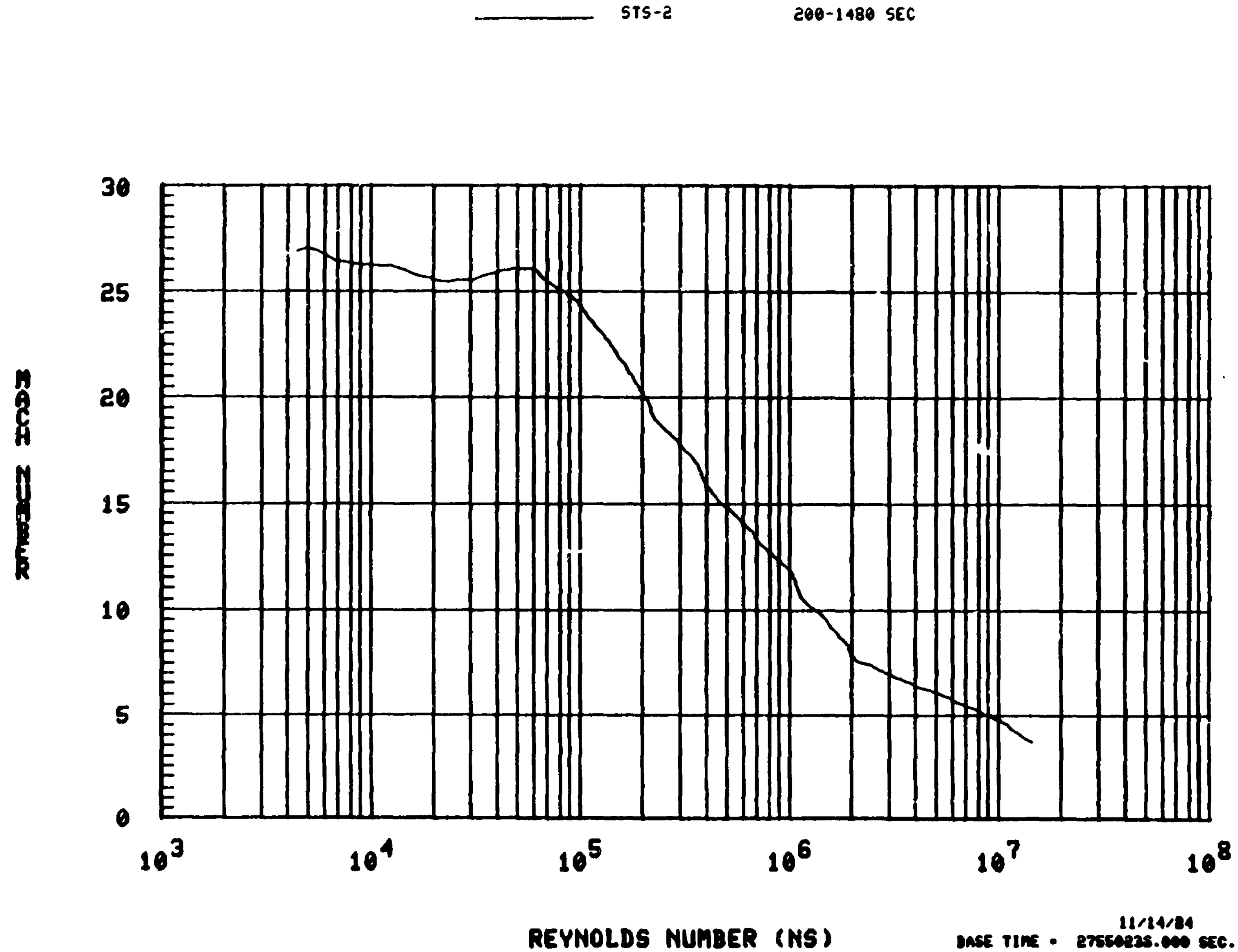

STS-3 (107 FT LENGTH) FLIGHT PARAMETER COMPARISON

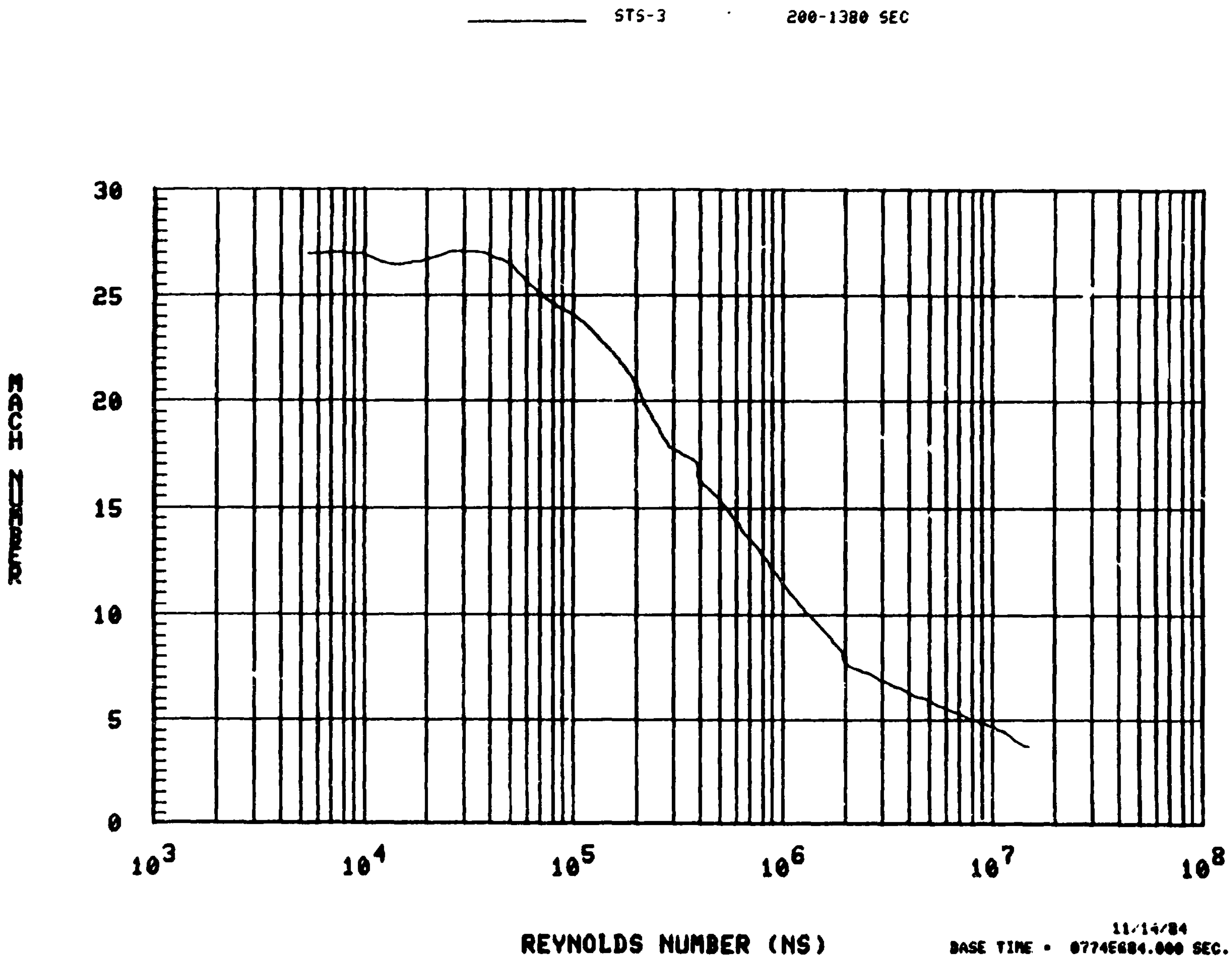

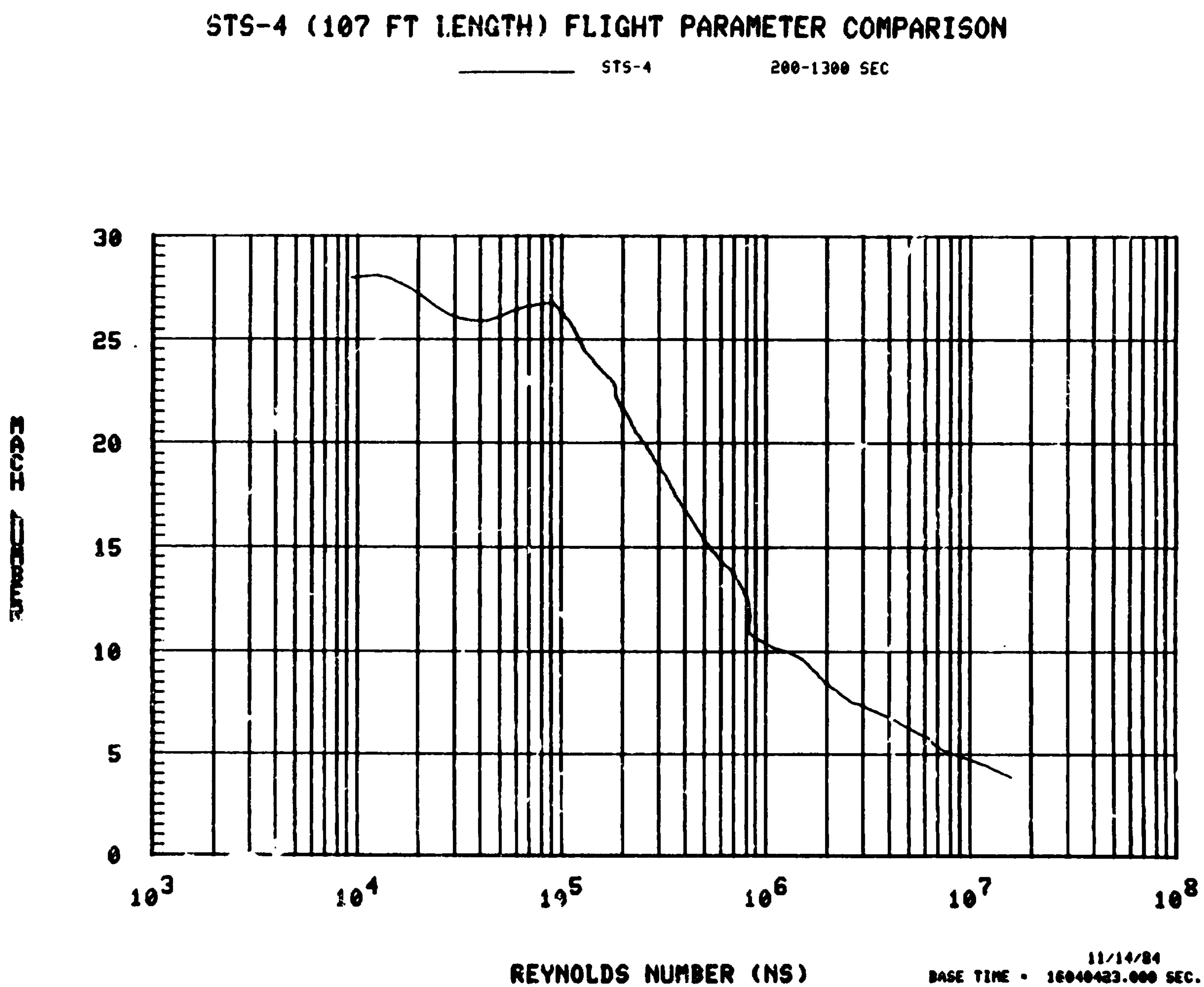

STS-4 (107 FT LENGTH) FLIGHT PARAMETER COMPARISON
STS-4 200-1300 SEC
MACH NUMBER
30
25
20
15
10
5
0
10^3
10^4
10^5
10^6
10^7
10^8
REYNOLDS NUMBER (NS)
11/14/84
BASE TIME = 16040423.000 SEC.

STS-5 (107 FT LENGTH) FLIGHT PARAMETER COMPARISON

STS-5 150-1350 SEC

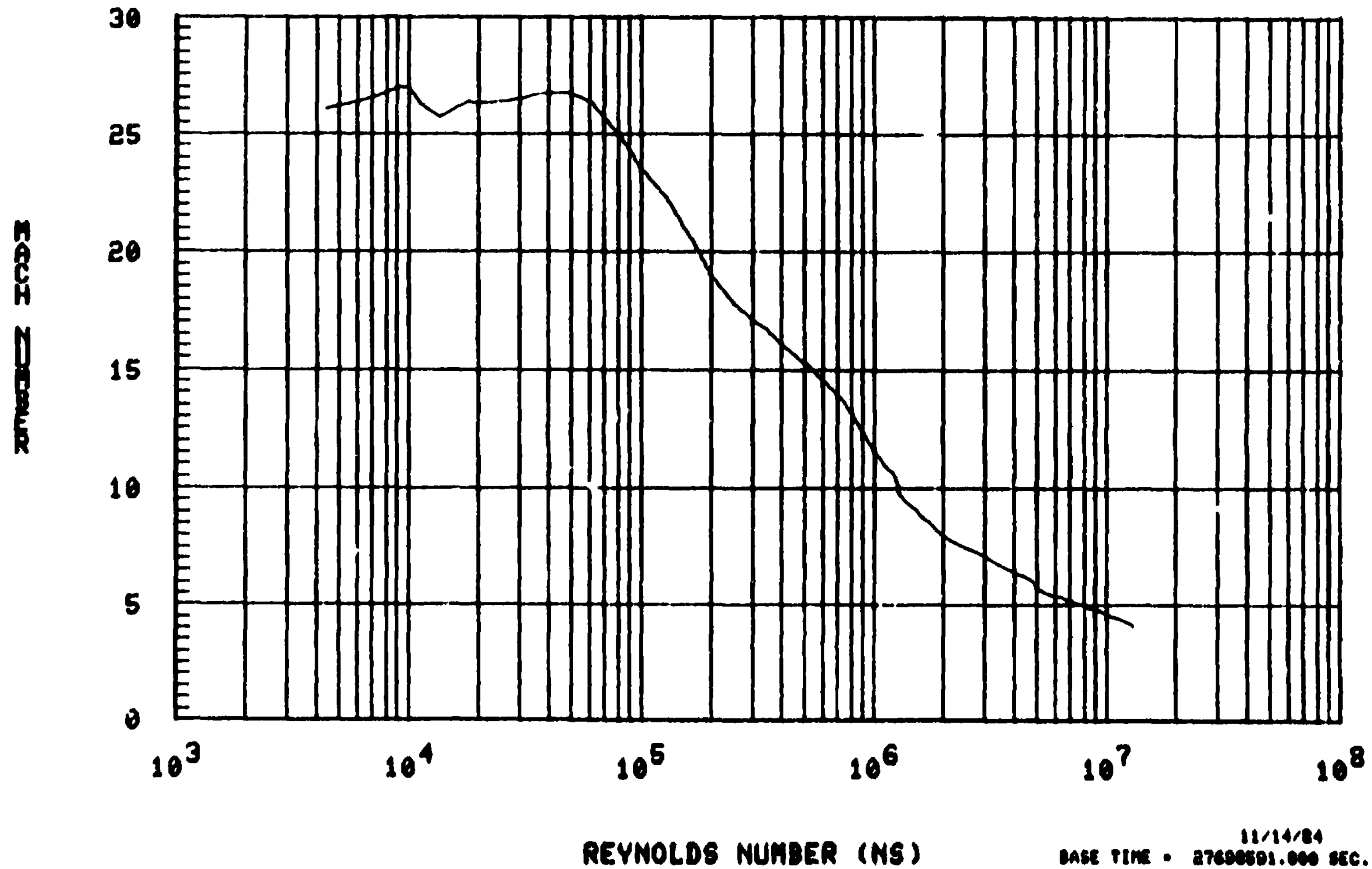

STS-1 (107 FT LENGTH) FLIGHT PARAMETER COMPARISON

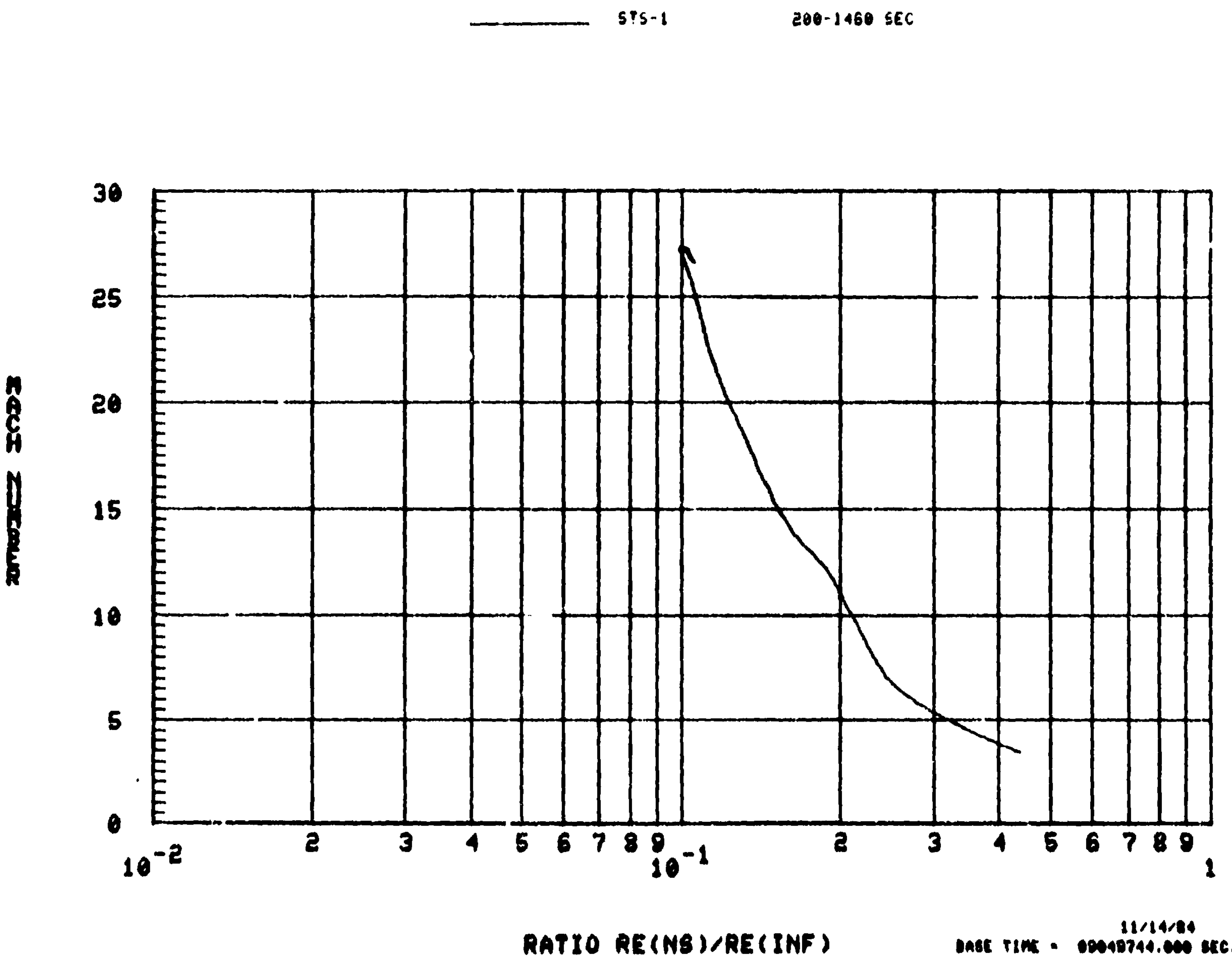

STS-2 (107 FT LENGTH) FLIGHT PARAMETER COMPARISON

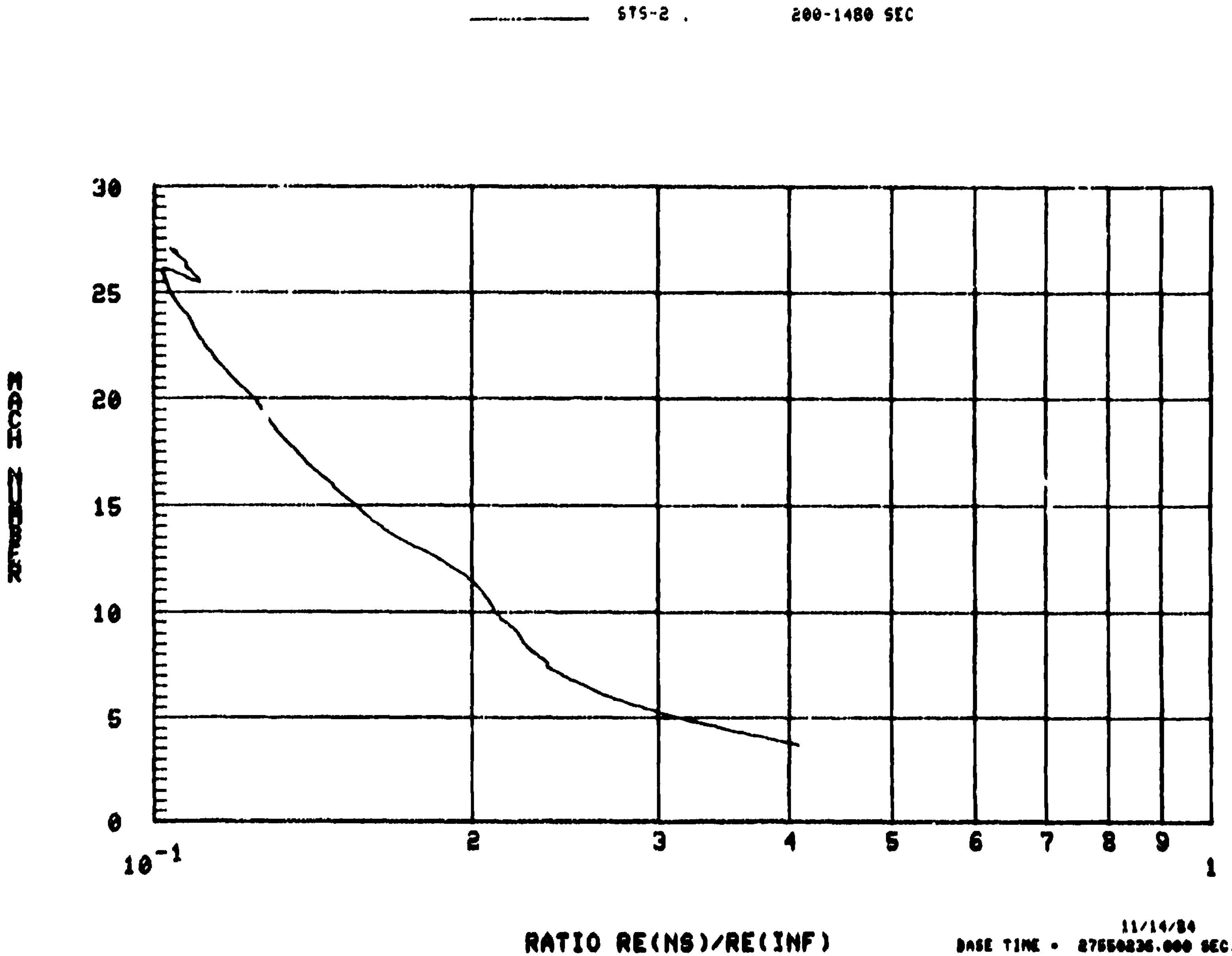

STS-3 (107 FT LENGTH) FLIGHT PARAMETER COMPARISON

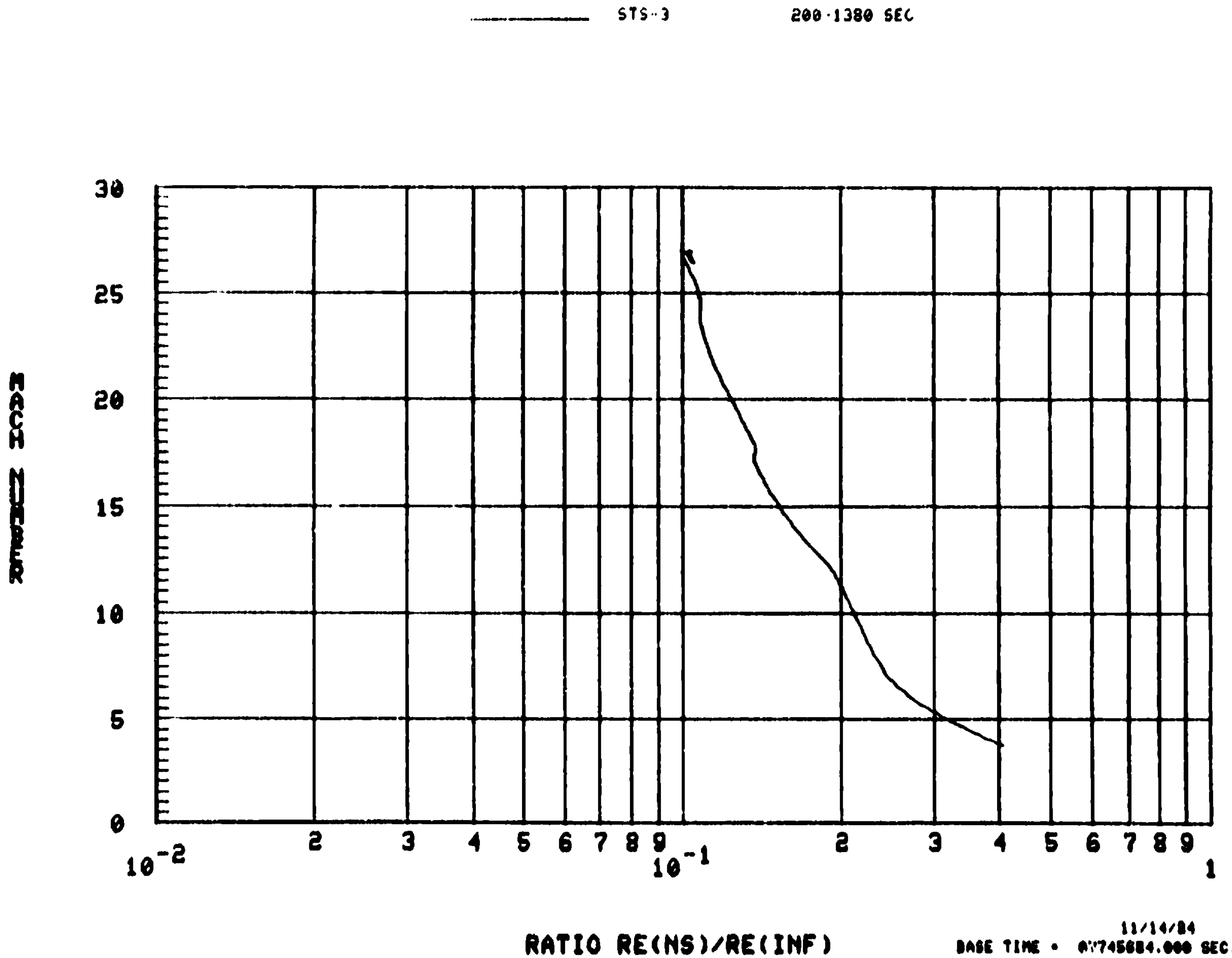

STS-4 (107 FT LENGTH) FLIGHT PARAMETER COMPARISON

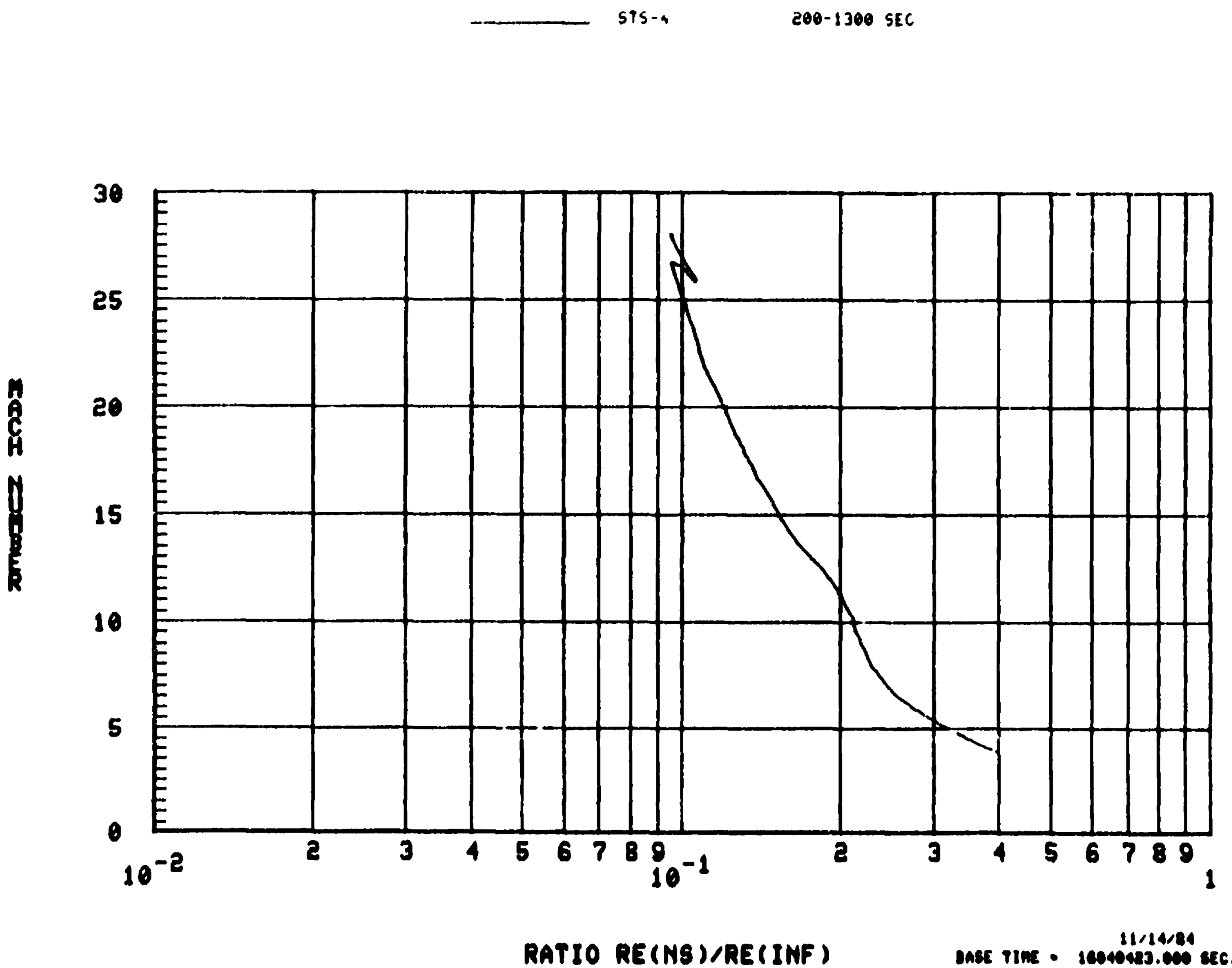

STS-5 (107 FT LENGTH) FLIGHT PARAMETER COMPARISON

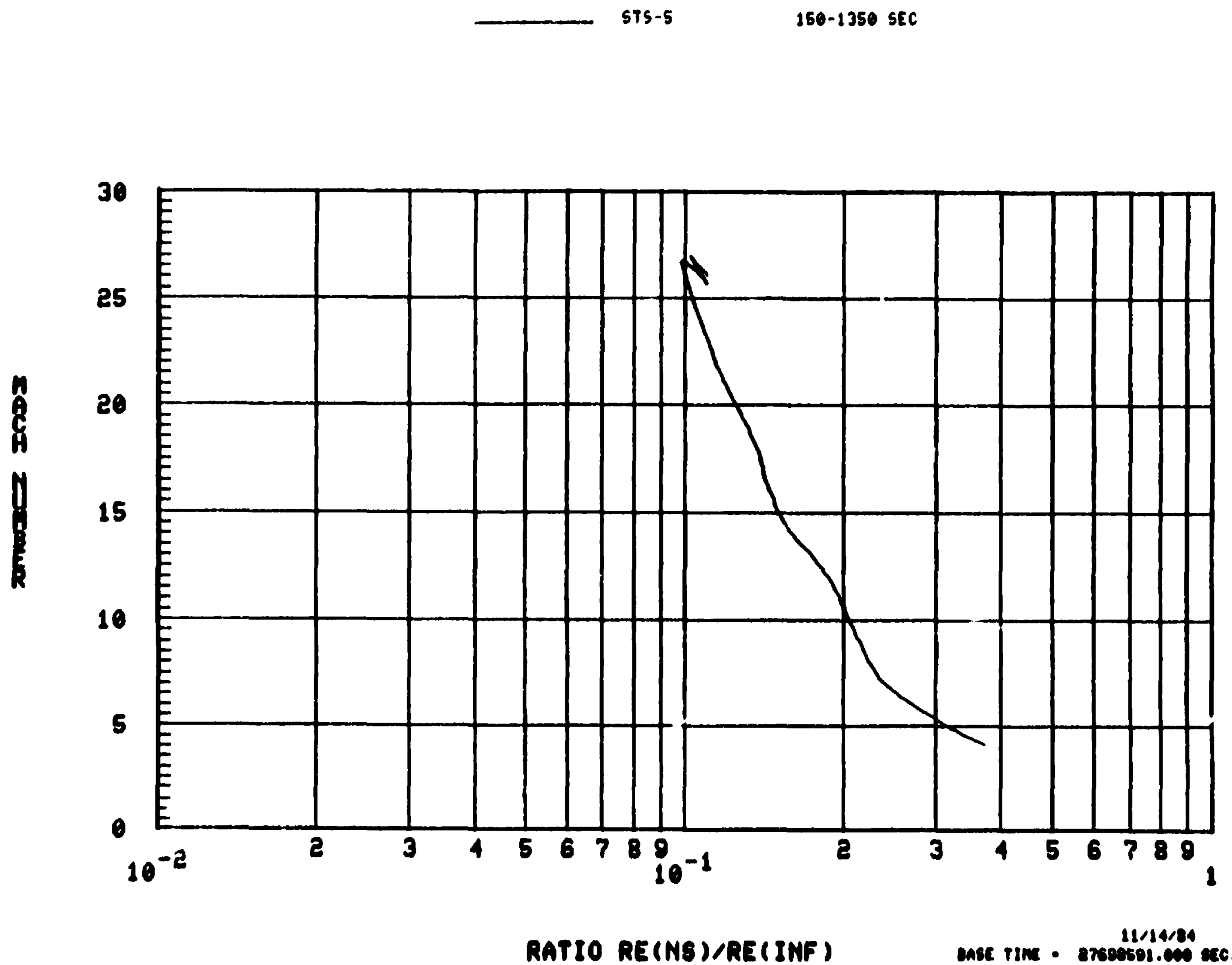

STS-1 (107 FT LENGTH) FLIGHT PARAMETER COMPARISON

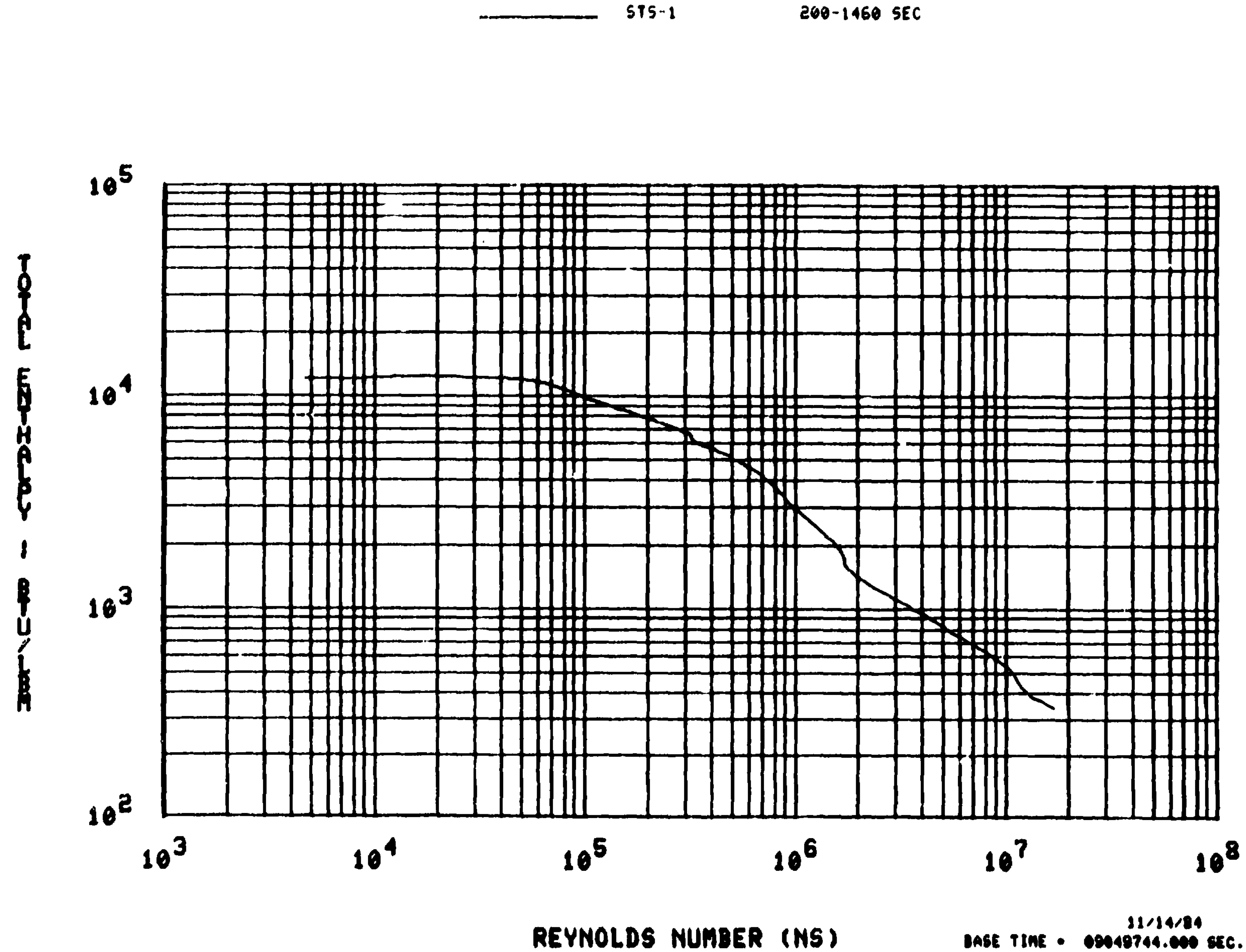

STS-2 (107 FT LENGTH) FLIGHT PARAMETER COMPARISON

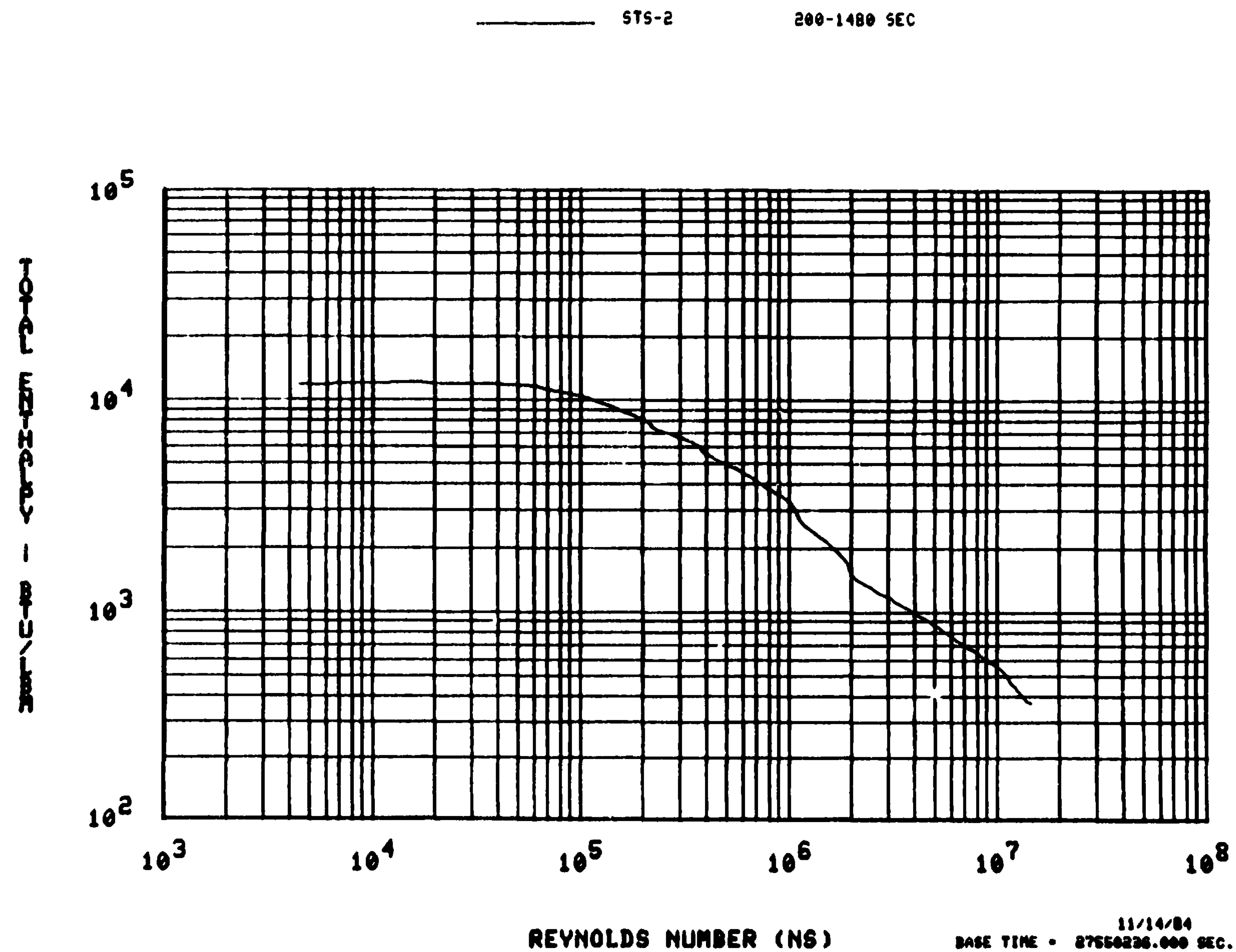

STS-3 (107 FT LENGTH) FLIGHT PARAMETER COMPARISON

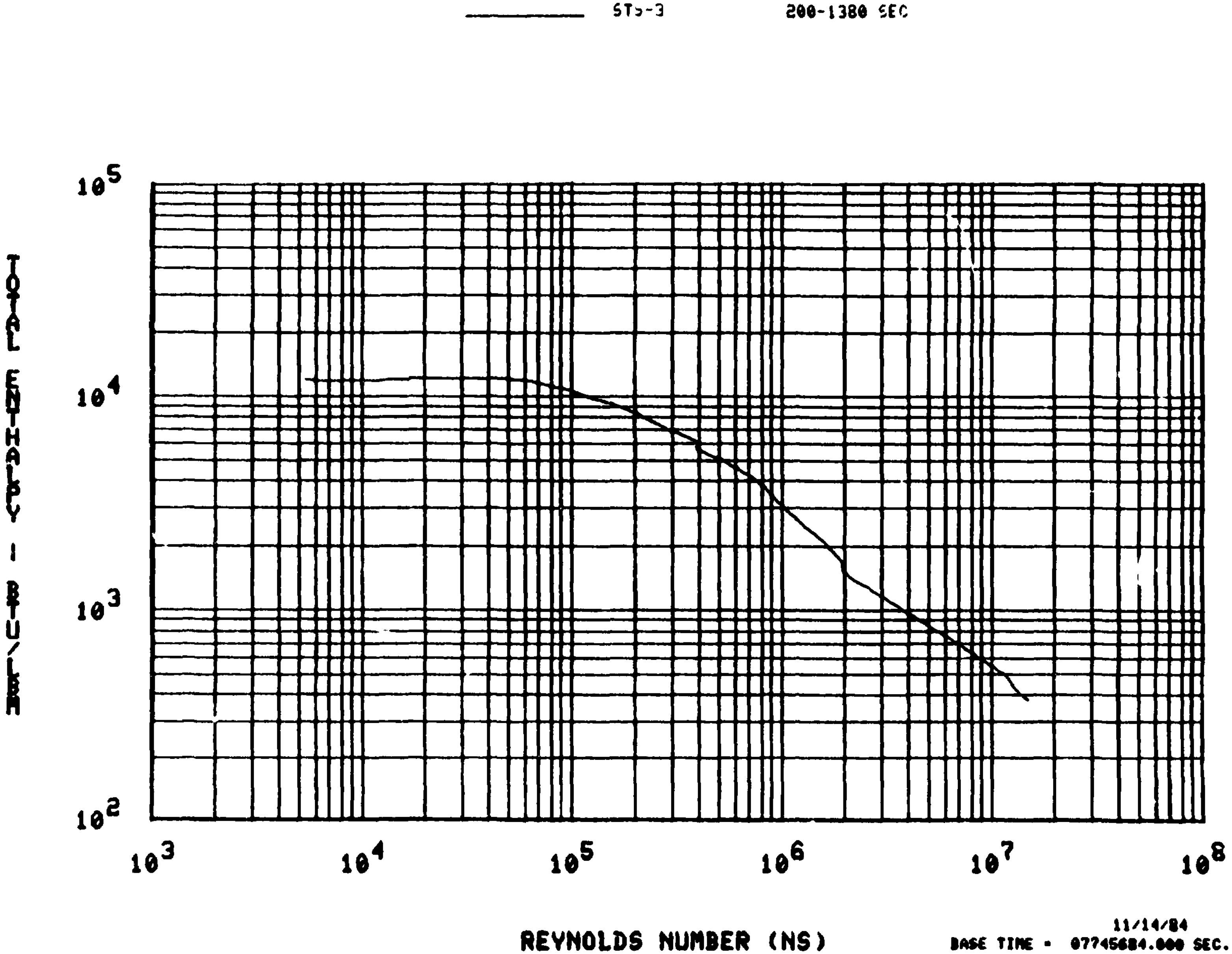

STS-4 (107 FT LENGTH) FLIGHT PARAMETER COMPARISON

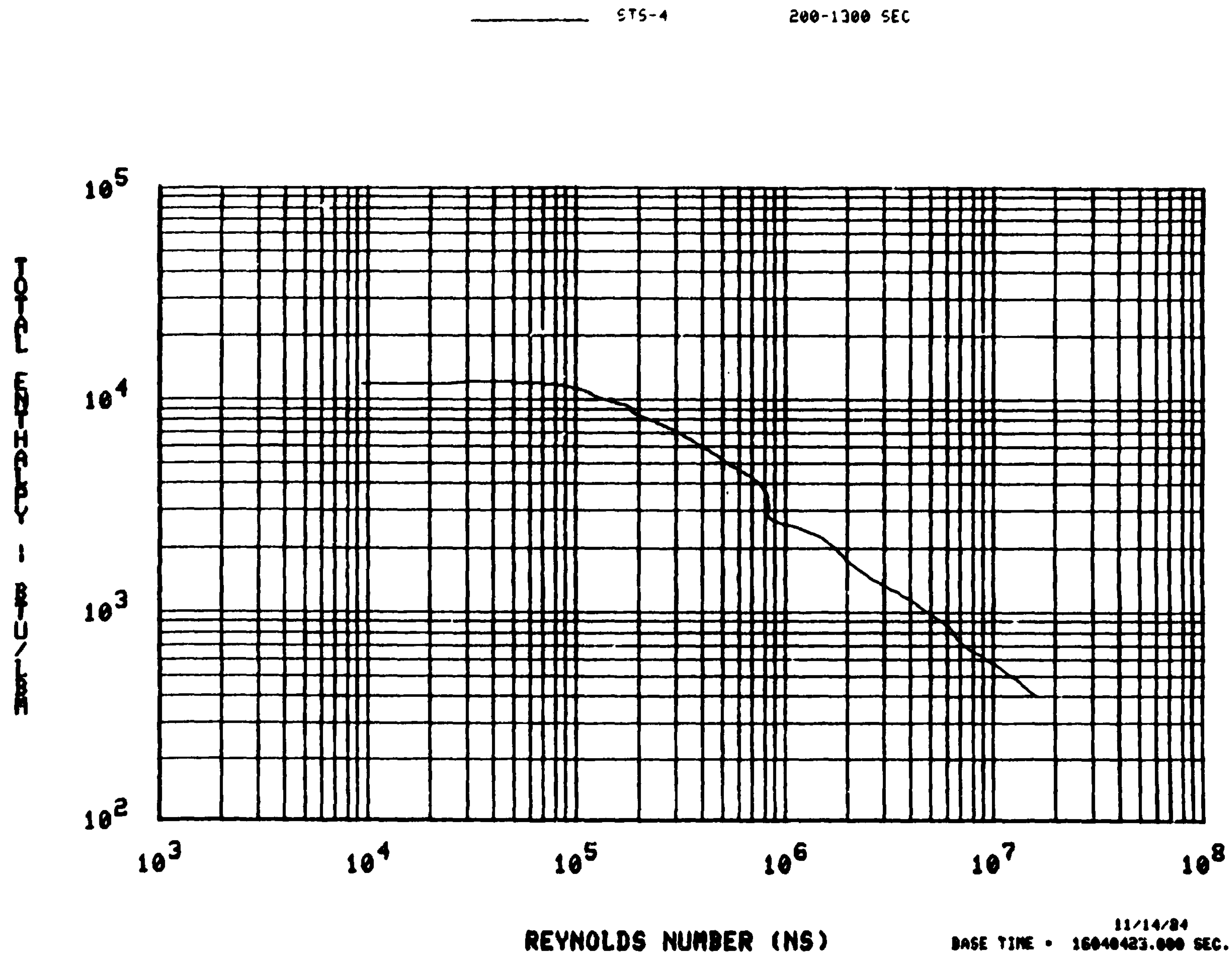

STS-5 (107 FT LENGTH) FLIGHT PARAMETER COMPARISON

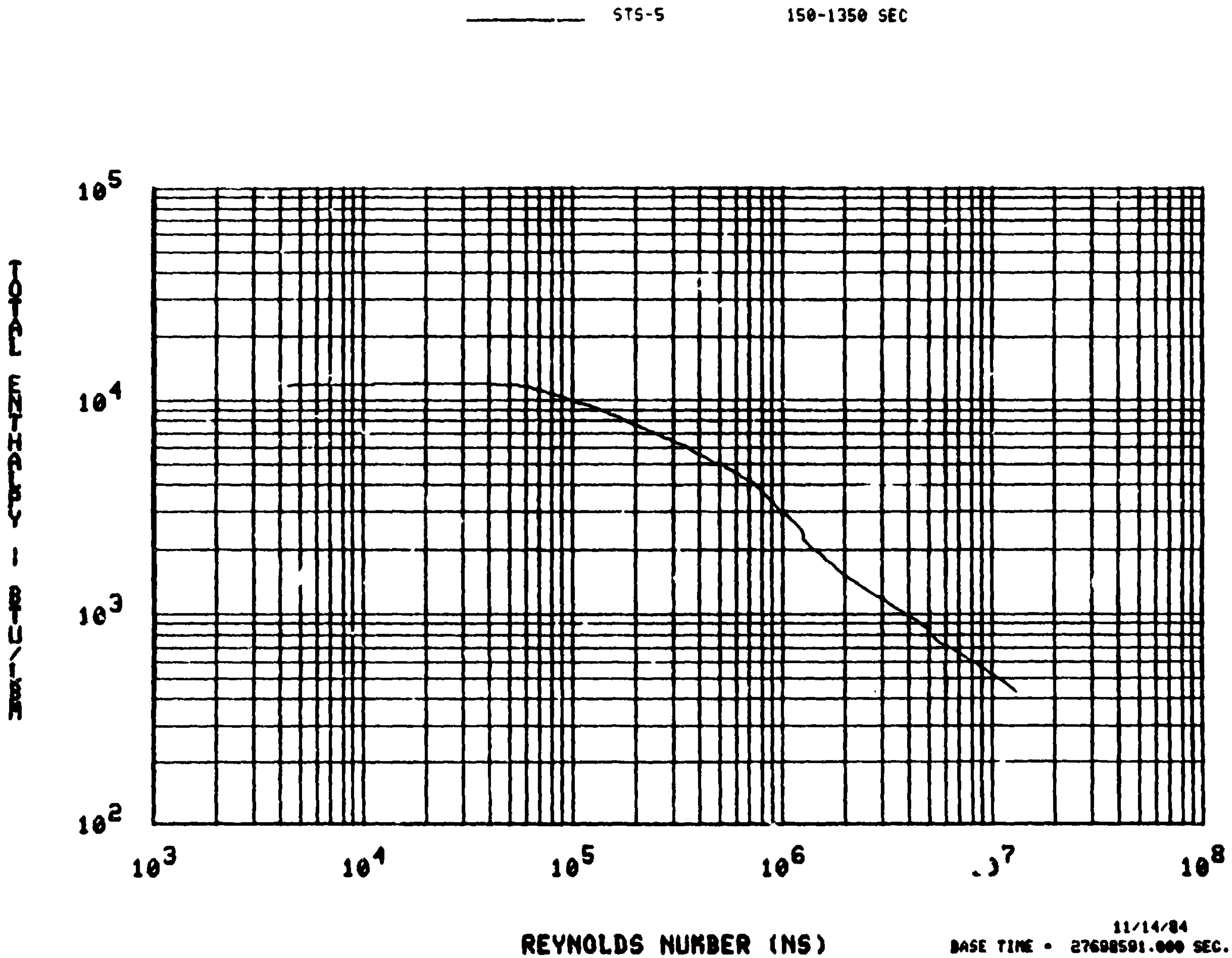

STS-1 (107 FT LENGTH) FLIGHT PARAMETER COMPARISON

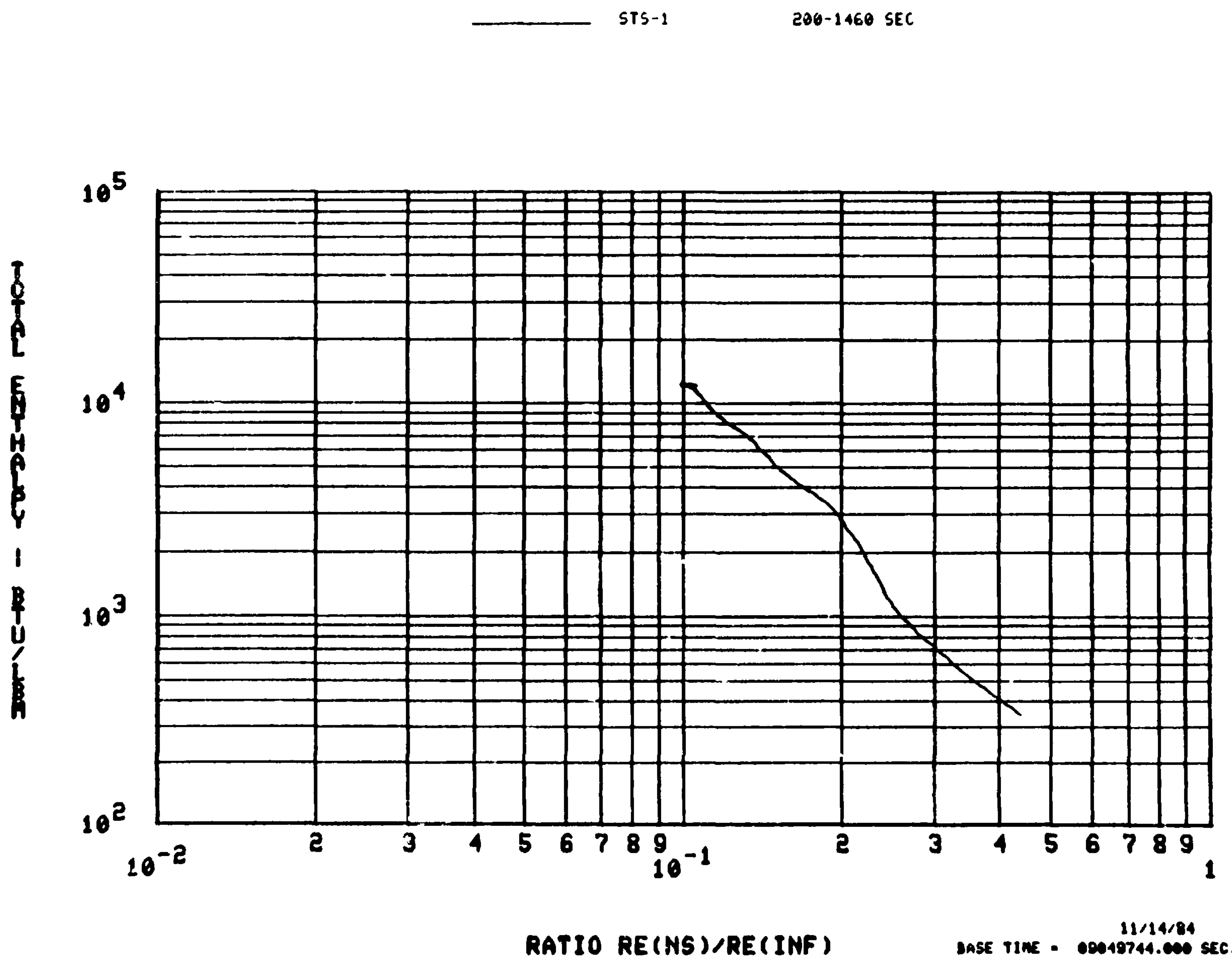

11/14/84
BASE TIME = 00049744.000 SEC.

STS-2 (107 FT LENGTH) FLIGHT PARAMETER COMPARISON

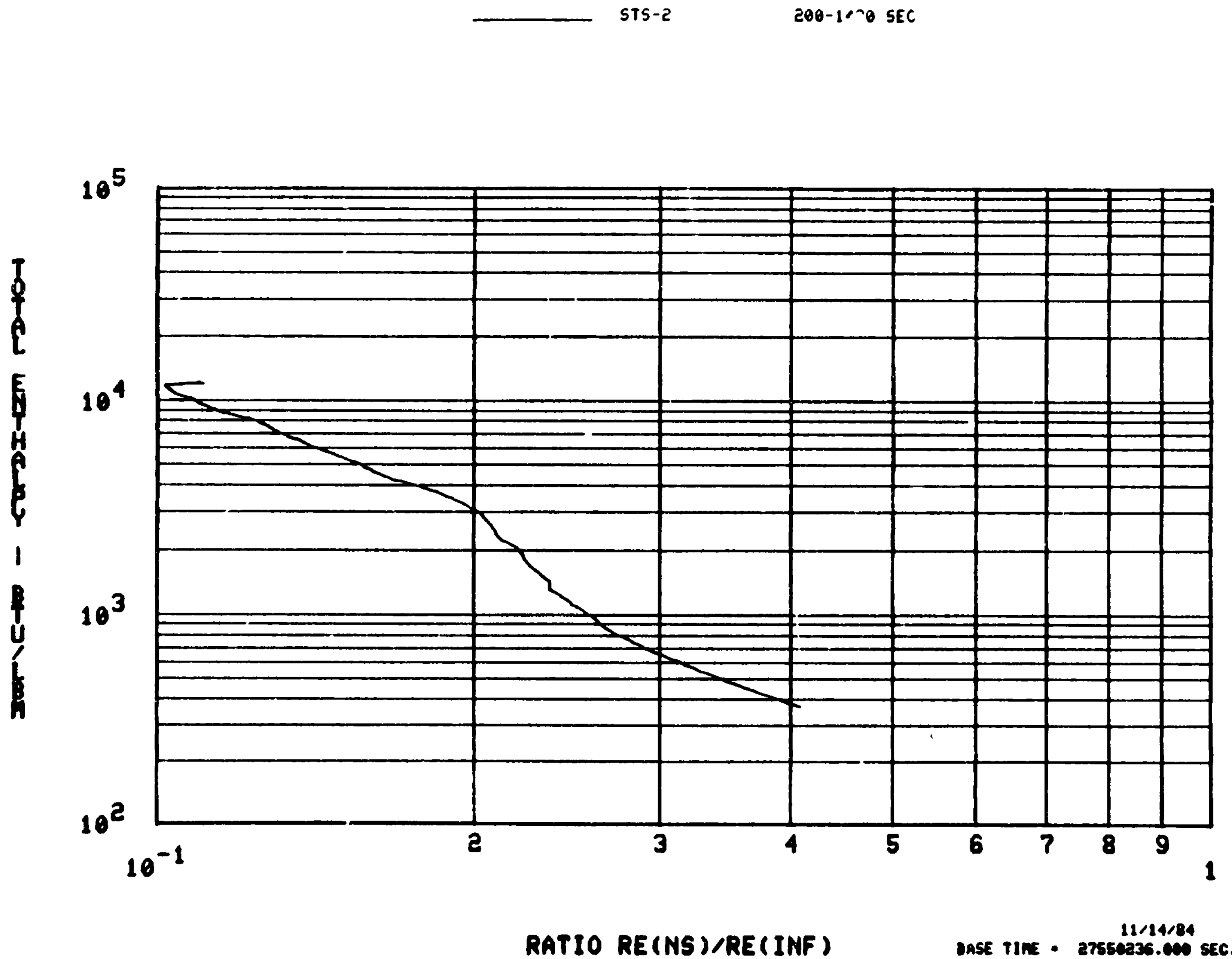

STS-3 (107 FT LENGTH) FLIGHT PARAMETER COMPARISON

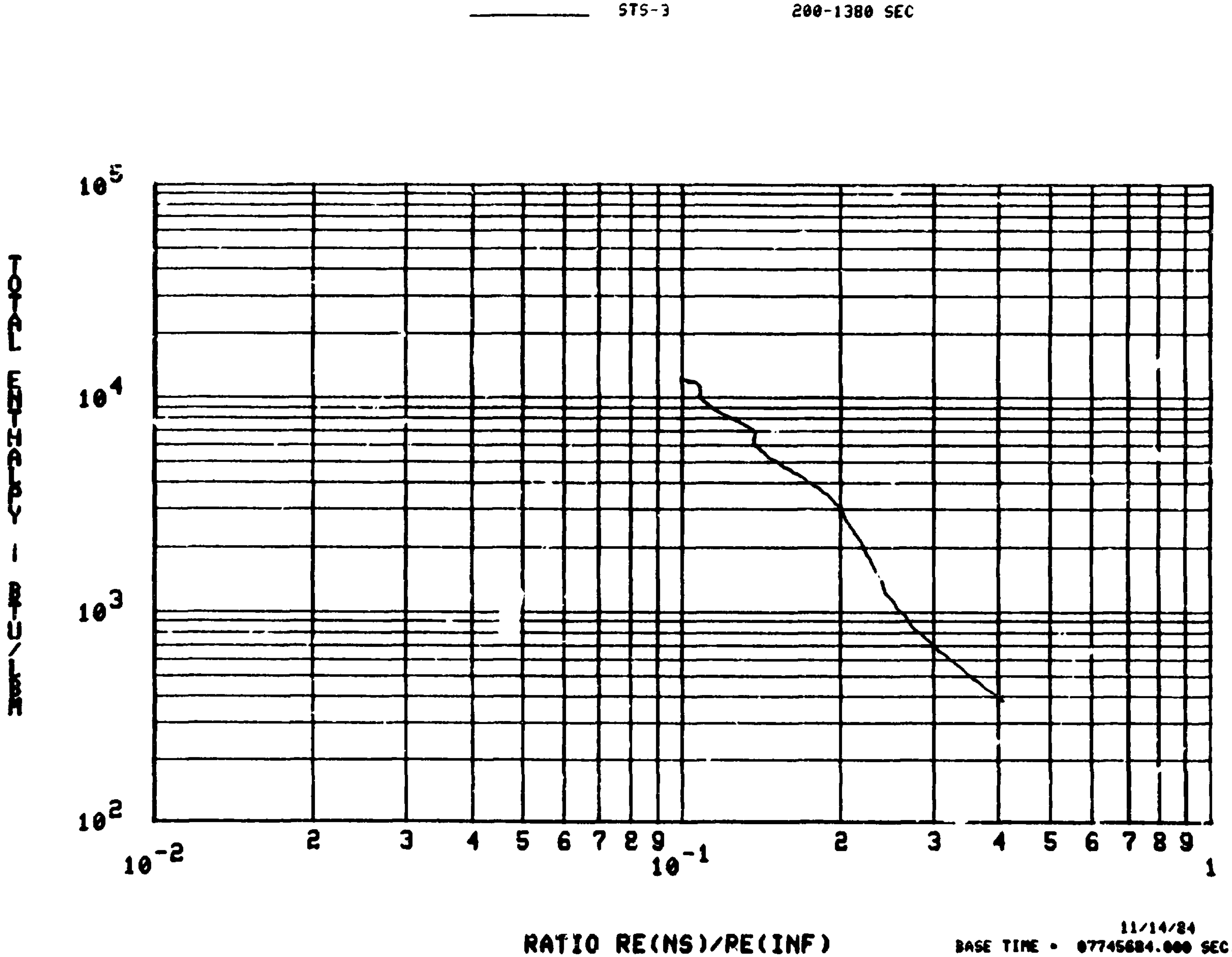

STS-4 (107 FT LENGTH) FLIGHT PARAMETER COMPARISON

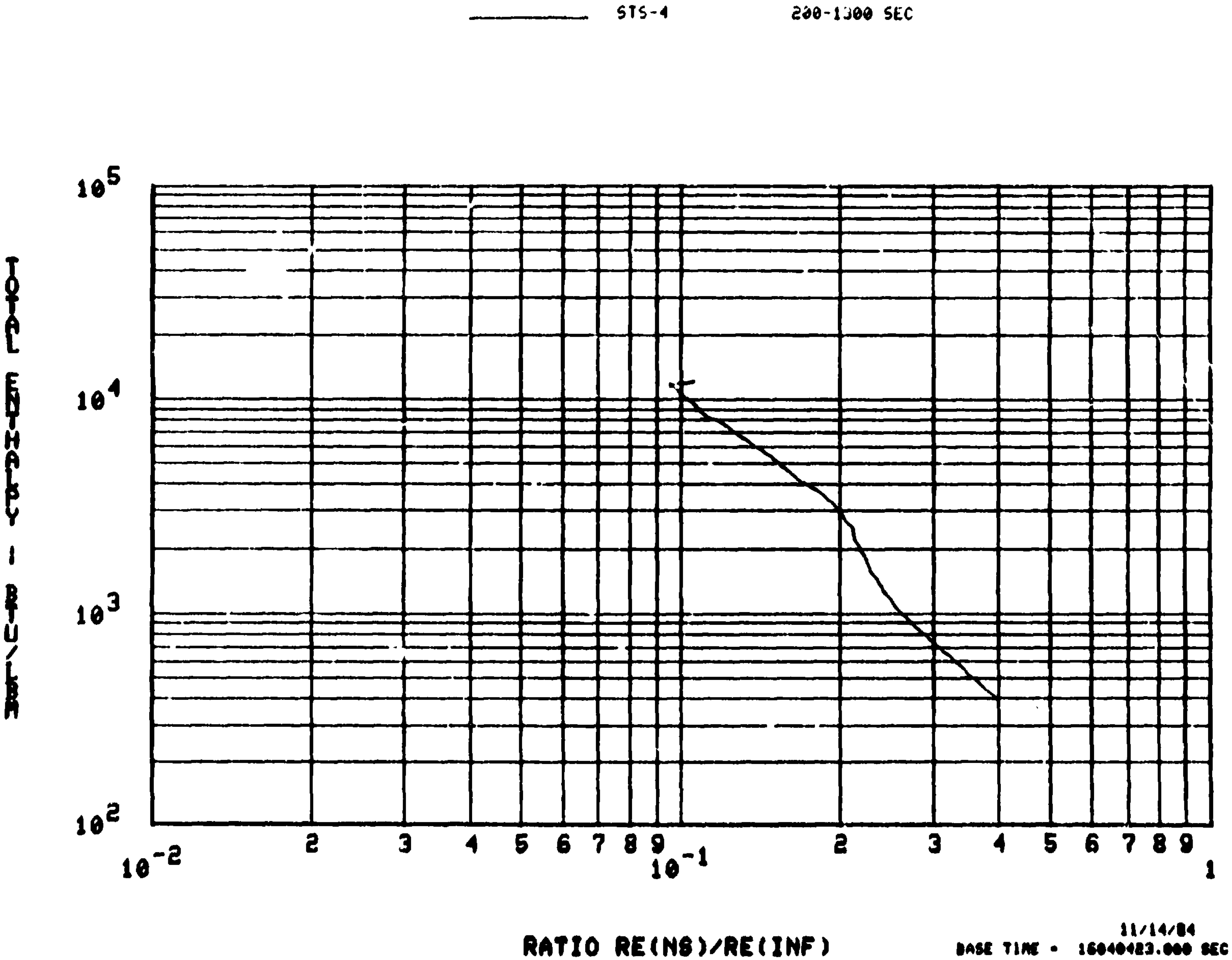

STS-5 (107 FT LENGTH) FLIGHT PARAMETER COMPARISON

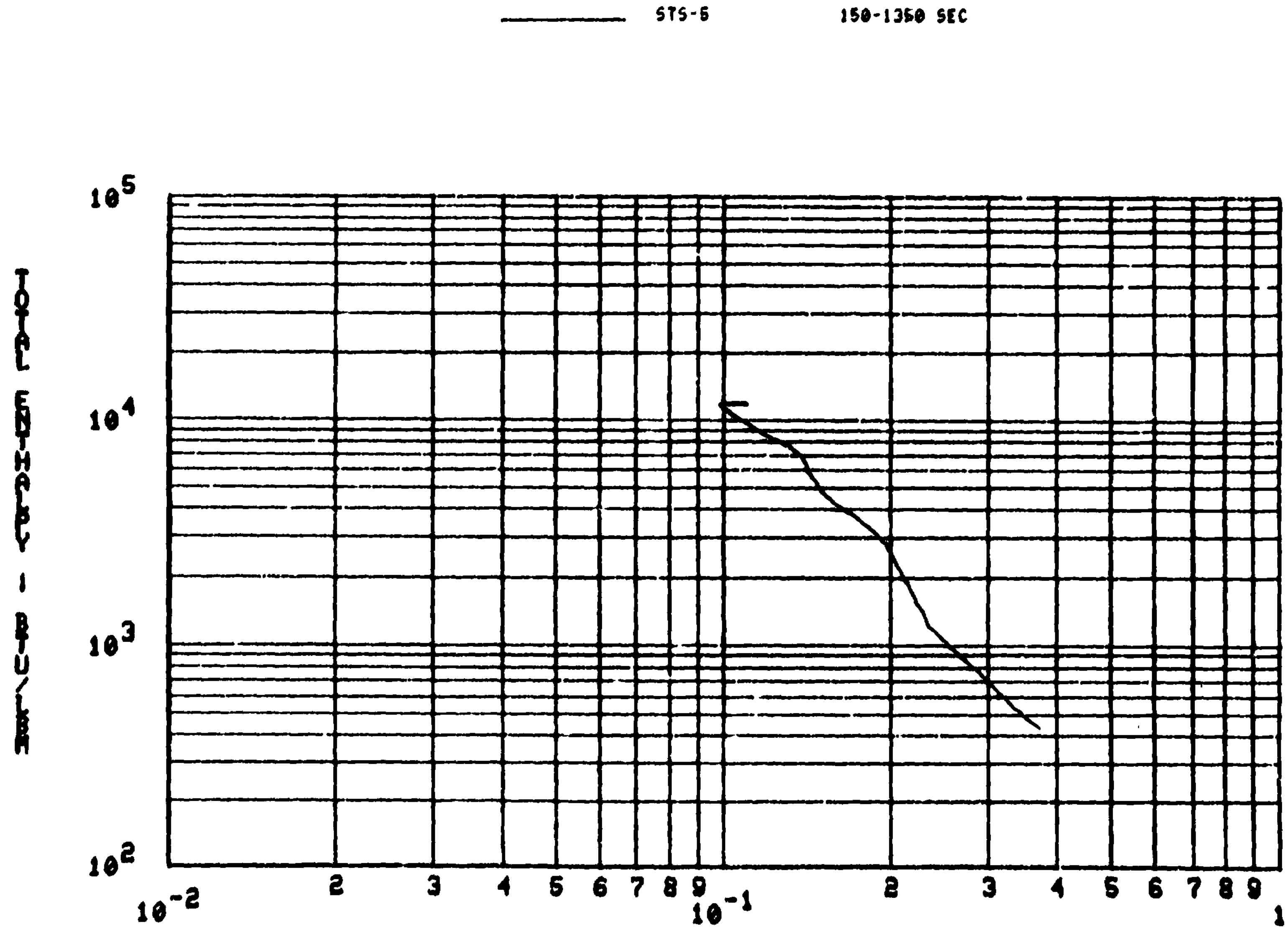

11/14/84
BASE TIME = 87508501.000 SEC.

STS-1 (107 FT LENGTH) FLIGHT PARAMETER COMPARISON

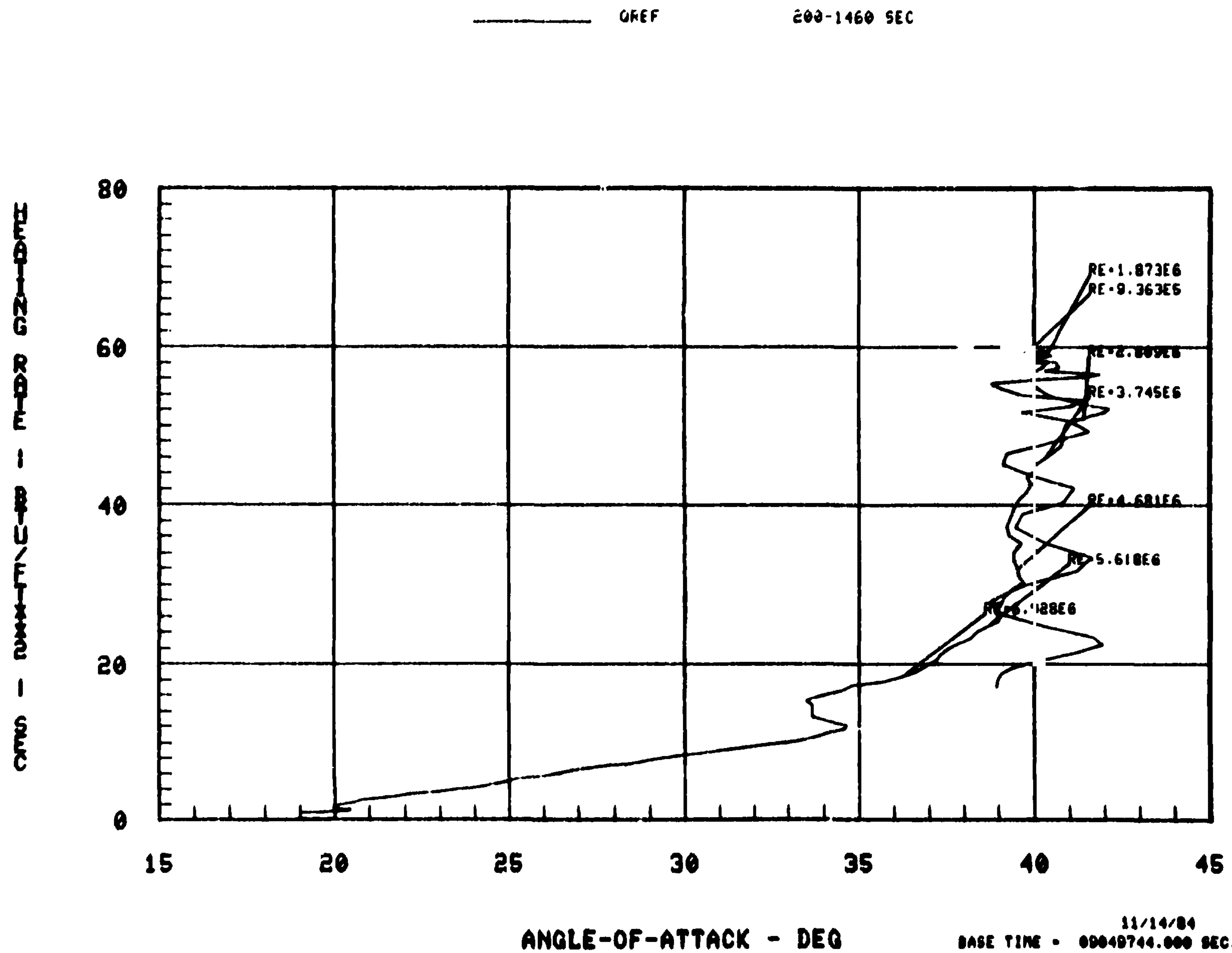

STS-2 (107 FT LENGTH) FLIGHT PARAMETER COMPARISON

QREF 200-1480 SEC

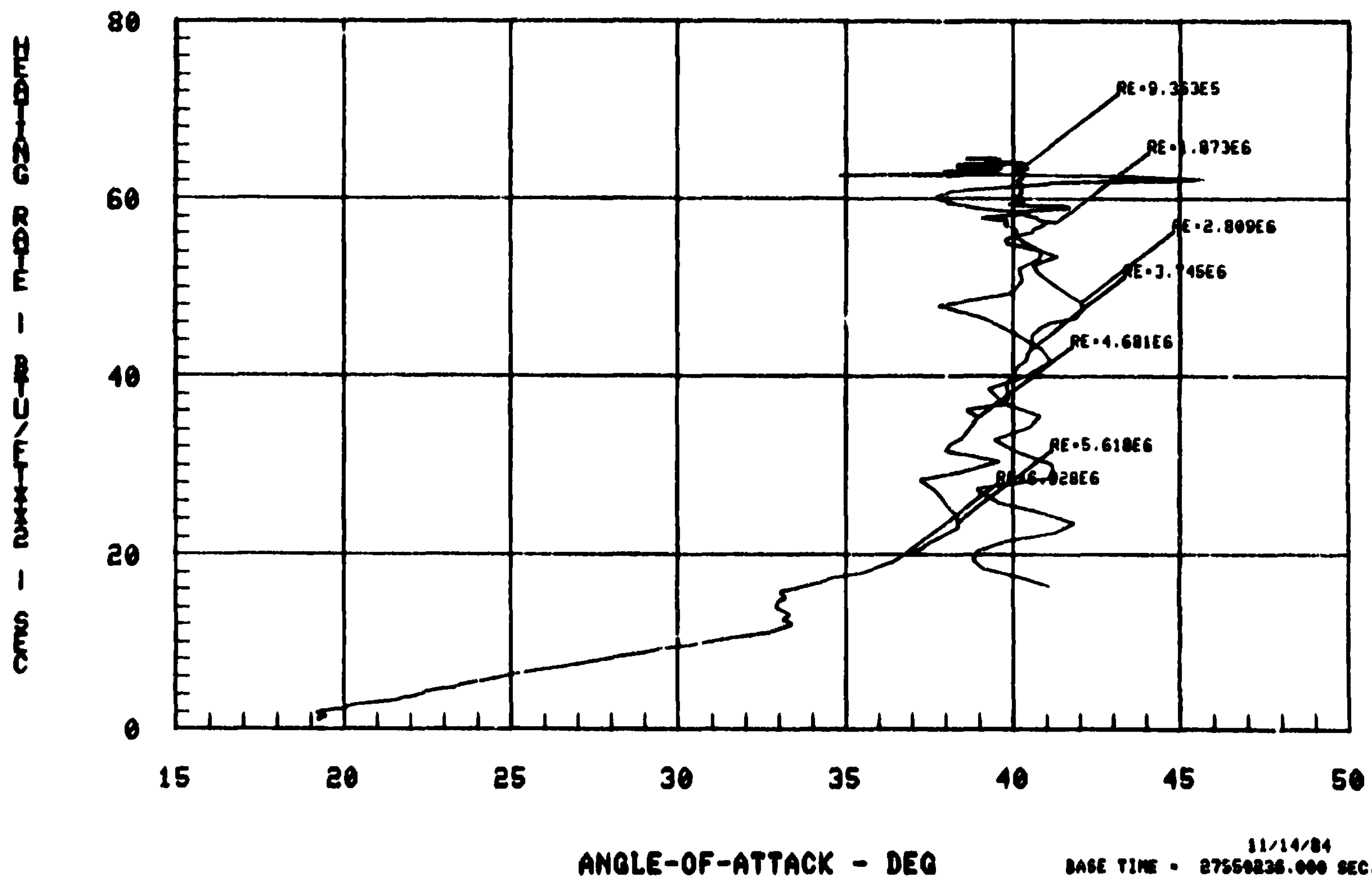

STS-3 (107 FT LENGTH) FLIGHT PARAMETER COMPARISON

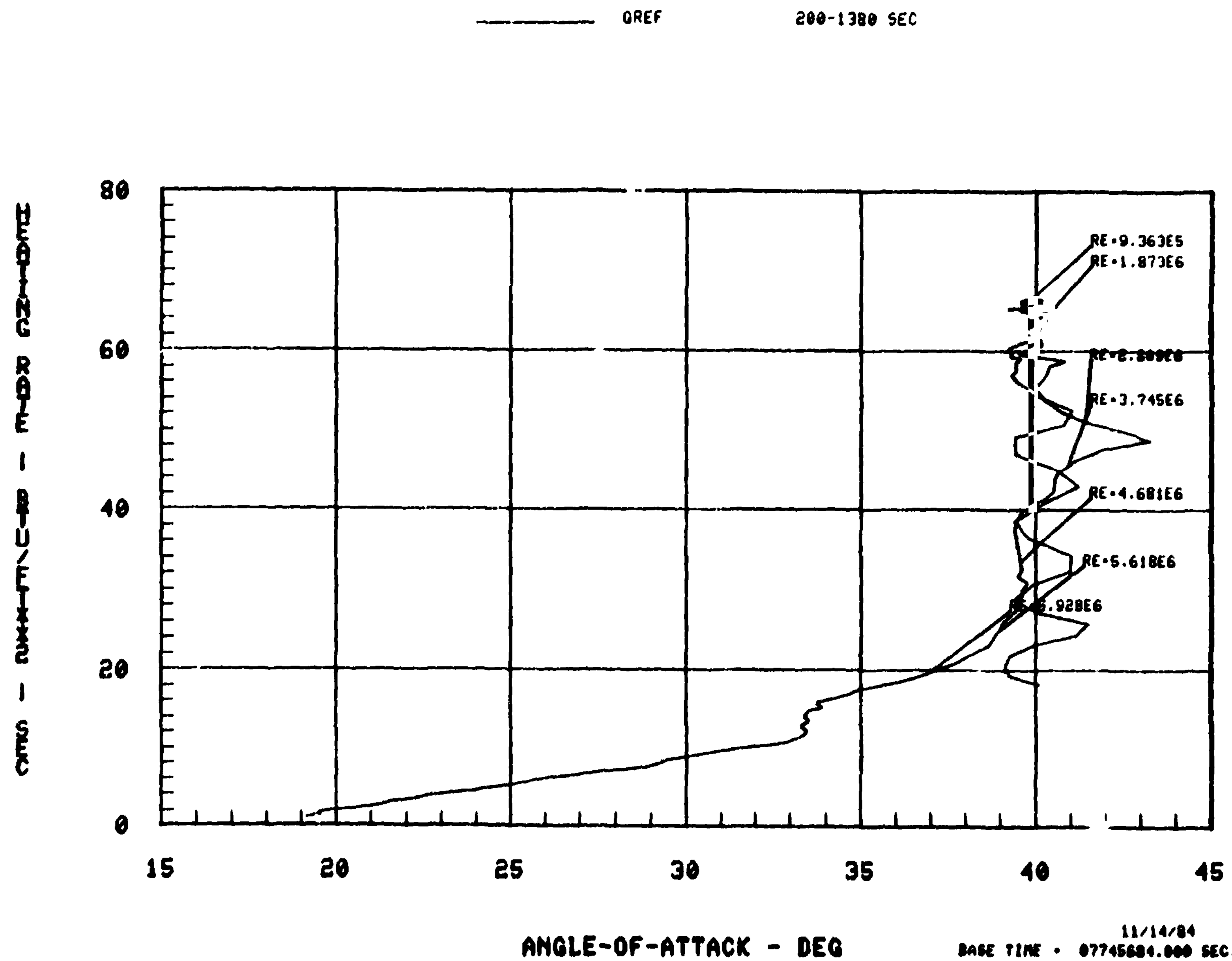

STS-4 (107 FT LENGTH) FLIGHT PARAMETER COMPARISON

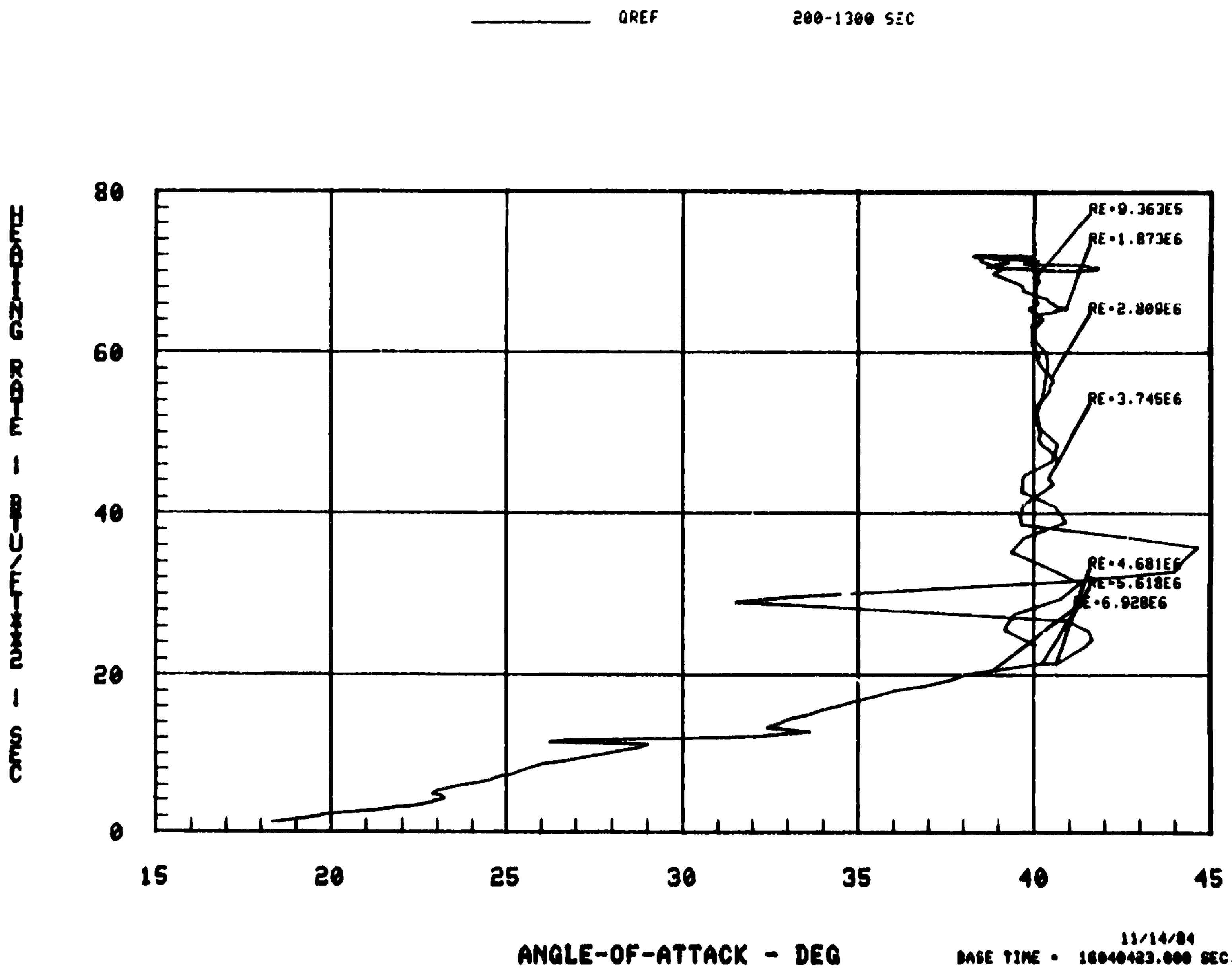

STS-5 (107 FT LENGTH) FLIGHT PARAMETER COMPARISON

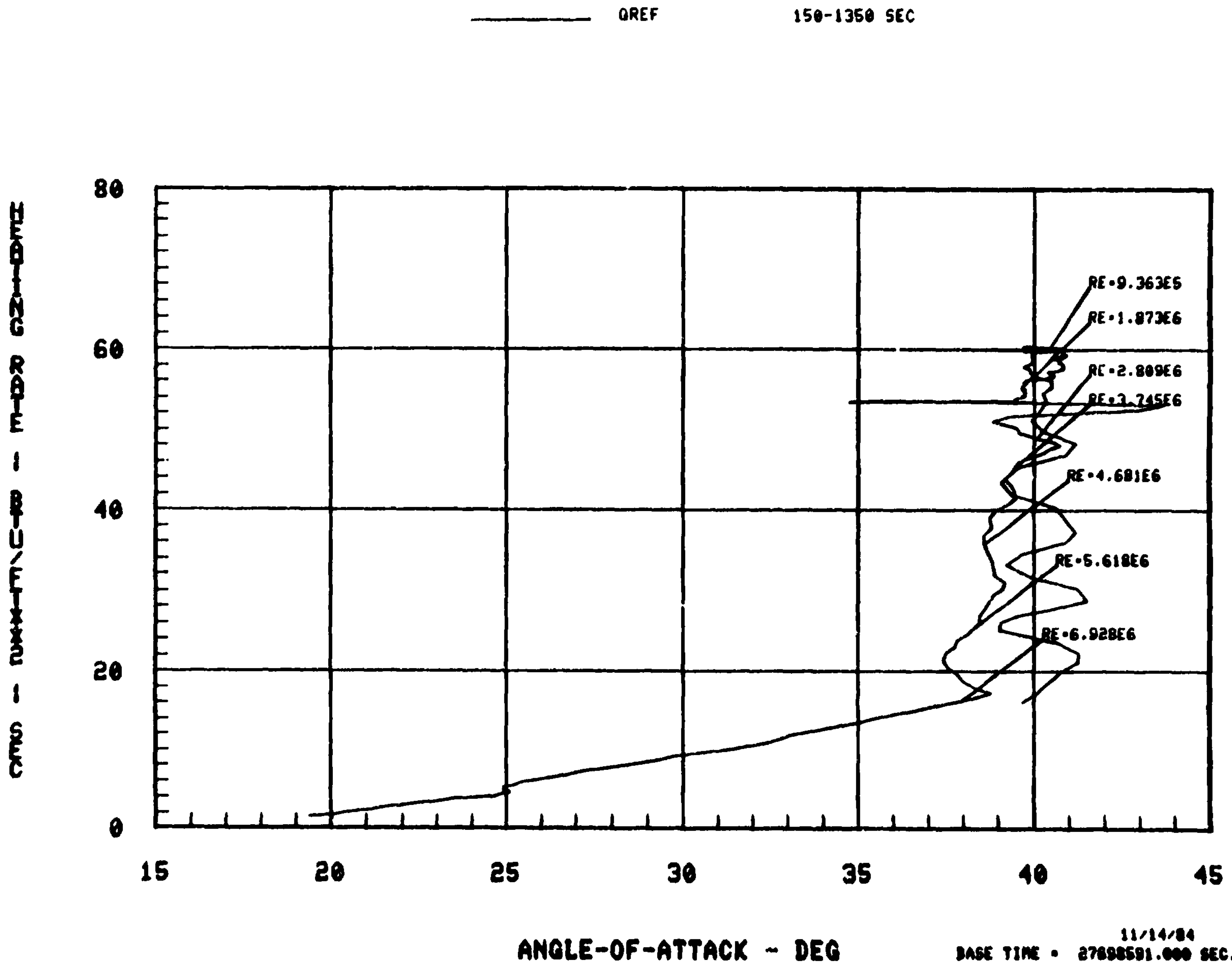

STS-1 (107 FT LENGTH) FLIGHT PARAMETER COMPARISON

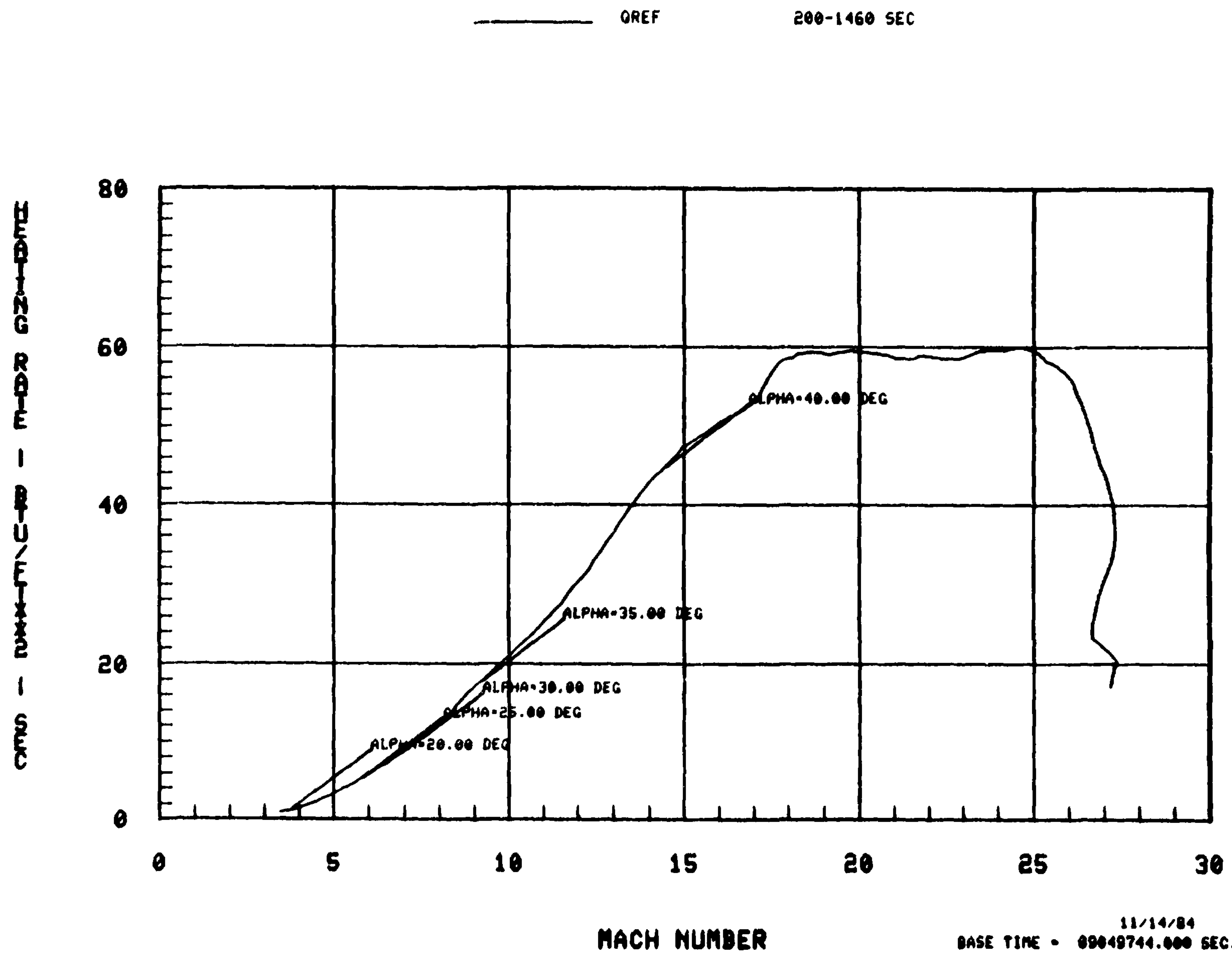

STS-2 (107 FT LENGTH) FLIGHT PARAMETER COMPARISON

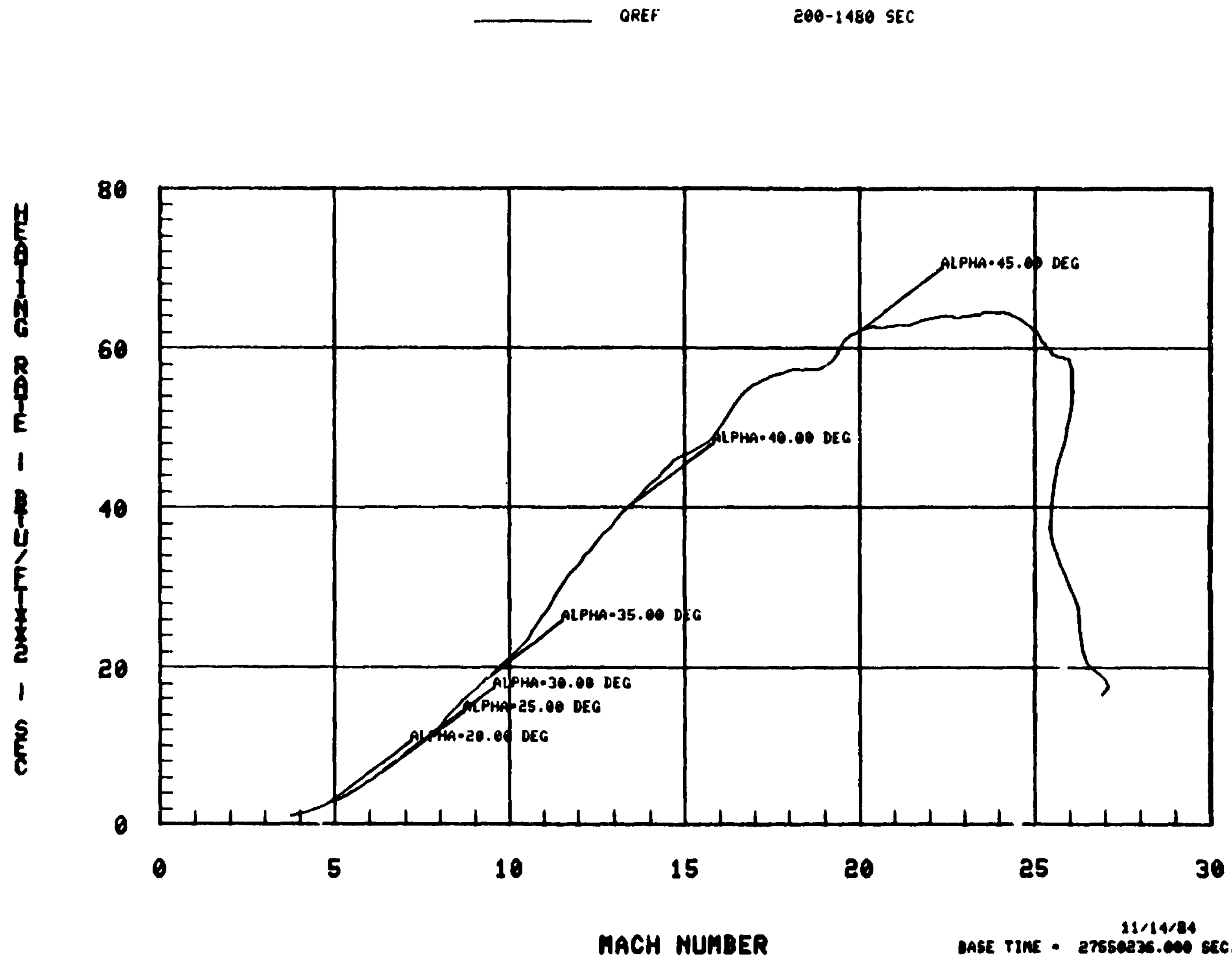

STS-3 (107 FT LENGTH) FLIGHT PARAMETER COMPARISON

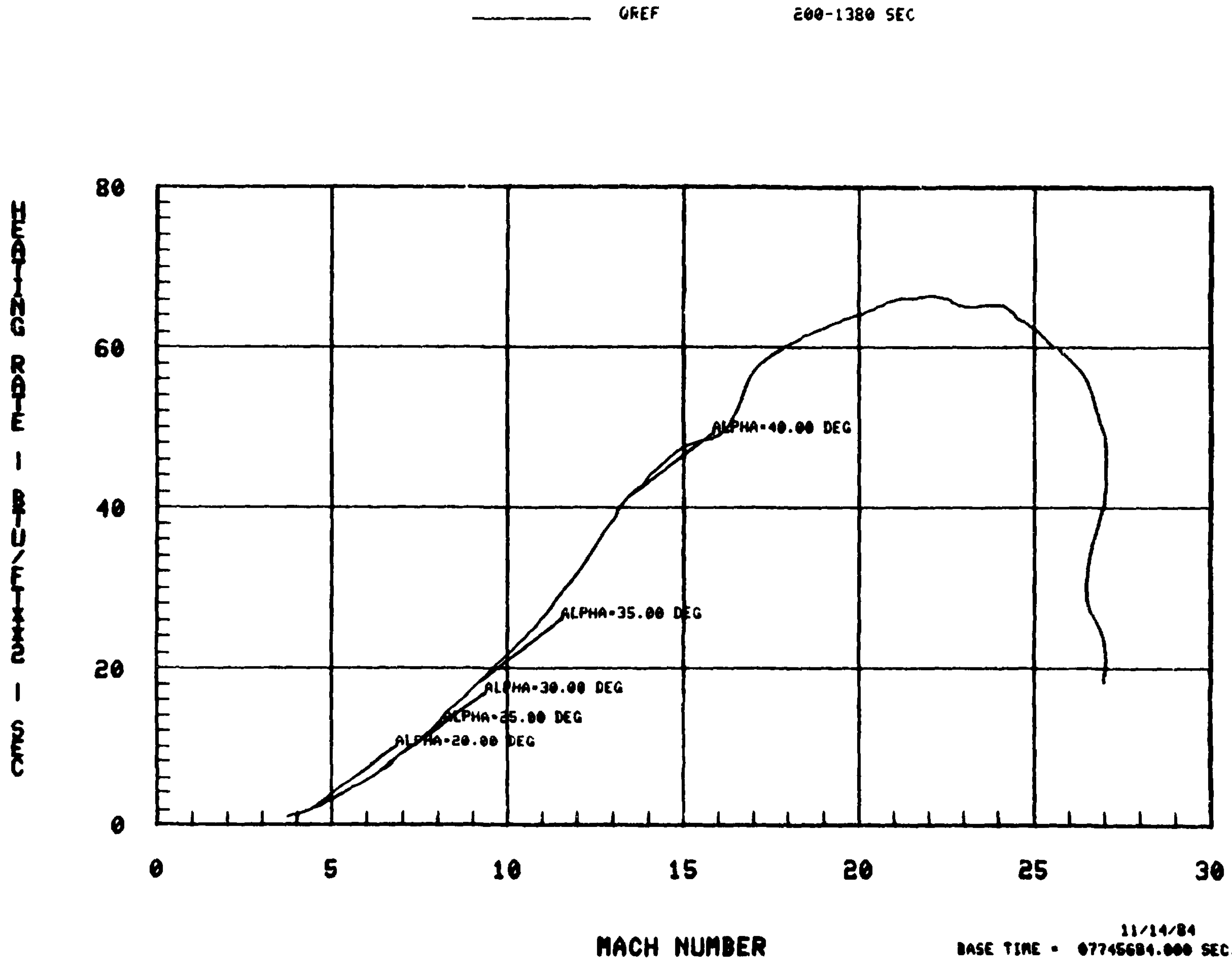

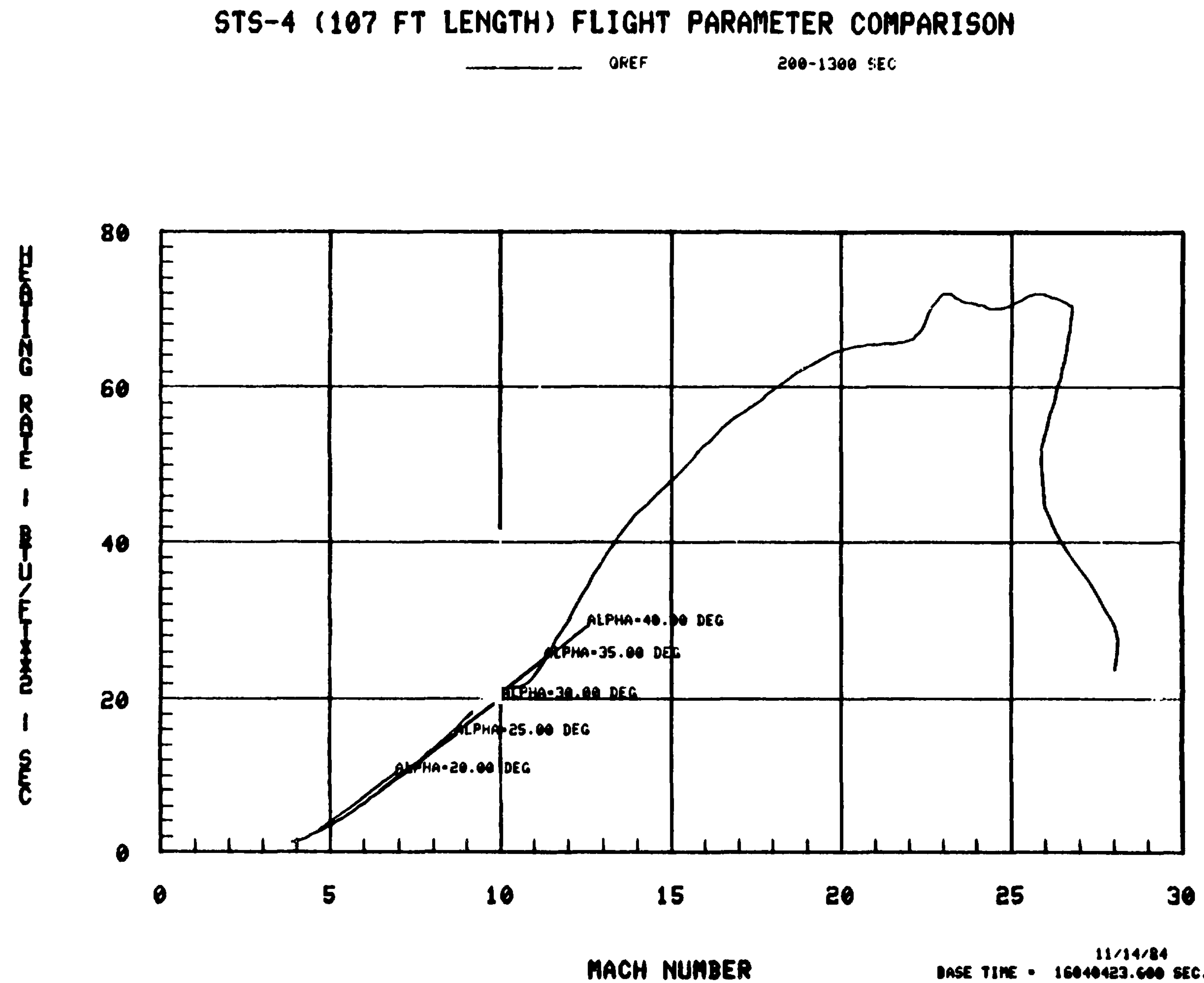

STS-4 (107 FT LENGTH) FLIGHT PARAMETER COMPARISON
QREF
200-1300 SEC
HEATING RATE - BTU/FT**2 - SEC
MACH NUMBER
ALPHA=40.00 DEG
ALPHA=35.00 DEG
ALPHA=30.00 DEG
ALPHA=25.00 DEG
ALPHA=20.00 DEG
0
20
40
60
80
0
5
10
15
20
25
30
11/14/84
BASE TIME = 16040423.600 SEC.

STS-5 (107 FT LENGTH) FLIGHT PARAMETER COMPARISON

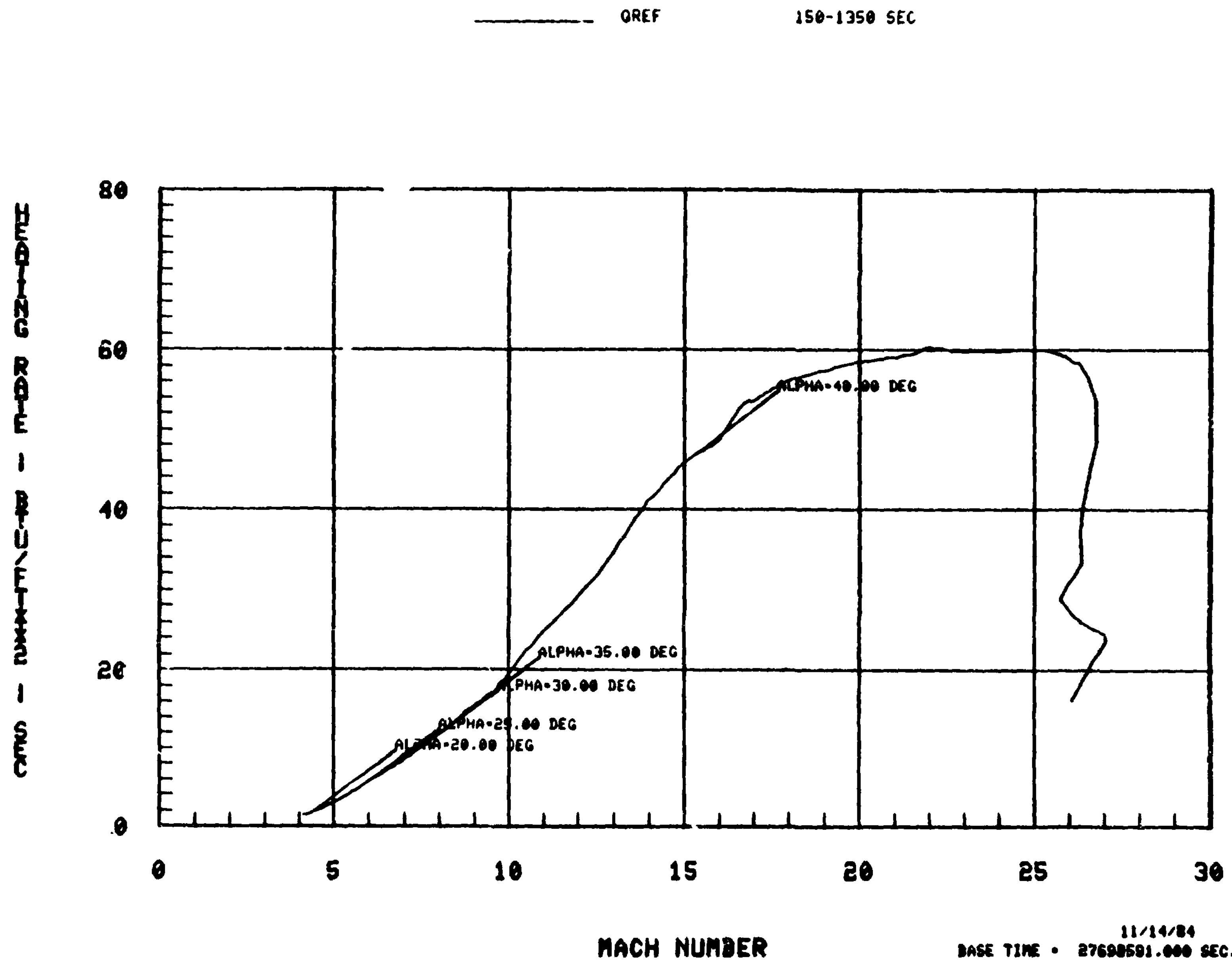

STS-1 (107 FT LENGTH) FLIGHT PARAMETER COMPARISON

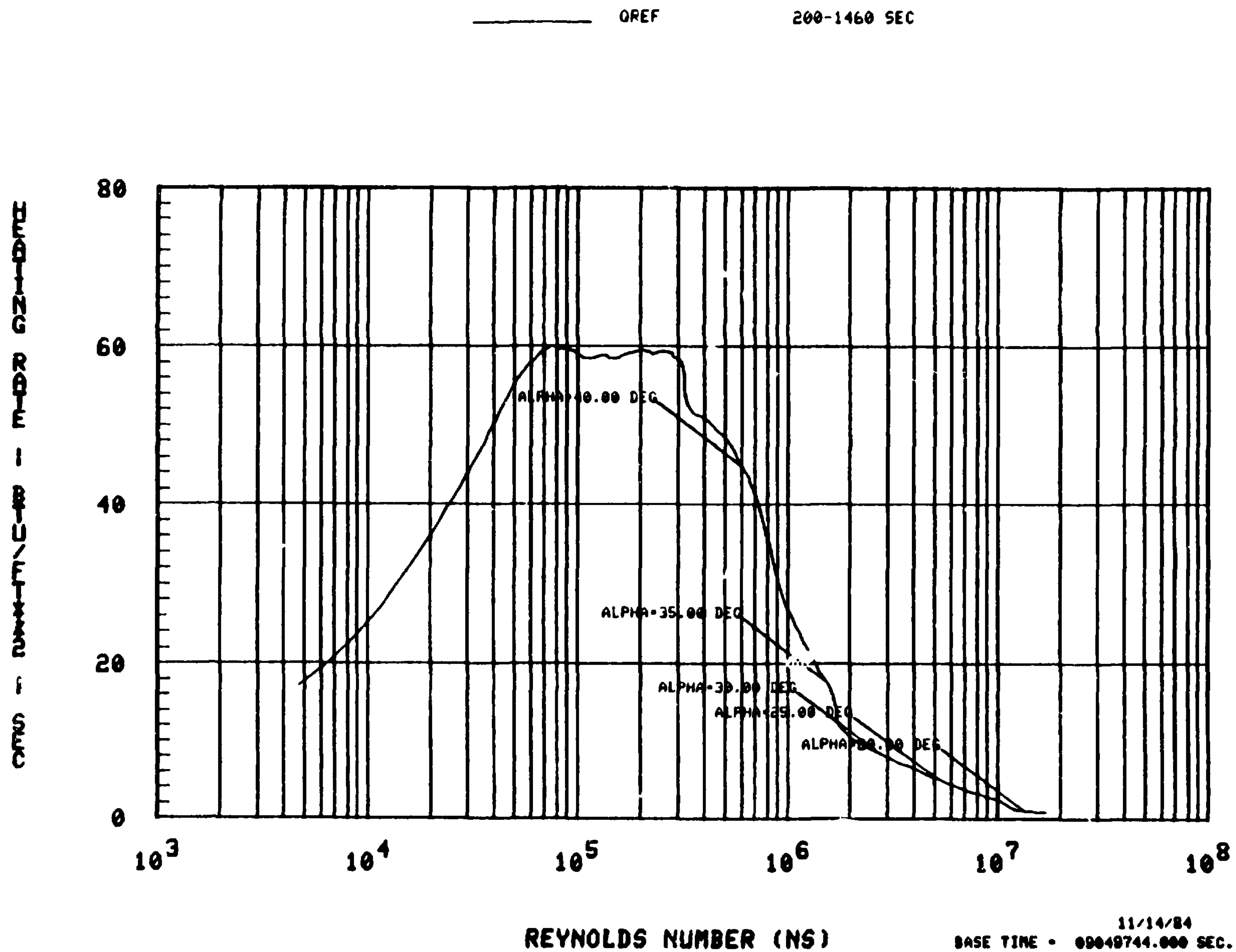

STS-2 (107 FT LENGTH) FLIGHT PARAMETER COMPARISON

QREF 200-1480 SEC

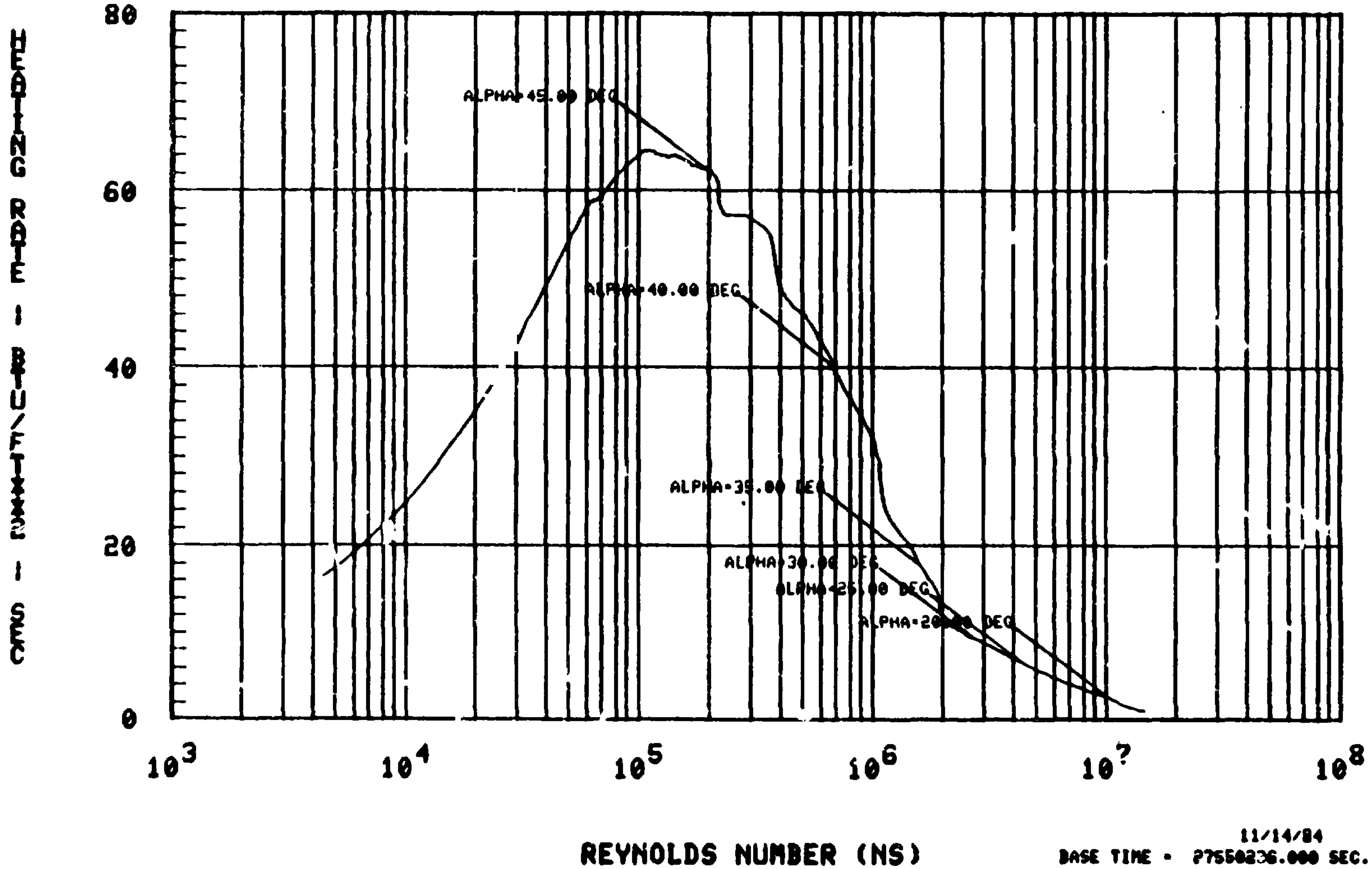

STS-3 (107 FT LENGTH) FLIGHT PARAMETER COMPARISON

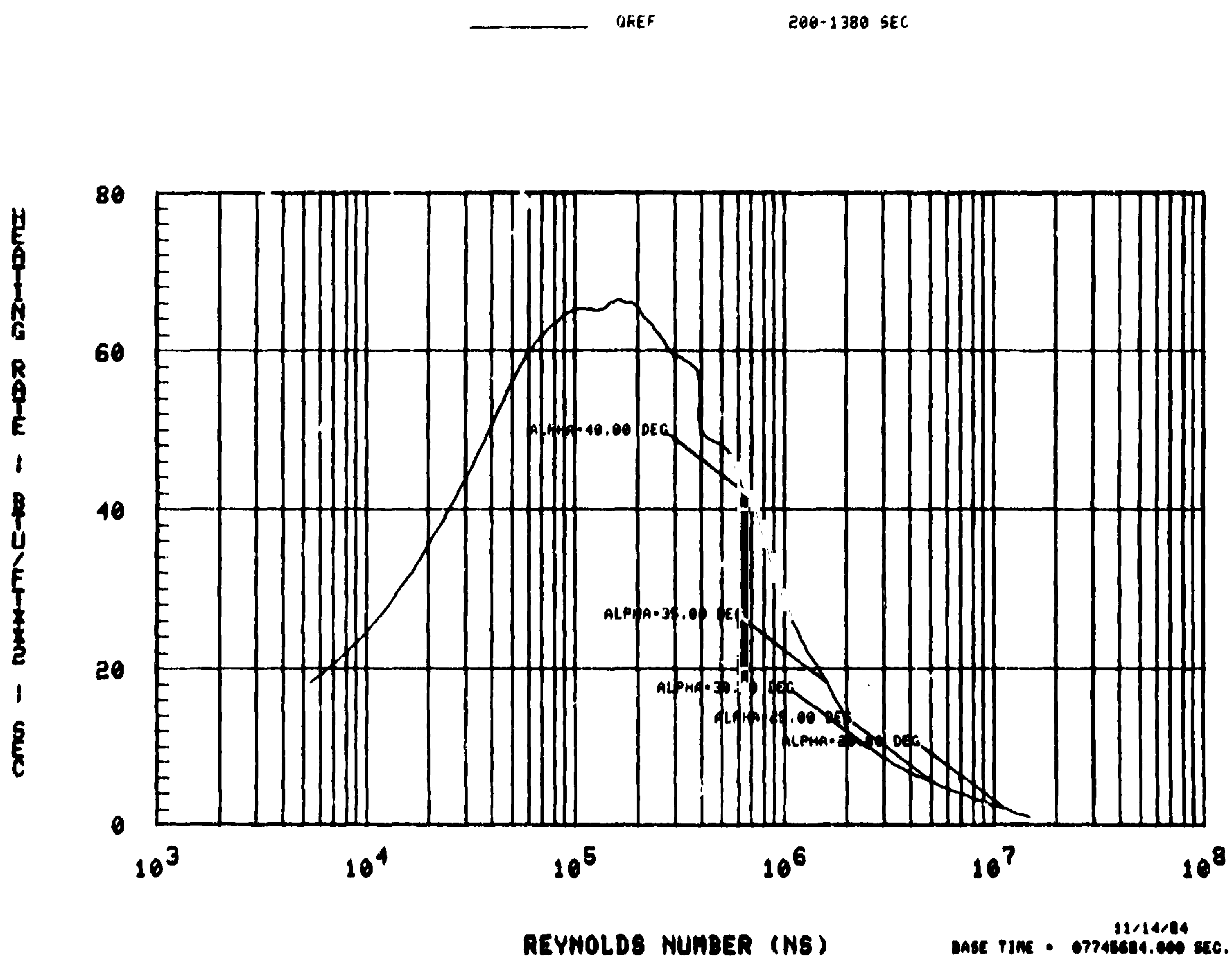

STS-4 (107 FT LENGTH) FLIGHT PARAMETER COMPARISON

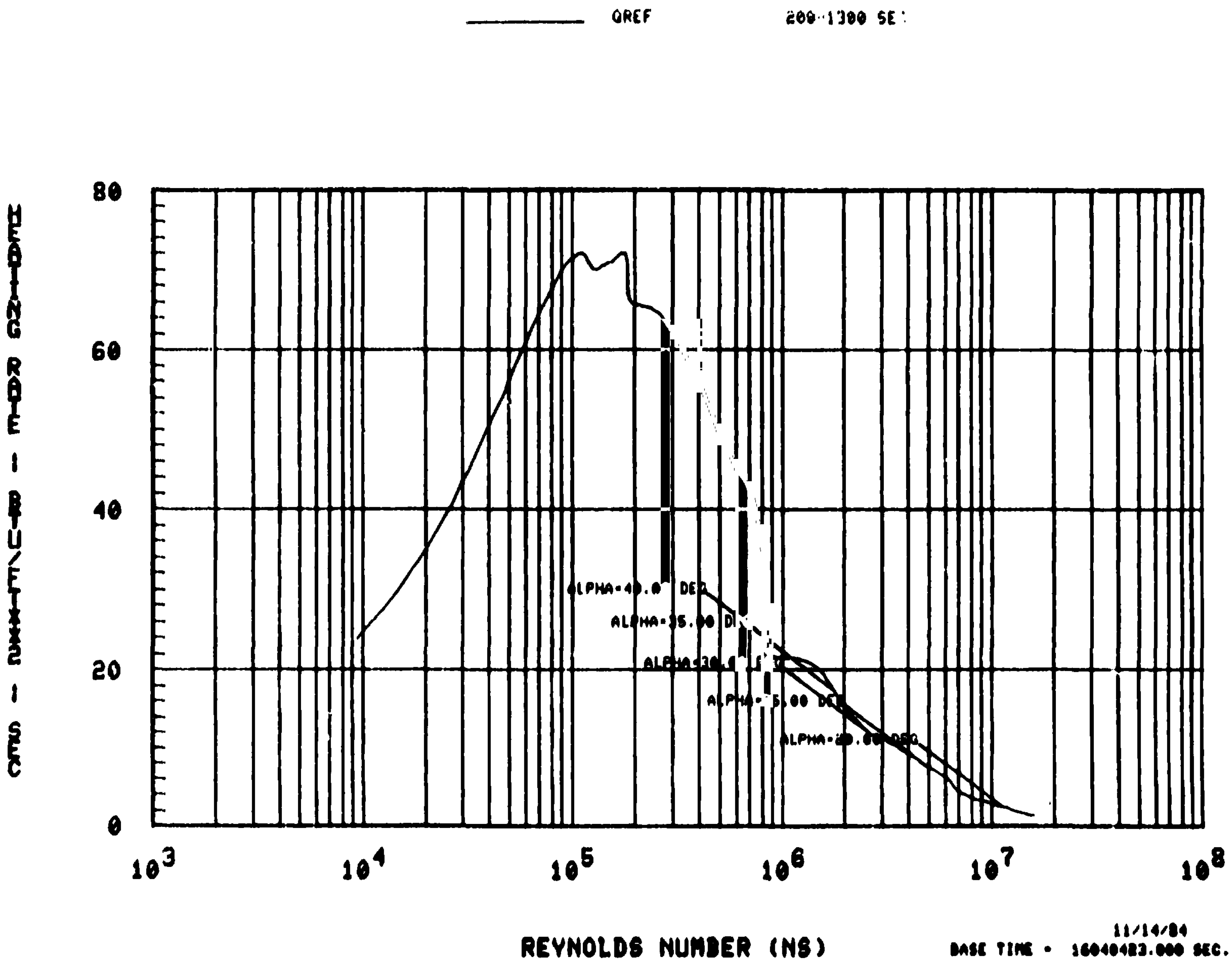

STS-5 (107 FT LENGTH) FLIGHT PARAMETER COMPARISON

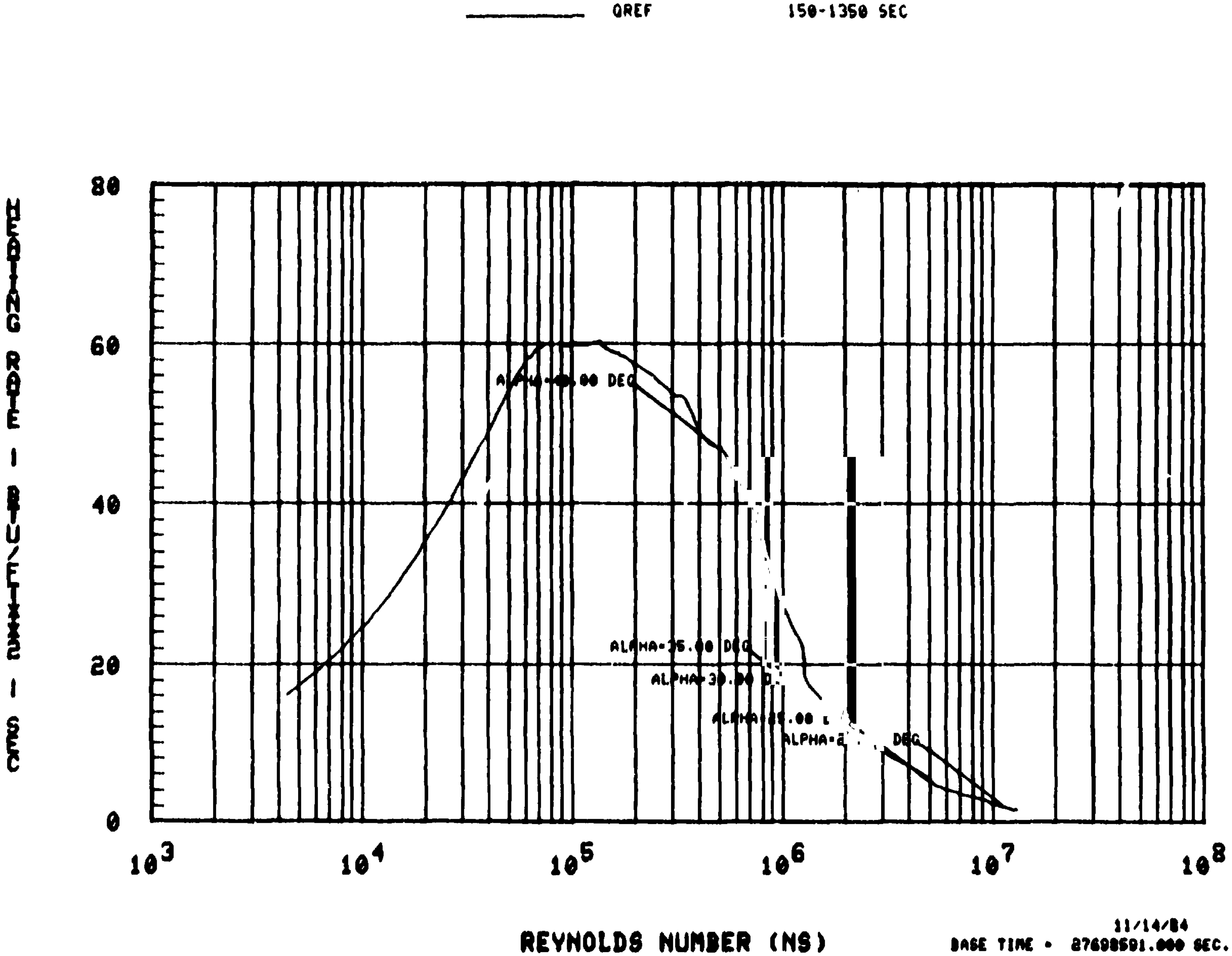

STS-1 (107 FT LENGTH) FLIGHT PARAMETER COMPARISON

HREF 200-1460 SEC

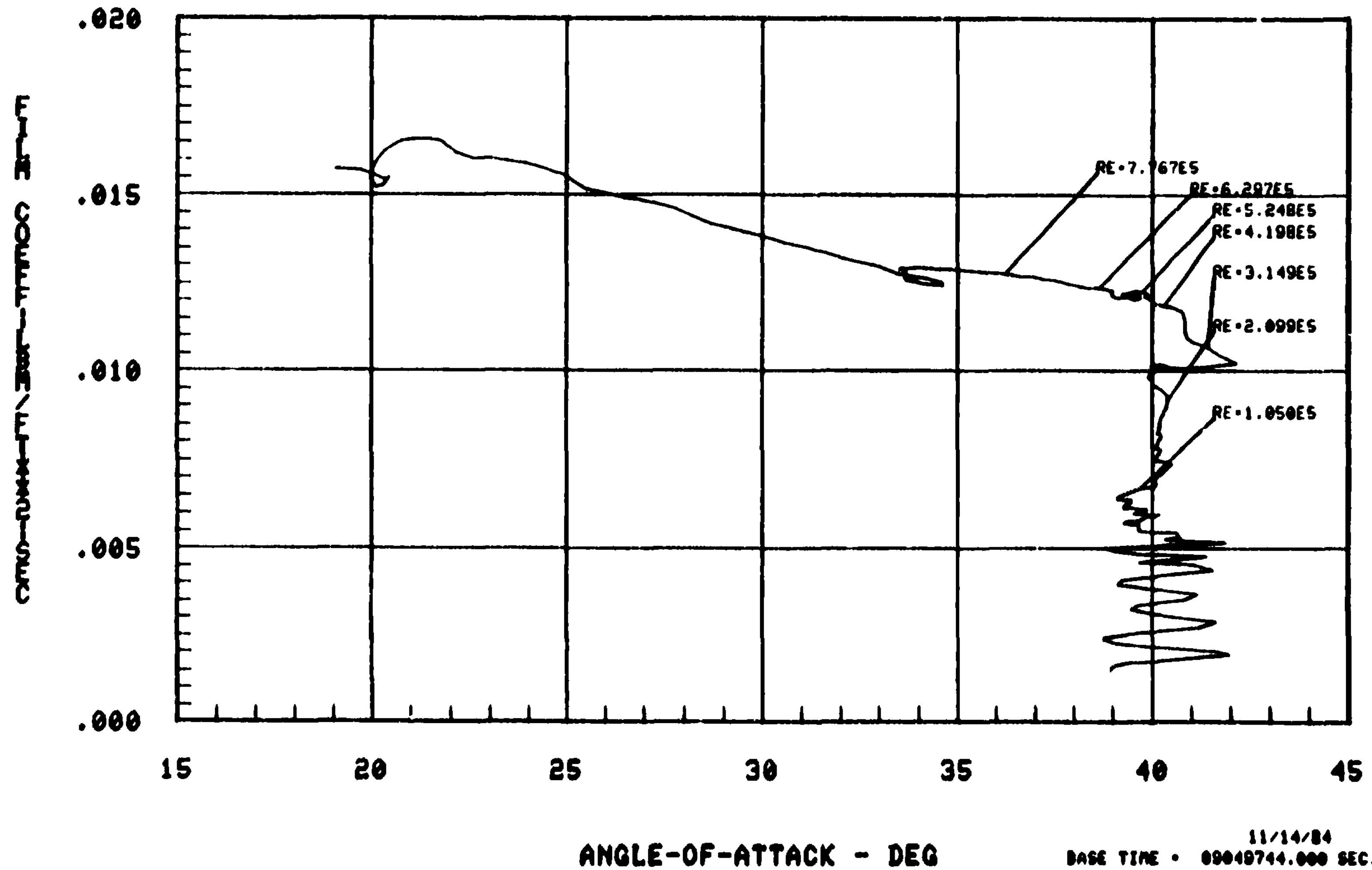

STS-2 (107 FT LENGTH) FLIGHT PARAMETER COMPARISON

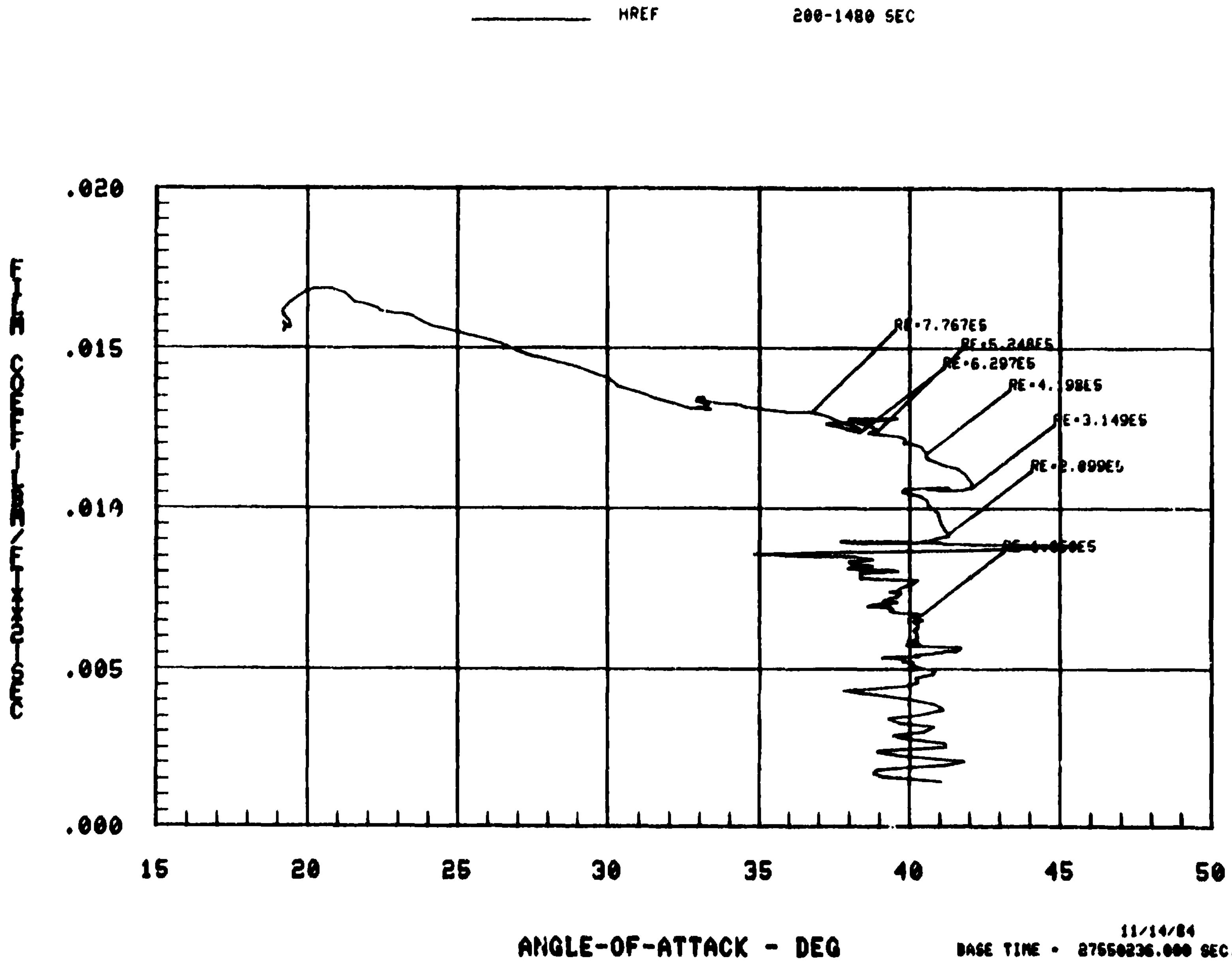

STS-3 (107 FT LENGTH) FLIGHT PARAMETER COMPARISON

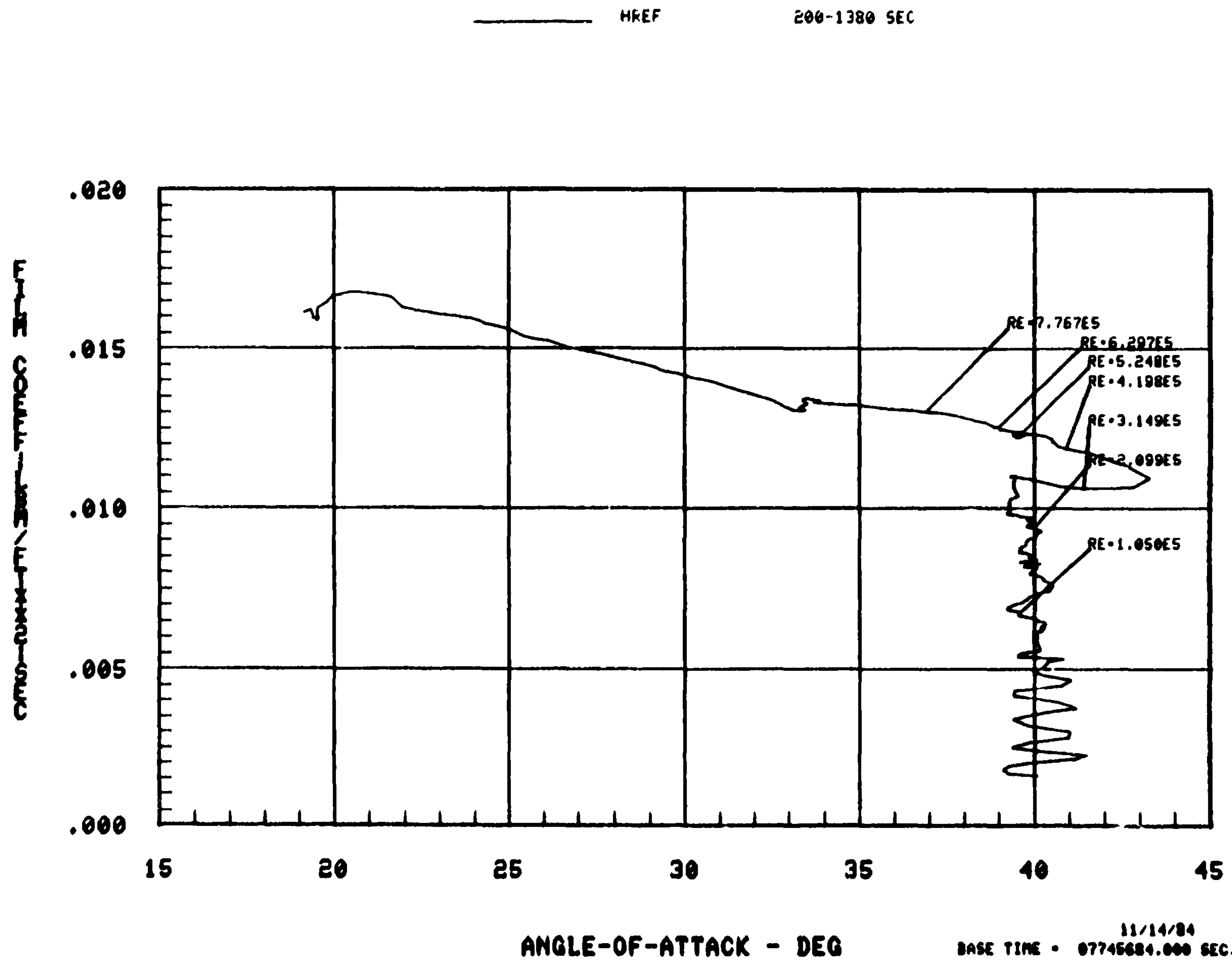

STS-4 (107 FT LENGTH) FLIGHT PARAMETER COMPARISON

HREF 200-1300 SEC

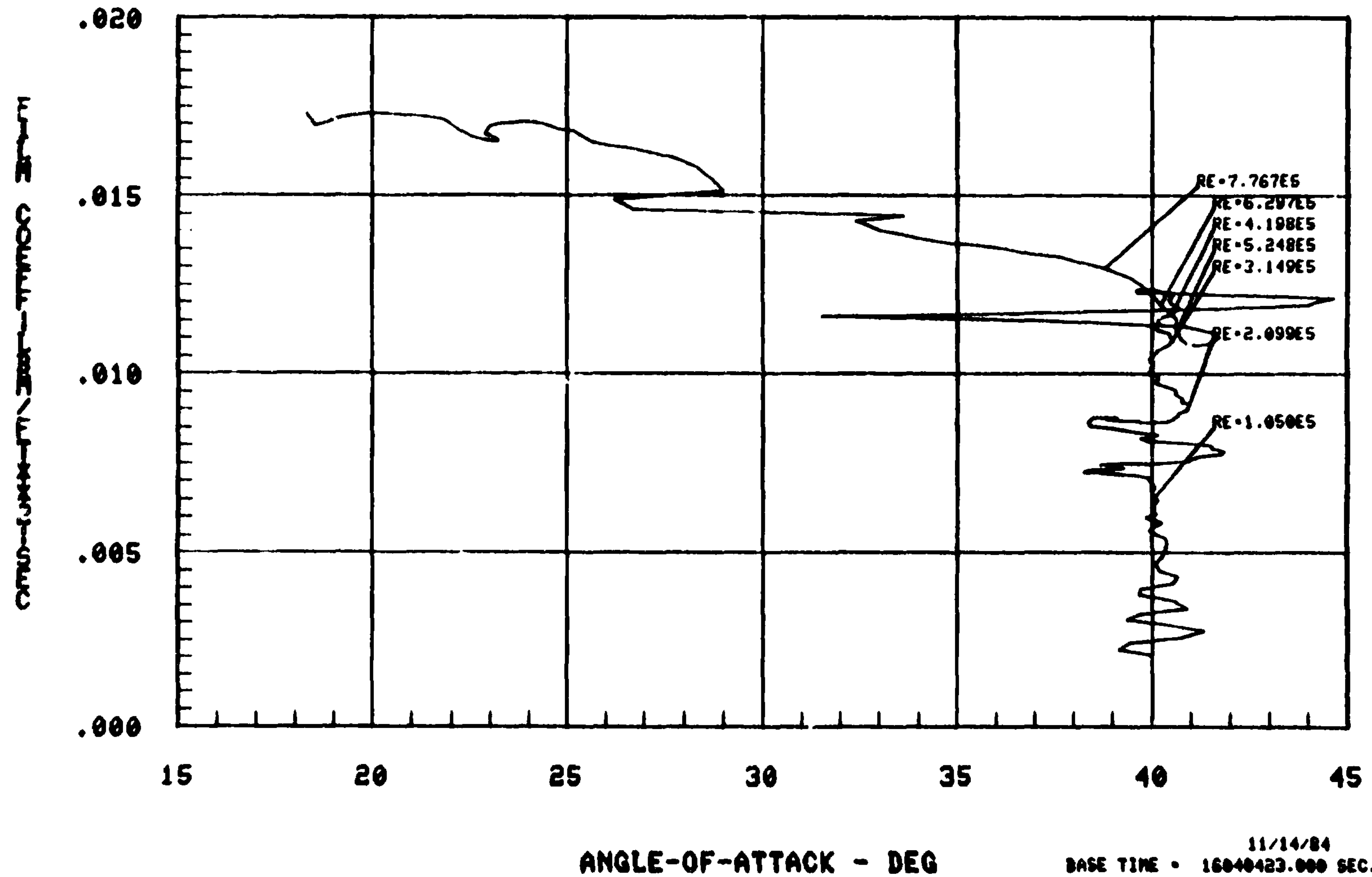

STS-5 (107 FT LENGTH) FLIGHT PARAMETER COMPARISON

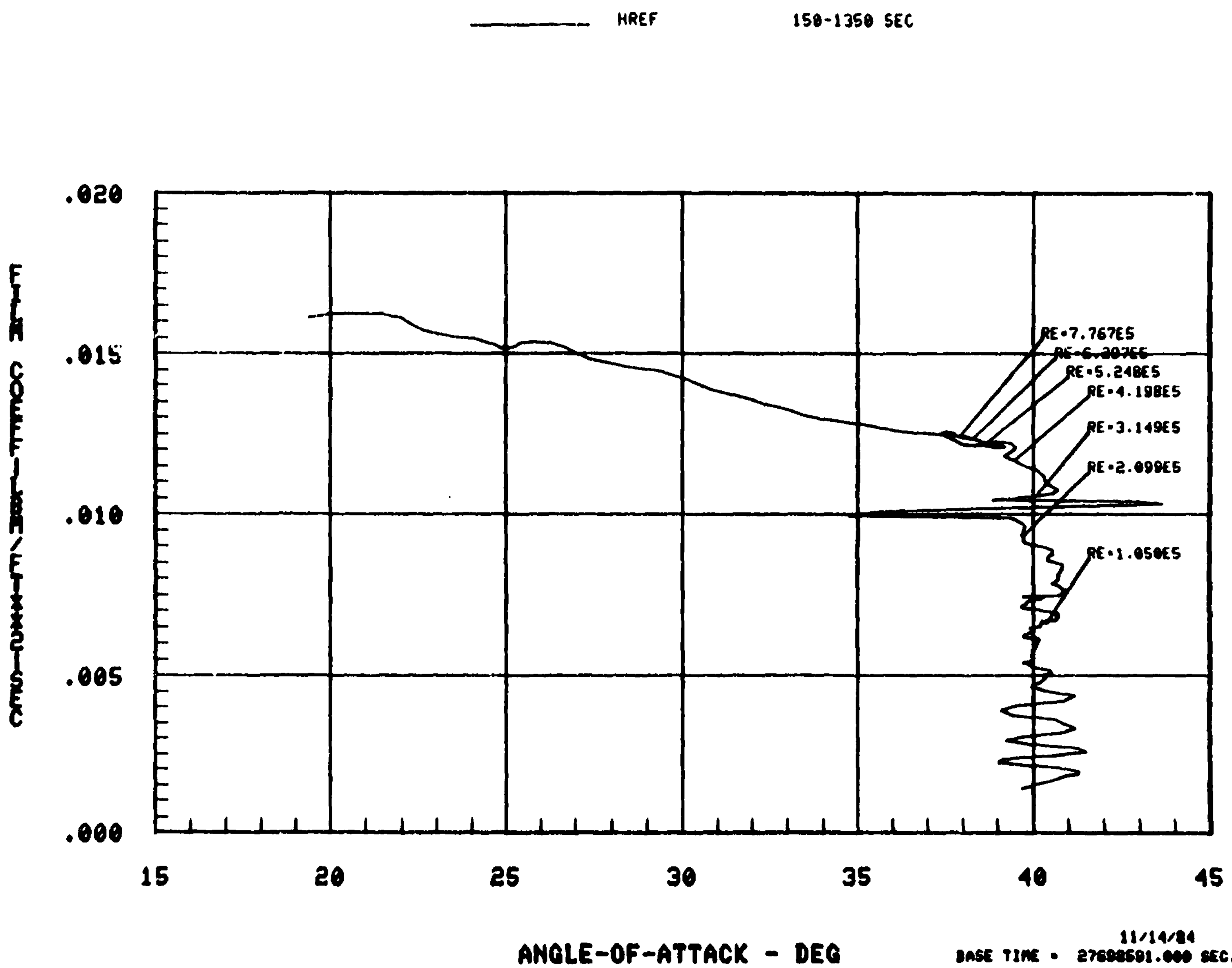

STS-1 (107 FT LENGTH) FLIGHT PARAMETER COMPARISON

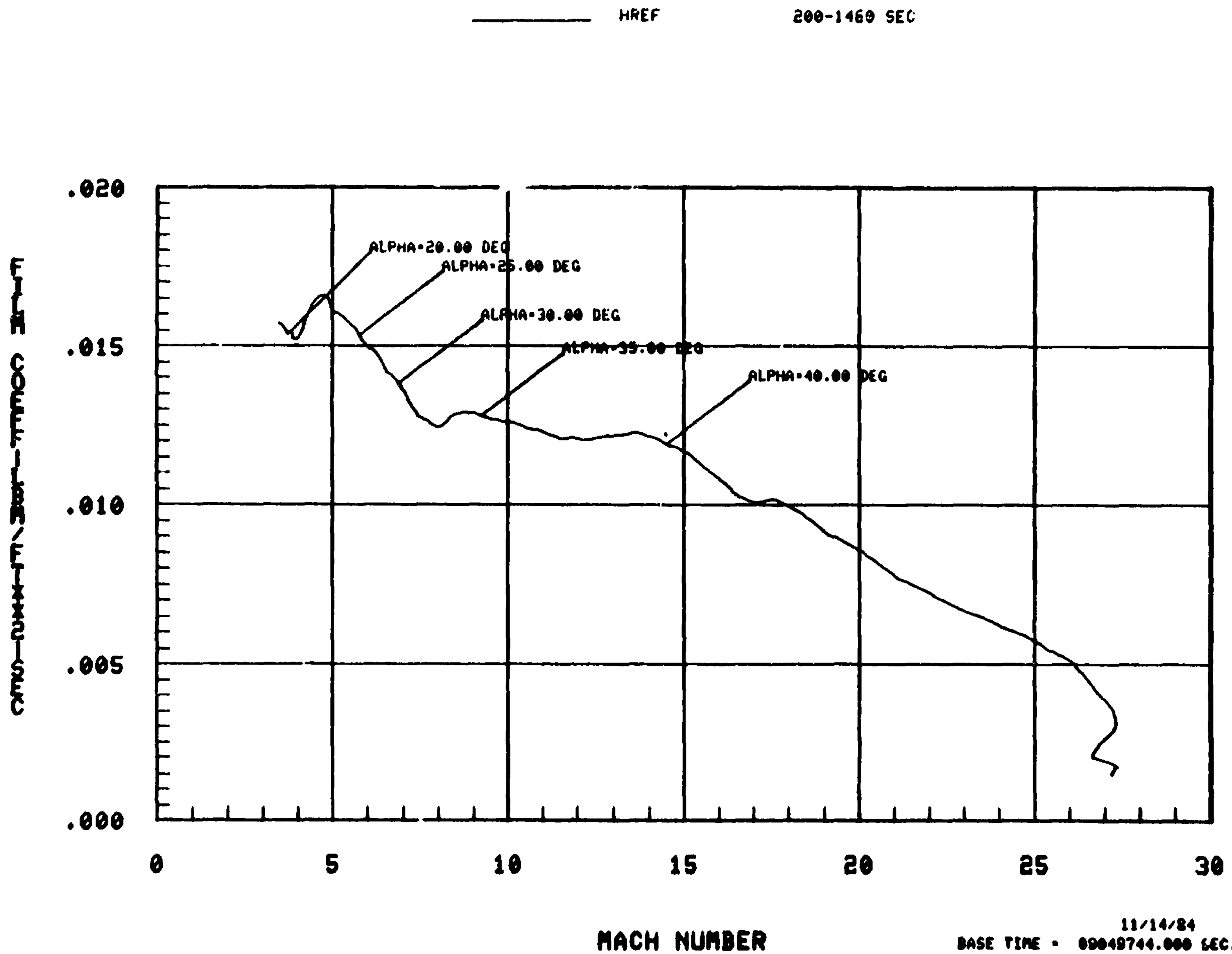

11/14/84
BASE TIME = 09048744.000 SEC.

STS-2 (107 FT LENGTH) FLIGHT PARAMETER COMPARISON

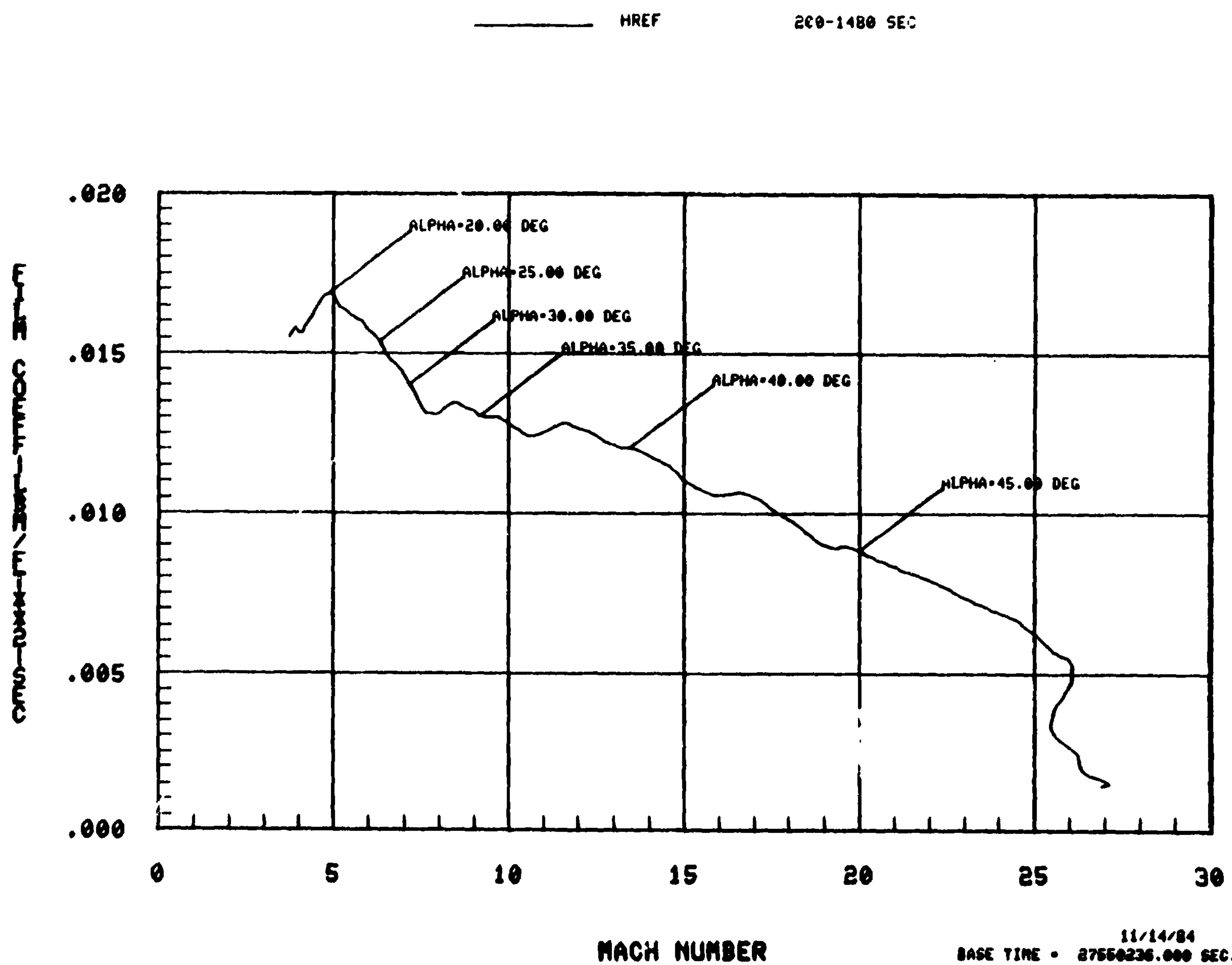

STS-3 (107 FT LENGTH) FLIGHT PARAMETER COMPARISON

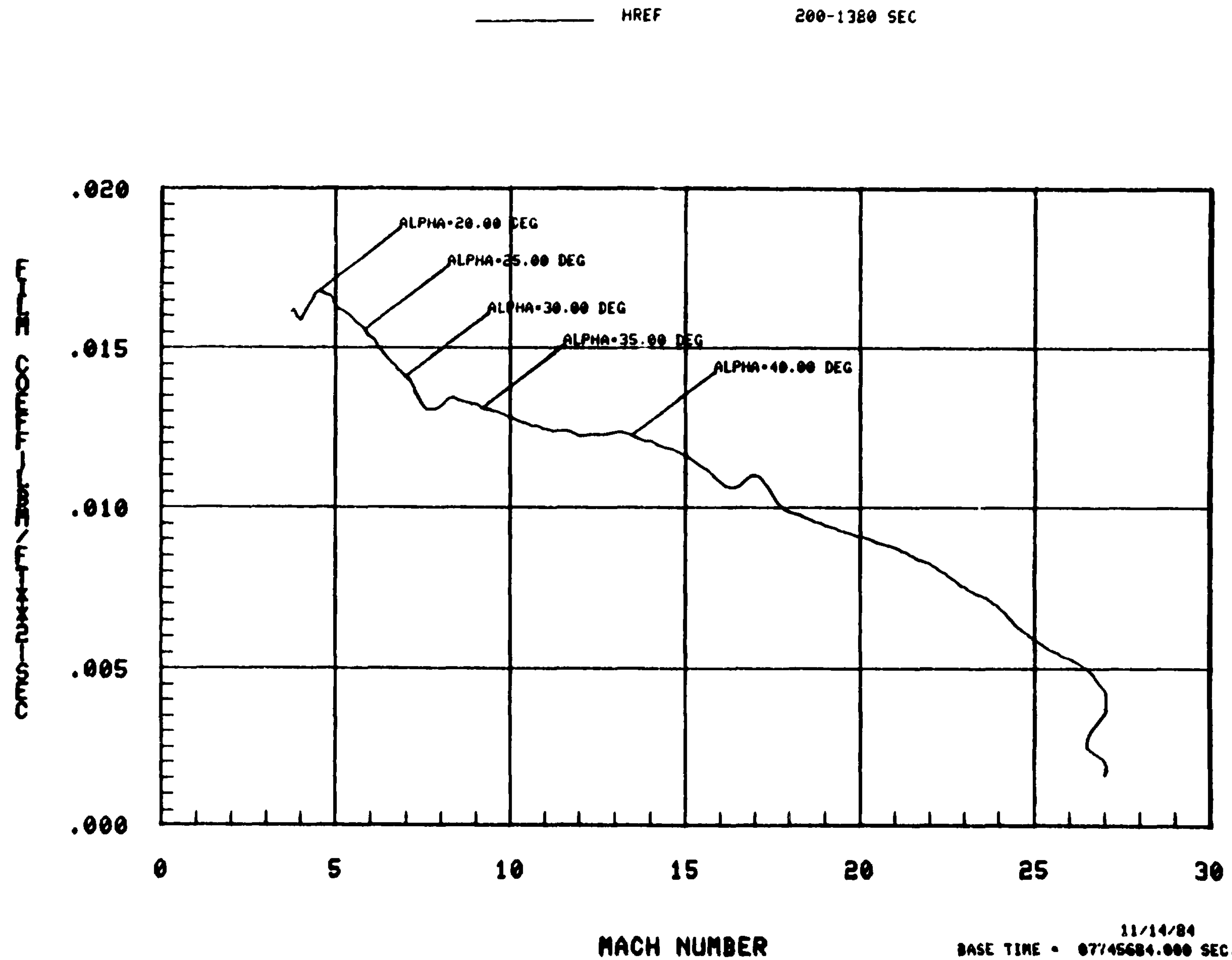

STS-4 (107 FT LENGTH) FLIGHT PARAMETER COMPARI⁚ON

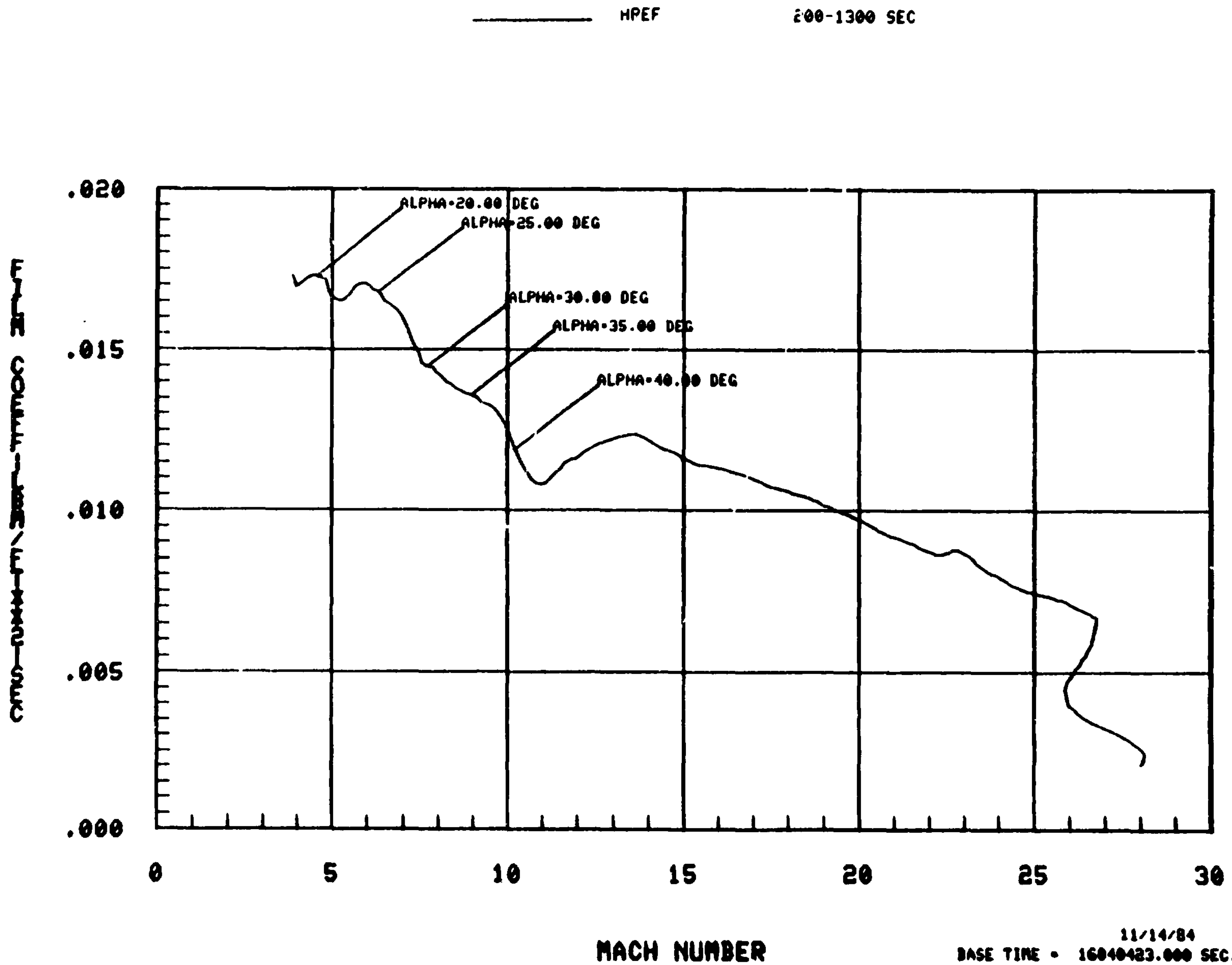

STS-5 (107 FT LENGTH) FLIGHT PARAMETER COMPARISON

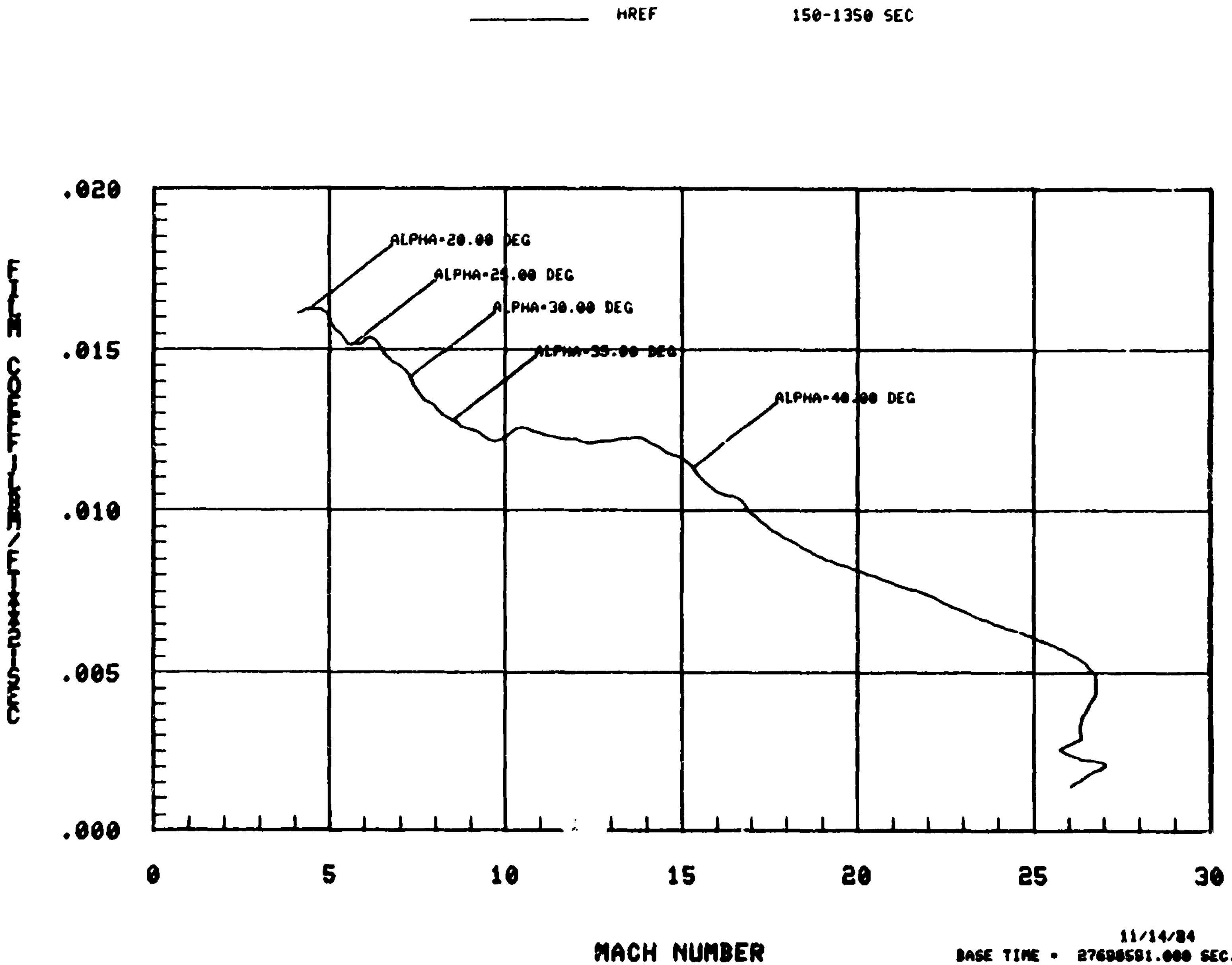

STS-1 (107 FT LENGTH) FLIGHT PARAMETER COMPARISON

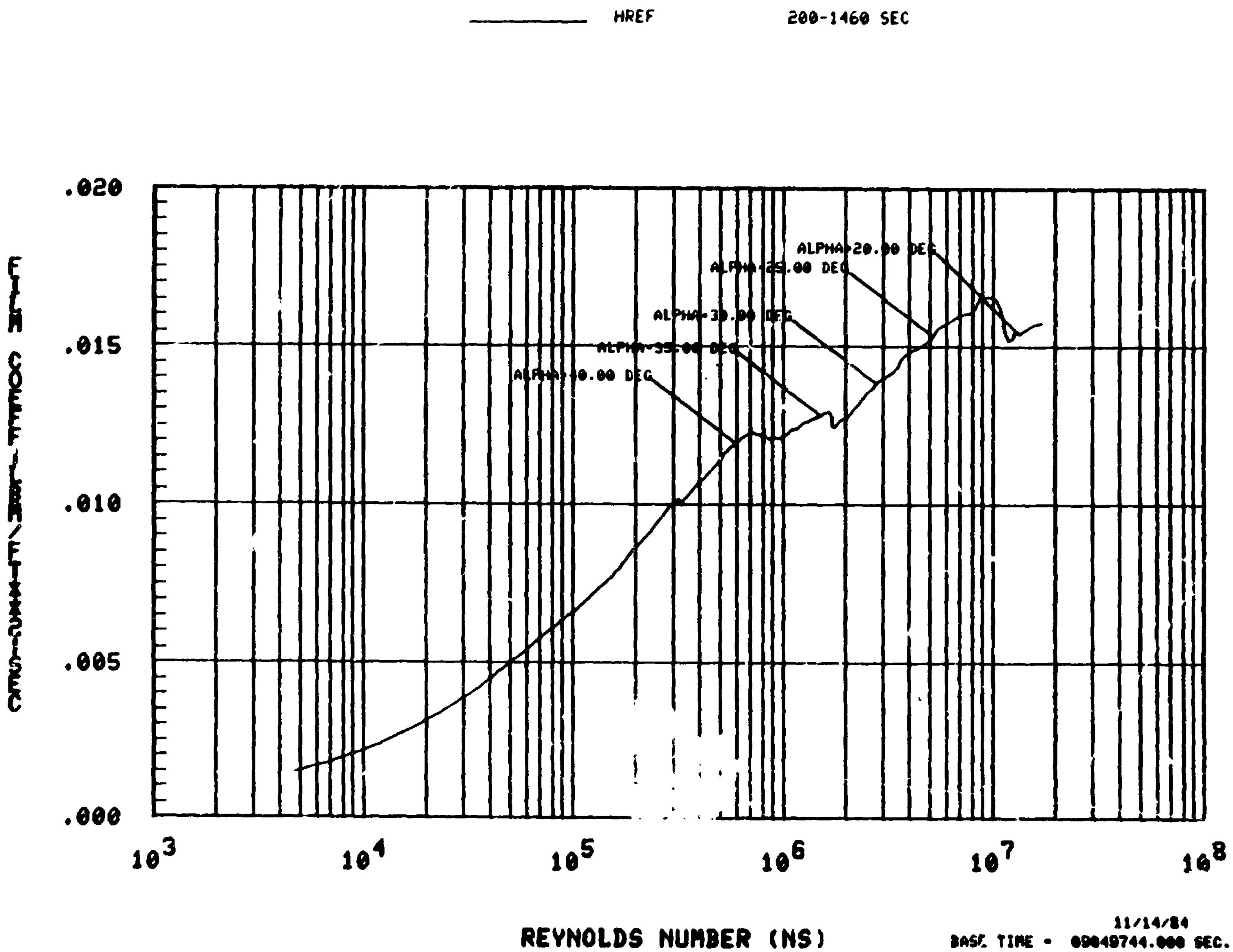

11/14/84
BASE TIME = 09049744.000 SEC.

STS-2 (107 FT LENGTH) FLIGHT PARAMETER COMPARISON

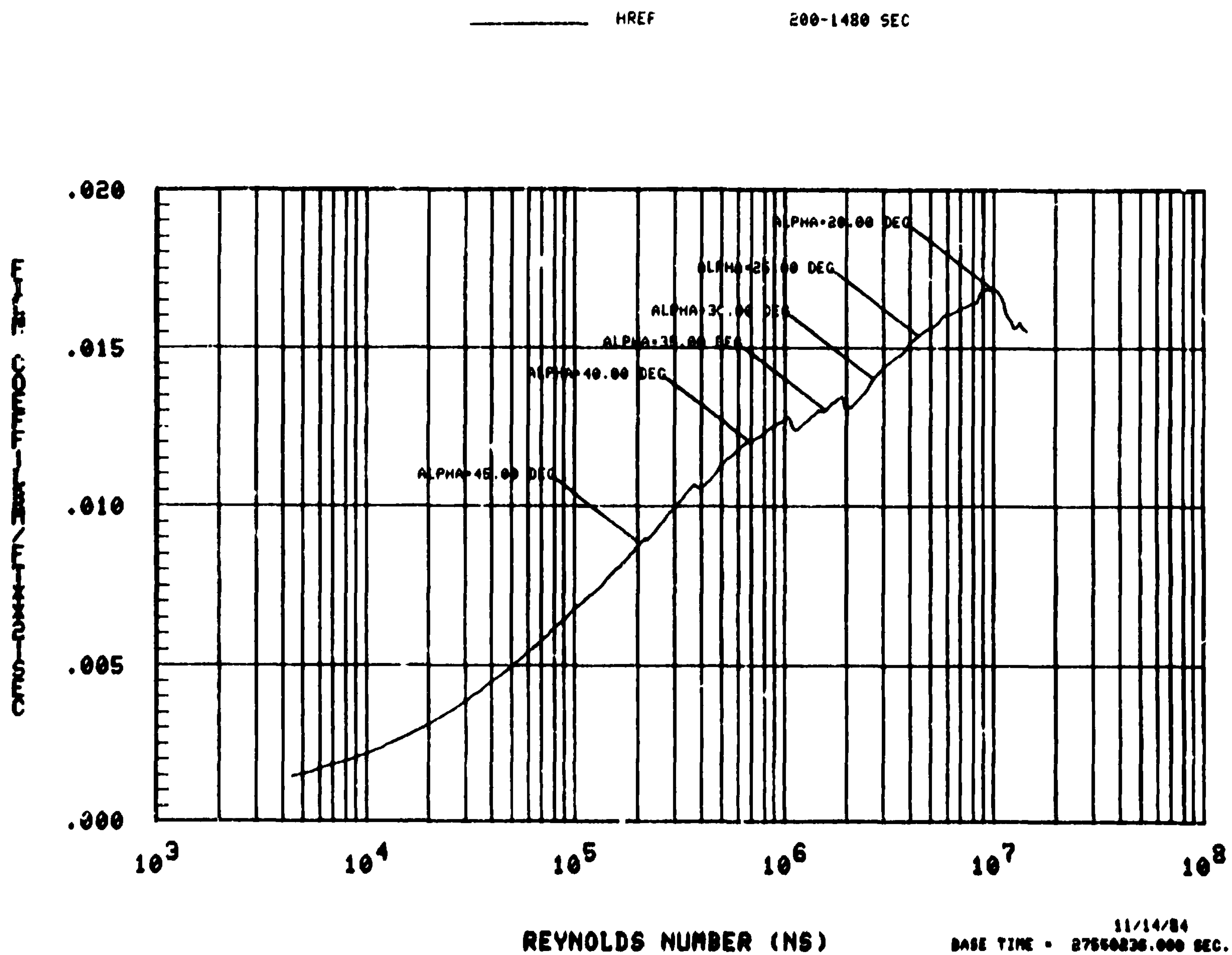

STS-3 (107 FT LENGTH) FLIGHT PARAMETER COMPARISON

HREF 200-1380 SEC

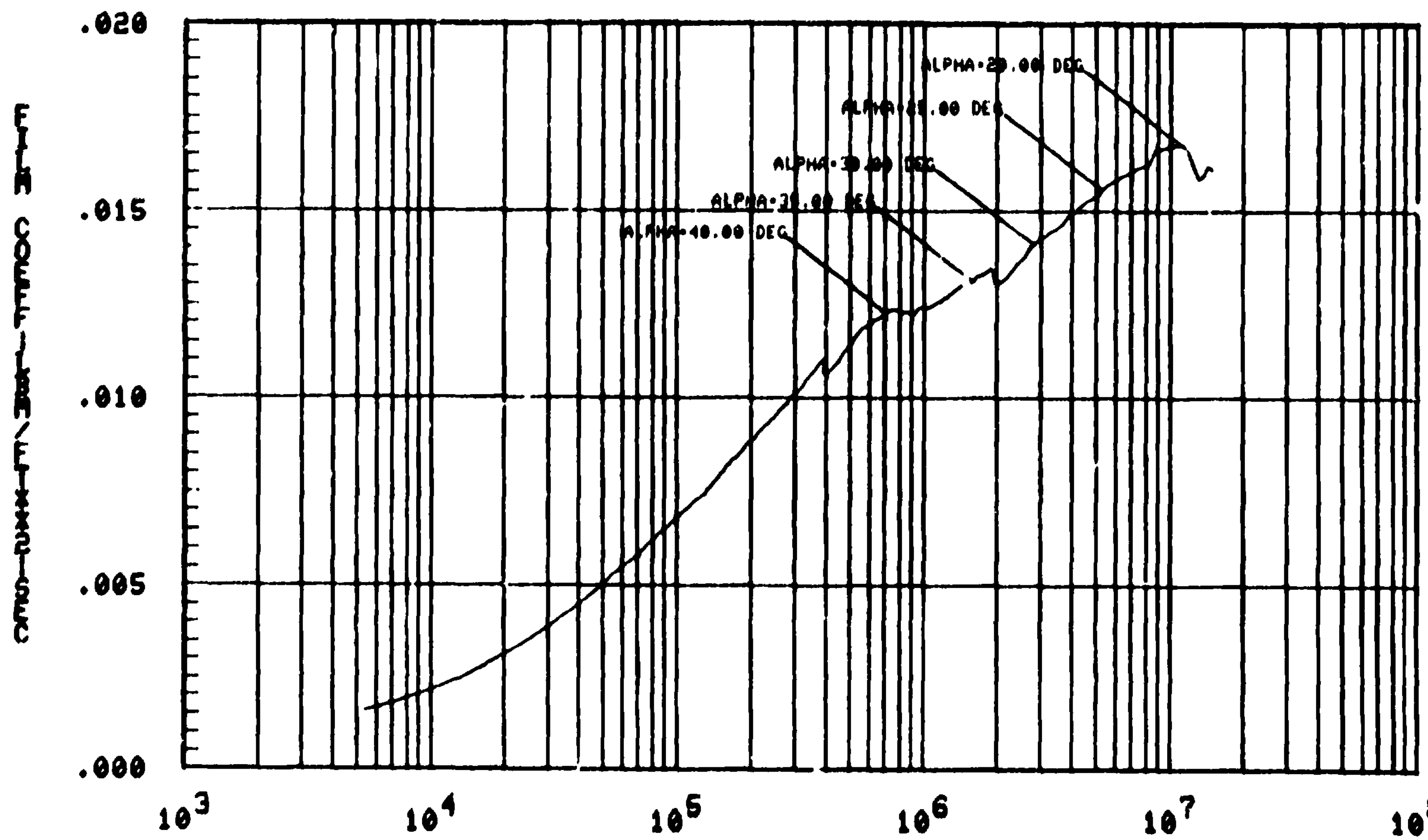

REYNOLDS NUMBER (NS)

11/14/84
BASE TIME = 077456684.000 SEC.

STS-4 (107 FT LENGTH) FLIGHT PARAMETER COMPARISON

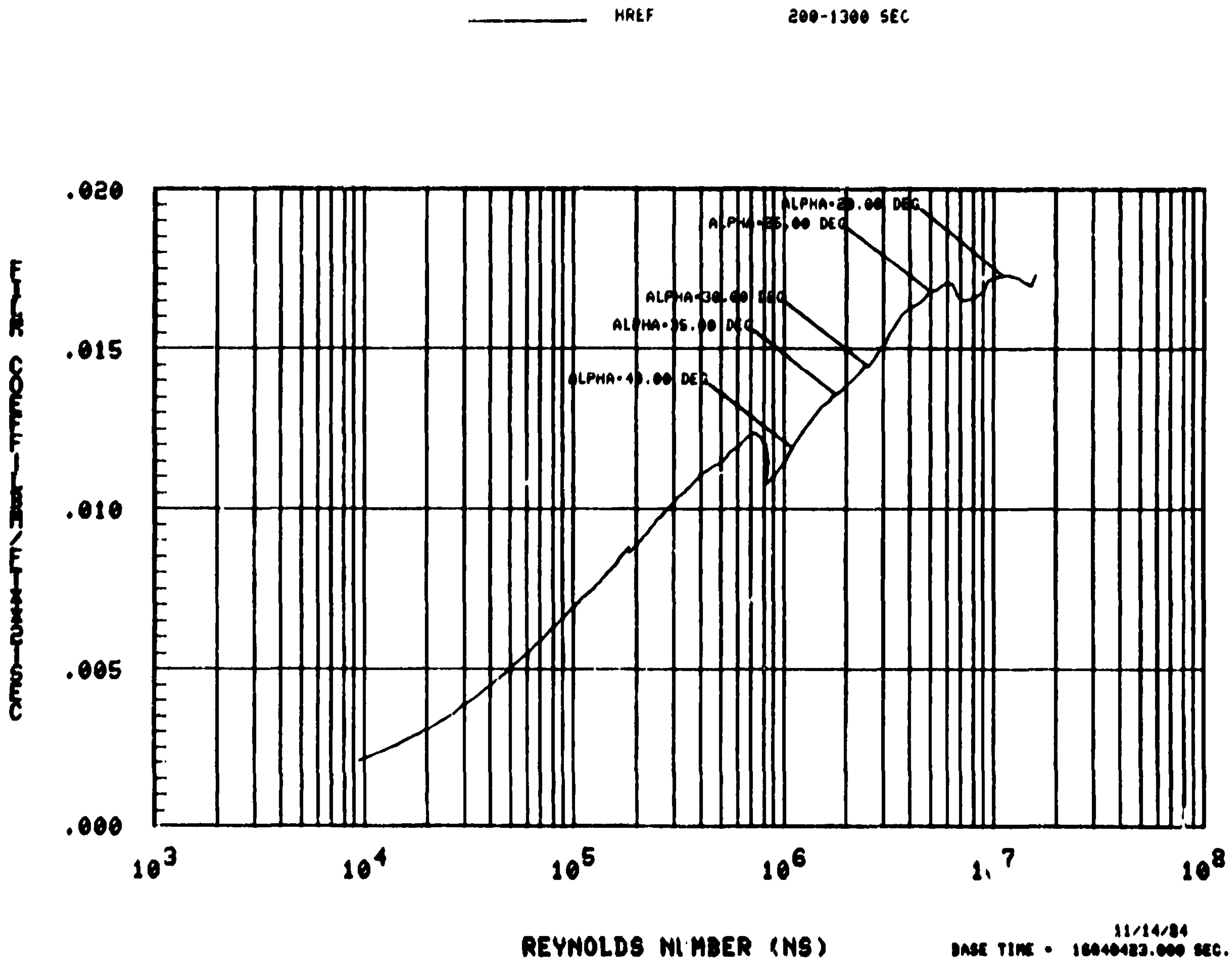

STS-5 (107 FT LENGTH) FLIGHT PARAMETER COMPARISON

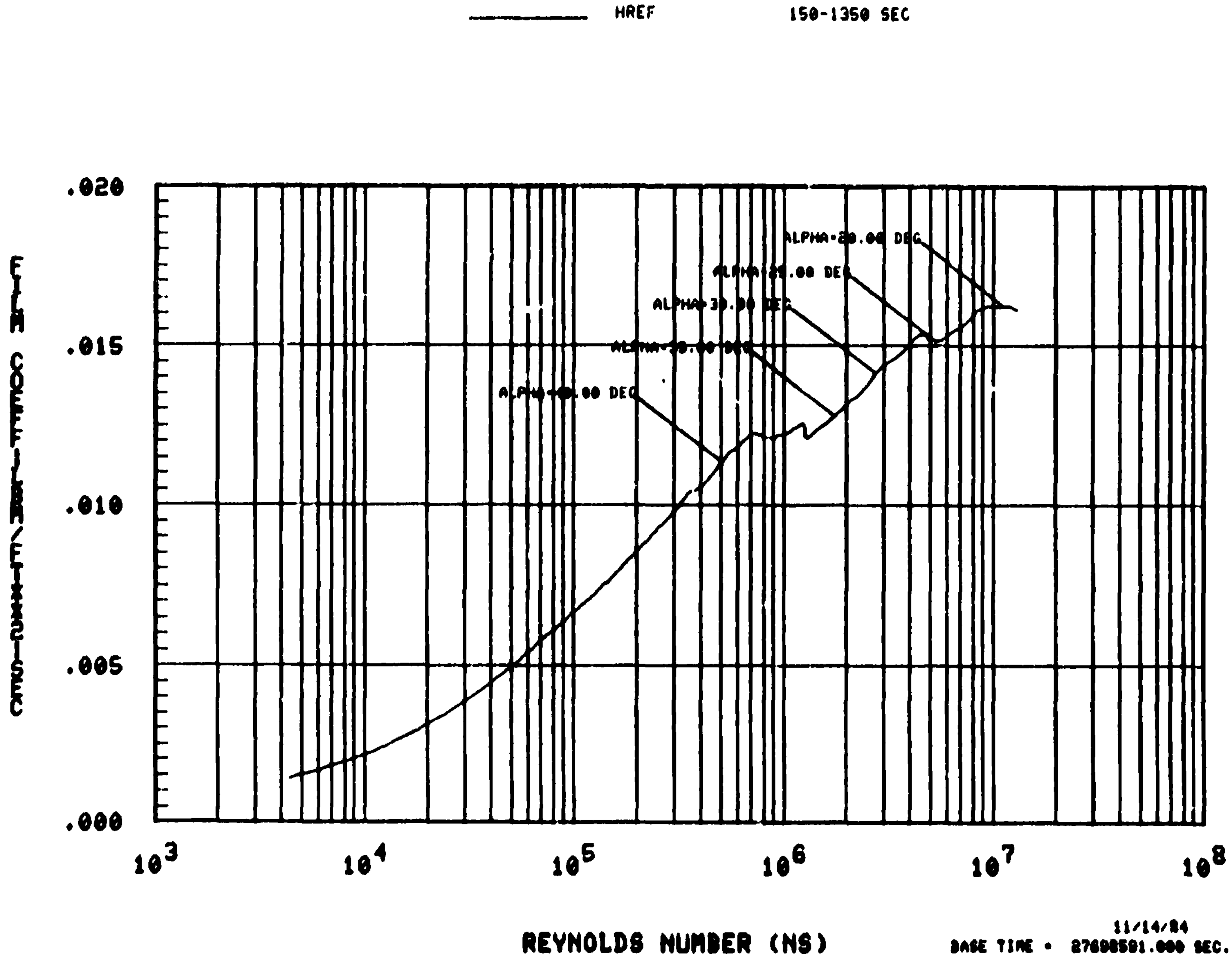

APPENDIX B

HEATING RATE COMPARISON -

INFLUENCE OF REYOLDS NUMBER

(40° ANGLE OF ATTACK) - INDIVIDUAL FLIGHTS

STS-2 LOWER CENTERLINE DISTRIBUTION

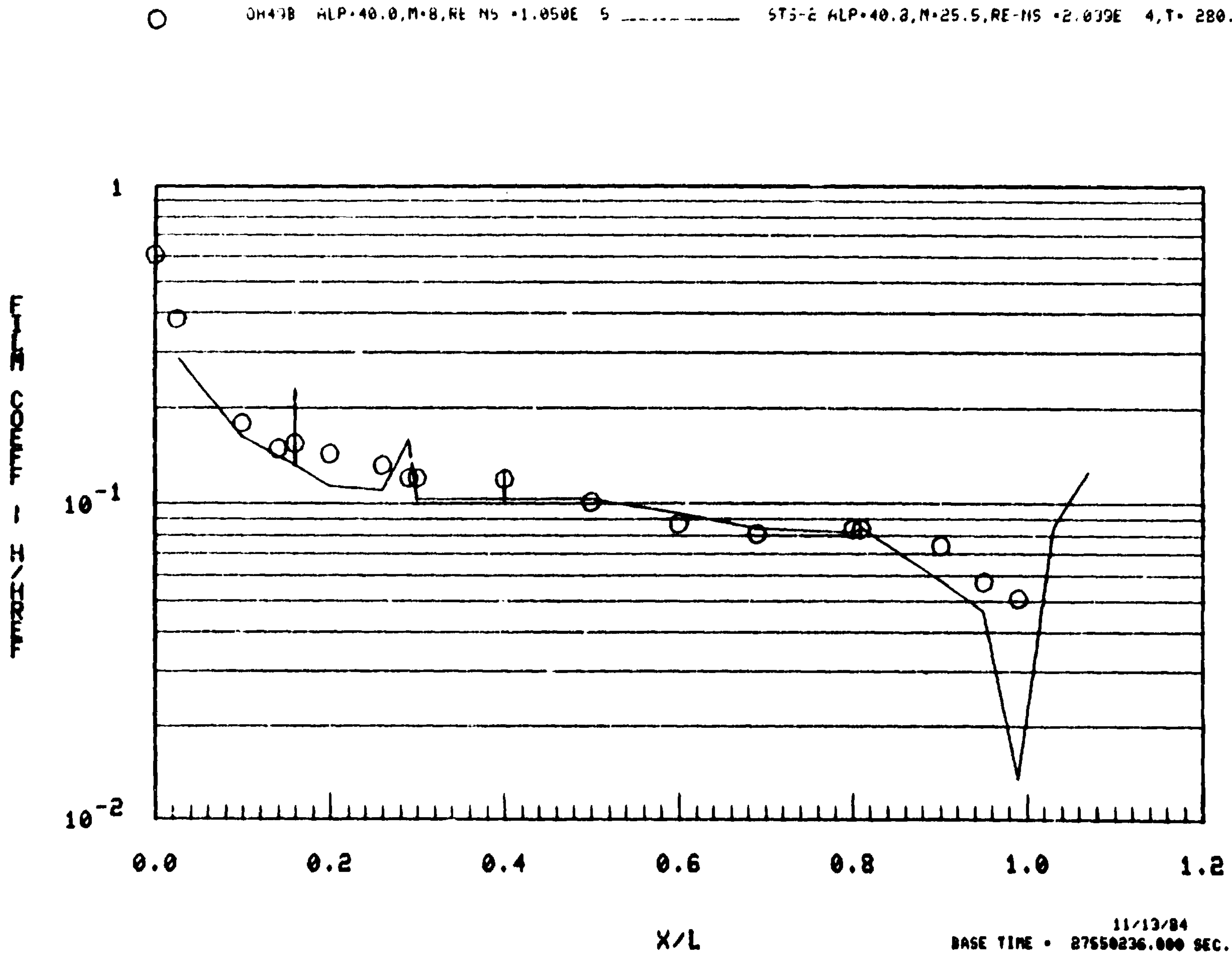

STS-2 LOWER CENTERLINE DISTRIBUTION

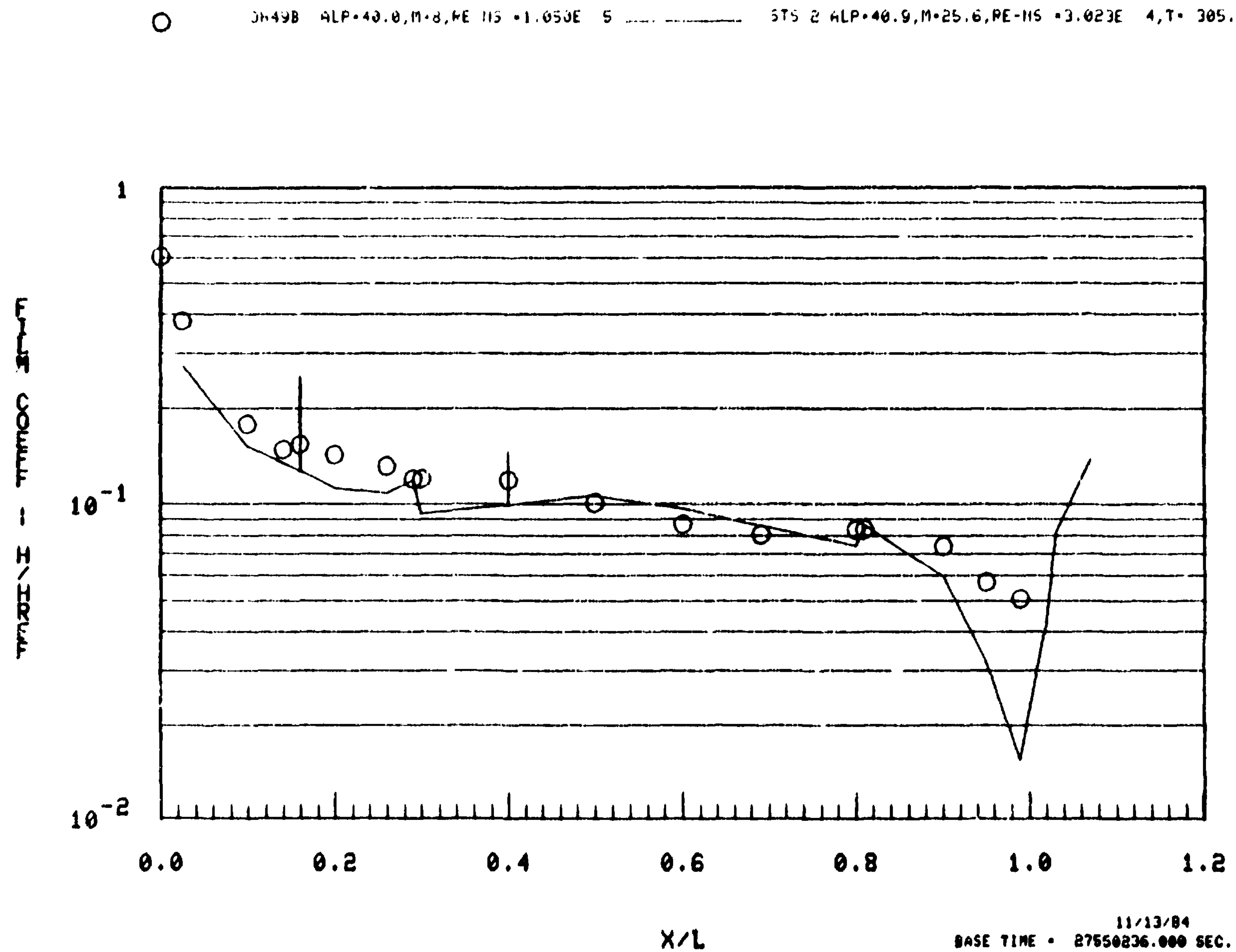

STS-2 LOWER CENTERLINE DISTRIBUTION

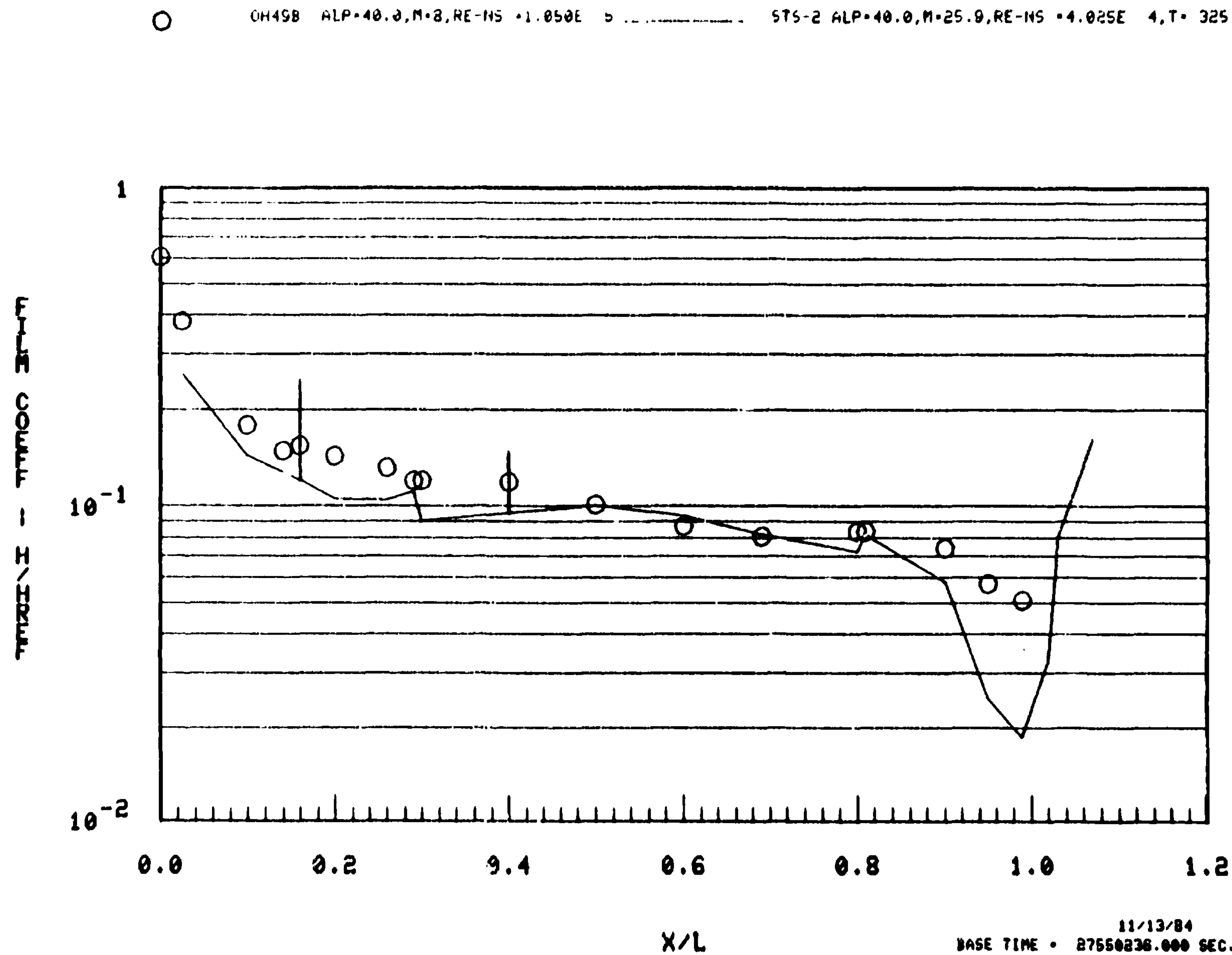

STS-2 LOWER CENTERLINE DISTRIBUTION

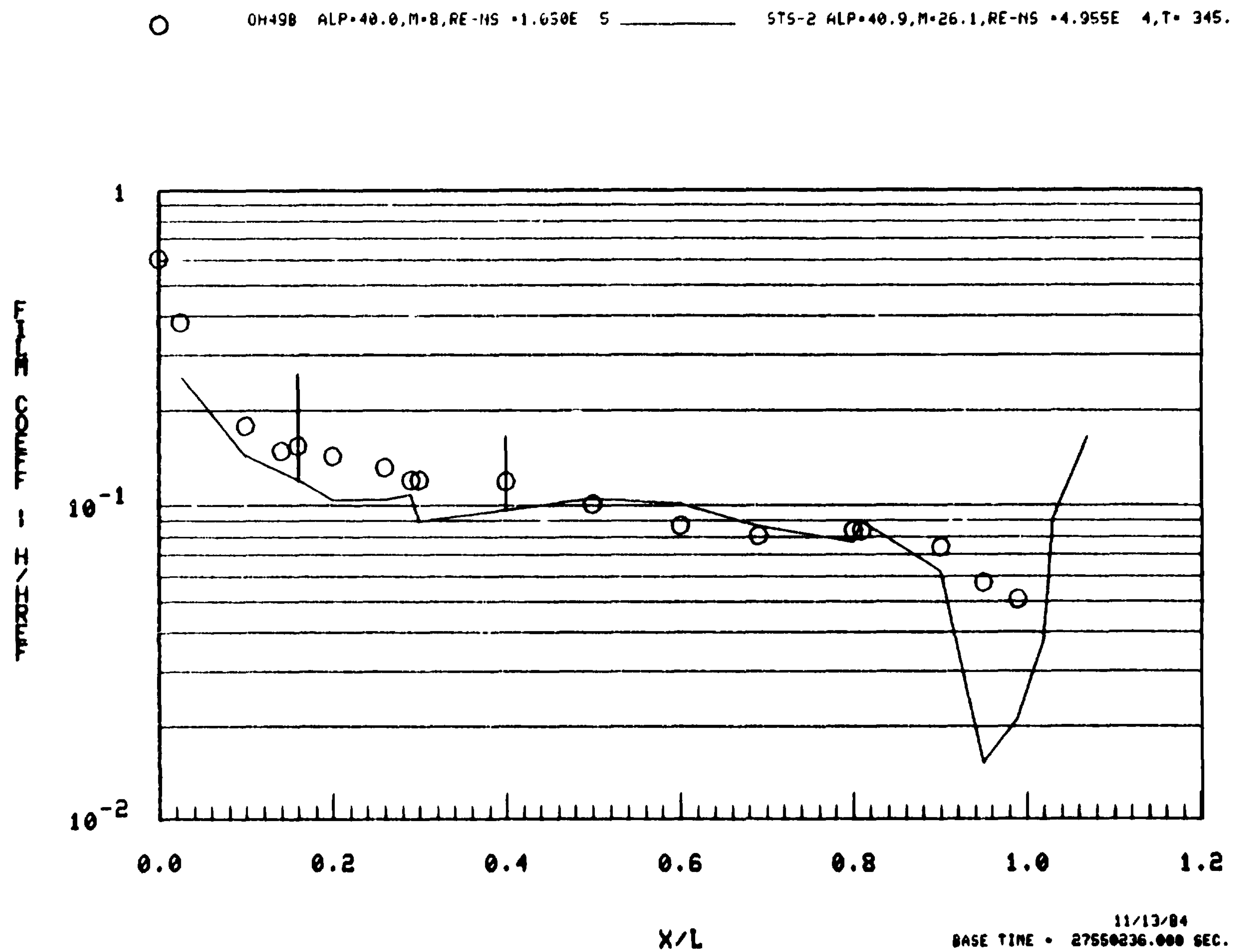

STS-2 LOWER CENTERLINE DISTRIBUTION

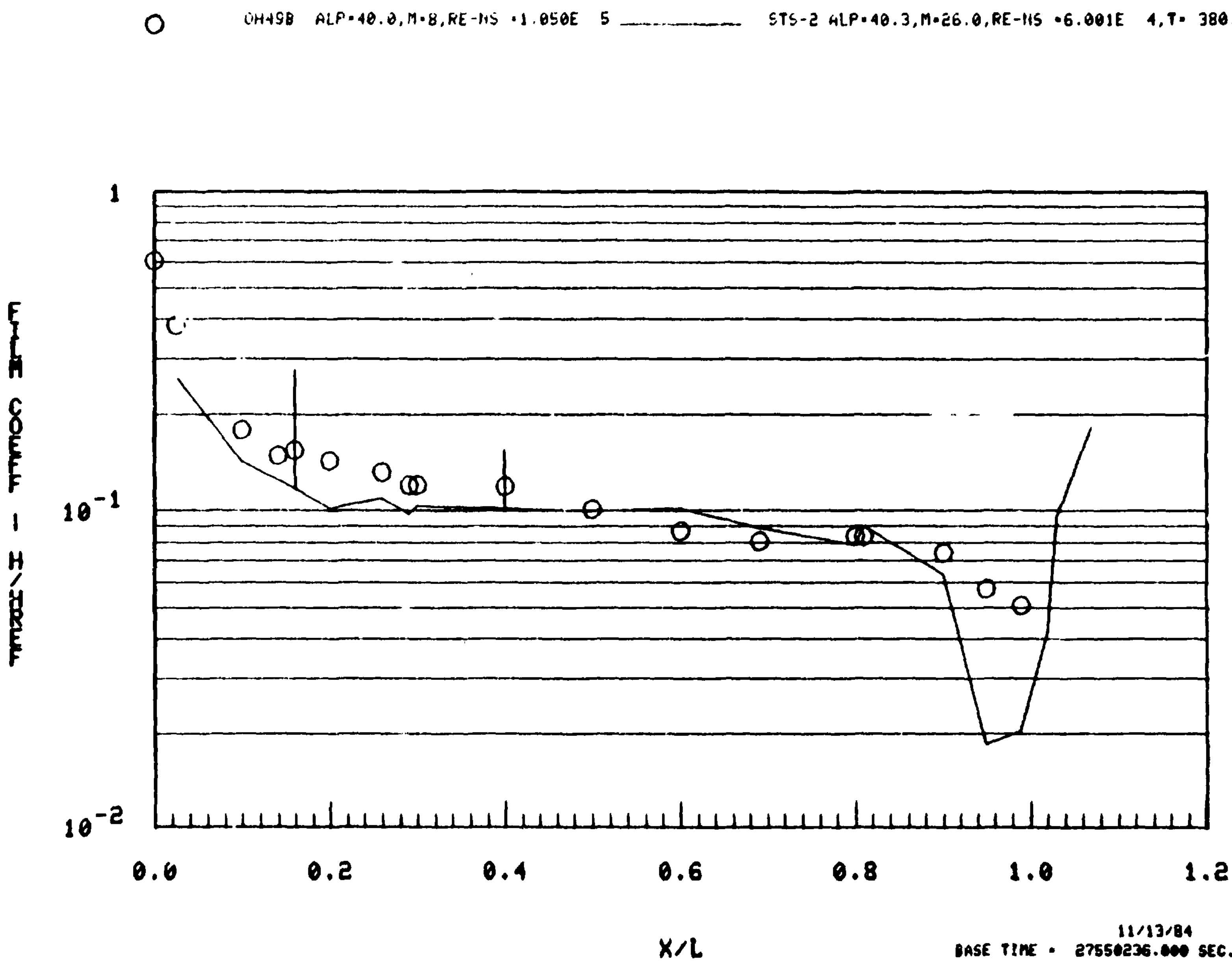

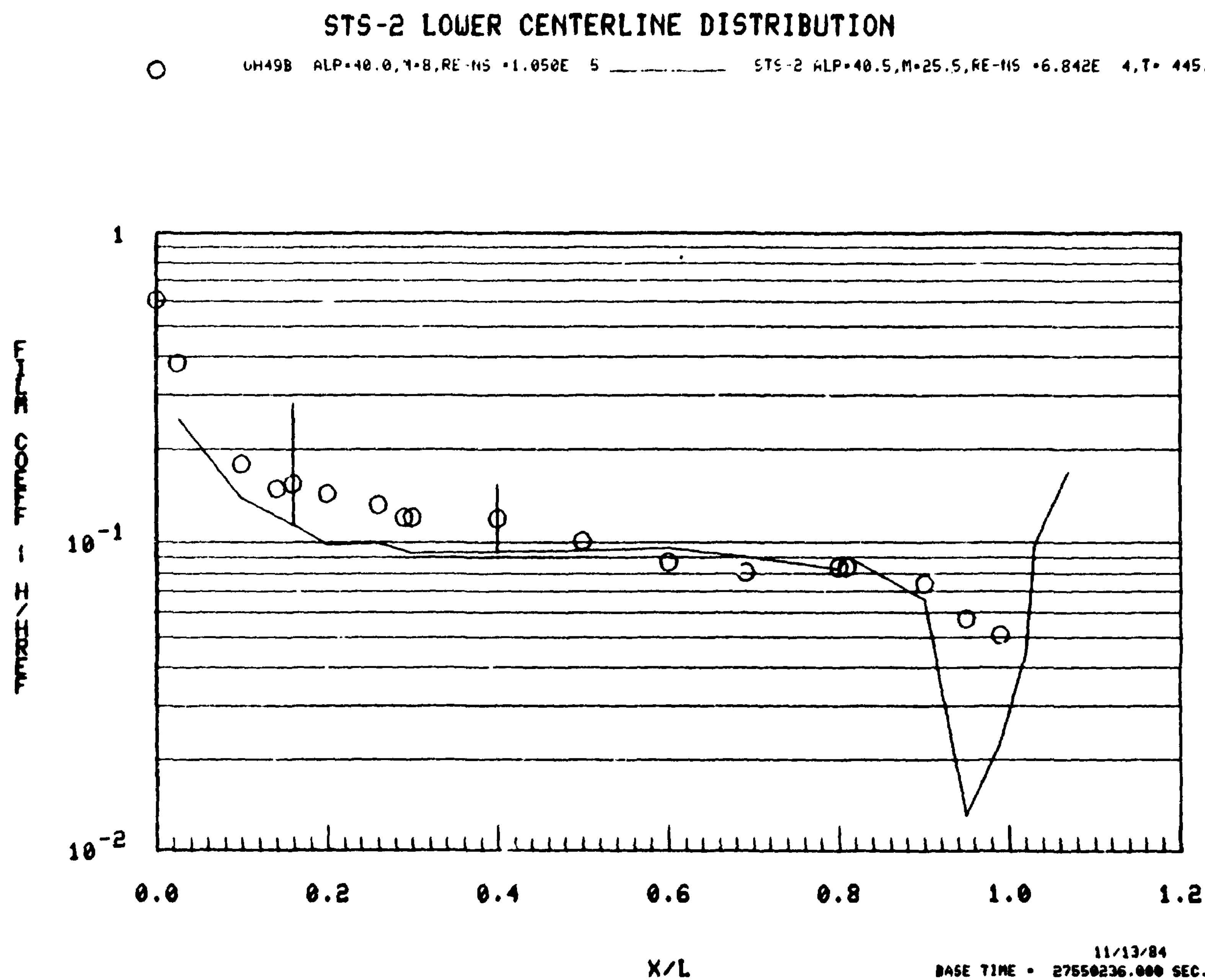
STS-2 LOWER CENTERLINE DISTRIBUTION
UH49B ALP=40.0,M=8,RE-NS =1.050E 5
STS-2 ALP=40.5,M=25.5,RE-NS =6.842E 4,T= 445.
1
10^-1
10^-2
FILM COEFF : H/HREF
0.0
0.2
0.4
0.6
0.8
1.0
1.2
X/L
11/13/84
BASE TIME = 27550236.000 SEC.

STS-2 LOWER CENTERLINE DISTRIBUTION

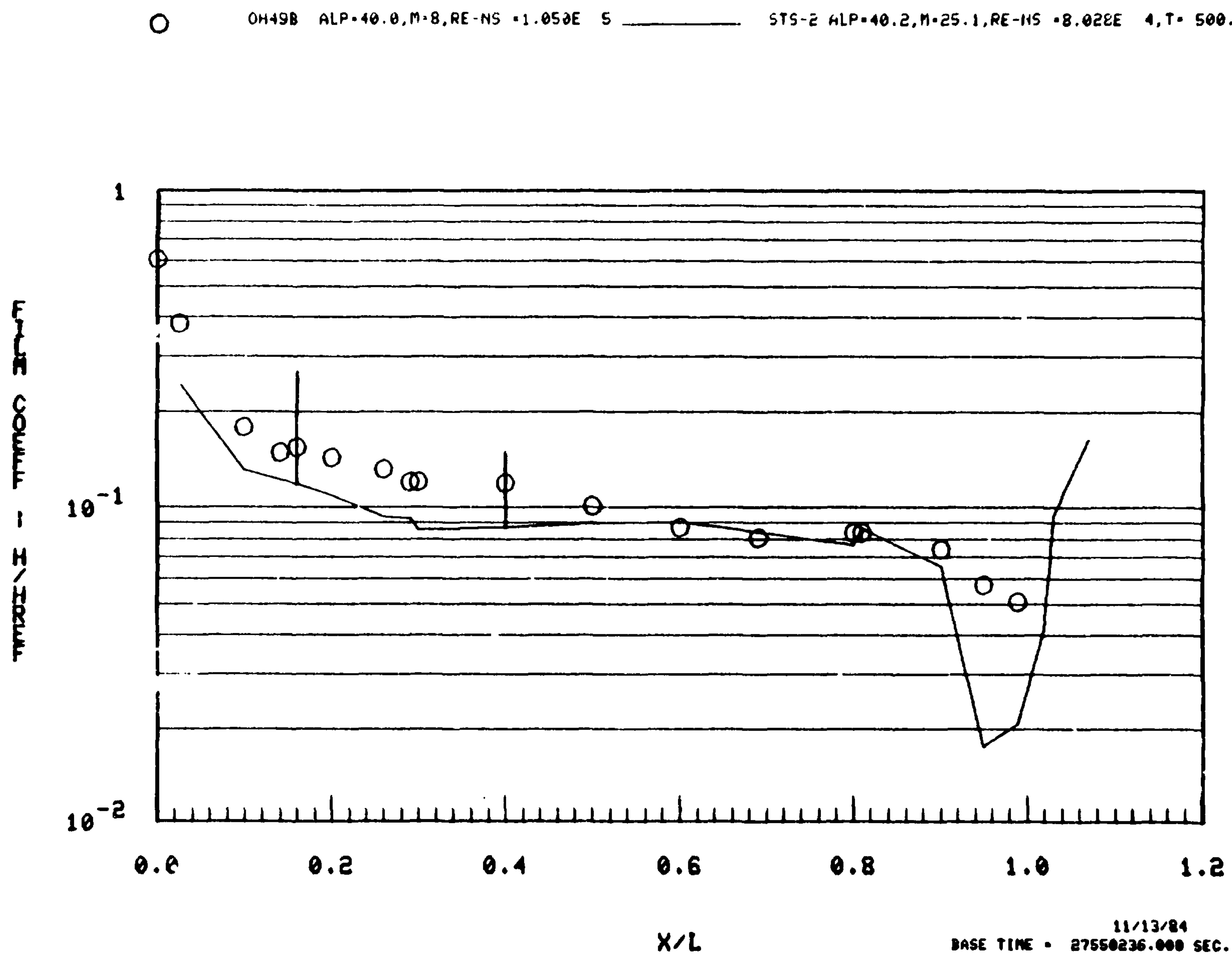

STS-2 LOWER CENTERLINE DISTRIBUTION

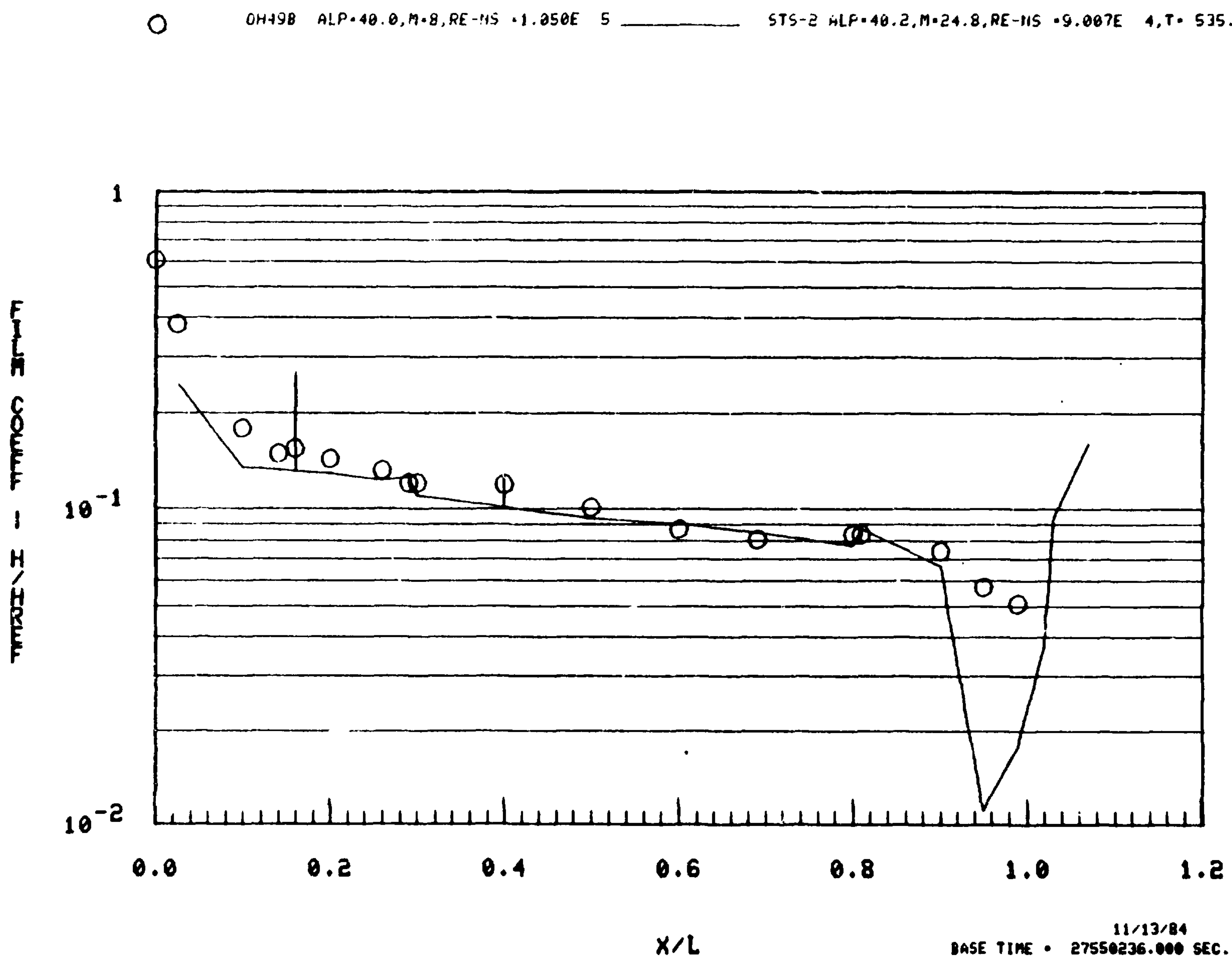

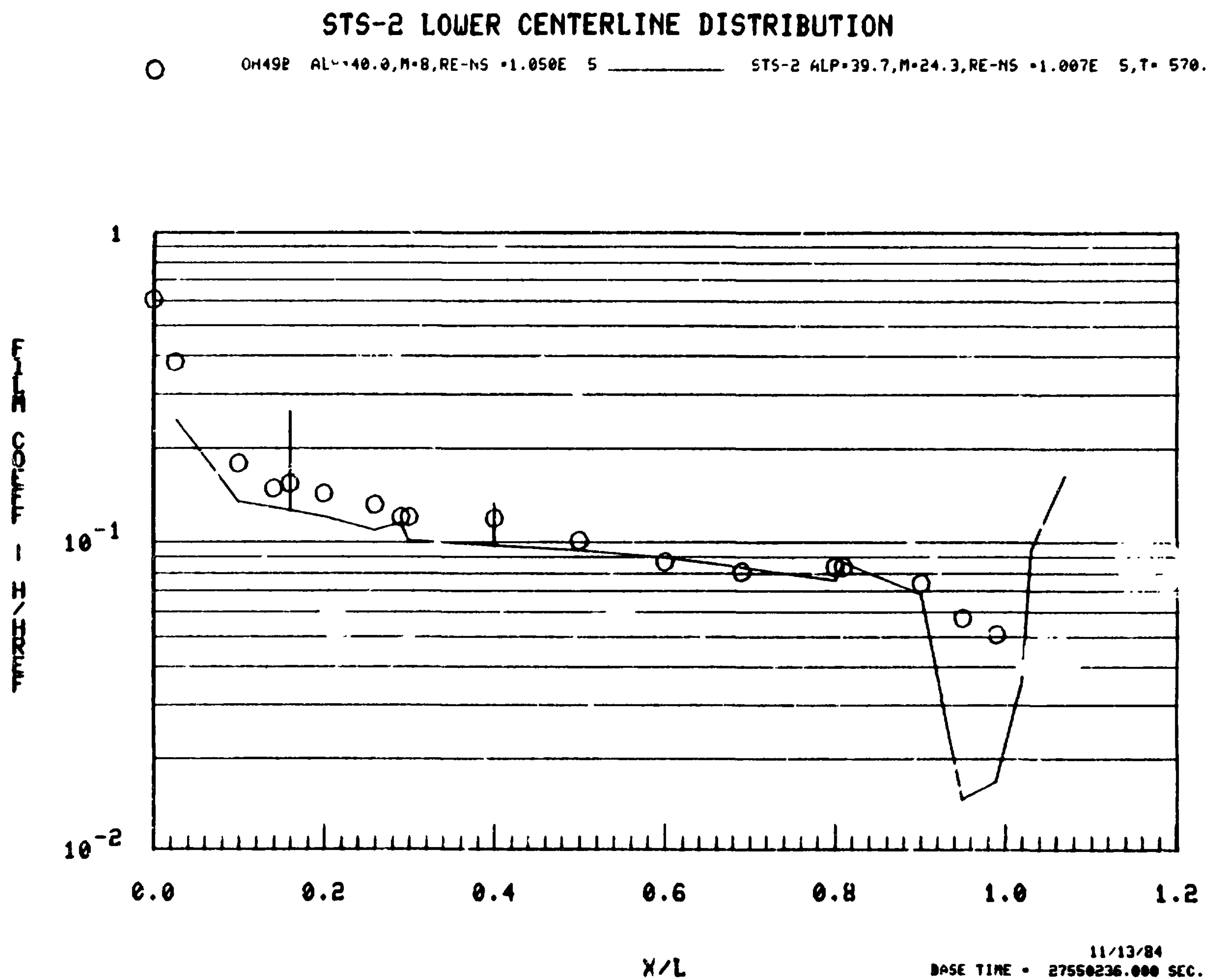
STS-2 LOWER CENTERLINE DISTRIBUTION
OH492 AL=40.0,M=8,RE-NS =1.050E 5
STS-2 ALP=39.7,M=24.3,RE-NS =1.007E 5,T= 570.
FILM COEFF - H/HREF
1
10^{-1}
10^{-2}
0.0
0.2
0.4
0.6
0.8
1.0
1.2
X/L
11/13/84
BASE TIME = 27550236.000 SEC.

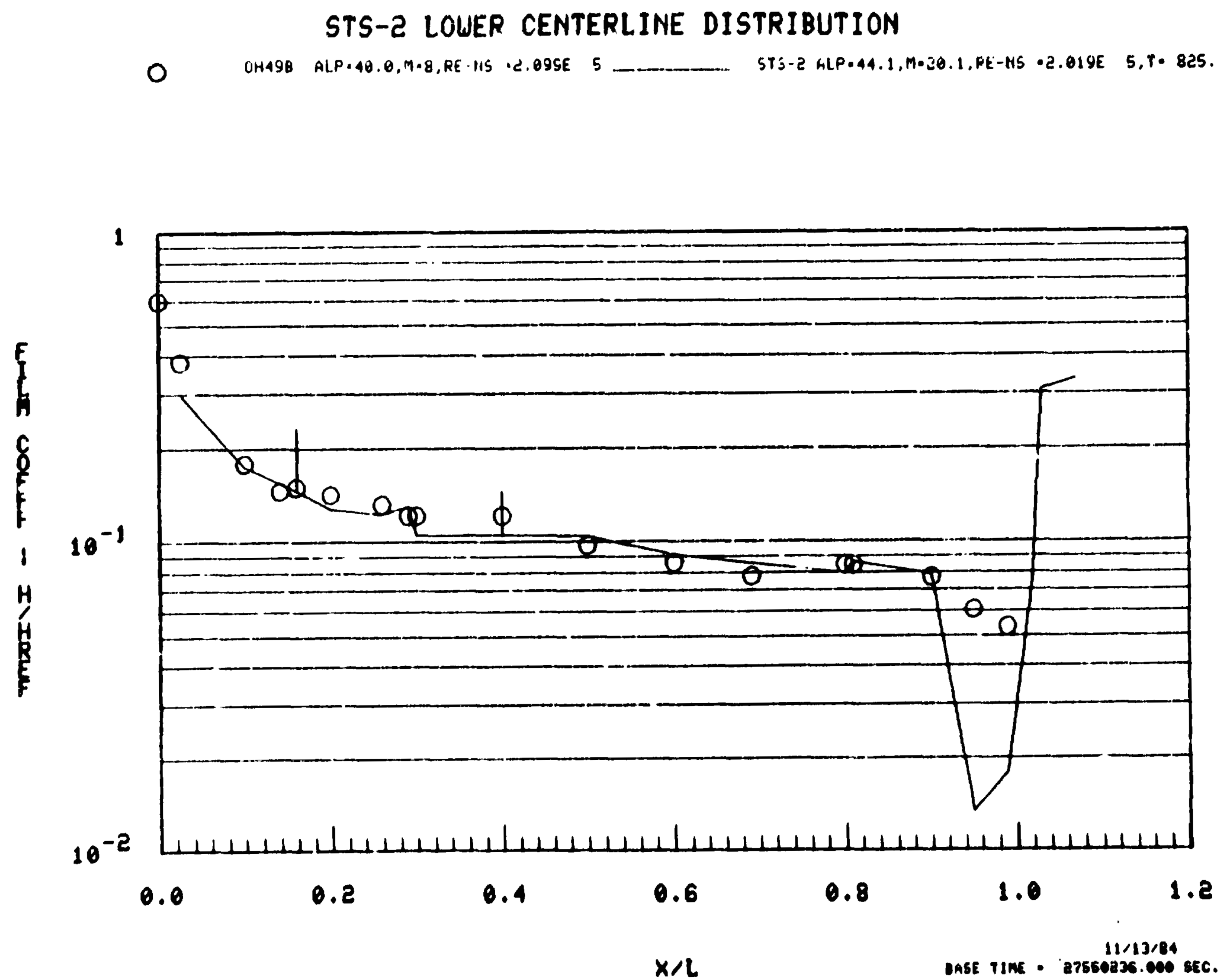

STS-2 LOWER CENTERLINE DISTRIBUTION
OH49B ALP=40.0,M=8,RE-NS =2.095E 5
STS-2 ALP=44.1,M=20.1,RE-NS =2.019E 5,T= 825.
1
10⁻¹
10⁻²
FILM COEFF : H/HREF
0.0
0.2
0.4
0.6
0.8
1.0
1.2
X/L
11/13/84
BASE TIME = 27560236.000 SEC.

STS-2 LOWER CENTERLINE DISTRIBUTION

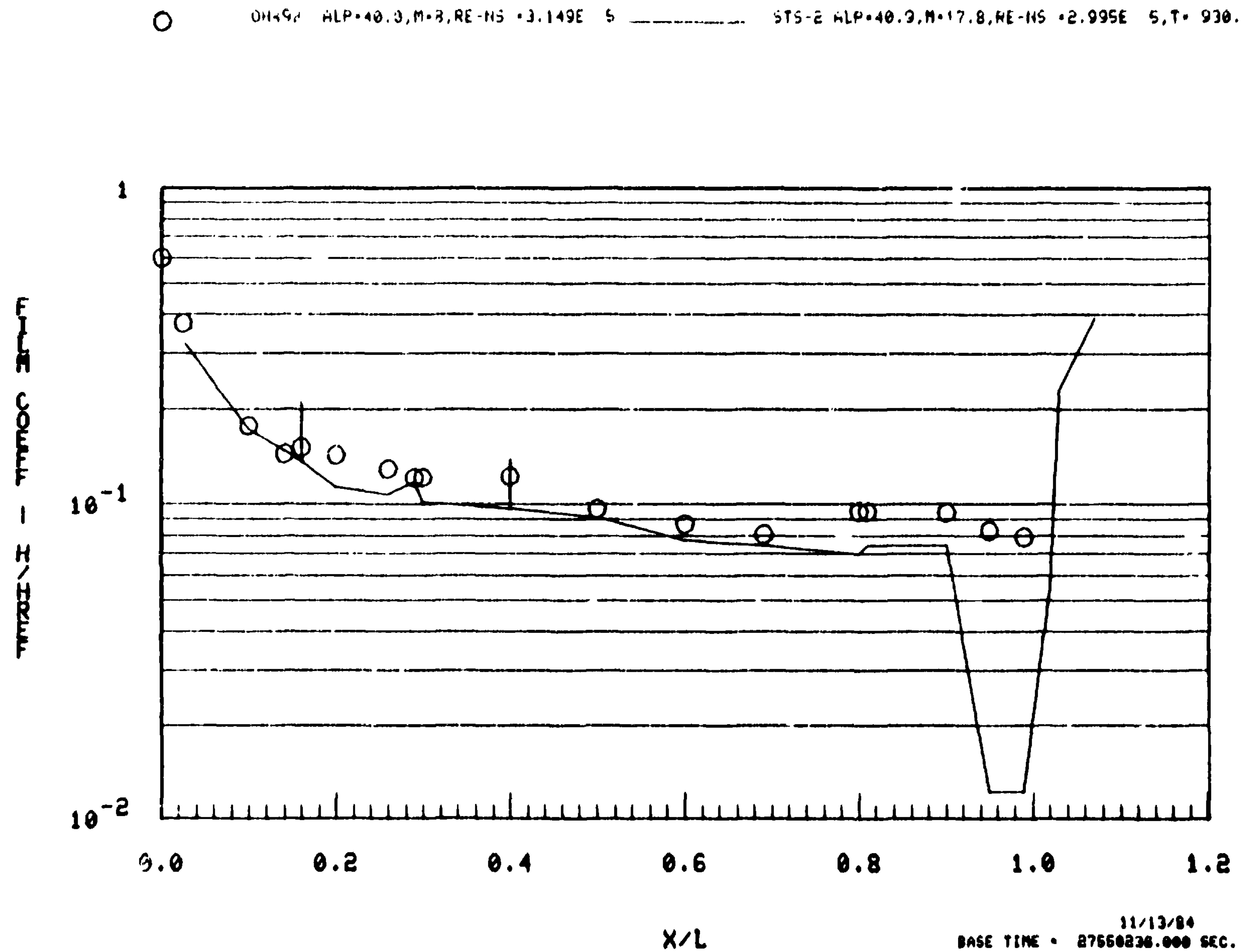

STS-2 LOWER CENTERLINE DISTRIBUTION

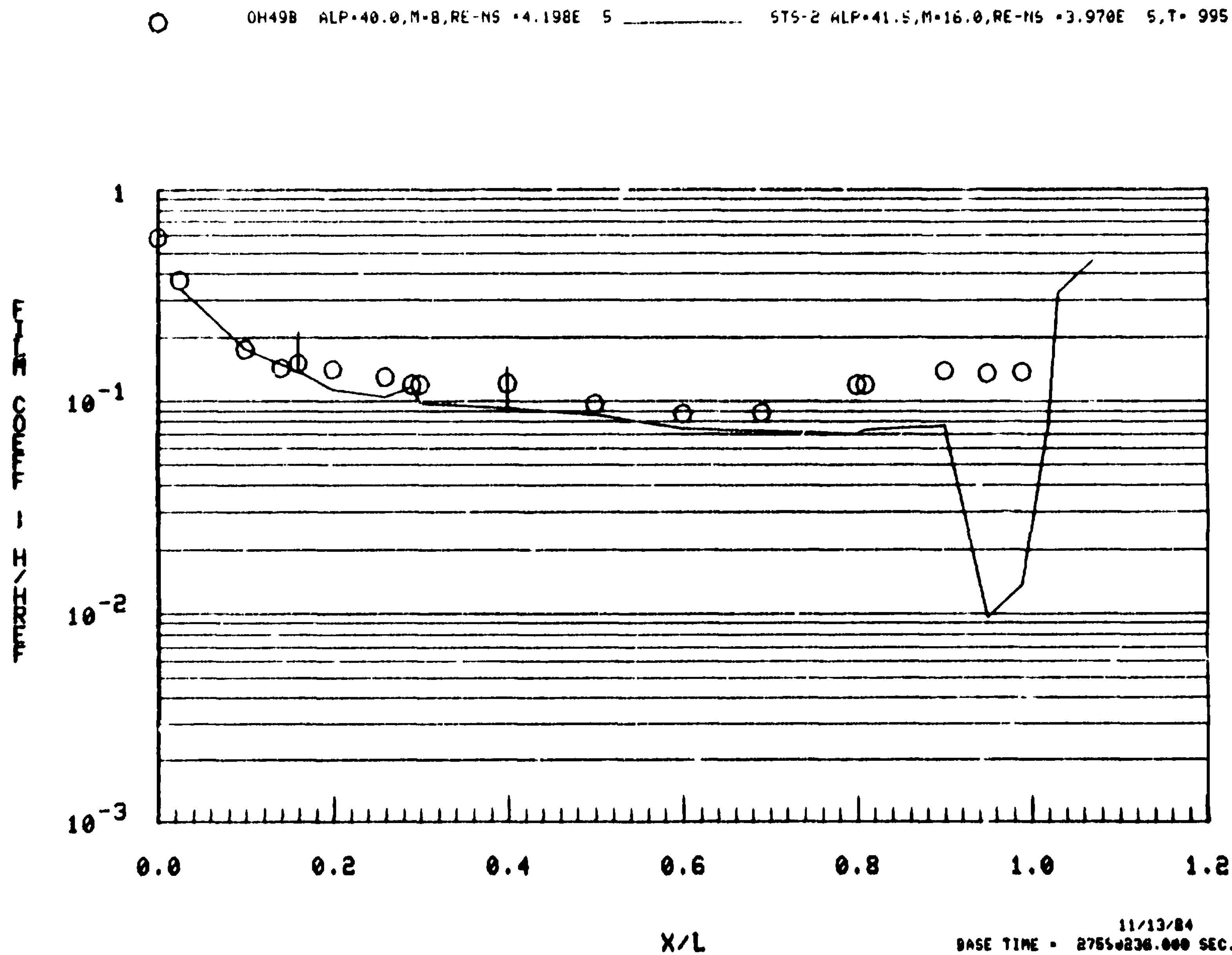

STS-2 LOWER CENTERLINE DISTRIBUTION

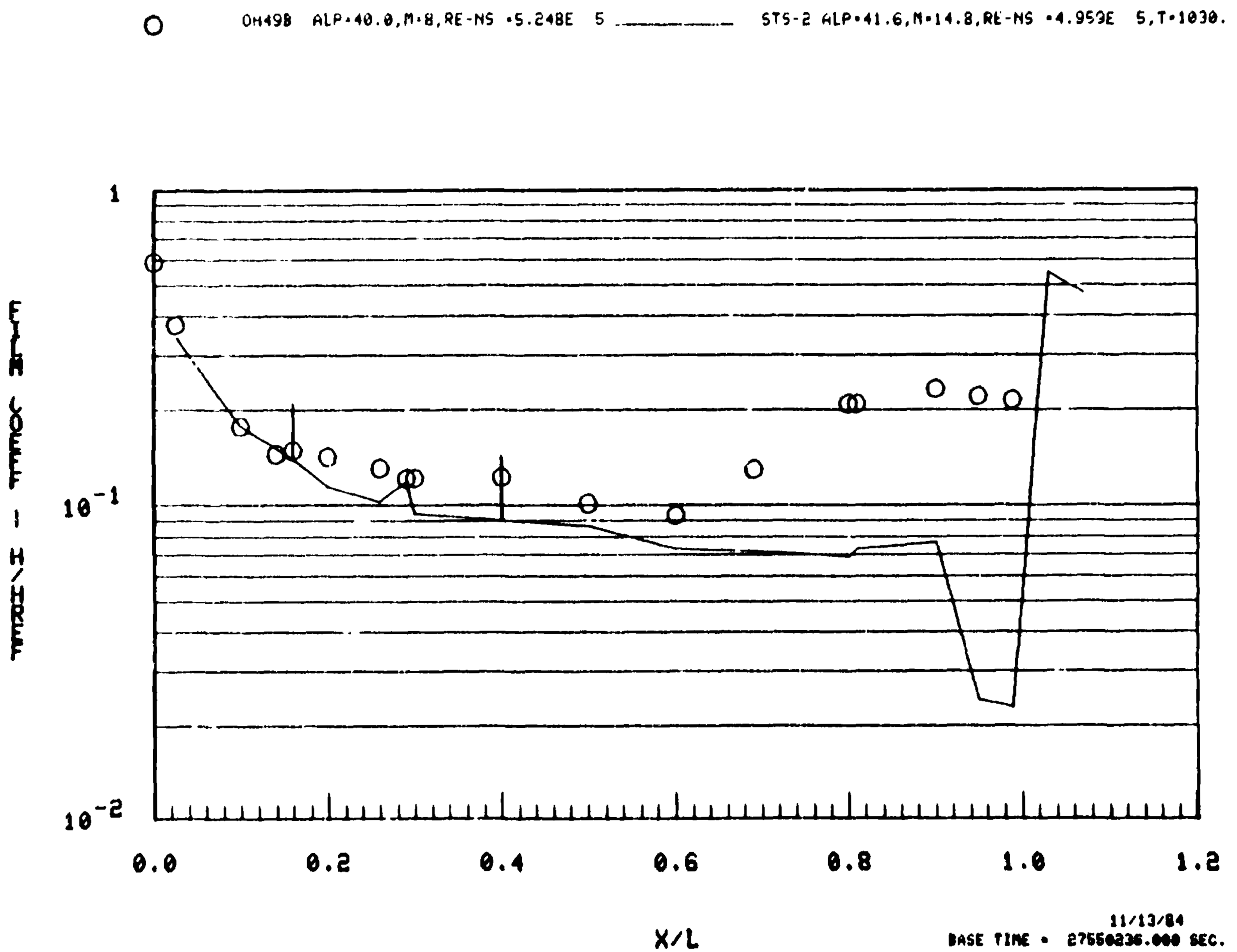

STS-2 LOWER CENTERLINE DISTRIBUTION

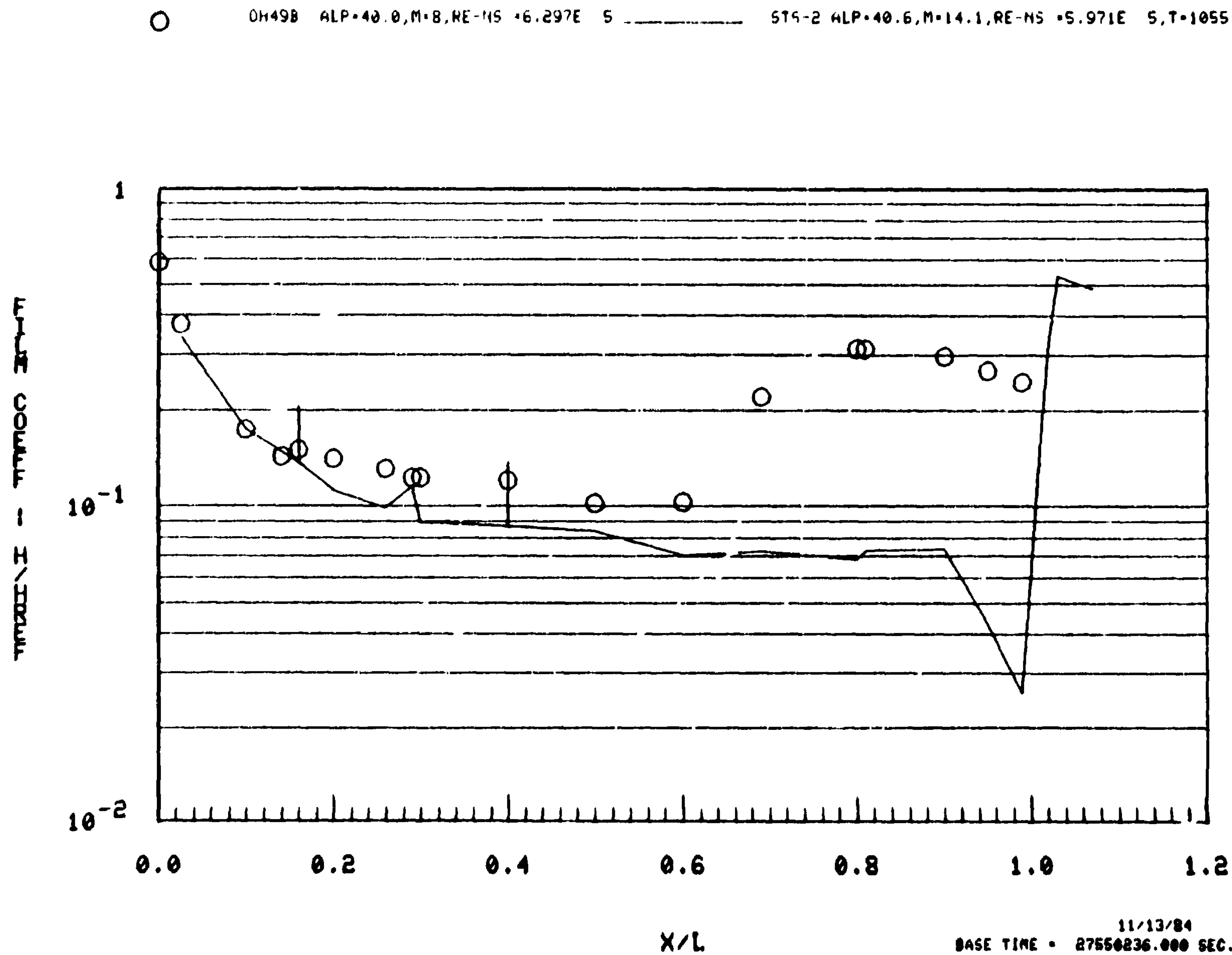

STS-2 LOWER CENTERLINE DISTRIBUTION

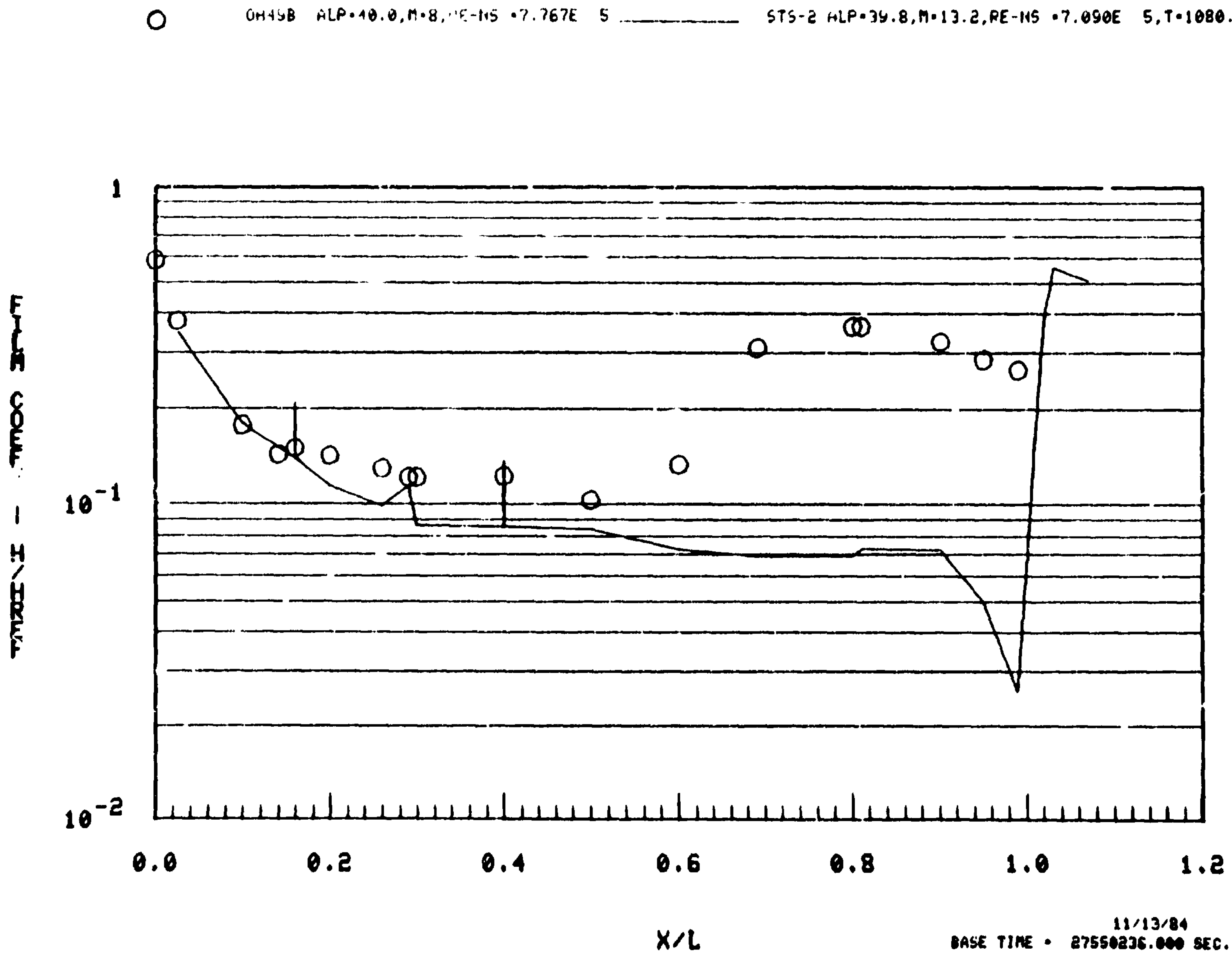

STS-2 LOWER CENTERLINE DISTRIBUTION

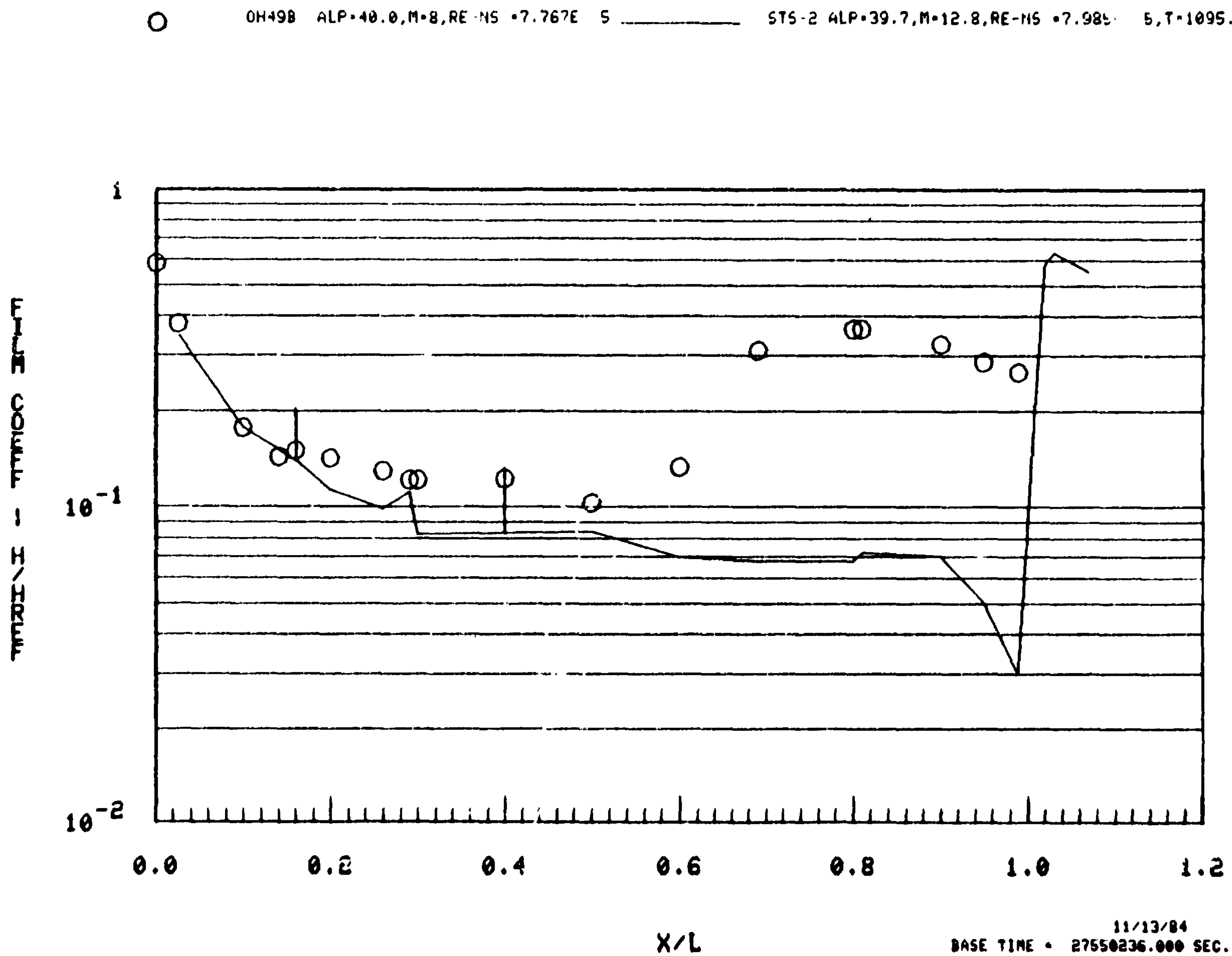

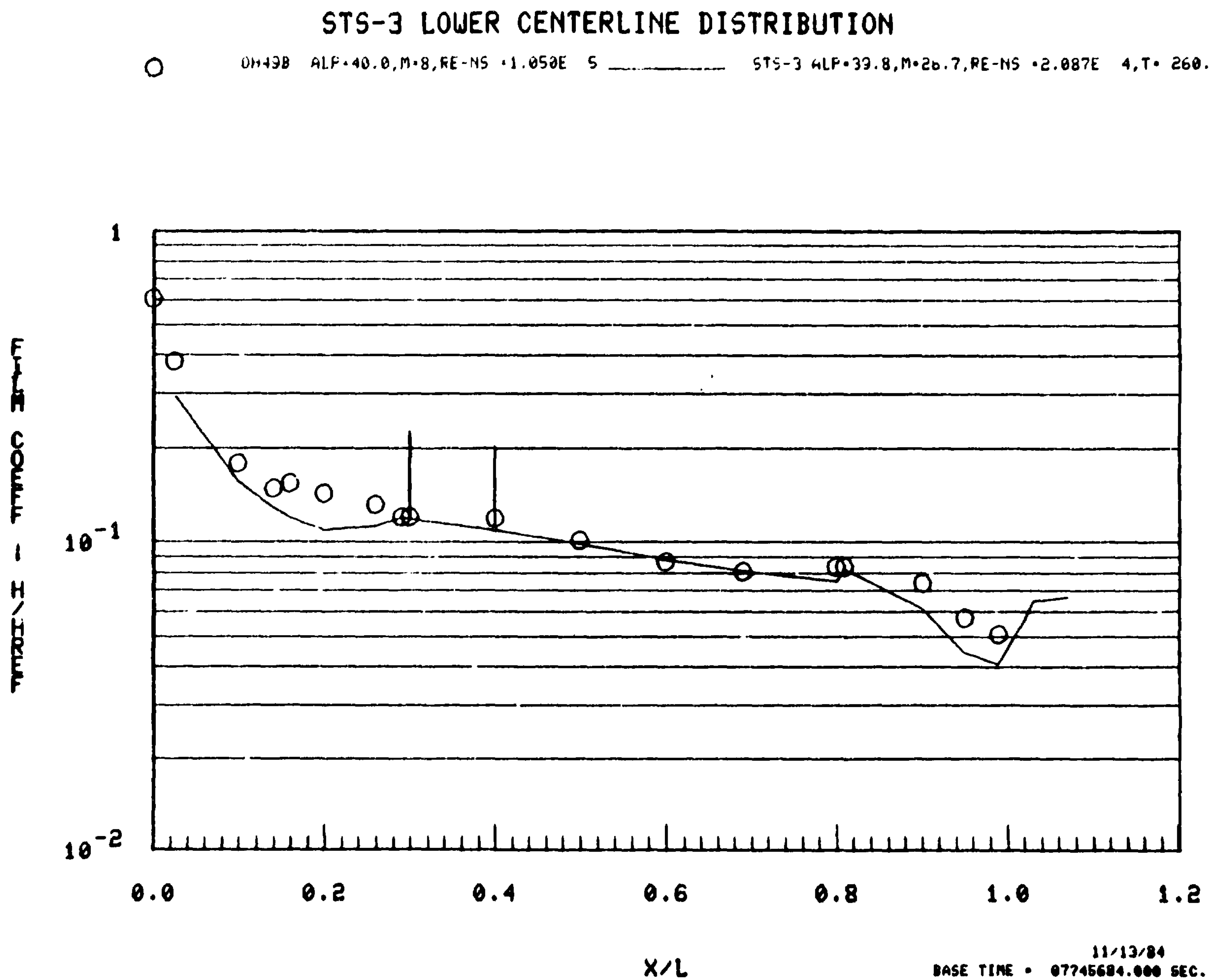

STS-3 LOWER CENTERLINE DISTRIBUTION
OH49B ALF=40.0,M=8,RE-NS =1.050E 5
STS-3 ALF=39.8,M=26.7,RE-NS =2.087E 4,T= 260.
1
10^{-1}
10^{-2}
FILM COEFF - H/HREF
0.0
0.2
0.4
0.6
0.8
1.0
1.2
X/L
11/13/84
BASE TIME = 07745684.000 SEC.

STS-3 LOWER CENTERLINE DISTRIBUTION

○ GH49B ALP=40.0,M=8,RE-NS =1.050E 5 ———— STS-3 ALP=40.6,M=27.0,RE-NS =3.142E 4,T= 280.

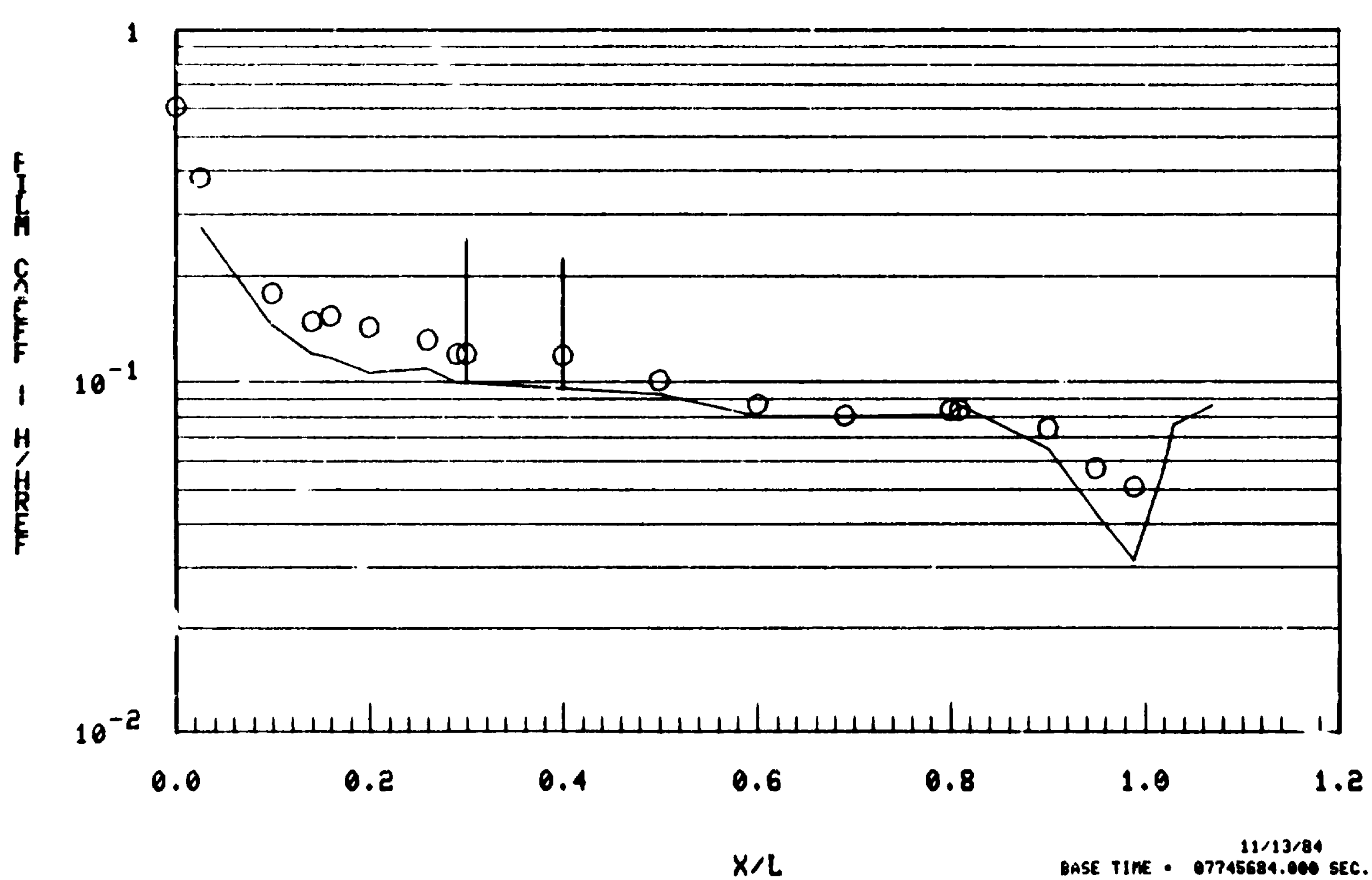

STS-3 LOWER CENTERLINE DISTRIBUTION

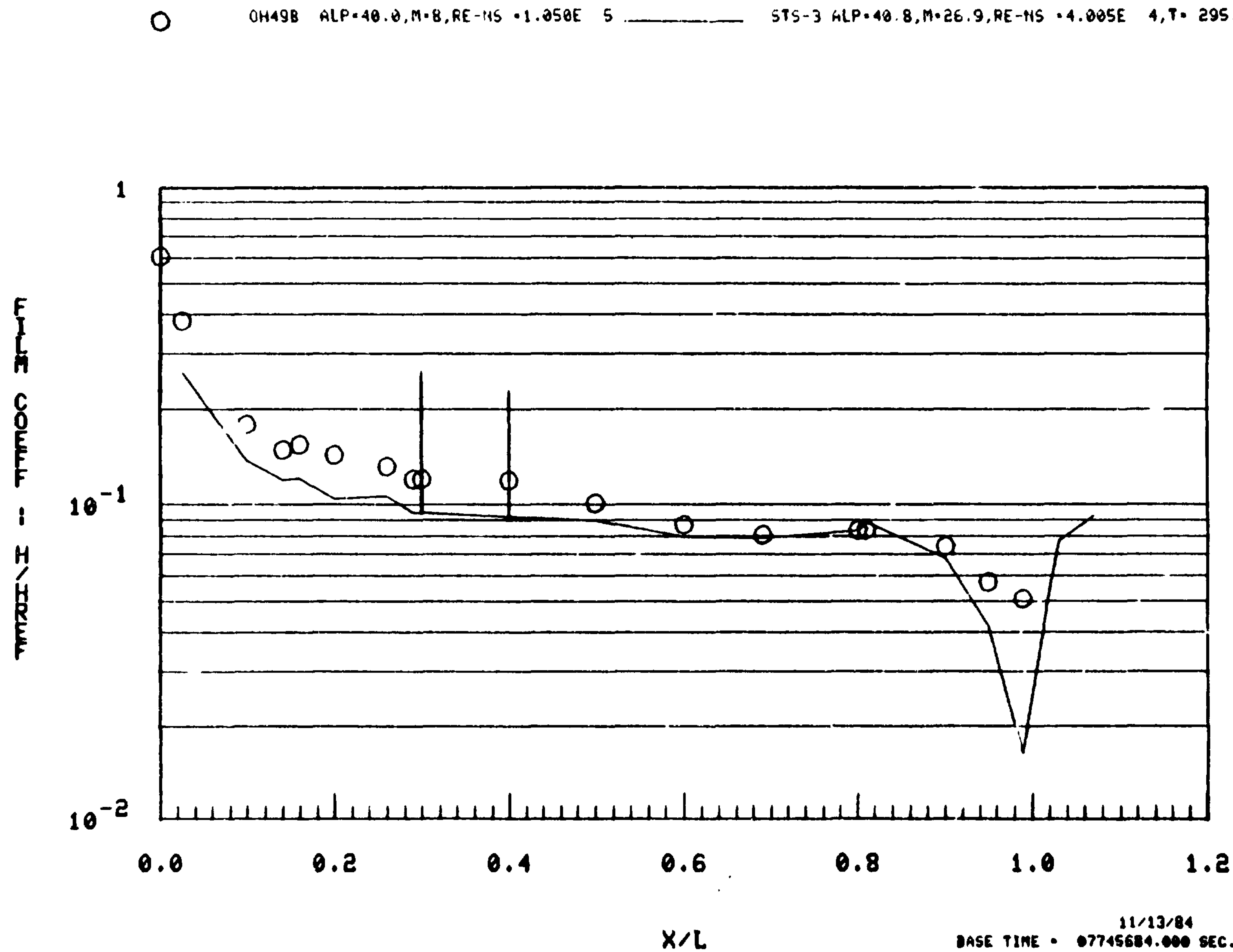

11/13/84
BASE TIME = 07745684.000 SEC.

STS-3 LOWER CENTERLINE DISTRIBUTION

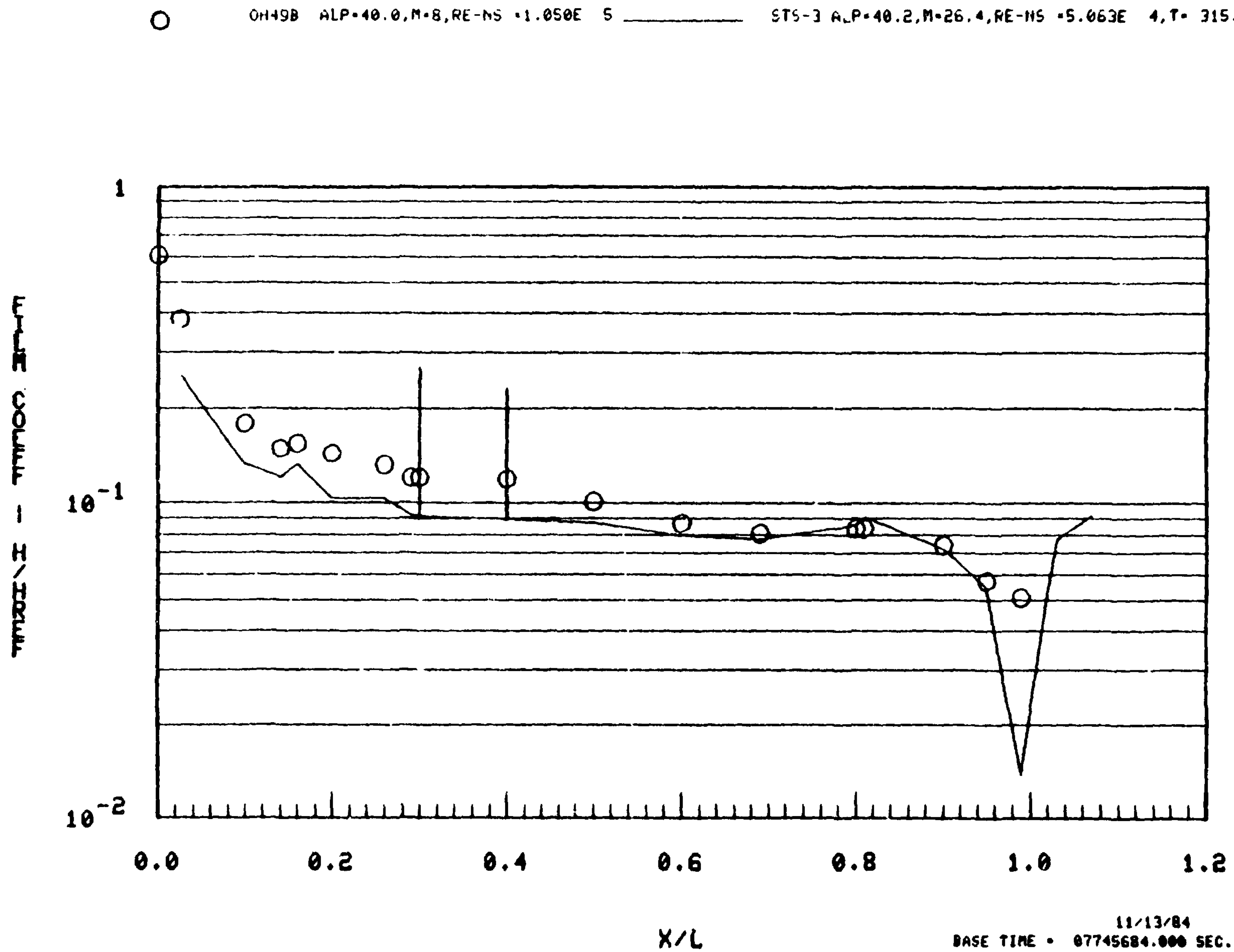

STS-3 LOWER CENTERLINE DISTRIBUTION

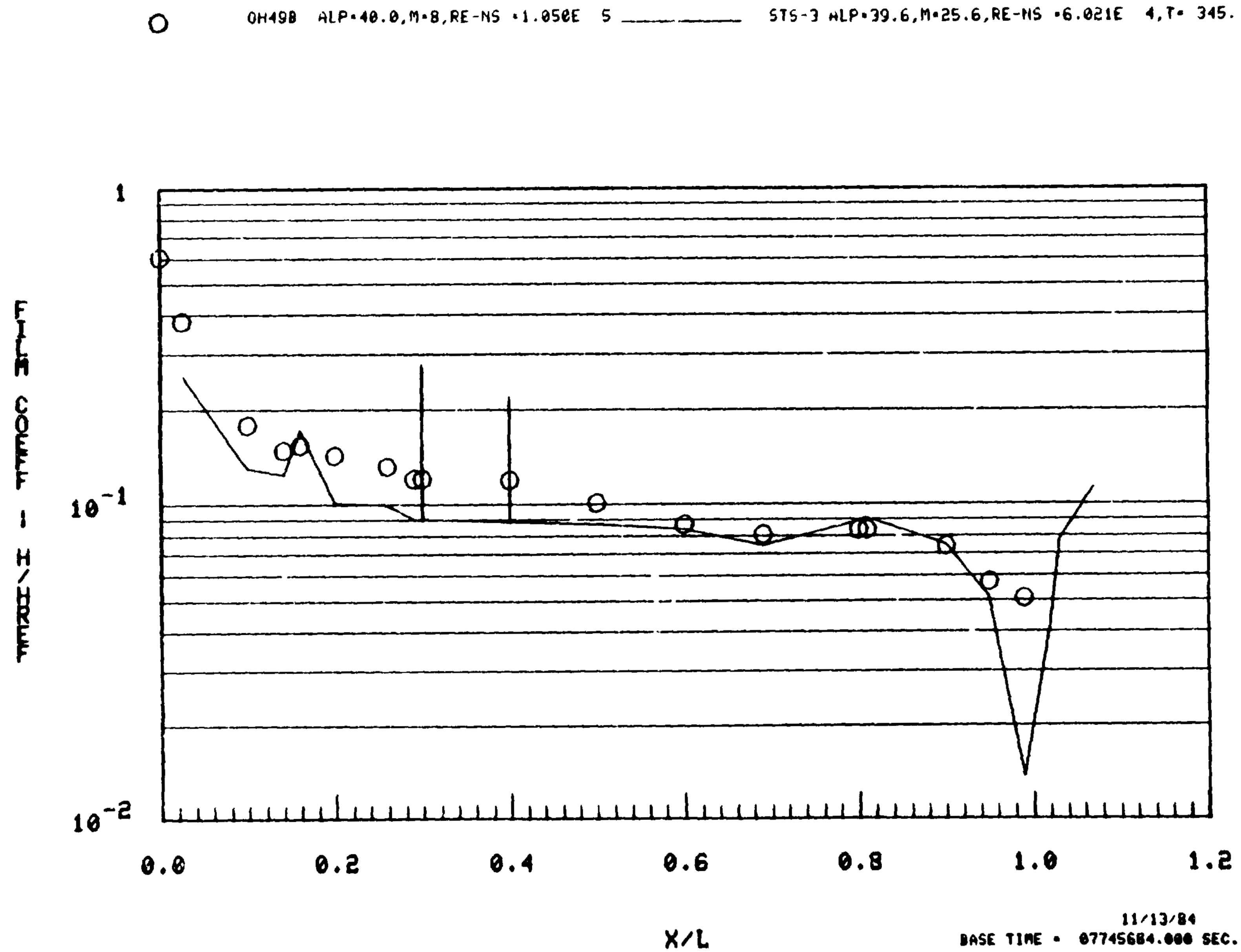

STS-3 LOWER CENTERLINE DISTRIBUTION

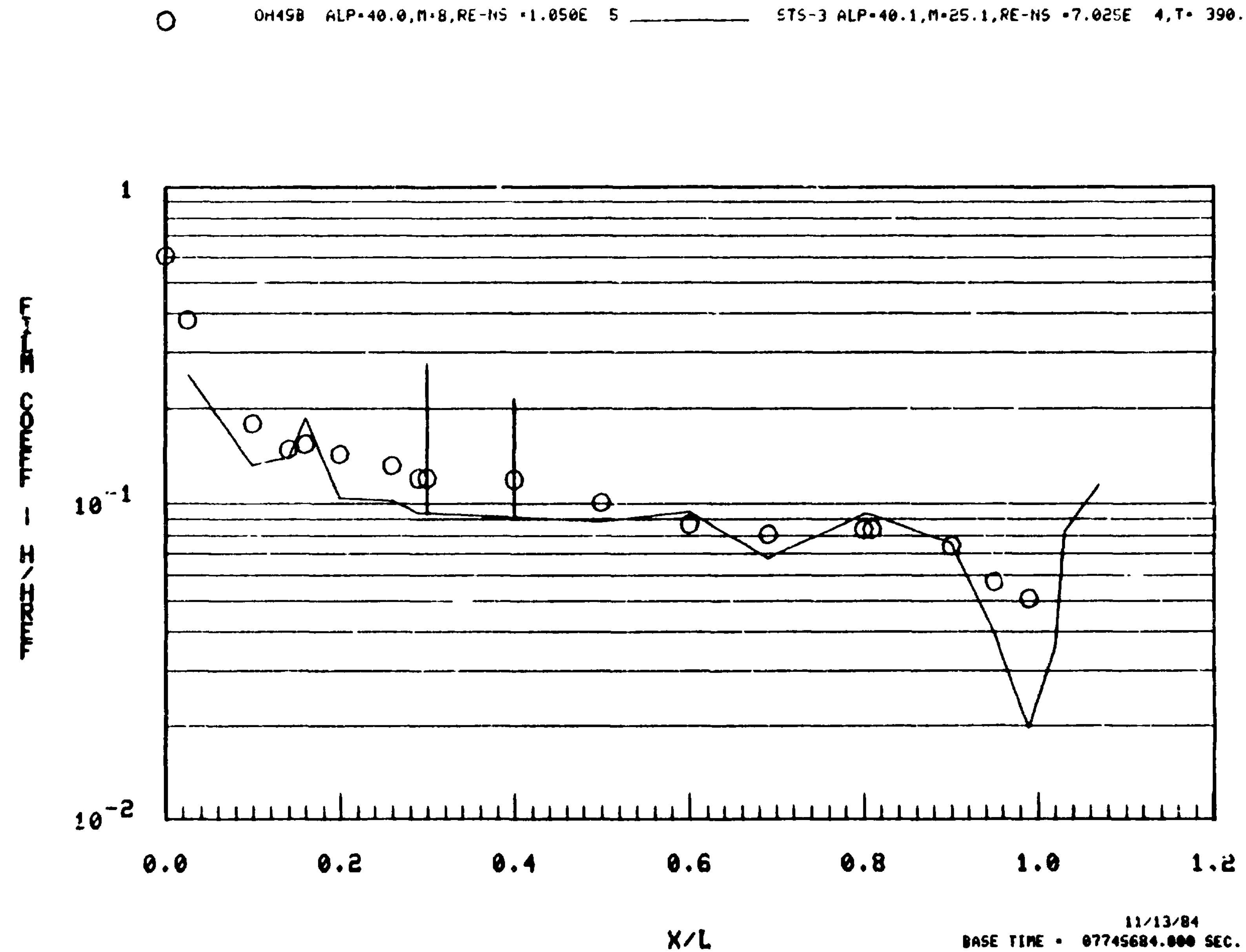

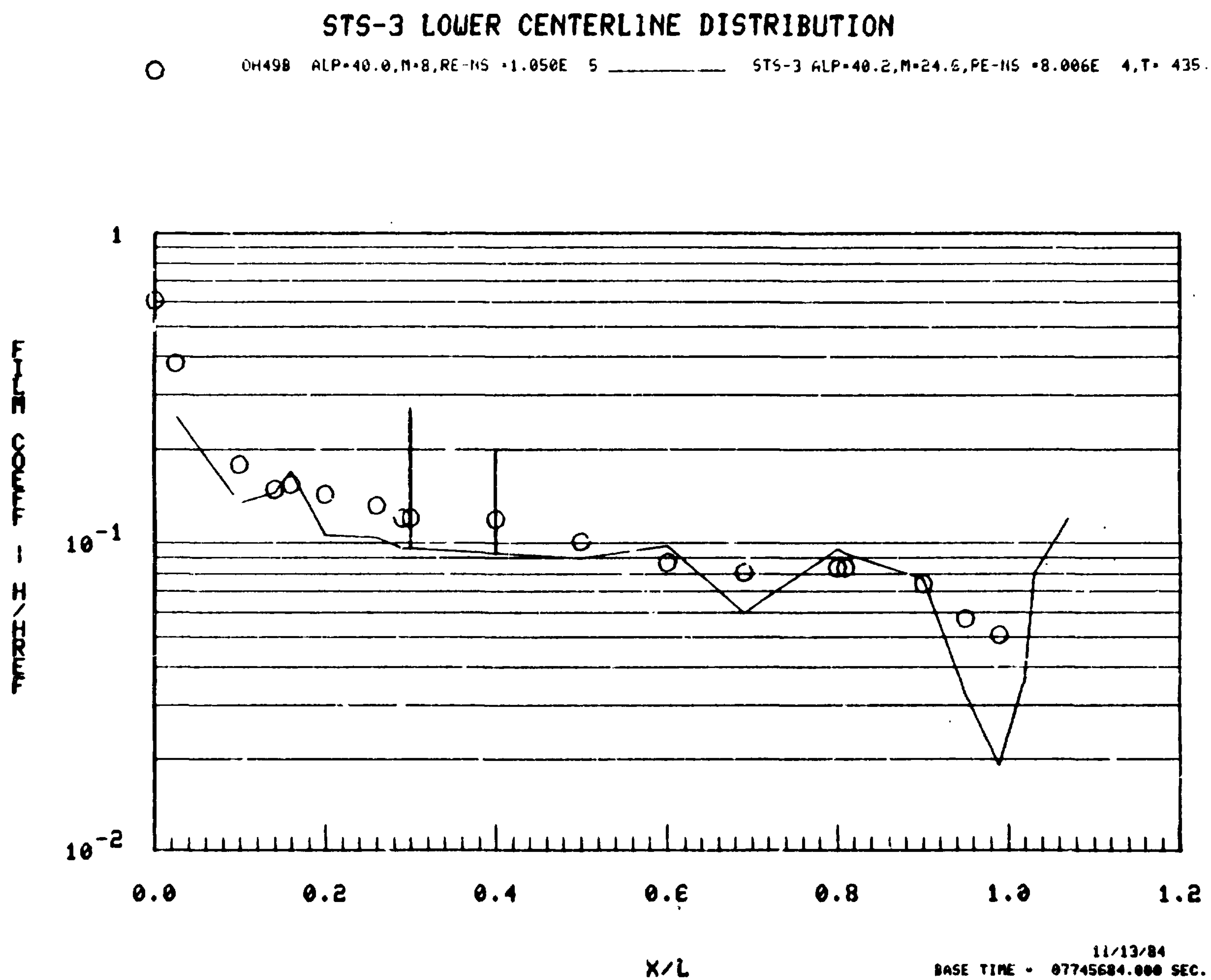

STS-3 LOWER CENTERLINE DISTRIBUTION
OH49B ALP=40.0,M=8,RE-NS =1.050E 5
STS-3 ALP=40.2,M=24.6,RE-NS =8.006E 4,T= 435.
1
10^{-1}
10^{-2}
FILM COEFF - H/HREF
0.0
0.2
0.4
0.6
0.8
1.0
1.2
X/L
11/13/84
BASE TIME = 07745684.000 SEC.

STS-3 LOWER CENTERLINE DISTRIBUTION

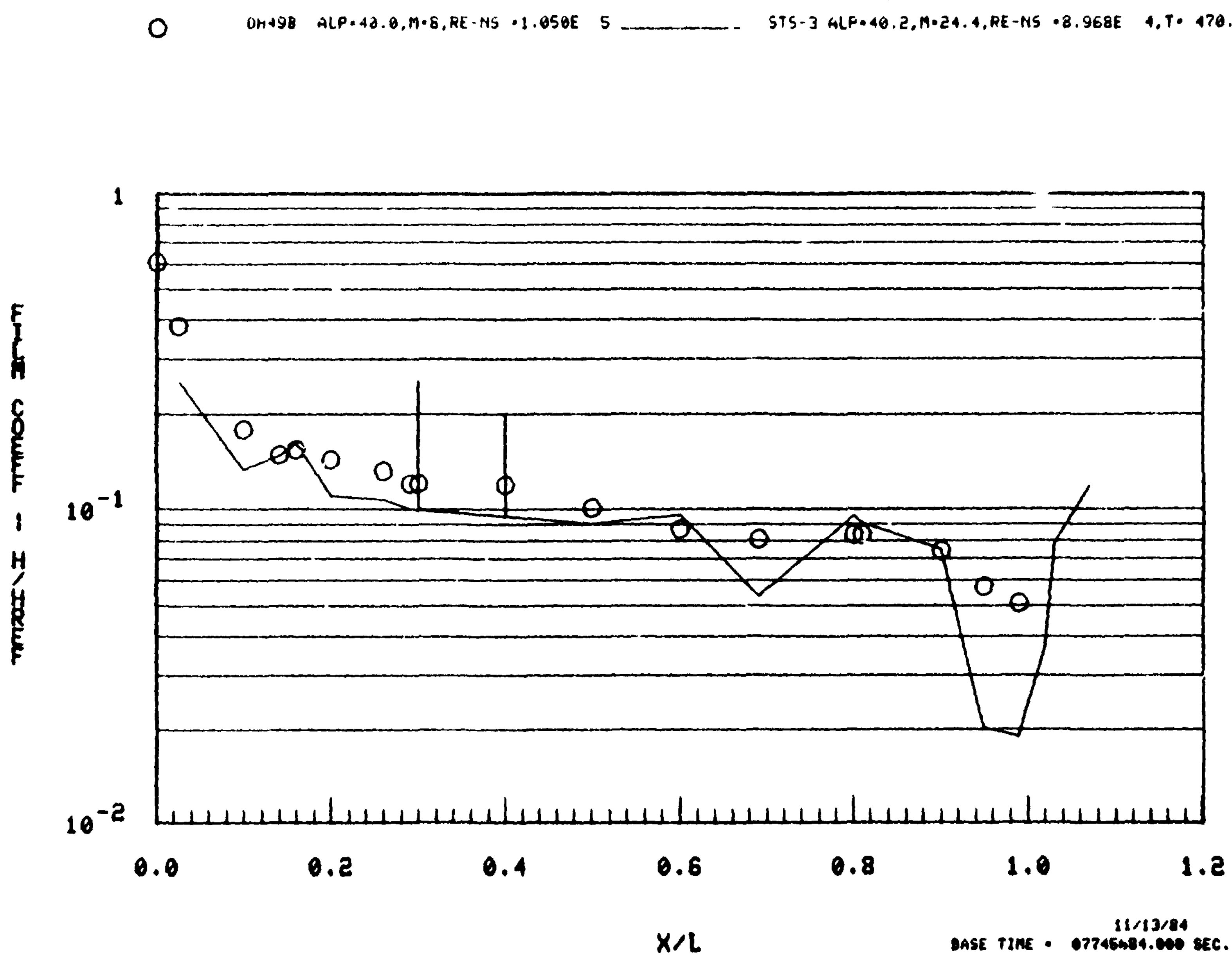

STS-3 LOWER CENTERLINE DISTRIBUTION

○ OH49B ALP=40.0,M=8,RE-NS =1.050E 5 ———— STS-3 ALP=39.6,M=24.1,RE-NS =1.005E 5,T= 505.

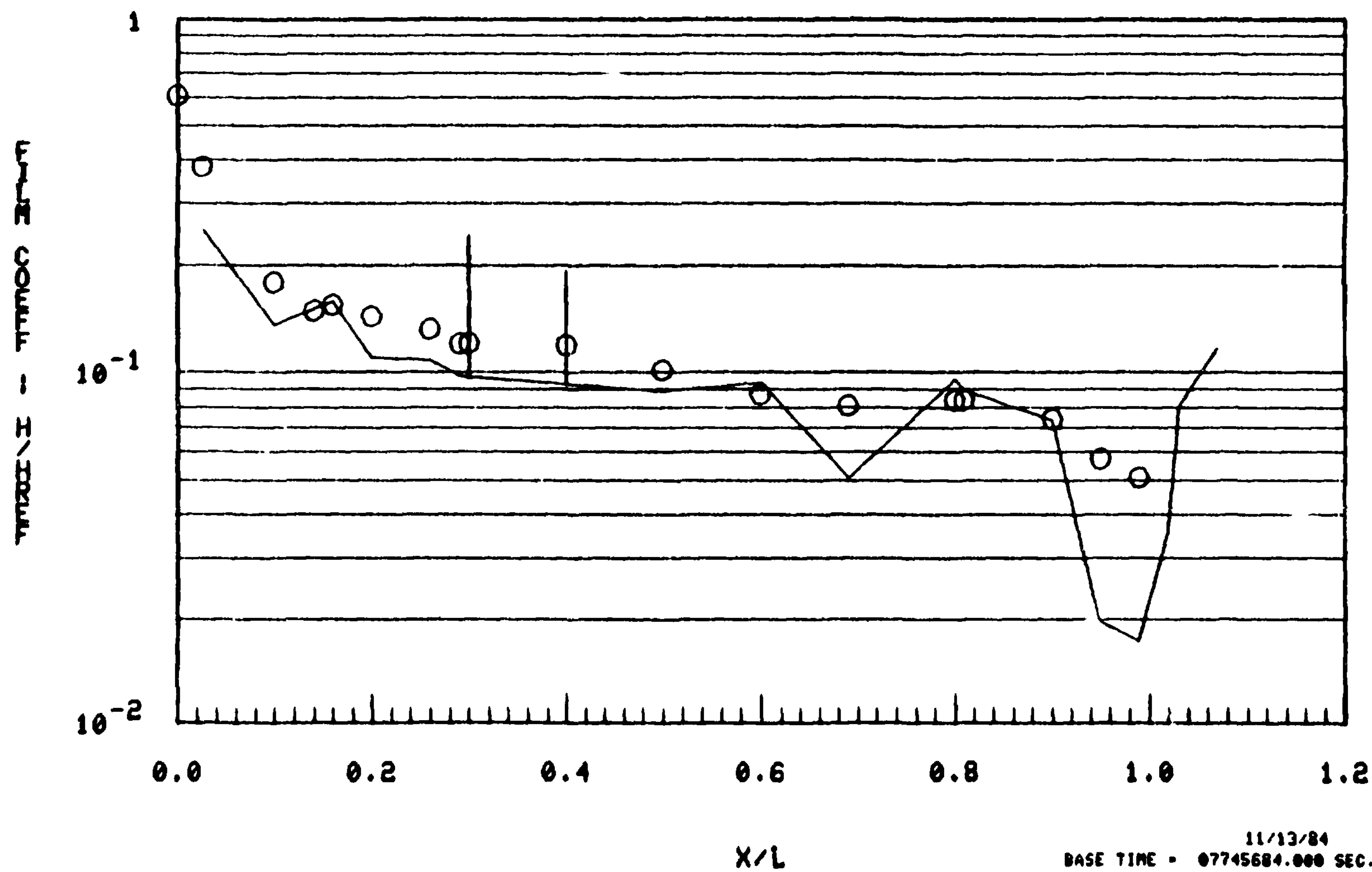

11/13/84
BASE TIME = 07745684.000 SEC.

STS-3 LOWER CENTERLINE DISTRIBUTION

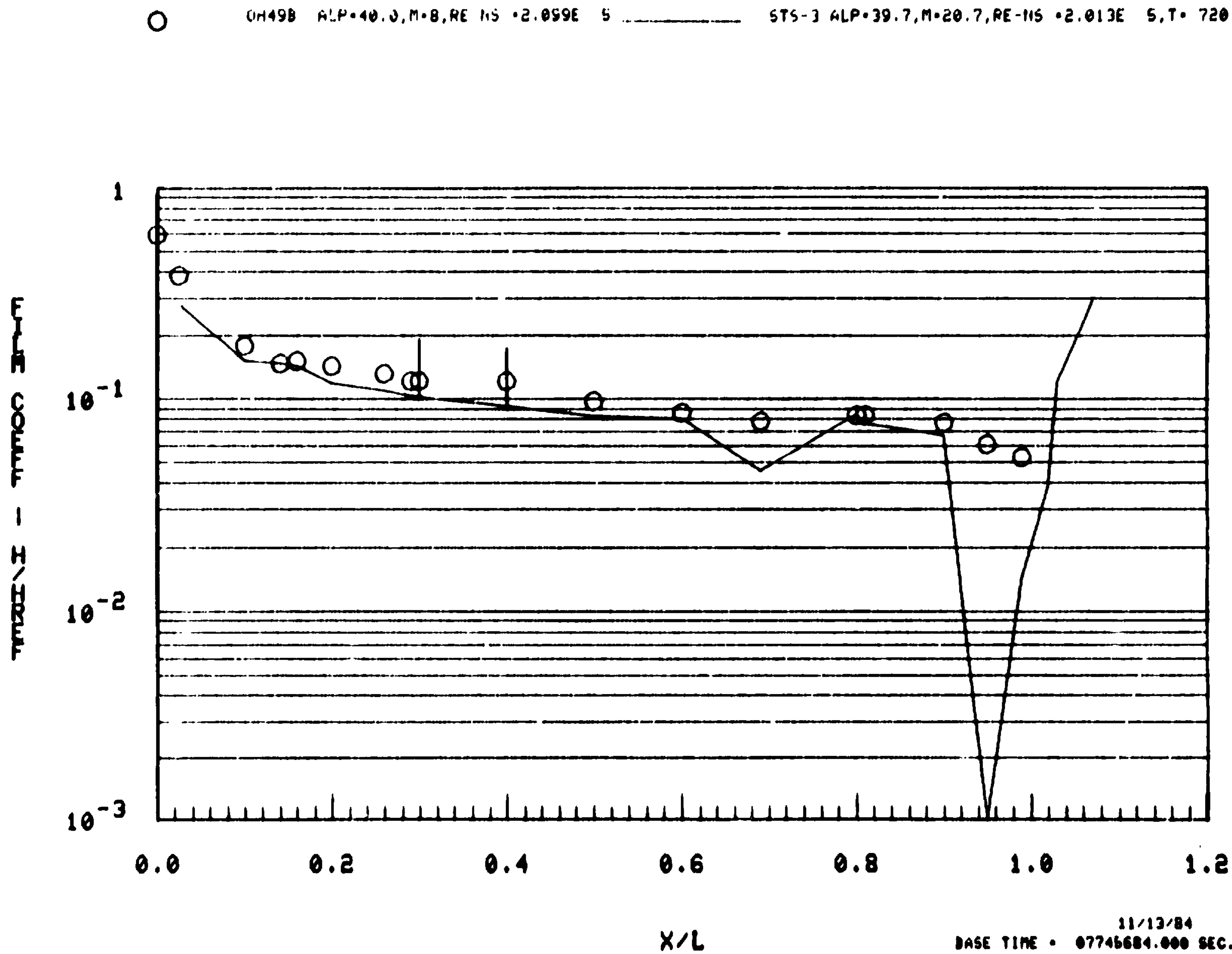

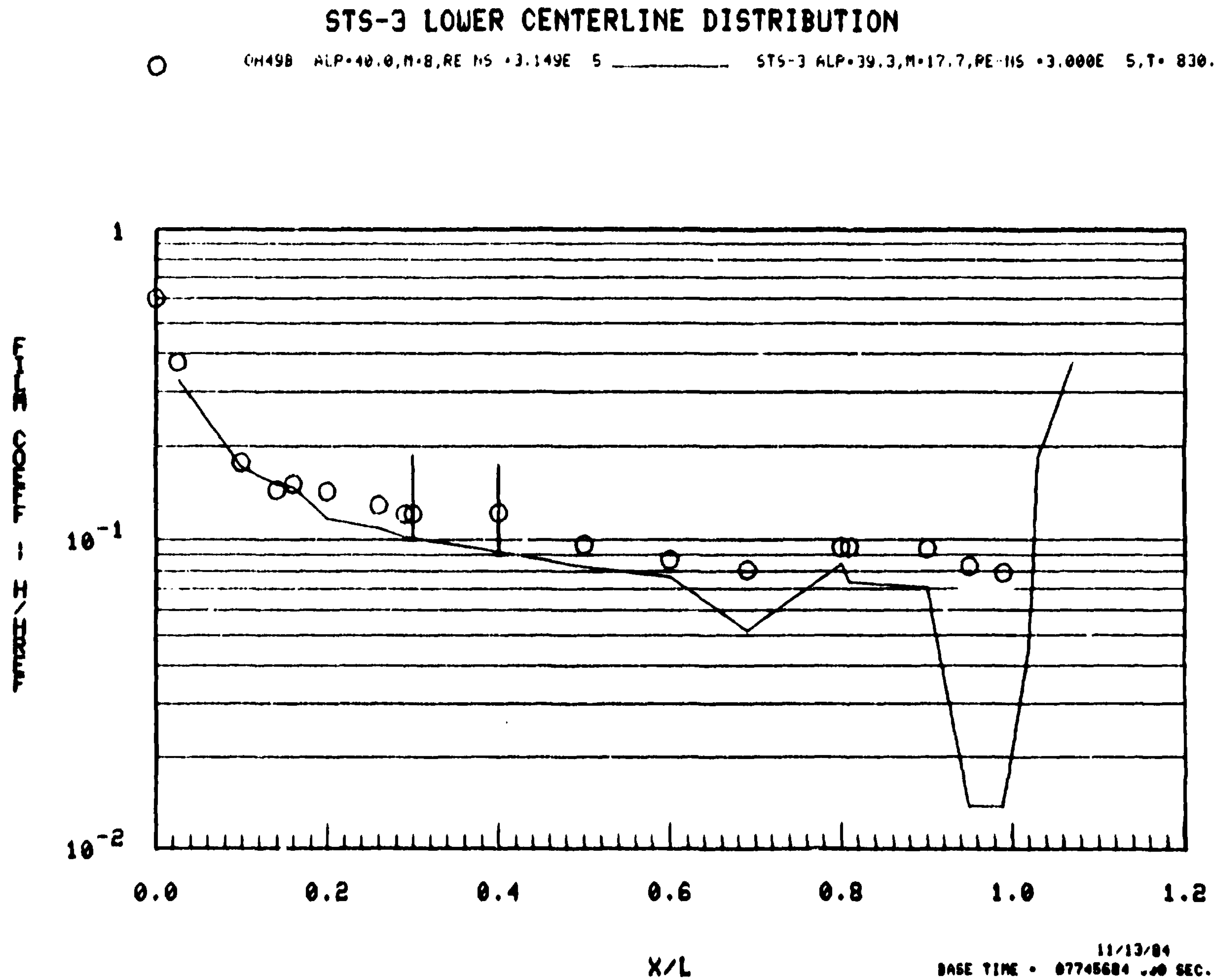

STS-3 LOWER CENTERLINE DISTRIBUTION
OH49B ALP=40.0,M=8,RE NS =3.149E 5
STS-3 ALP=39.3,M=17.7,RE NS =3.000E 5,T= 830.
1
10^{-1}
10^{-2}
FILM COEFF : H/HREF
0.0
0.2
0.4
0.6
0.8
1.0
1.2
X/L
11/13/84
BASE TIME = 07745684 .00 SEC.

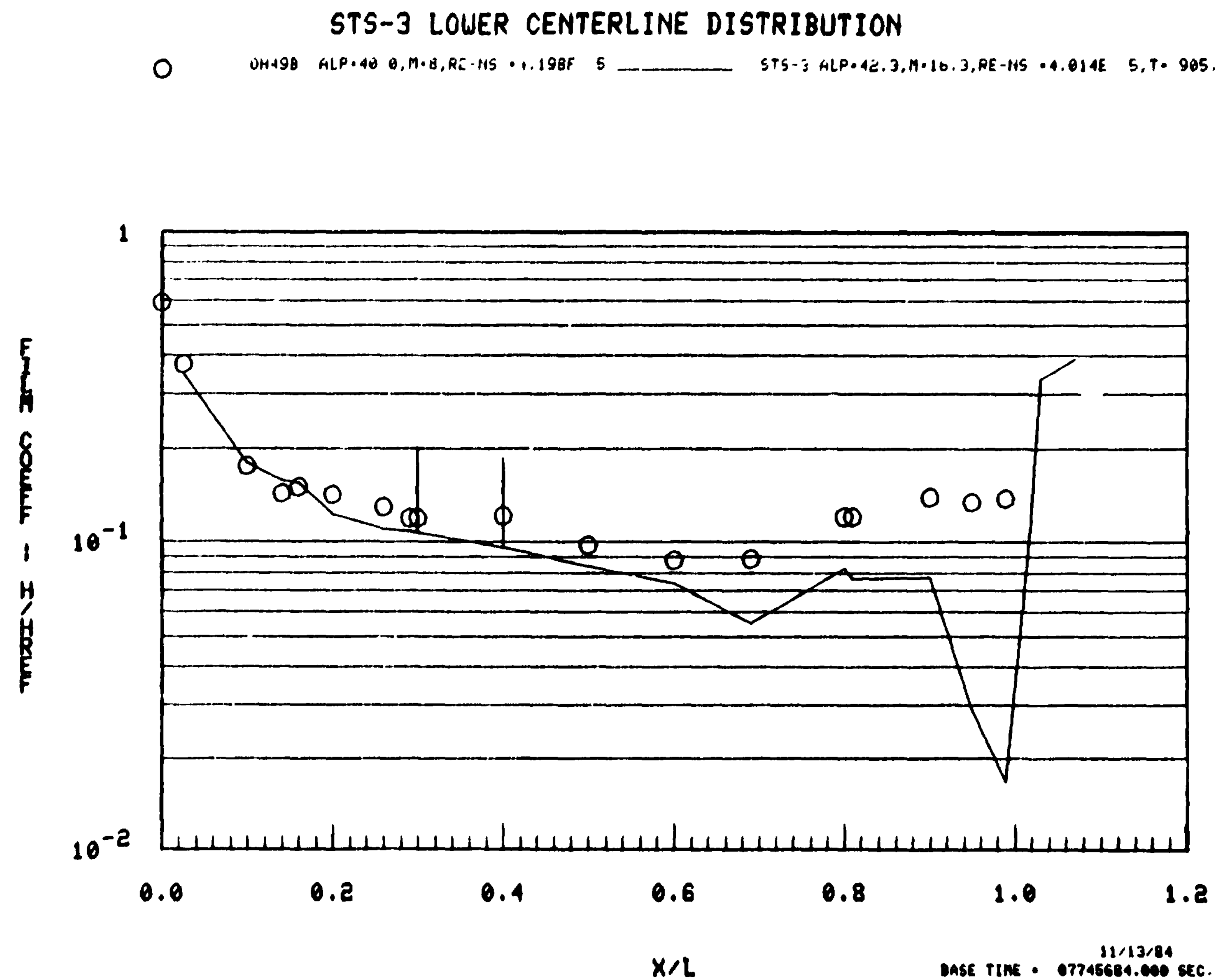
STS-3 LOWER CENTERLINE DISTRIBUTION
OH49B ALP=40.0,M=8,RE-NS =1.198E 5
STS-3 ALP=42.3,M=16.3,RE-NS =4.014E 5,T= 905.
1
10^{-1}
10^{-2}
FILM COEFF - H/HREF
0.0
0.2
0.4
0.6
0.8
1.0
1.2
X/L
11/13/84
BASE TIME = 07745684.000 SEC.

STS-3 LOWER CENTERLINE DISTRIBUTION

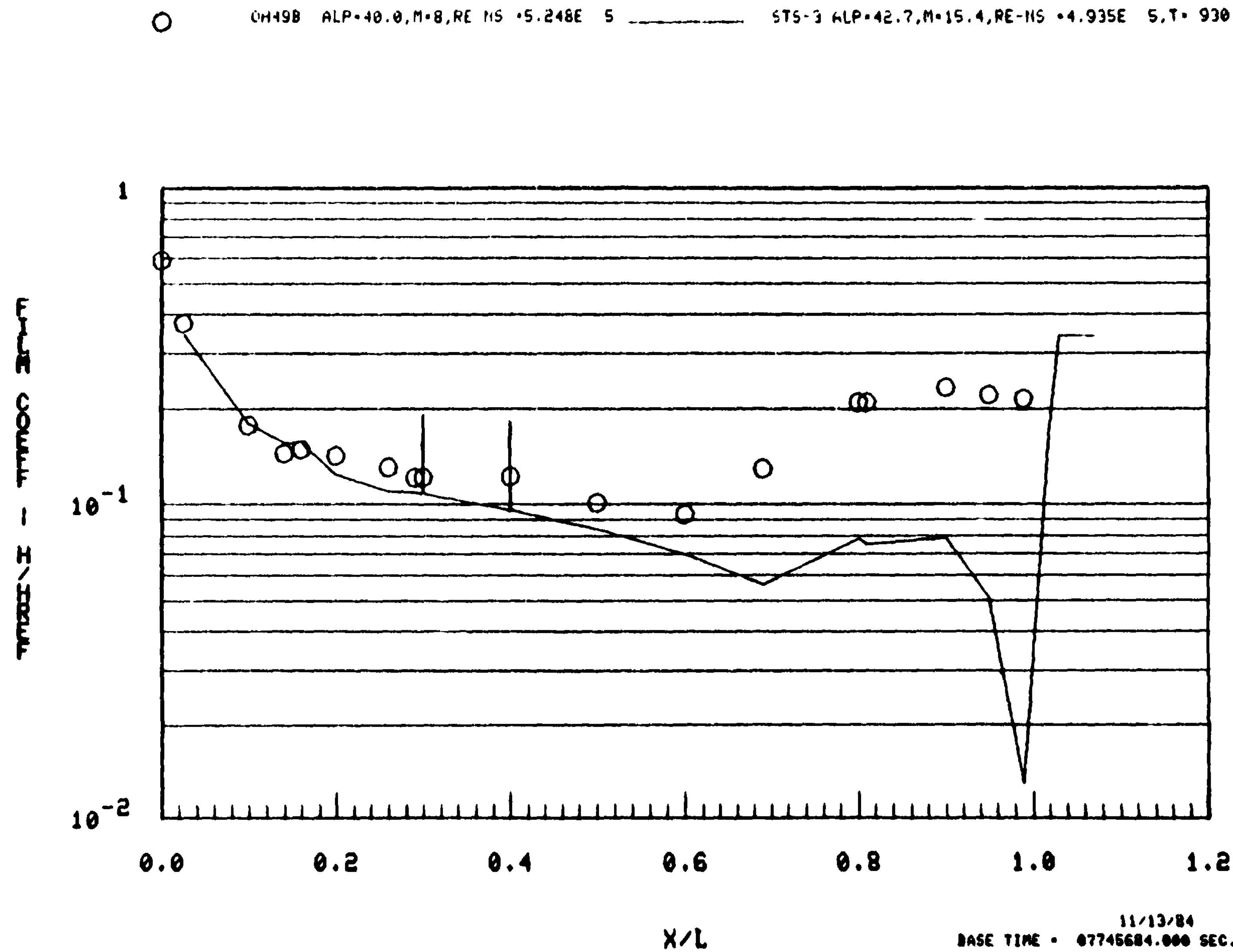

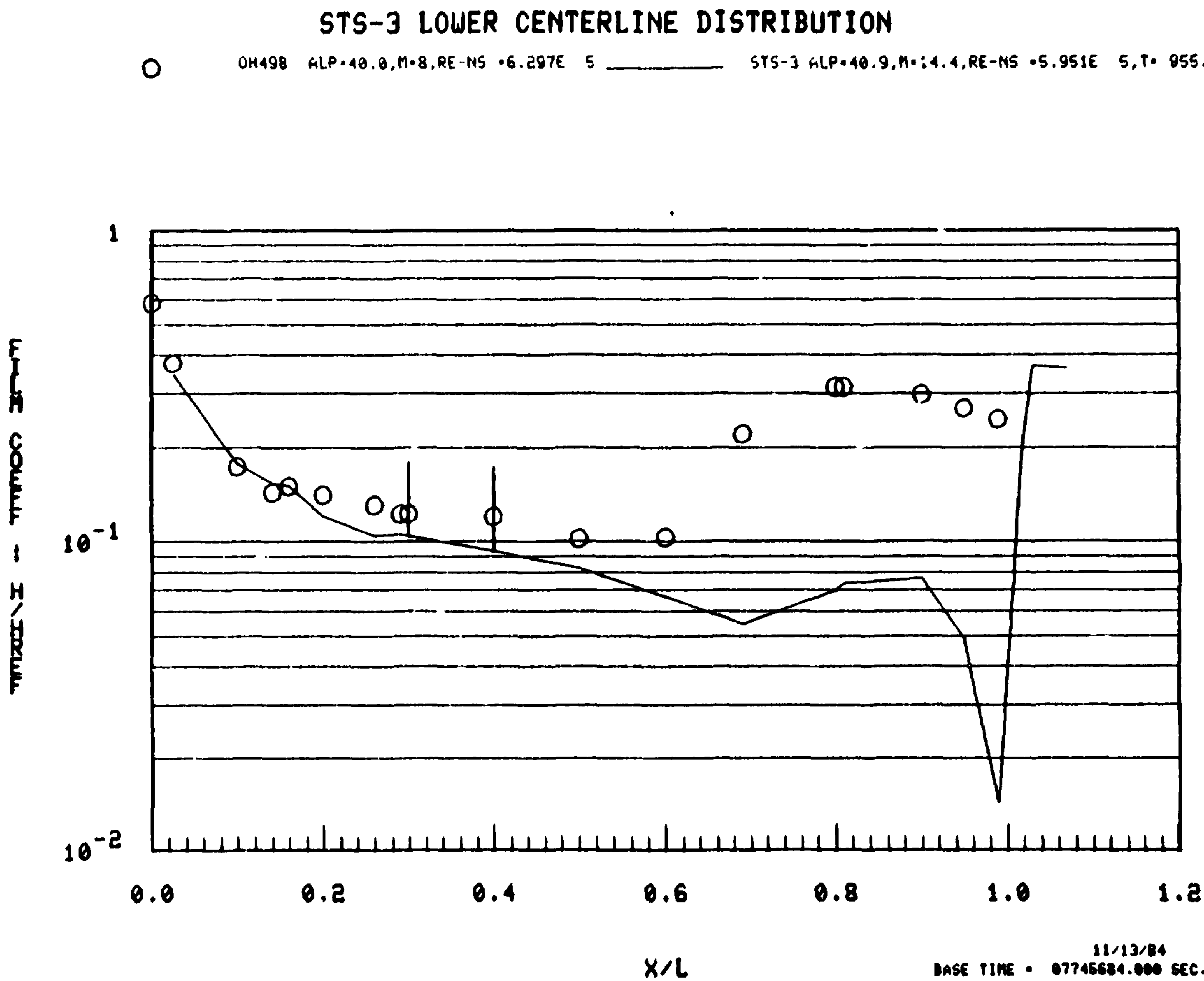

STS-3 LOWER CENTERLINE DISTRIBUTION
OH498 ALP=40.0,M=8,RE-NS =6.297E 5
STS-3 ALP=40.9,M=14.4,RE-NS =5.951E 5,T= 955.
1
10^{-1}
10^{-2}
FILM COEFF : H/HREF
0.0
0.2
0.4
0.6
0.8
1.0
1.2
X/L
11/13/84
BASE TIME = 07745684.000 SEC.

STS-3 LOWER CENTERLINE DISTRIBUTION

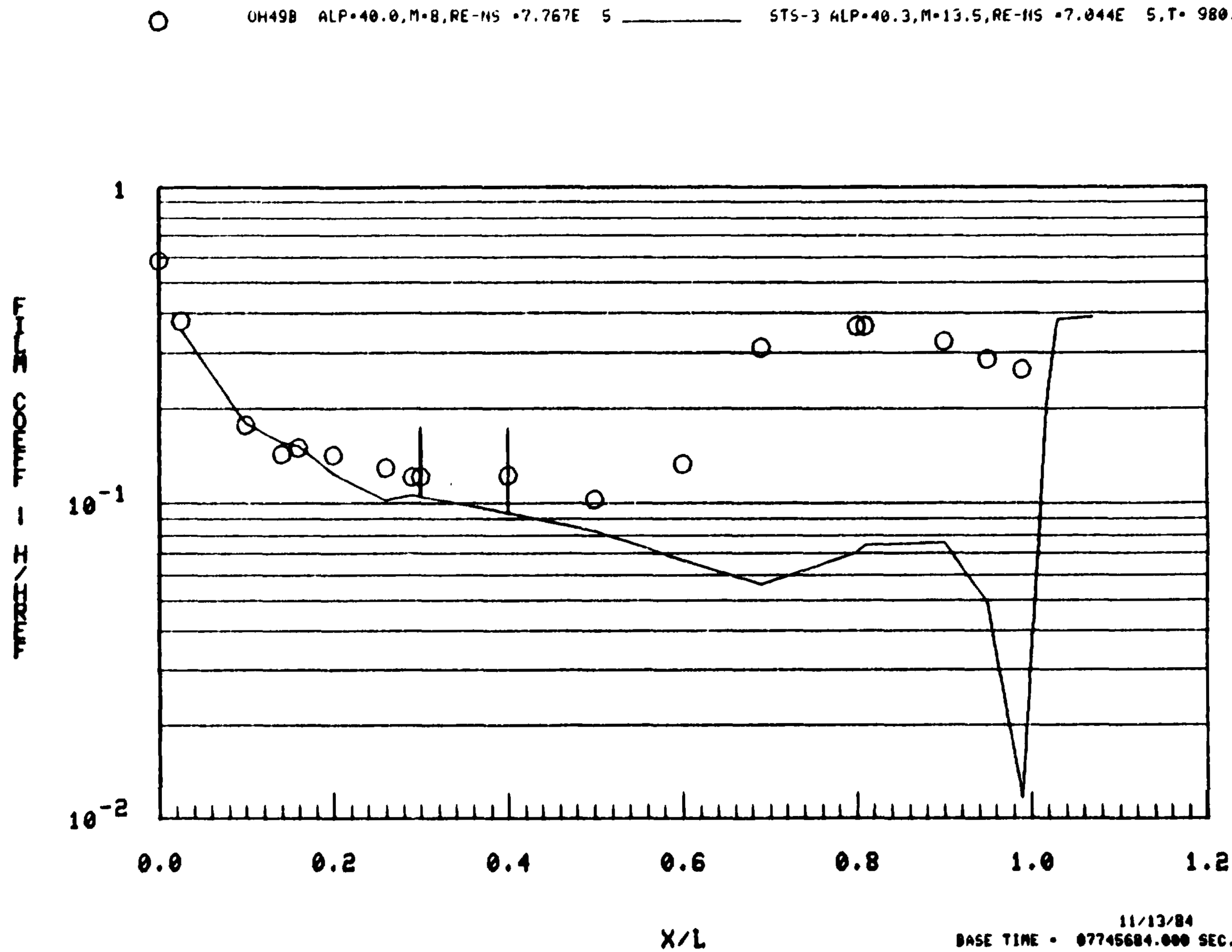

STS-3 LOWER CENTERLINE DISTRIBUTION

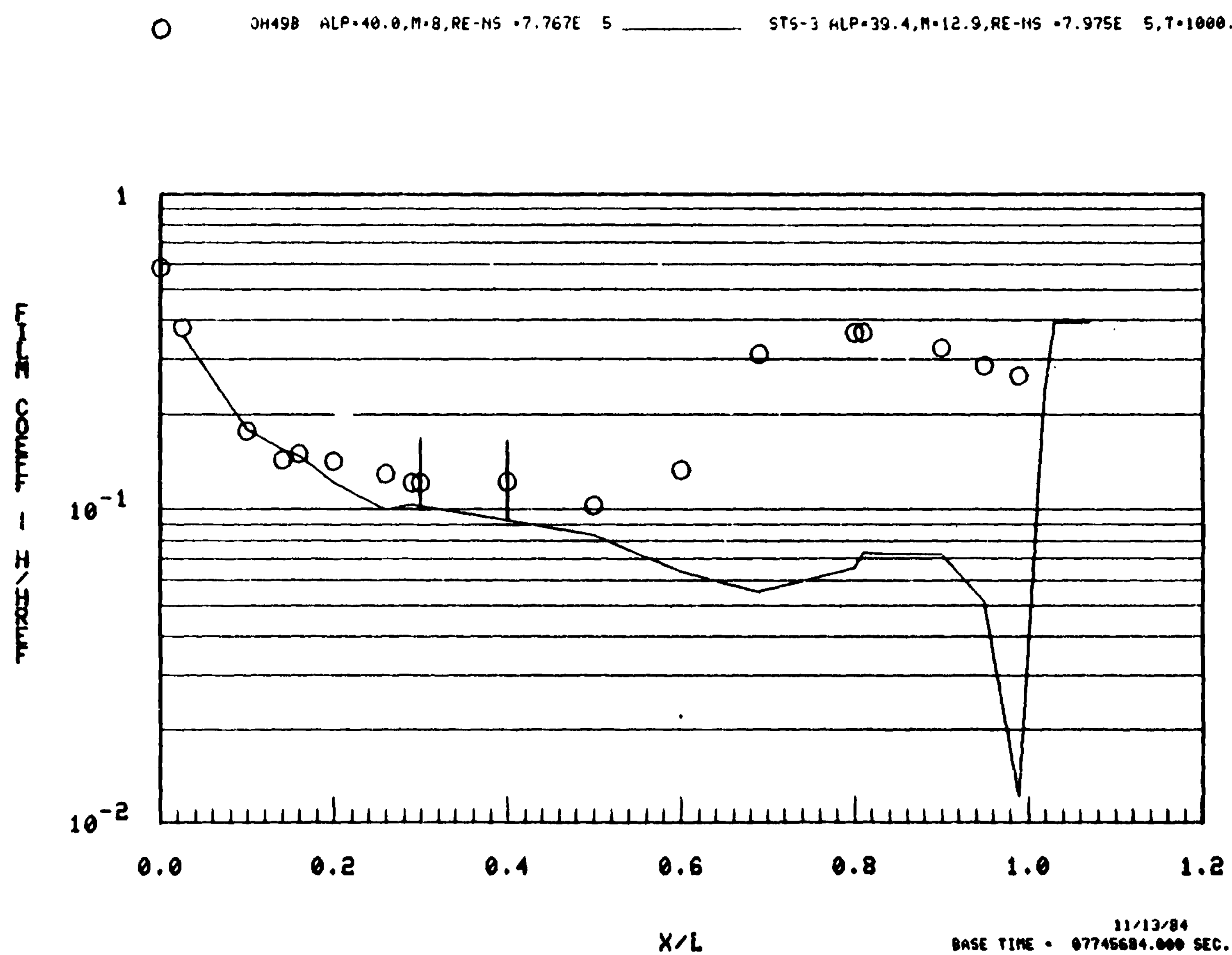

STS-5 LOWER CENTERLINE DISTRIBUTION

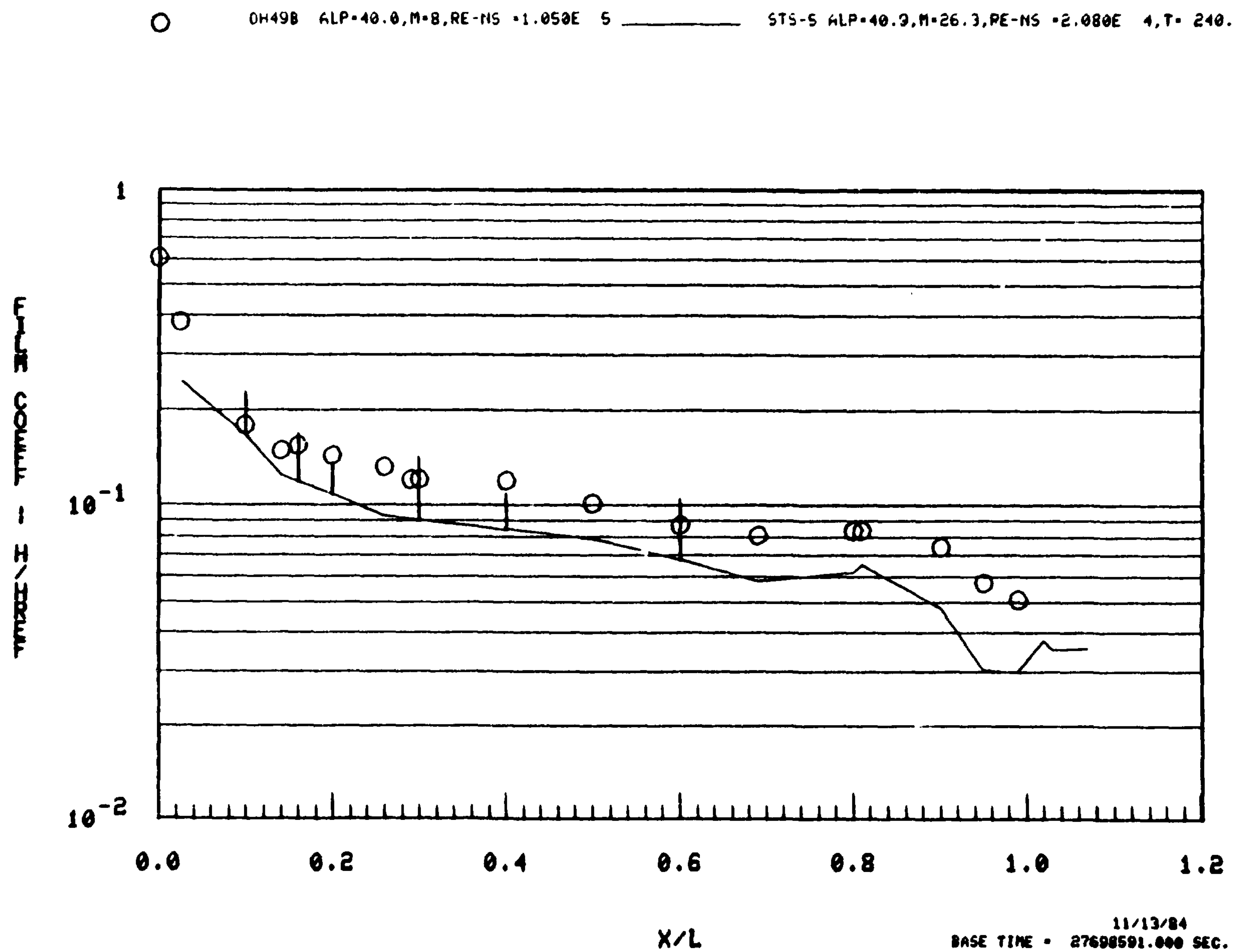

STS-5 LOWER CENTERLINE DISTRIBUTION

○ OH49B ALP=40.0,M=8,RE-NS =1.050E 5 ———— STS-5 ALP=39.1,M=26.5,RE-NS =3.056E 4,T= 265.

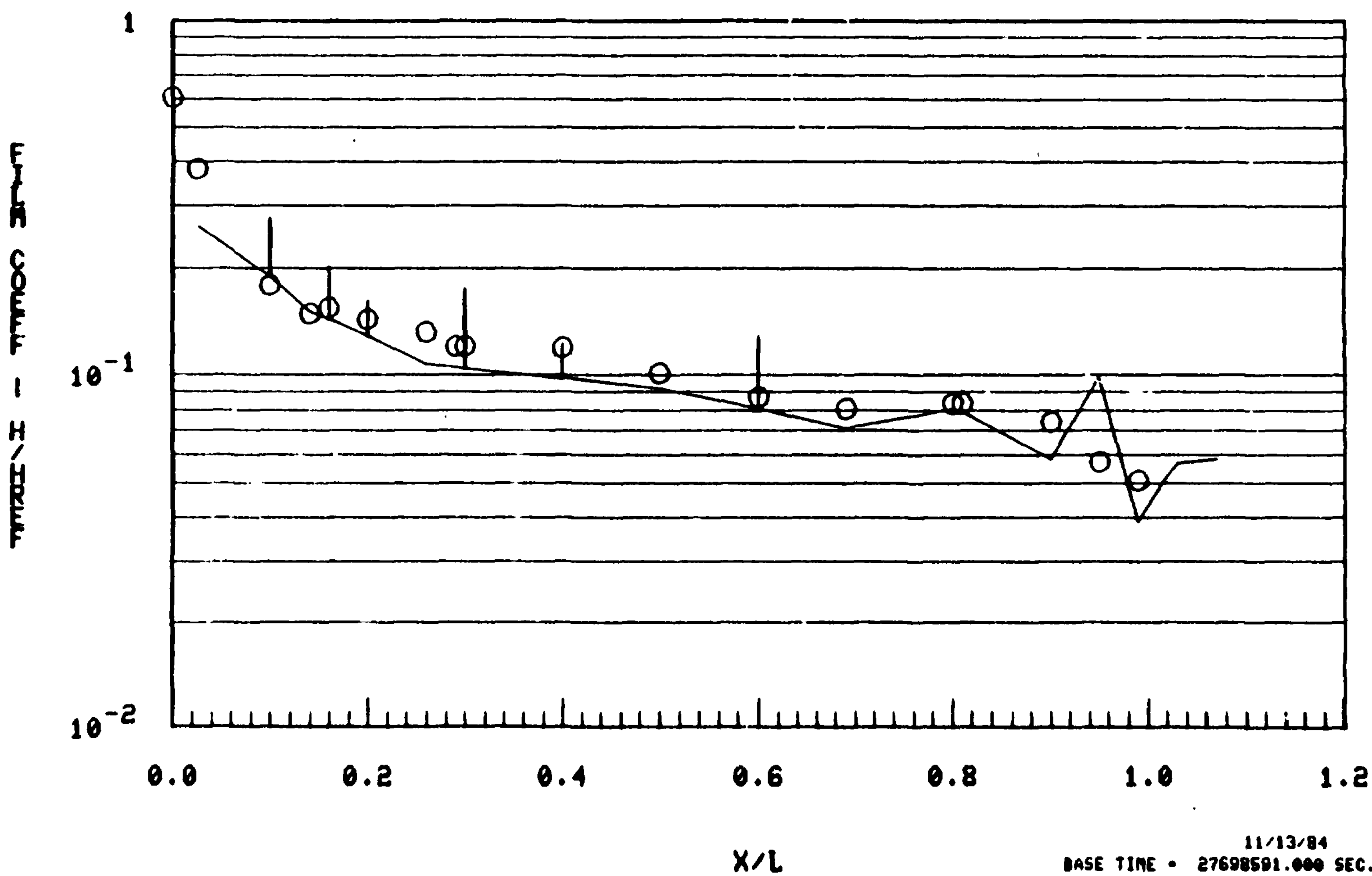

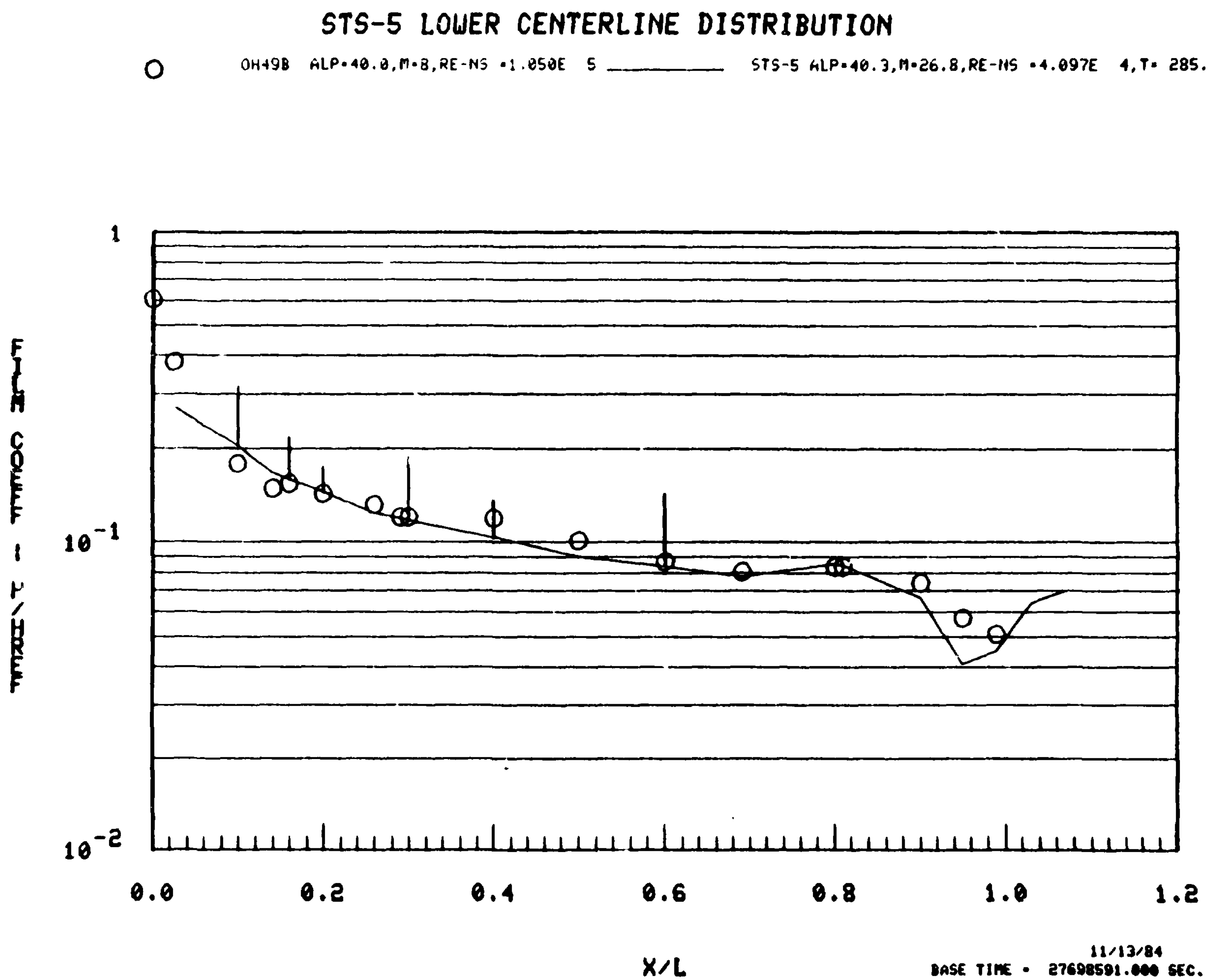
STS-5 LOWER CENTERLINE DISTRIBUTION
OH49B ALP=40.0,M=8,RE-NS =1.050E 5
STS-5 ALP=40.3,M=26.8,RE-NS =4.097E 4,T= 285.
FILM COEFF - H/HREF
1
10^{-1}
10^{-2}
0.0
0.2
0.4
0.6
0.8
1.0
1.2
X/L
11/13/84
BASE TIME = 27698591.000 SEC.

STS-5 LOWER CENTERLINE DISTRIBUTION

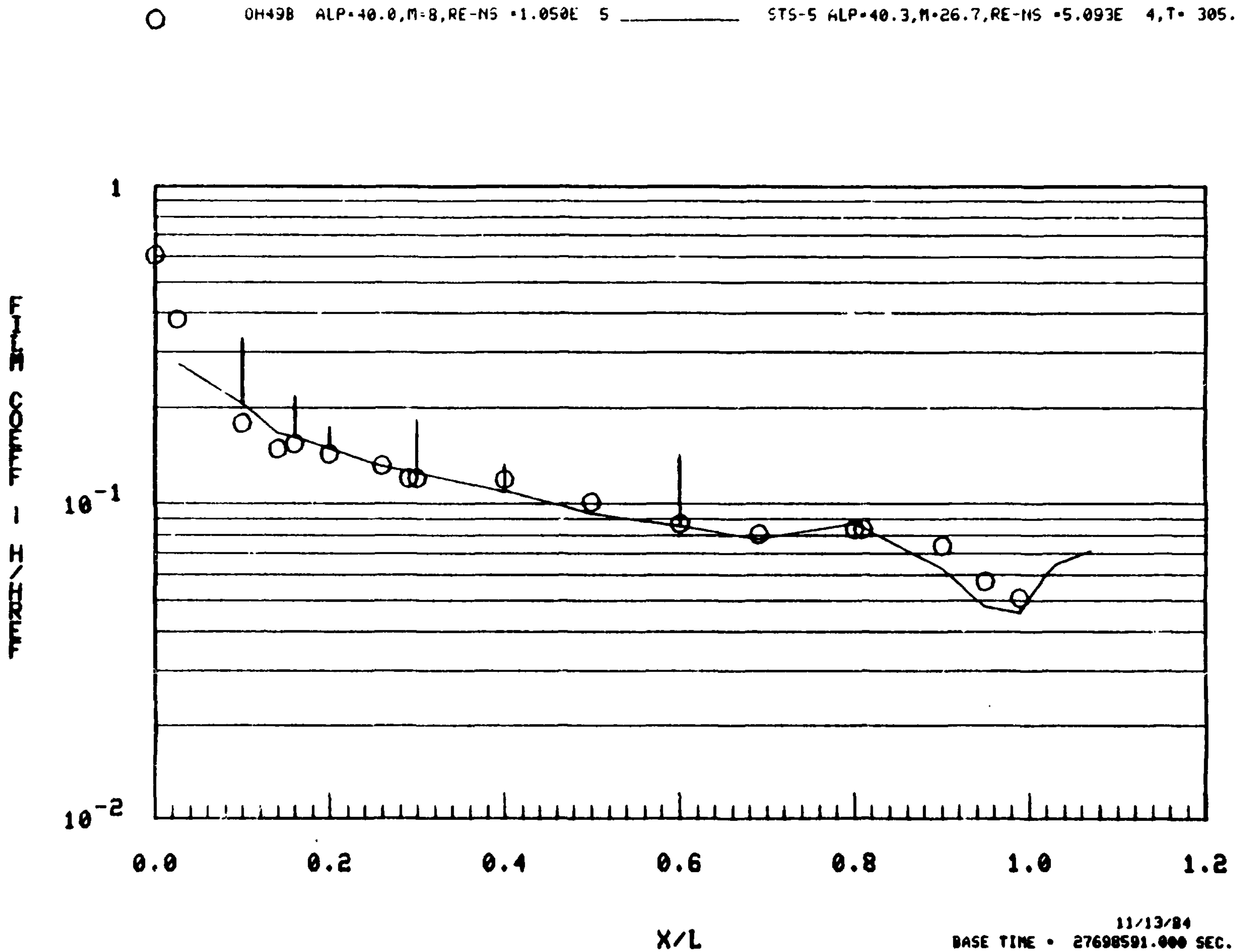

STS-5 LOWER CENTERLINE DISTRIBUTION

○ OH49B ALP=40.0,M=8,RE-NS =1.050E 5 ———— STS-5 ALP=39.7,M=26.3,RE-NS =6.030E 4,T= 335.

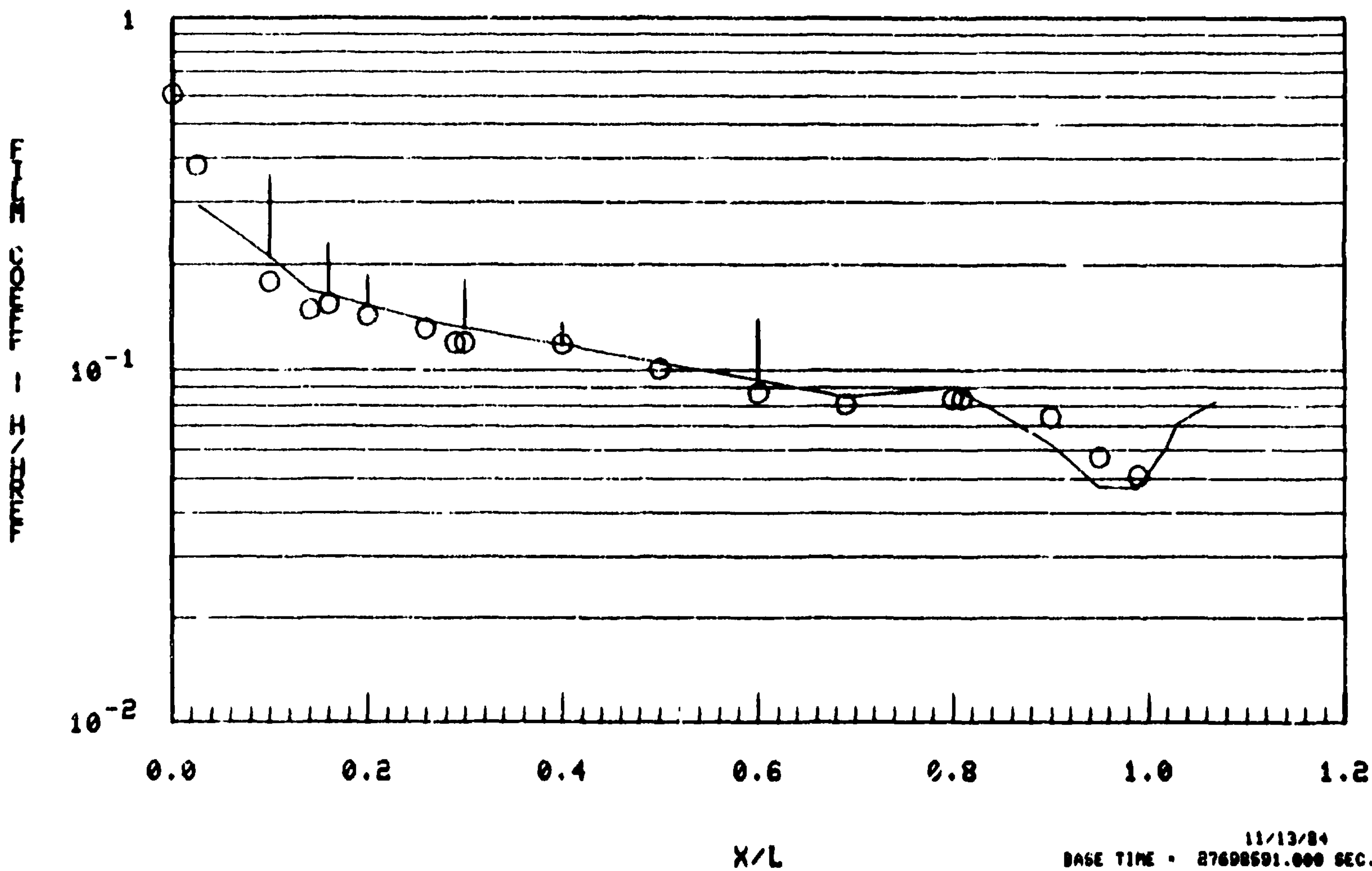

STS-5 LOWER CENTERLINE DISTRIBUTION

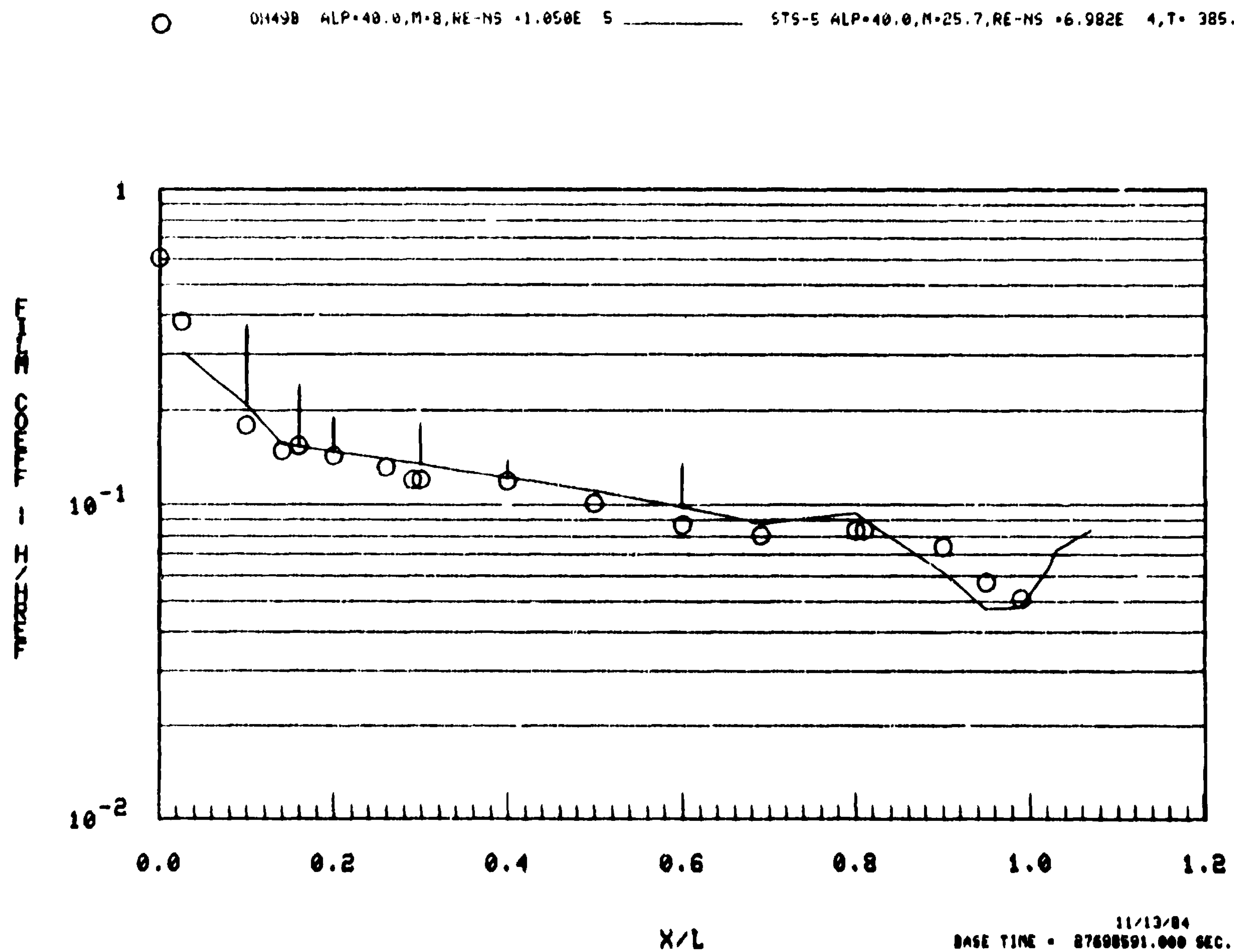

STS-5 LOWER CENTERLINE DISTRIBUTION

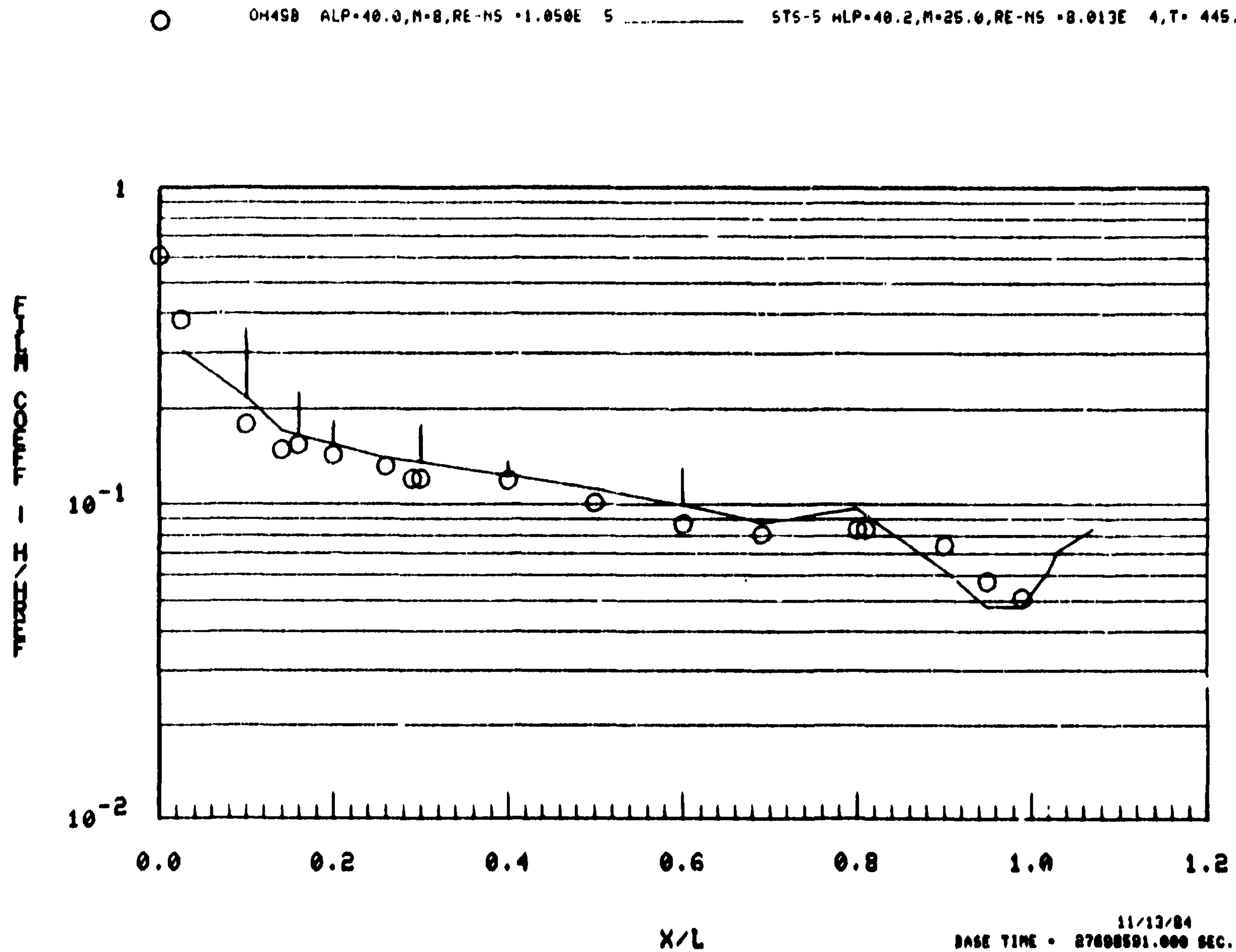

STS-5 LOWER CENTERLINE DISTRIBUTION

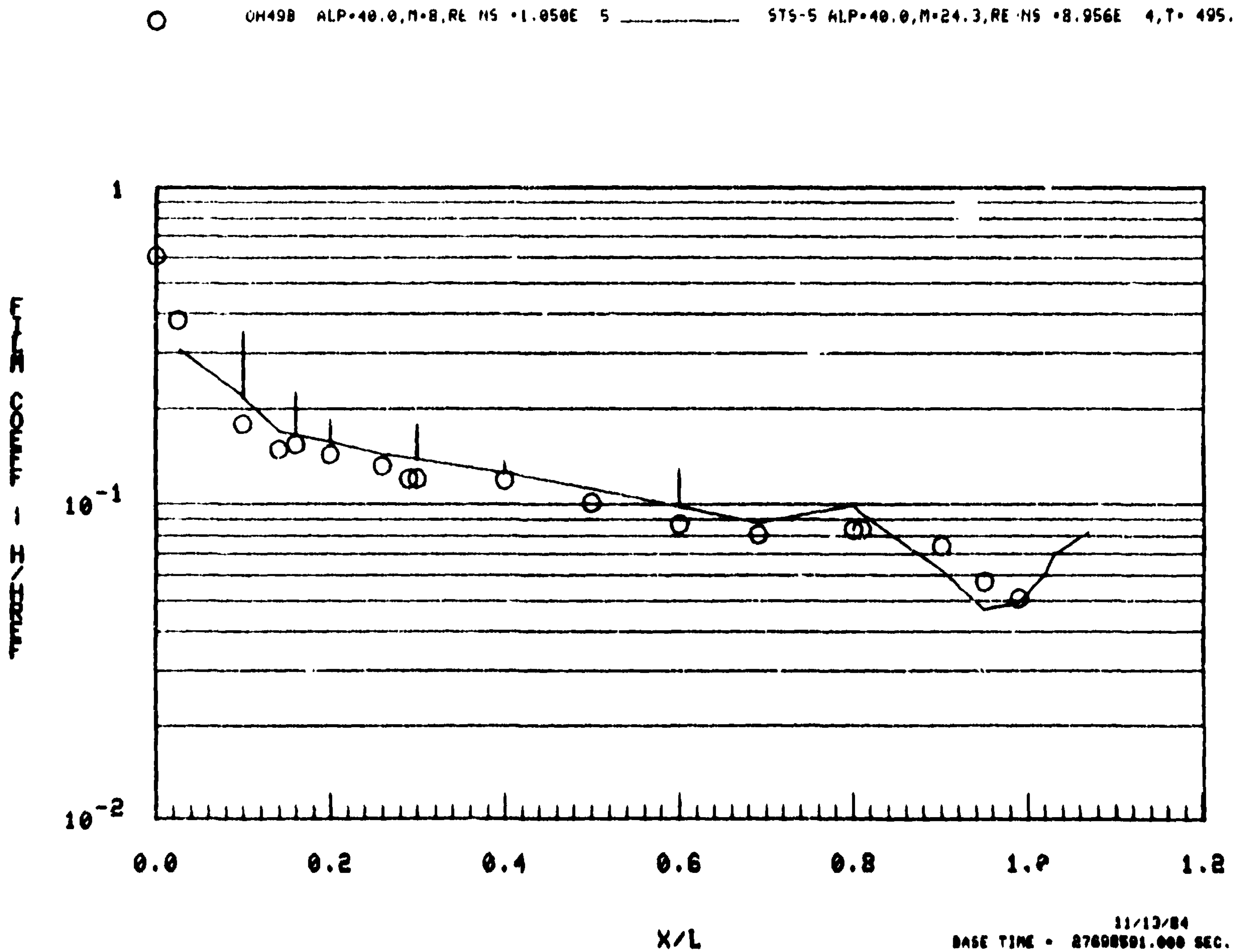

STS-5 LOWER CENTERLINE DISTRIBUTION

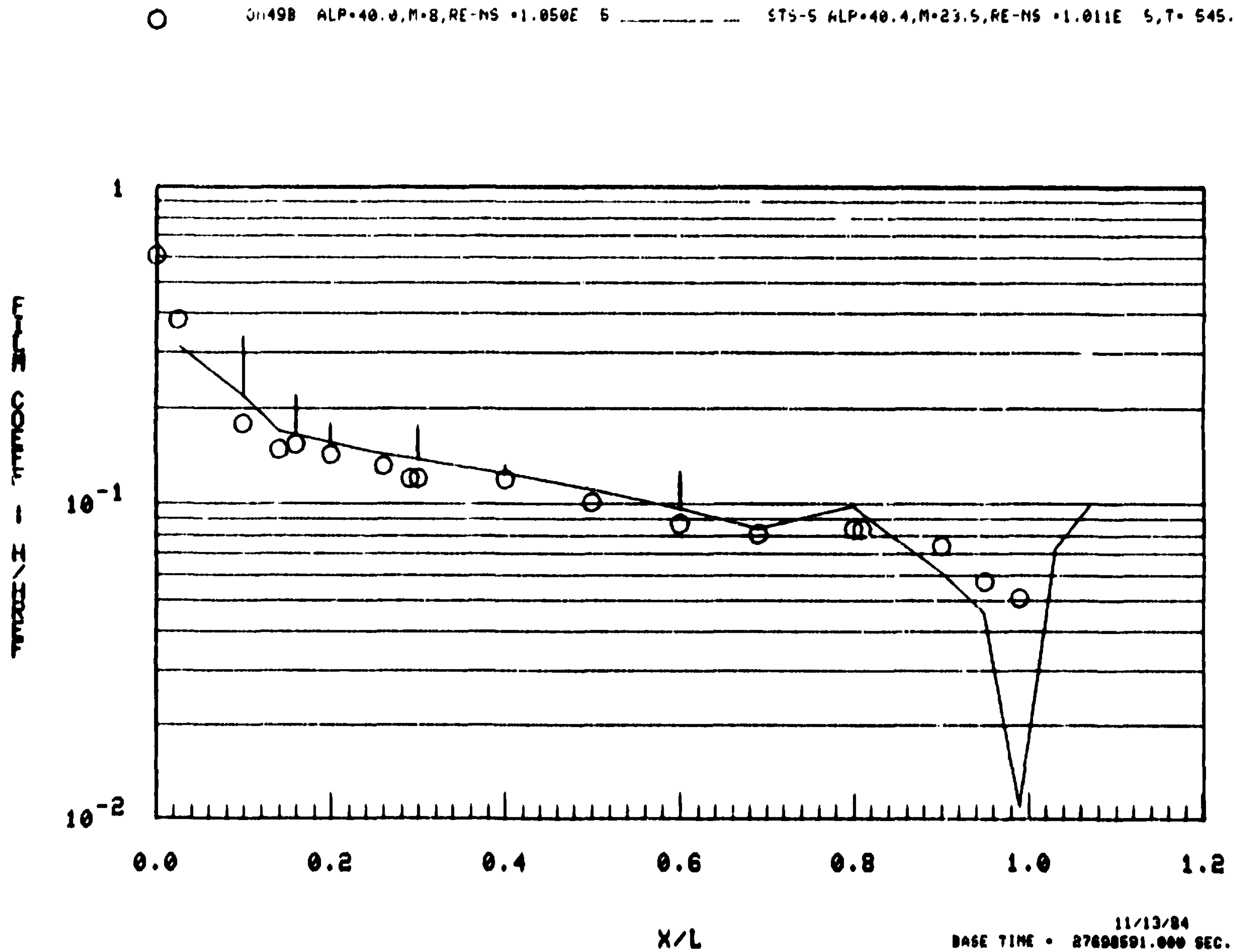

11/13/84
BASE TIME = 27698591.000 SEC.

STS-5 LOWER CENTERLINE DISTRIBUTION

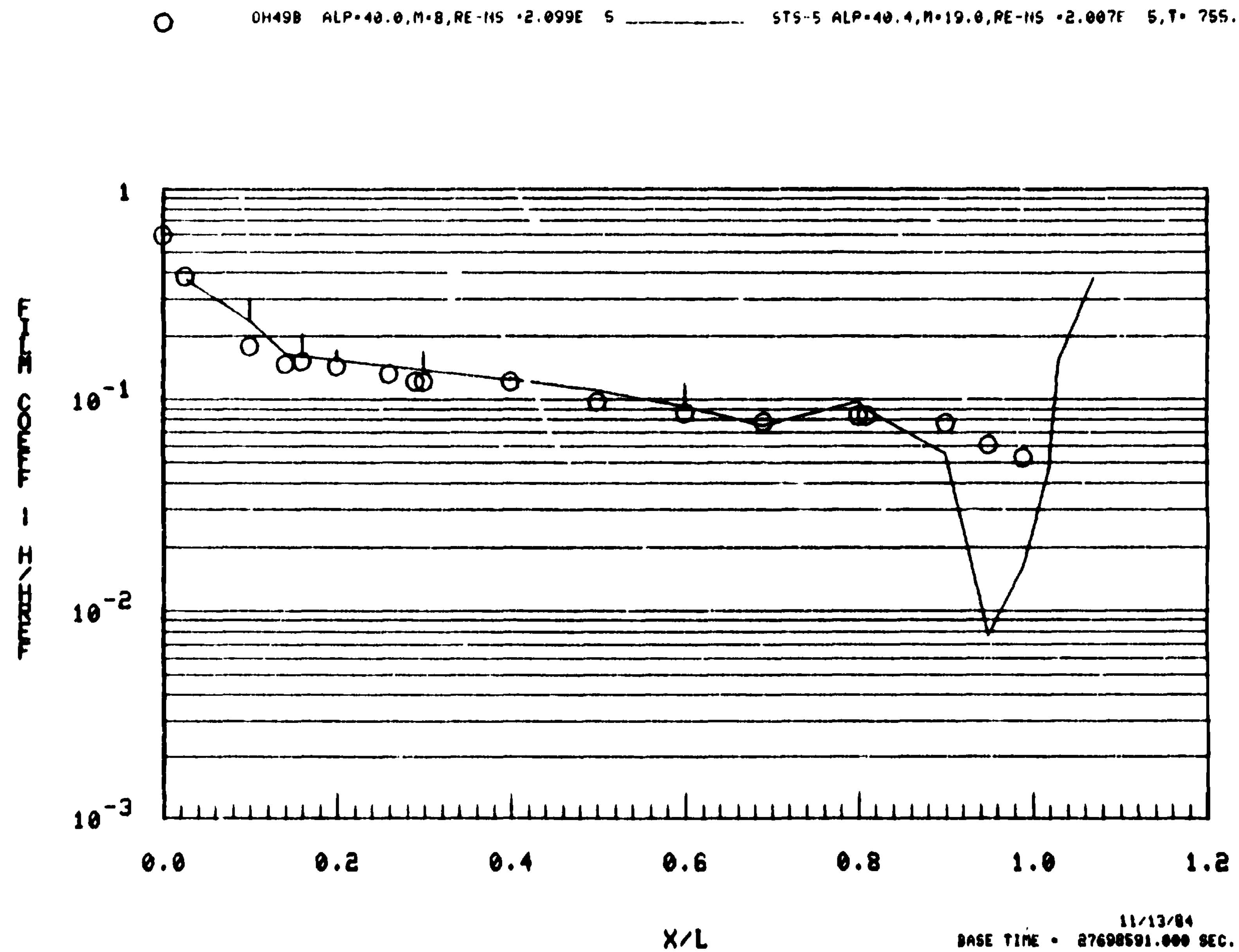

STS-5 LOWER CENTERLINE DISTRIBUTION

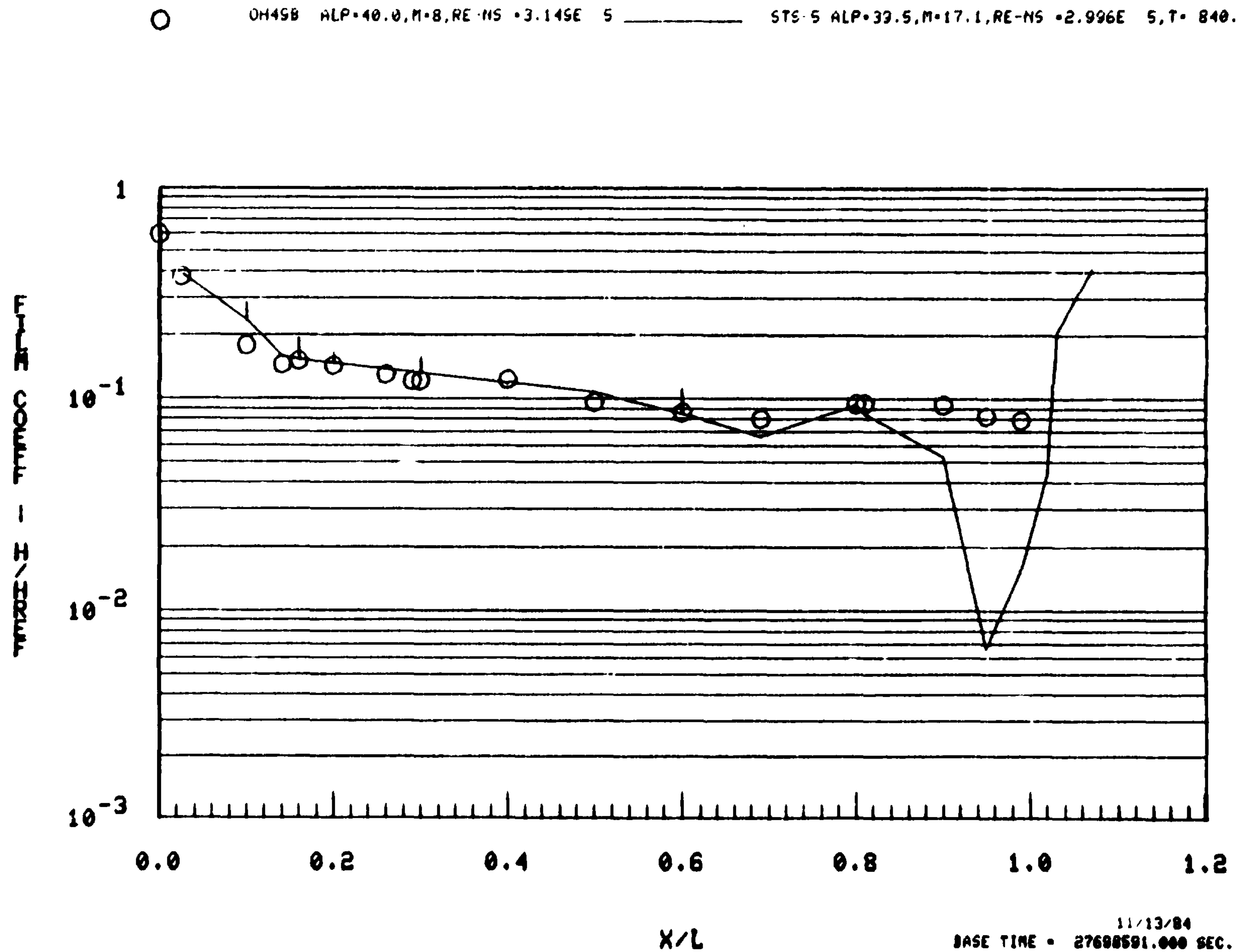

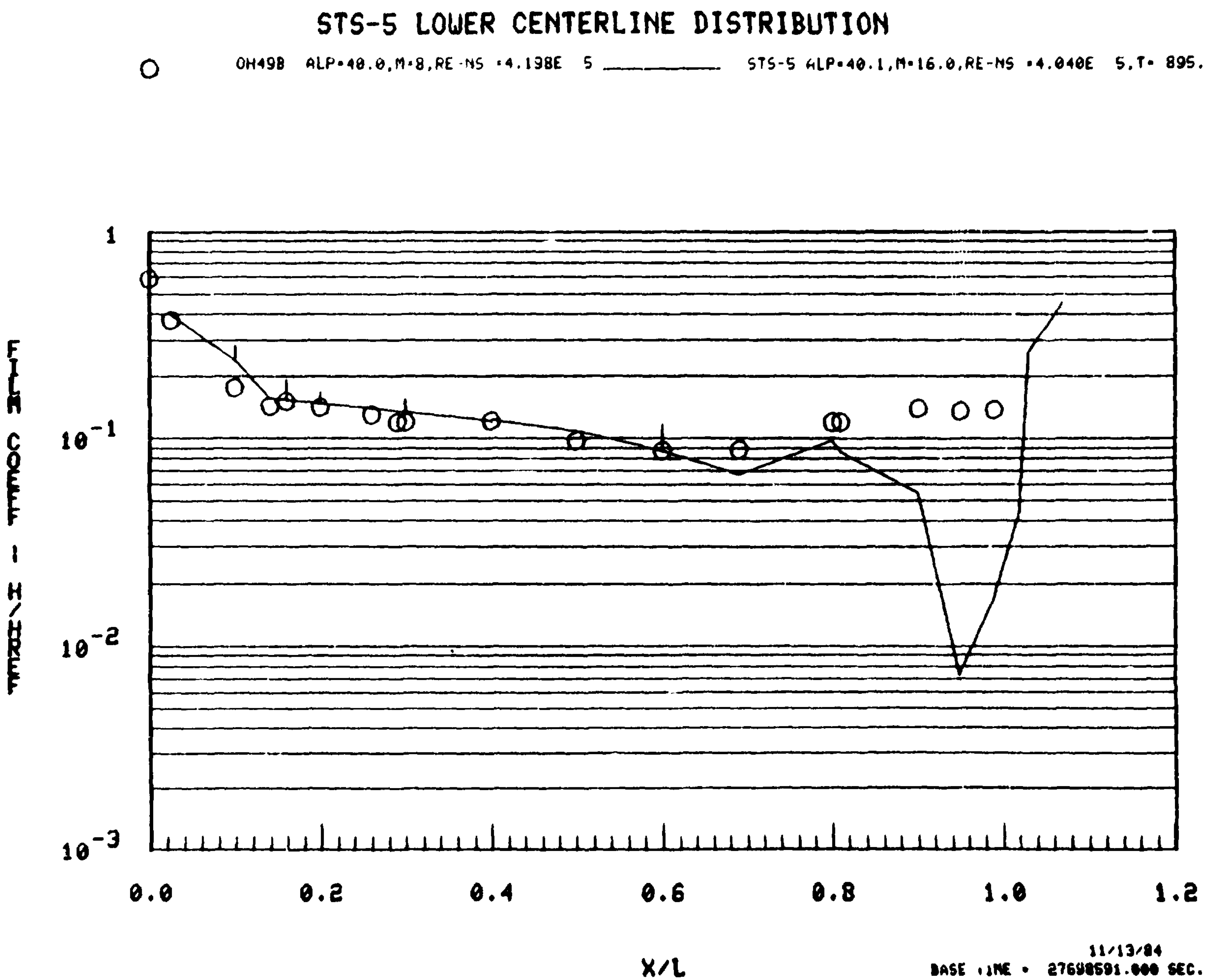
STS-5 LOWER CENTERLINE DISTRIBUTION
OH49B ALP=40.0,M=8,RE-NS =4.138E 5
STS-5 ALP=40.1,M=16.0,RE-NS =4.040E 5,T= 895.
FILM COEFF - H/HREF
1
10^{-1}
10^{-2}
10^{-3}
0.0
0.2
0.4
0.6
0.8
1.0
1.2
X/L
11/13/84
BASE TIME = 27698591.000 SEC.

STS-5 LOWER CENTERLINE DISTRIBUTION

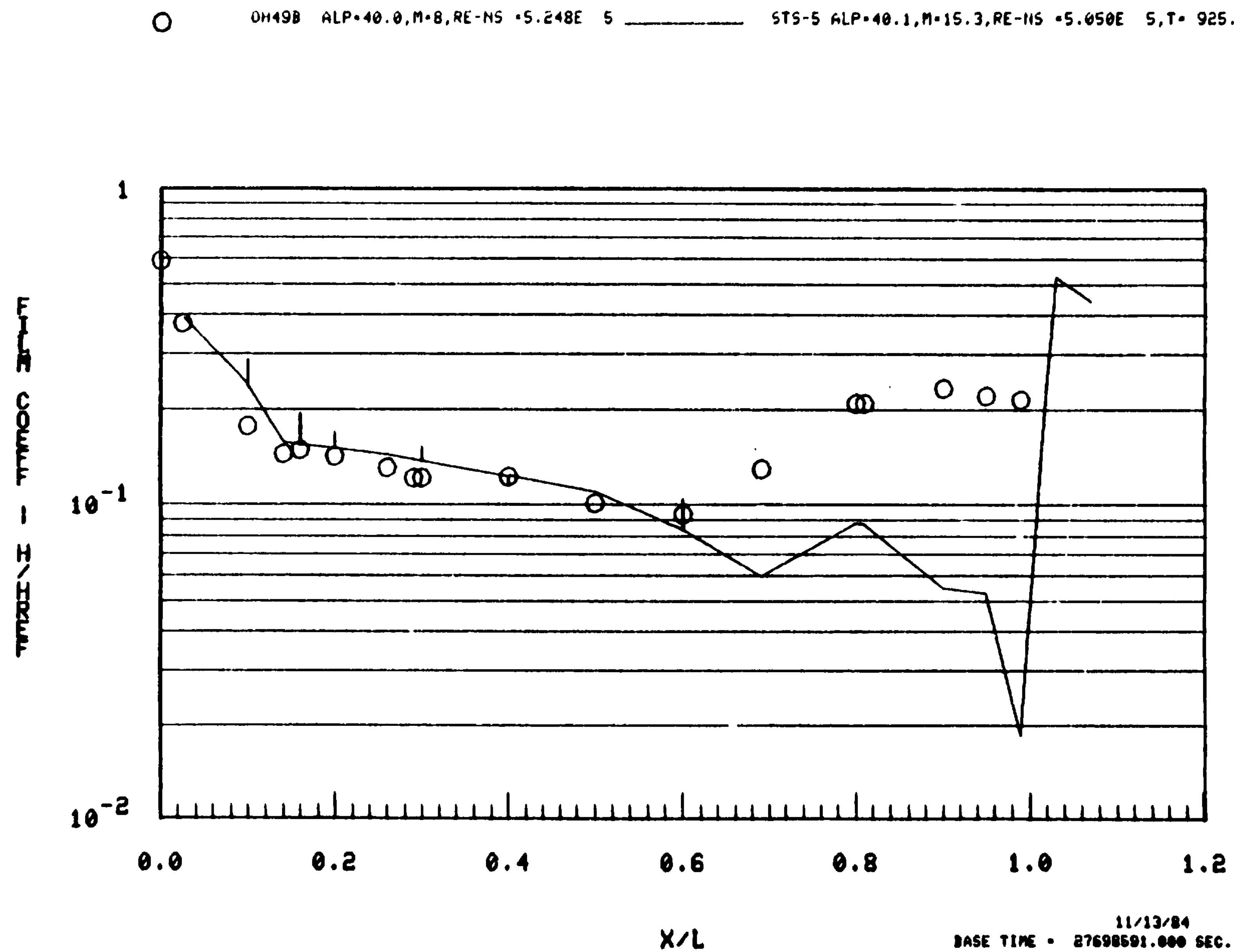

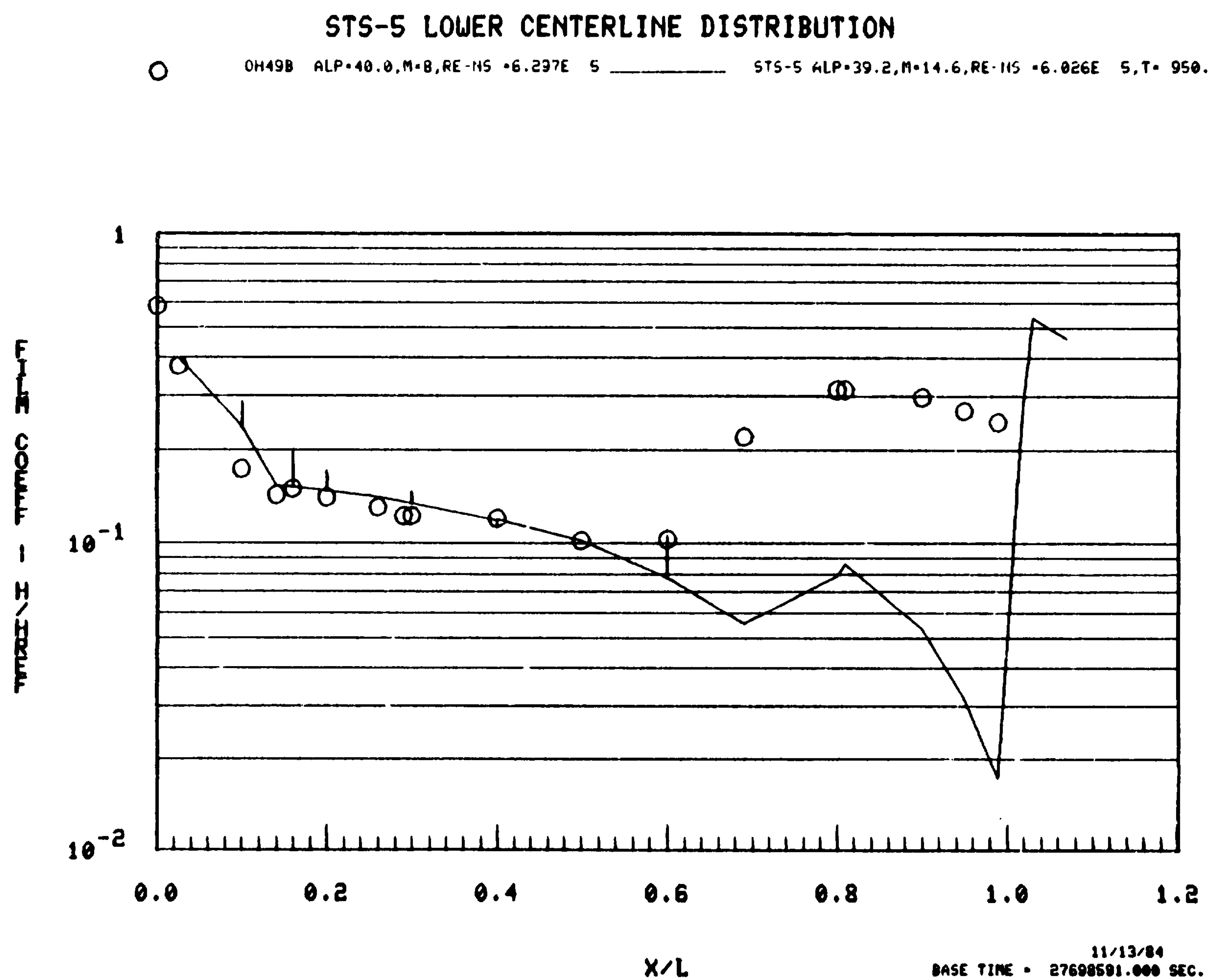
STS-5 LOWER CENTERLINE DISTRIBUTION
OH49B ALP=40.0,M=8,RE-NS =6.297E 5
STS-5 ALP=39.2,M=14.6,RE-NS =6.026E 5,T= 950.
FILM COEFF : H/HREF
1
10^{-1}
10^{-2}
0.0
0.2
0.4
0.6
0.8
1.0
1.2
X/L
11/13/84
BASE TIME = 27698591.000 SEC.

STS-5 LOWER CENTERLINE DISTRIBUTION

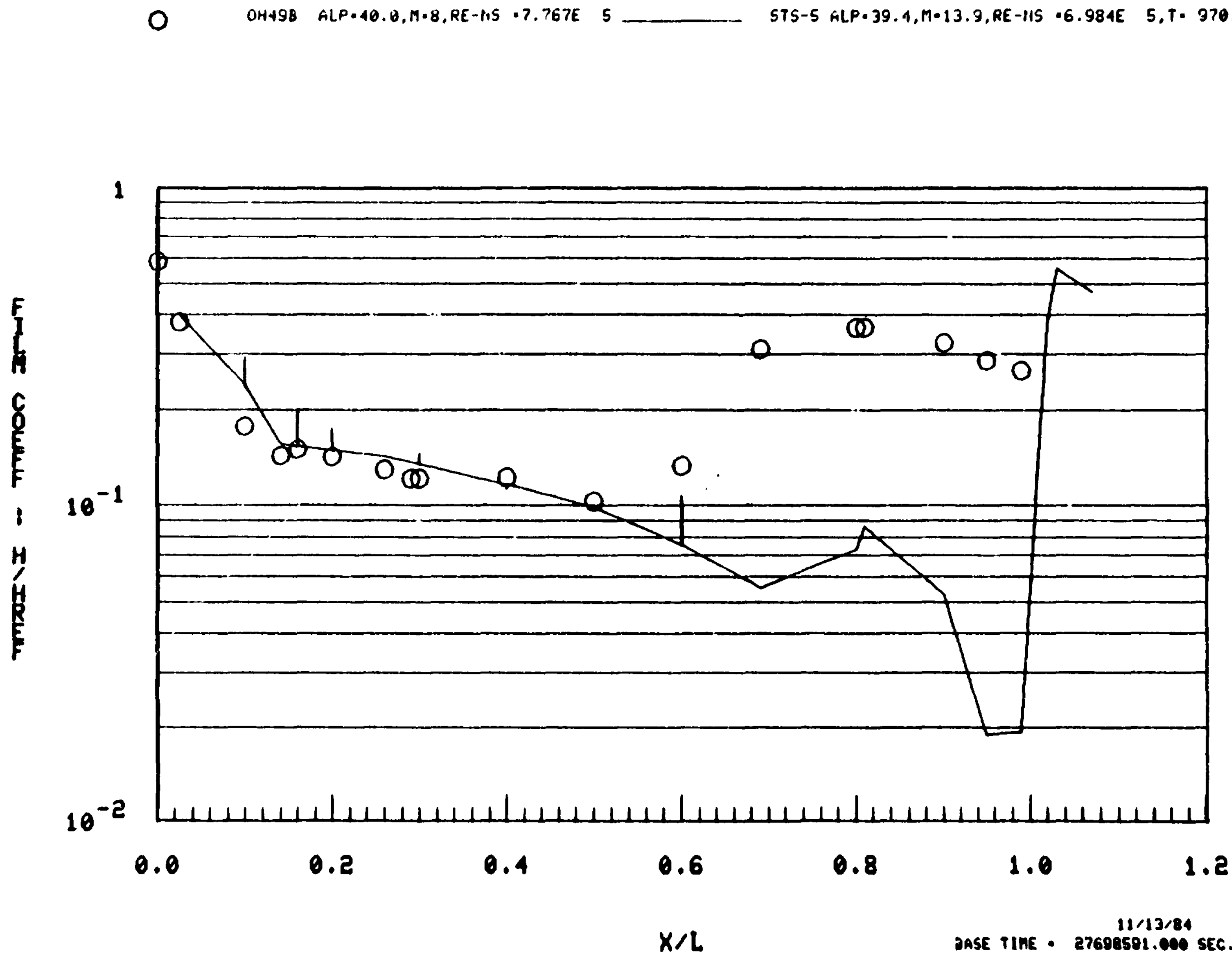

STS-5 LOWER CENTERLINE DISTRIBUTION

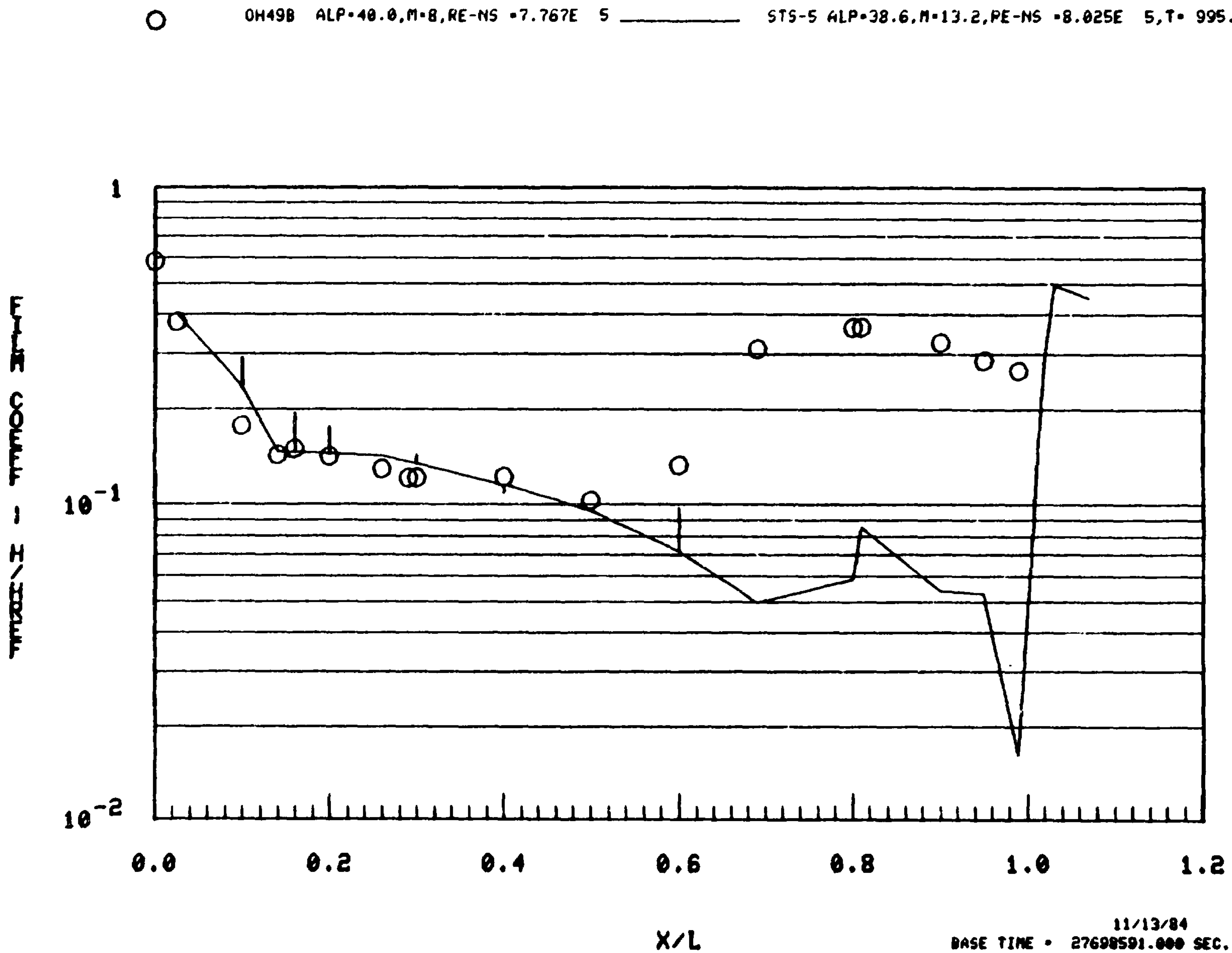

STS-2 LOWER CENTERLINE DISTRIBUTION

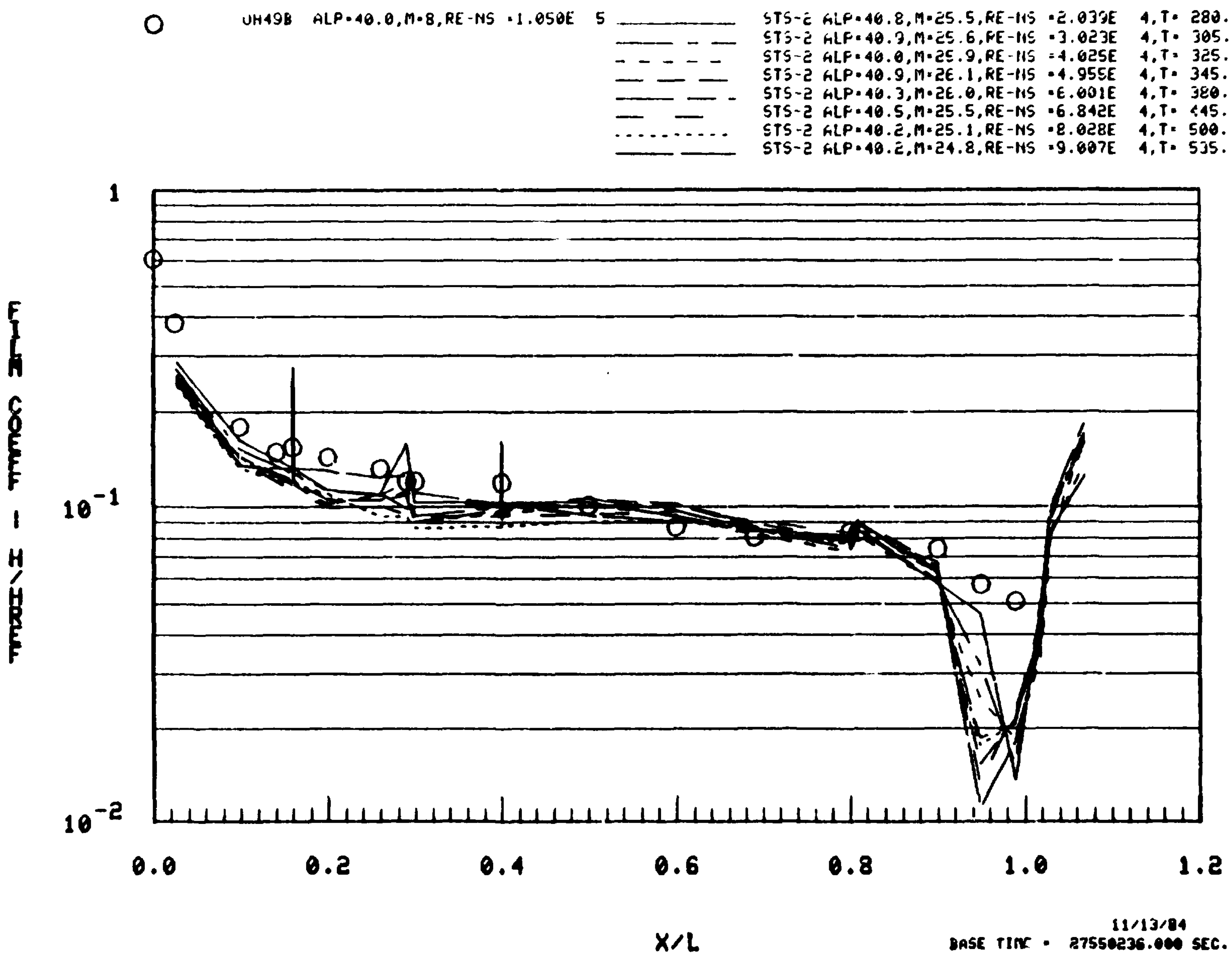

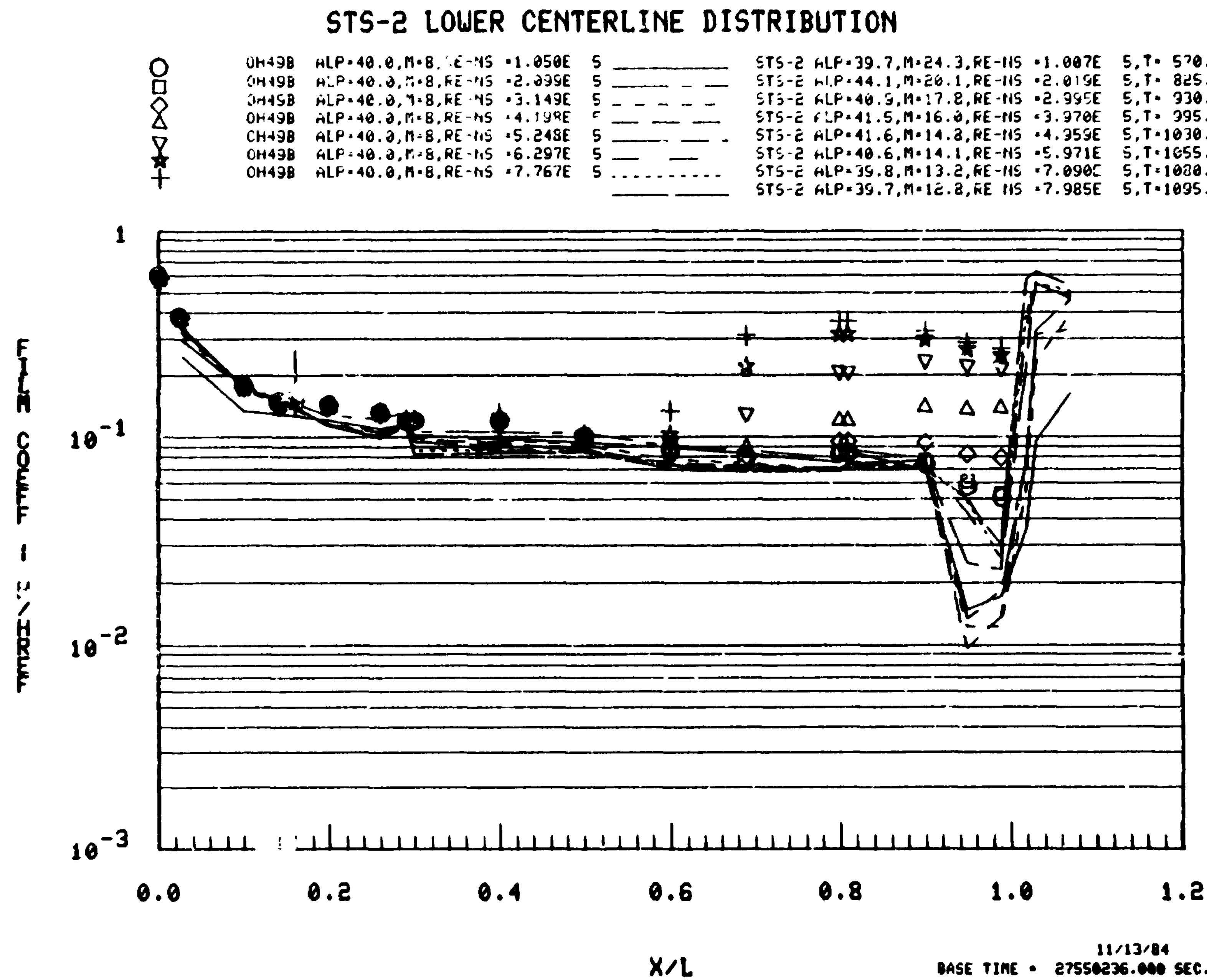

STS-2 LOWER CENTERLINE DISTRIBUTION
OH49B ALP=40.0,M=8,RE-NS =1.050E 5
OH49B ALP=40.0,M=8,RE-NS =2.099E 5
OH49B ALP=40.0,M=8,RE-NS =3.149E 5
OH49B ALP=40.0,M=8,RE-NS =4.198E 5
OH49B ALP=40.0,M=8,RE-NS =5.248E 5
OH49B ALP=40.0,M=8,RE-NS =6.297E 5
OH49B ALP=40.0,M=8,RE-NS =7.767E 5
STS-2 ALP=39.7,M=24.3,RE-NS =1.007E 5,T= 570.
STS-2 ALP=44.1,M=20.1,RE-NS =2.019E 5,T= 825.
STS-2 ALP=40.9,M=17.8,RE-NS =2.995E 5,T= 930.
STS-2 ALP=41.5,M=16.0,RE-NS =3.970E 5,T= 995.
STS-2 ALP=41.6,M=14.8,RE-NS =4.959E 5,T=1030.
STS-2 ALP=40.6,M=14.1,RE-NS =5.971E 5,T=1055.
STS-2 ALP=39.8,M=13.2,RE-NS =7.090E 5,T=1080.
STS-2 ALP=39.7,M=12.8,RE NS =7.985E 5,T=1095.
FILM COEFF H/HREF
1
10^{-1}
10^{-2}
10^{-3}
0.0
0.2
0.4
0.6
0.8
1.0
1.2
X/L
11/13/84
BASE TIME = 27550236.000 SEC.

STS-3 LOWER CENTERLINE DISTRIBUTION

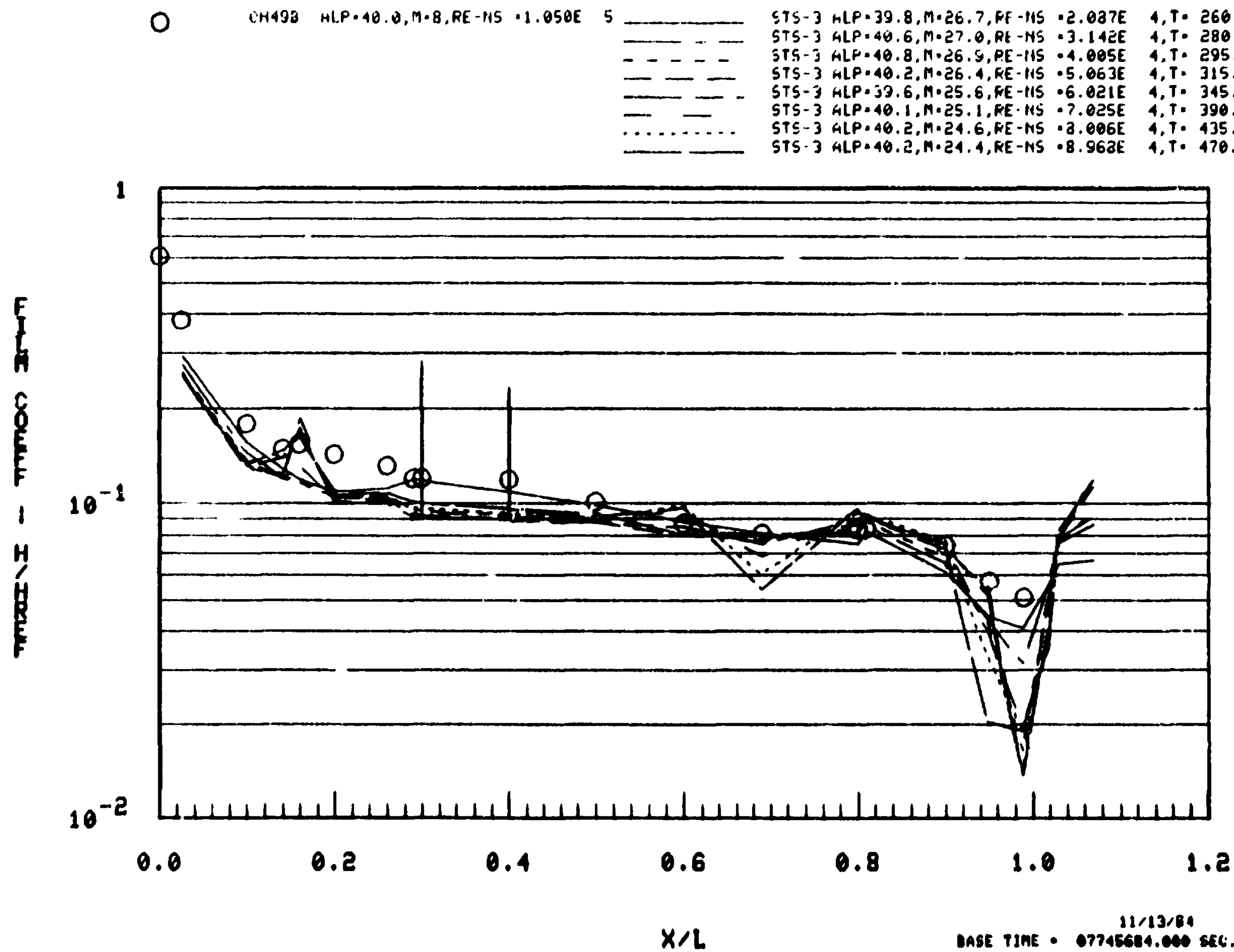

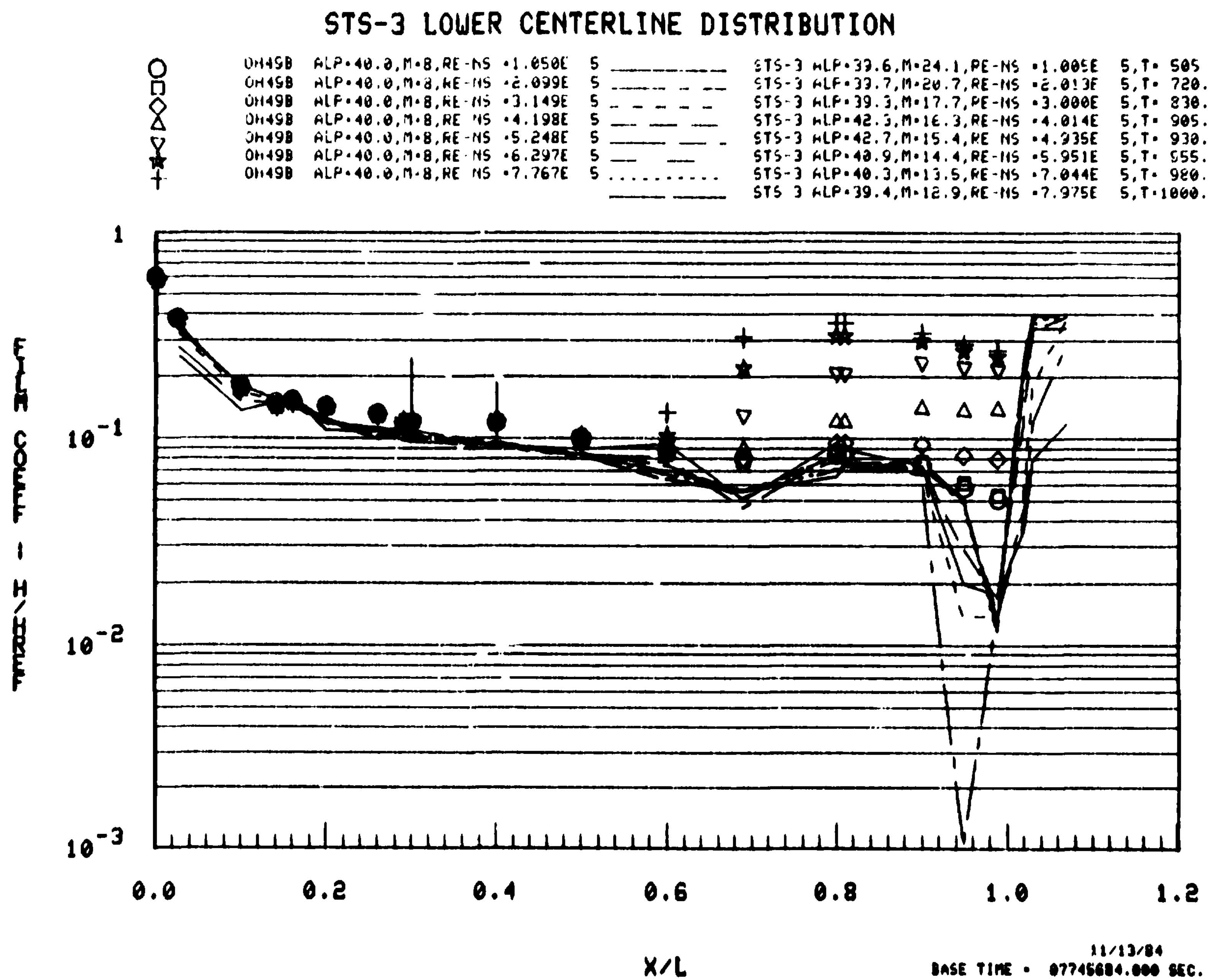
STS-3 LOWER CENTERLINE DISTRIBUTION
OH49B ALP=40.0,M=8,RE-NS =1.050E 5
OH49B ALP=40.0,M=8,RE-NS =2.099E 5
OH49B ALP=40.0,M=8,RE-NS =3.149E 5
OH49B ALP=40.0,M=8,RE-NS =4.198E 5
OH49B ALP=40.0,M=8,RE-NS =5.248E 5
OH49B ALP=40.0,M=8,RE-NS =6.297E 5
OH49B ALP=40.0,M=8,RE-NS =7.767E 5
STS-3 ALP=39.6,M=24.1,RE-NS =1.005E 5,T= 505
STS-3 ALP=39.7,M=20.7,RE-NS =2.013E 5,T= 720.
STS-3 ALP=39.3,M=17.7,RE-NS =3.000E 5,T= 830.
STS-3 ALP=42.3,M=16.3,RE-NS =4.014E 5,T= 905.
STS-3 ALP=42.7,M=15.4,RE-NS =4.935E 5,T= 930.
STS-3 ALP=40.9,M=14.4,RE-NS =5.951E 5,T= 955.
STS-3 ALP=40.3,M=13.5,RE-NS =7.044E 5,T= 980.
STS 3 ALP=39.4,M=12.9,RE-NS =7.975E 5,T=1000.
FILM COEFF : H/HREF
1
10⁻¹
10⁻²
10⁻³
0.0
0.2
0.4
0.6
0.8
1.0
1.2
X/L
11/13/84
BASE TIME = 07745684.000 SEC.

STS-5 LOWER CENTERLINE DISTRIBUTION

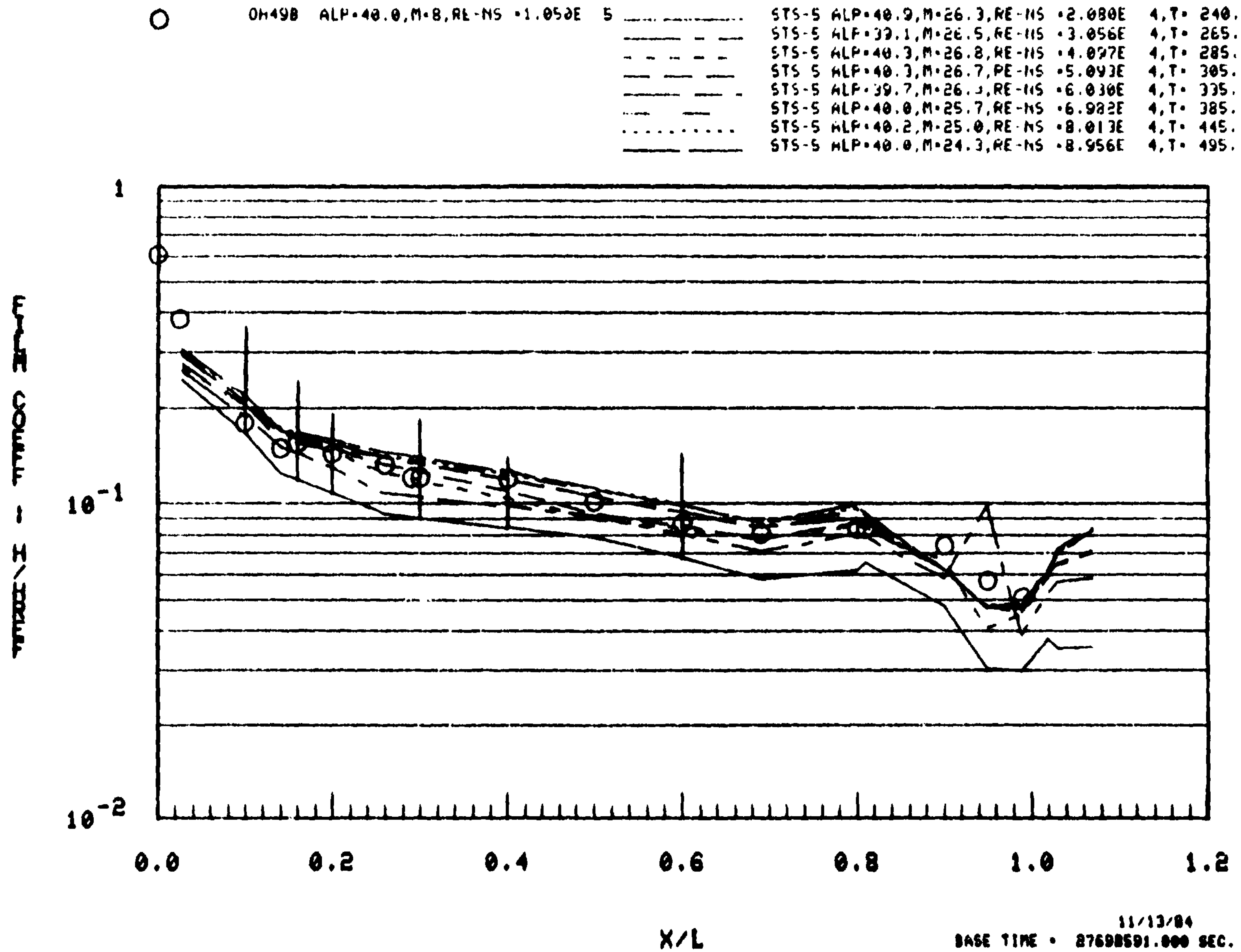

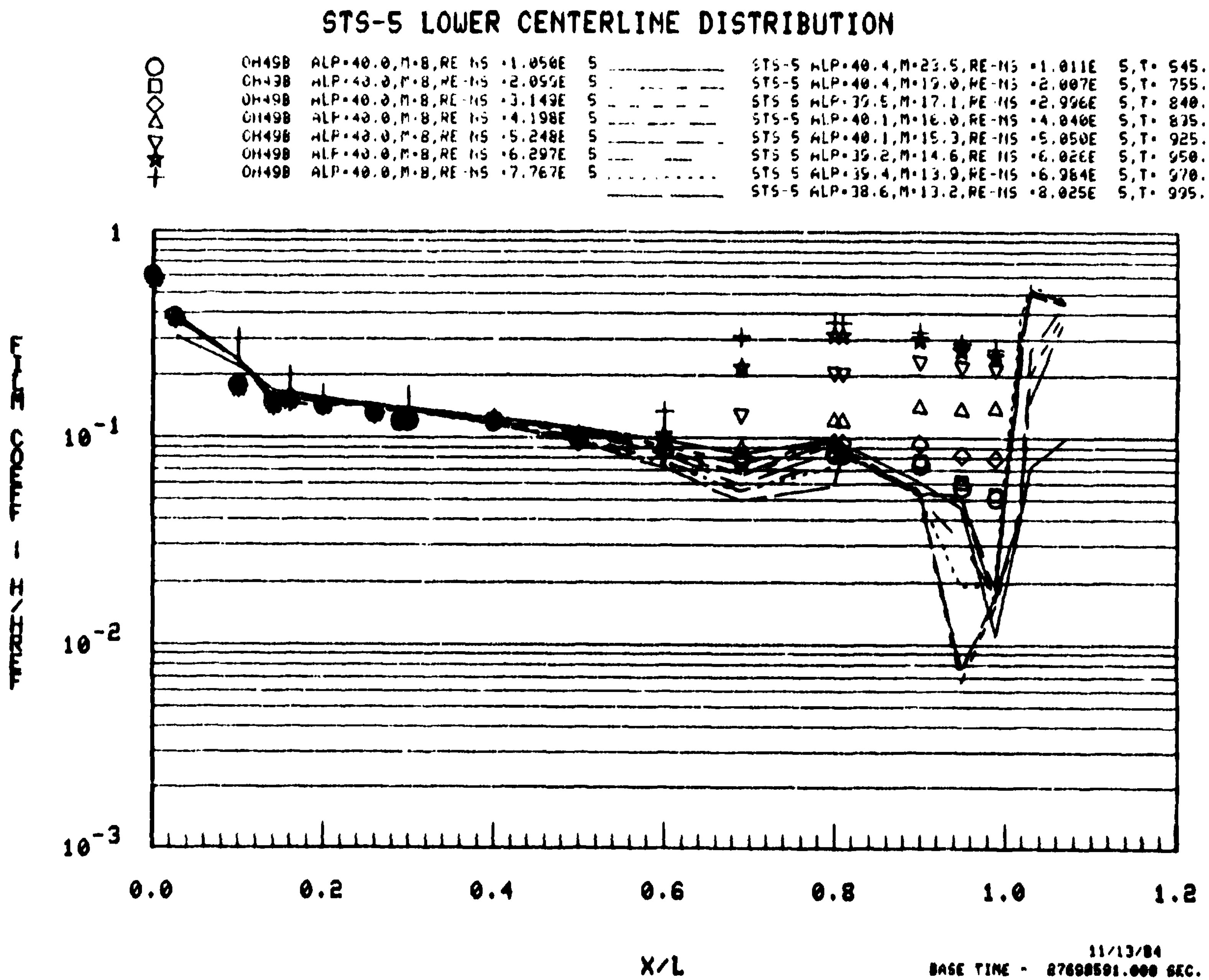

STS-5 LOWER CENTERLINE DISTRIBUTION
OH49B ALP=40.0,M=8,RE-NS =1.050E 5
OH49B ALP=40.0,M=8,RE-NS =2.099E 5
OH49B ALP=40.0,M=8,RE-NS =3.149E 5
OH49B ALP=40.0,M=8,RE-NS =4.198E 5
OH49B ALP=40.0,M=8,RE-NS =5.248E 5
OH49B ALP=40.0,M=8,RE-NS =6.297E 5
OH49B ALP=40.0,M=8,RE-NS =7.767E 5
STS-5 ALP=40.4,M=23.5,RE-NS =1.011E 5,T= 545.
STS-5 ALP=40.4,M=19.0,RE-NS =2.007E 5,T= 755.
STS-5 ALP=39.5,M=17.1,RE-NS =2.996E 5,T= 840.
STS-5 ALP=40.1,M=16.0,RE-NS =4.040E 5,T= 835.
STS-5 ALP=40.1,M=15.3,RE-NS =5.050E 5,T= 925.
STS-5 ALP=39.2,M=14.6,RE-NS =6.026E 5,T= 950.
STS-5 ALP=39.4,M=13.9,RE-NS =6.984E 5,T= 970.
STS-5 ALP=38.6,M=13.2,RE-NS =8.025E 5,T= 995.
FILM COEFF - H/HREF
1
10-1
10-2
10-3
0.0
0.2
0.4
0.6
0.8
1.0
1.2
X/L
11/13/84
BASE TIME - 87698591.000 SEC.

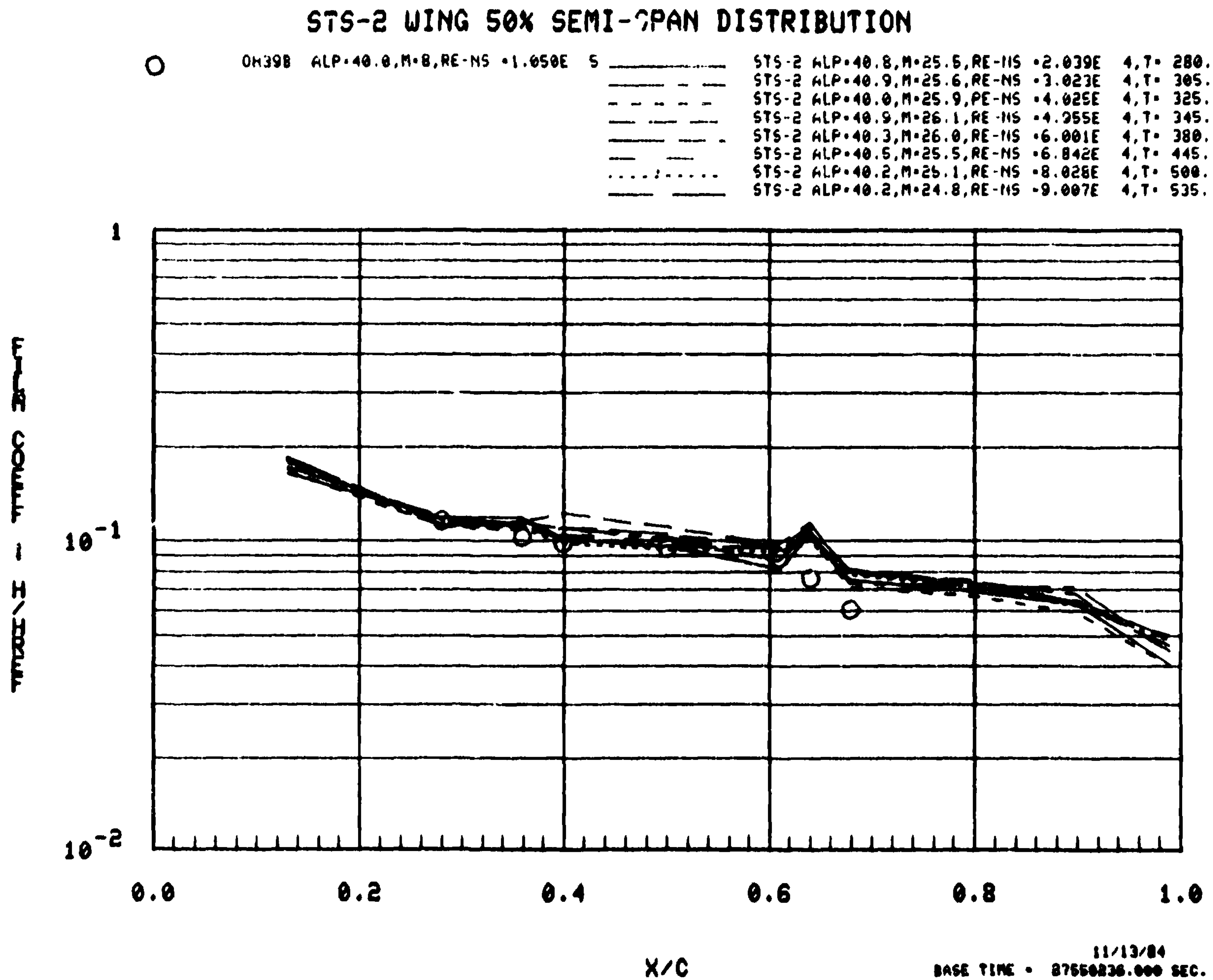
STS-2 WING 50% SEMI-SPAN DISTRIBUTION
OH39B ALP=40.0,M=8,RE-NS =1.050E 5
STS-2 ALP=40.8,M=25.5,RE-NS =2.039E 4,T= 280.
STS-2 ALP=40.9,M=25.6,RE-NS =3.023E 4,T= 305.
STS-2 ALP=40.0,M=25.9,RE-NS =4.025E 4,T= 325.
STS-2 ALP=40.9,M=26.1,RE-NS =4.955E 4,T= 345.
STS-2 ALP=40.3,M=26.0,RE-NS =6.001E 4,T= 380.
STS-2 ALP=40.5,M=25.5,RE-NS =6.842E 4,T= 445.
STS-2 ALP=40.2,M=26.1,RE-NS =8.028E 4,T= 500.
STS-2 ALP=40.2,M=24.8,RE-NS =9.007E 4,T= 535.
FILM COEFF - H/HREF
1
10^{-1}
10^{-2}
0.0
0.2
0.4
0.6
0.8
1.0
X/C
11/13/84
BASE TIME = 87550236.000 SEC.

STS-2 WING 50% SEMI-SPAN DISTRIBUTION

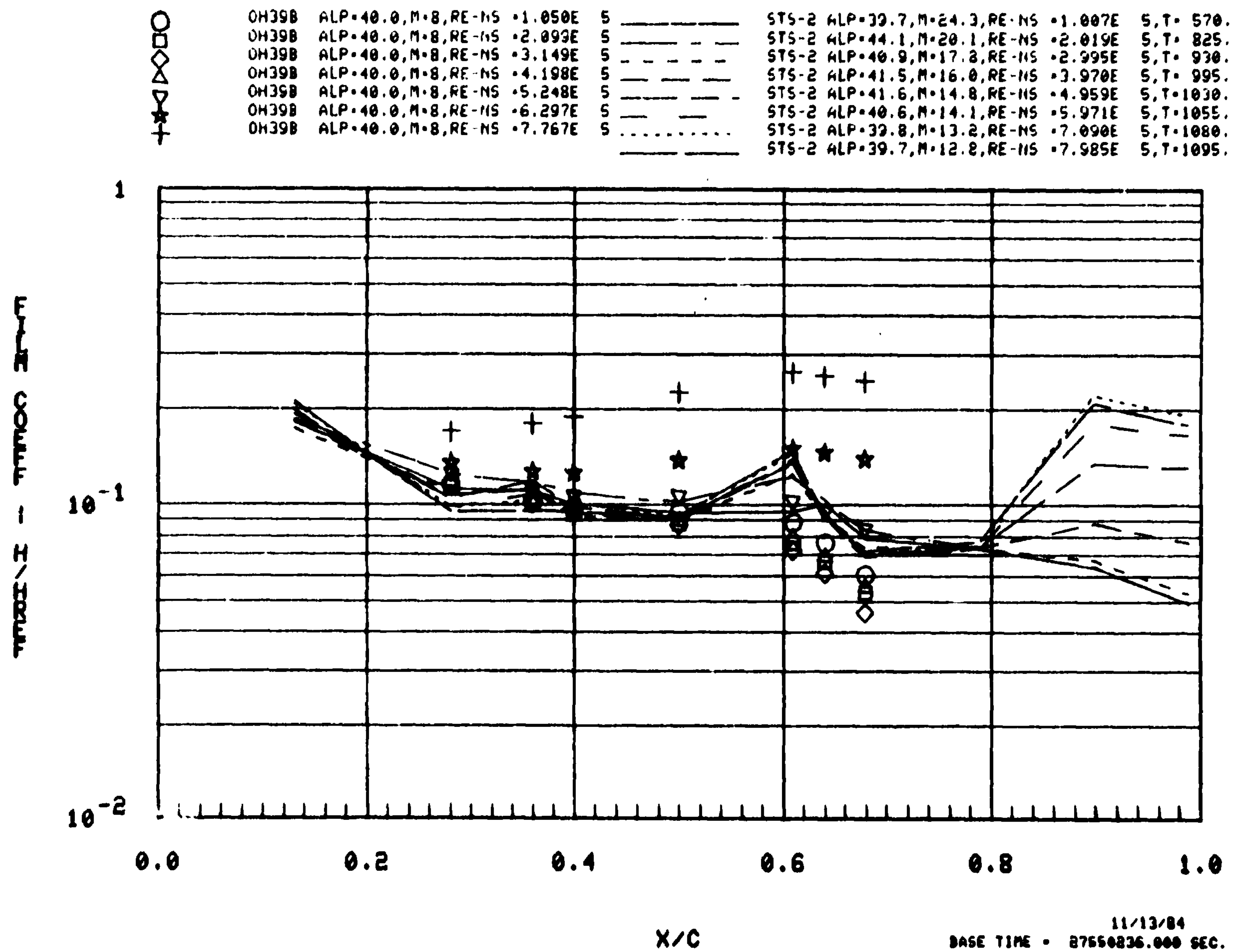

11/13/84
BASE TIME = 87550836.000 SEC.

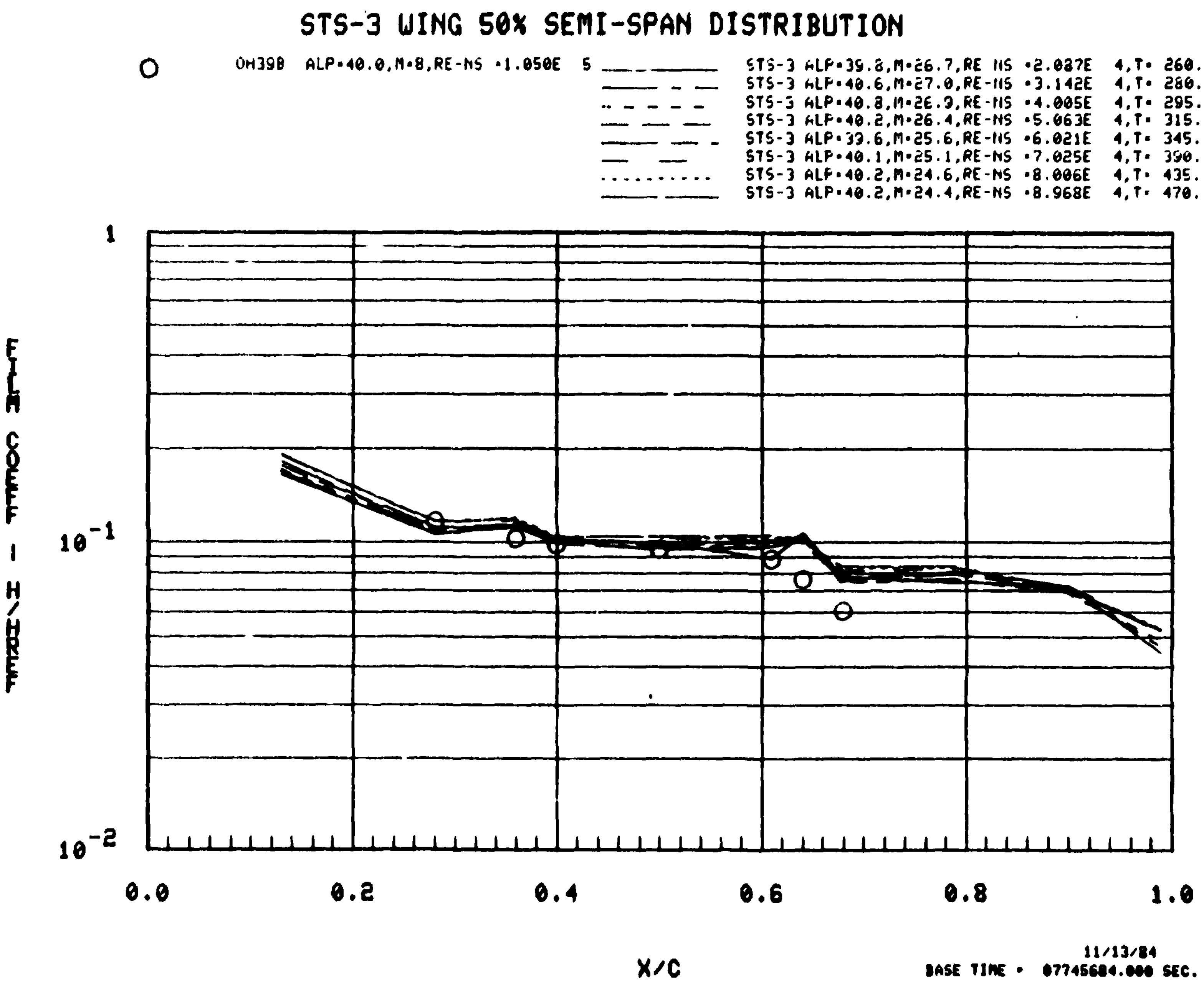

STS-3 WING 50% SEMI-SPAN DISTRIBUTION
OH39B ALP=40.0,M=8,RE-NS =1.050E 5
STS-3 ALP=39.8,M=26.7,RE NS =2.087E 4,T= 260.
STS-3 ALP=40.6,M=27.0,RE-NS =3.142E 4,T= 280.
STS-3 ALP=40.8,M=26.9,RE-NS =4.005E 4,T= 295.
STS-3 ALP=40.2,M=26.4,RE-NS =5.063E 4,T= 315.
STS-3 ALP=39.6,M=25.6,RE-NS =6.021E 4,T= 345.
STS-3 ALP=40.1,M=25.1,RE-NS =7.025E 4,T= 390.
STS-3 ALP=40.2,M=24.6,RE-NS =8.006E 4,T= 435.
STS-3 ALP=40.2,M=24.4,RE-NS =8.968E 4,T= 470.
FILM COEFF - H/HREF
1
10^-1
10^-2
0.0
0.2
0.4
0.6
0.8
1.0
X/C
11/13/84
BASE TIME = 07745684.000 SEC.

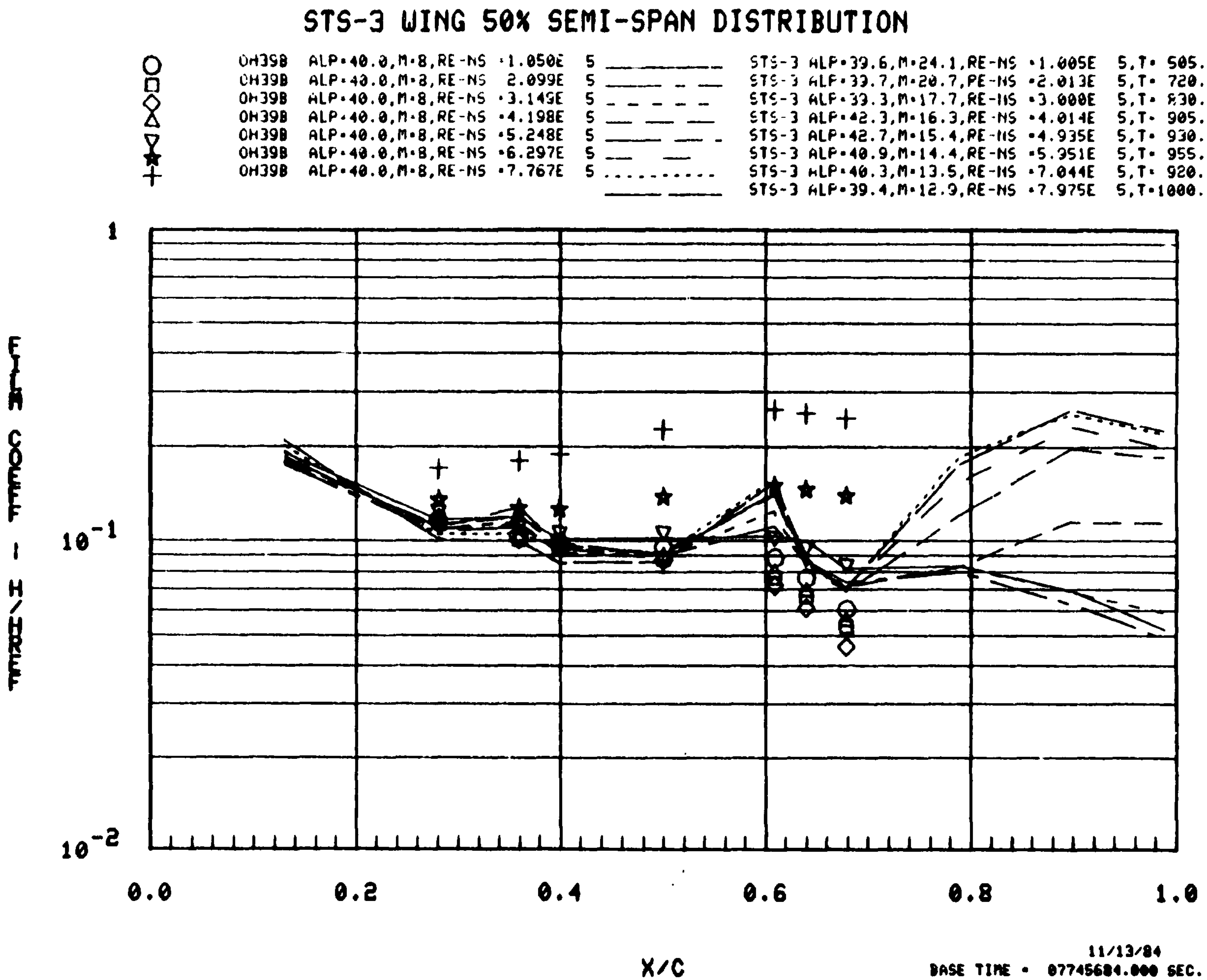

STS-3 WING 50% SEMI-SPAN DISTRIBUTION
OH39B ALP=40.0,M=8,RE-NS =1.050E 5
OH39B ALP=40.0,M=8,RE-NS 2.099E 5
OH39B ALP=40.0,M=8,RE-NS =3.149E 5
OH39B ALP=40.0,M=8,RE-NS =4.198E 5
OH39B ALP=40.0,M=8,RE-NS =5.248E 5
OH39B ALP=40.0,M=8,RE-NS =6.297E 5
OH39B ALP=40.0,M=8,RE-NS =7.767E 5
STS-3 ALP=39.6,M=24.1,RE-NS =1.005E 5,T= 505.
STS-3 ALP=39.7,M=20.7,RE-NS =2.013E 5,T= 720.
STS-3 ALP=39.3,M=17.7,RE-NS =3.000E 5,T= 830.
STS-3 ALP=42.3,M=16.3,RE-NS =4.014E 5,T= 905.
STS-3 ALP=42.7,M=15.4,RE-NS =4.935E 5,T= 930.
STS-3 ALP=40.9,M=14.4,RE-NS =5.951E 5,T= 955.
STS-3 ALP=40.3,M=13.5,RE-NS =7.044E 5,T= 920.
STS-3 ALP=39.4,M=12.9,RE-NS =7.975E 5,T=1000.
FILM COEFF - H/HREF
1
10^{-1}
10^{-2}
0.0
0.2
0.4
0.6
0.8
1.0
X/C
11/13/84
BASE TIME = 07745684.000 SEC.

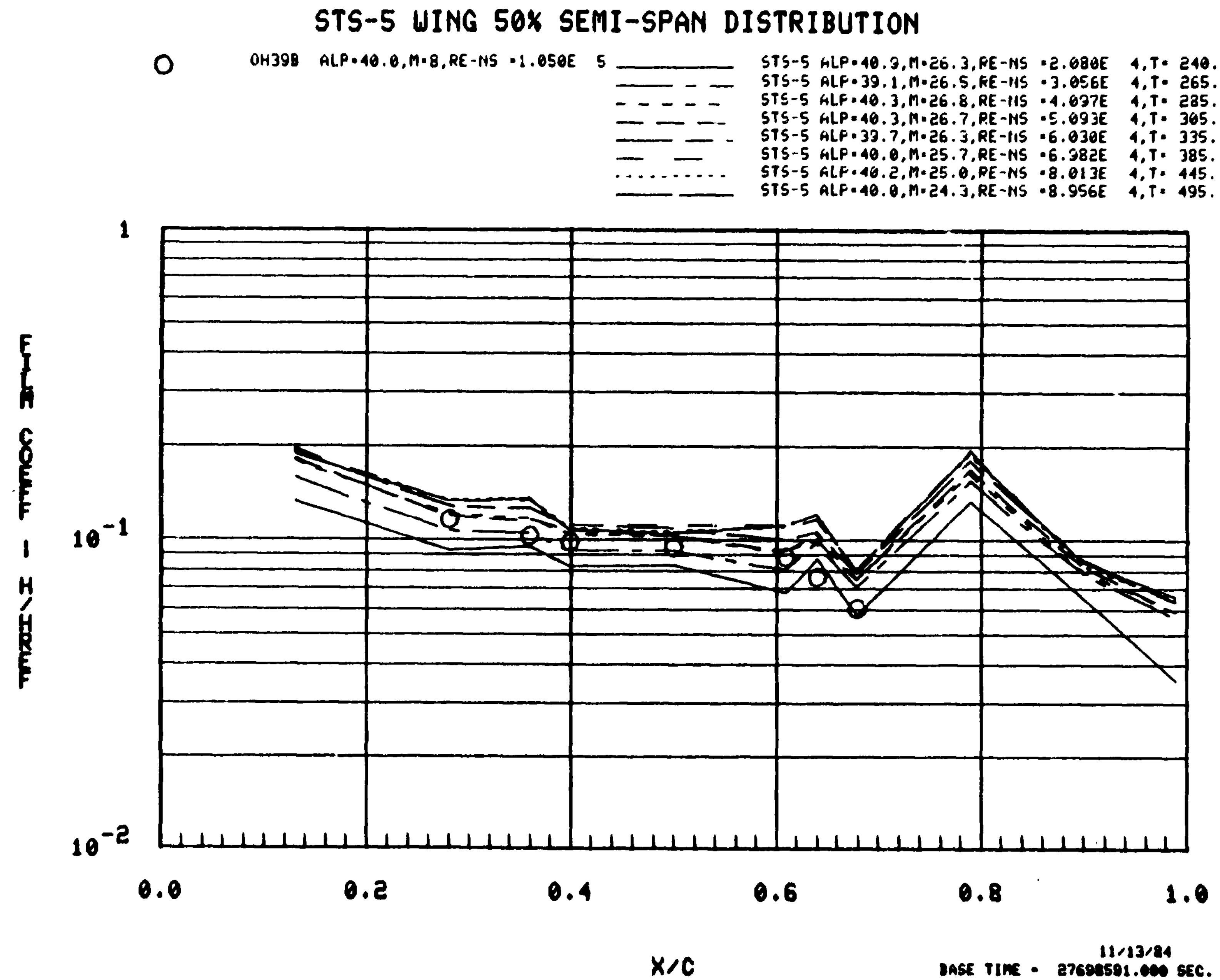

STS-5 WING 50% SEMI-SPAN DISTRIBUTION
OH39B ALP=40.0,M=8,RE-NS =1.050E 5
STS-5 ALP=40.9,M=26.3,RE-NS =2.080E 4,T= 240.
STS-5 ALP=39.1,M=26.5,RE-NS =3.056E 4,T= 265.
STS-5 ALP=40.3,M=26.8,RE-NS =4.037E 4,T= 285.
STS-5 ALP=40.3,M=26.7,RE-NS =5.093E 4,T= 305.
STS-5 ALP=39.7,M=26.3,RE-NS =6.030E 4,T= 335.
STS-5 ALP=40.0,M=25.7,RE-NS =6.982E 4,T= 385.
STS-5 ALP=40.2,M=25.0,RE-NS =8.013E 4,T= 445.
STS-5 ALP=40.0,M=24.3,RE-NS =8.956E 4,T= 495.
FILM COEFF - H/HREF
1
10^{-1}
10^{-2}
0.0
0.2
0.4
0.6
0.8
1.0
X/C
11/13/84
BASE TIME = 27698591.000 SEC.

STS-5 WING 50% SEMI-SPAN DISTRIBUTION

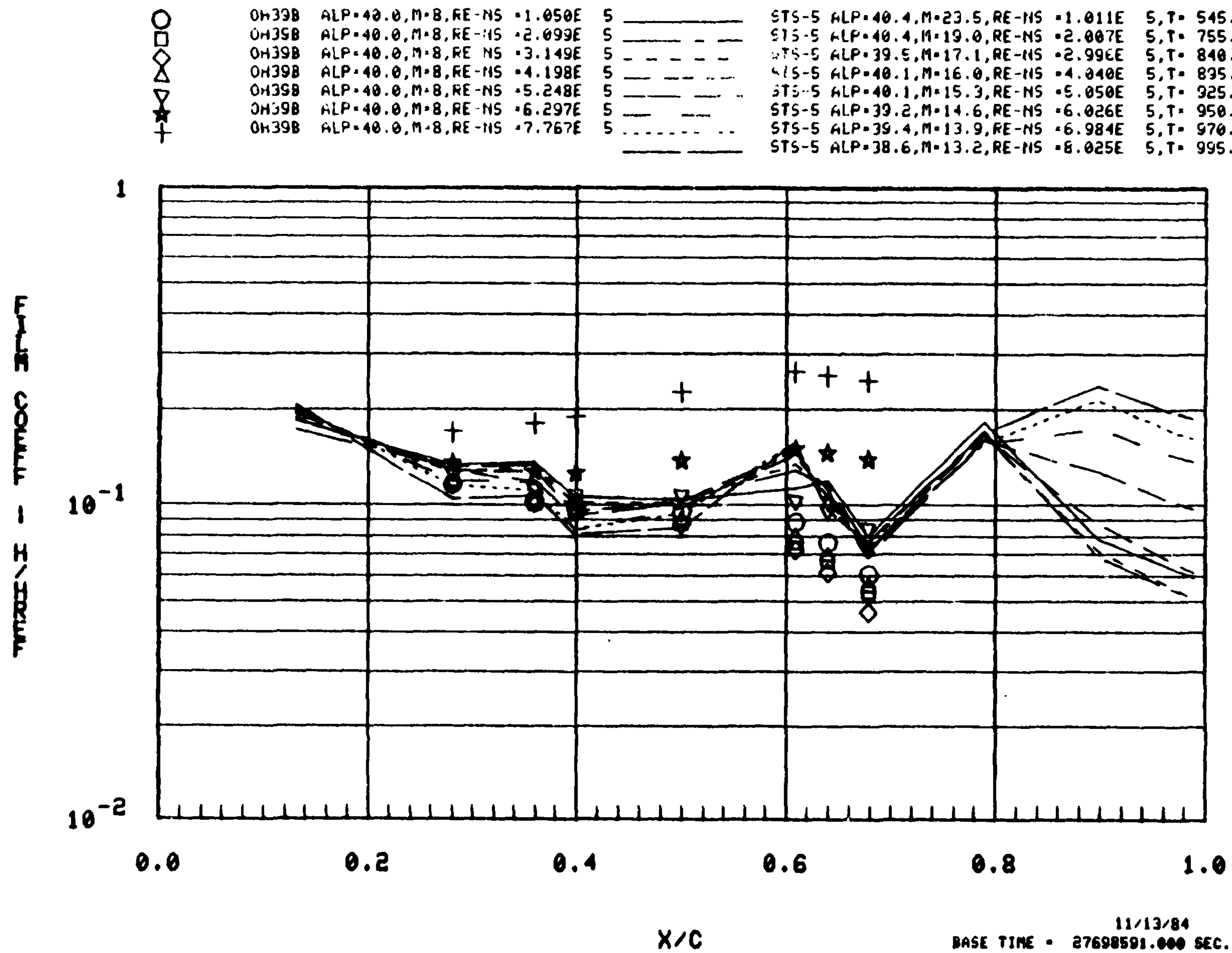

11/13/84
BASE TIME = 27698591.000 SEC.

STS-2 WING 80% SEMI-SPAN DISTRIBUTION

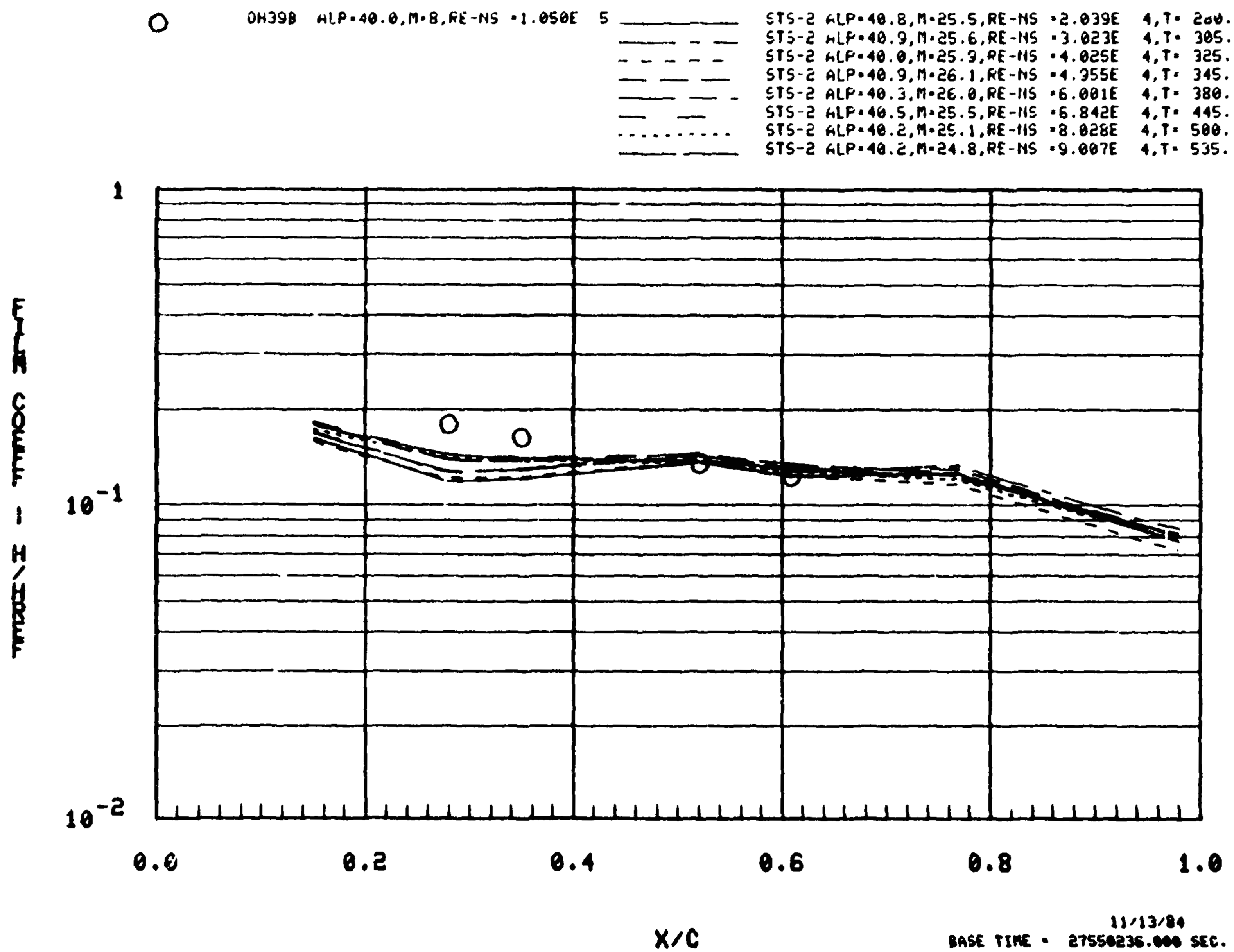

11/13/84
BASE TIME = 27550236.000 SEC.

STS-2 WING 80% SEMI-SPAN DISTRIBUTION

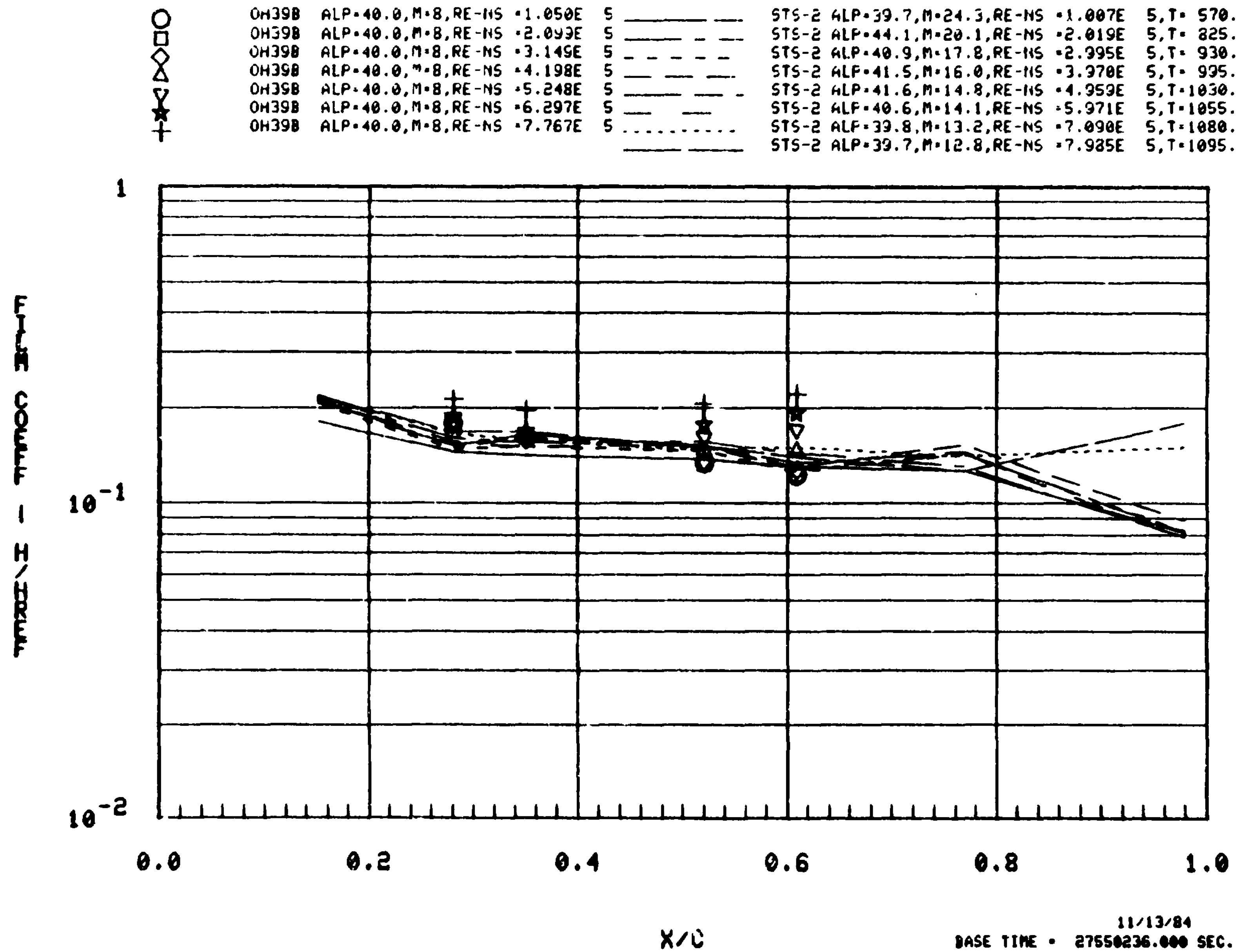

STS-3 WING 80% SEMI-SPAN DISTRIBUTION

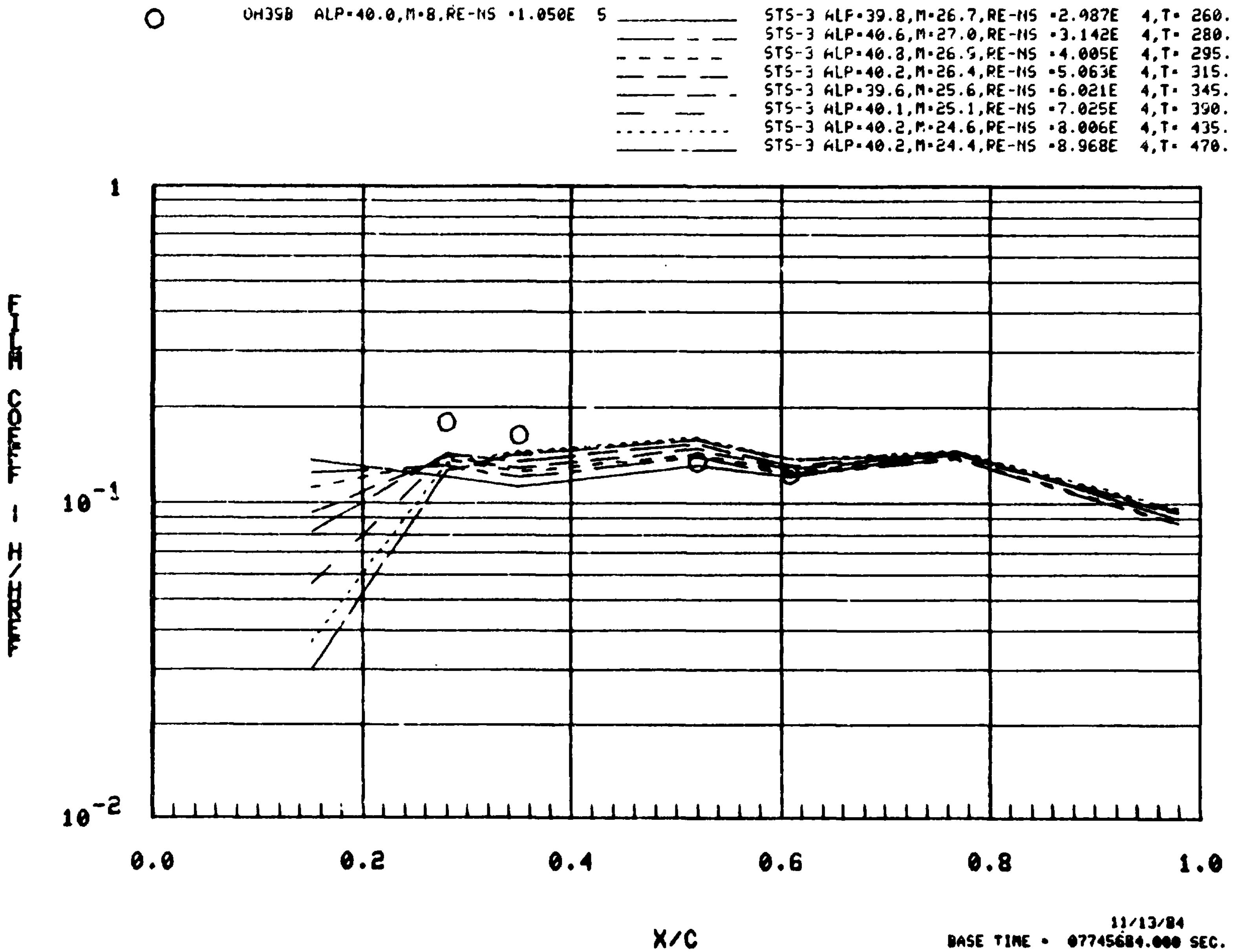

STS-3 WING 80% SEMI-SPAN DISTRIBUTION

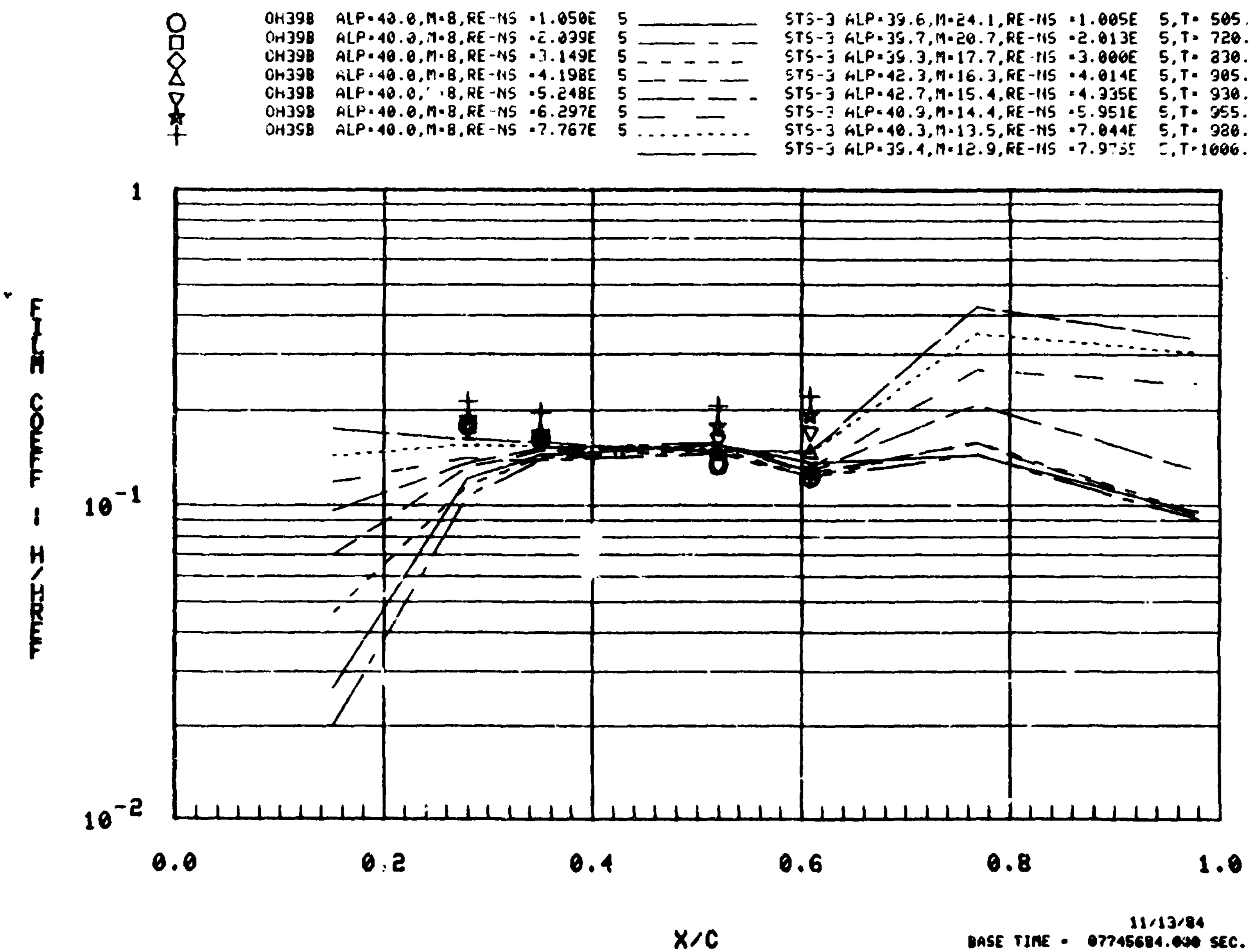

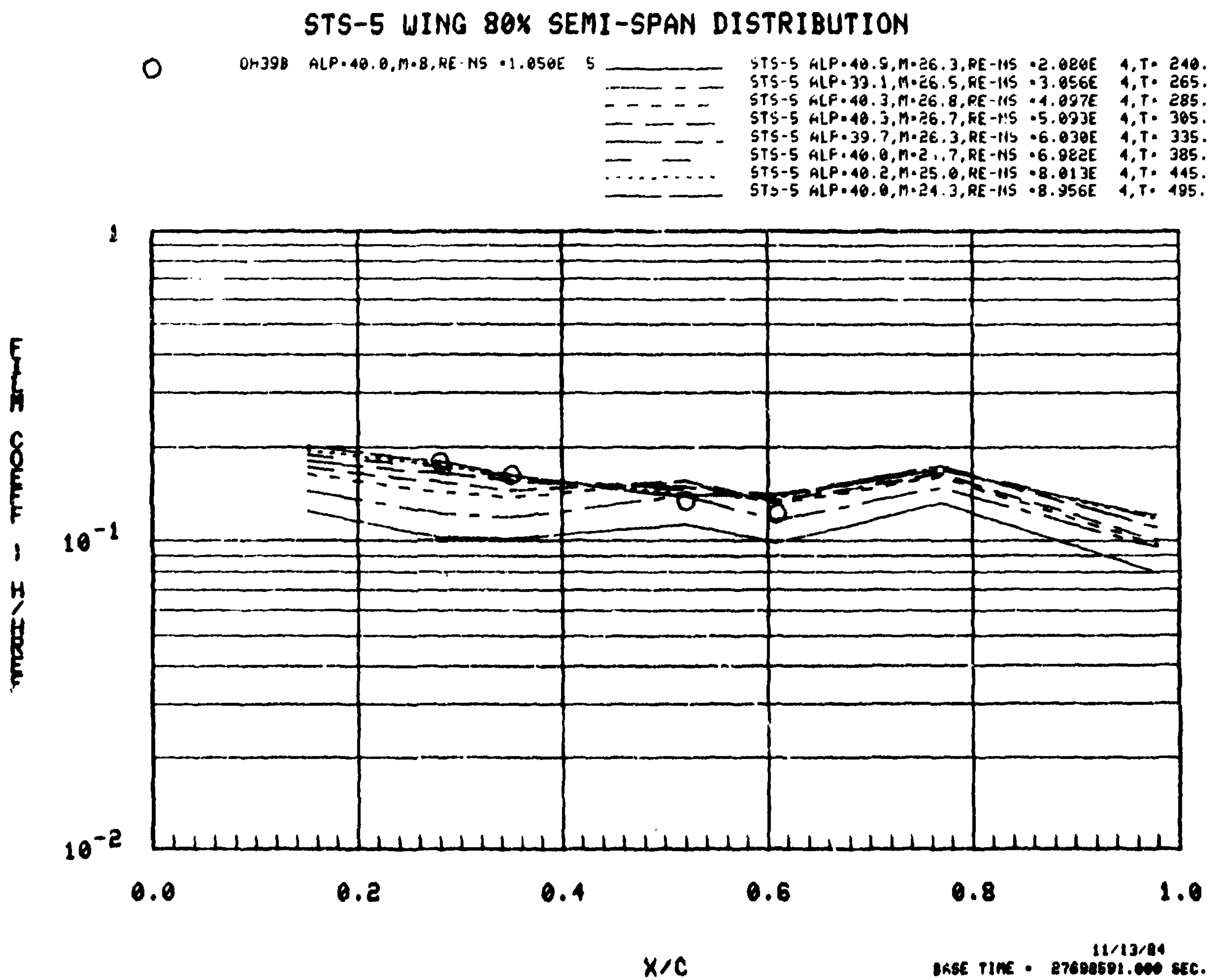

STS-5 WING 80% SEMI-SPAN DISTRIBUTION
OH39B ALP=40.0,M=8,RE-NS =1.050E 5
STS-5 ALP=40.9,M=26.3,RE-NS =2.020E 4,T= 240.
STS-5 ALP=39.1,M=26.5,RE-NS =3.056E 4,T= 265.
STS-5 ALP=40.3,M=26.8,RE-NS =4.097E 4,T= 285.
STS-5 ALP=40.3,M=26.7,RE-NS =5.093E 4,T= 305.
STS-5 ALP=39.7,M=26.3,RE-NS =6.030E 4,T= 335.
STS-5 ALP=40.0,M=2 .7,RE-NS =6.922E 4,T= 385.
STS-5 ALP=40.2,M=25.0,RE-NS =8.013E 4,T= 445.
STS-5 ALP=40.0,M=24.3,RE-NS =8.956E 4,T= 495.
FILM COEFF - H/HREF
1
10^{-1}
10^{-2}
0.0
0.2
0.4
0.6
0.8
1.0
X/C
11/13/84
BASE TIME = 27698591.000 SEC.

STS-5 WING 80% SEMI-SPAN DISTRIBUTION

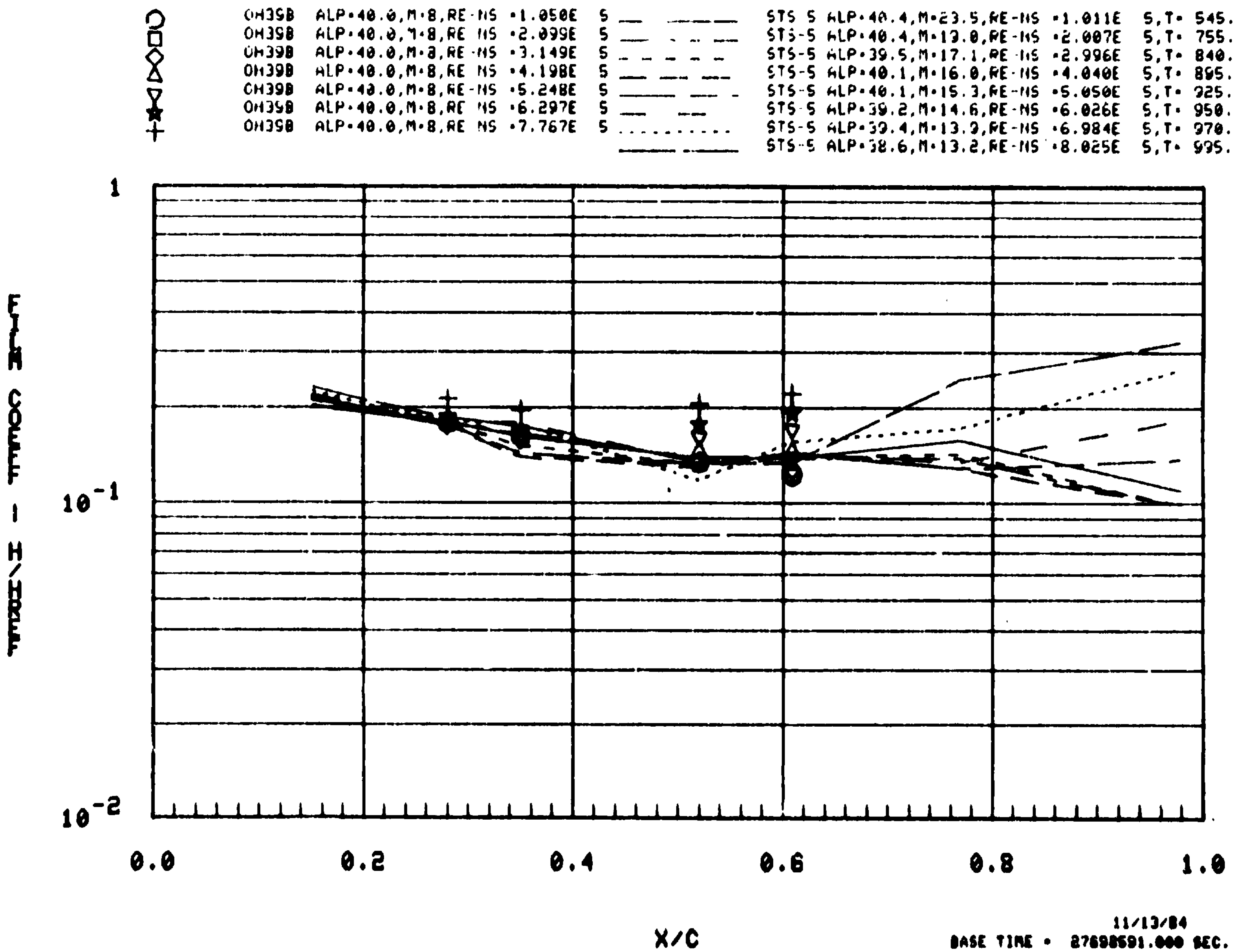

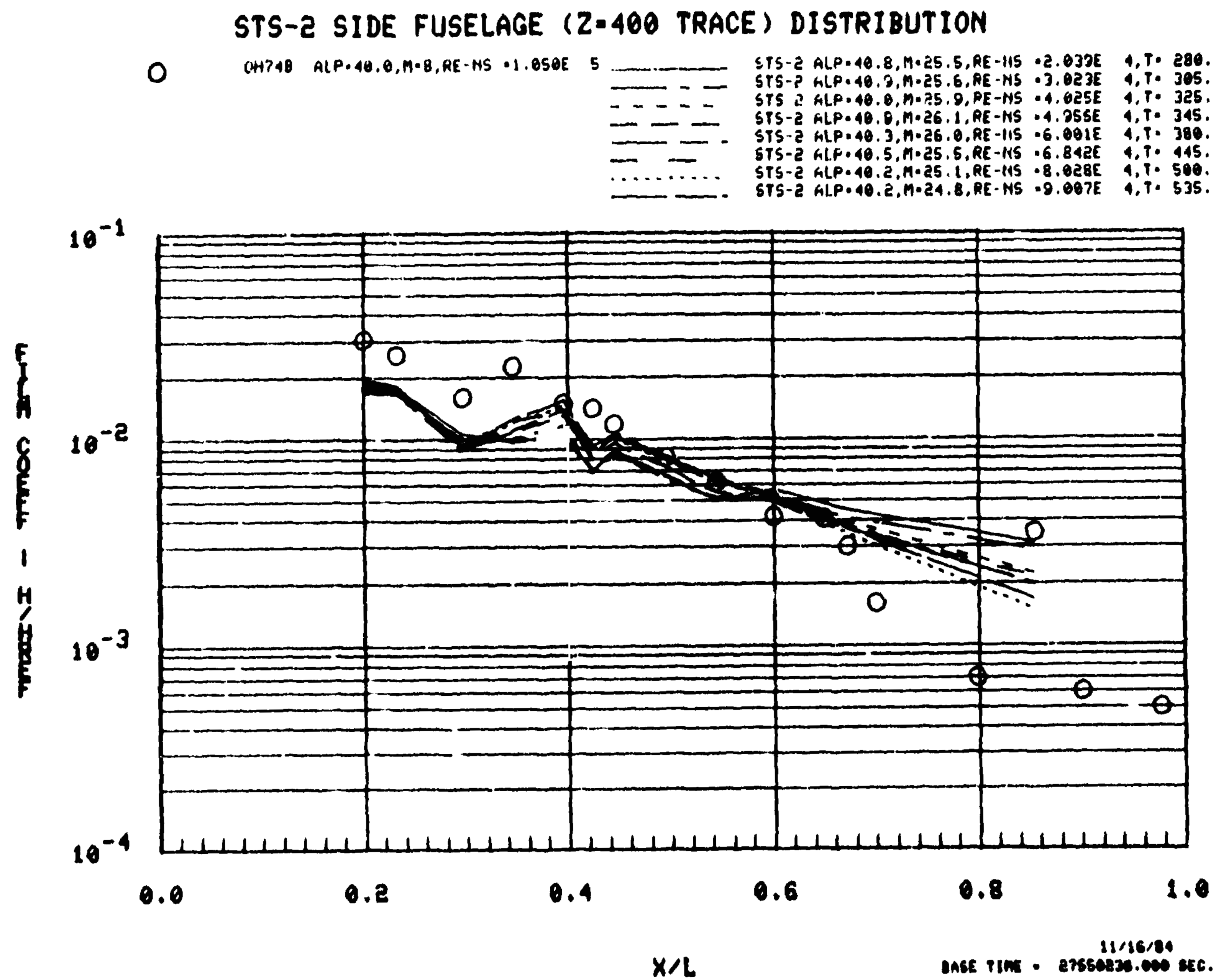

STS-2 SIDE FUSELAGE (Z=400 TRACE) DISTRIBUTION
OH74B ALP=40.0,M=8,RE-NS =1.050E 5
STS-2 ALP=40.8,M=25.5,RE-NS =2.039E 4,T= 280.
STS-2 ALP=40.9,M=25.6,RE-NS =3.023E 4,T= 305.
STS 2 ALP=40.0,M=25.9,RE-NS =4.025E 4,T= 325.
STS-2 ALP=40.0,M=26.1,RE-NS =4.955E 4,T= 345.
STS-2 ALP=40.3,M=26.0,RE-NS =6.001E 4,T= 380.
STS-2 ALP=40.5,M=25.5,RE-NS =6.842E 4,T= 445.
STS-2 ALP=40.2,M=25.1,RE-NS =8.028E 4,T= 500.
STS-2 ALP=40.2,M=24.8,RE-NS =9.007E 4,T= 535.
FILM COEFF : H/HREF
10^{-1}
10^{-2}
10^{-3}
10^{-4}
0.0
0.2
0.4
0.6
0.8
1.0
X/L
11/16/84
BASE TIME = 27550830.000 SEC.

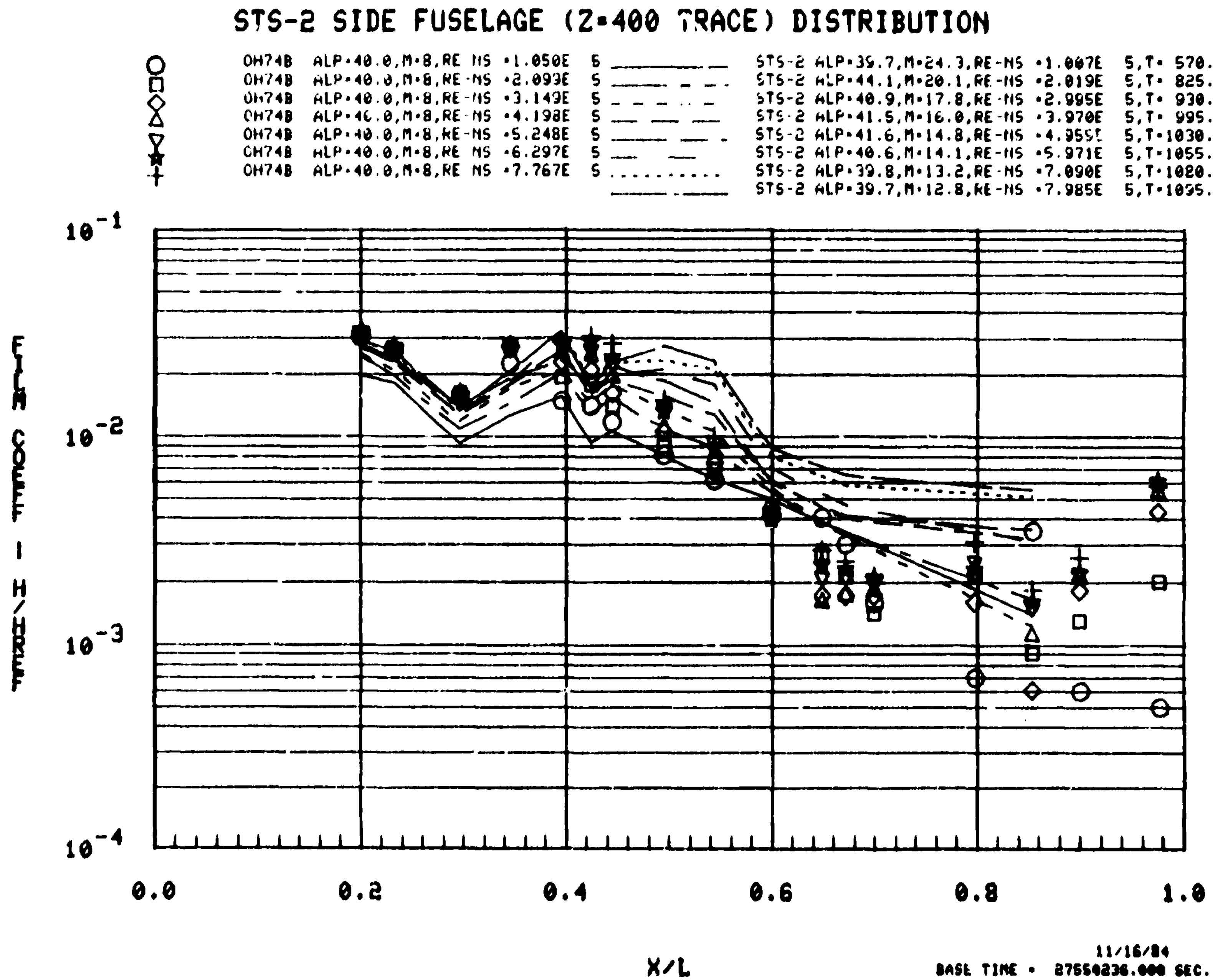
STS-2 SIDE FUSELAGE (Z=400 TRACE) DISTRIBUTION
OH74B ALP=40.0,M=8,RE-NS =1.050E 5
OH74B ALP=40.0,M=8,RE-NS =2.093E 5
OH74B ALP=40.0,M=8,RE-NS =3.149E 5
OH74B ALP=40.0,M=8,RE-NS =4.198E 5
OH74B ALP=40.0,M=8,RE-NS =5.248E 5
OH74B ALP=40.0,M=8,RE-NS =6.297E 5
OH74B ALP=40.0,M=8,RE-NS =7.767E 5
STS-2 ALP=39.7,M=24.3,RE-NS =1.007E 5,T= 570.
STS-2 ALP=44.1,M=20.1,RE-NS =2.019E 5,T= 825.
STS-2 ALP=40.9,M=17.8,RE-NS =2.995E 5,T= 930.
STS-2 ALP=41.5,M=16.0,RE-NS =3.970E 5,T= 995.
STS-2 ALP=41.6,M=14.8,RE-NS =4.955E 5,T=1030.
STS-2 ALP=40.6,M=14.1,RE-NS =5.971E 5,T=1055.
STS-2 ALP=39.8,M=13.2,RE-NS =7.090E 5,T=1080.
STS-2 ALP=39.7,M=12.8,RE-NS =7.985E 5,T=1095.
FILM COEFF | H/HREF
10^-1
10^-2
10^-3
10^-4
0.0
0.2
0.4
0.6
0.8
1.0
X/L
11/16/84
BASE TIME = 27550236.000 SEC.

STS-3 SIDE FUSELAGE (Z=400 TRACE) DISTRIBUTION

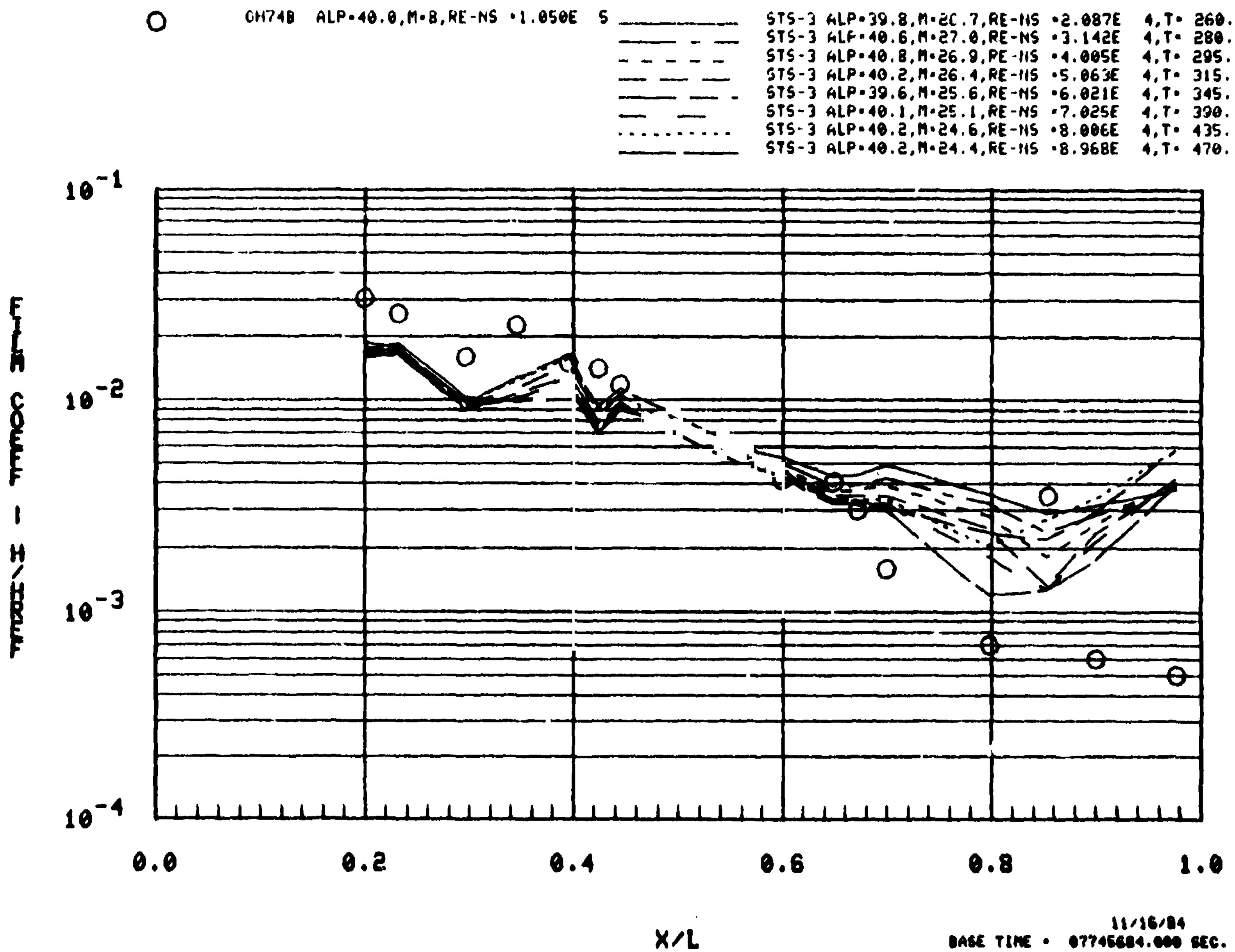

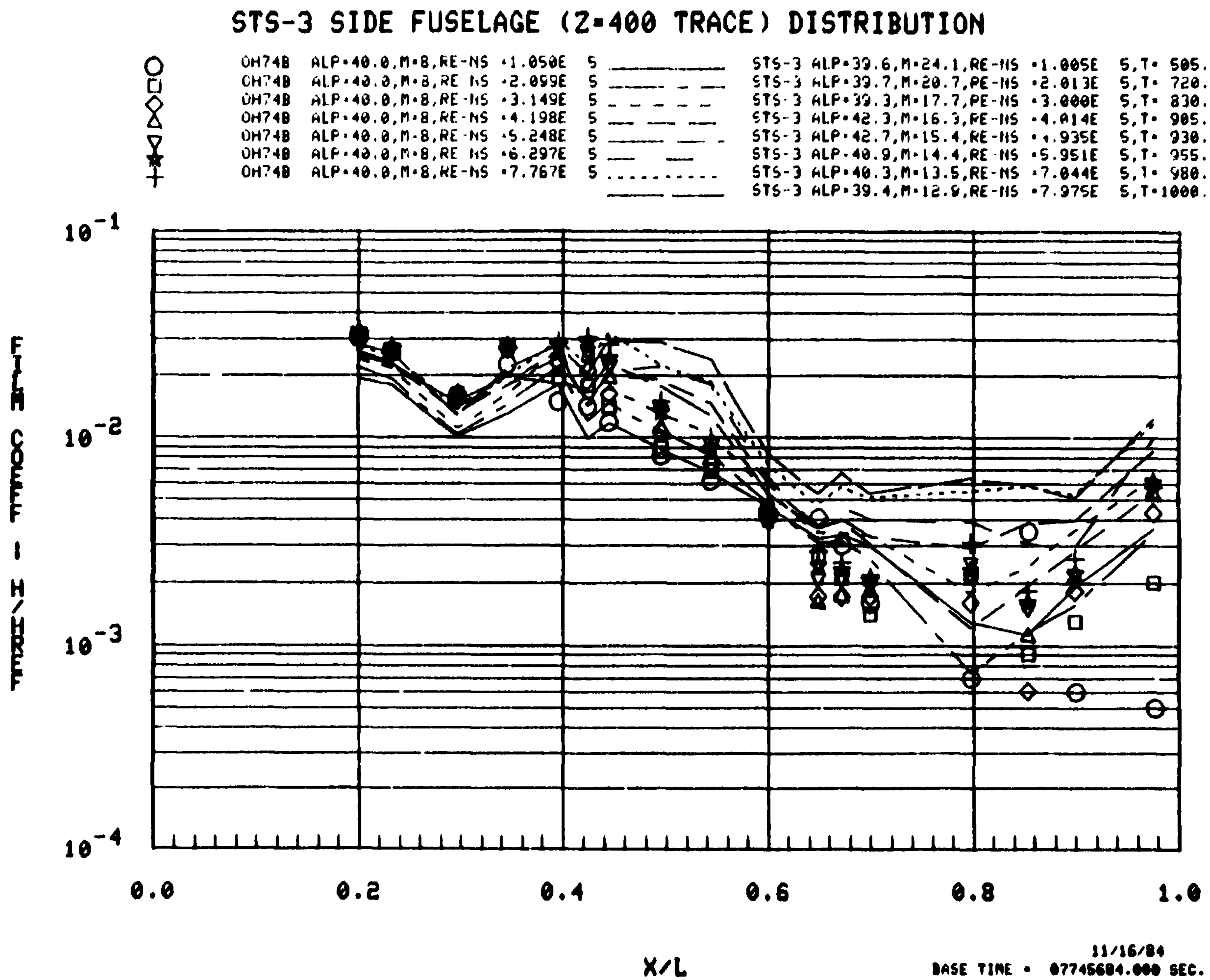

STS-3 SIDE FUSELAGE (Z=400 TRACE) DISTRIBUTION
OH74B ALP=40.0,M=8,RE-NS =1.050E 5
OH74B ALP=40.0,M=8,RE-NS =2.099E 5
OH74B ALP=40.0,M=8,RE-NS =3.149E 5
OH74B ALP=40.0,M=8,RE-NS =4.198E 5
OH74B ALP=40.0,M=8,RE-NS =5.248E 5
OH74B ALP=40.0,M=8,RE-NS =6.297E 5
OH74B ALP=40.0,M=8,RE-NS =7.767E 5
STS-3 ALP=39.6,M=24.1,RE-NS =1.005E 5,T= 505.
STS-3 ALP=39.7,M=20.7,RE-NS =2.013E 5,T= 720.
STS-3 ALP=39.3,M=17.7,RE-NS =3.000E 5,T= 830.
STS-3 ALP=42.3,M=16.3,RE-NS =4.014E 5,T= 905.
STS-3 ALP=42.7,M=15.4,RE-NS =4.935E 5,T= 930.
STS-3 ALP=40.9,M=14.4,RE-NS =5.951E 5,T= 955.
STS-3 ALP=40.3,M=13.5,RE-NS =7.044E 5,T= 980.
STS-3 ALP=39.4,M=12.9,RE-NS =7.975E 5,T=1000.
FILM COEFF : H/HREF
X/L
11/16/84
BASE TIME = 07745684.000 SEC.

STS-5 SIDE FUSELAGE (Z=400 TRACE) DISTRIBUTION

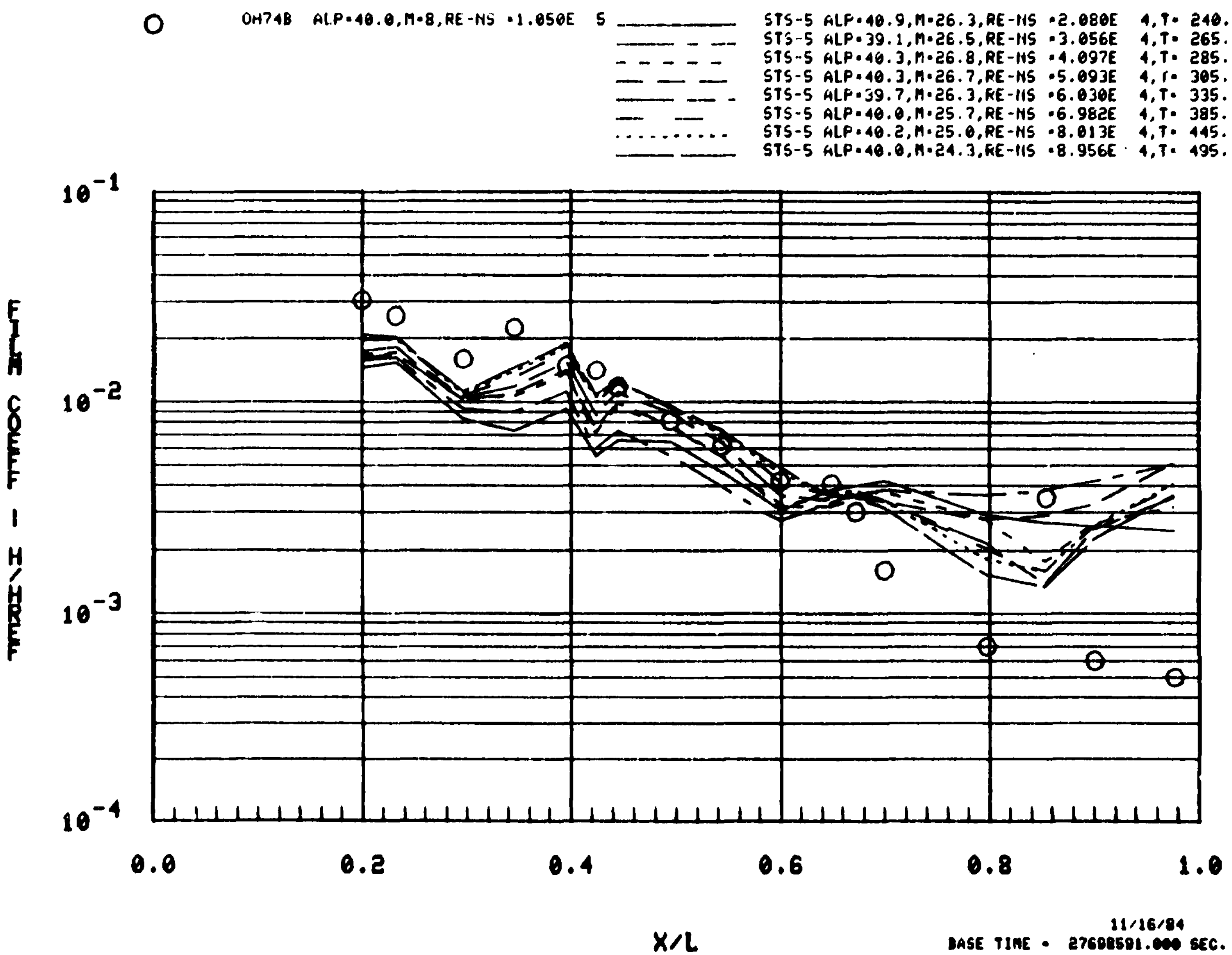

11/16/84
BASE TIME = 27608591.000 SEC.

STS-5 SIDE FUSELAGE (Z=400 TRACE) DISTRIBUTION

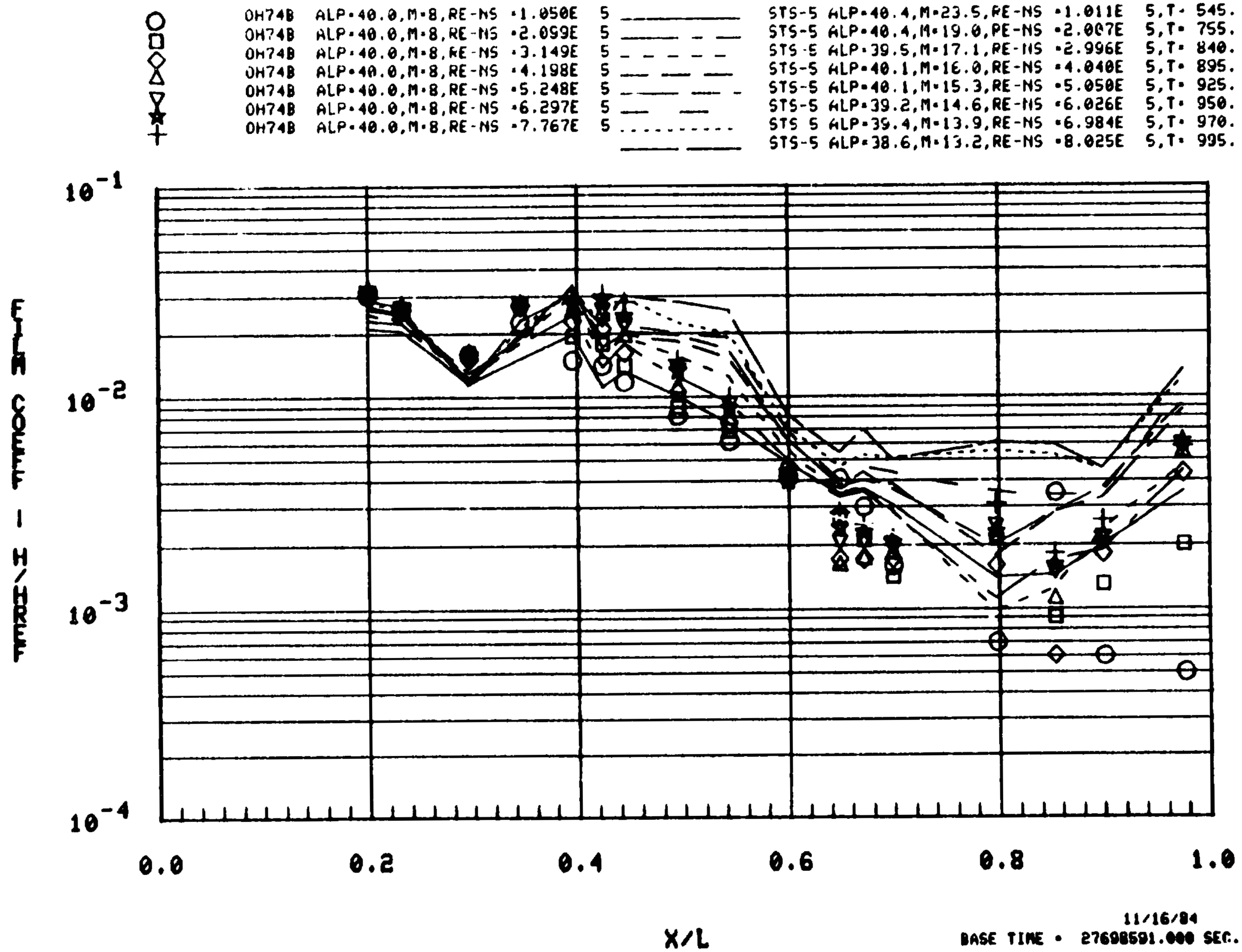

STS-2 SIDE PLB DOOR (Z=440 TRACE) DISTRIBUTION

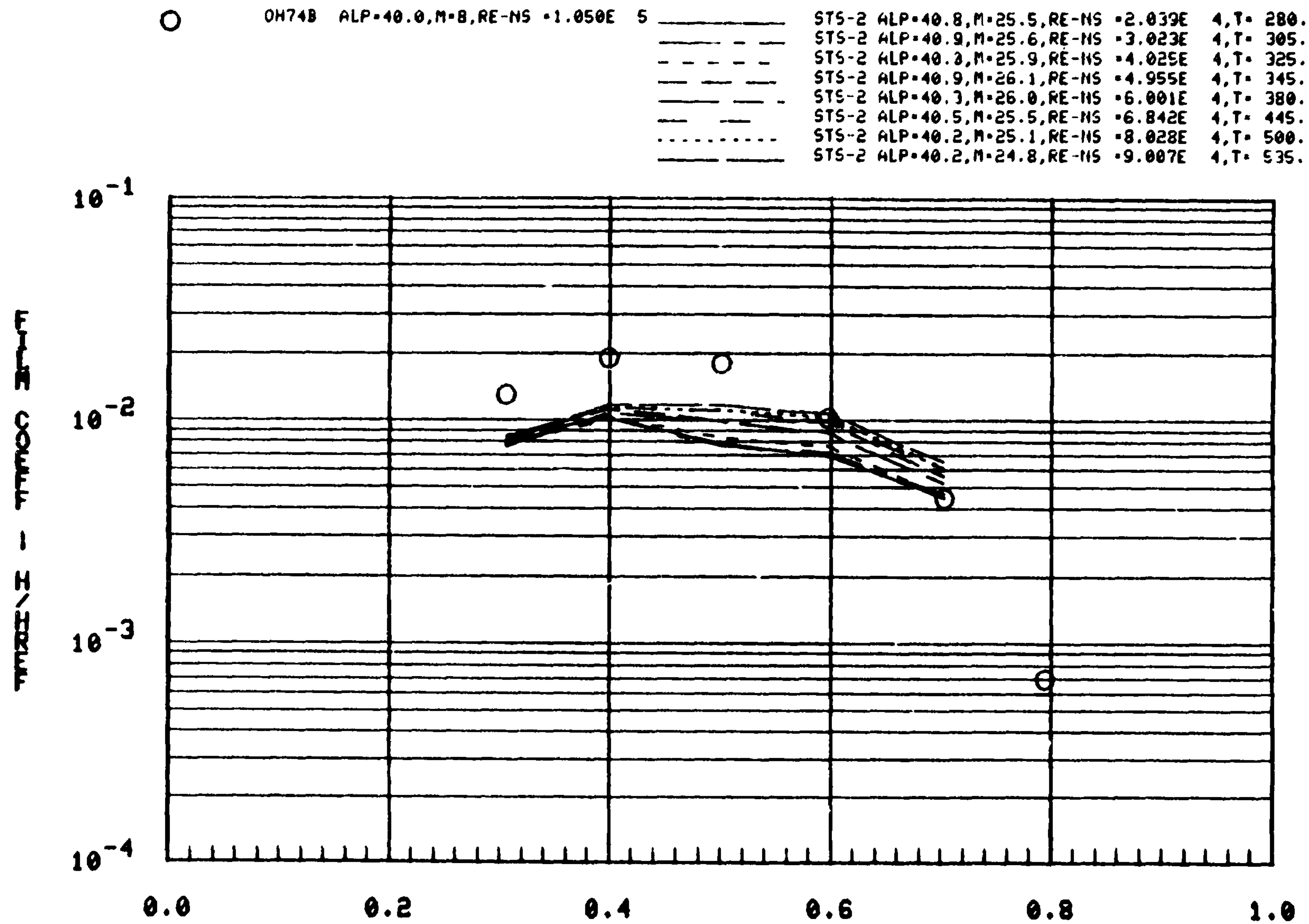

11/16/84
BASE TIME = 27550236.000 SEC.

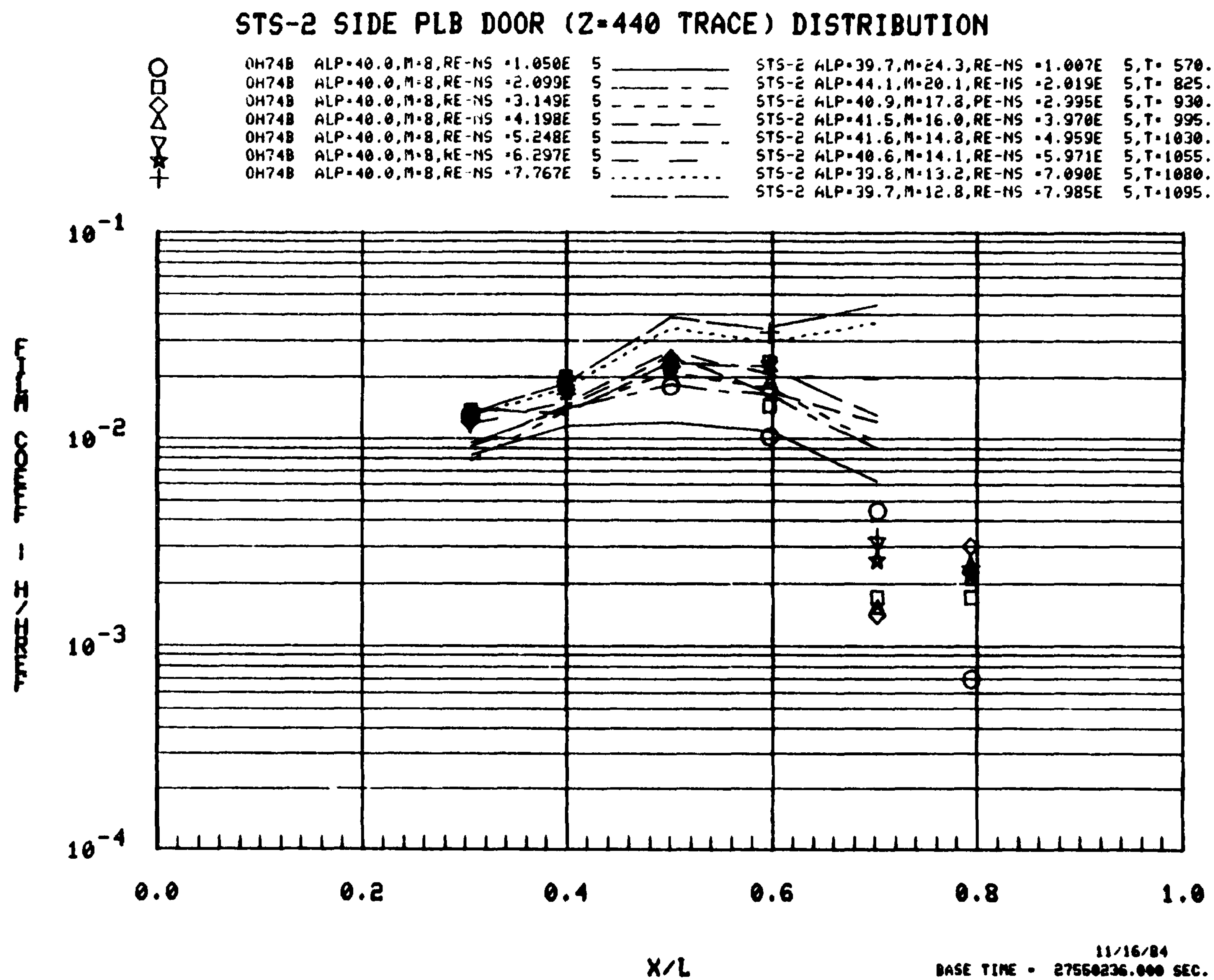

STS-2 SIDE PLB DOOR (Z=440 TRACE) DISTRIBUTION
OH74B ALP=40.0,M=8,RE-NS =1.050E 5
OH74B ALP=40.0,M=8,RE-NS =2.099E 5
OH74B ALP=40.0,M=8,RE-NS =3.149E 5
OH74B ALP=40.0,M=8,RE-NS =4.198E 5
OH74B ALP=40.0,M=8,RE-NS =5.248E 5
OH74B ALP=40.0,M=8,RE-NS =6.297E 5
OH74B ALP=40.0,M=8,RE-NS =7.767E 5
STS-2 ALP=39.7,M=24.3,RE-NS =1.007E 5,T= 570.
STS-2 ALP=44.1,M=20.1,RE-NS =2.019E 5,T= 825.
STS-2 ALP=40.9,M=17.8,RE-NS =2.995E 5,T= 930.
STS-2 ALP=41.5,M=16.0,RE-NS =3.970E 5,T= 995.
STS-2 ALP=41.6,M=14.8,RE-NS =4.959E 5,T=1030.
STS-2 ALP=40.6,M=14.1,RE-NS =5.971E 5,T=1055.
STS-2 ALP=39.8,M=13.2,RE-NS =7.090E 5,T=1080.
STS-2 ALP=39.7,M=12.8,RE-NS =7.985E 5,T=1095.
FILM COEFF - H/HREF
10^{-1}
10^{-2}
10^{-3}
10^{-4}
0.0
0.2
0.4
0.6
0.8
1.0
X/L
11/16/84
BASE TIME = 27550236.000 SEC.

STS-3 SIDE PLB DOOR (Z=440 TRACE) DISTRIBUTION

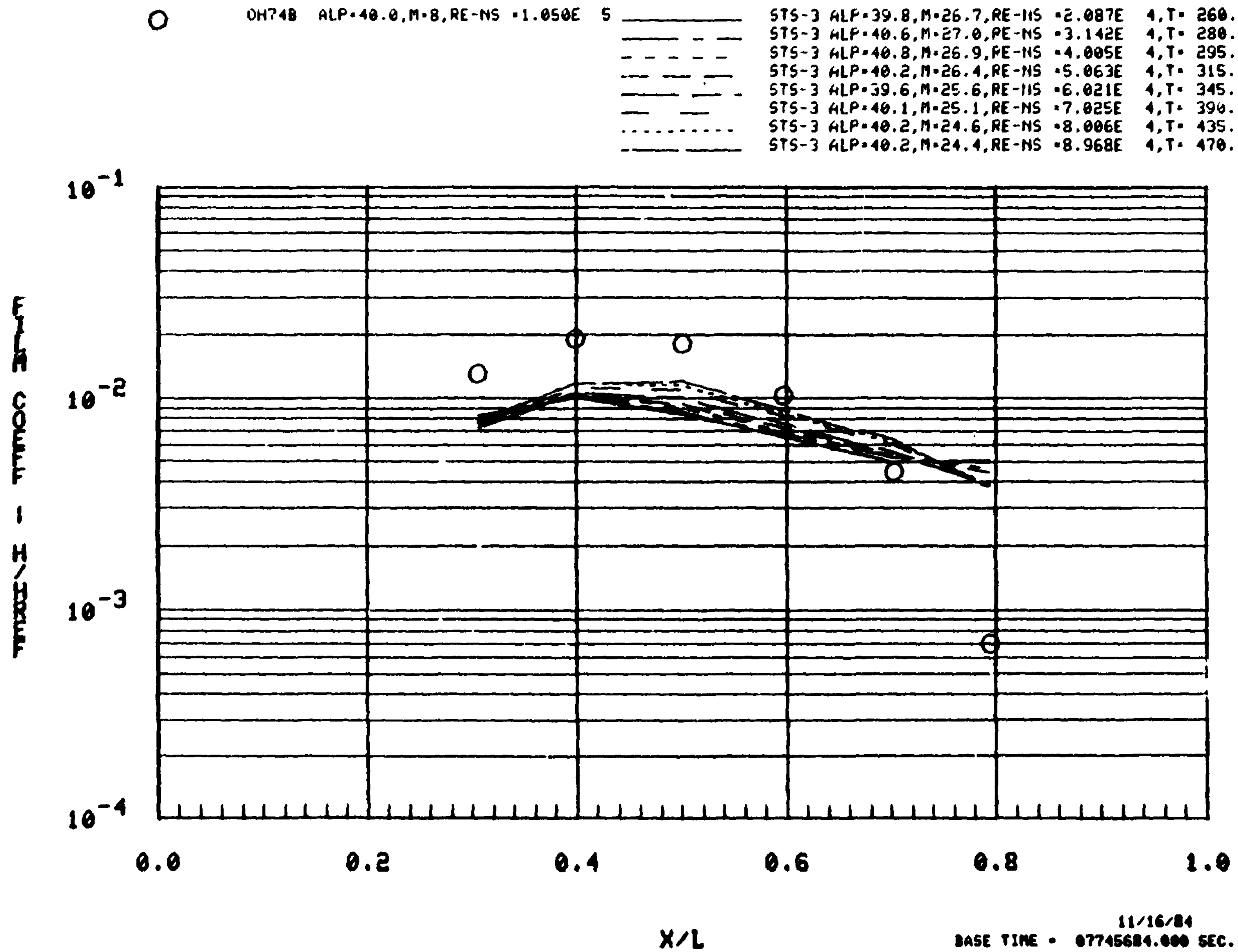

11/16/84
BASE TIME = 07745684.000 SEC.

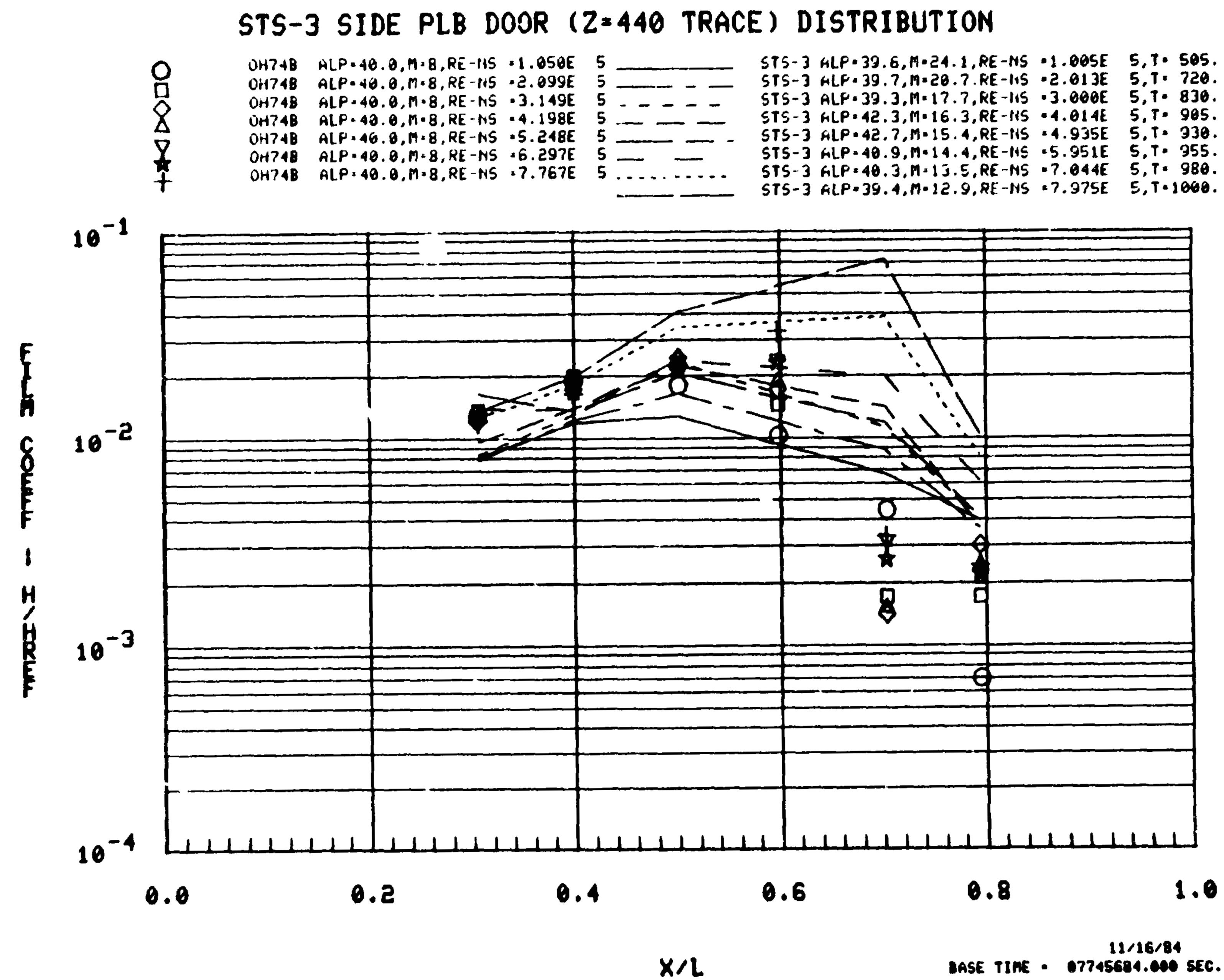

STS-3 SIDE PLB DOOR (Z=440 TRACE) DISTRIBUTION
OH74B ALP=40.0,M=8,RE-NS =1.050E 5
OH74B ALP=40.0,M=8,RE-NS =2.099E 5
OH74B ALP=40.0,M=8,RE-NS =3.149E 5
OH74B ALP=40.0,M=8,RE-NS =4.198E 5
OH74B ALP=40.0,M=8,RE-NS =5.248E 5
OH74B ALP=40.0,M=8,RE-NS =6.297E 5
OH74B ALP=40.0,M=8,RE-NS =7.767E 5
STS-3 ALP=39.6,M=24.1,RE-NS =1.005E 5,T= 505.
STS-3 ALP=39.7,M=20.7,RE-NS =2.013E 5,T= 720.
STS-3 ALP=39.3,M=17.7,RE-NS =3.000E 5,T= 830.
STS-3 ALP=42.3,M=16.3,RE-NS =4.014E 5,T= 905.
STS-3 ALP=42.7,M=15.4,RE-NS =4.935E 5,T= 930.
STS-3 ALP=40.9,M=14.4,RE-NS =5.951E 5,T= 955.
STS-3 ALP=40.3,M=13.5,RE-NS =7.044E 5,T= 980.
STS-3 ALP=39.4,M=12.9,RE-NS =7.975E 5,T=1000.
10^{-1}
10^{-2}
10^{-3}
10^{-4}
FILM COEFF - H/HREF
0.0
0.2
0.4
0.6
0.8
1.0
X/L
11/16/84
BASE TIME = 07745684.000 SEC.

STS-5 SIDE PLB DOOR (Z=440 TRACE) DISTRIBUTION

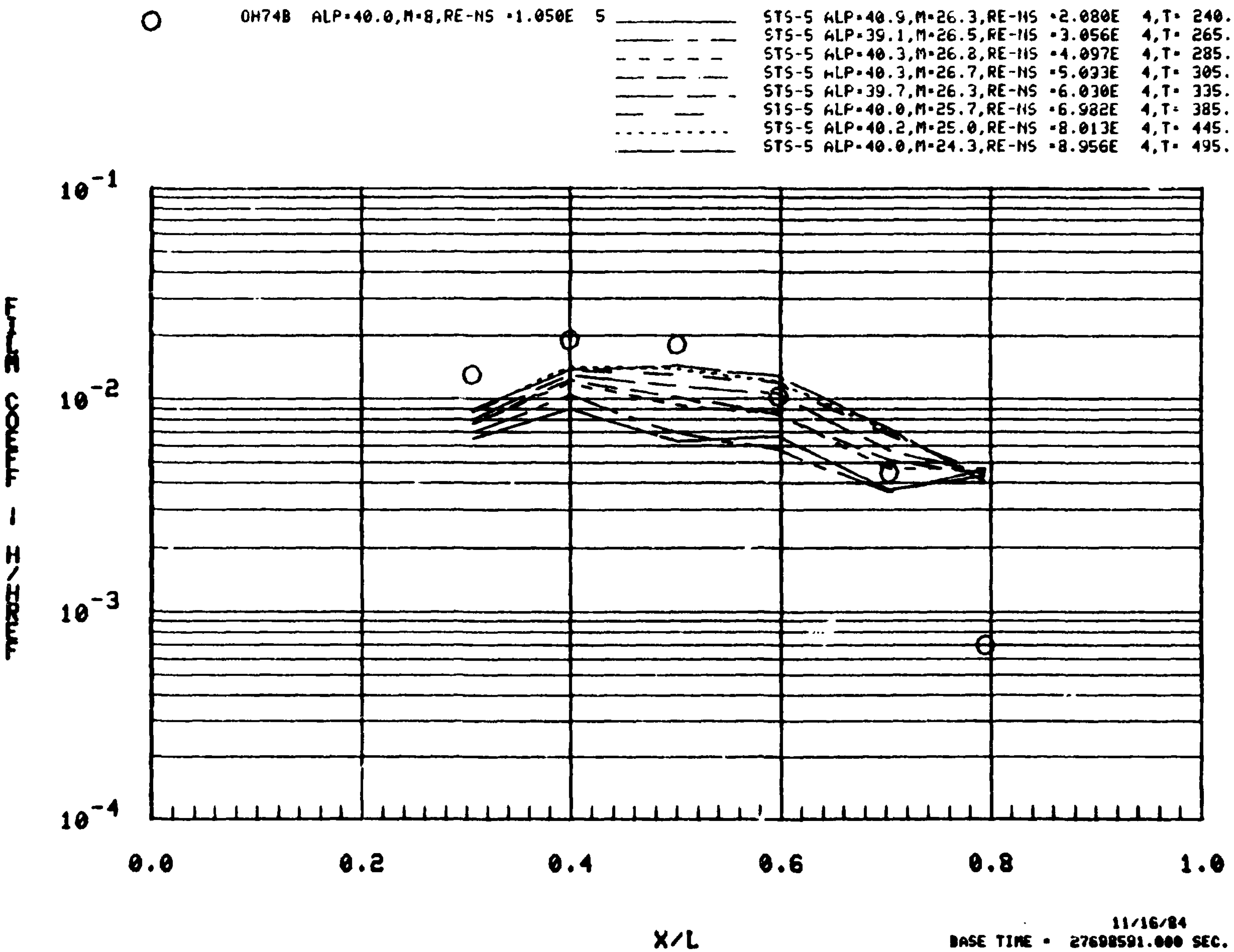

11/16/84
BASE TIME = 27698591.000 SEC.

STS-5 SIDE PLB DOOR (Z=440 TRACE) DISTRIBUTION

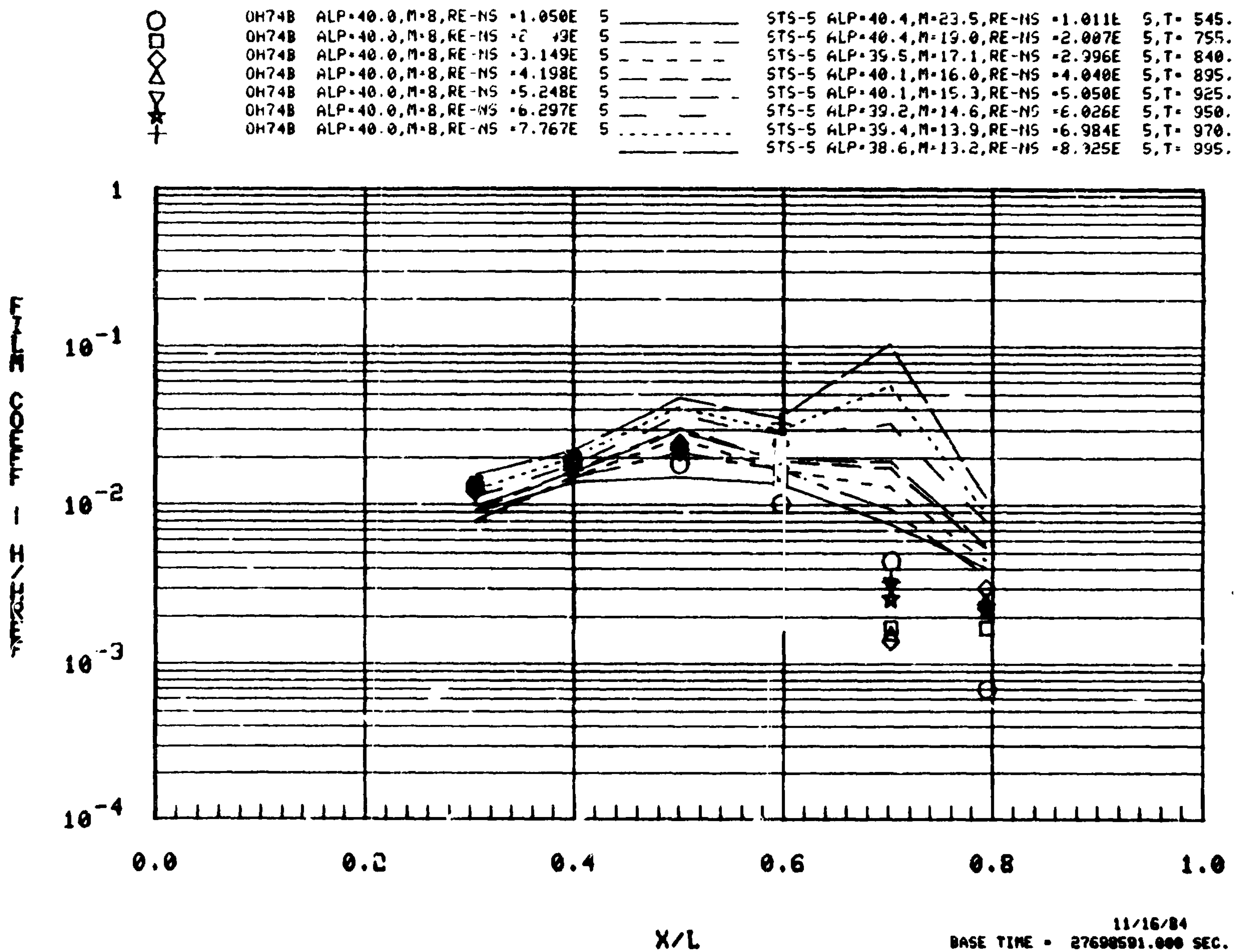

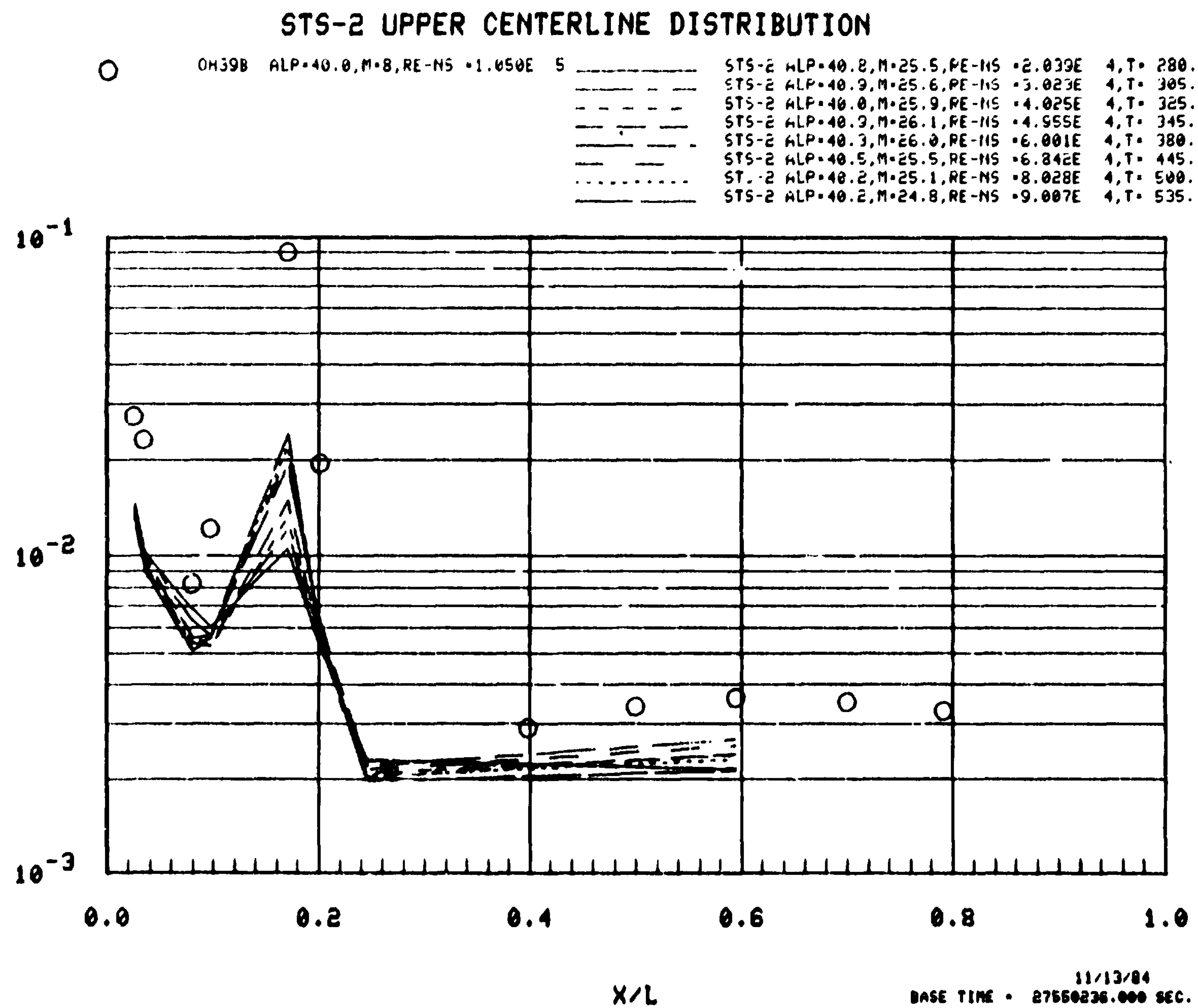
STS-2 UPPER CENTERLINE DISTRIBUTION
OH39B ALP=40.0,M=8,RE-NS =1.050E 5
STS-2 ALP=40.8,M=25.5,RE-NS =2.039E 4,T= 280.
STS-2 ALP=40.9,M=25.6,RE-NS =3.023E 4,T= 305.
STS-2 ALP=40.0,M=25.9,RE-NS =4.025E 4,T= 325.
STS-2 ALP=40.9,M=26.1,RE-NS =4.955E 4,T= 345.
STS-2 ALP=40.3,M=26.0,RE-NS =6.001E 4,T= 380.
STS-2 ALP=40.5,M=25.5,RE-NS =6.842E 4,T= 445.
ST.-2 ALP=40.2,M=25.1,RE-NS =8.028E 4,T= 500.
STS-2 ALP=40.2,M=24.8,RE-NS =9.007E 4,T= 535.
10^-1
10^-2
10^-3
FILM COEFF - H/HREF
0.0
0.2
0.4
0.6
0.8
1.0
X/L
11/13/84
BASE TIME = 27550236.000 SEC.

B-80

STS-2 UPPER CENTERLINE DISTRIBUTION

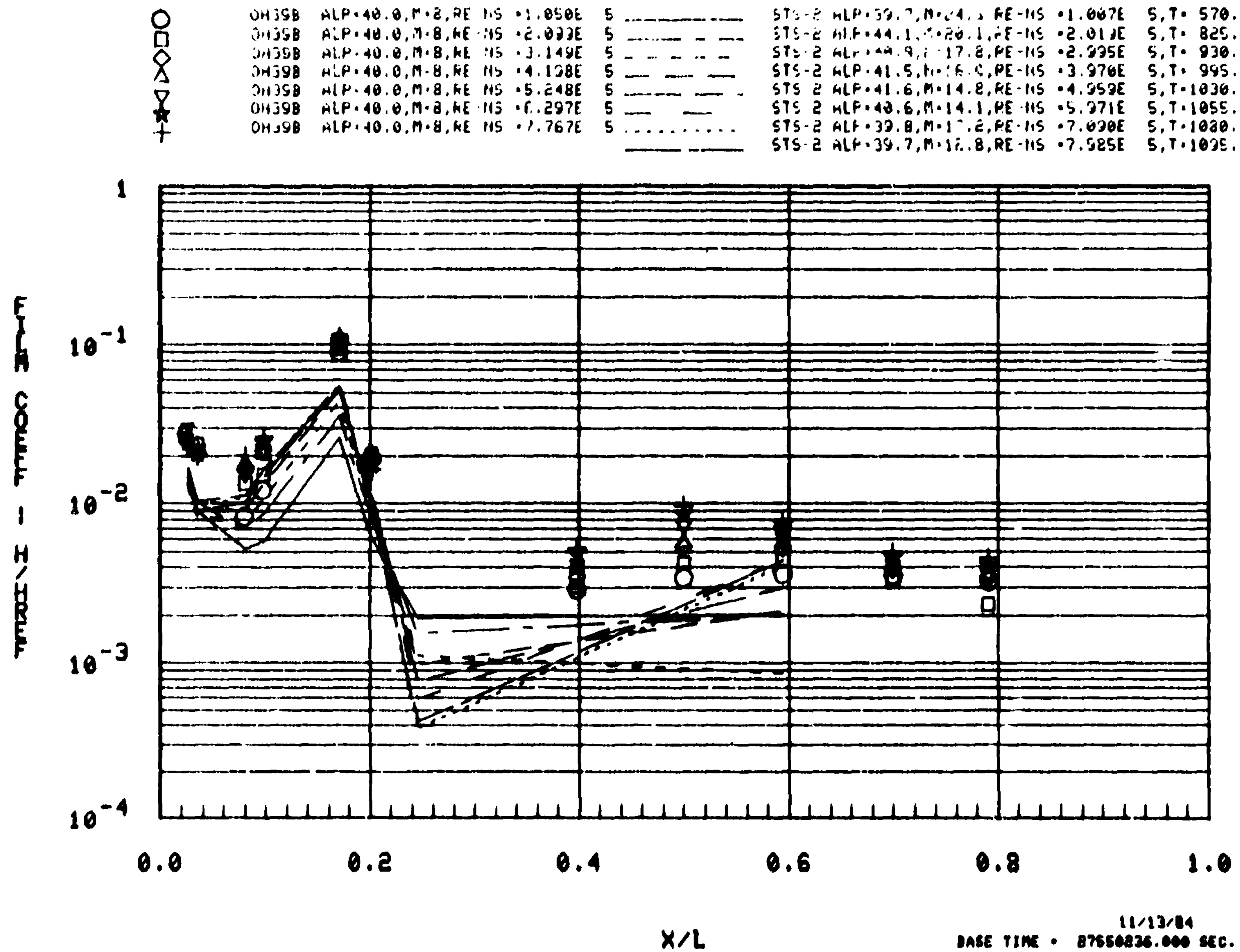

STS-3 UPPER CENTERLINE DISTRIBUTION

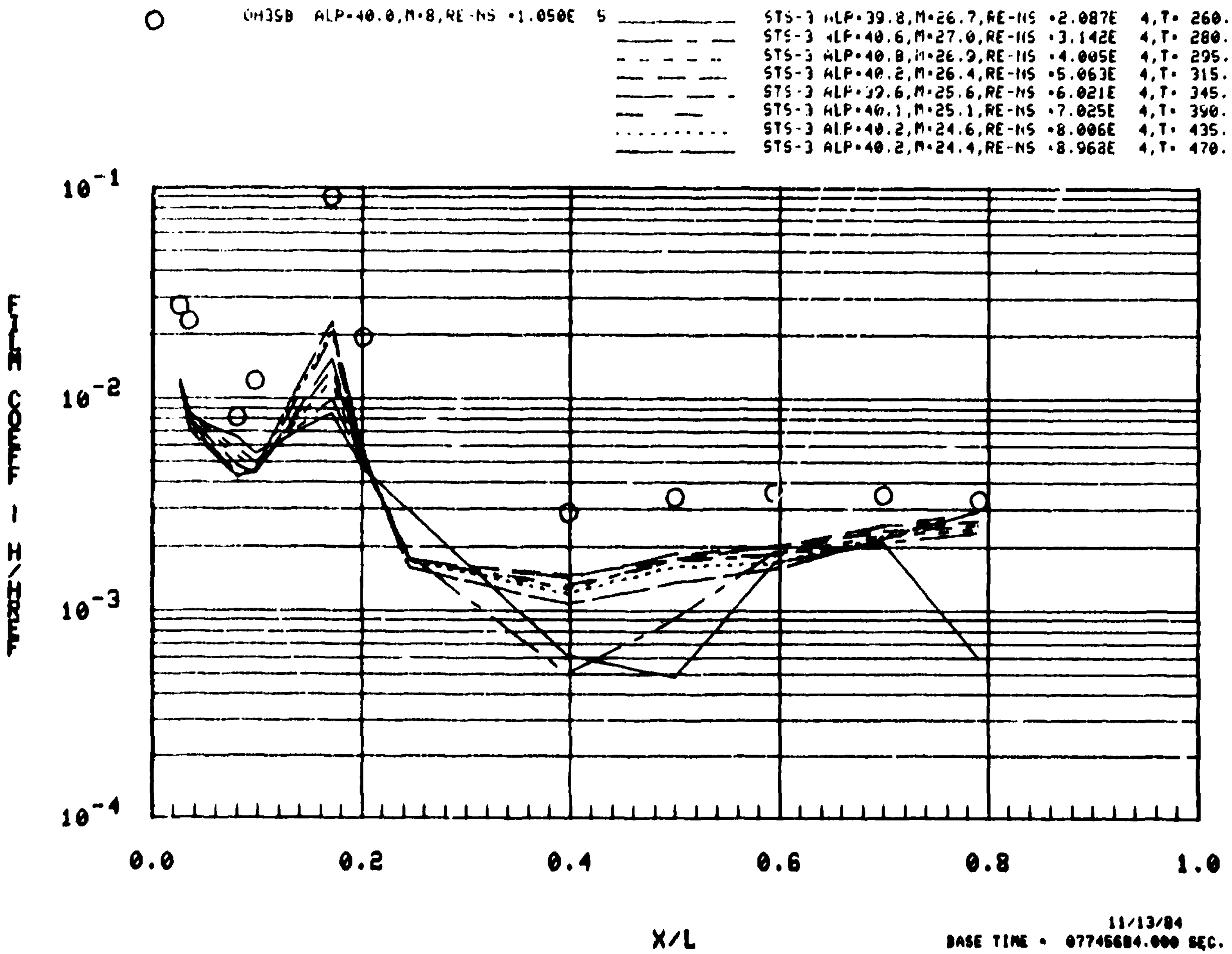

STS-3 UPPER CENTERLINE DISTRIBUTION

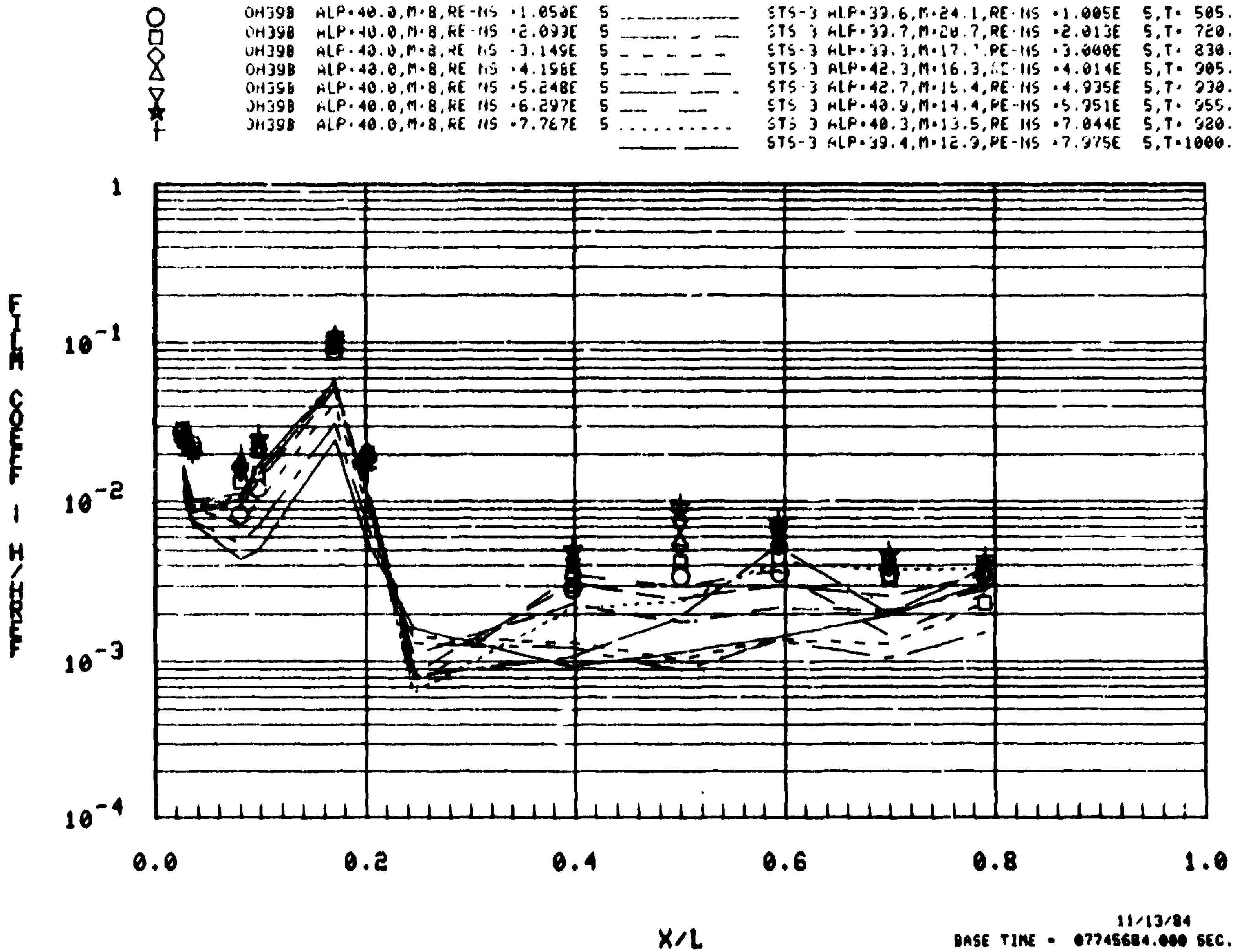

STS-5 UPPER CENTERLINE DISTRIBUTION

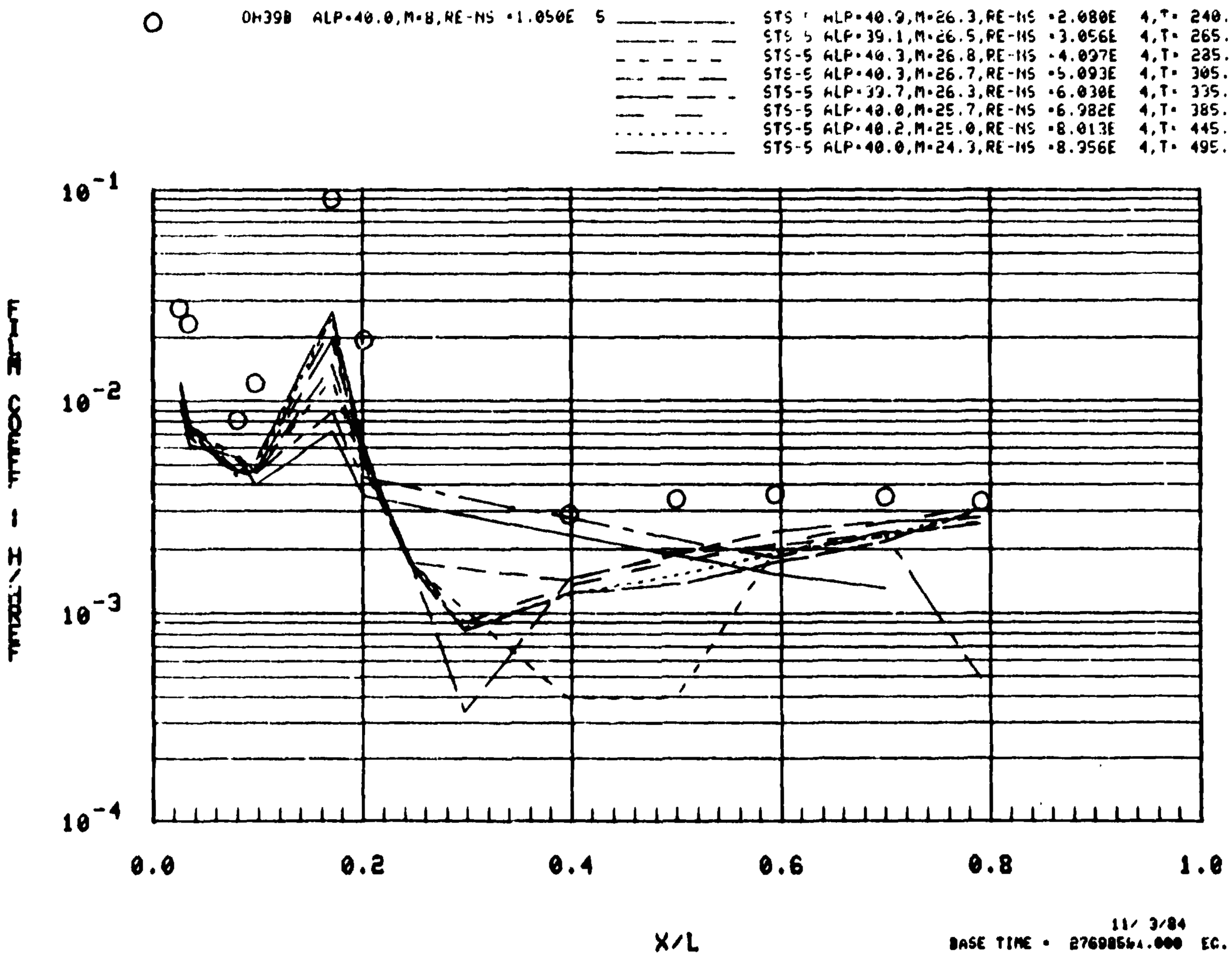

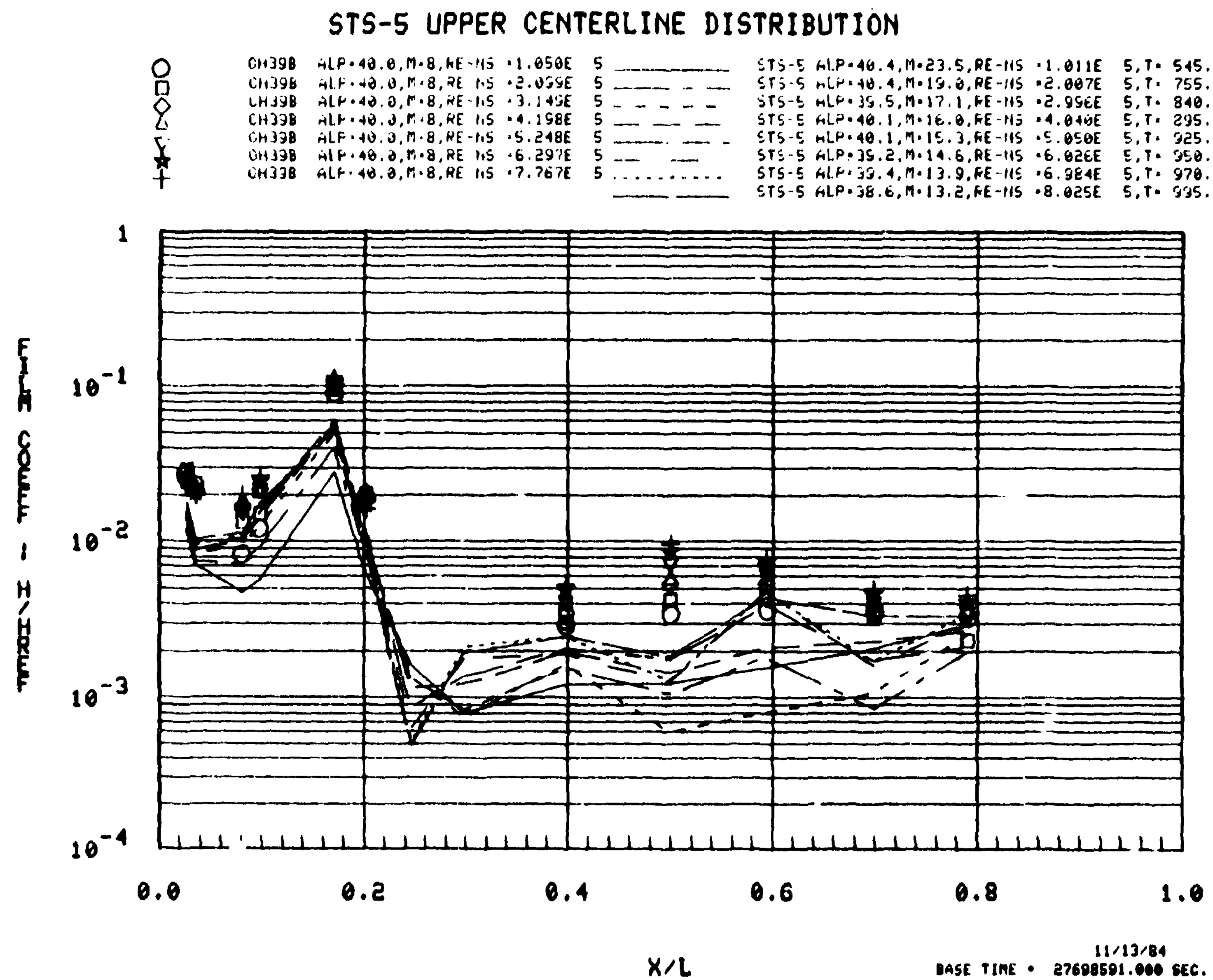
STS-5 UPPER CENTERLINE DISTRIBUTION
CH39B ALP=40.0,M=8,RE-NS =1.050E 5
CH39B ALP=40.0,M=8,RE-NS =2.099E 5
CH39B ALP=40.0,M=8,RE-NS =3.149E 5
CH39B ALP=40.0,M=8,RE-NS =4.198E 5
CH39B ALP=40.0,M=8,RE-NS =5.248E 5
CH39B ALP=40.0,M=8,RE-NS =6.297E 5
CH39B ALP=40.0,M=8,RE-NS =7.767E 5
STS-5 ALP=40.4,M=23.5,RE-NS =1.011E 5,T= 545.
STS-5 ALP=40.4,M=19.0,RE-NS =2.007E 5,T= 755.
STS-5 ALP=39.5,M=17.1,RE-NS =2.996E 5,T= 840.
STS-5 ALP=40.1,M=16.0,RE-NS =4.040E 5,T= 895.
STS-5 ALP=40.1,M=15.3,RE-NS =5.050E 5,T= 925.
STS-5 ALP=39.2,M=14.6,RE-NS =6.026E 5,T= 950.
STS-5 ALP=39.4,M=13.9,RE-NS =6.984E 5,T= 970.
STS-5 ALP=38.6,M=13.2,RE-NS =8.025E 5,T= 995.
FILM COEFF : H/HREF
1
10^{-1}
10^{-2}
10^{-3}
10^{-4}
0.0
0.2
0.4
0.6
0.8
1.0
X/L
11/13/84
BASE TIME = 27698591.000 SEC.

STS-2 OMS POD TRACE 3 DISTRIBUTION

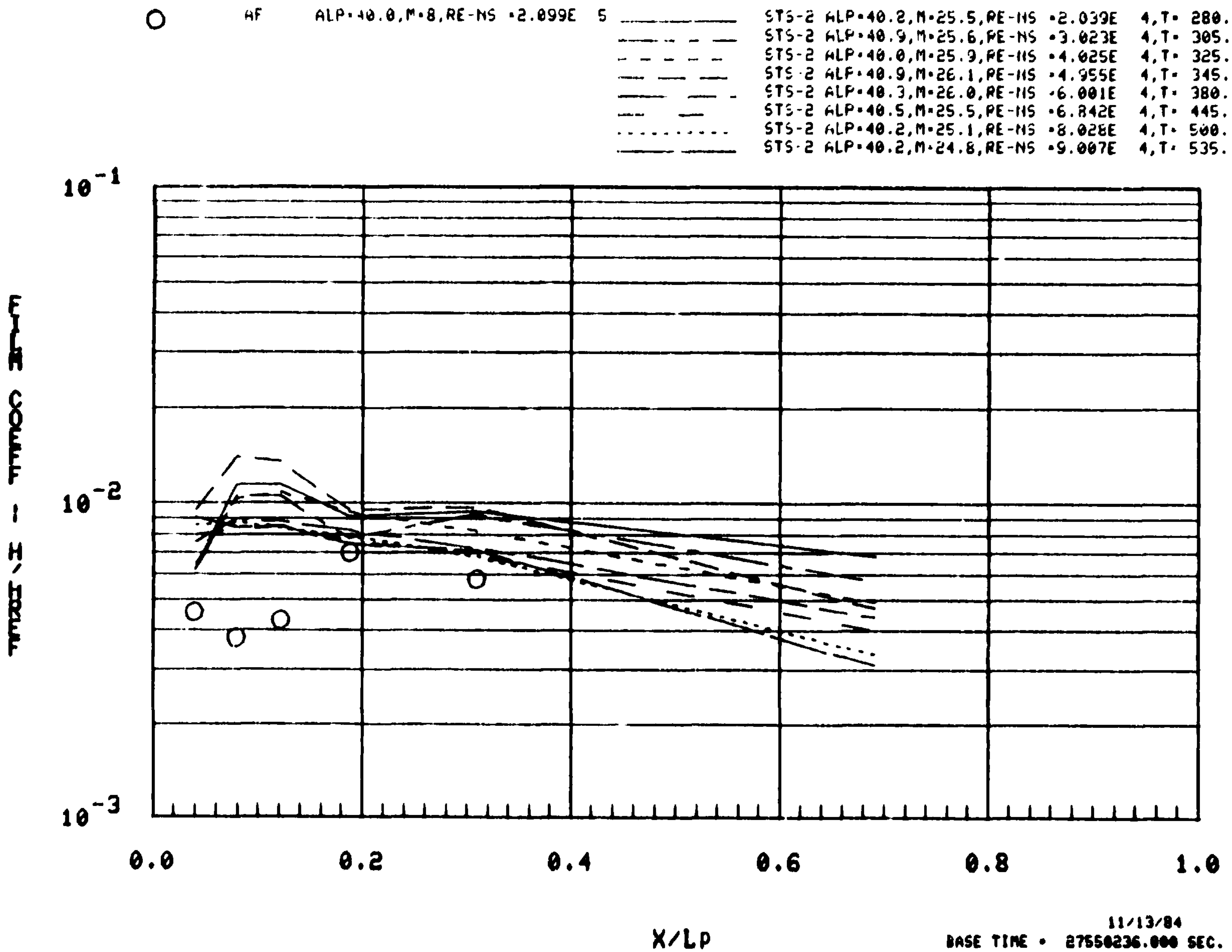

STS-2 OMS POD TRACE 3 DISTRIBUTION

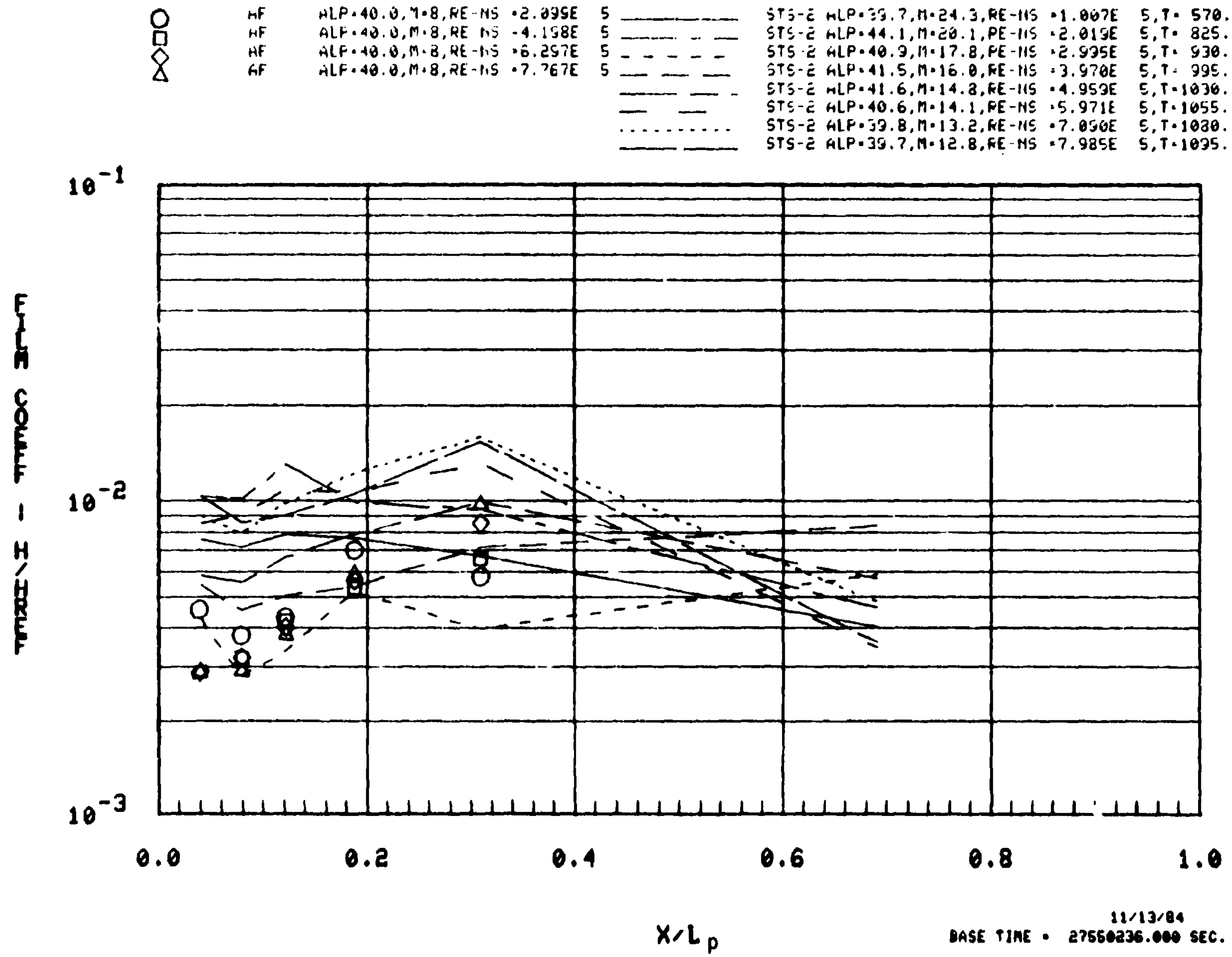

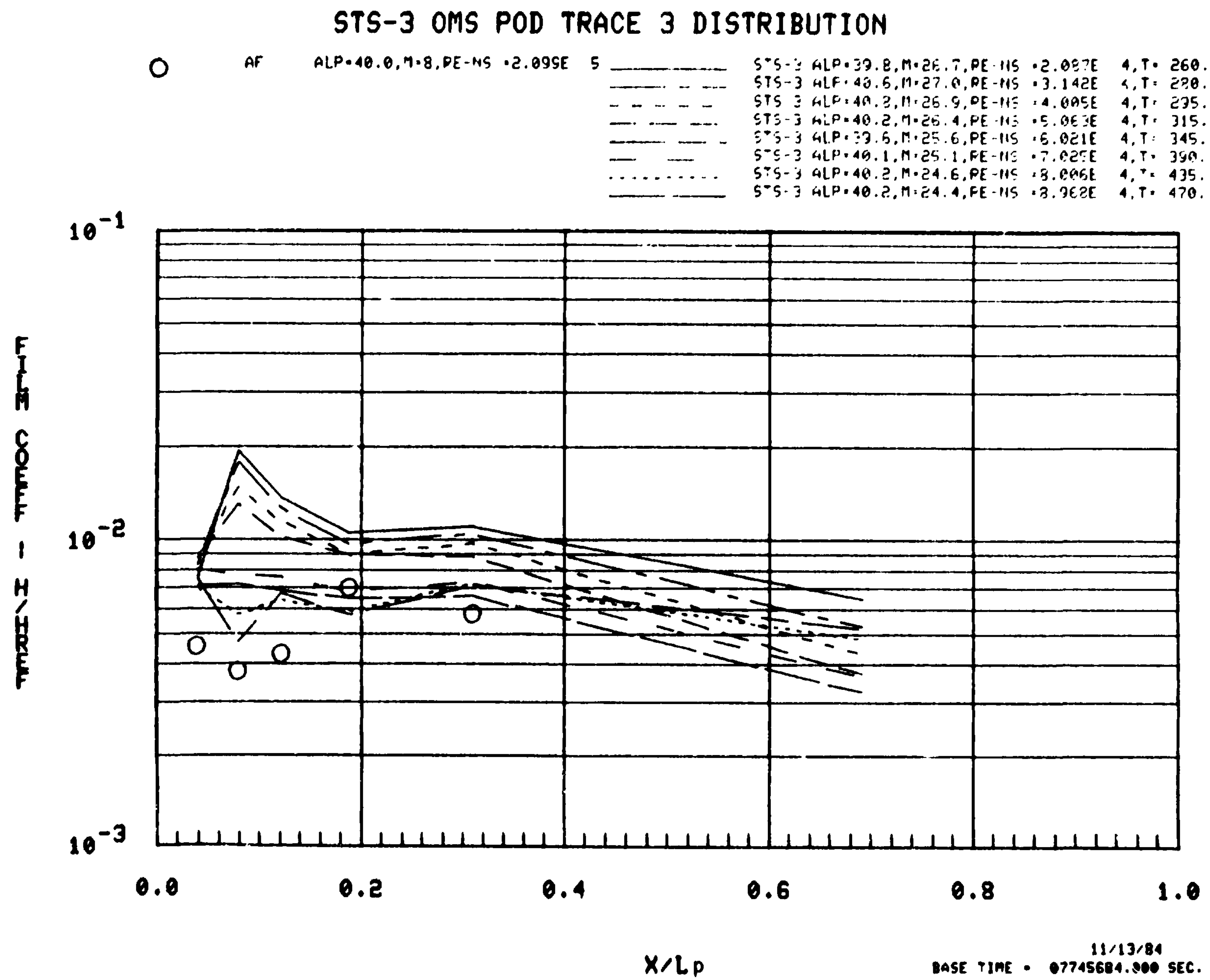
STS-3 OMS POD TRACE 3 DISTRIBUTION
AF ALP=40.0,M=8,PE-NS =2.099E 5
STS-3 ALP=39.8,M=26.7,PE-NS =2.097E 4,T= 260.
STS-3 ALP=40.6,M=27.0,PE-NS =3.142E 4,T= 280.
STS 3 ALP=40.3,M=26.9,PE-NS =4.005E 4,T= 295.
STS-3 ALP=40.2,M=26.4,PE-NS =5.063E 4,T= 315.
STS-3 ALP=39.6,M=25.6,PE-NS =6.021E 4,T= 345.
STS-3 ALP=40.1,M=25.1,PE-NS =7.025E 4,T= 390.
STS-3 ALP=40.2,M=24.6,PE-NS =8.006E 4,T= 435.
STS-3 ALP=40.2,M=24.4,PE-NS =8.968E 4,T= 470.
10^{-1}
10^{-2}
10^{-3}
FILM COEFF , H/HREF
0.0
0.2
0.4
0.6
0.8
1.0
X/Lp
11/13/84
BASE TIME = 07745684.000 SEC.

STS-3 OMS POD TRACE 3 DISTRIBUTION

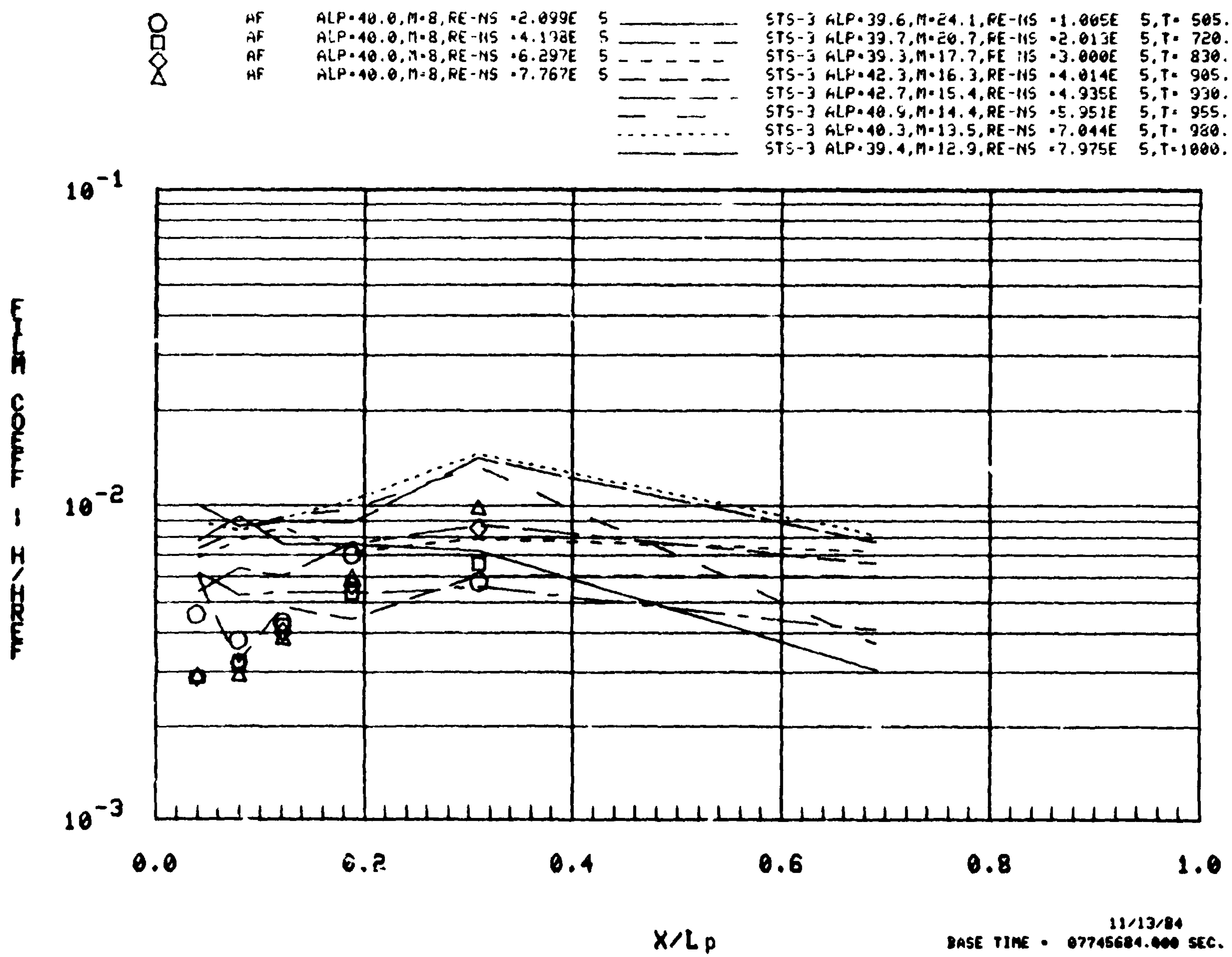

STS-5 OMS POD TRACE 3 DISTRIBUTION

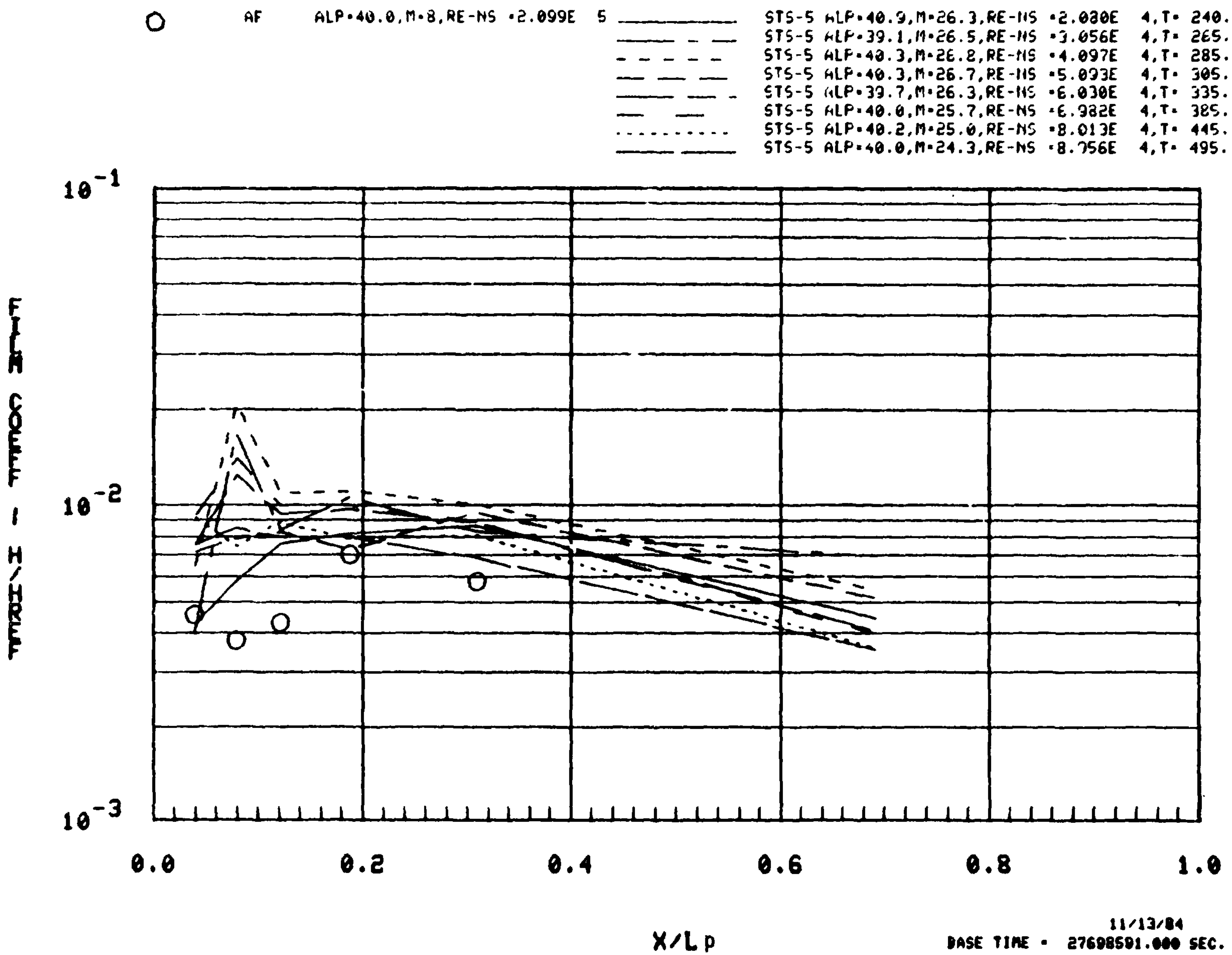

STS-5 OMS POD TRACE 3 DISTRIBUTION

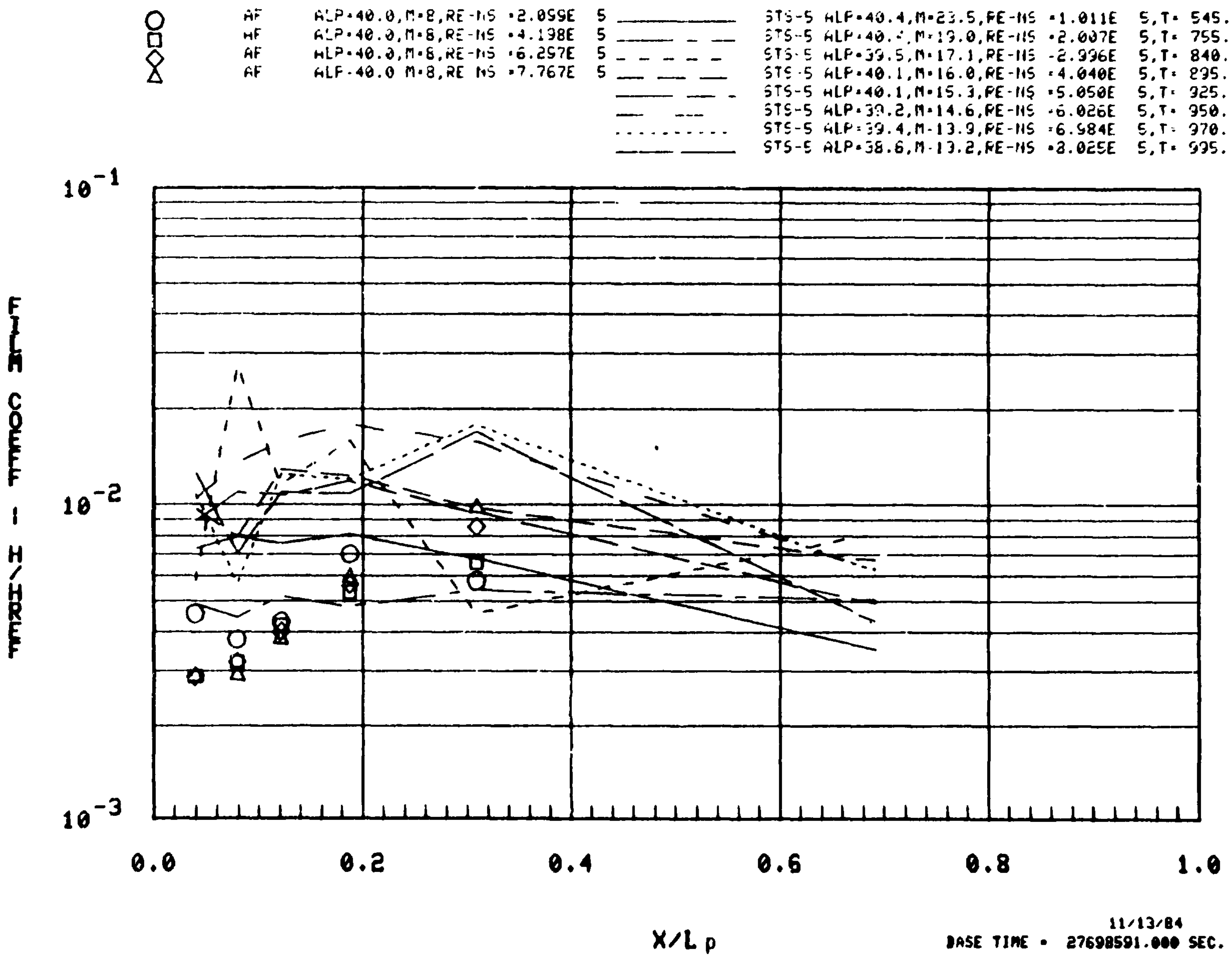

11/13/84
BASE TIME = 27698591.000 SEC.

APPENDIX C

HEATING RATE COMPARISON AT

WIND TUNNEL CONDITIONS - COMPOSITE FLIGHTS

LOWER CENTERLINE DISTRIBUTION

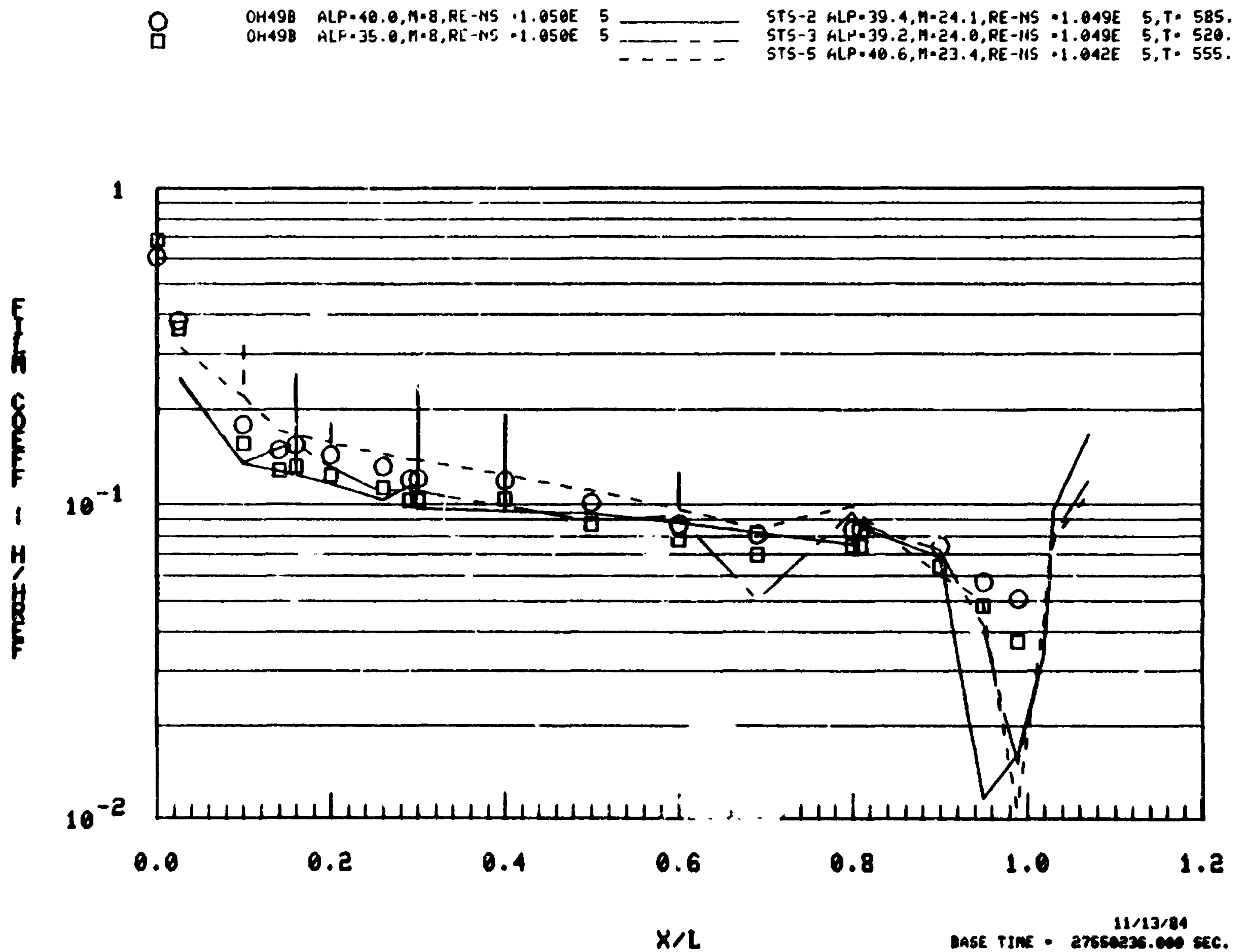

LOWER CENTERLINE DISTRIBUTION

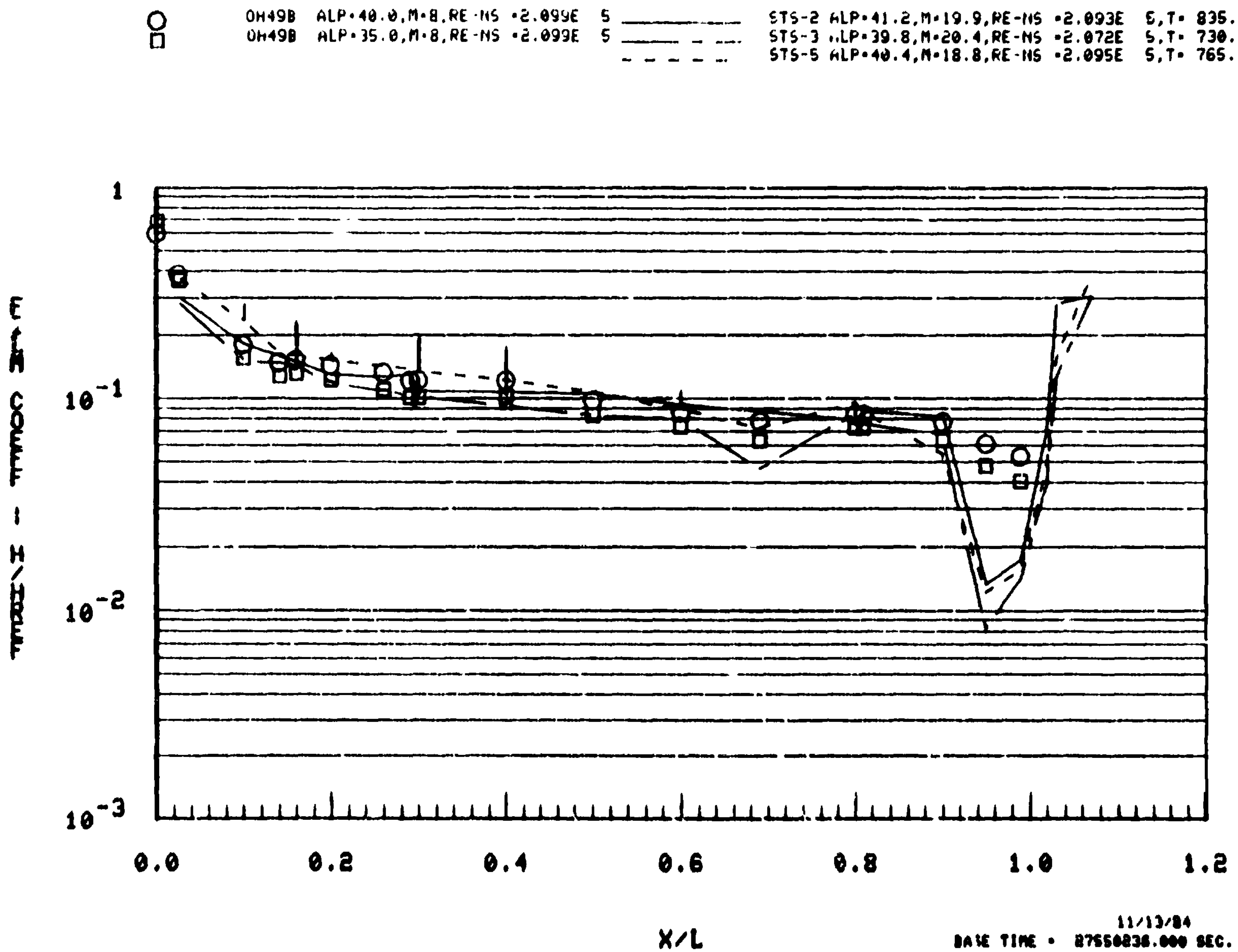

LOWER CENTERLINE DISTRIBUTION

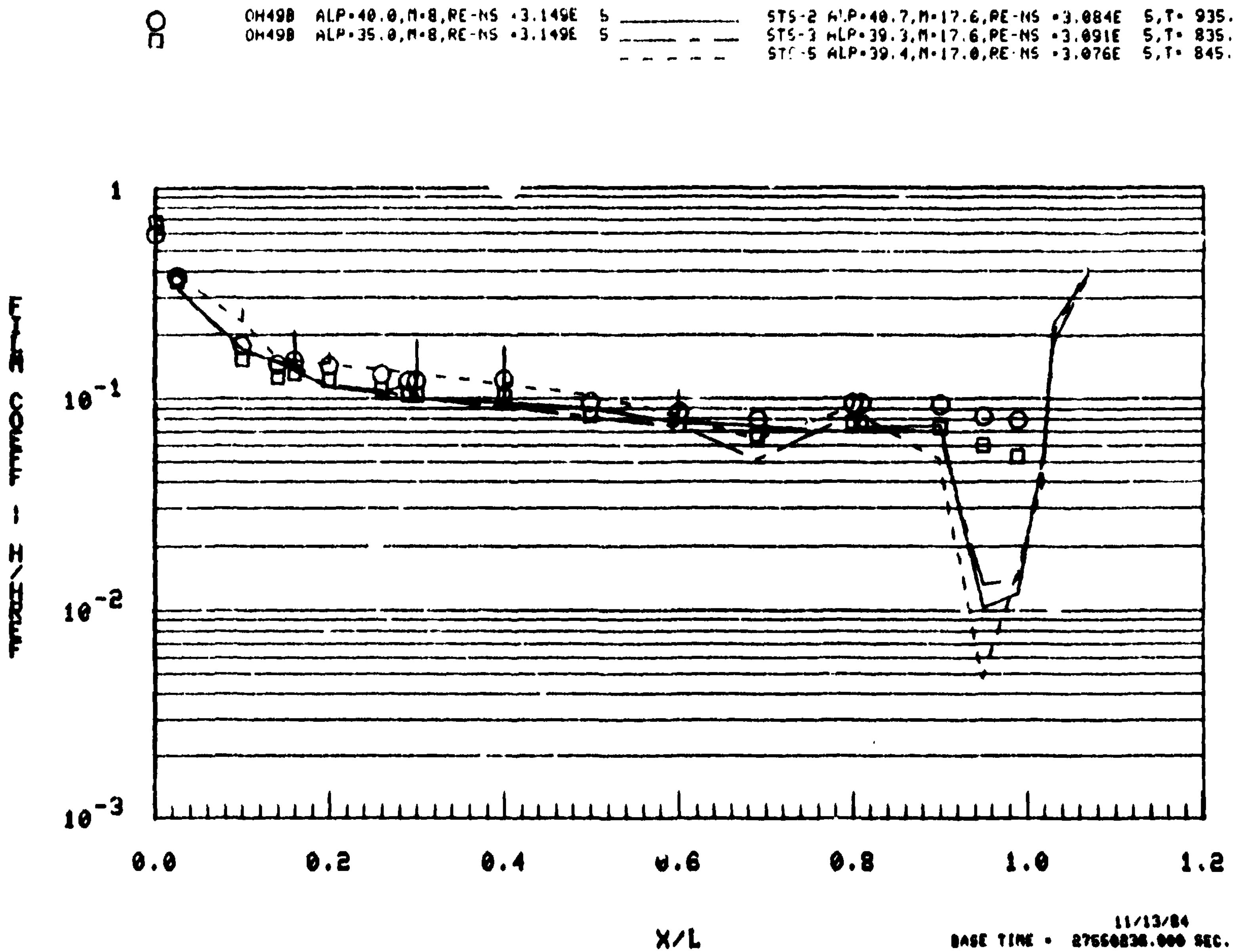

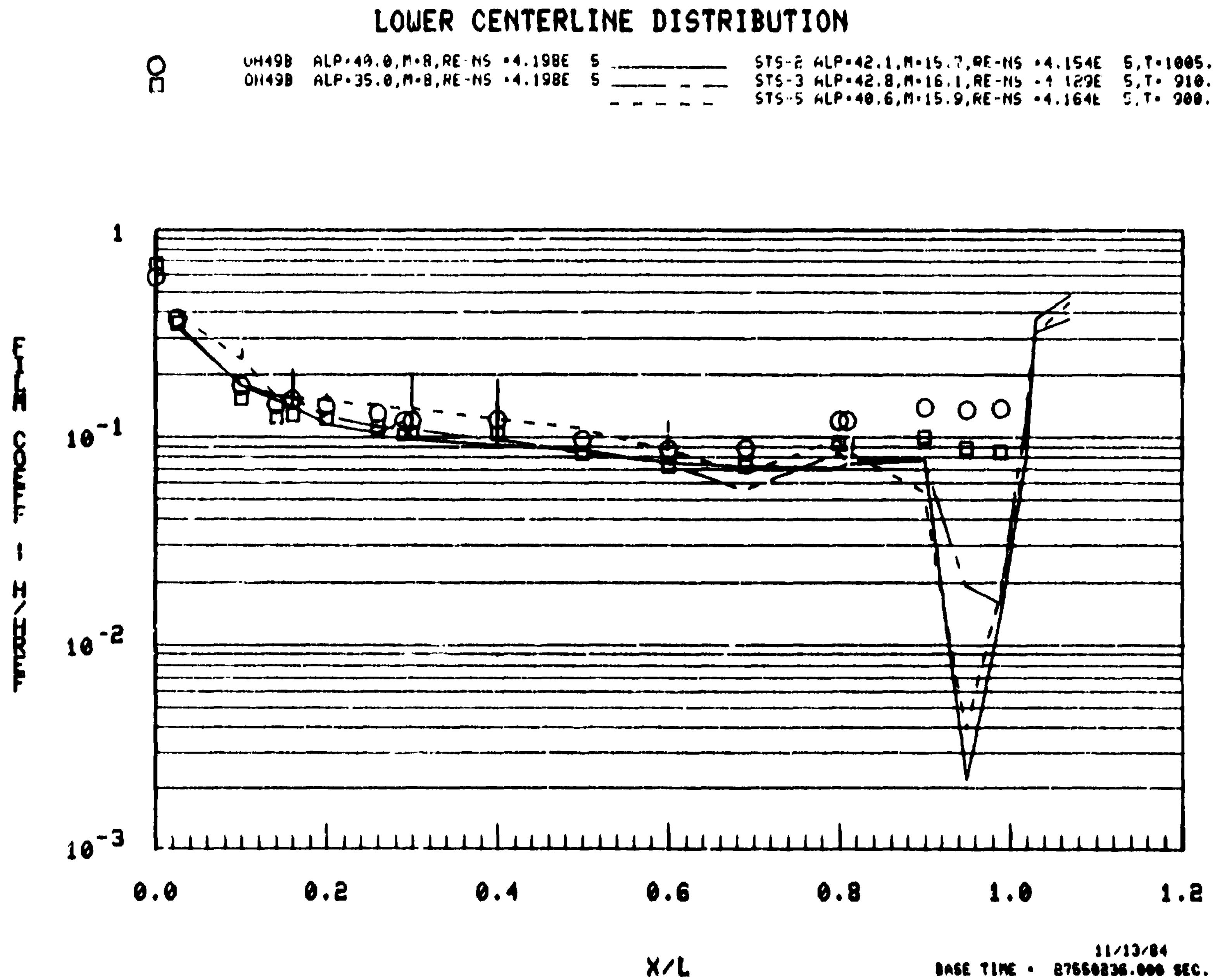

LOWER CENTERLINE DISTRIBUTION
OH49B ALP=40.0,M=8,RE-NS =4.198E 5
OH49B ALP=35.0,M=8,RE-NS =4.198E 5
STS-2 ALP=42.1,M=15.7,RE-NS =4.154E 5,T=1005.
STS-3 ALP=42.8,M=16.1,RE-NS =4.129E 5,T= 910.
STS-5 ALP=40.6,M=15.9,RE-NS =4.164E 5,T= 900.
FILM COEFF - H/HREF
X/L
11/13/84
BASE TIME = 27550236.000 SEC.

LOWER CENTERLINE DISTRIBUTION

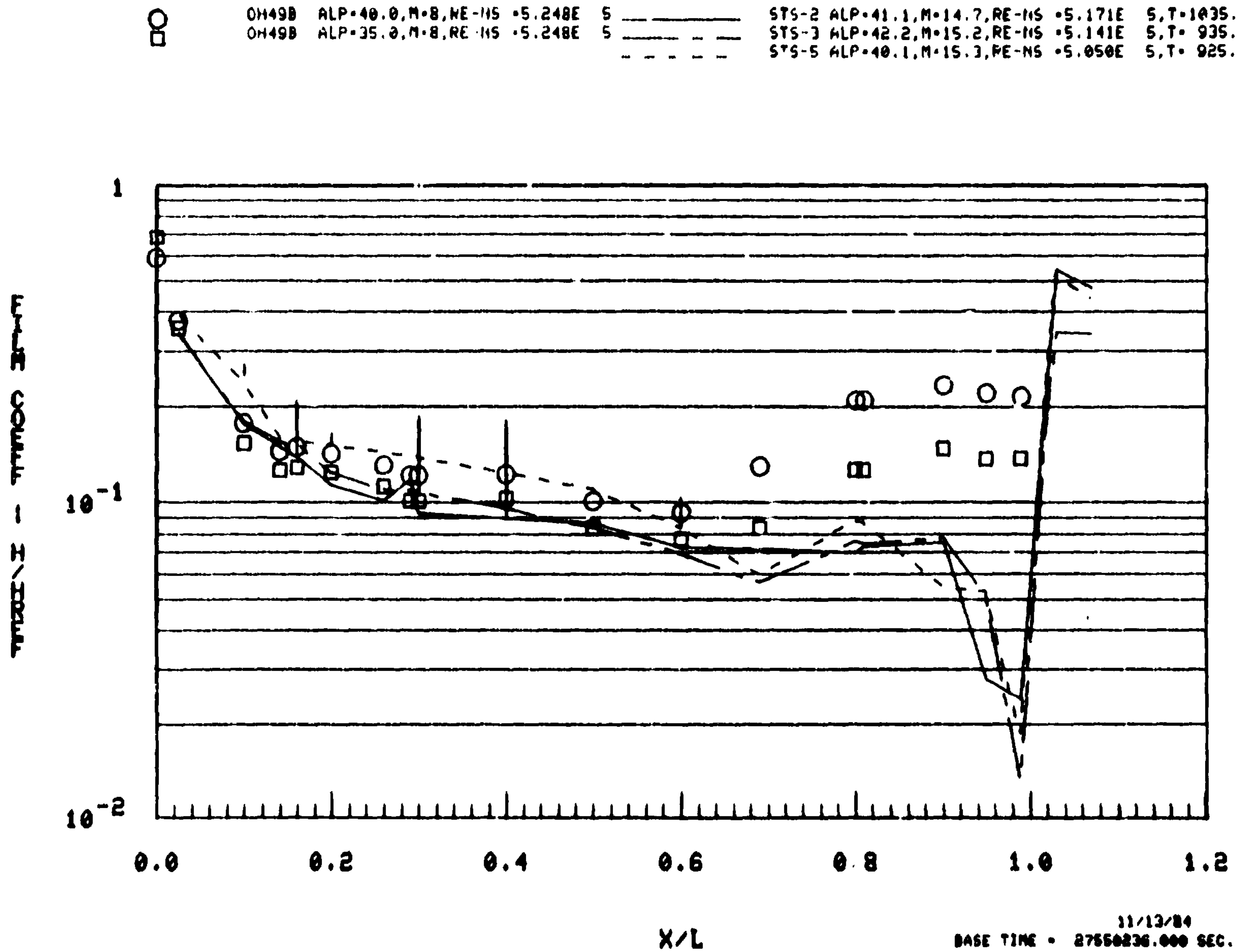

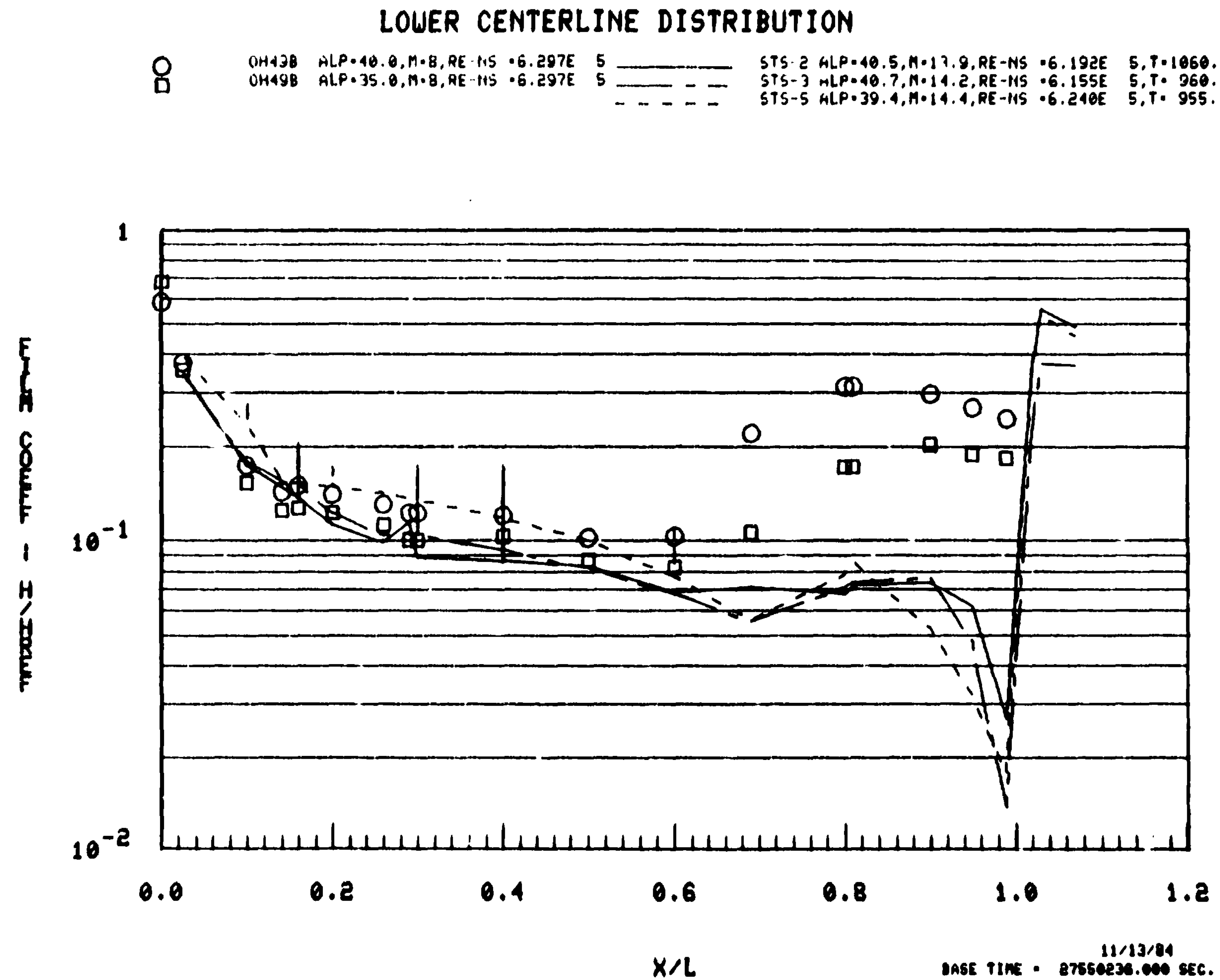

LOWER CENTERLINE DISTRIBUTION
OH43B ALP=40.0,M=8,RE-NS =6.297E 5
OH49B ALP=35.0,M=8,RE-NS =6.297E 5
STS-2 ALP=40.5,M=13.9,RE-NS =6.192E 5,T=1060.
STS-3 ALP=40.7,M=14.2,RE-NS =6.155E 5,T= 960.
STS-5 ALP=39.4,M=14.4,RE-NS =6.240E 5,T= 955.
FILM COEFF - H/HREF
1
10^-1
10^-2
0.0
0.2
0.4
0.6
0.8
1.0
1.2
X/L
11/13/84
BASE TIME = 27550236.000 SEC.

LOWER CENTERLINE DISTRIBUTION

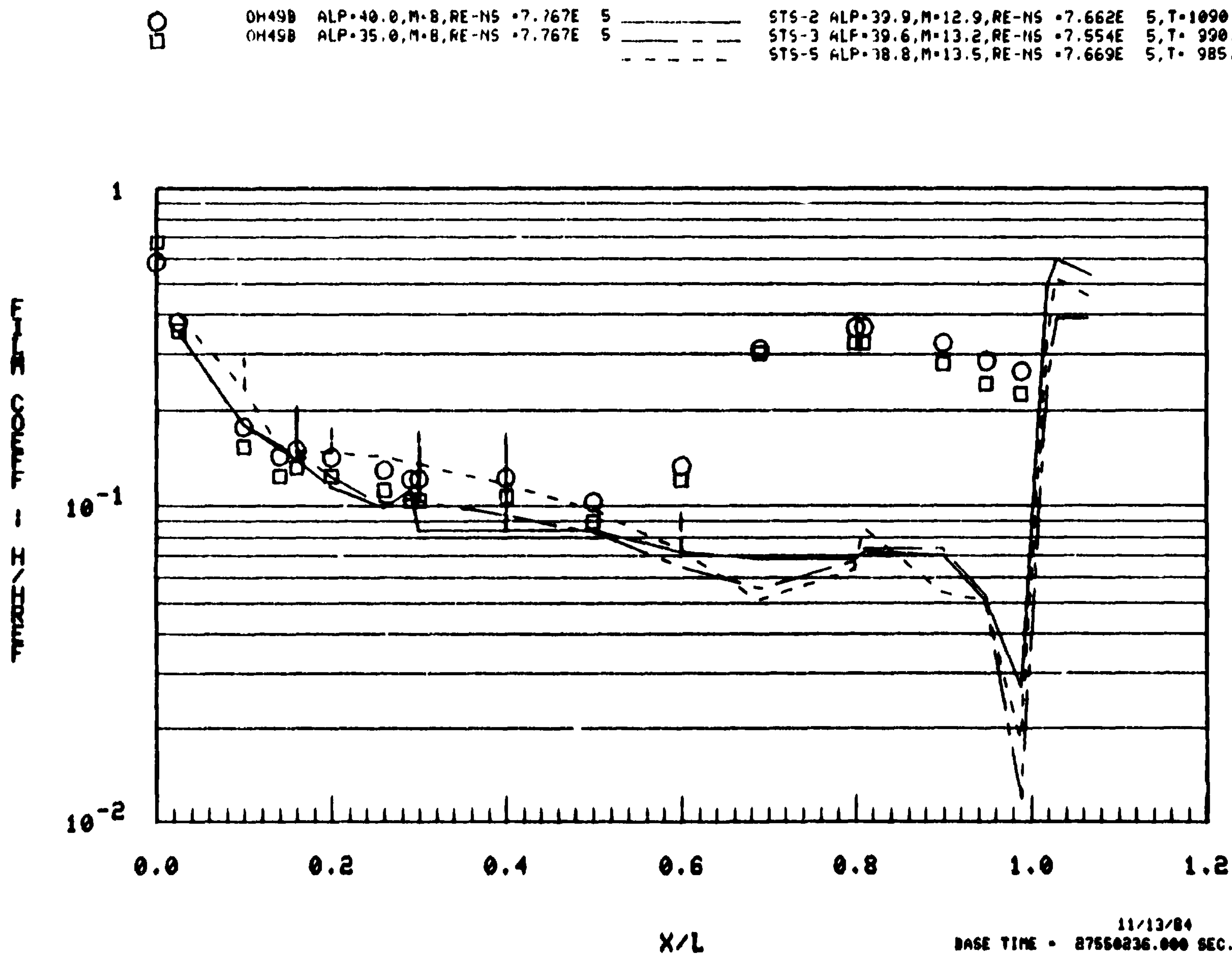

WING 50% SEMI-SPAN DISTRIBUTION

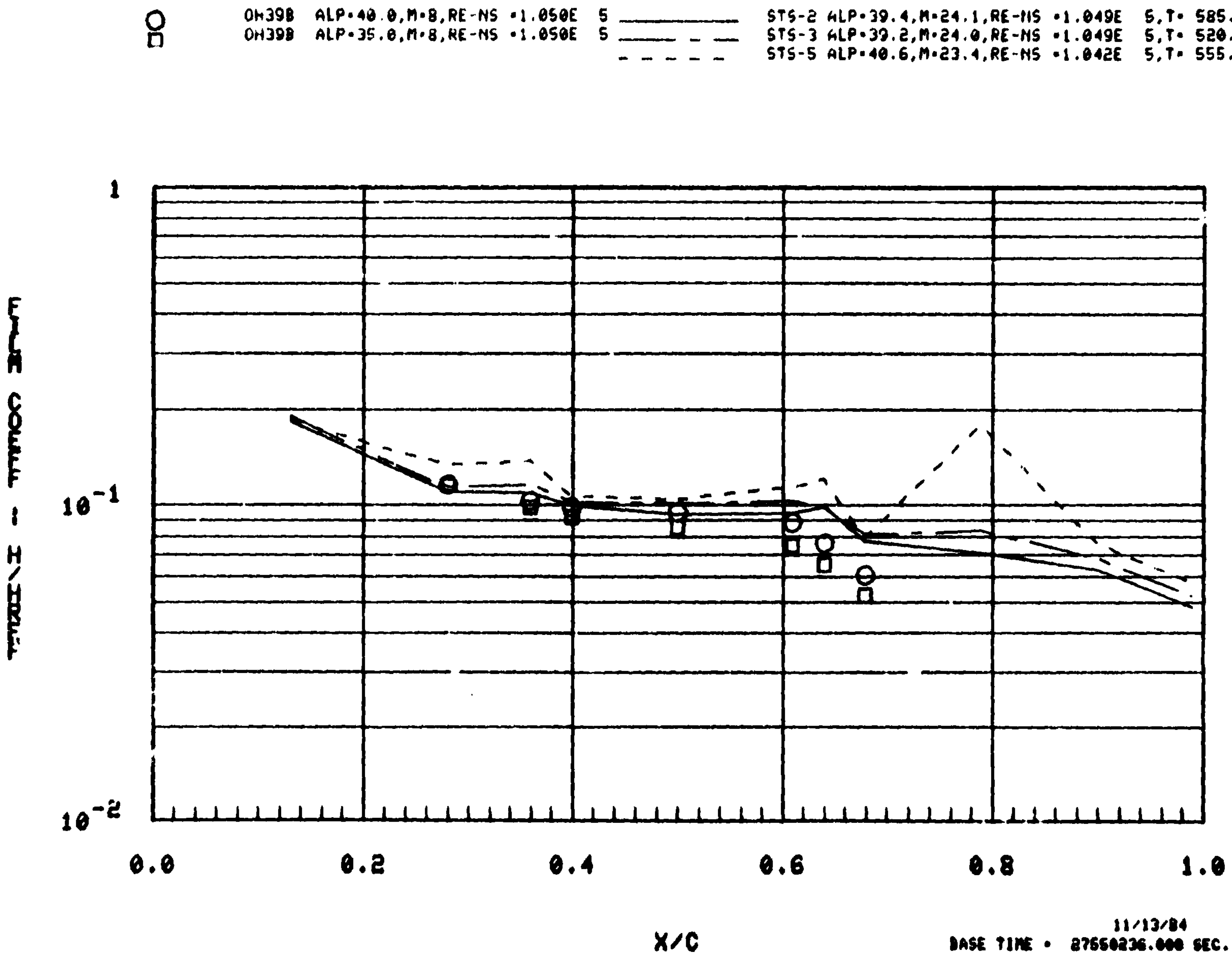

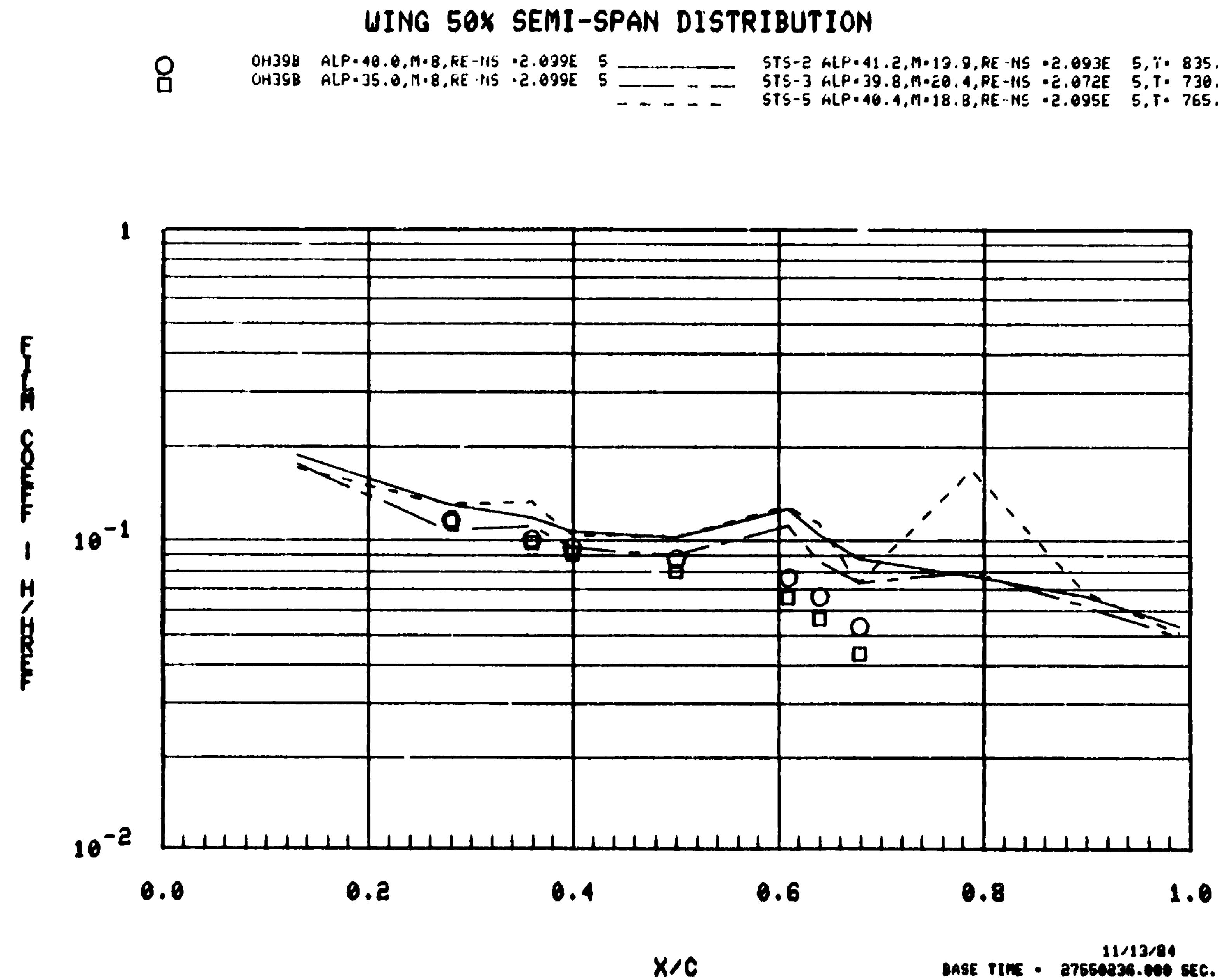

WING 50% SEMI-SPAN DISTRIBUTION
OH39B ALP=40.0,M=8,RE-NS =2.099E 5
OH39B ALP=35.0,M=8,RE-NS =2.099E 5
STS-2 ALP=41.2,M=19.9,RE-NS =2.093E 5,T= 835.
STS-3 ALP=39.8,M=20.4,RE-NS =2.072E 5,T= 730.
STS-5 ALP=40.4,M=18.8,RE-NS =2.095E 5,T= 765.
FILM COEFF - H/HREF
1
10^-1
10^-2
0.0
0.2
0.4
0.6
0.8
1.0
X/C
11/13/84
BASE TIME = 27660236.000 SEC.

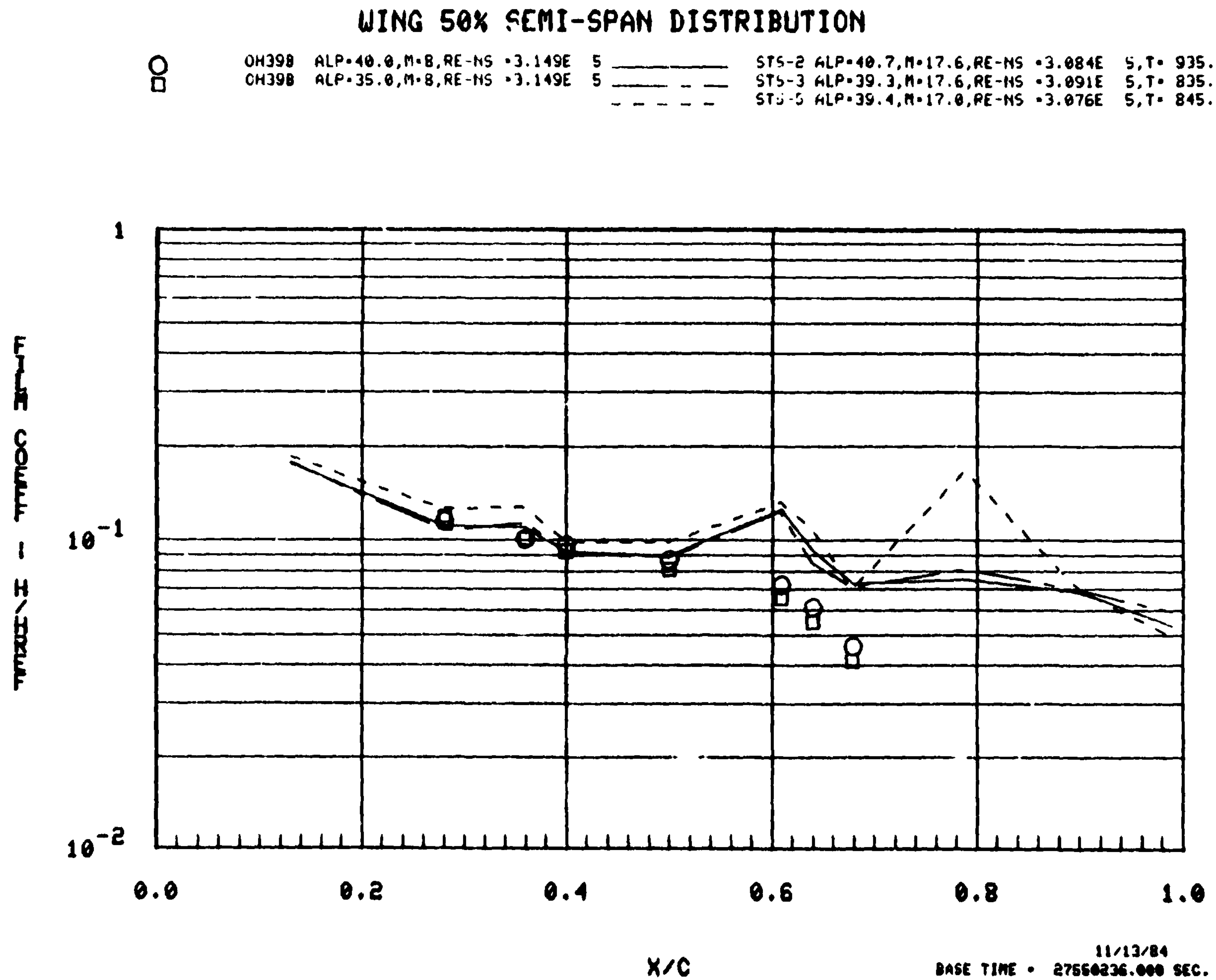
WING 50% SEMI-SPAN DISTRIBUTION
OH39B ALP=40.0,M=8,RE-NS =3.149E 5
OH39B ALP=35.0,M=8,RE-NS =3.149E 5
STS-2 ALP=40.7,M=17.6,RE-NS =3.084E 5,T= 935.
STS-3 ALP=39.3,M=17.6,RE-NS =3.091E 5,T= 835.
STS-5 ALP=39.4,M=17.0,RE-NS =3.076E 5,T= 845.
1
10^-1
10^-2
FILM COEFF - H/HREF
0.0
0.2
0.4
0.6
0.8
1.0
X/C
11/13/84
BASE TIME = 27560236.000 SEC.

WING 50% SEMI-SPAN DISTRIBUTION

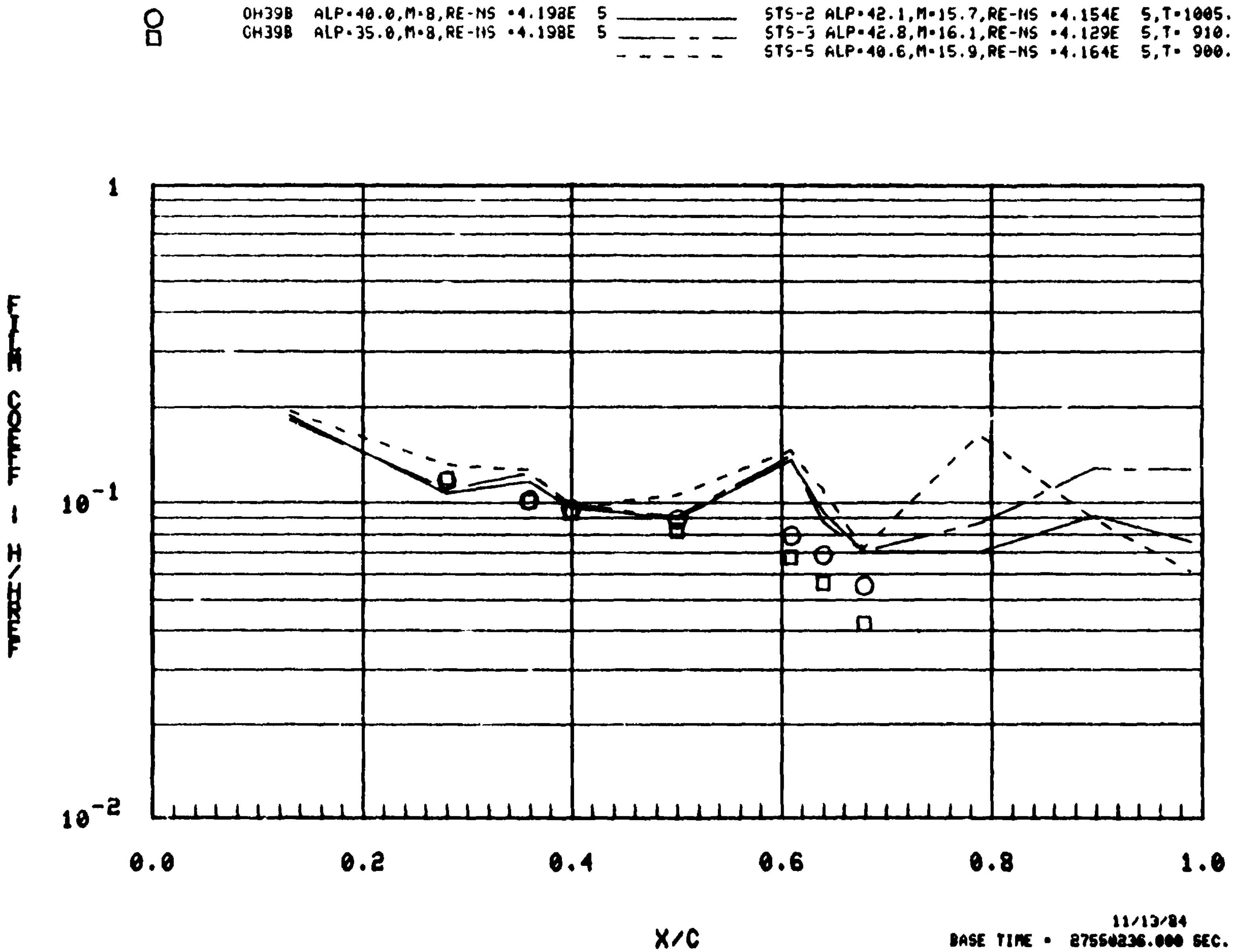

11/13/84
BASE TIME = 27550236.000 SEC.

WING 50% SEMI-SPAN DISTRIBUTION

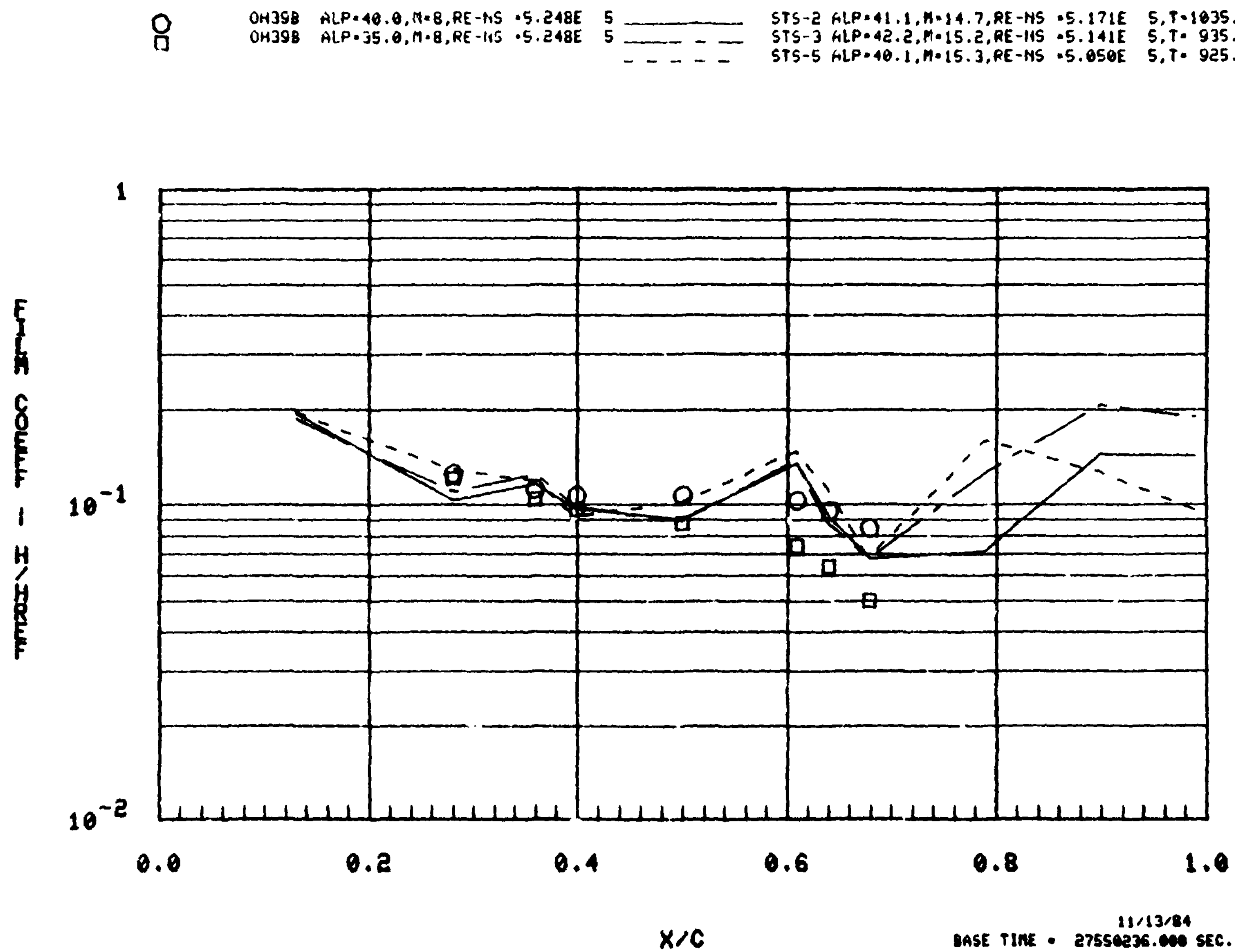

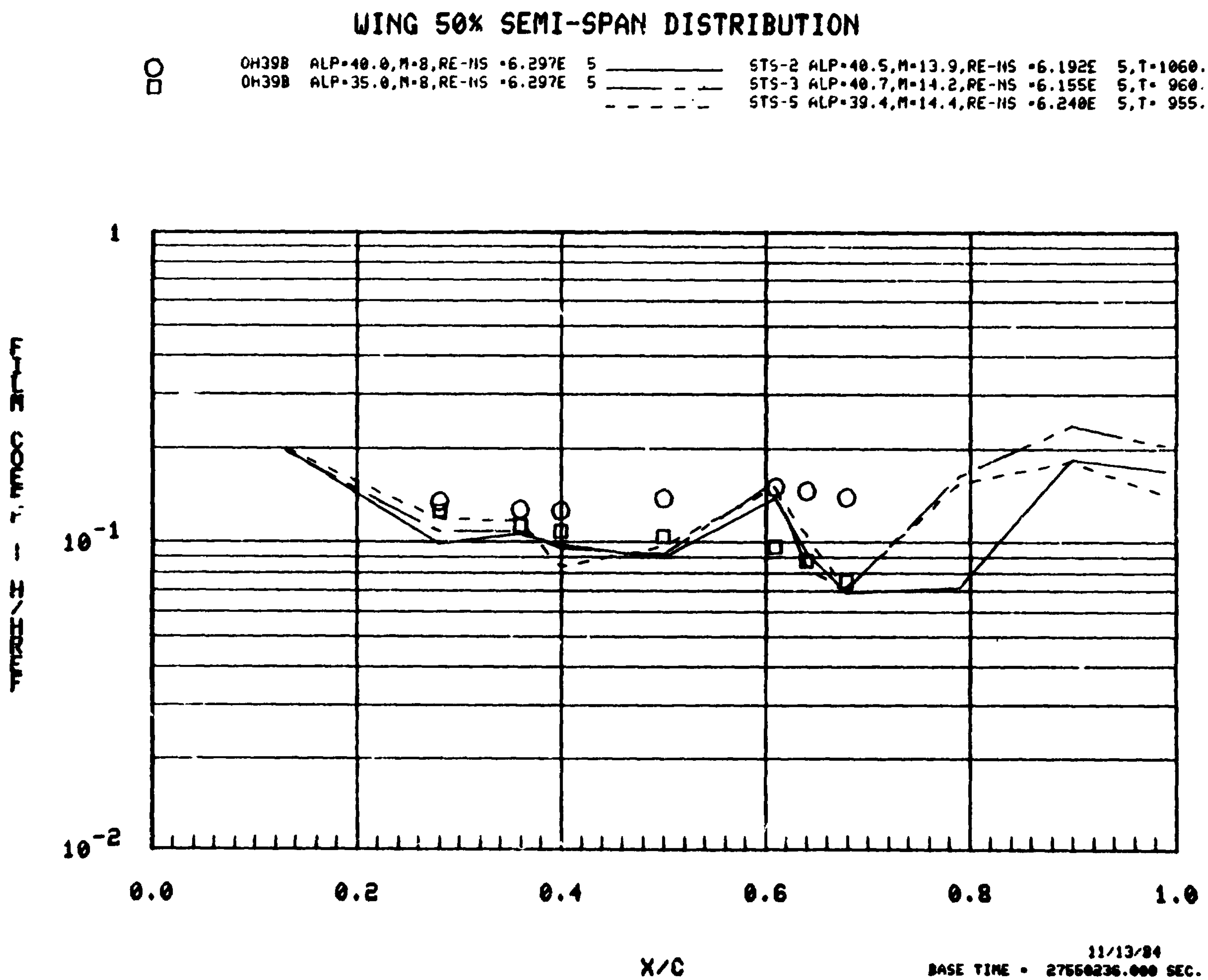
WING 50% SEMI-SPAN DISTRIBUTION
OH39B ALP=40.0,M=8,RE-NS =6.297E 5
OH39B ALP=35.0,M=8,RE-NS =6.297E 5
STS-2 ALP=40.5,M=13.9,RE-NS =6.192E 5,T=1060.
STS-3 ALP=40.7,M=14.2,RE-NS =6.155E 5,T= 960.
STS-5 ALP=39.4,M=14.4,RE-NS =6.240E 5,T= 955.
FILM COEF. - H/HREF
1
10^{-1}
10^{-2}
0.0
0.2
0.4
0.6
0.8
1.0
X/C
11/13/84
BASE TIME = 27560236.000 SEC.

WING 50% SEMI-SPAN DISTRIBUTION

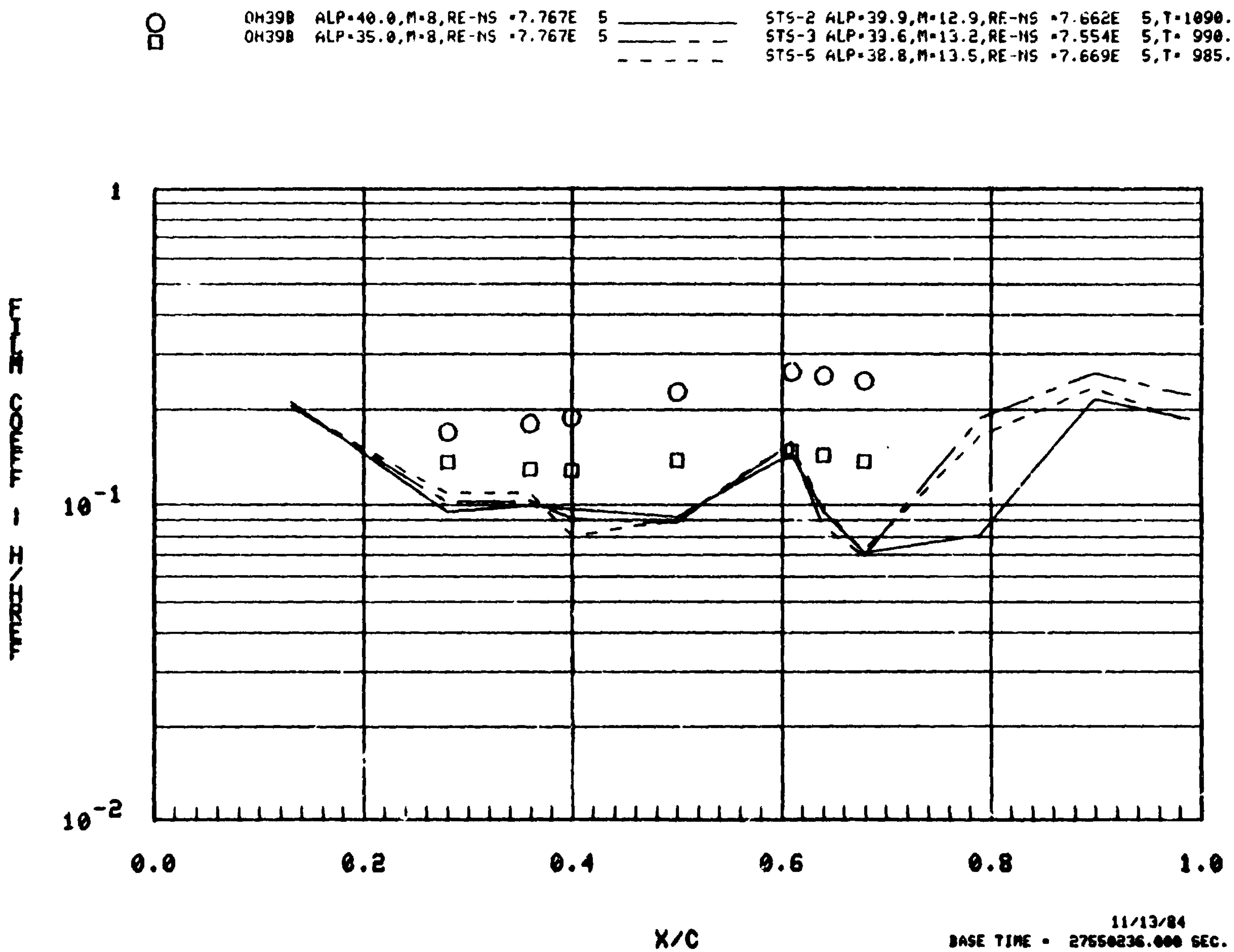

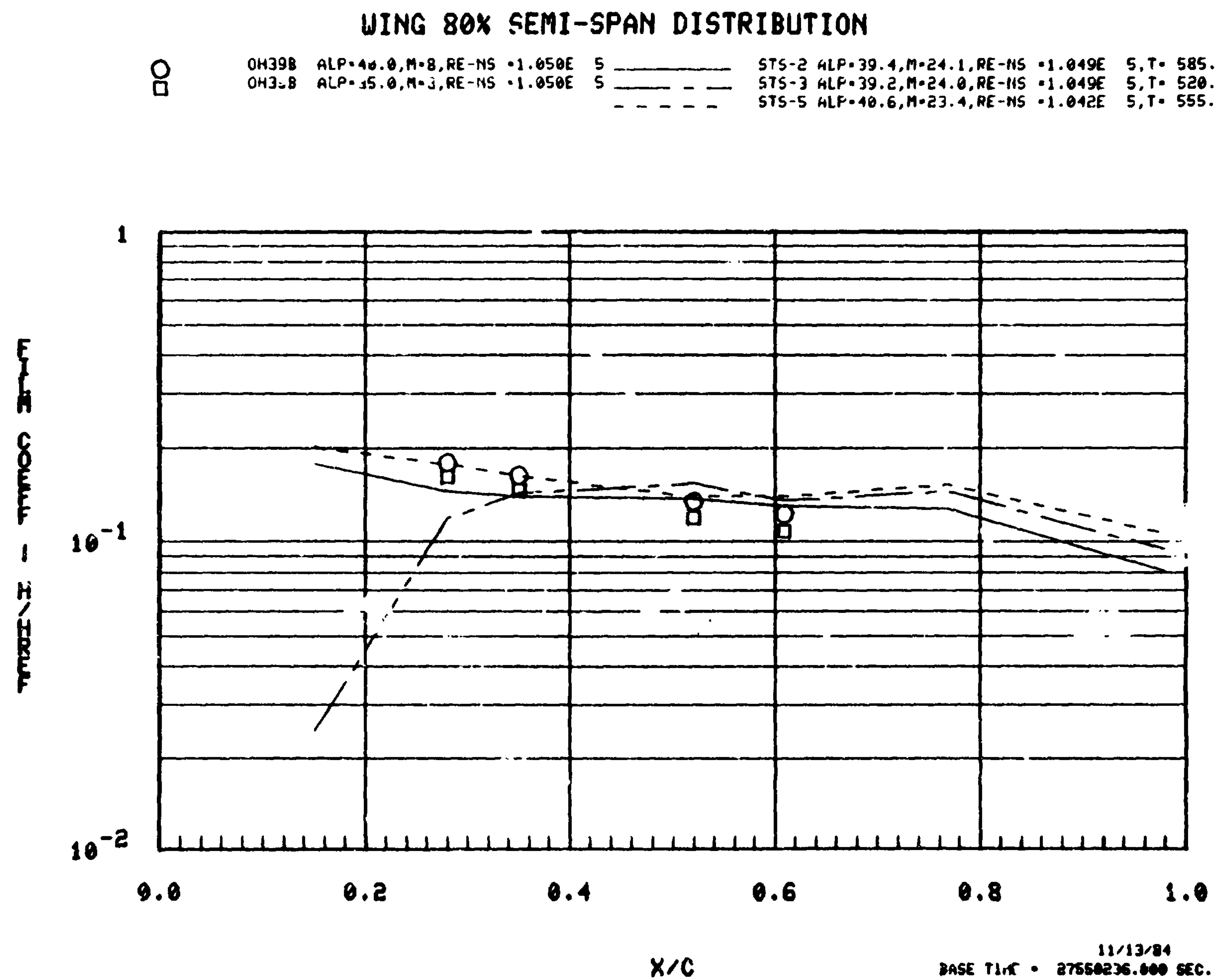

WING 80% SEMI-SPAN DISTRIBUTION
OH39B ALP=40.0,M=8,RE-NS =1.050E 5
OH39B ALP=35.0,M=8,RE-NS =1.050E 5
STS-2 ALP=39.4,M=24.1,RE-NS =1.049E 5,T= 585.
STS-3 ALP=39.2,M=24.0,RE-NS =1.049E 5,T= 520.
STS-5 ALP=40.6,M=23.4,RE-NS =1.042E 5,T= 555.
1
10-1
10-2
FILM COEFF : H/HREF
0.0
0.2
0.4
0.6
0.8
1.0
X/C
11/13/84
BASE TIME = 27550236.000 SEC.

WING 80% SEMI-SPAN DISTRIBUTION

○	OH3.J ALP=40.0,M=8,RE-NS =2.099E 5	STS-2 ALP=41.2,M=19.9,RE-NS =2.093E 5,T= 835.
□	OH39B ALP=35.0,M=8,RE-NS =2.099E 5	STS-3 ALP=39.8,M=20.4,RE-NS =2.072E 5,T= 730.
		STS-5 ALP=40.4,M=18.8,RE-NS =2.095E 5,T= 765.

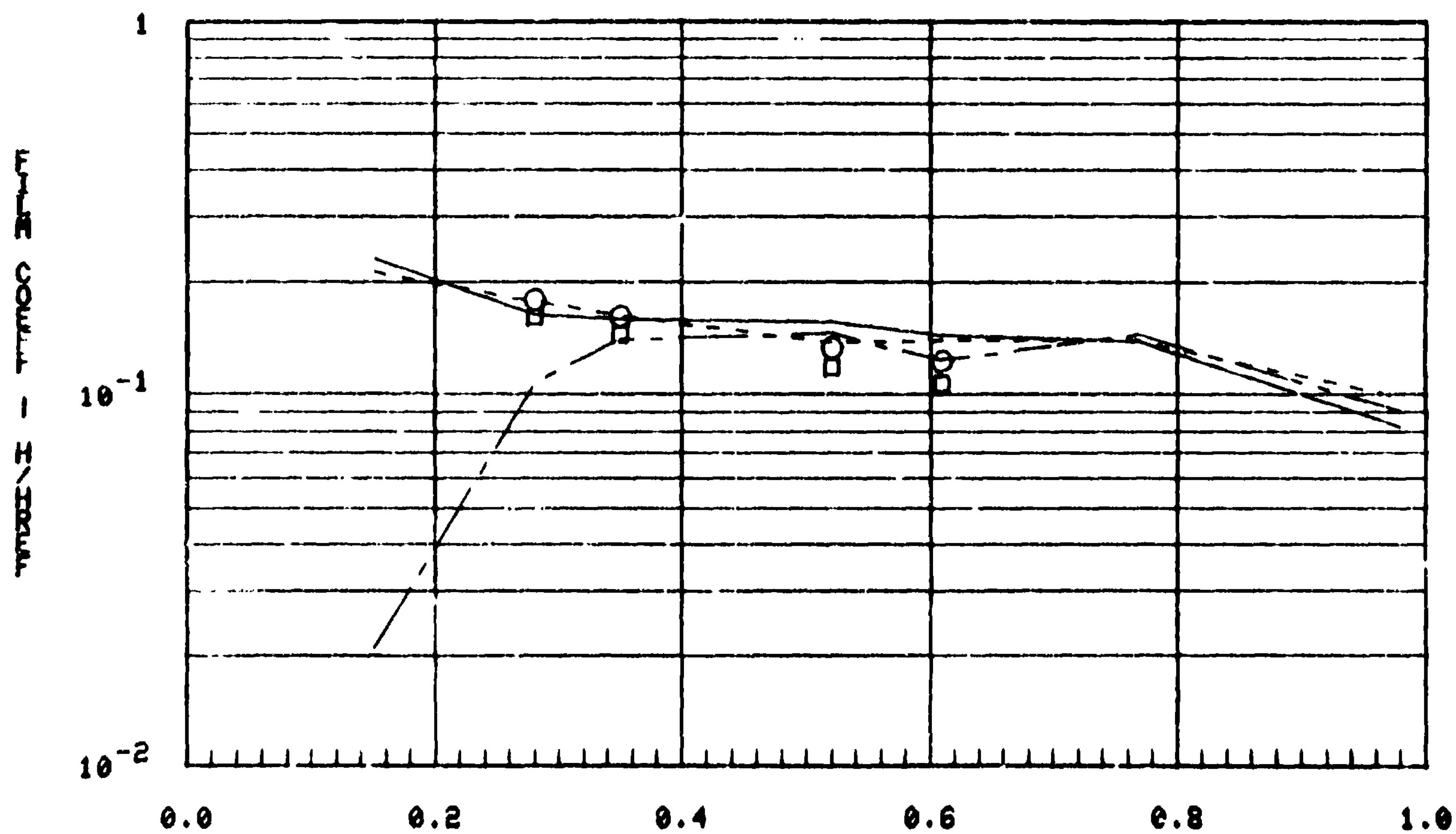

11/13/84
BASE TIME = 27550236.000 SEC.

WING 80% SEMI-SPAN DISTRIBUTION

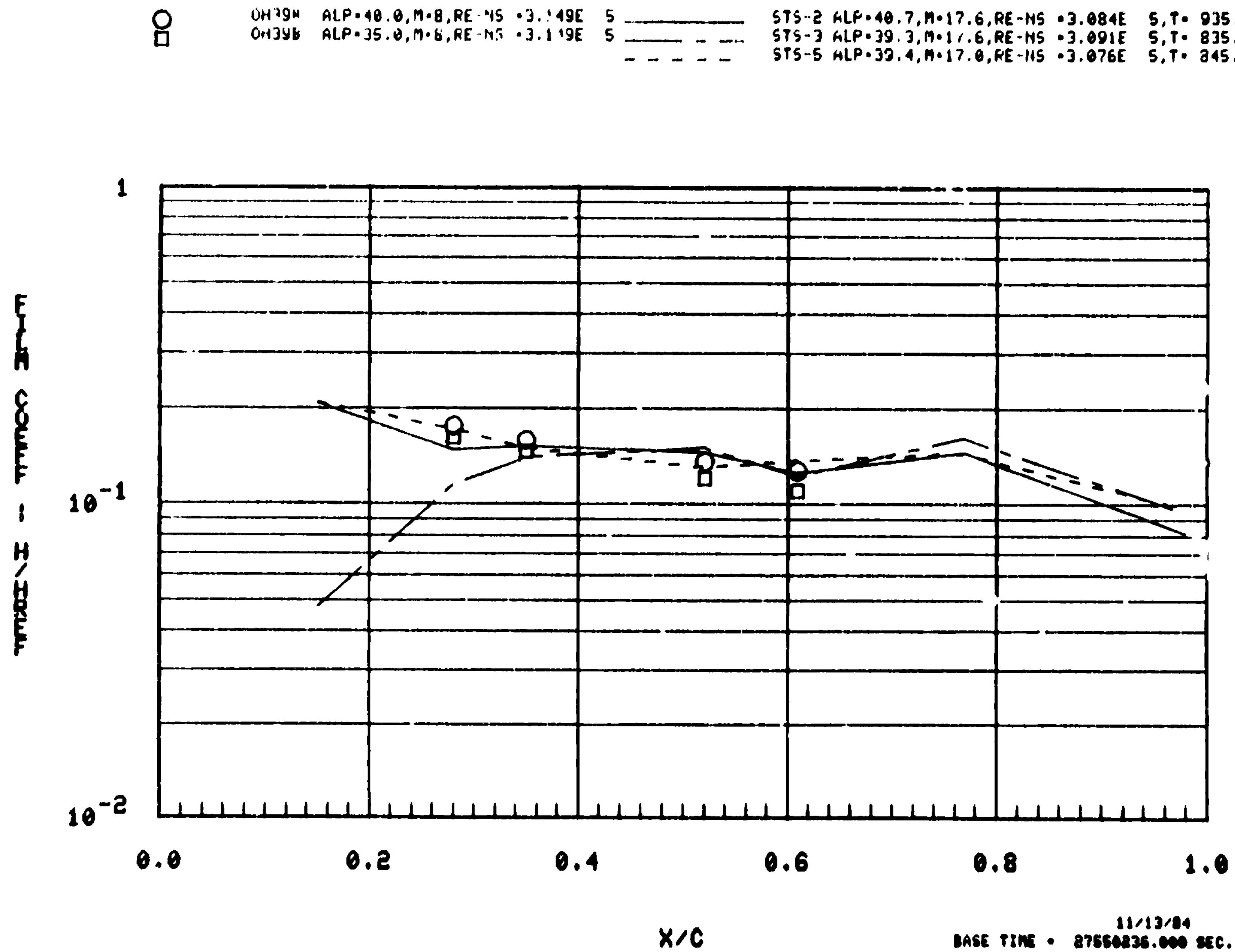

WING 80% SEMI-SPAN DISTRIBUTION

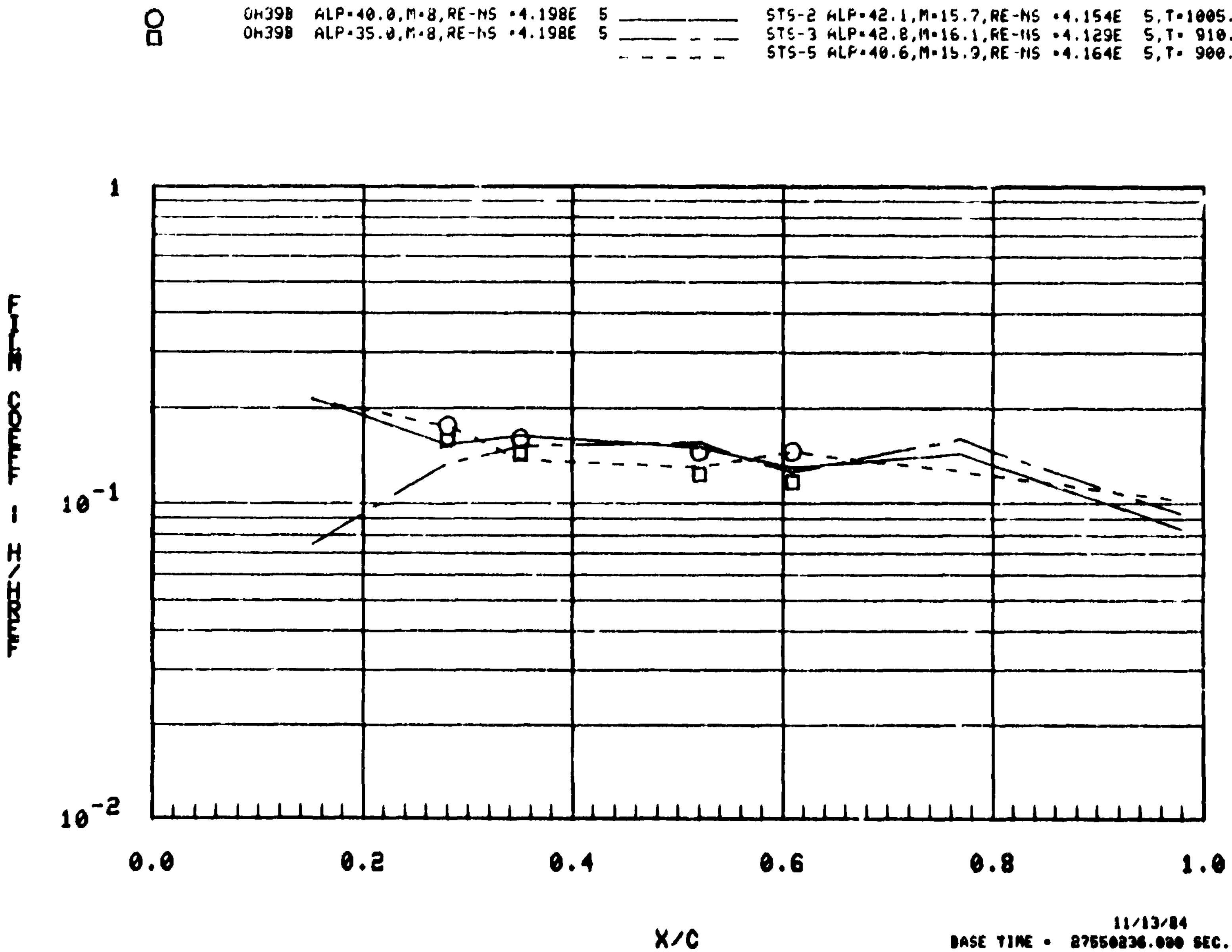

WING 80% SEMI-SPAN DISTRIBUTION

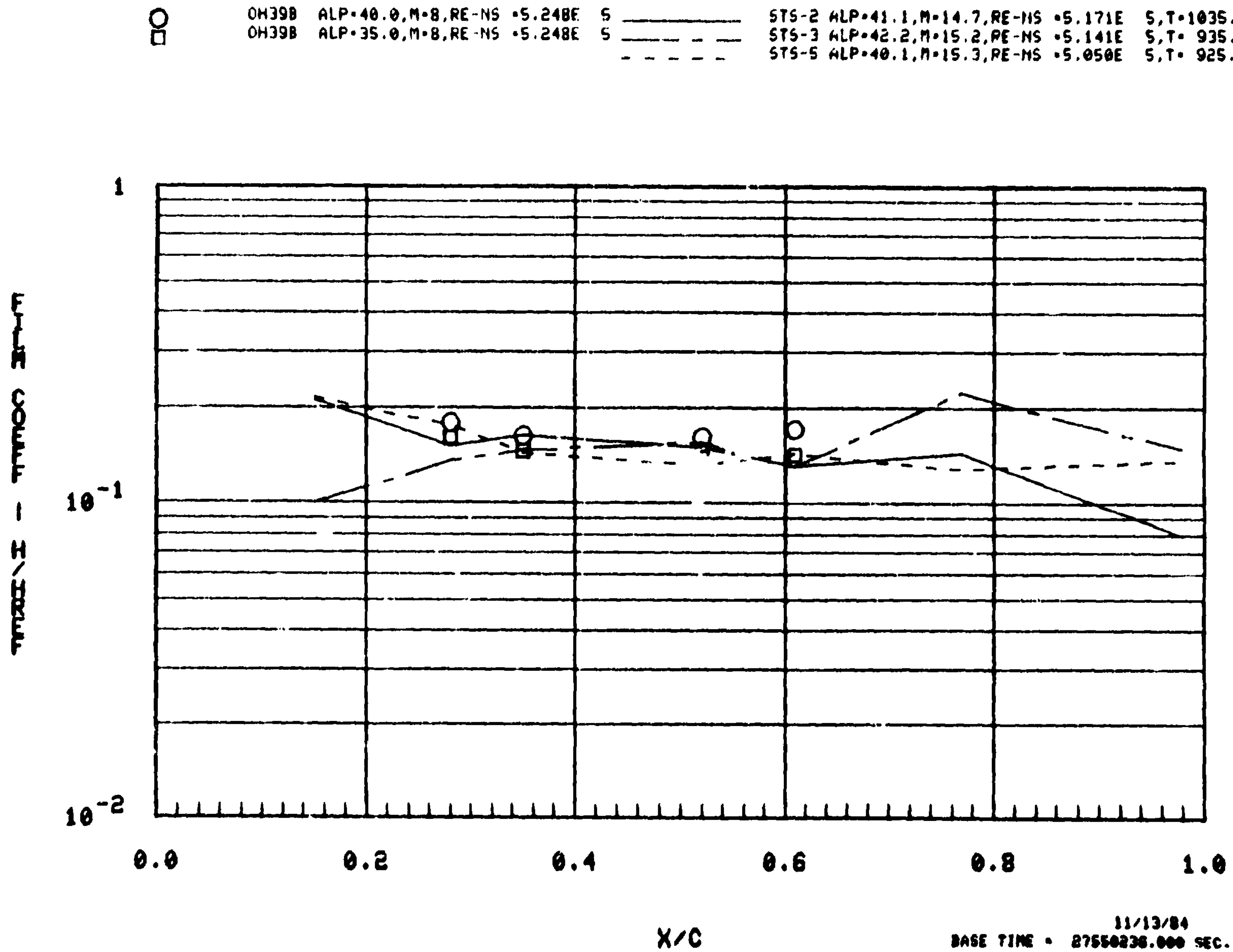

11/13/84
BASE TIME = 27550236.000 SEC.

WING 80% SEMI-SPAN DISTRIBUTION

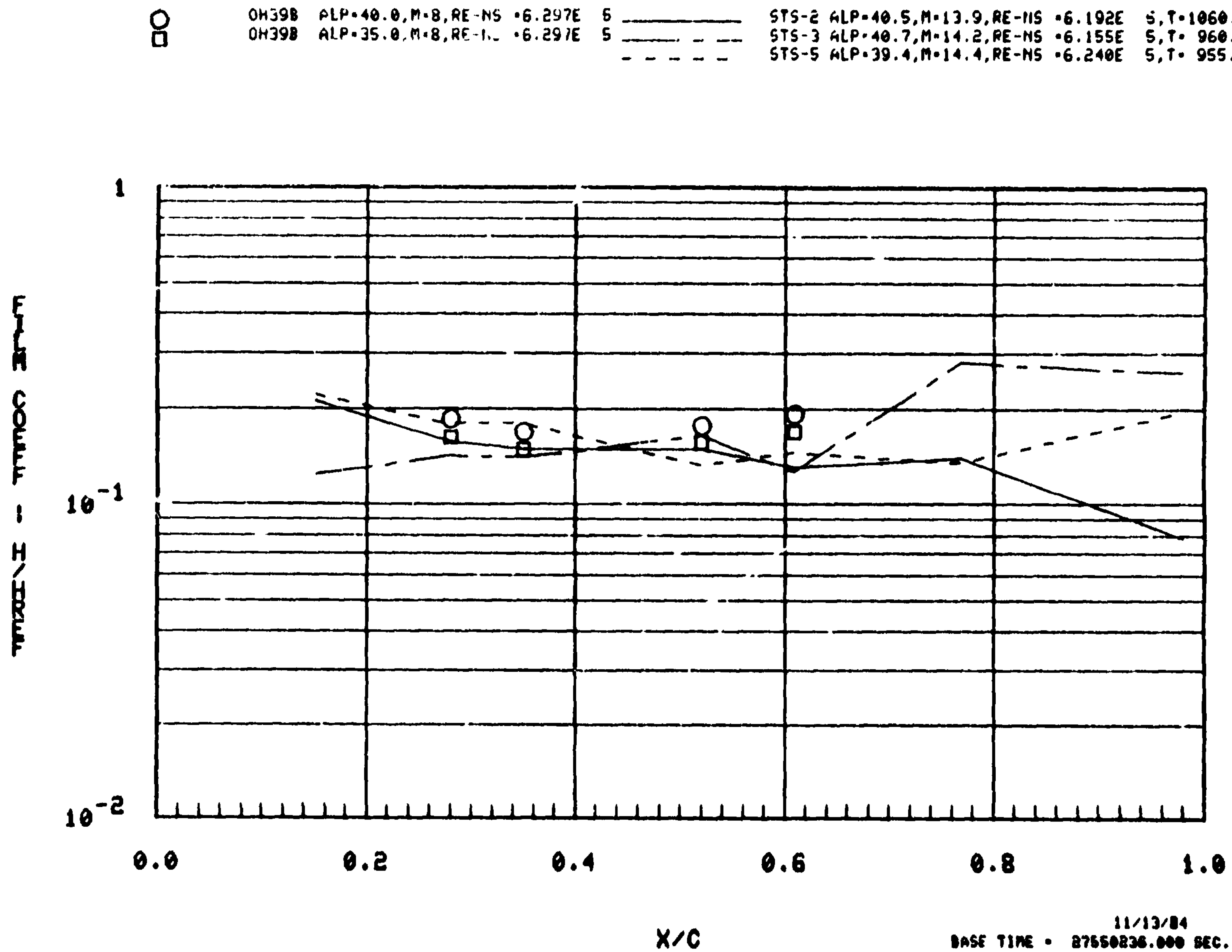

WING 80% SEMI-SPAN DISTRIBUTION

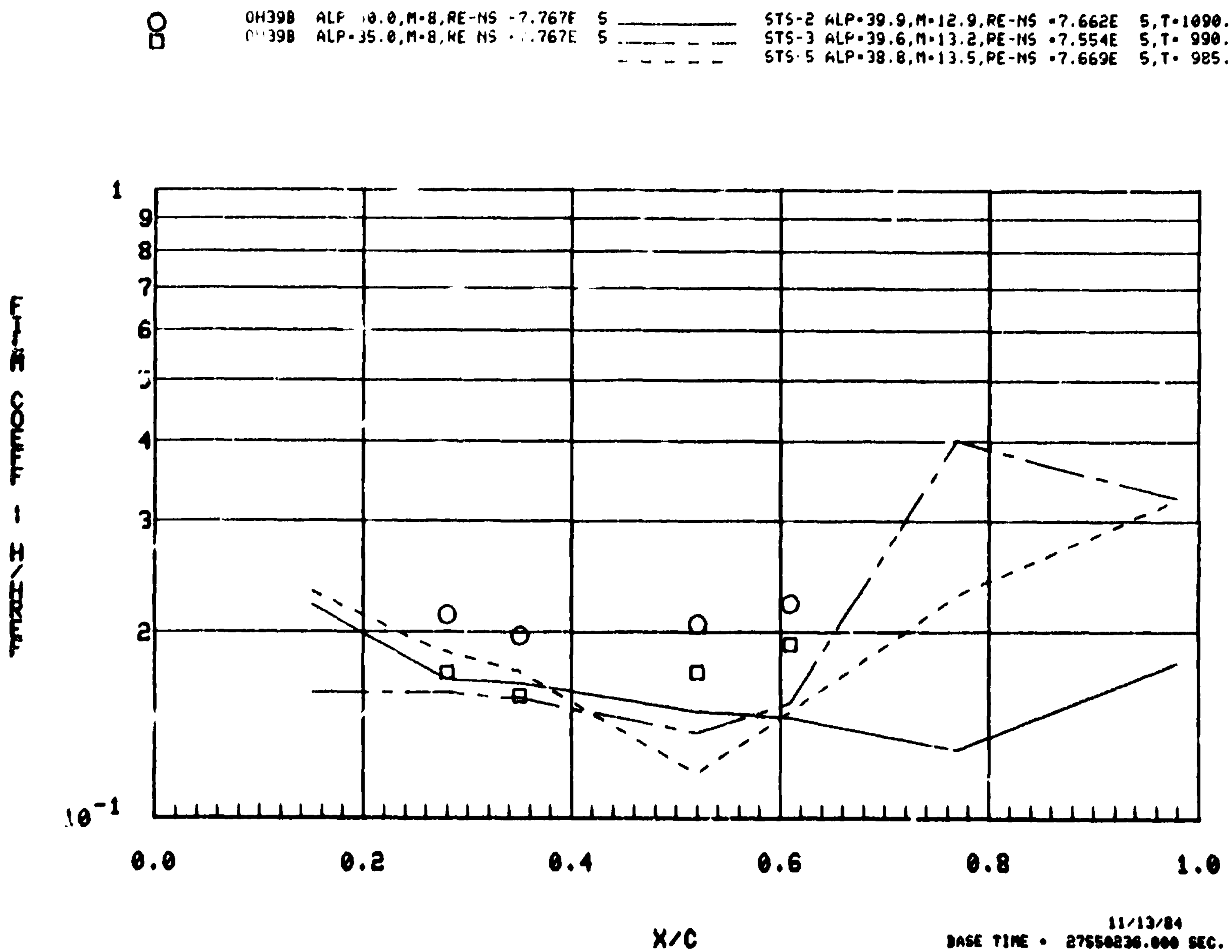

SIDE FUSELAGE (Z=400 TRACE) DISTRIBUTION

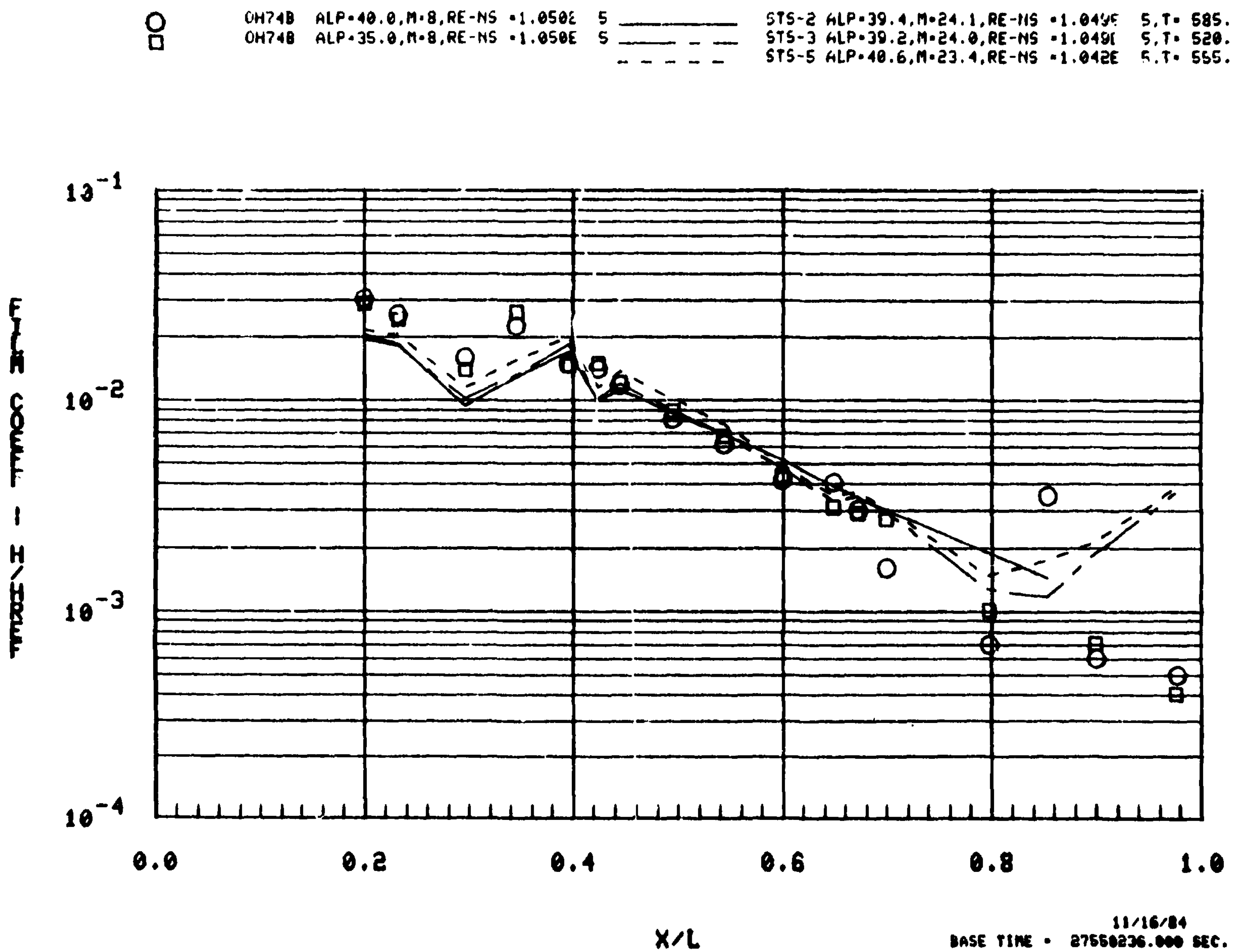

SIDE FUSELAGE (Z=400 TRACE) DISTRIBUTION

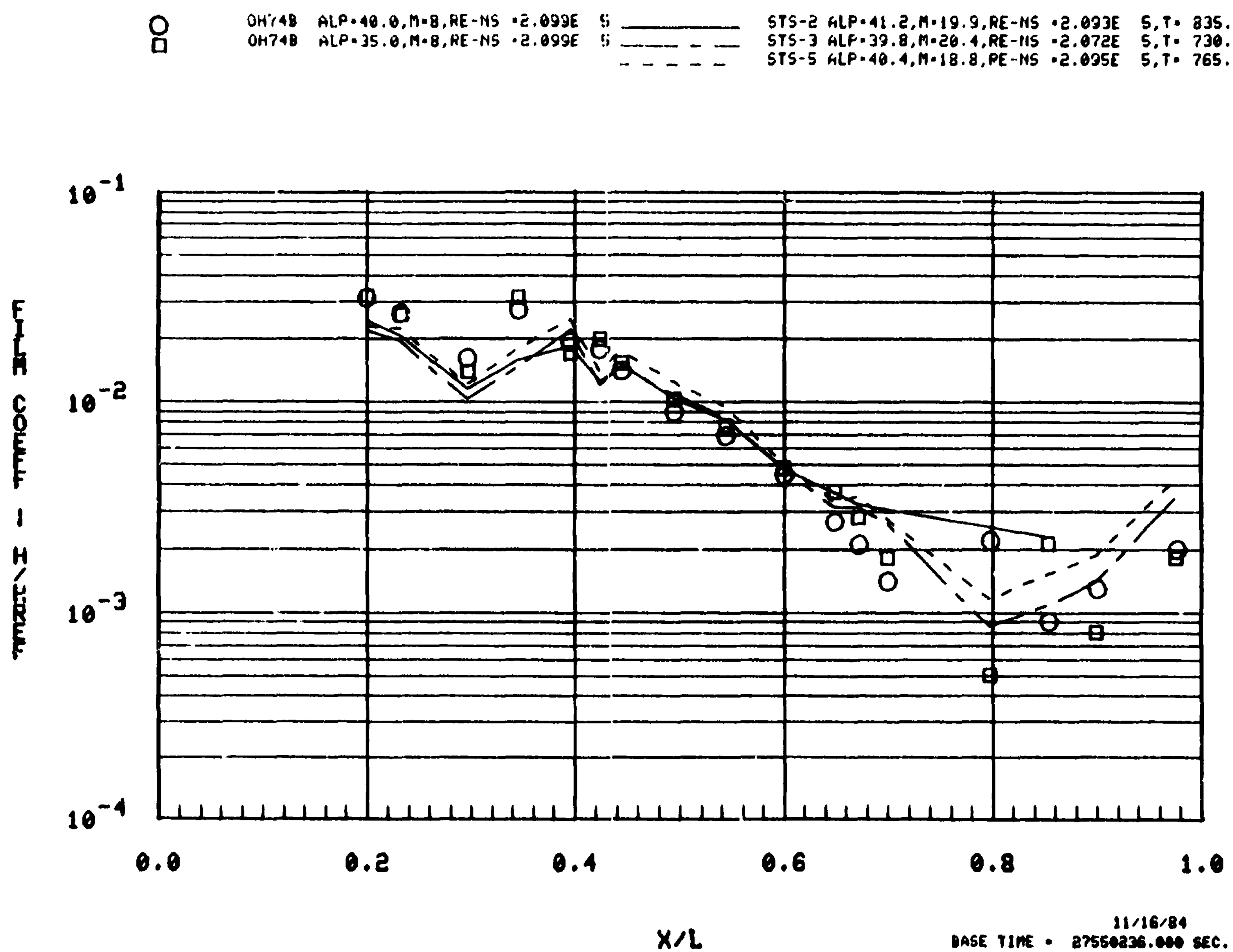

SIDE FUSELAGE (Z=400 TRACE) DISTRIBUTION

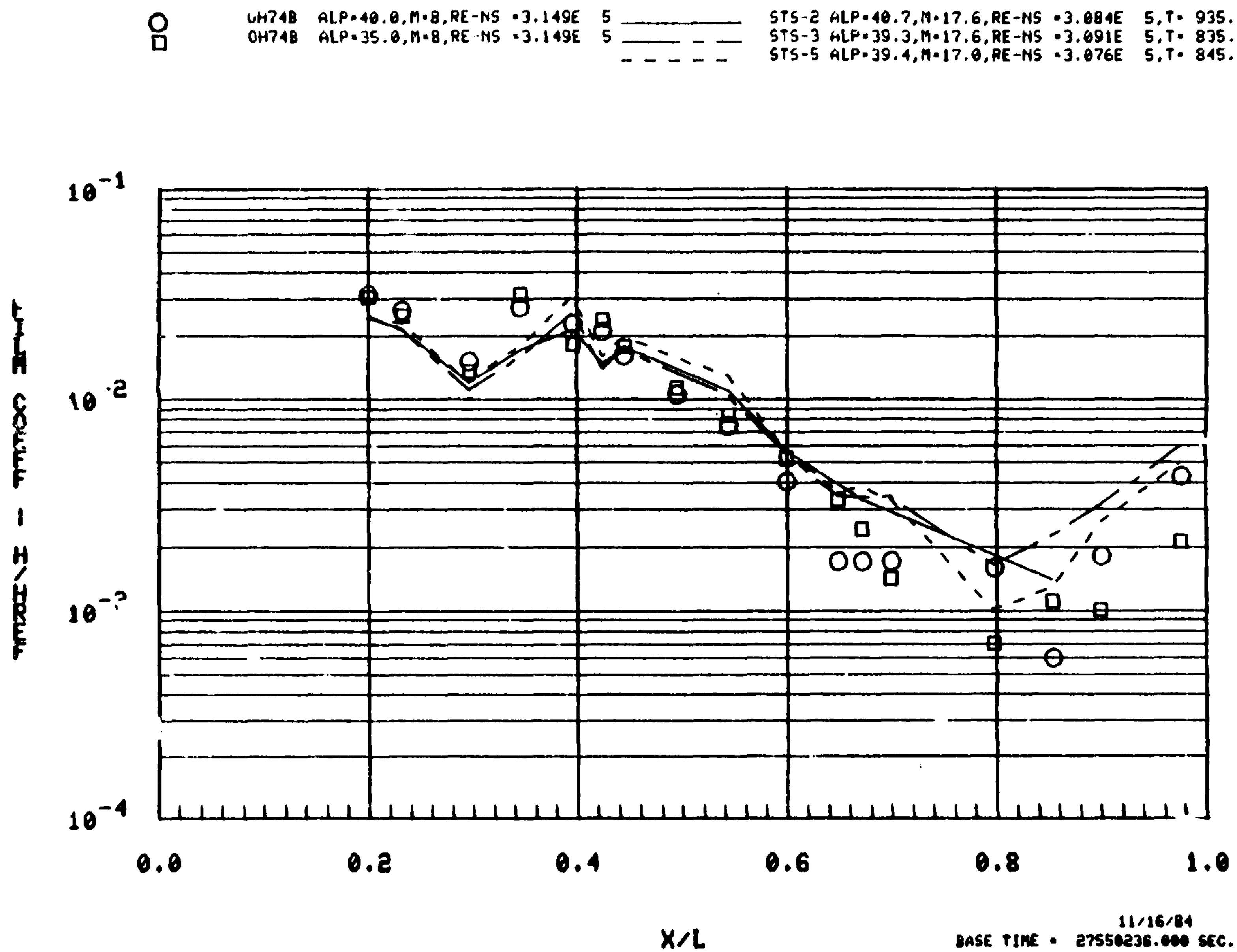

SIDE FUSELAGE (Z=400 TRACE) DISTRIBUTION

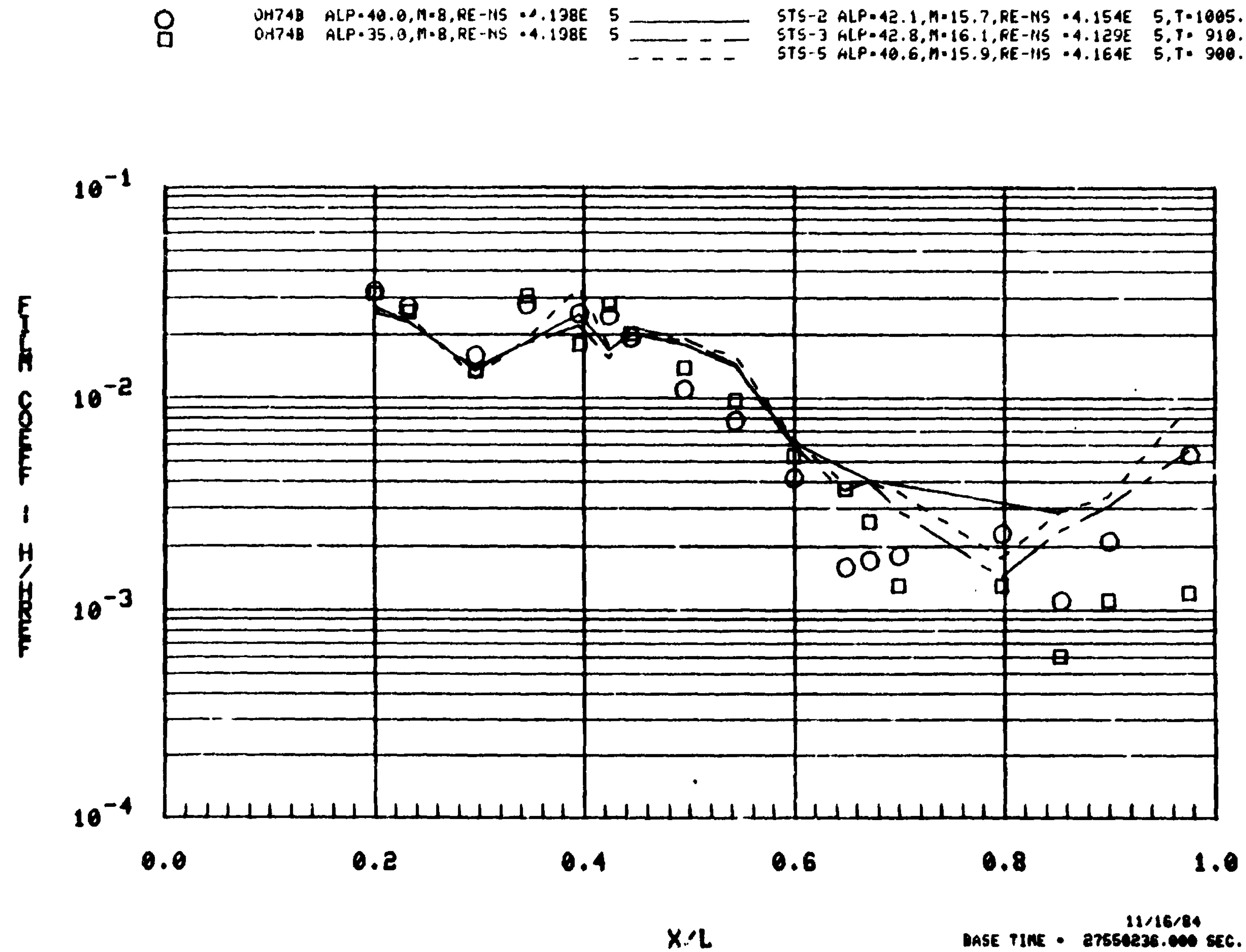

SIDE FUSELAGE (Z=400 TRACE) DISTRIBUTION

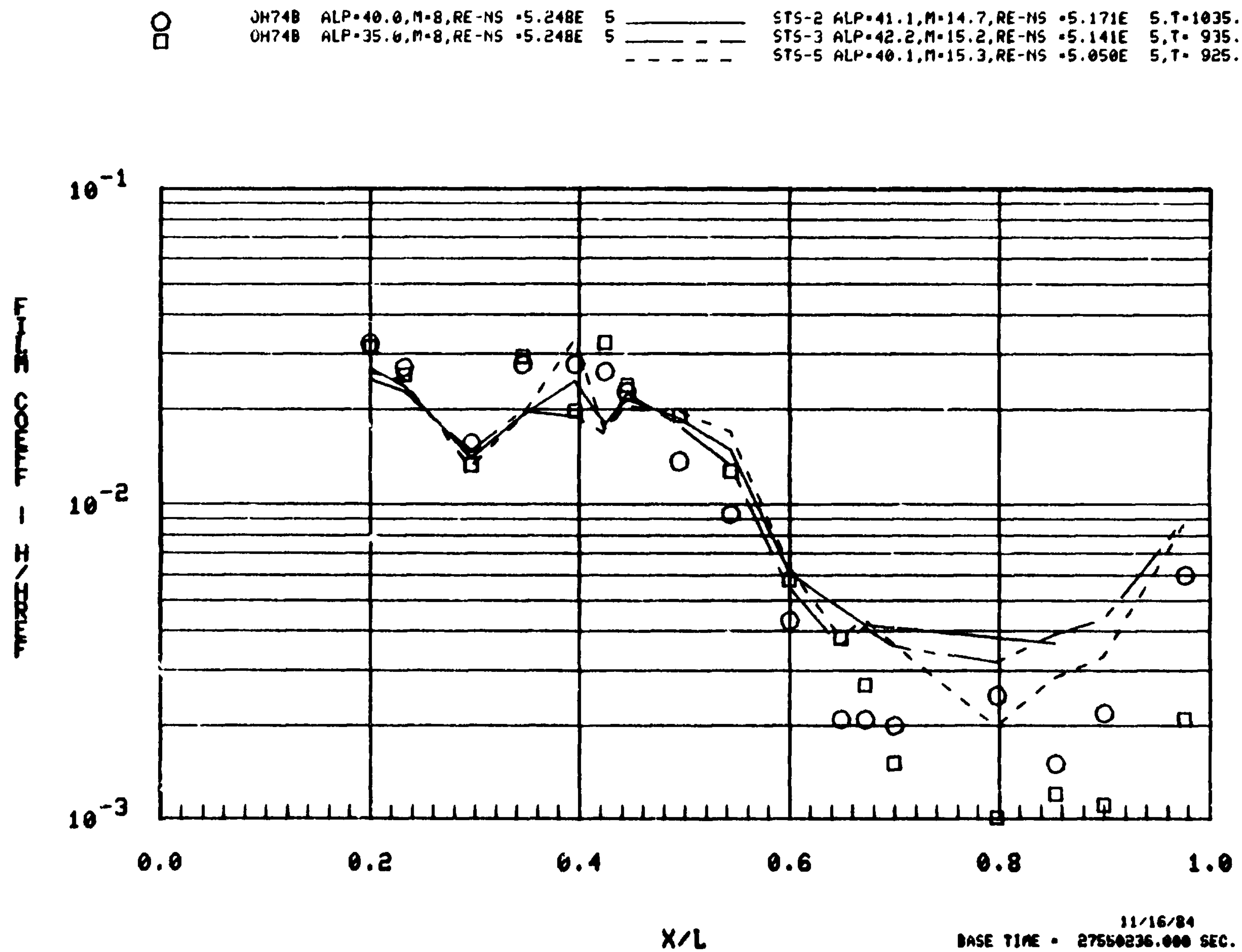

SIDE FUSELAGE (Z=400 TRACE) DISTRIBUTION

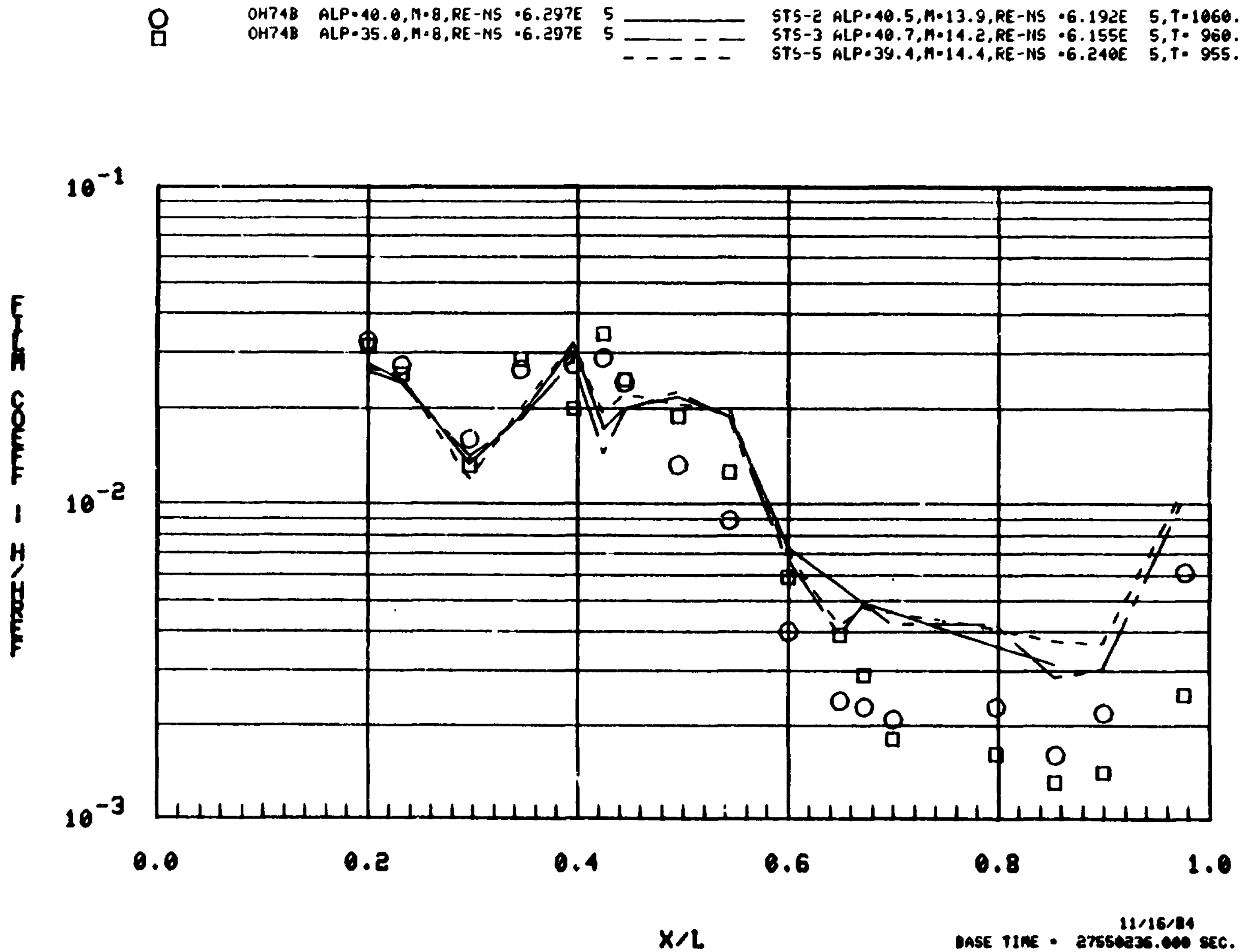

SIDE FUSELAGE (Z=400 TRACE) DISTRIBUTION

○	OH74B ALP=40.0,M=8,RE-NS =7.347E 5	————	STS-2 ALP=39.8,M=13.2,RE-NS =7.090E 5,T=1080.
□	OH74B ALP=35.0,M=8,RE-NS =7.347E 5	—— — —	STS-3 ALP=40.0,M=13.3,RE-NS =7.313E 5,T= 985.
		— — — — —	STS-5 ALP=38.9,M=13.8,RE-NS =7.235E 5,T= 975.

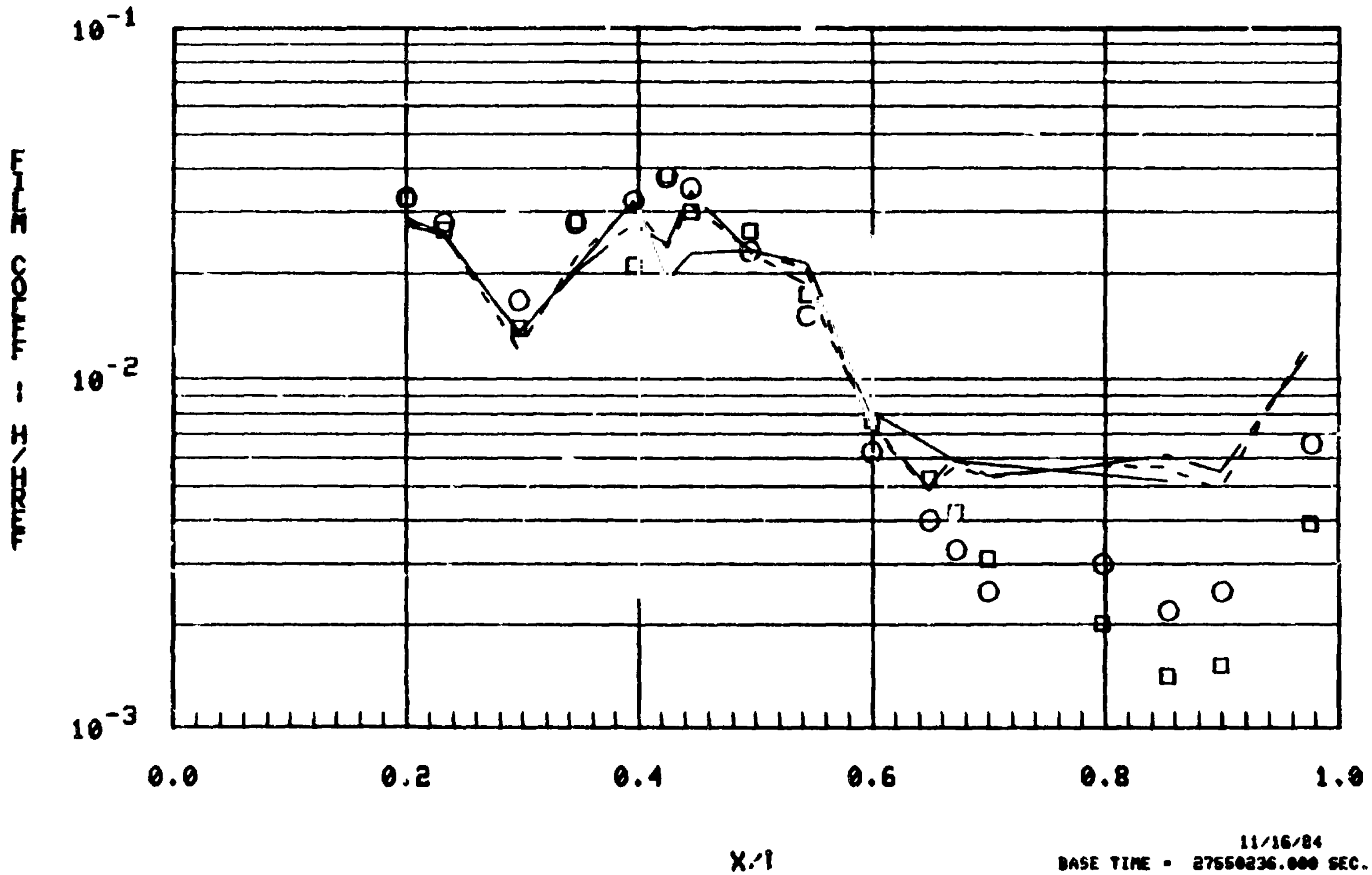

SIDE FUSELAGE (Z=400 TRACE) DISTRIBUTION

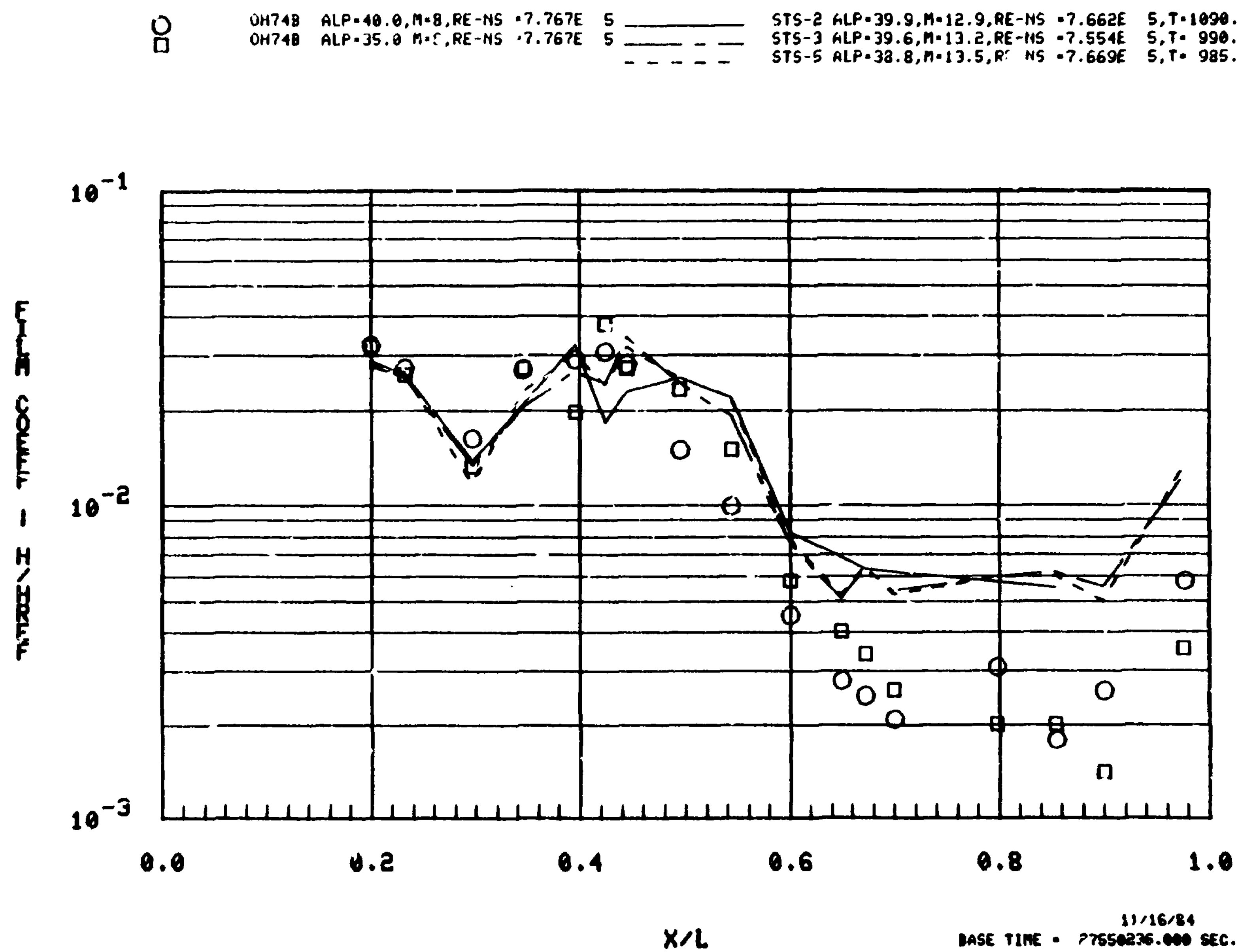

SIDE PLB DOOR (Z=440 TRACE) DISTRIBUTION

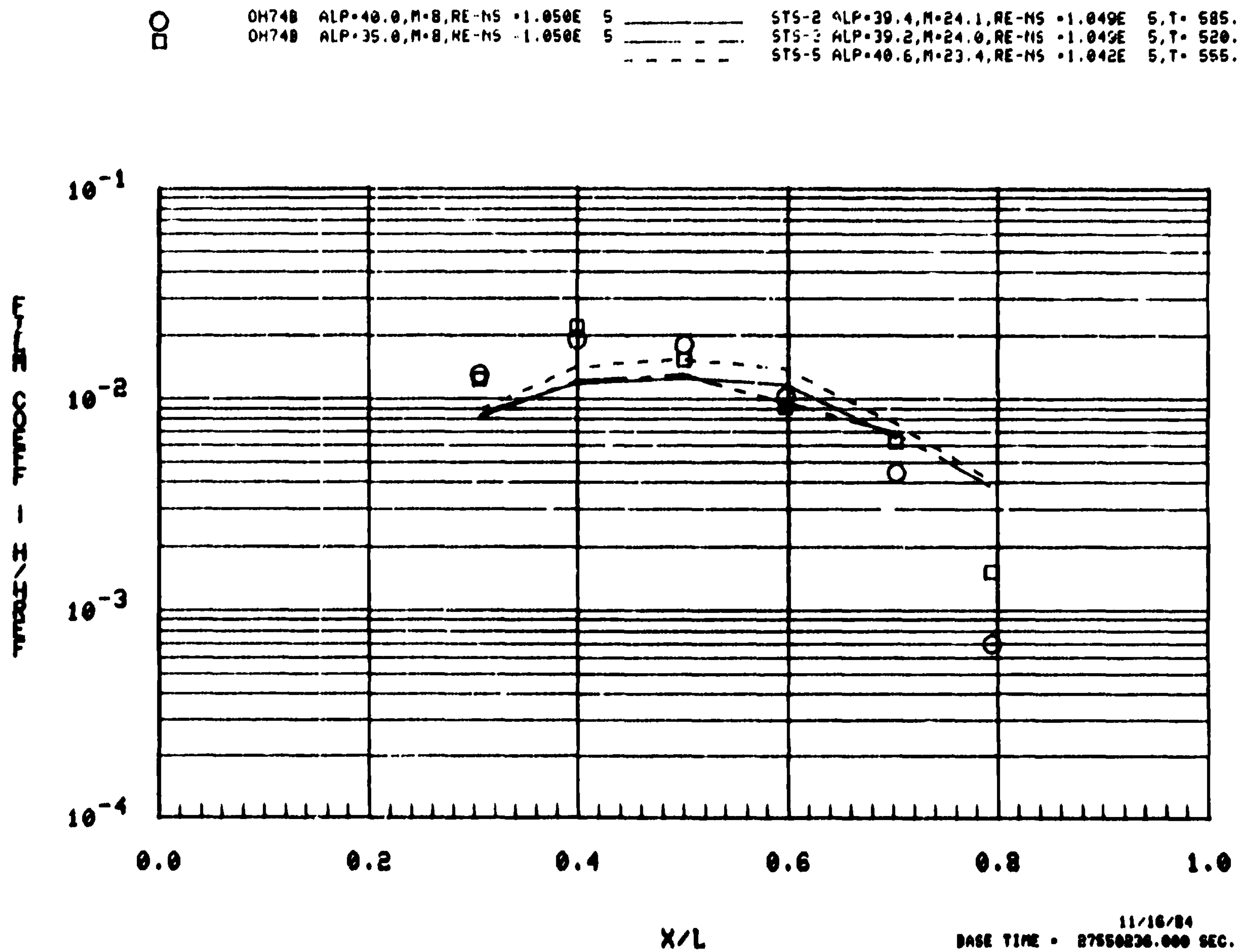

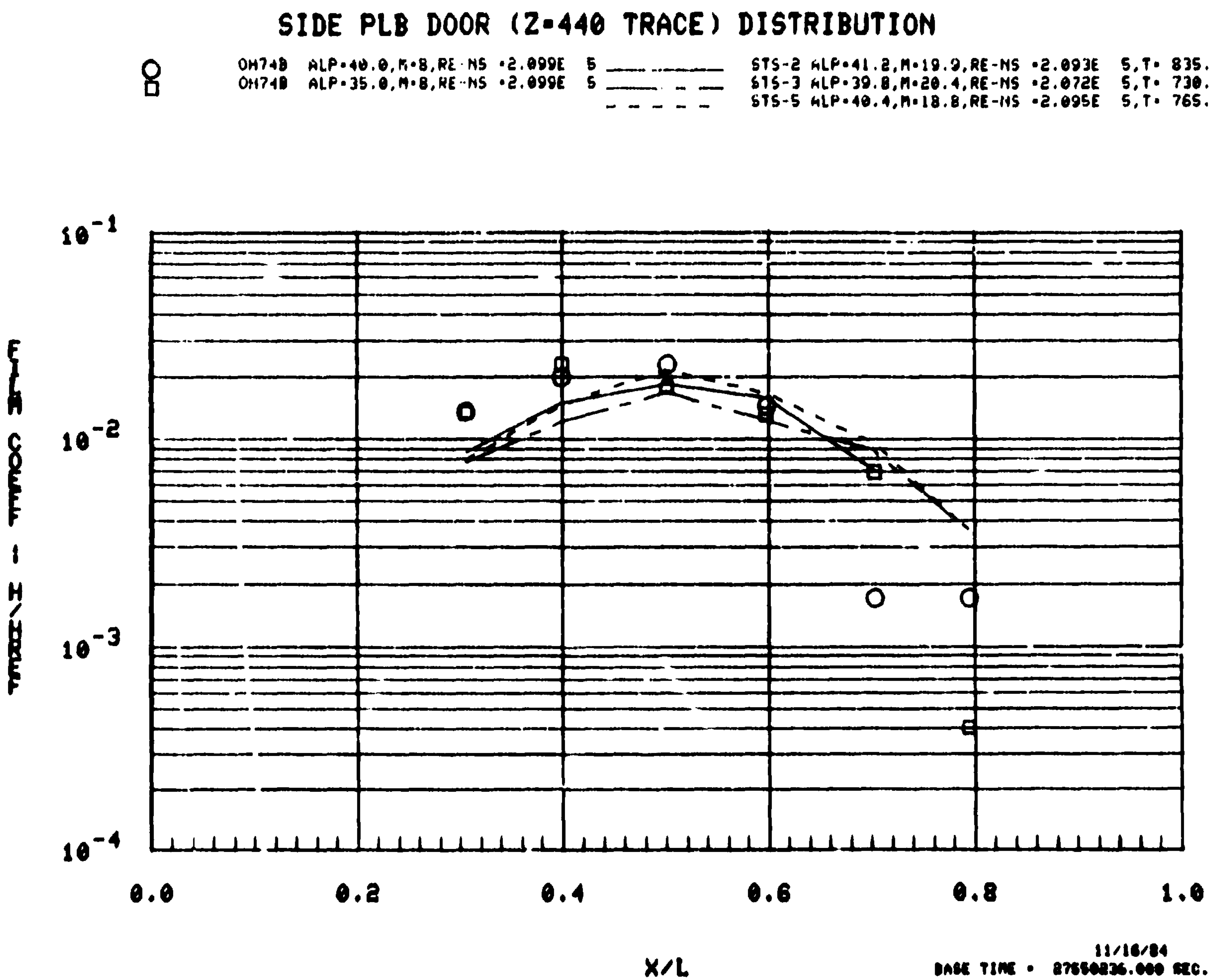
SIDE PLB DOOR (Z=440 TRACE) DISTRIBUTION
OH74B ALP=40.0,M=8,RE-NS =2.099E 5
OH74B ALP=35.0,M=8,RE-NS =2.099E 5
STS-2 ALP=41.2,M=19.9,RE-NS =2.093E 5,T= 835.
STS-3 ALP=39.8,M=20.4,RE-NS =2.072E 5,T= 730.
STS-5 ALP=40.4,M=18.8,RE-NS =2.095E 5,T= 765.
FILM COEFF : H/HREF
10^{-1}
10^{-2}
10^{-3}
10^{-4}
0.0
0.2
0.4
0.6
0.8
1.0
X/L
11/16/84
BASE TIME = 87550836.000 SEC.

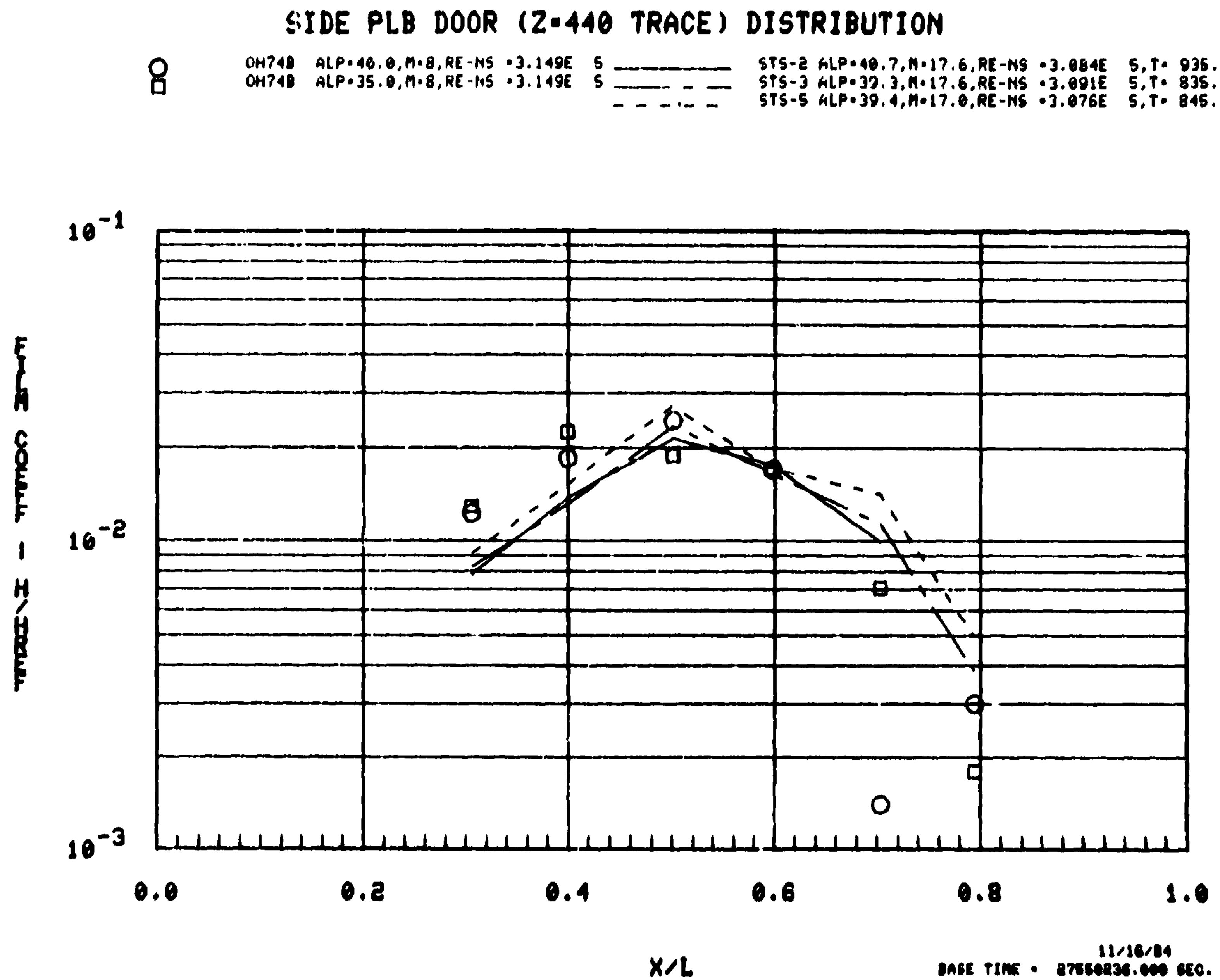

SIDE PLB DOOR (Z=440 TRACE) DISTRIBUTION
OH74B ALP=40.0,M=8,RE-NS =3.149E 5
OH74B ALP=35.0,M=8,RE-NS =3.149E 5
STS-2 ALP=40.7,M=17.6,RE-NS =3.084E 5,T= 935.
STS-3 ALP=39.3,M=17.6,RE-NS =3.091E 5,T= 835.
STS-5 ALP=39.4,M=17.0,RE-NS =3.076E 5,T= 846.
FILM COEFF - H/HREF
X/L
11/16/84
BASE TIME = 27550236.000 SEC.

SIDE PLB DOOR (Z=440 TRACE) DISTRIBUTION

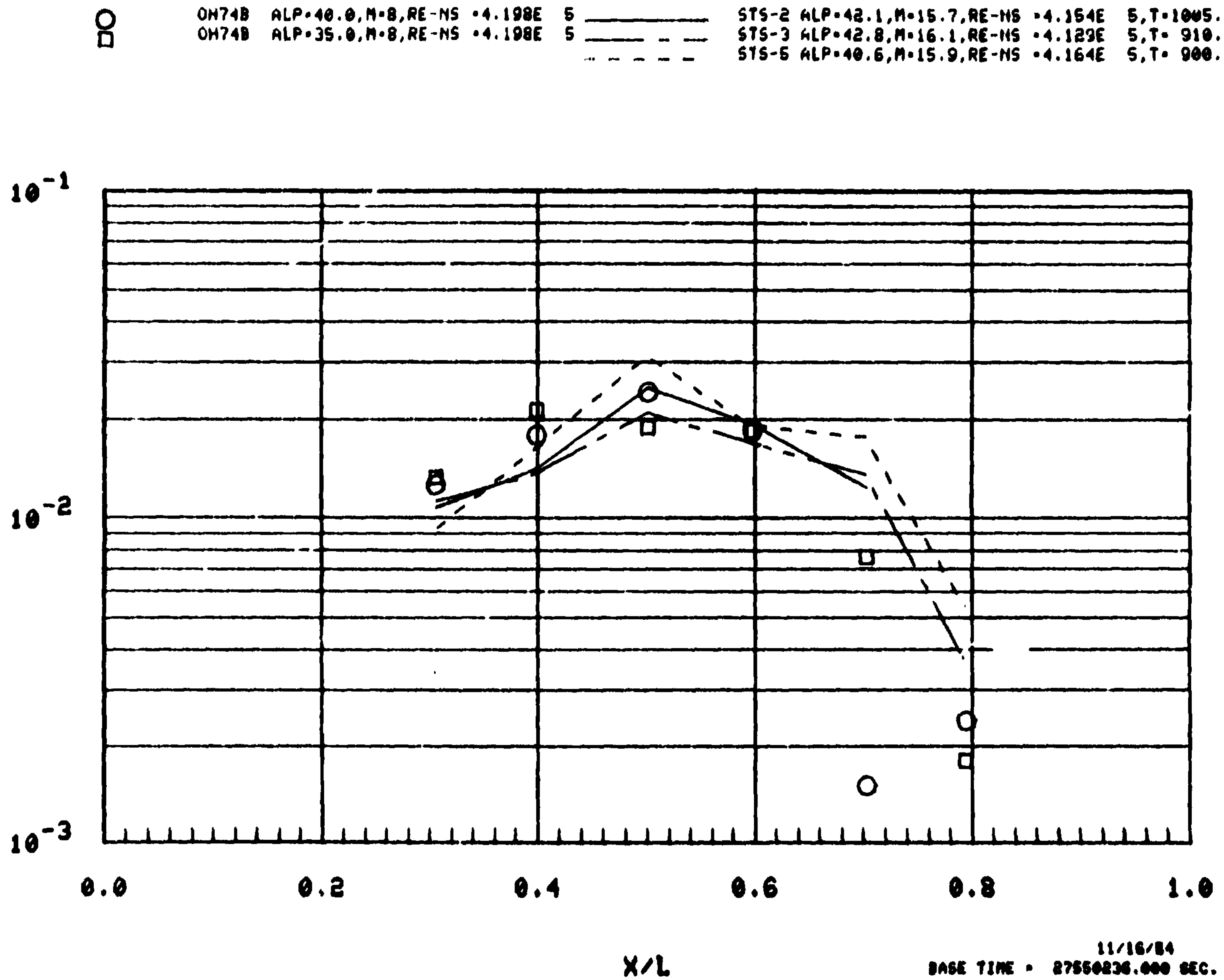

11/16/84
BASE TIME = 27556236.000 SEC.

SIDE PLB DOOR (Z=440 TRACE) DISTRIBUTION

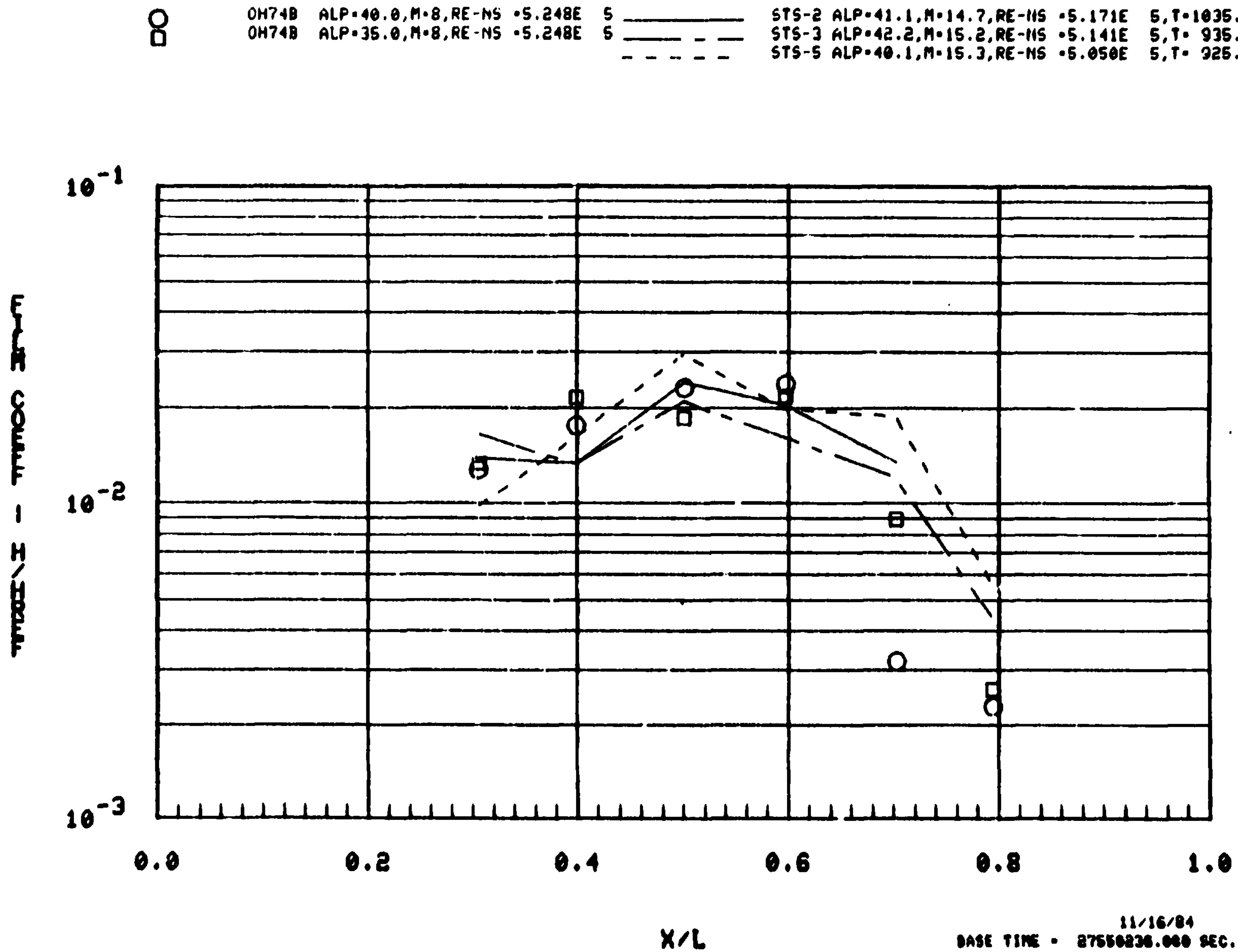

SIDE PLB DOOR (Z=440 TRACE) DISTRIBUTION

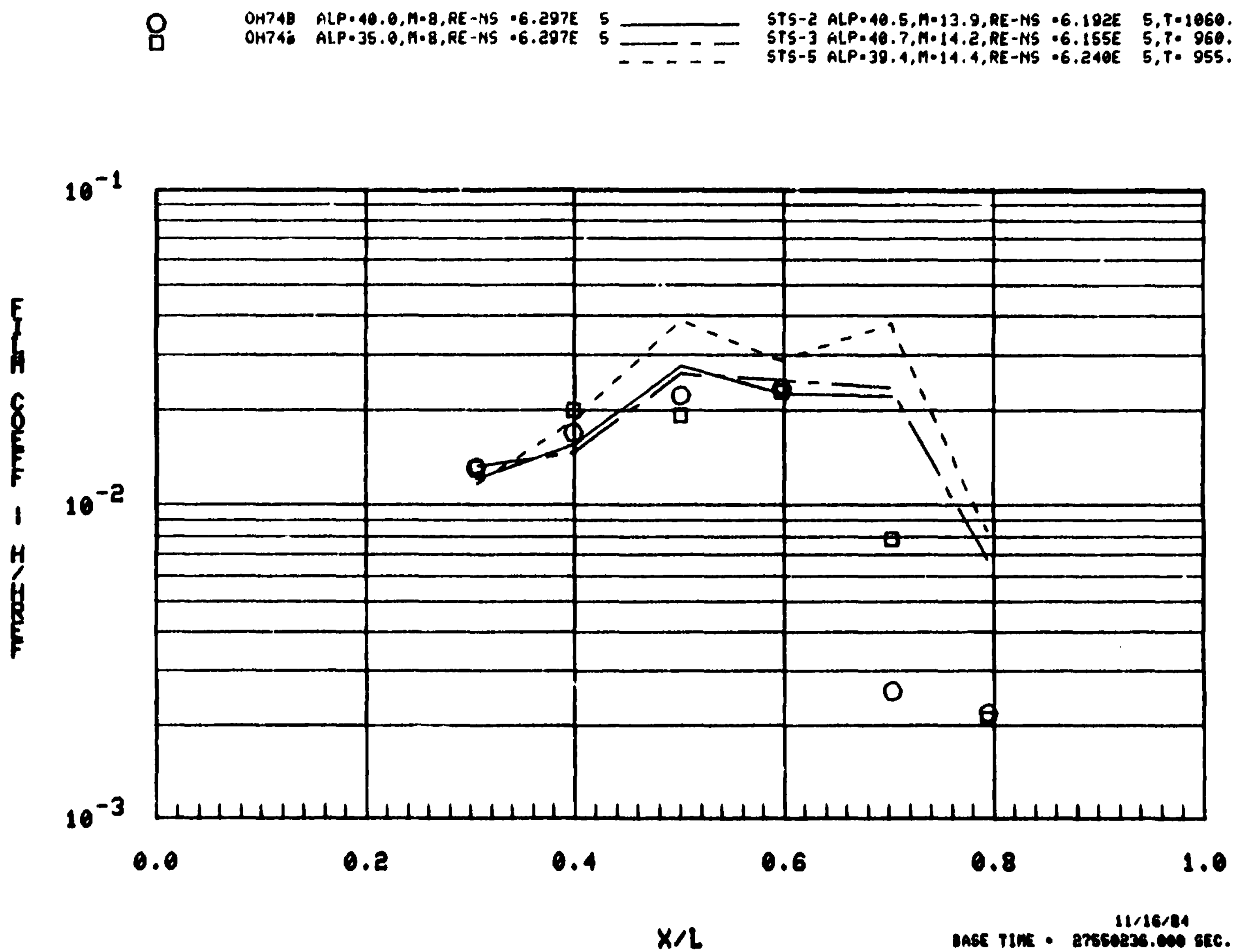

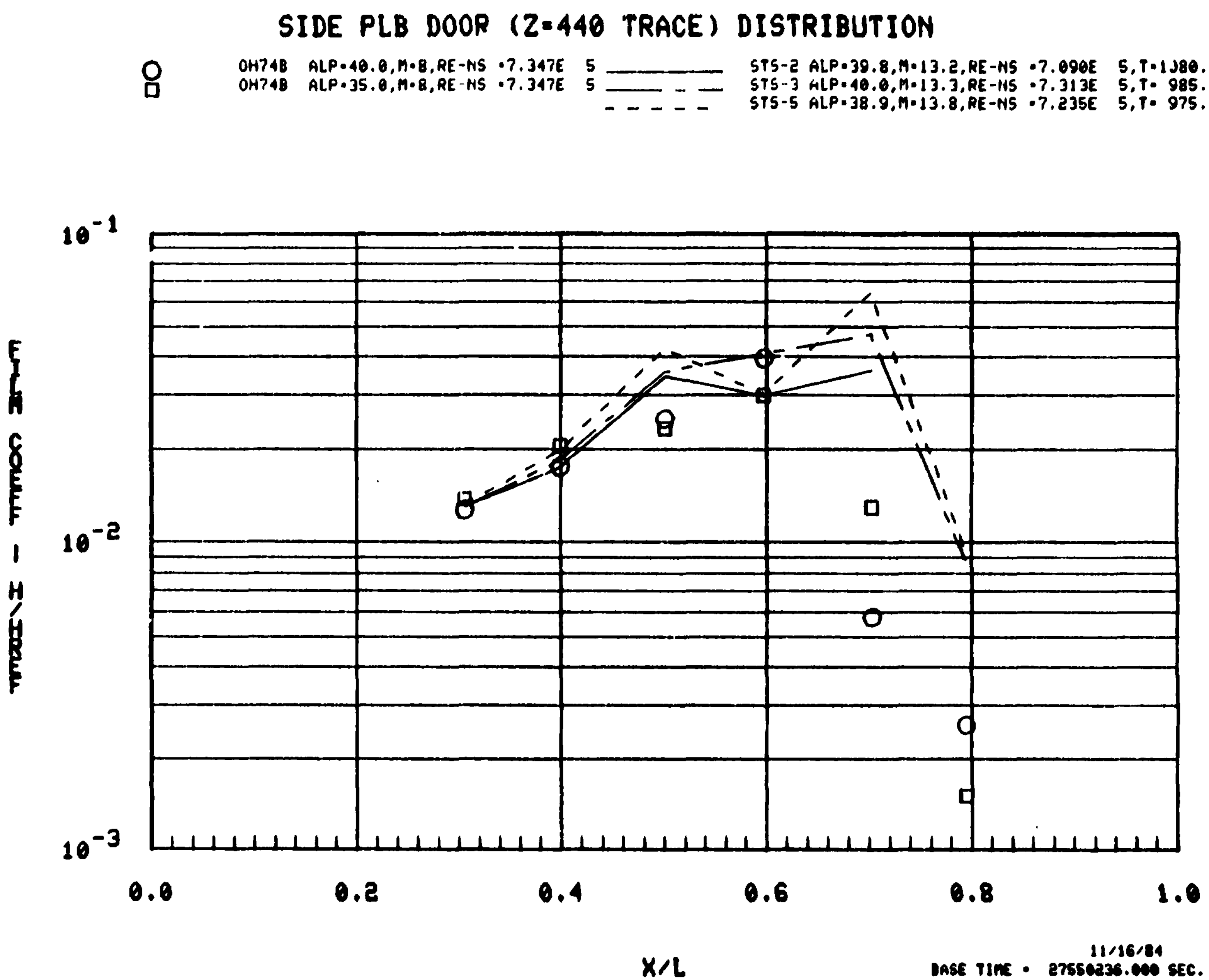

SIDE PLB DOOR (Z=440 TRACE) DISTRIBUTION
OH74B ALP=40.0,M=8,RE-NS =7.347E 5
OH74B ALP=35.0,M=8,RE-NS =7.347E 5
STS-2 ALP=39.8,M=13.2,RE-NS =7.090E 5,T=1380.
STS-3 ALP=40.0,M=13.3,RE-NS =7.313E 5,T= 985.
STS-5 ALP=38.9,M=13.8,RE-NS =7.235E 5,T= 975.
FILM COEFF - H/HREF
10^-1
10^-2
10^-3
0.0
0.2
0.4
0.6
0.8
1.0
X/L
11/16/84
BASE TIME = 27550236.000 SEC.

SIDE PLB DOOR (Z=440 TRACE) DISTRIBUTION

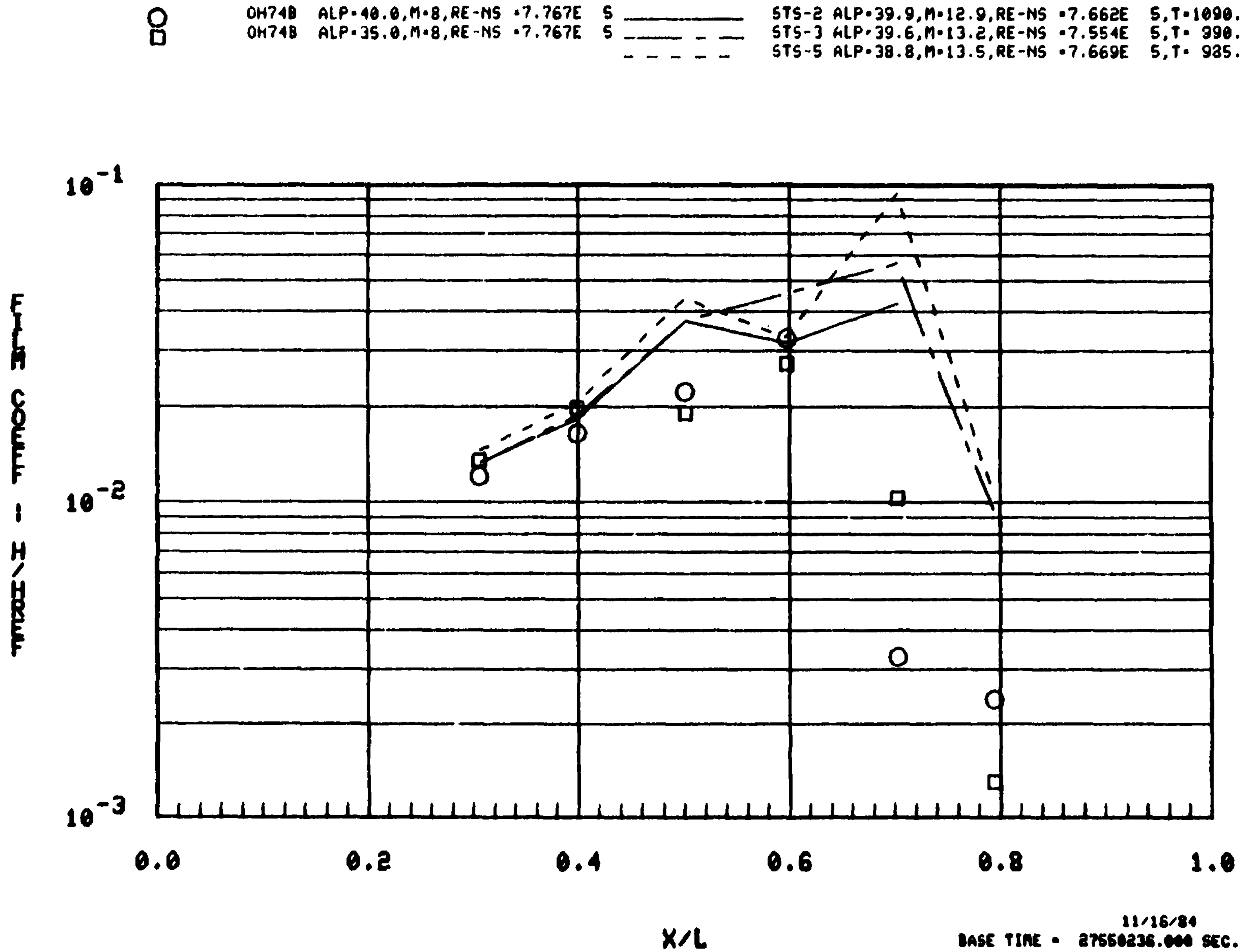

UPPER CENTERLINE DISTRIBUTION

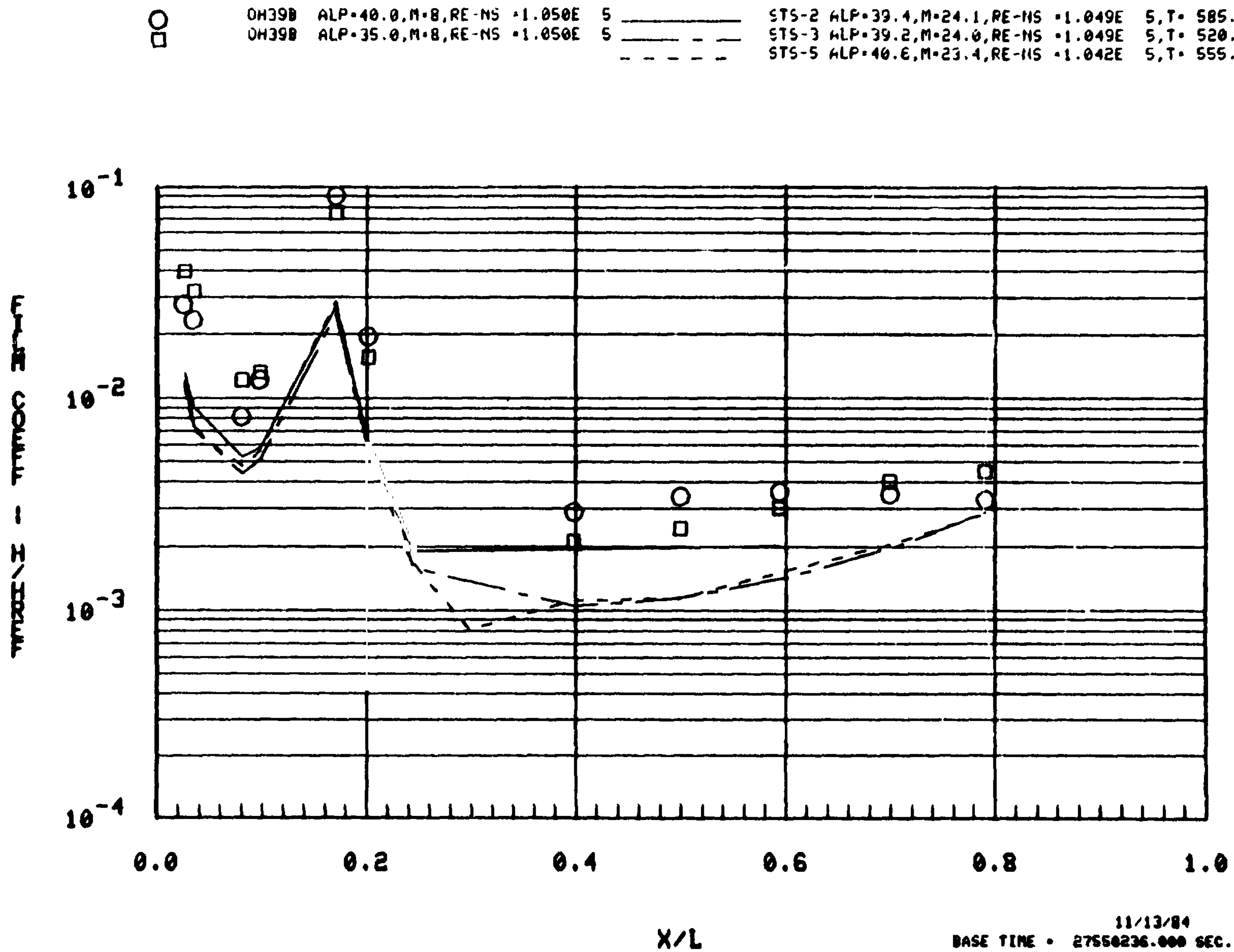

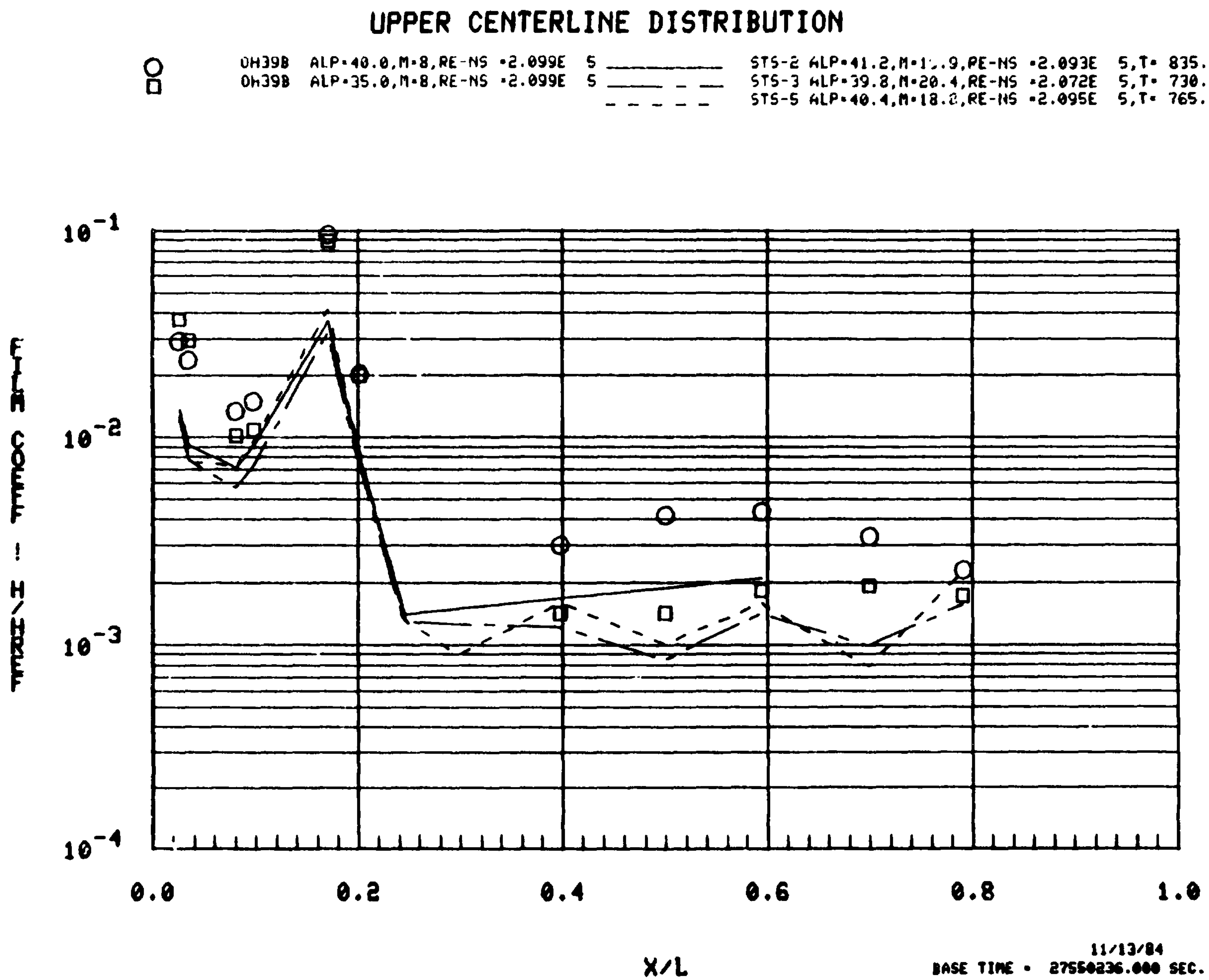
UPPER CENTERLINE DISTRIBUTION
OH39B ALP=40.0,M=8,RE-NS =2.099E 5
OH39B ALP=35.0,M=8,RE-NS =2.099E 5
STS-2 ALP=41.2
STS-3 ALP=39.8,M=20.4,RE-NS =2.072E 5,T= 730.
STS-5 ALP=40.4,RE-NS =2.095E 5,T= 765.
10^{-1}
10^{-2}
10^{-3}
10^{-4}
FILM COEFF ! H/HREF
0.0
0.2
0.4
0.6
0.8
1.0
X/L
11/13/84
BASE TIME = 27550236.000 SEC.

UPPER CENTERLINE DISTRIBUTION

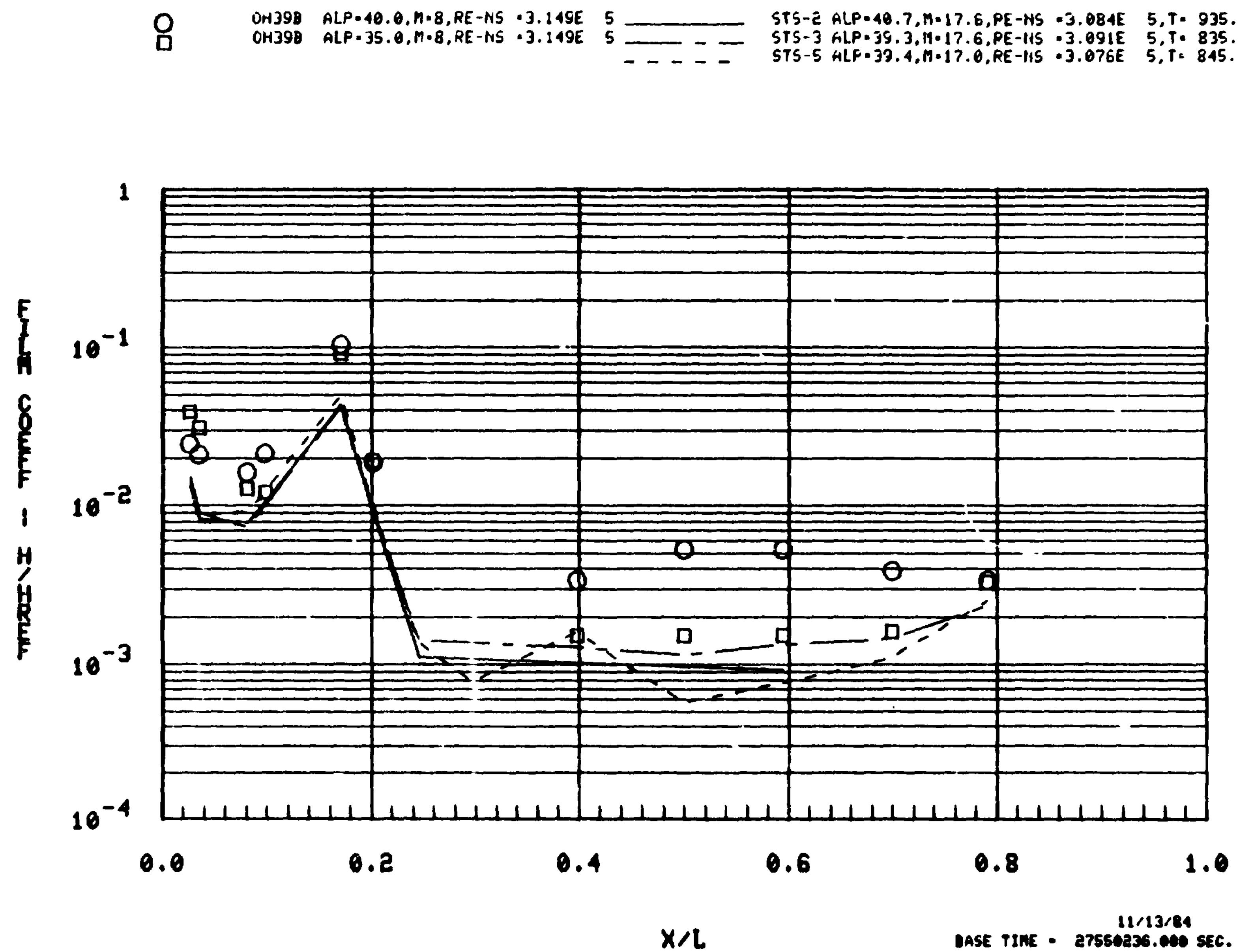

UPPER CENTERLINE DISTRIBUTION

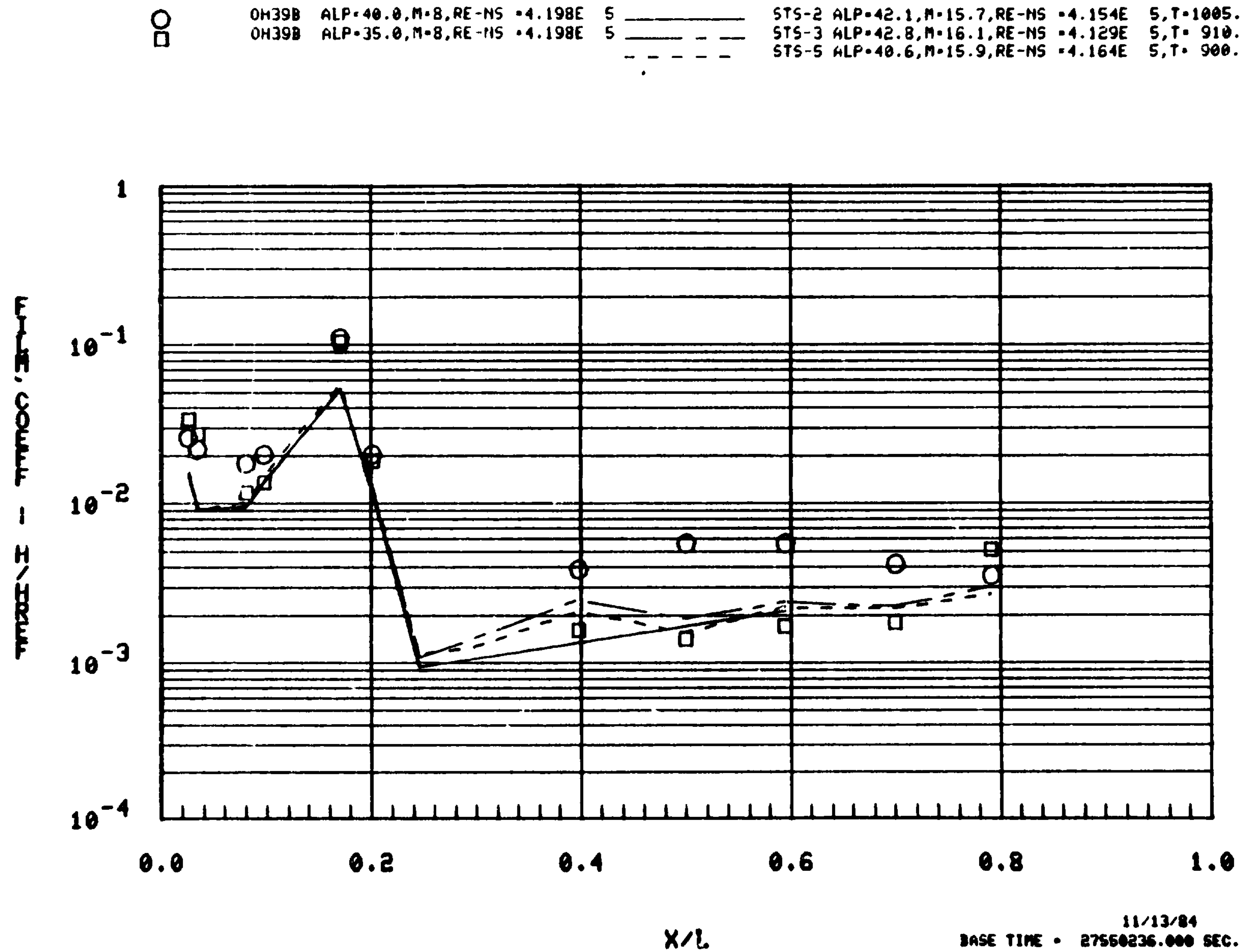

UPPER CENTERLINE DISTRIBUTION

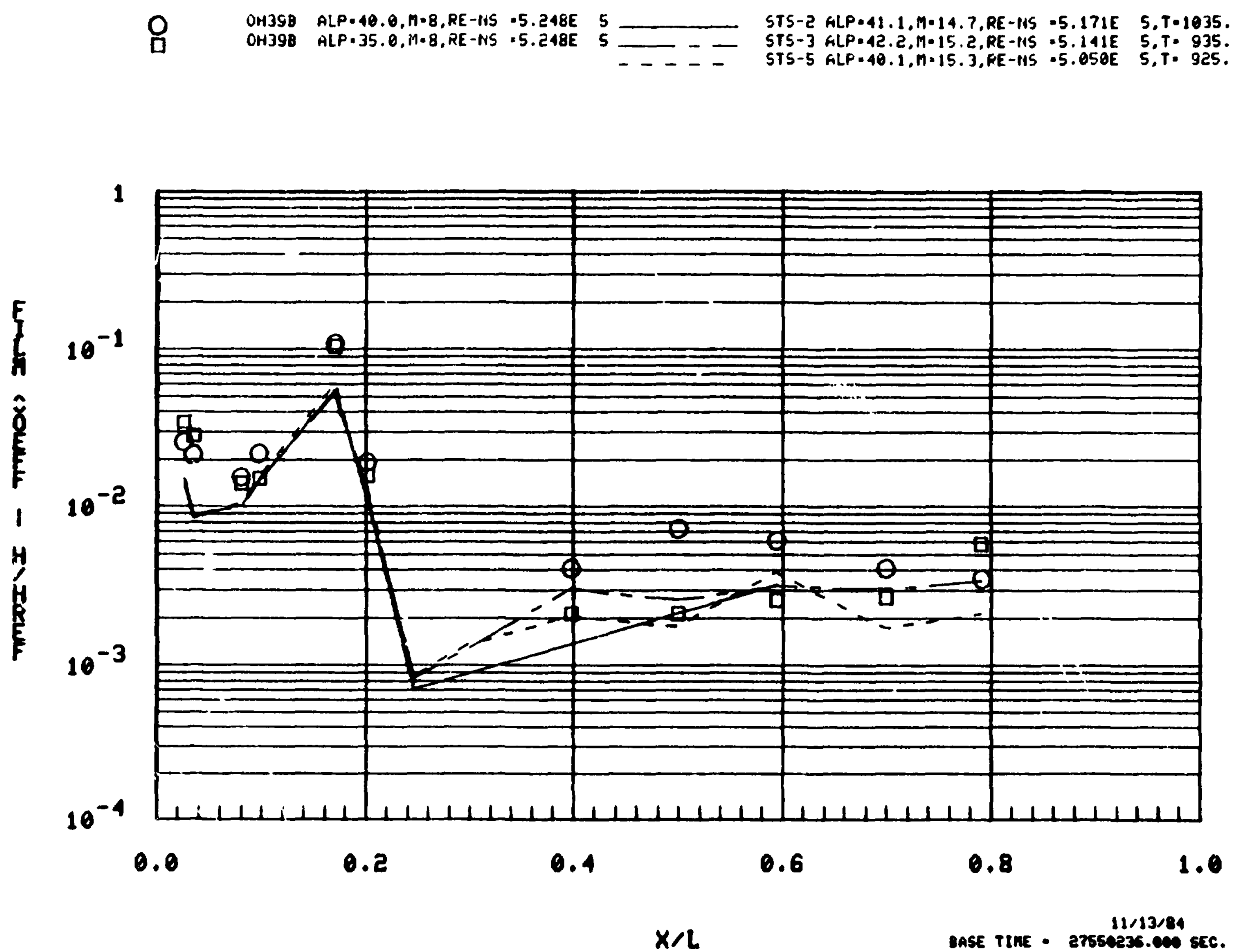

11/13/84
BASE TIME = 27550236.000 SEC.

UPPER CENTERLINE DISTRIBUTION

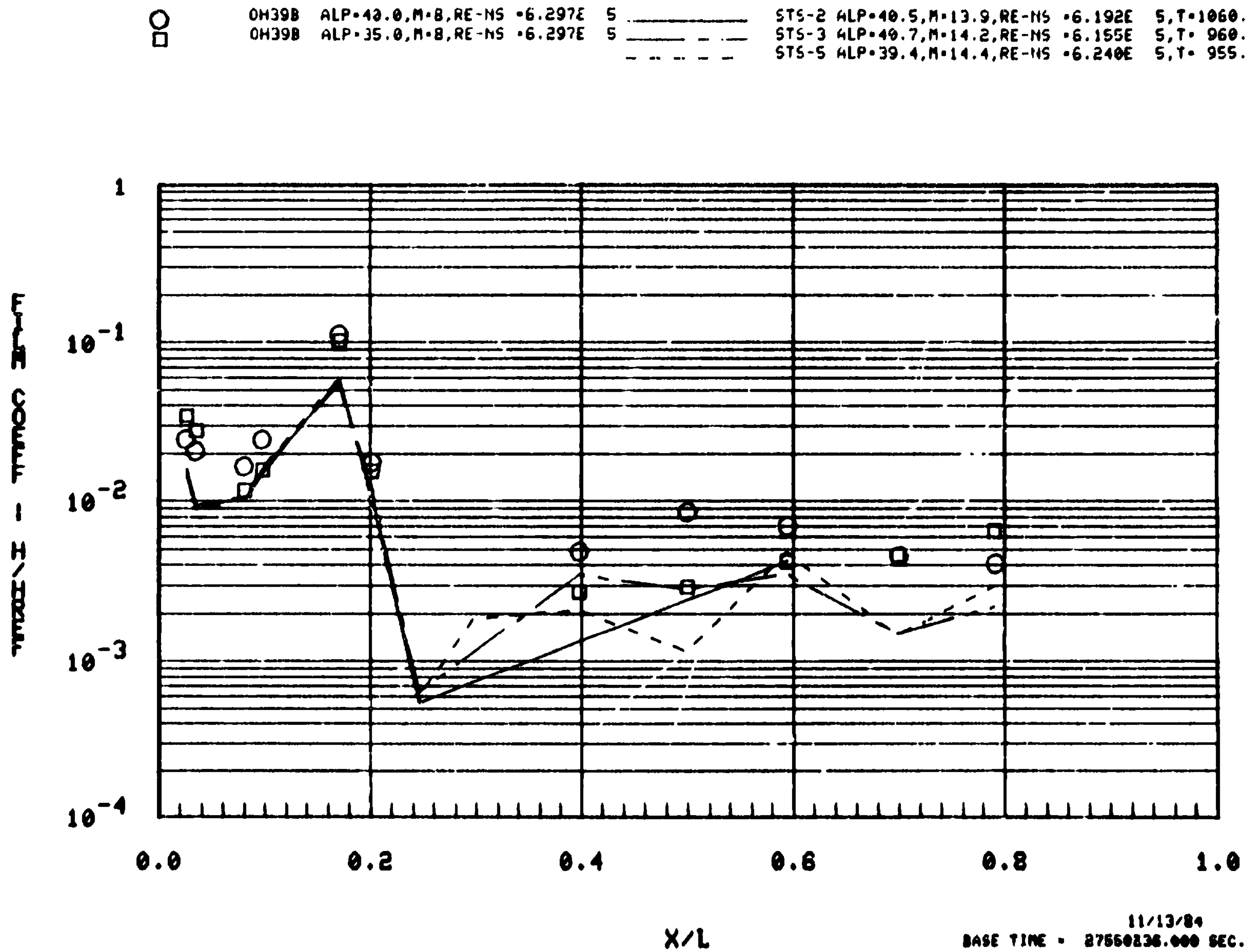

UPPER CENTERLINE DISTRIBUTION

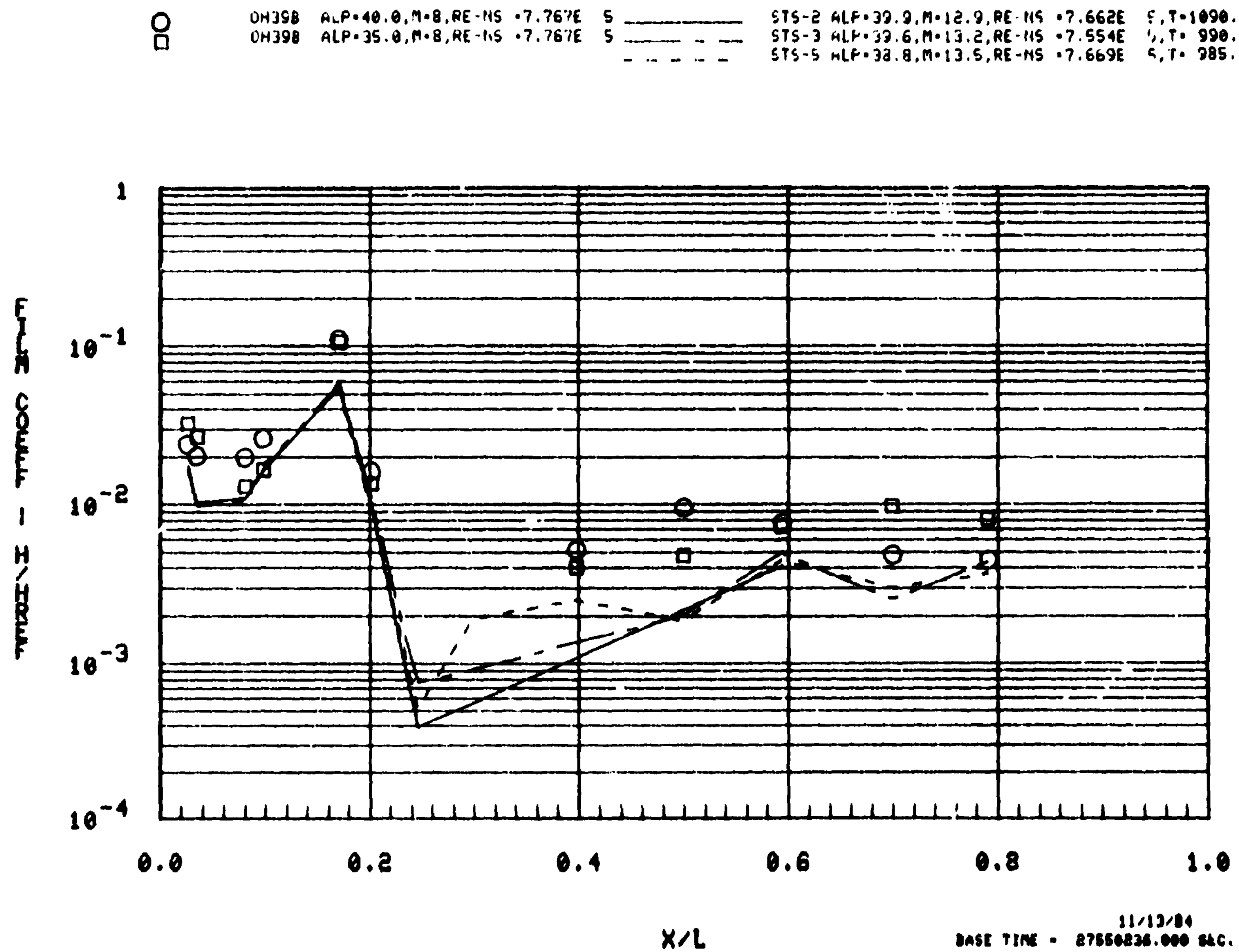

11/13/84
BASE TIME = 87550236.000 SEC.

OMS POD TRACE 3 DISTRIBUTION

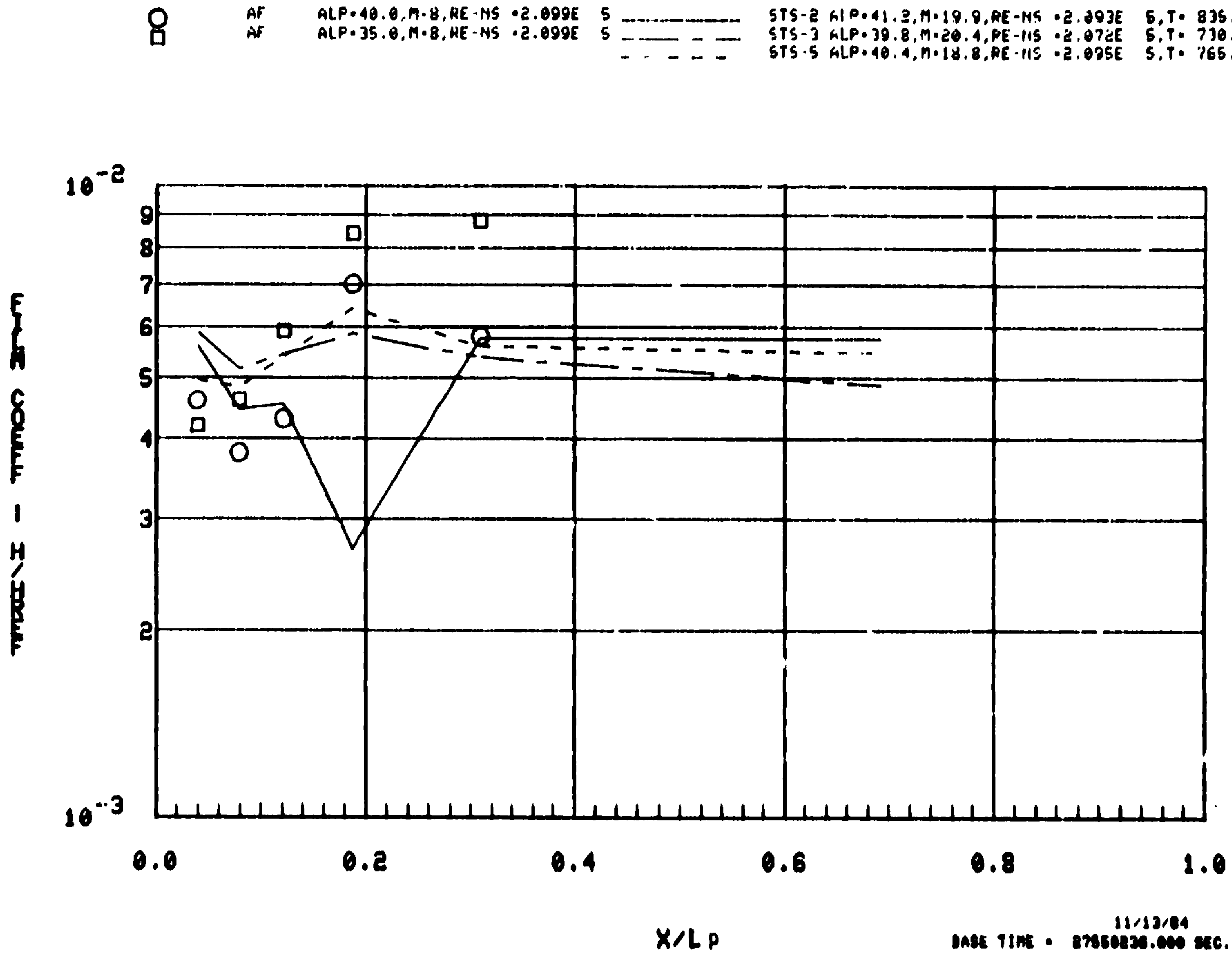

OMS POD TRACE 3 DISTRIBUTION

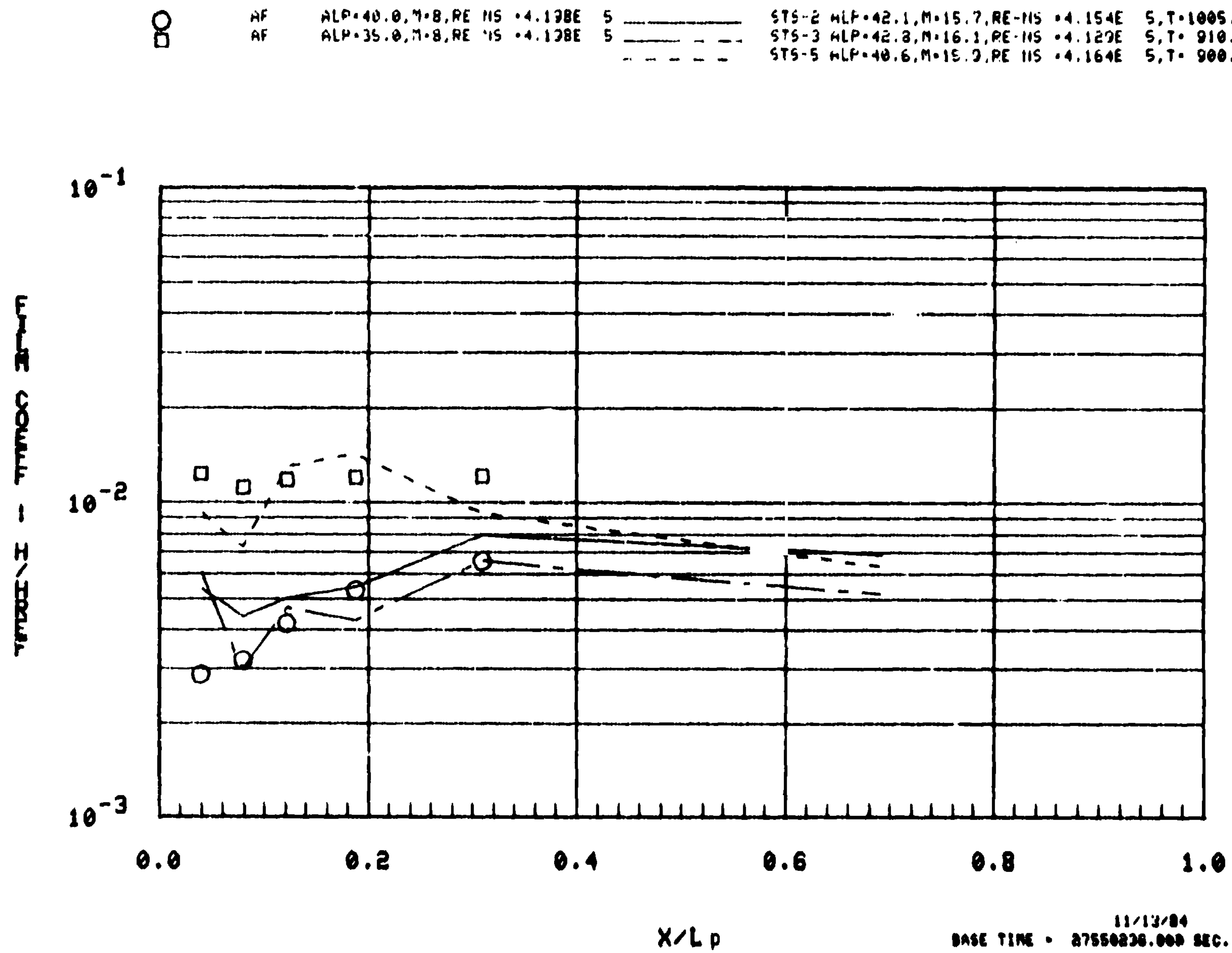

OMS POD TRACE 3 DISTRIBUTION

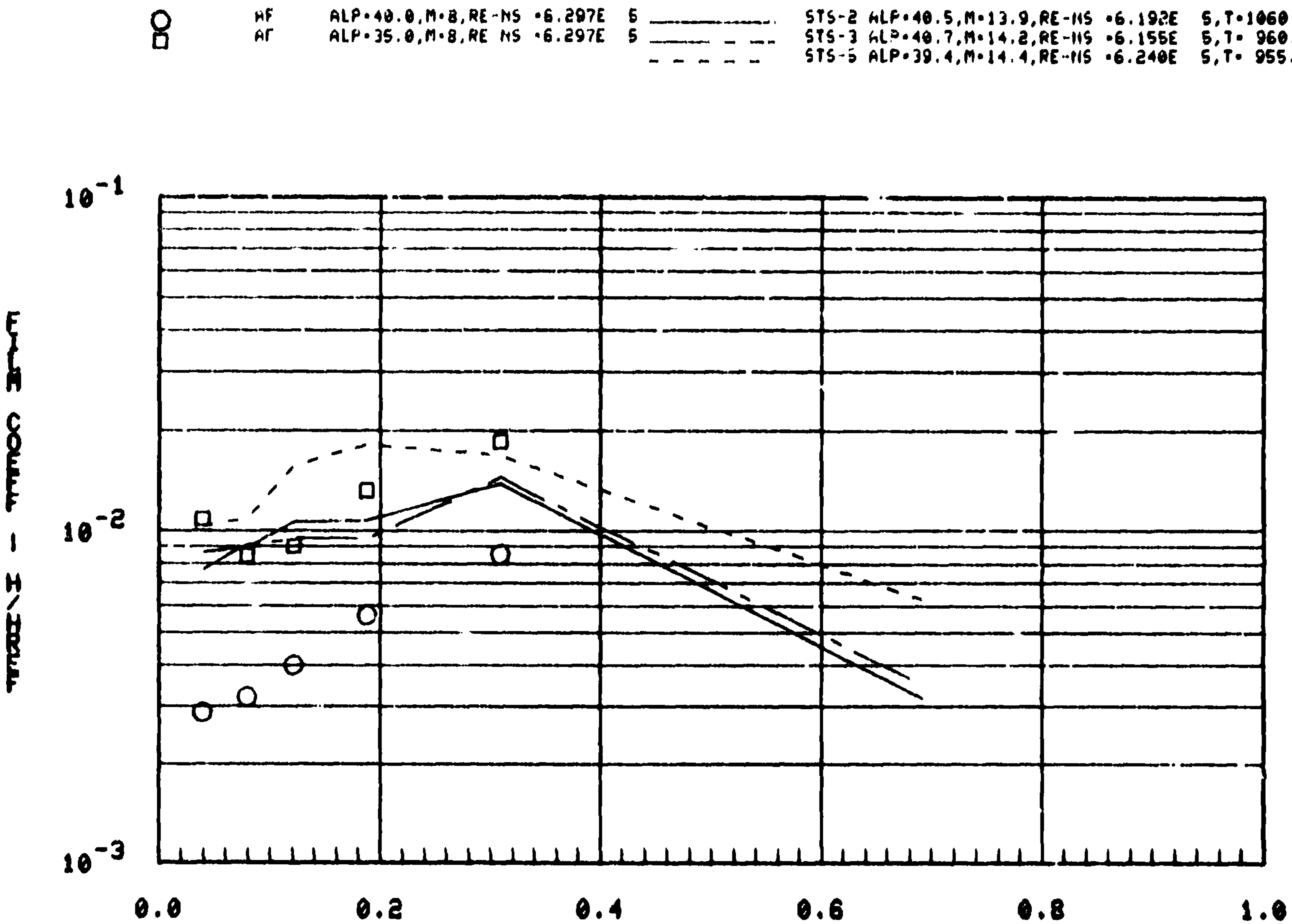

11/13/84
BASE TIME = 27550236.000 SEC.

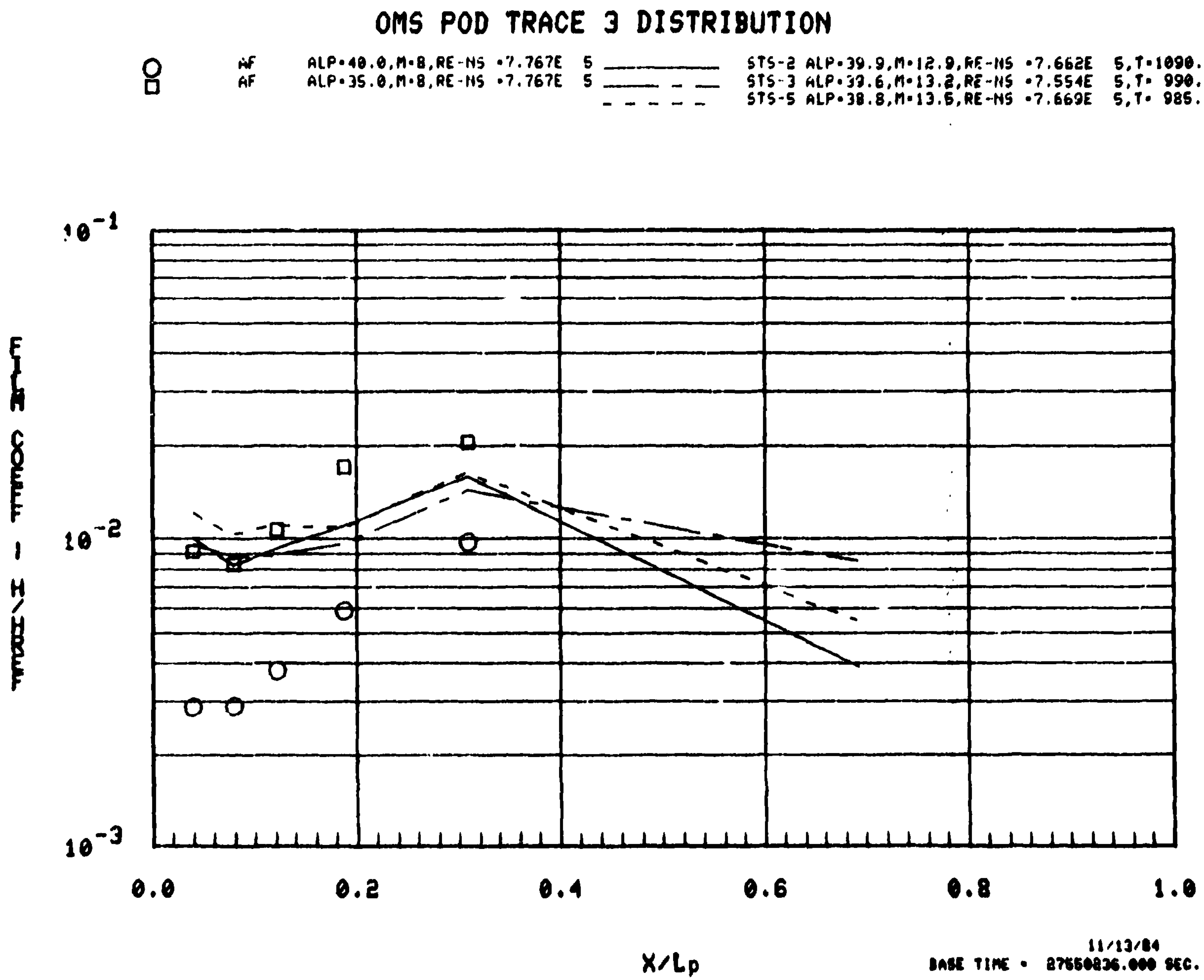

OMS POD TRACE 3 DISTRIBUTION
AF ALP=40.0,M=8,RE-NS =7.767E 5
AF ALP=35.0,M=8,RE-NS =7.767E 5
STS-2 ALP=39.9,M=12.9,RE-NS =7.662E 5,T=1090.
STS-3 ALP=39.6,M=13.2,RE-NS =7.554E 5,T= 990.
STS-5 ALP=38.8,M=13.5,RE-NS =7.669E 5,T= 985.
FILM COEFF : H/HREF
X/Lp
11/13/84
BASE TIME = 27550836.000 SEC.

APPENDIX D

HEATING RATE COMPARISON -

INFLUENCE OF ANGLE OF ATTACK

(CONSTANT REYNOLDS NUMBERS) INDIVIDUAL FLIGHTS

STS-2 LOWER CENTERLINE DISTRIBUTION

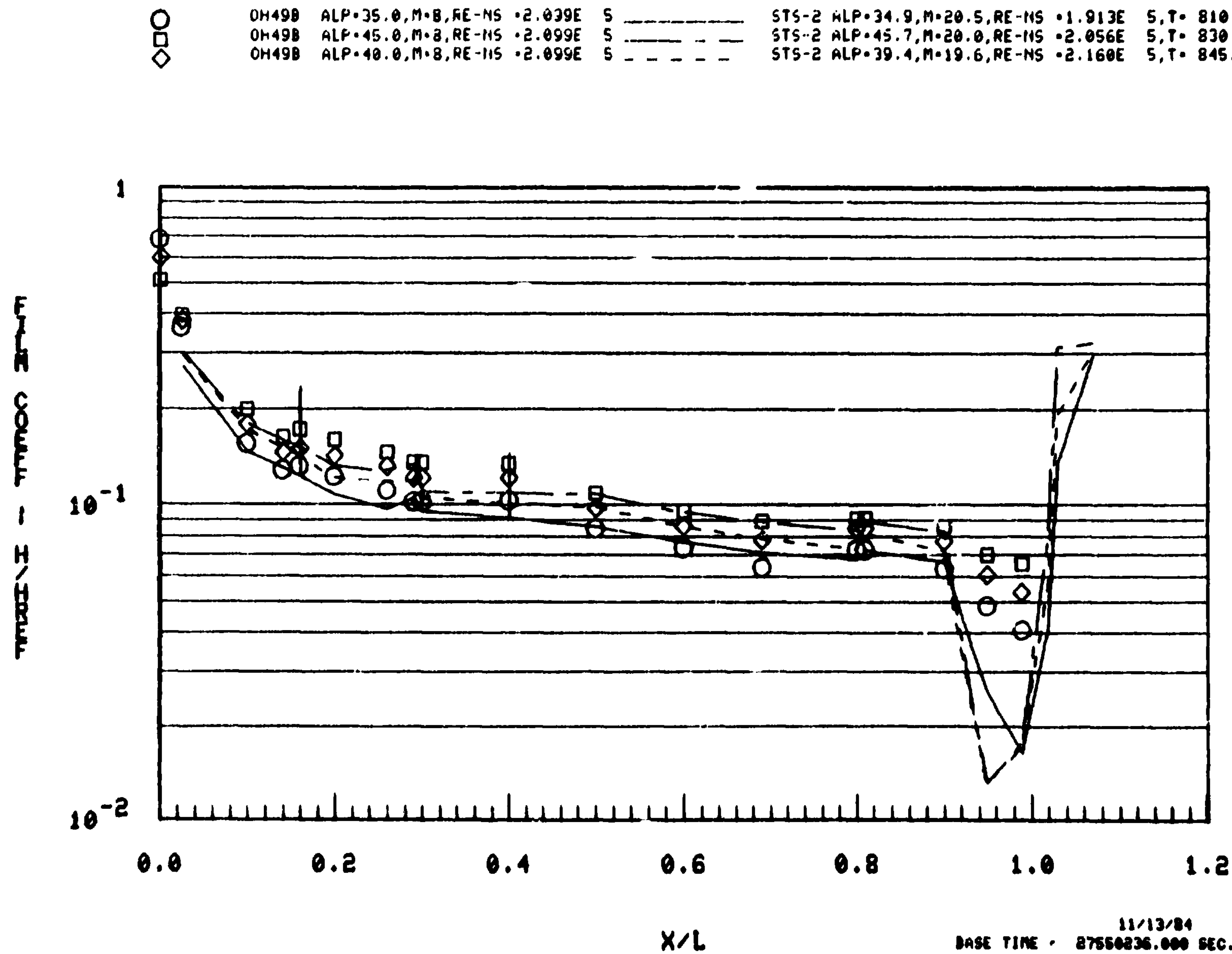

STS-5 LOWER CENTERLINE DISTRIBUTION

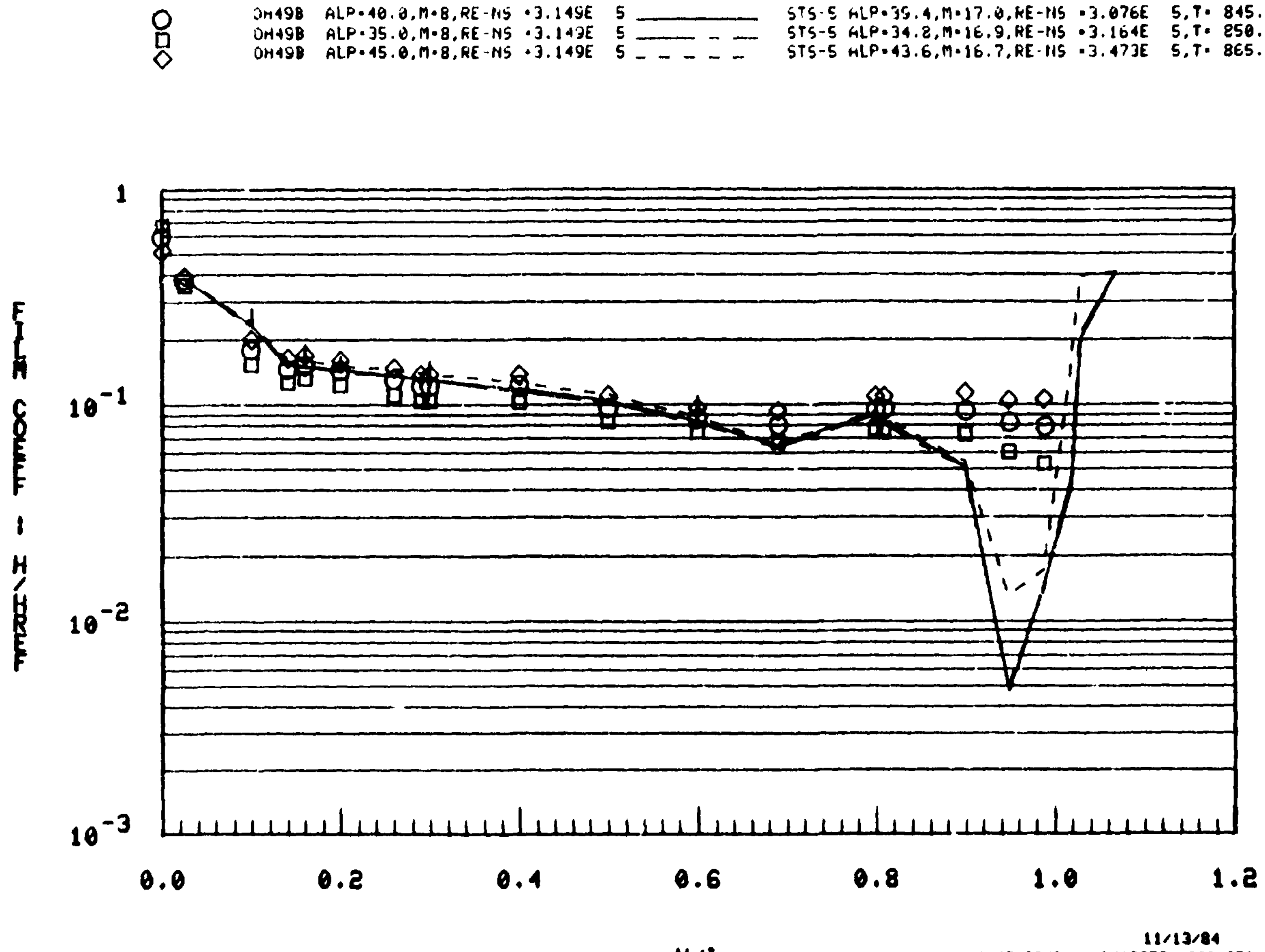

11/13/84
BASE TIME = 27698591.000 SEC.

STS-3 LOWER CENTERLINE DISTRIBUTION

○ OH49B ALP=40.0,M=8,RE-NS =4.198E 5 ——— STS-3 ALP=40.4,M=16.7,RE-NS =3.933E 5,T= 890.
□ OH49B ALP=45.0,M=8,RE-NS =4.198E 5 — — — STS-3 ALP=43.3,M=15.8,RE-NS =4.492E 5,T= 920.

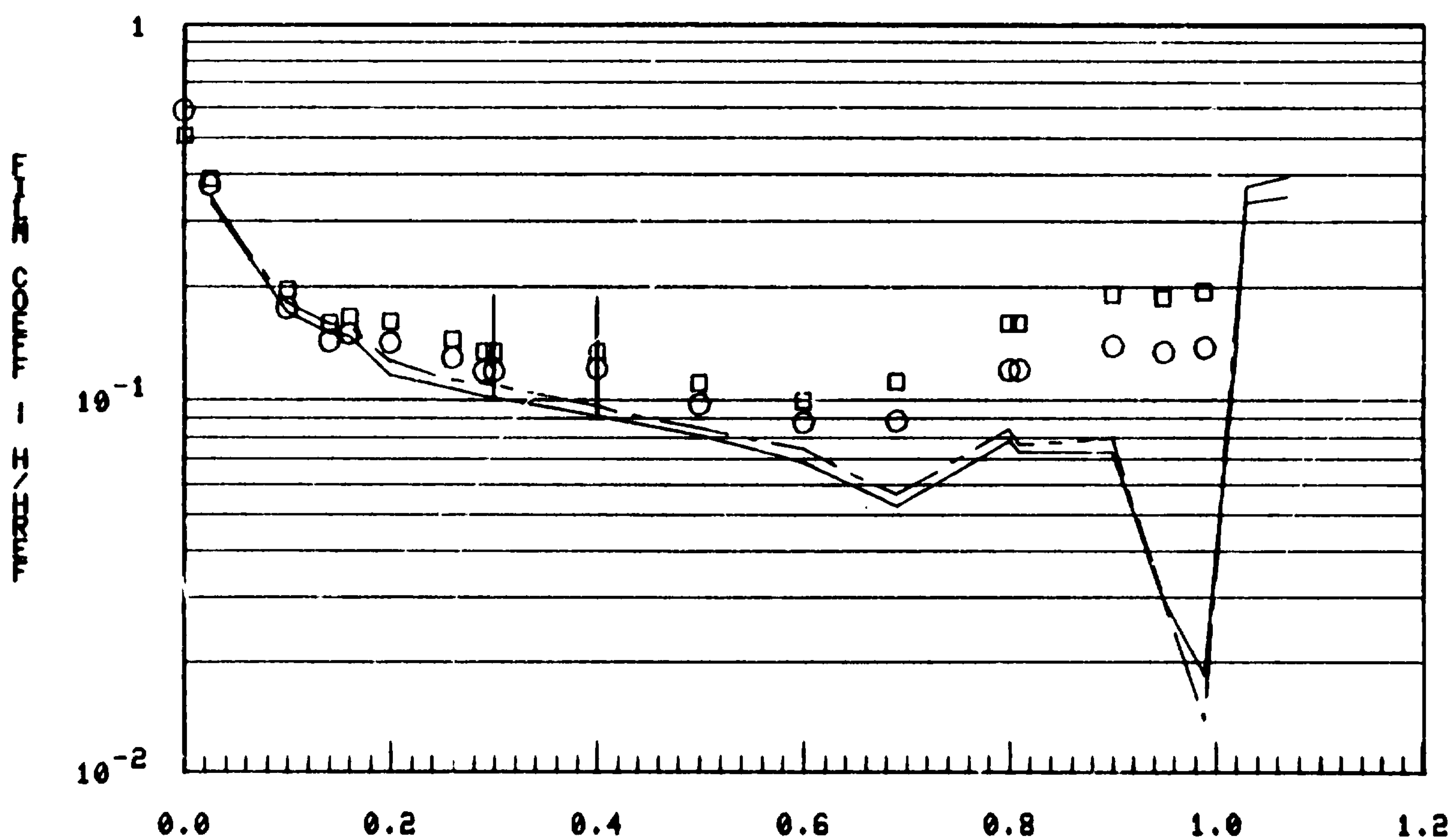

11/13/84
BASE TIME = 07745684.000 SEC.

STS-4 LOWER CENTERLINE DISTRIBUTION

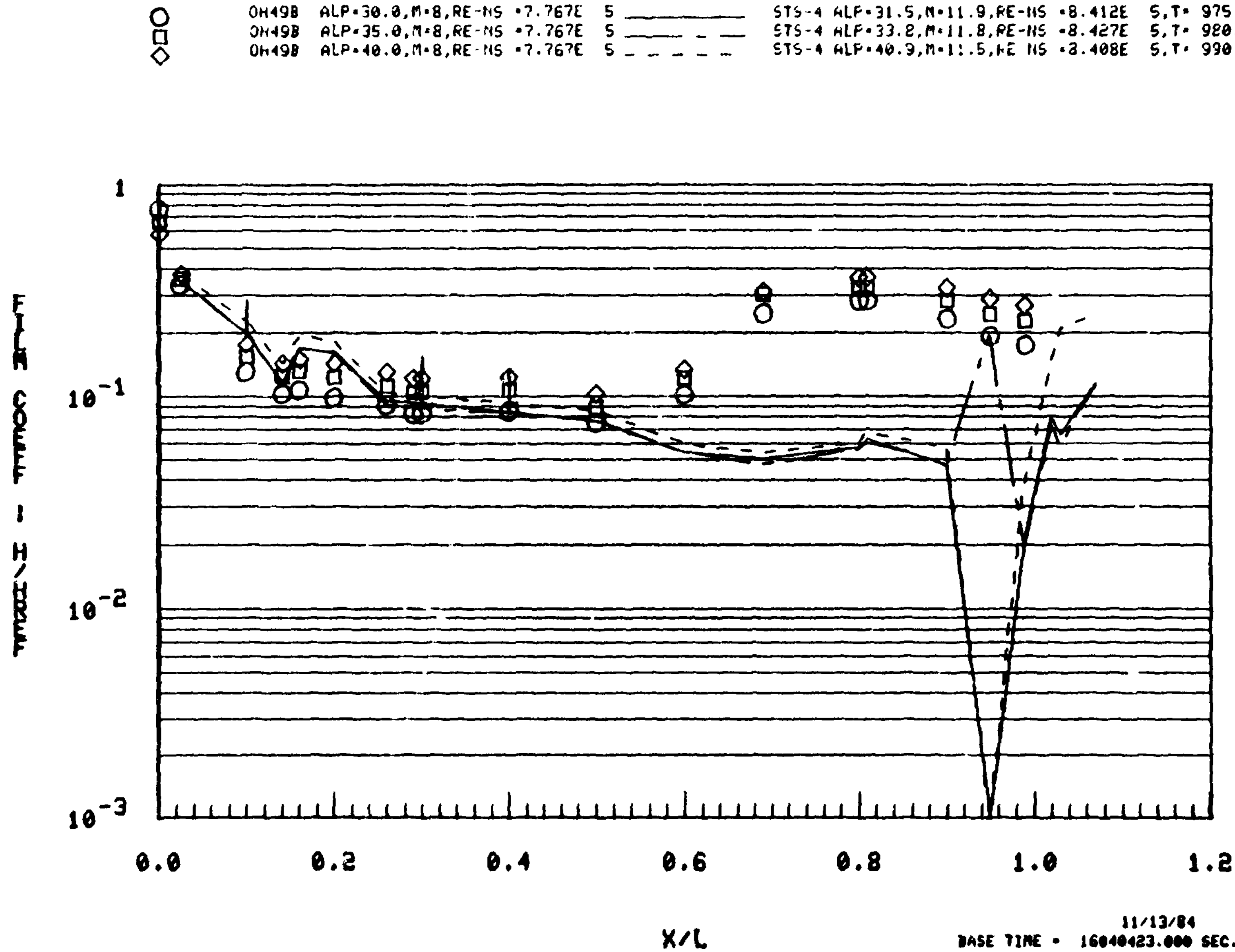

11/13/84
BASE TIME = 16040423.000 SEC.

STS-4 LOWER CENTERLINE DISTRIBUTION

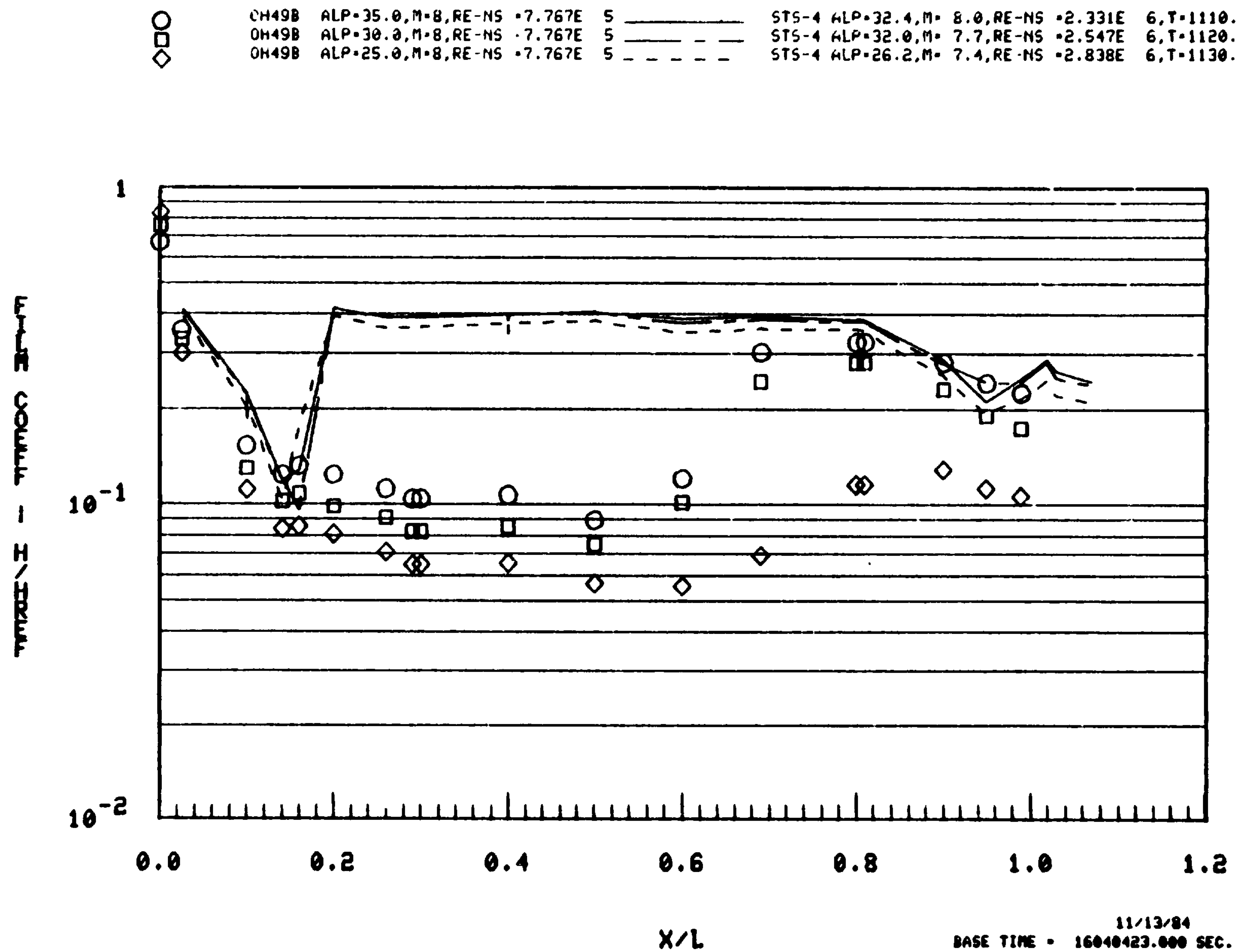

11/13/84
BASE TIME = 16040423.000 SEC.

STS-2 WING 50% SEMI-SPAN DISTRIBUTION

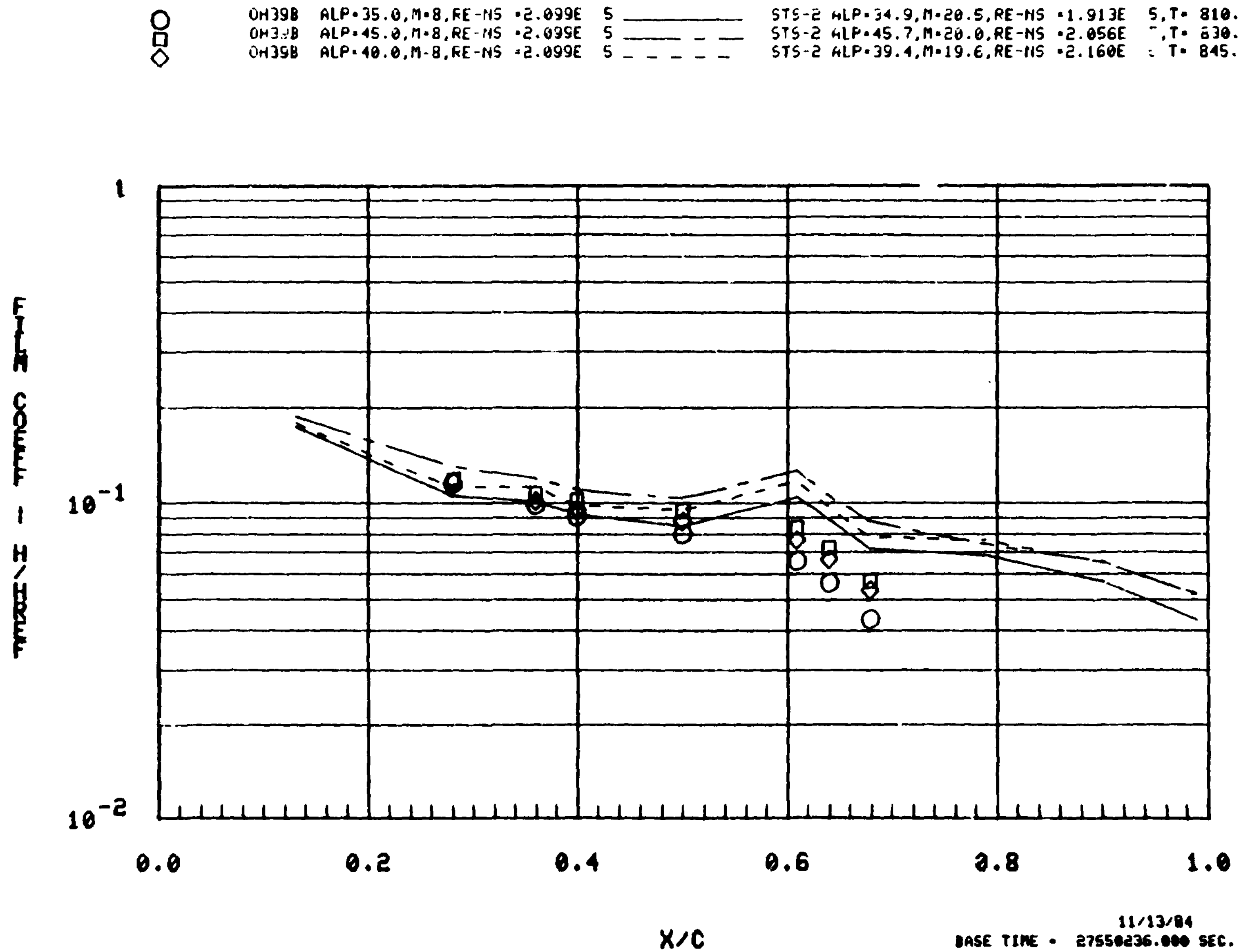

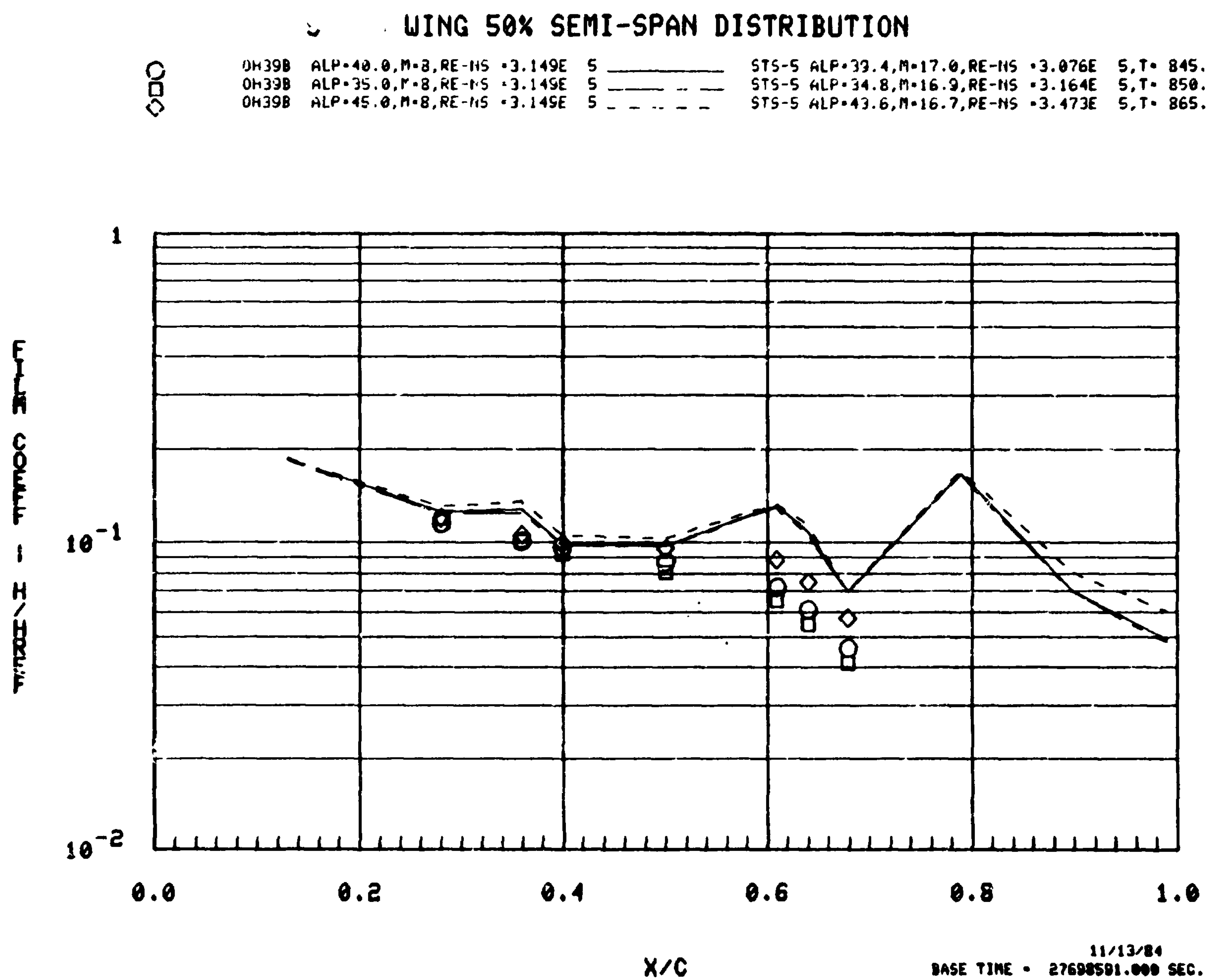

WING 50% SEMI-SPAN DISTRIBUTION
OH39B ALP=40.0,M=8,RE-NS =3.149E 5 STS-5 ALP=39.4,M=17.0,RE-NS =3.076E 5,T= 845.
OH39B ALP=35.0,M=8,RE-NS =3.149E 5 STS-5 ALP=34.8,M=16.9,RE-NS =3.164E 5,T= 850.
OH39B ALP=45.0,M=8,RE-NS =3.149E 5 STS-5 ALP=43.6,M=16.7,RE-NS =3.473E 5,T= 865.
FILM COEFF : H/HREF
1
10^-1
10^-2
0.0
0.2
0.4
0.6
0.8
1.0
X/C
11/13/84
BASE TIME = 27698591.000 SEC.

STTS-3 WING 50% SEMI-SPAN DISTRIBUTIC

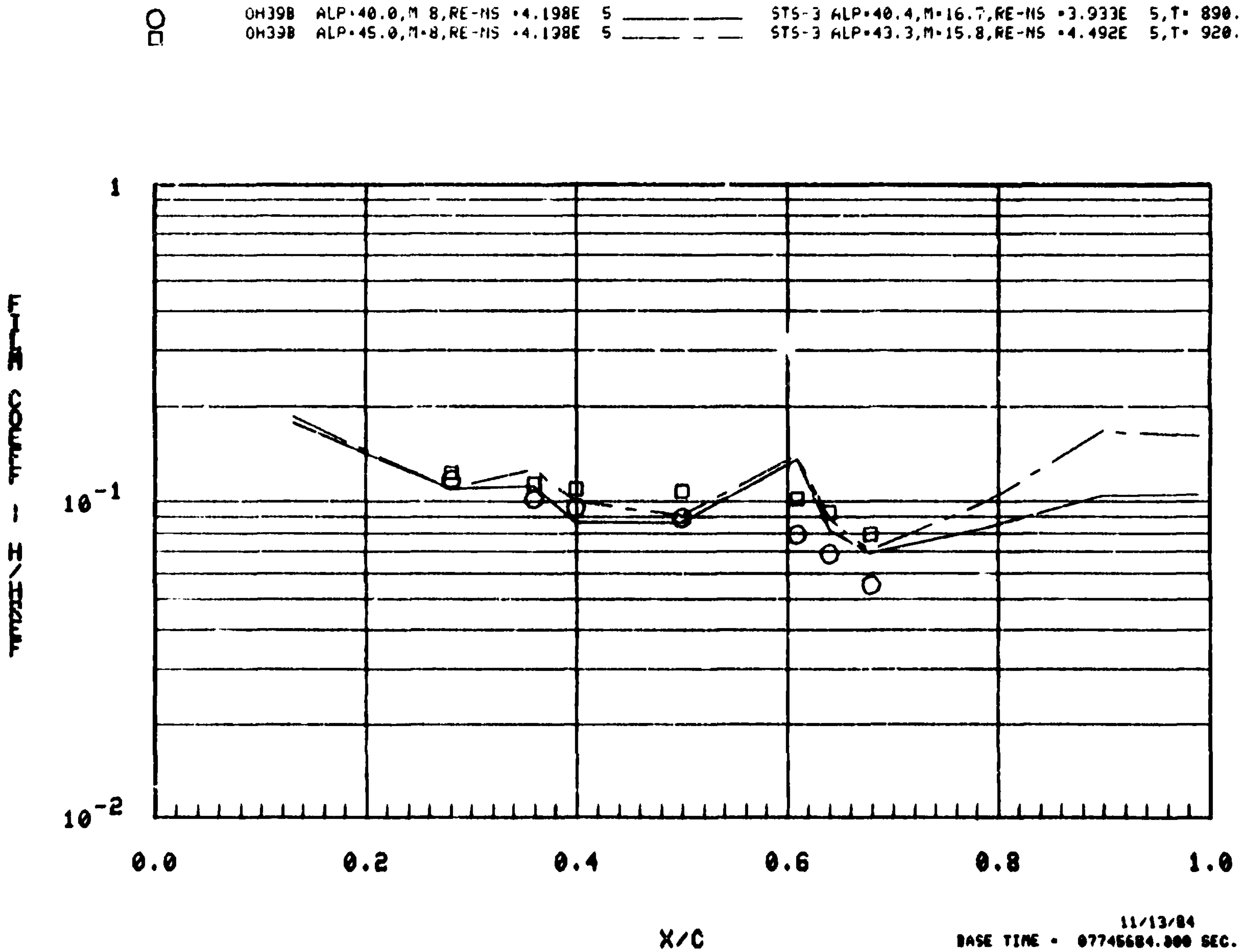

STS-4 WING 50% SEMI-SPAN DISTRIBUTION

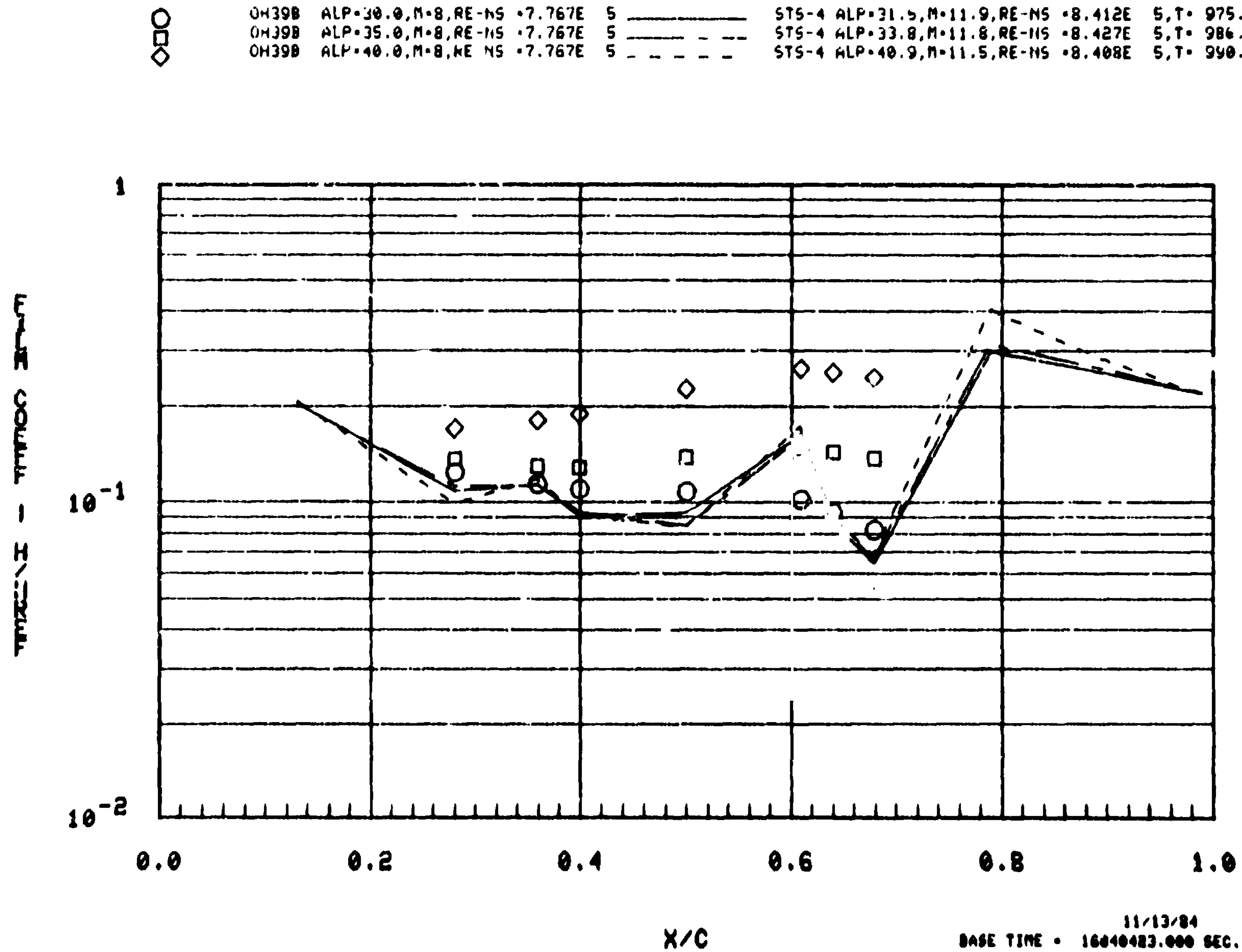

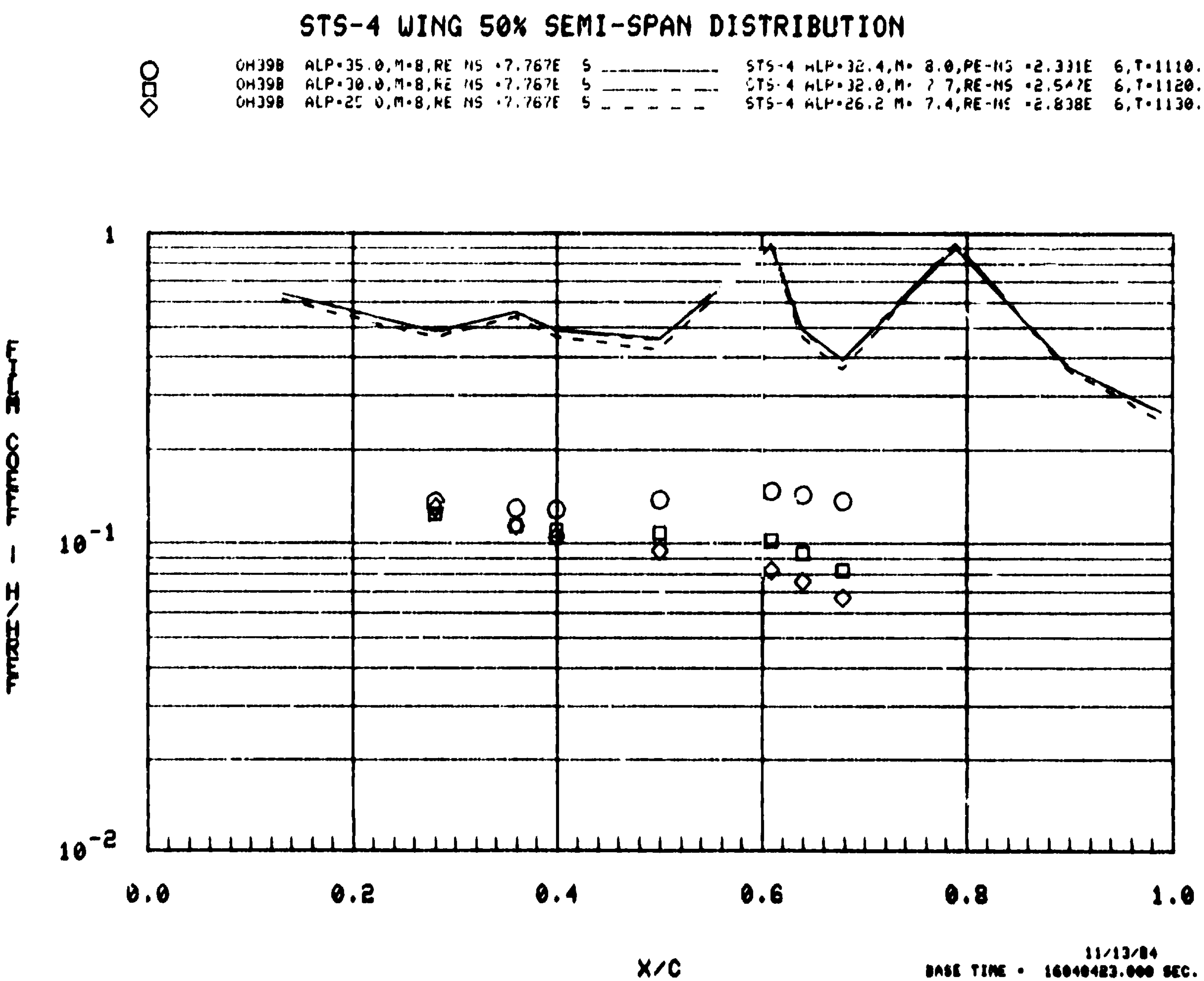

STS-4 WING 50% SEMI-SPAN DISTRIBUTION
OH39B ALP=35.0,M=8,RE NS =7.767E 5
OH39B ALP=30.0,M=8,RE NS =7.767E 5
OH39B ALP=25.0,M=8,RE NS =7.767E 5
STS-4 ALP=32.4,M= 8.0,RE-NS =2.331E 6,T=1110.
STS-4 ALP=32.0,M= 7.7,RE-NS =2.547E 6,T=1120.
STS-4 ALP=26.2 M= 7.4,RE-NS =2.838E 6,T=1130.
1
10^{-1}
10^{-2}
FILM COEFF - H/HREF
0.0
0.2
0.4
0.6
0.8
1.0
X/C
11/13/84
BASE TIME = 16040423.000 SEC.

STS-2 WING 80% SEMI-SPAN DISTRIBUTION

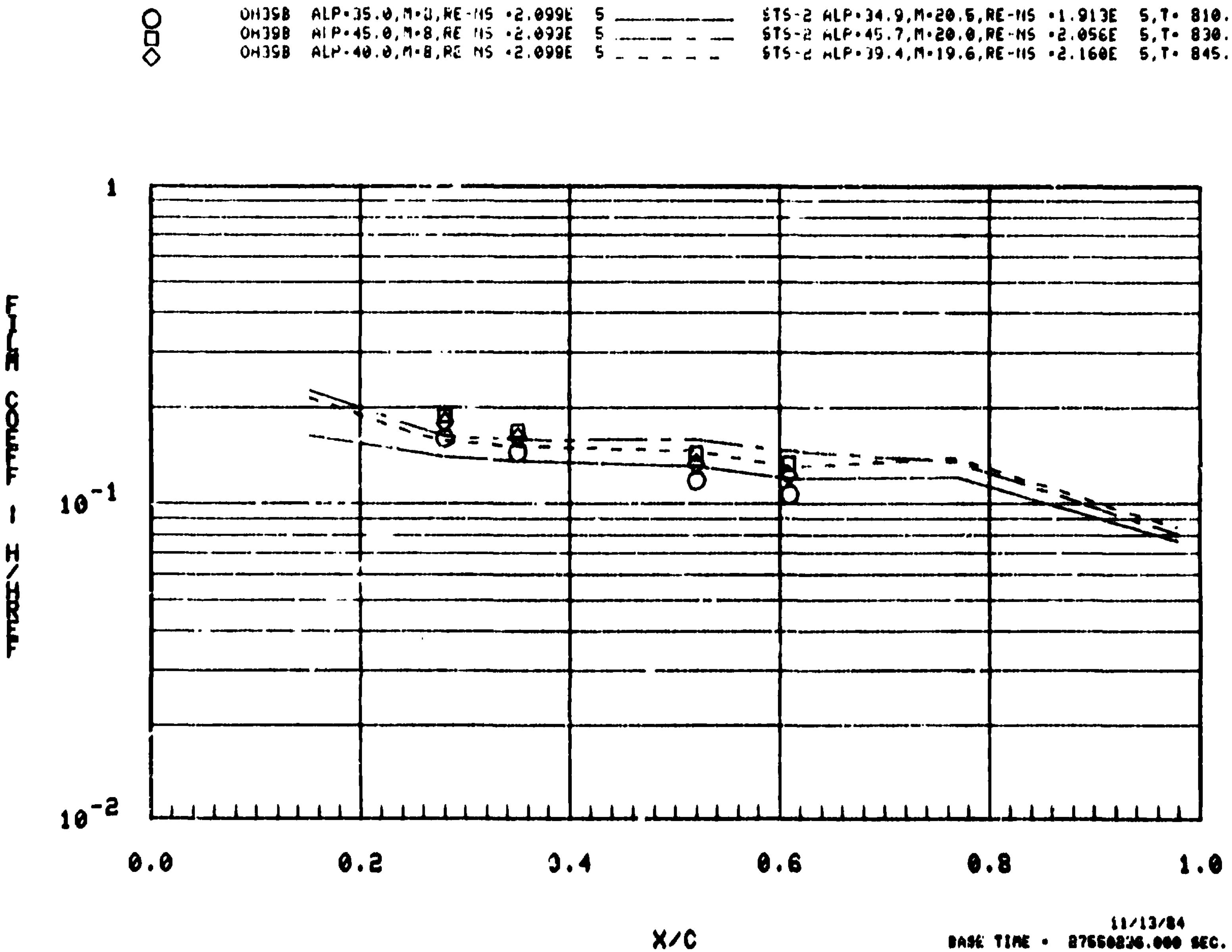

STS-5 WING 80% SEMI-SPAN DISTRIBUTION

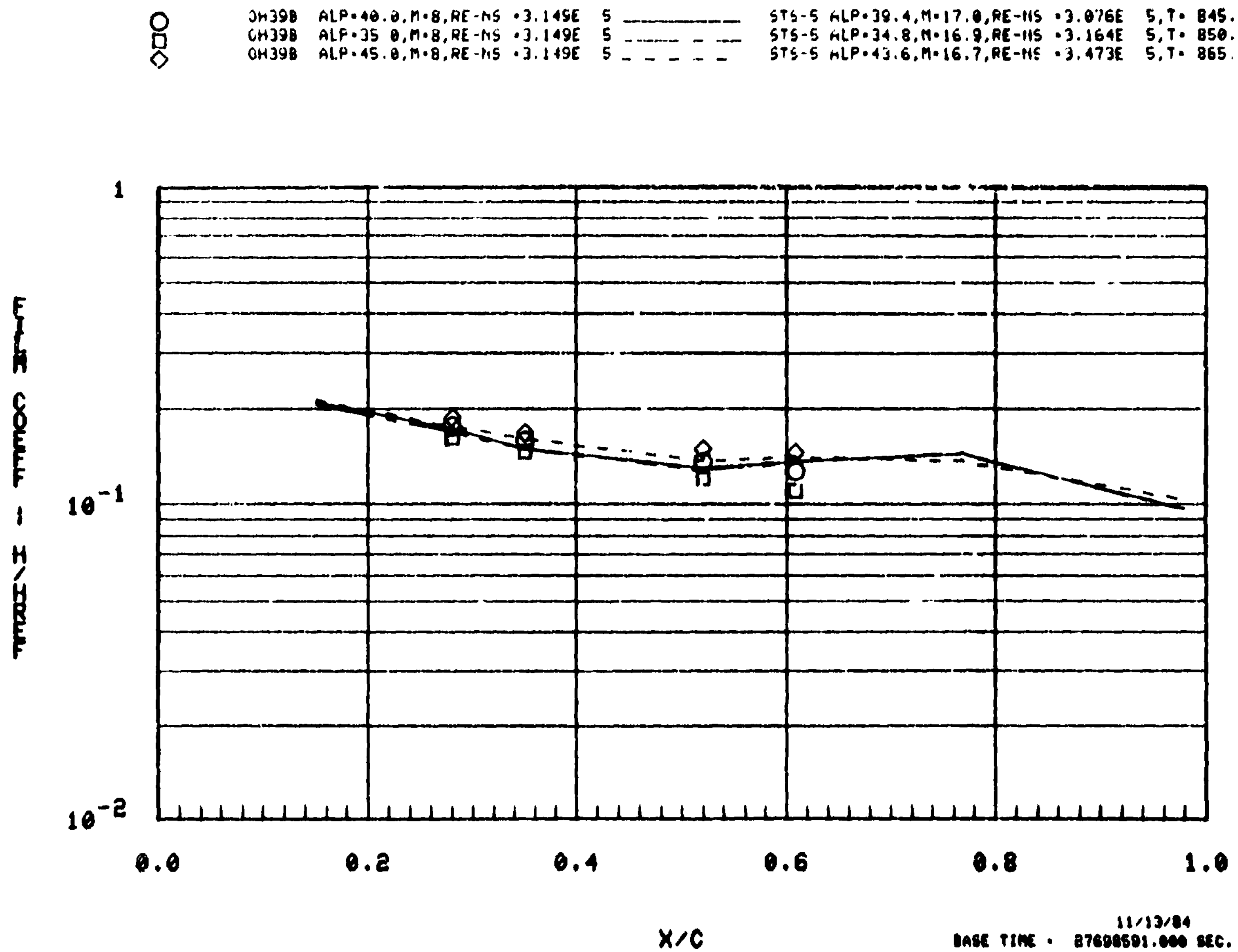

STS-3 WING 80% SEMI-SPAN DISTRIBUTION

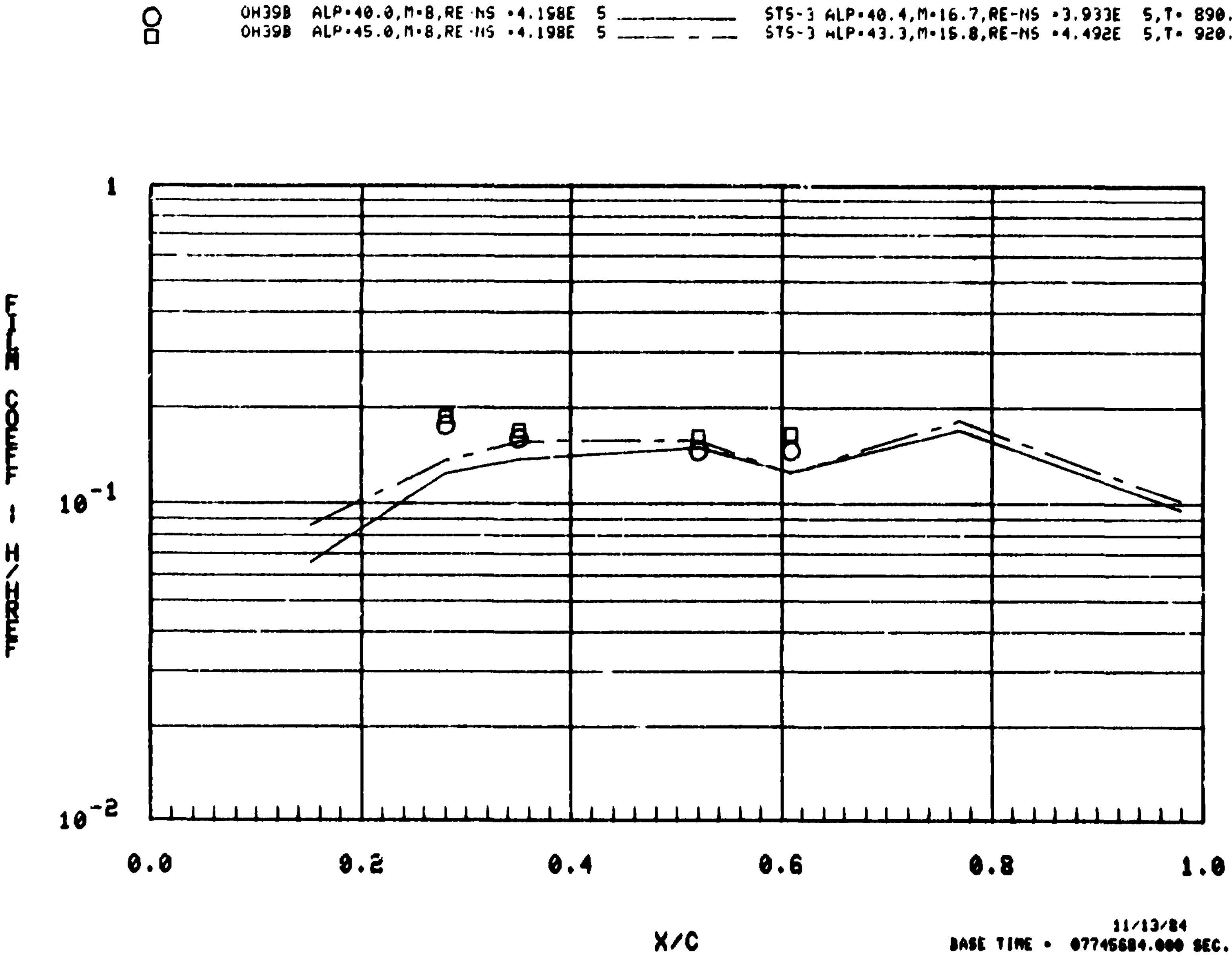

11/13/84
BASE TIME = 07745684.000 SEC.

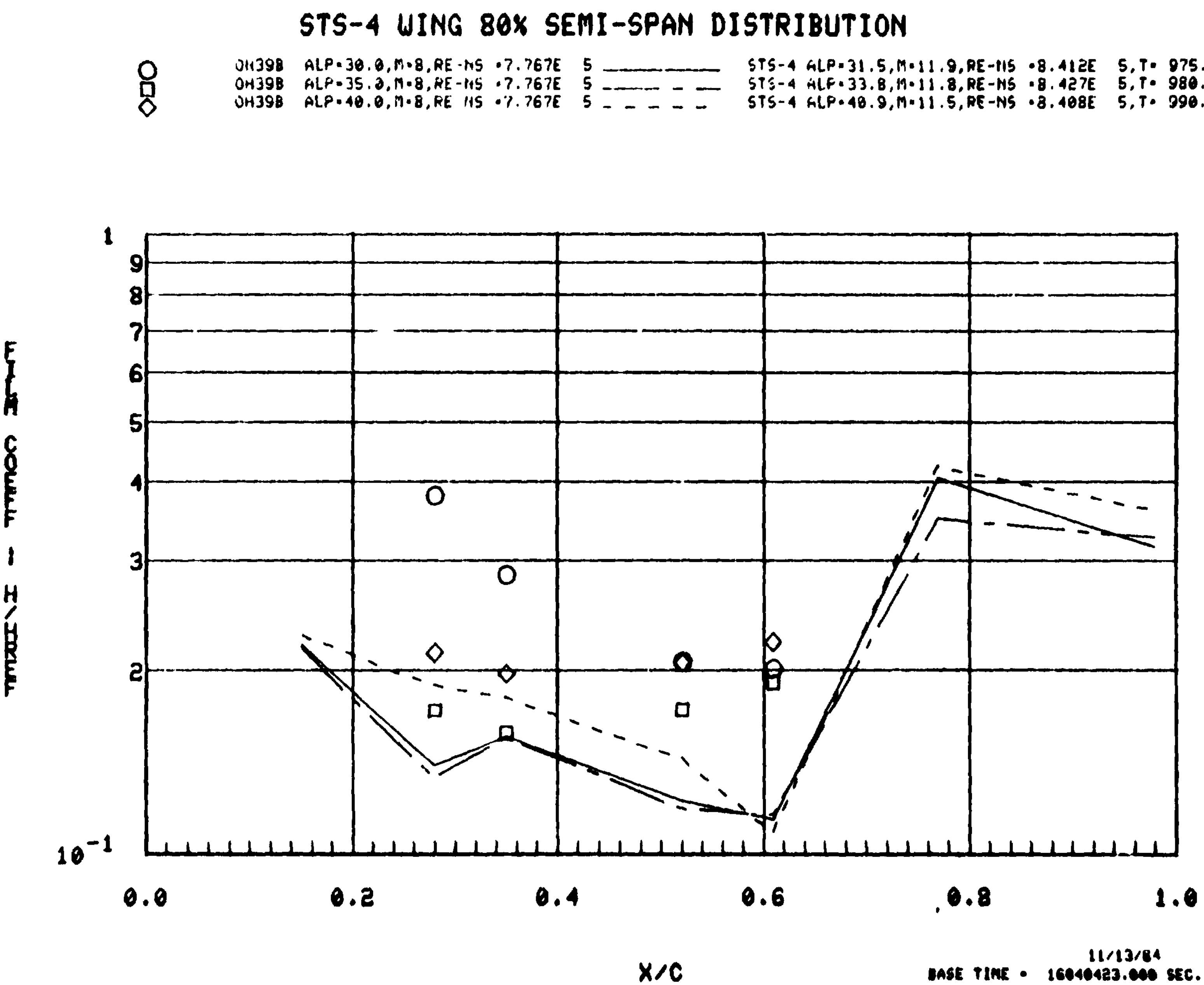
STS-4 WING 80% SEMI-SPAN DISTRIBUTION
OH39B ALP=30.0,M=8,RE-NS =7.767E 5
OH39B ALP=35.0,M=8,RE-NS =7.767E 5
OH39B ALP=40.0,M=8,RE NS =7.767E 5
STS-4 ALP=31.5,M=11.9,RE-NS =8.412E 5,T= 975.
STS-4 ALP=33.8,M=11.8,RE-NS =8.427E 5,T= 980.
STS-4 ALP=40.9,M=11.5,RE-NS =8.408E 5,T= 990.
FILM COEFF : H/HREF
X/C
11/13/84
BASE TIME = 16040423.000 SEC.

STS-4 WING 80% SEMI-SPAN DISTRIBUTION

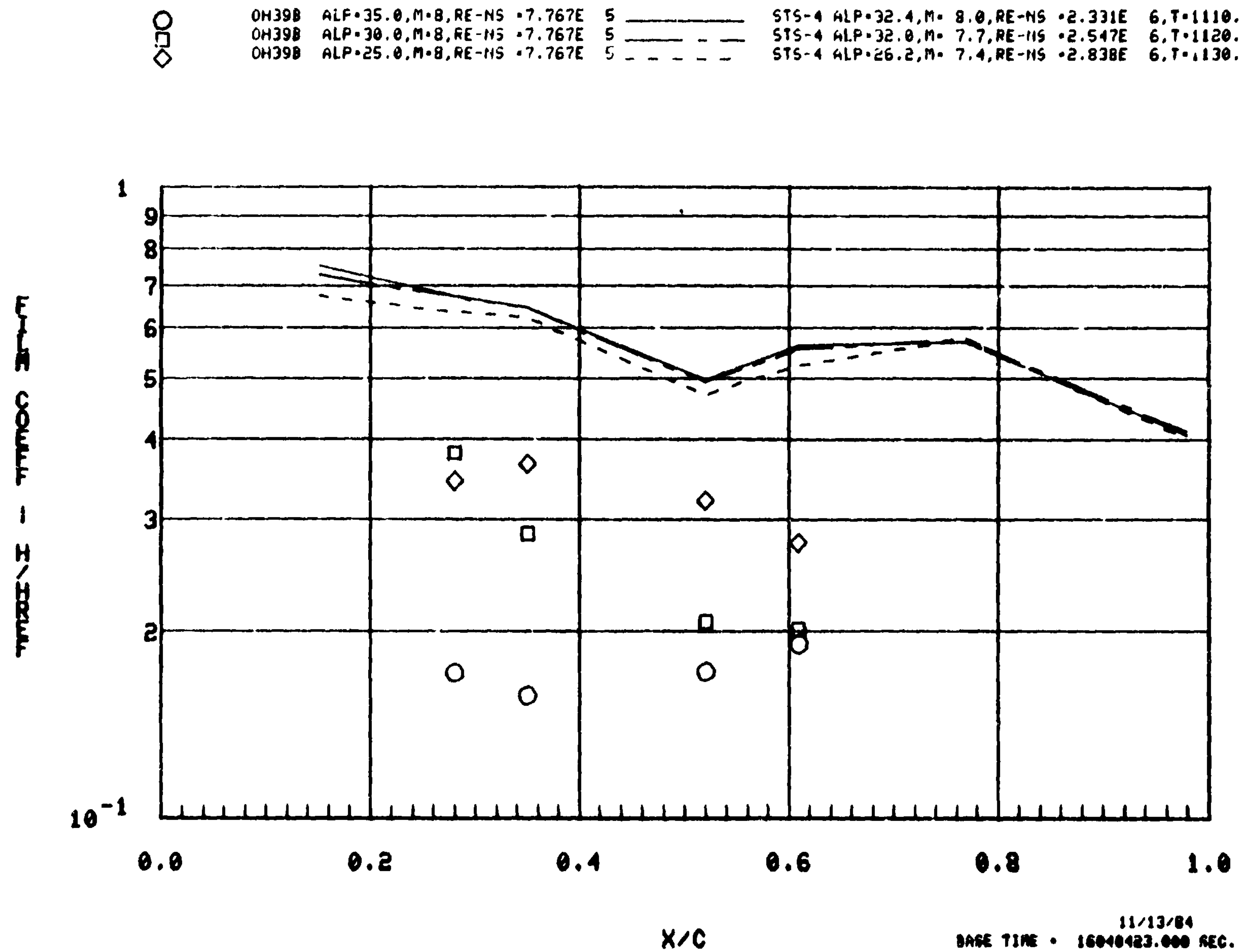

STS-2 SIDE FUSELAGE (Z=400 TRACE) DISTRIBUTION

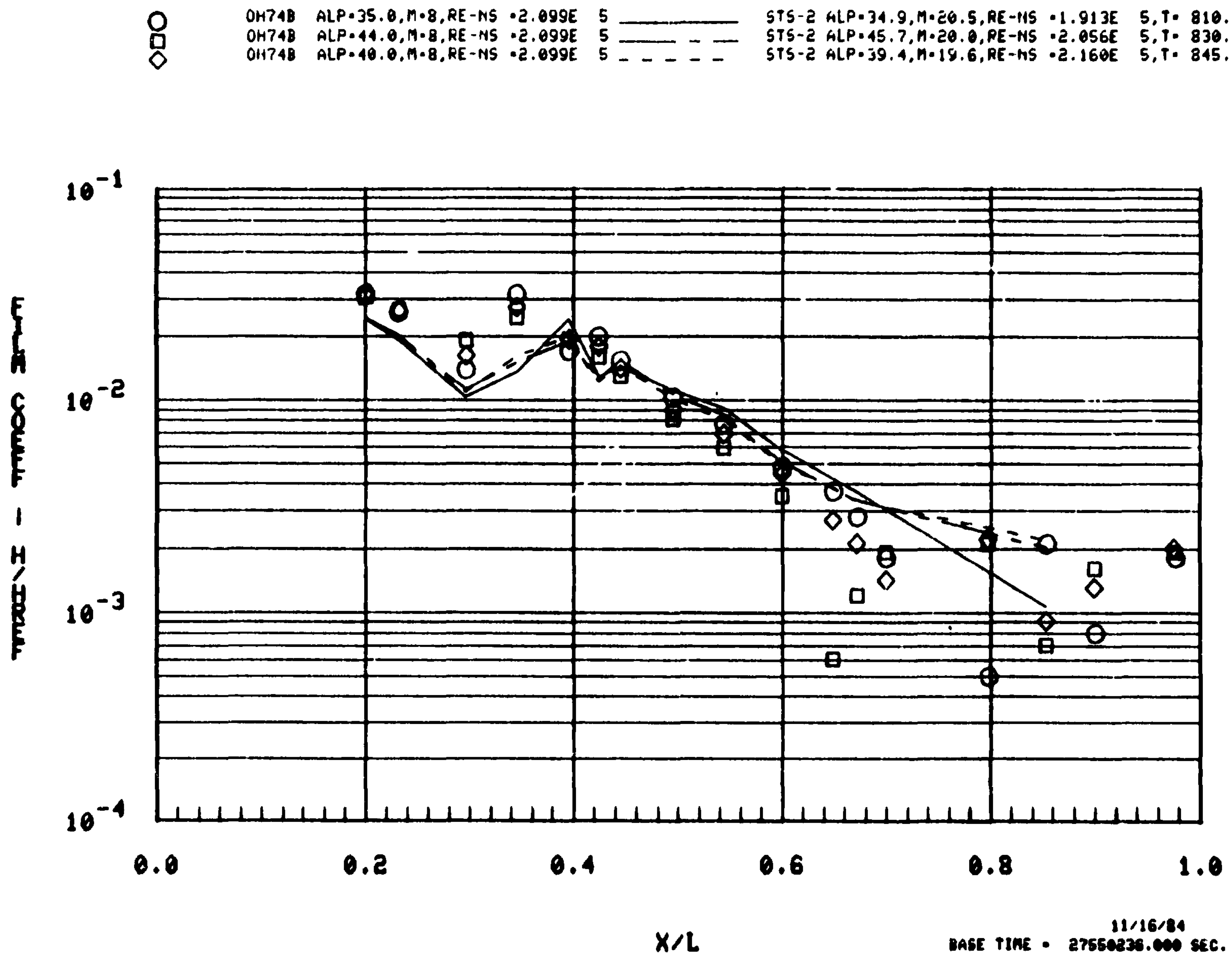

11/16/84
BASE TIME = 27550236.000 SEC.

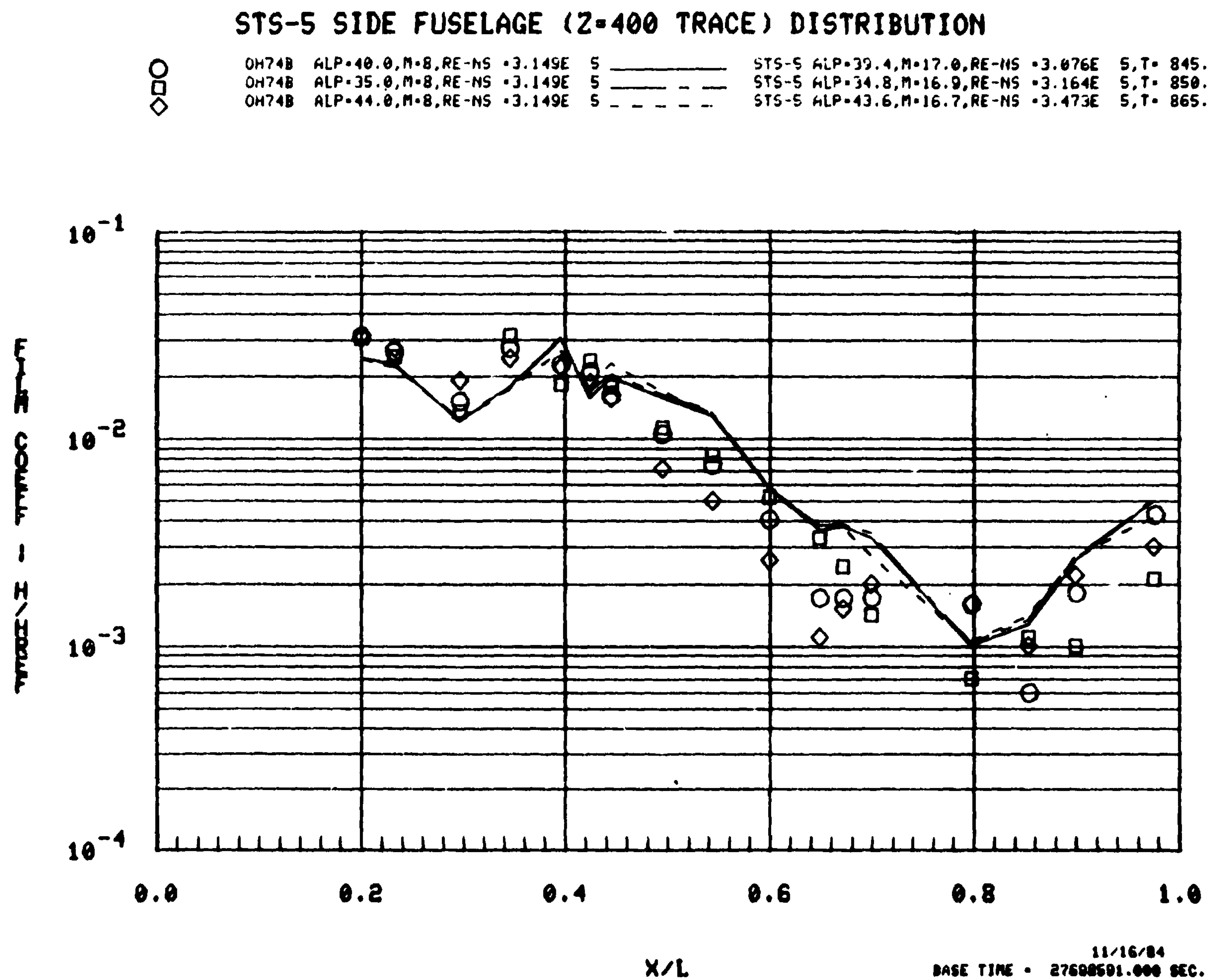

STS-5 SIDE FUSELAGE (Z=400 TRACE) DISTRIBUTION
OH74B ALP=40.0,M=8,RE-NS =3.149E 5
STS-5 ALP=39.4,M=17.0,RE-NS =3.076E 5,T= 845.
OH74B ALP=35.0,M=8,RE-NS =3.149E 5
STS-5 ALP=34.8,M=16.9,RE-NS =3.164E 5,T= 850.
OH74B ALP=44.0,M=8,RE-NS =3.149E 5
STS-5 ALP=43.6,M=16.7,RE-NS =3.473E 5,T= 865.
FILM COEFF = H/HREF
10^{-1}
10^{-2}
10^{-3}
10^{-4}
0.0
0.2
0.4
0.6
0.8
1.0
X/L
11/16/84
BASE TIME = 27608591.000 SEC.

STS-3 SIDE FUSELAGE (Z=400 TRACE) DISTRIBUTION

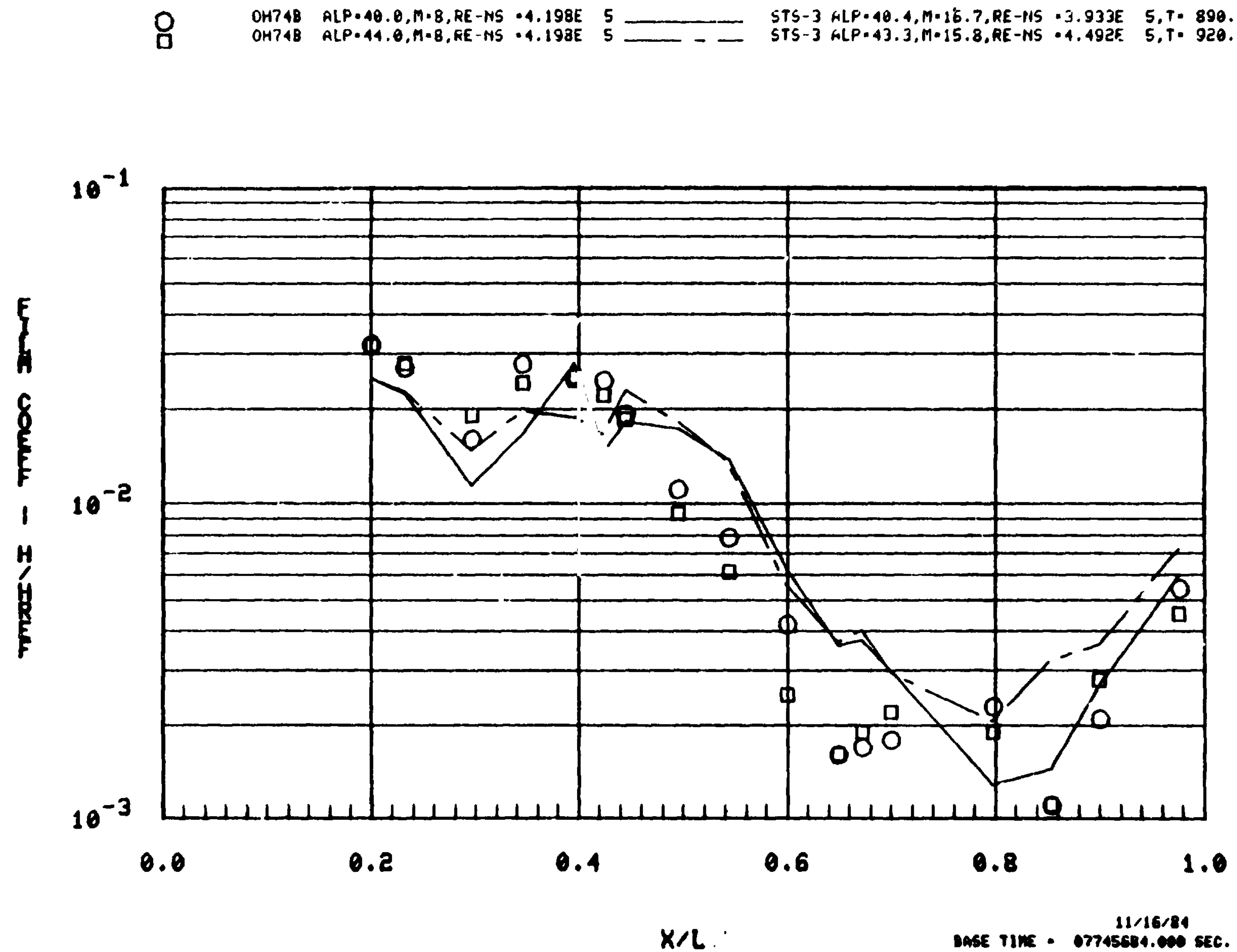

STS-4 SIDE FUSELAGE (Z=400 TRACE) DISTRIBUTION

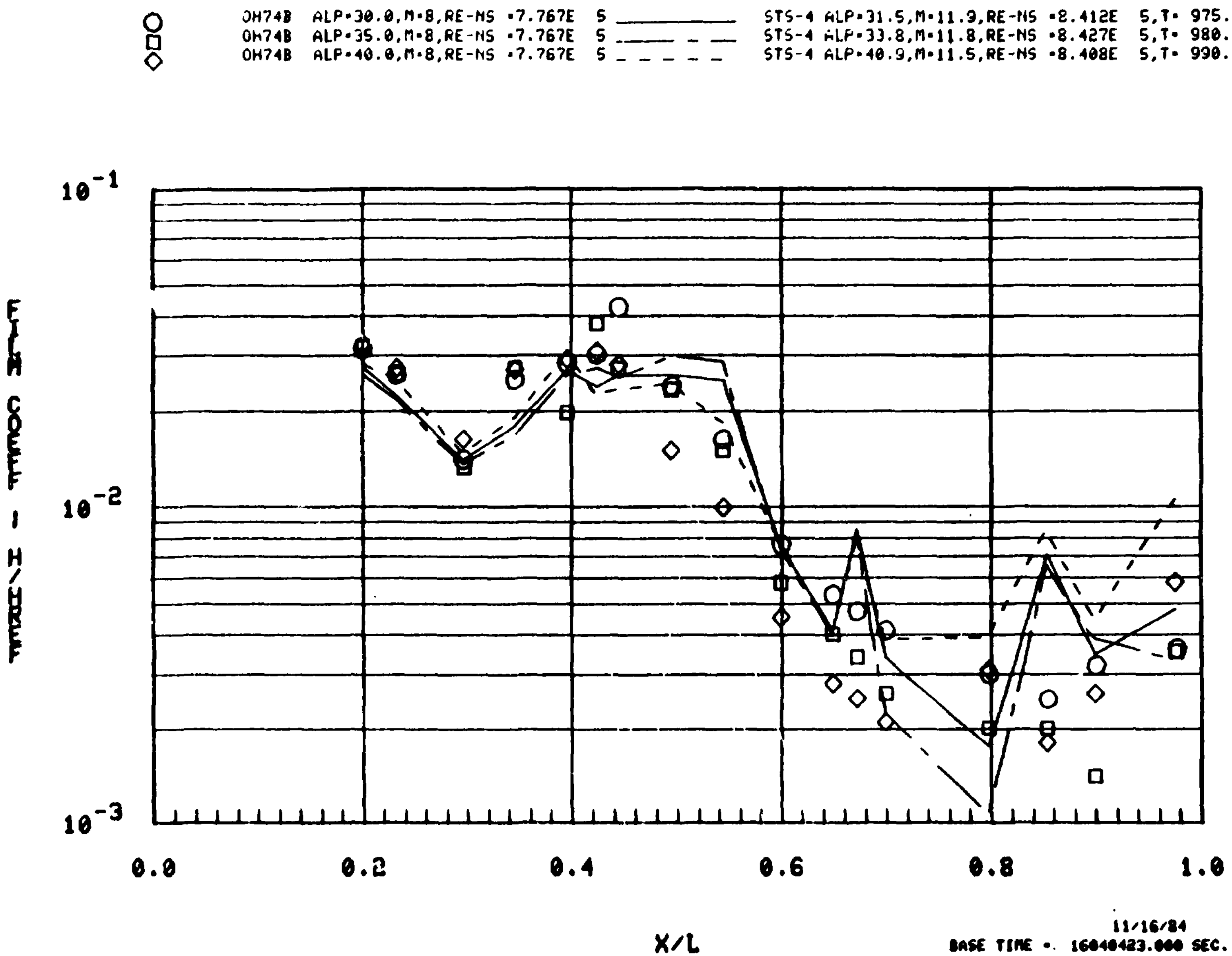

STS-4 SIDE FUSELAGE (Z=400 TRACE) DISTRIBUTION

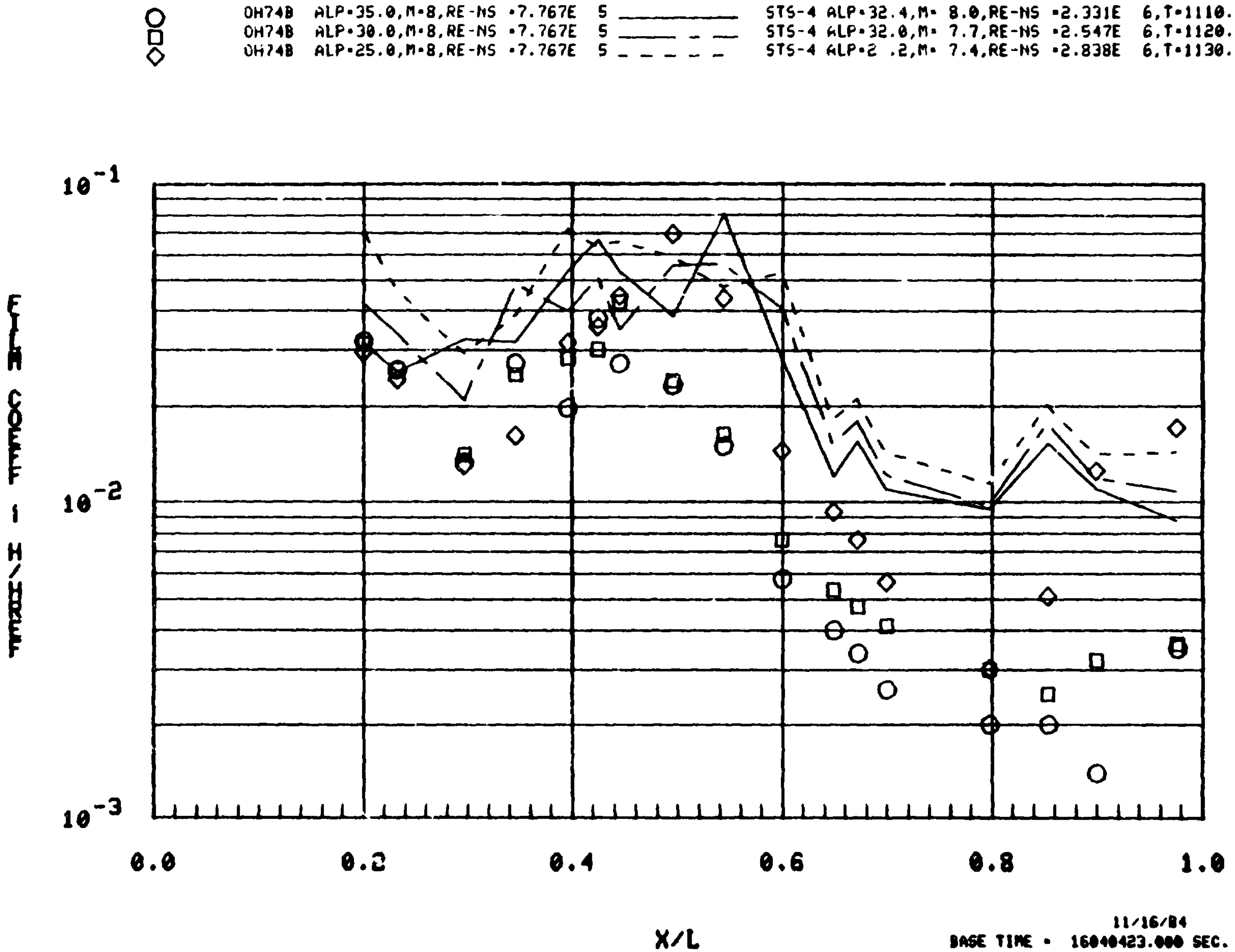

STS-2 SIDE PLB DOOR (Z=440 TRACE) DISTRIBUTION

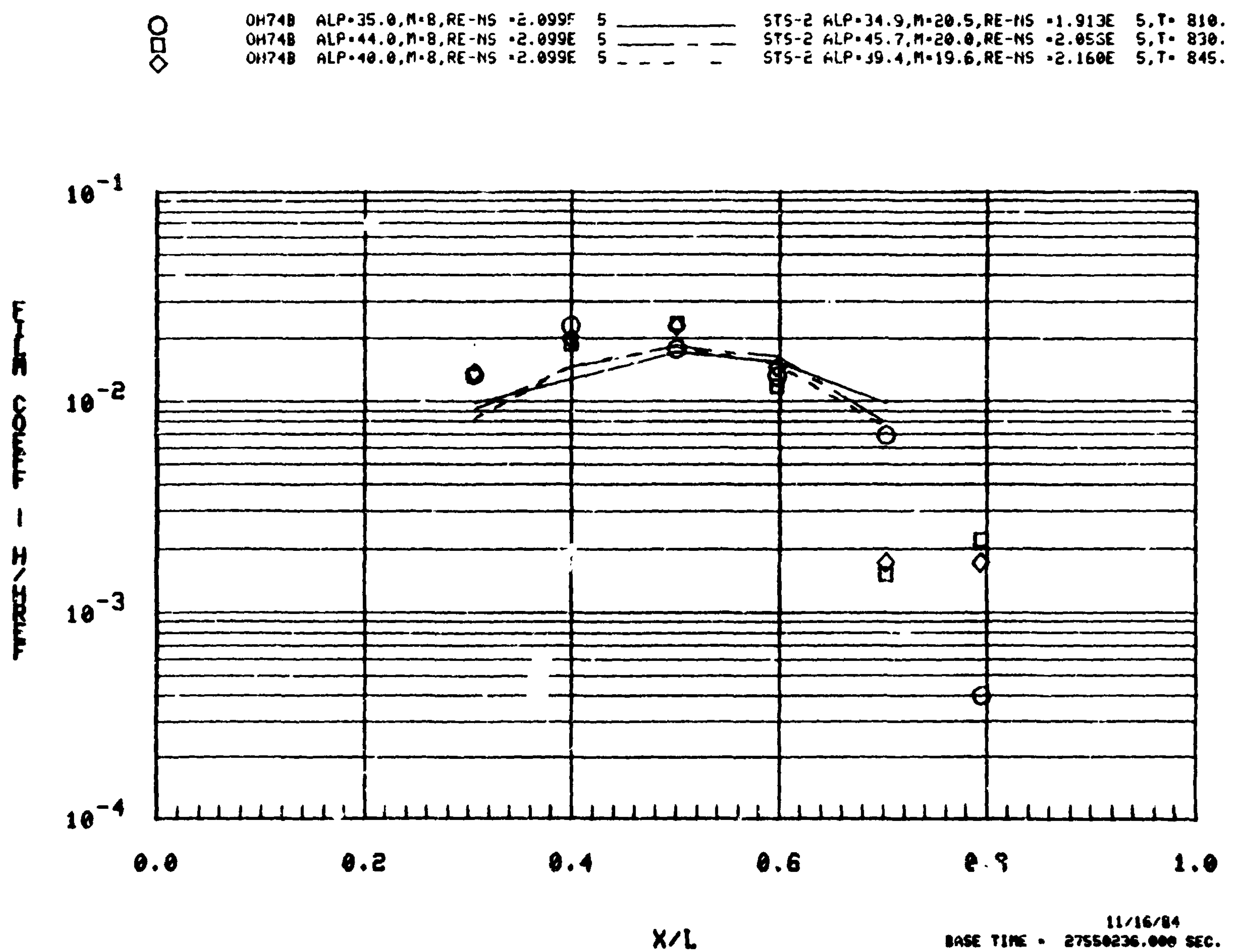

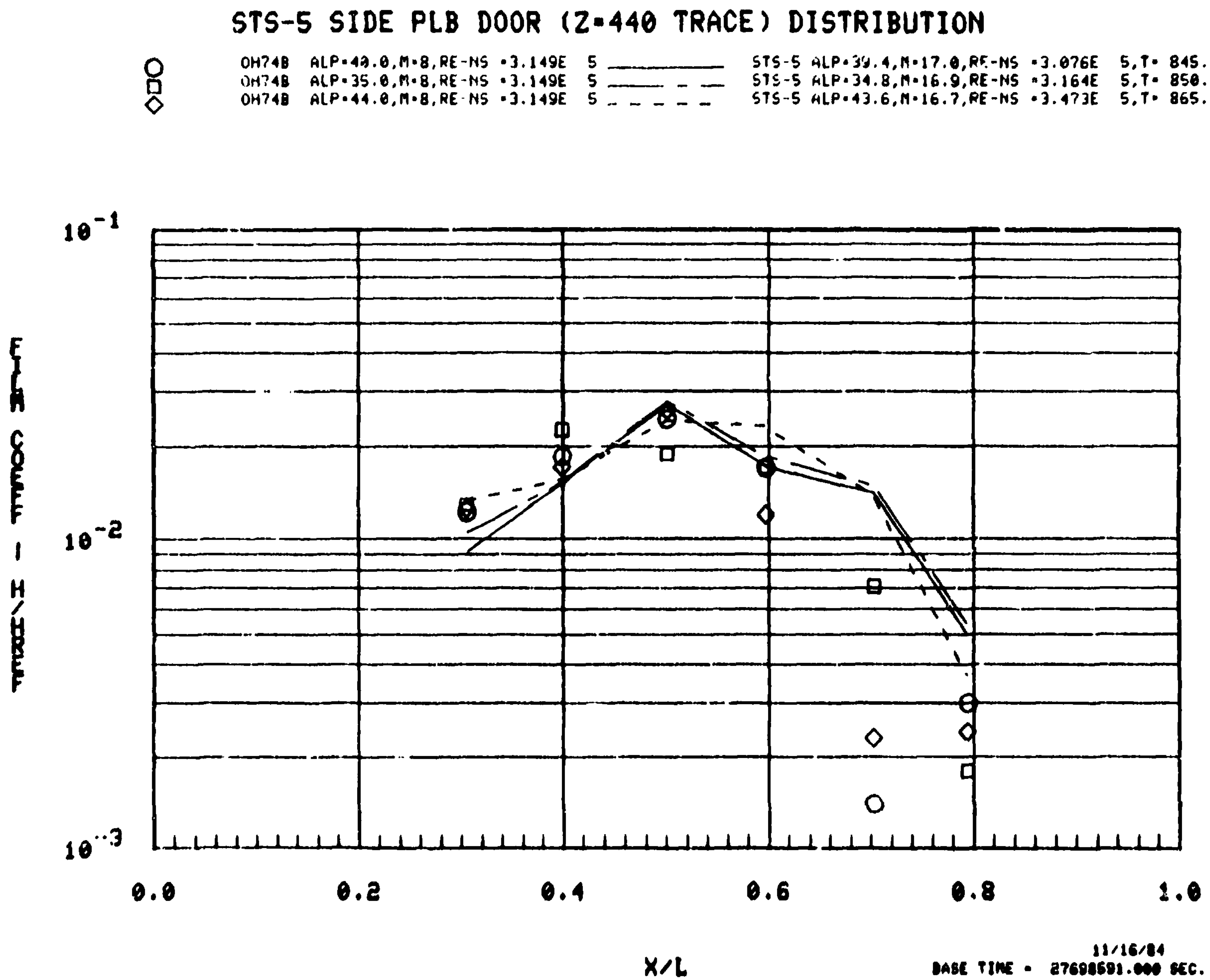

STS-5 SIDE PLB DOOR (Z=440 TRACE) DISTRIBUTION
OH74B ALP=40.0,M=8,RE-NS =3.149E 5
OH74B ALP=35.0,M=8,RE-NS =3.149E 5
OH74B ALP=44.0,M=8,RE-NS =3.149E 5
STS-5 ALP=39.4,M=17.0,RE-NS =3.076E 5,T= 845.
STS-5 ALP=34.8,M=16.9,RE-NS =3.164E 5,T= 850.
STS-5 ALP=43.6,M=16.7,RE-NS =3.473E 5,T= 865.
10^{-1}
10^{-2}
10^{-3}
FILM COEFF : H/HREF
0.0
0.2
0.4
0.6
0.8
1.0
X/L
11/16/84
BASE TIME = 27698591.000 SEC.

STS-3 SIDE PLB DOOR (Z=440 TRACE) DISTRIBUTION

○ OH74B ALP=40.0,M=8,RE-NS =4.198E 5 ———— STS-3 ALP=40.4,M=16.7,RE-NS =3.933E 5,T= 890.

□ OH74B ALP=44.0,M=8,RE-NS =4.198E 5 — — — STS-3 ALP=43.3,M=15.8,RE-NS =4.492E 5,T= 920.

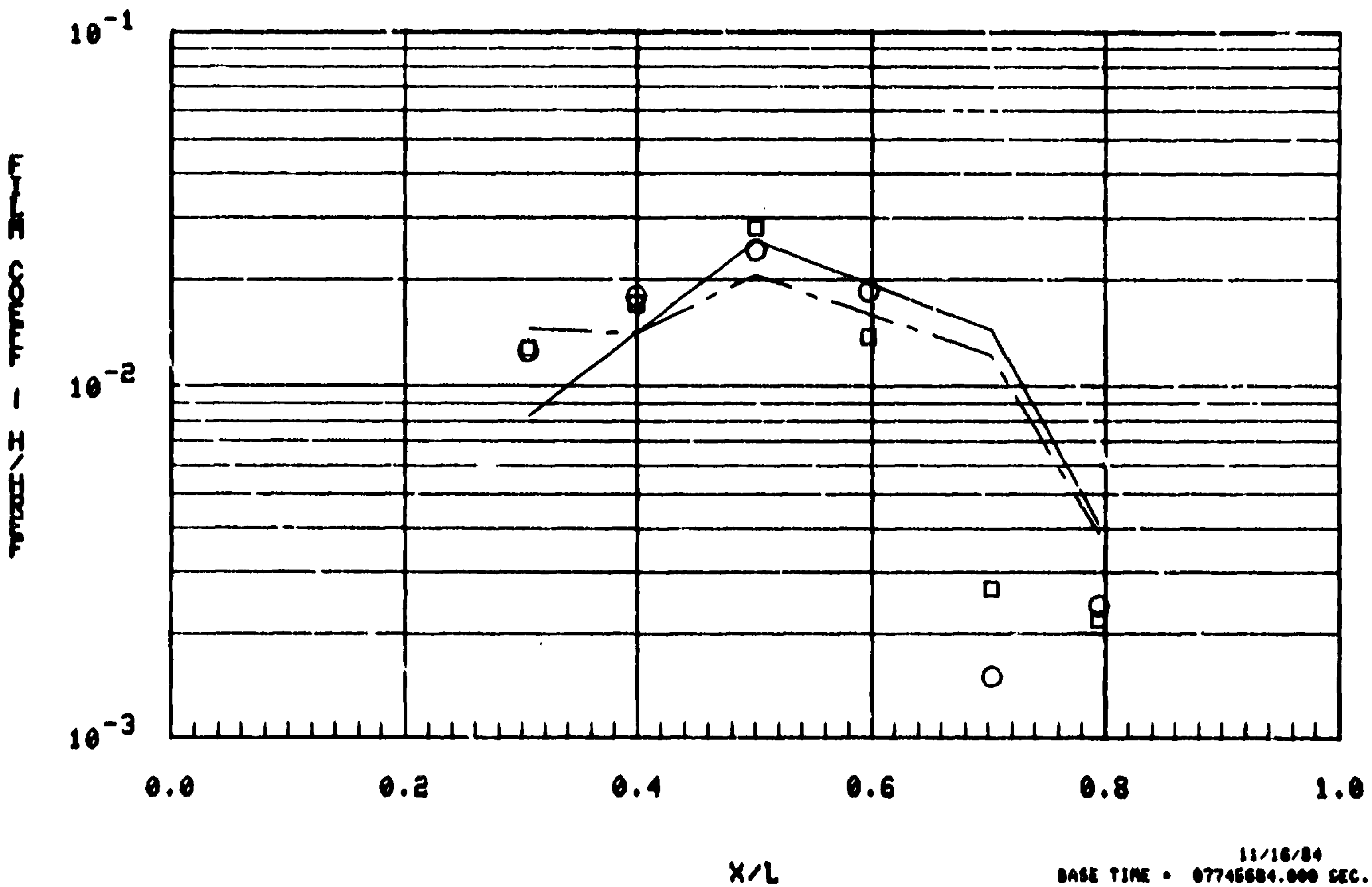

11/16/84
BASE TIME = 07745684.000 SEC.

STS-4 SIDE PLB DOOR (Z=440 TRACE) DISTRIBUTION

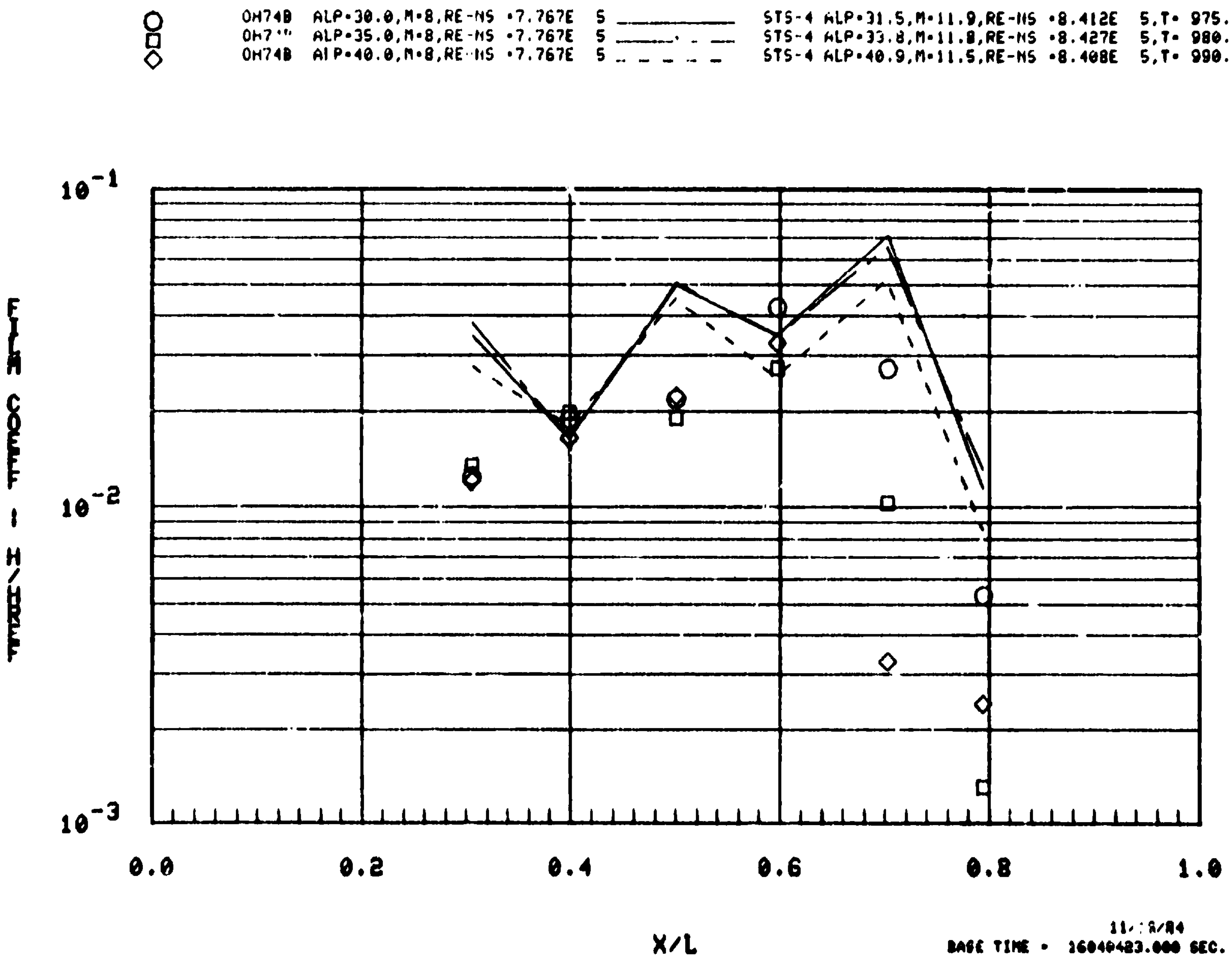

11/ /84
BASE TIME = 16040423.000 SEC.

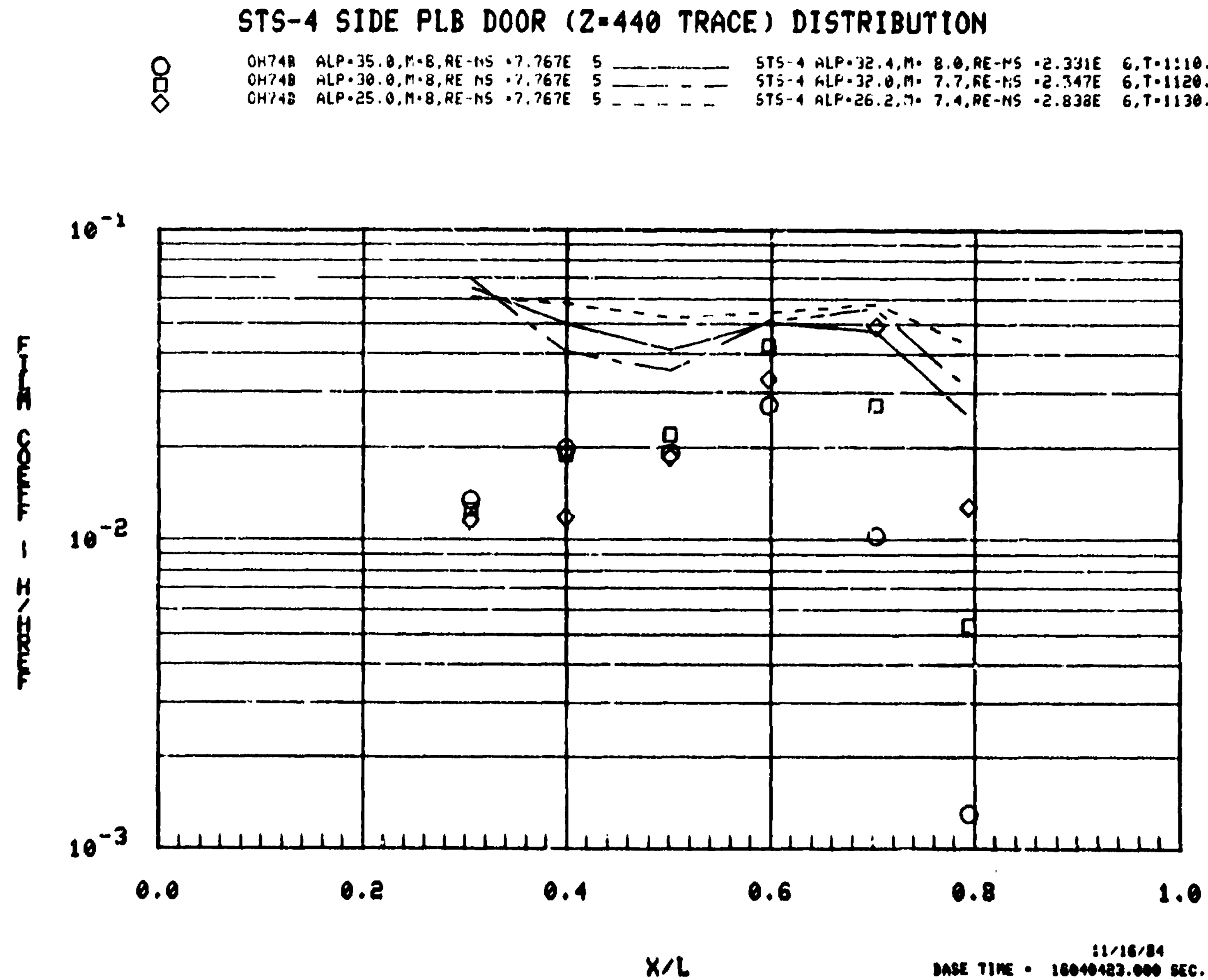

STS-4 SIDE PLB DOOR (Z=440 TRACE) DISTRIBUTION
OH74B ALP=35.0,M=8,RE-NS =7.767E 5
OH74B ALP=30.0,M=8,RE NS =7.767E 5
OH74B ALP=25.0,M=8,RE-NS =7.767E 5
STS-4 ALP=32.4,M= 8.0,RE-NS =2.331E 6,T=1110.
STS-4 ALP=32.0,M= 7.7,RE-NS =2.347E 6,T=1120.
STS-4 ALP=26.2,M= 7.4,RE-NS =2.838E 6,T=1130.
FILM COEFF - H/HREF
X/L
11/16/84
BASE TIME = 16040423.000 SEC.

STS-2 UPPER CENTERLINE DISTRIBUTION

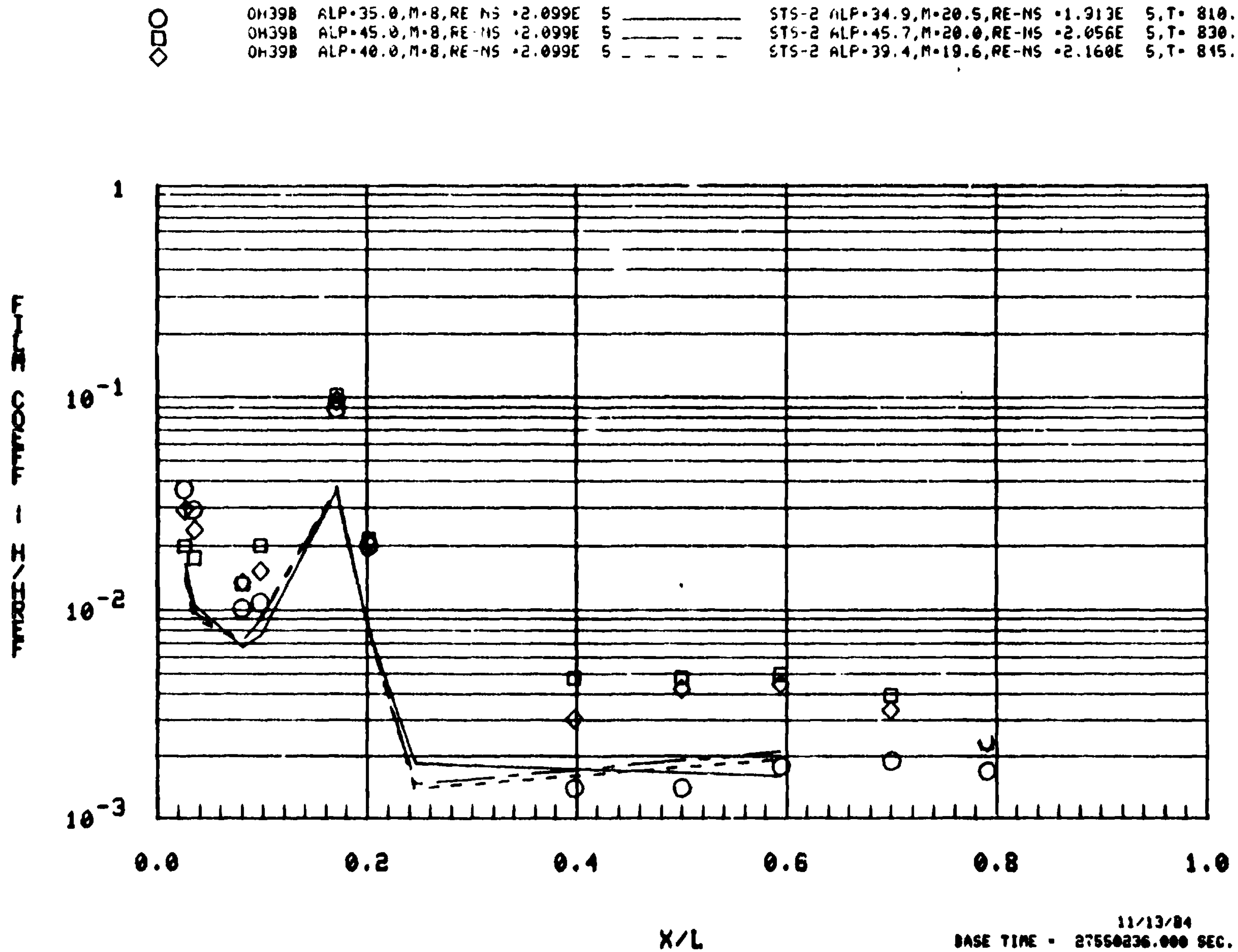

STS-5 UPPER CENTERLINE DISTRIBUTION

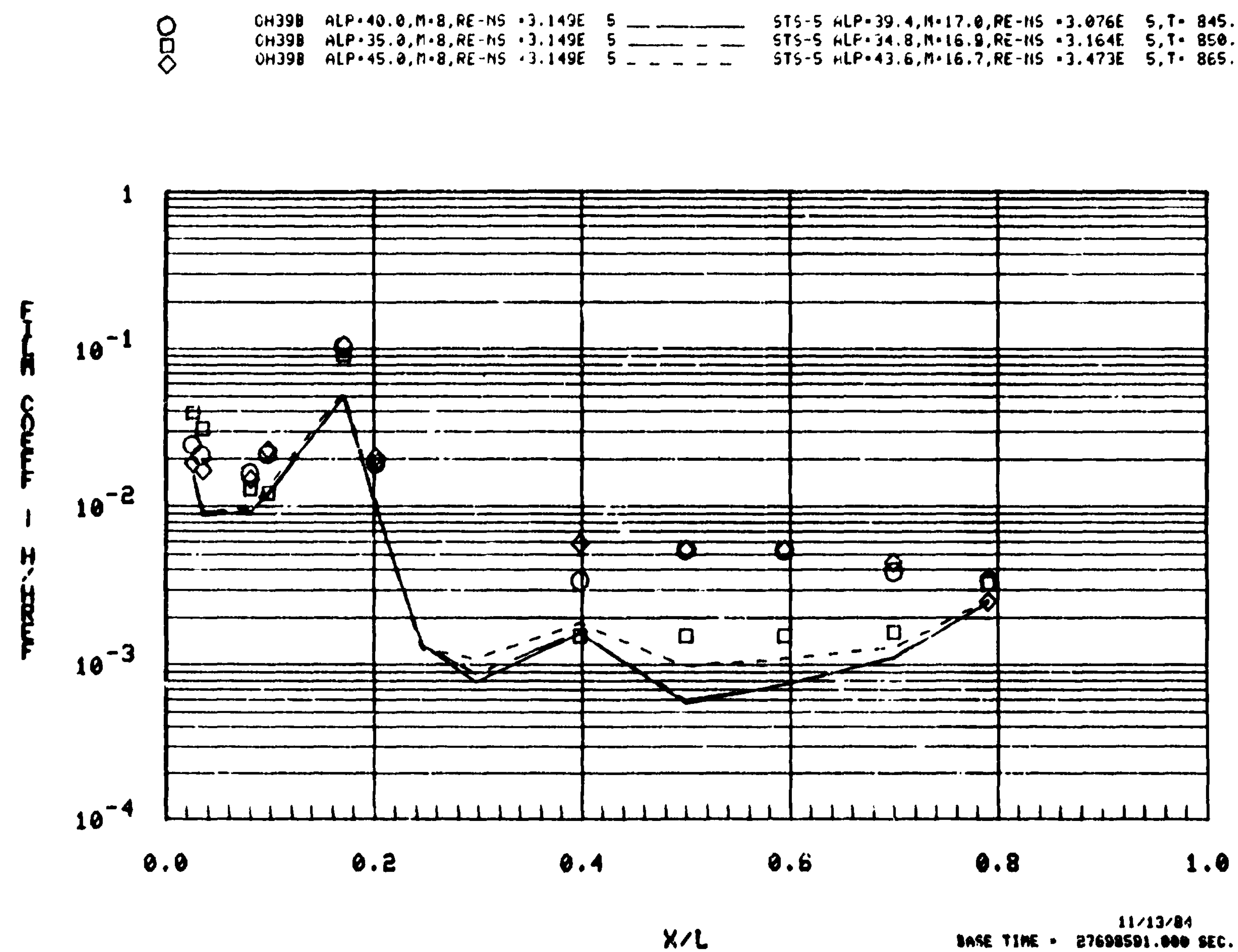

STS-3 UPPER CENTERLINE DISTRIBUTION

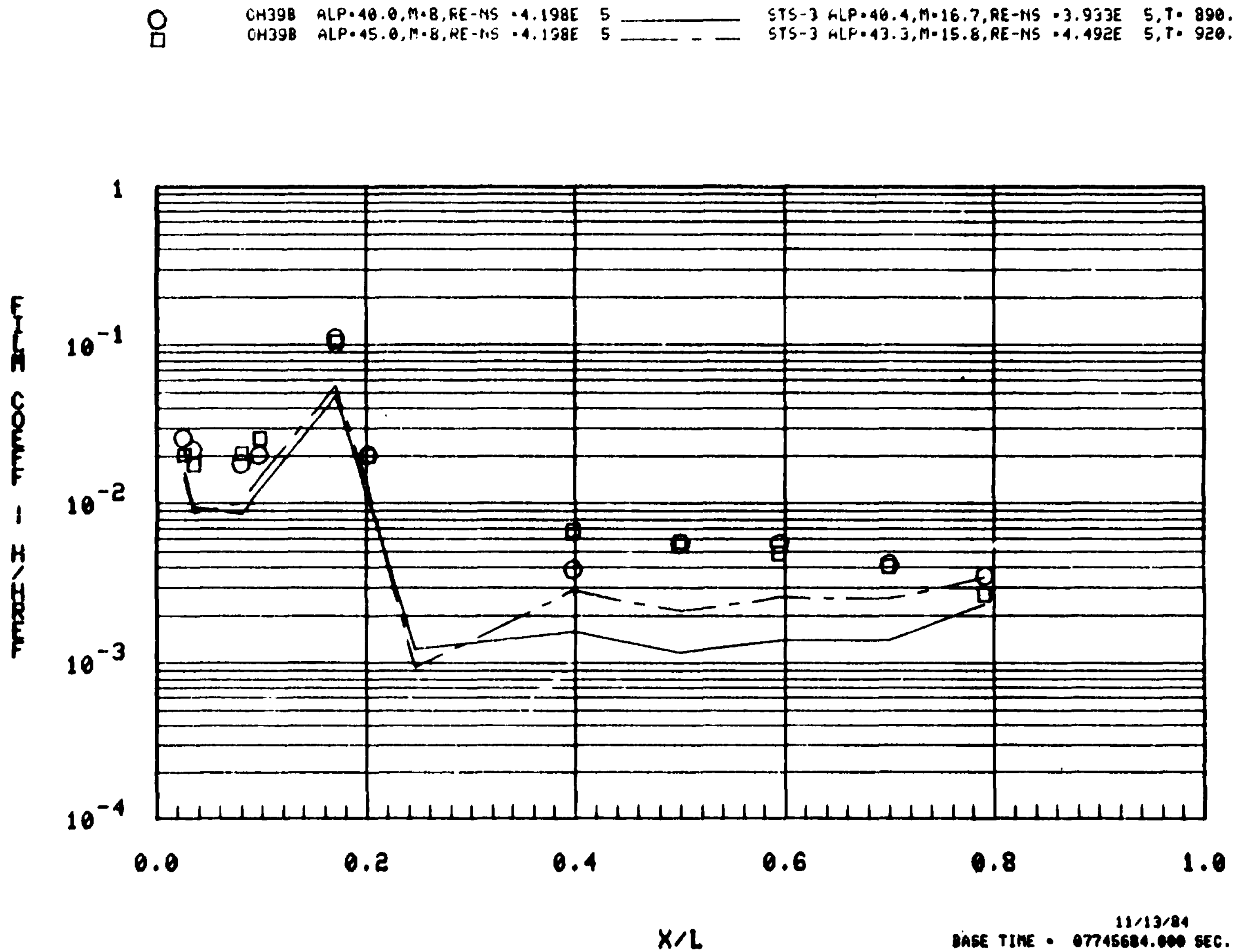

STS-4 UPPER CENTERLINE DISTRIBUTION

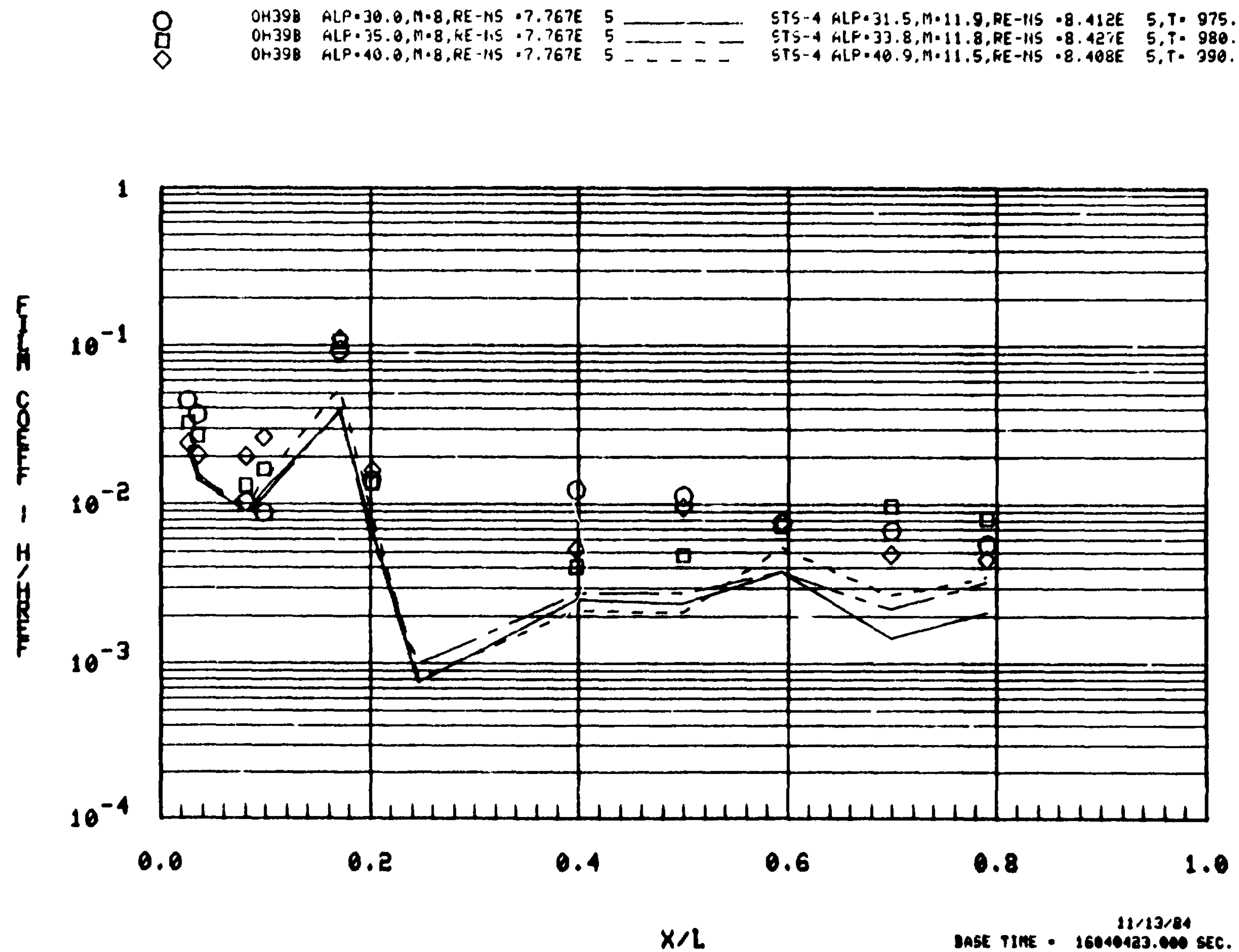

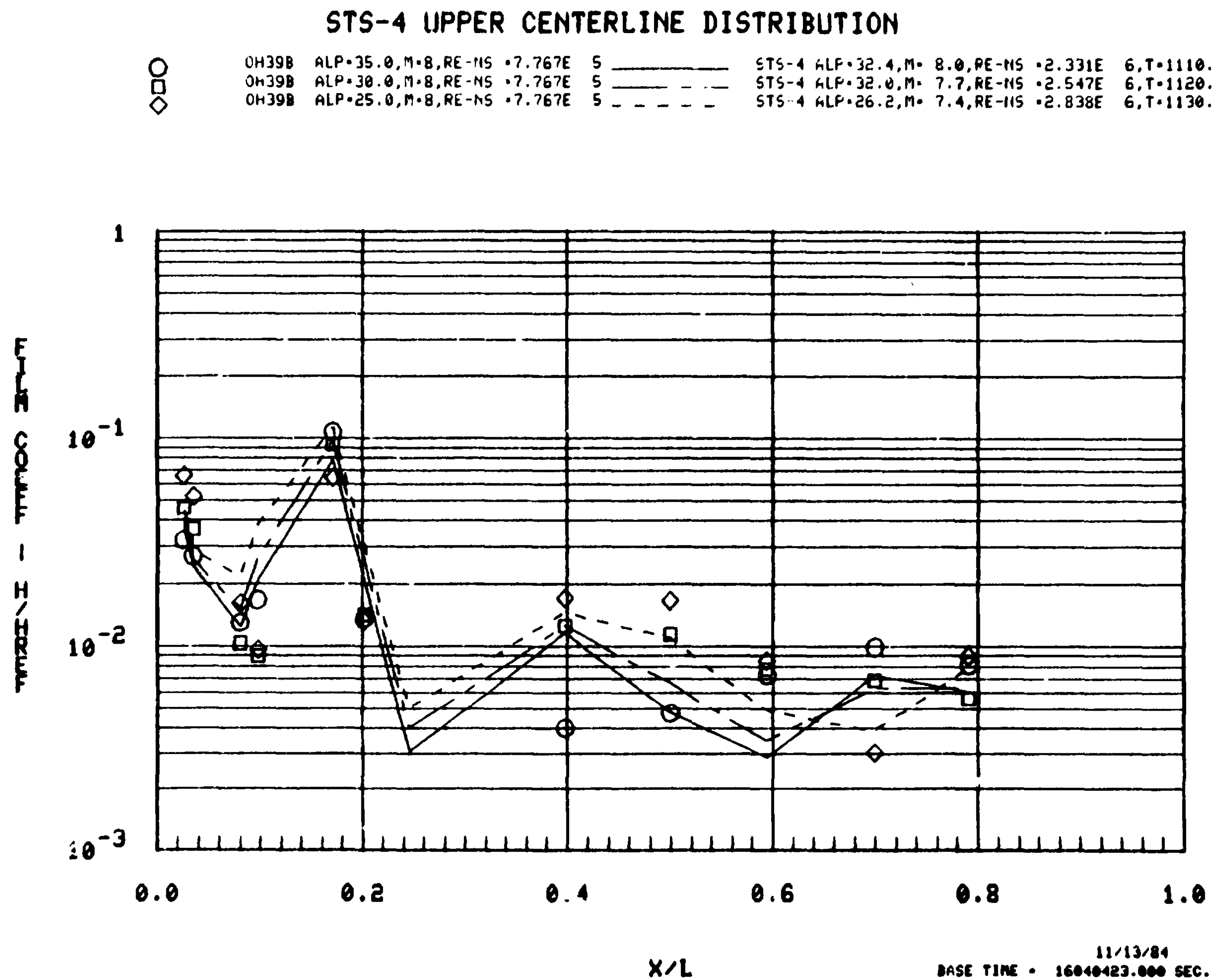
STS-4 UPPER CENTERLINE DISTRIBUTION
OH39B ALP=35.0,M=8,RE-NS =7.767E 5 STS-4 ALP=32.4,M= 8.0,RE-NS =2.331E 6,T=1110.
OH39B ALP=30.0,M=8,RE-NS =7.767E 5 STS-4 ALP=32.0,M= 7.7,RE-NS =2.547E 6,T=1120.
OH39B ALP=25.0,M=8,RE-NS =7.767E 5 STS-4 ALP=26.2,M= 7.4,RE-NS =2.838E 6,T=1130.
FILM COEFF - H/HREF
1
10^{-1}
10^{-2}
10^{-3}
0.0
0.2
0.4
0.6
0.8
1.0
X/L
11/13/84
BASE TIME = 16040423.000 SEC.

STS-2 OMS POD TRACE 3 DISTRIBUTION

○	AF	ALP=35.0,M=8,RE-NS =2.099E 5	————	STS-2 ALP=34.9,M=20.5,RE-NS =1.913E 5,T= 810.
□	AF	ALP=40.0,M=8,RE-NS =2.099E 5	—— — —	STS-2 ALP=45.7,M=20.0,RE-NS =2.056E 5,T= 830.
◇	AF	ALP=40.0,M=8,RE-NS =2.099E 5	— — — —	STS-2 ALP=39.4,M=19.6,RE-NS =2.160E 5,T= 845.

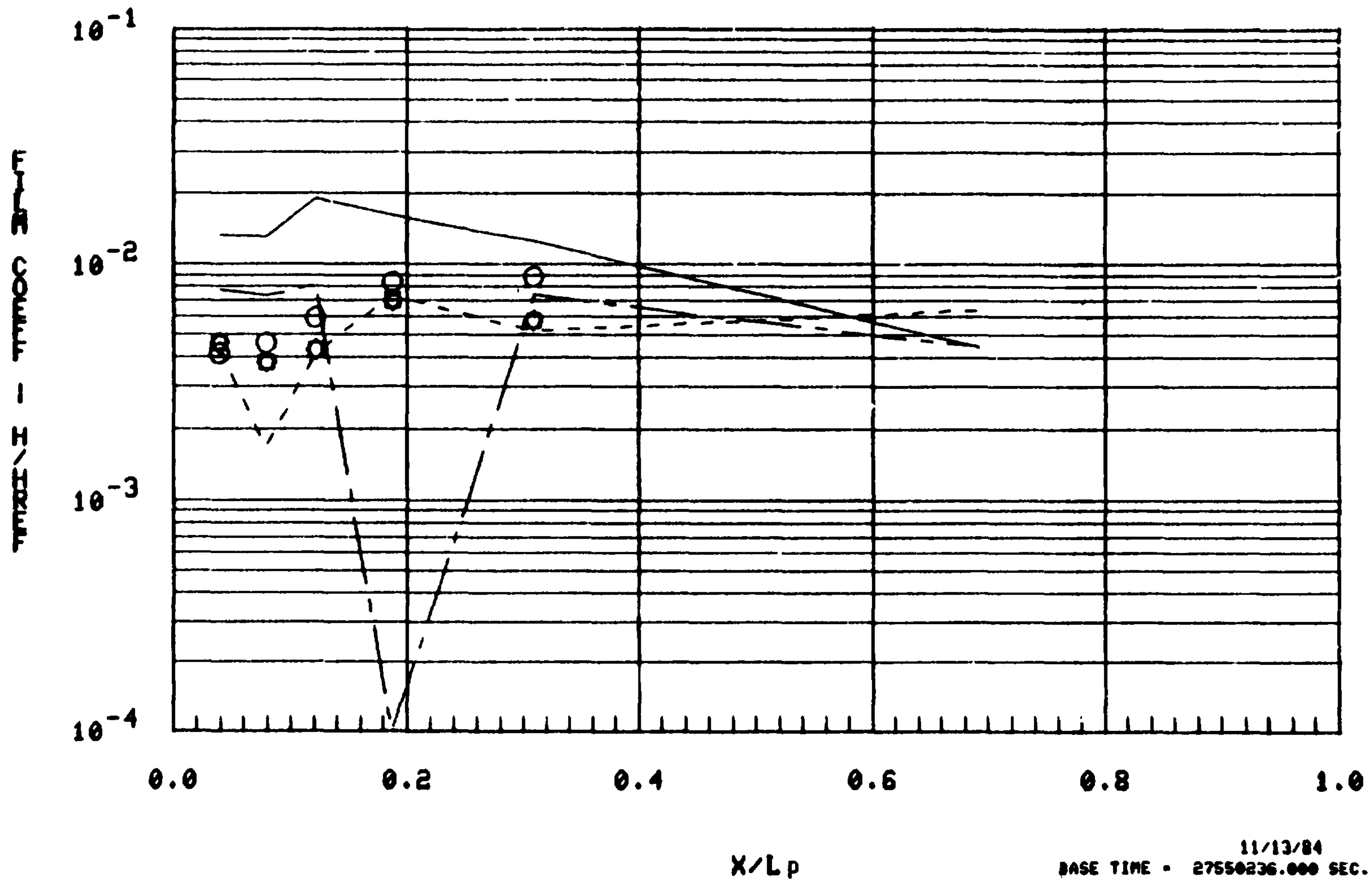

STS-5 OMS POD TRACE 3 DISTRIBUTION

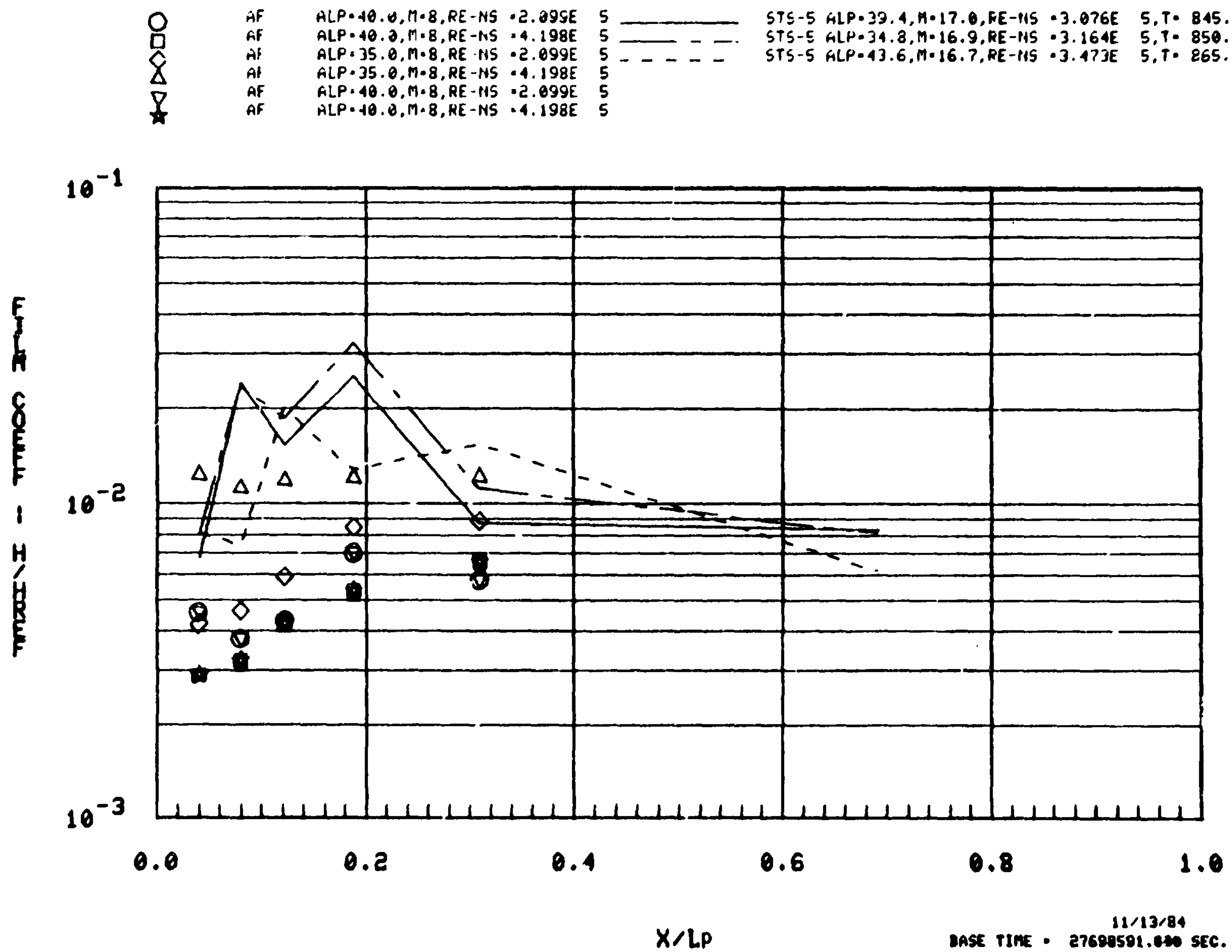

STS-3 OMS POD TRACE 3 DISTRIBUTION

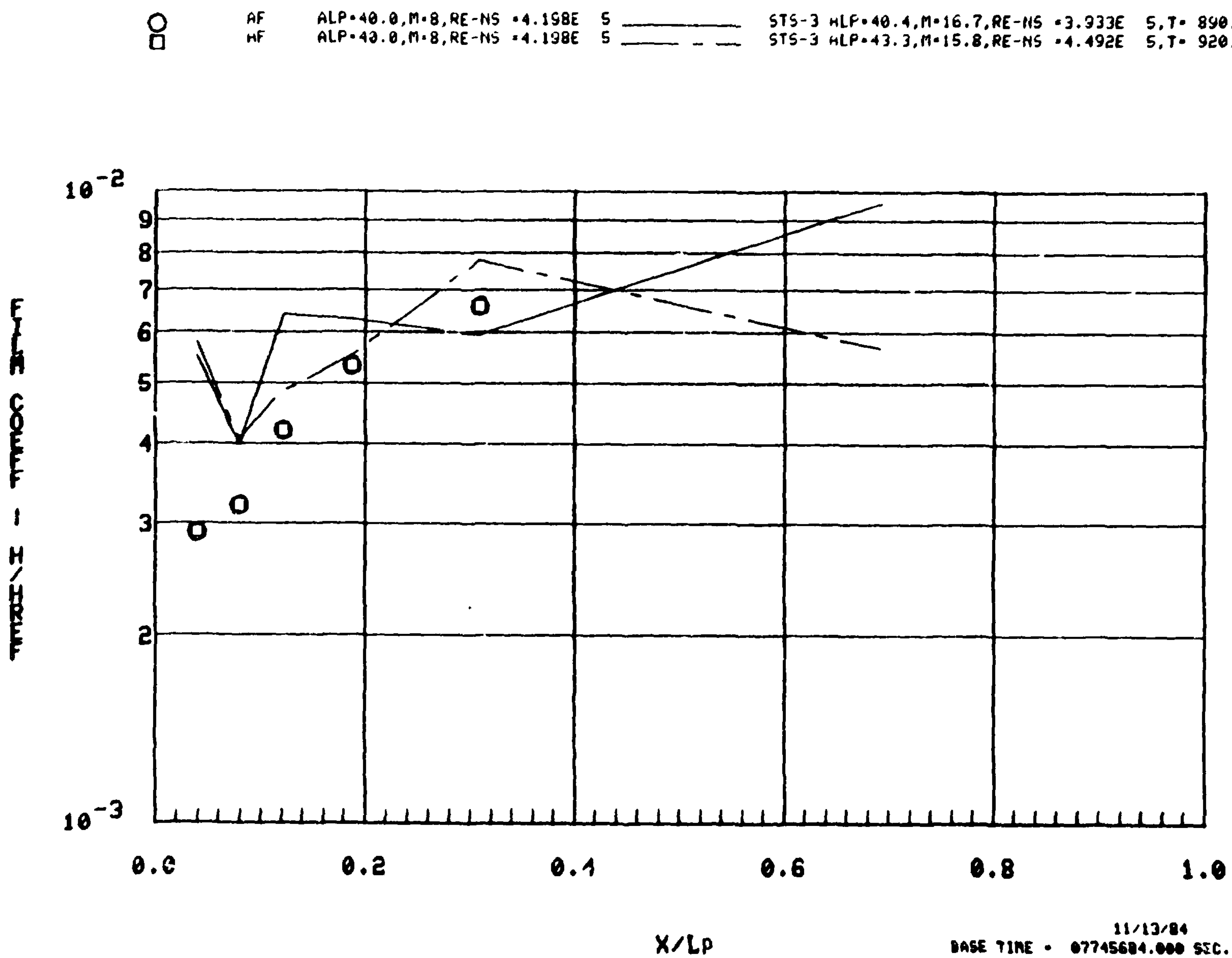

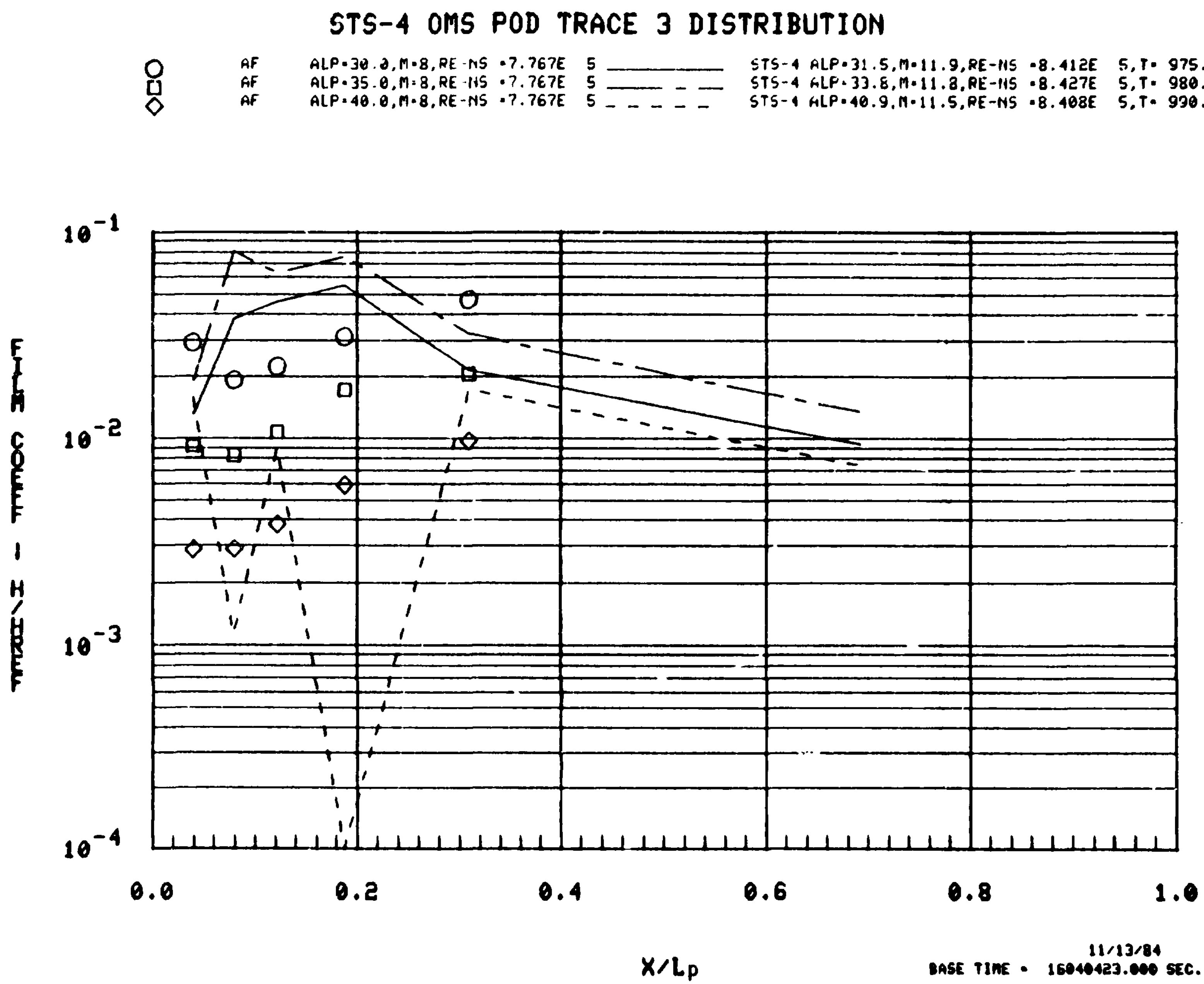

STS-4 OMS POD TRACE 3 DISTRIBUTION
AF ALP=30.0,M=8,RE-NS =7.767E 5
AF ALP=35.0,M=8,RE-NS =7.767E 5
AF ALP=40.0,M=8,RE-NS =7.767E 5
STS-4 ALP=31.5,M=11.9,RE-NS =8.412E 5,T= 975.
STS-4 ALP=33.8,M=11.8,RE-NS =8.427E 5,T= 980.
STS-4 ALP=40.9,M=11.5,RE-NS =8.408E 5,T= 990.
FILM COEFF - H/HREF
X/Lp
11/13/84
BASE TIME = 16040423.000 SEC.

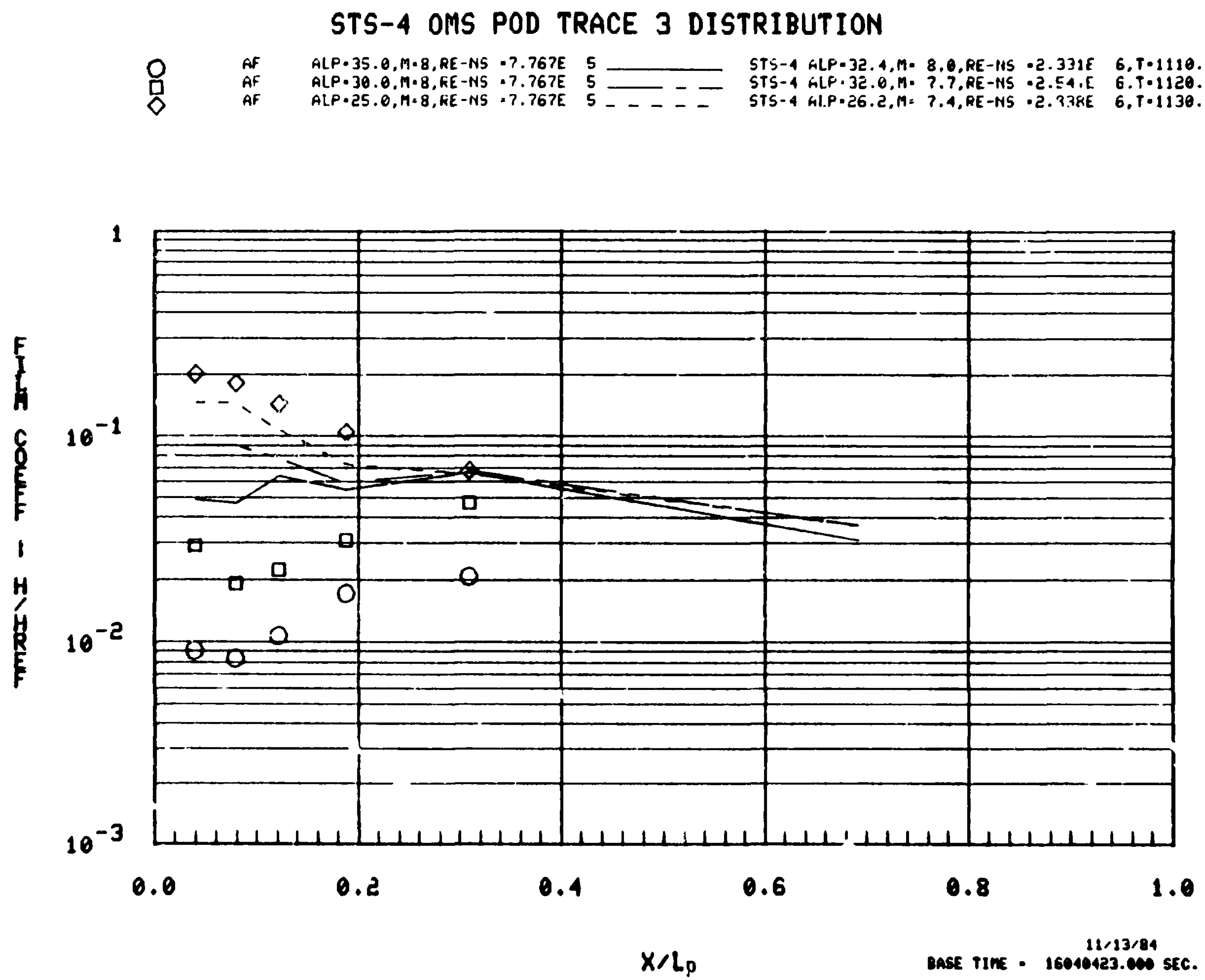
STS-4 OMS POD TRACE 3 DISTRIBUTION
AF ALP=35.0,M=8,RE-NS =7.767E 5
AF ALP=30.0,M=8,RE-NS =7.767E 5
AF ALP=25.0,M=8,RE-NS =7.767E 5
STS-4 ALP=32.4,M= 8.0,RE-NS =2.331E 6,T=1110.
STS-4 ALP=32.0,M= 7.7,RE-NS =2.54.E 6,T=1120.
STS-4 ALP=26.2,M= 7.4,RE-NS =2.338E 6,T=1130.
FILM COEFF : H/HREF
1
10^-1
10^-2
10^-3
0.0
0.2
0.4
0.6
0.8
1.0
X/Lp
11/13/84
BASE TIME = 16040423.000 SEC.

APPENDIX E

HEATING RATE COMPARISON -

INFLUENCE OF ANGLE OF ATTACK

(VARIABLE REYNOLDS NUMBERS) COMPOSITE FLIGHTS

LOWER CENTERLINE DISTRIBUTION

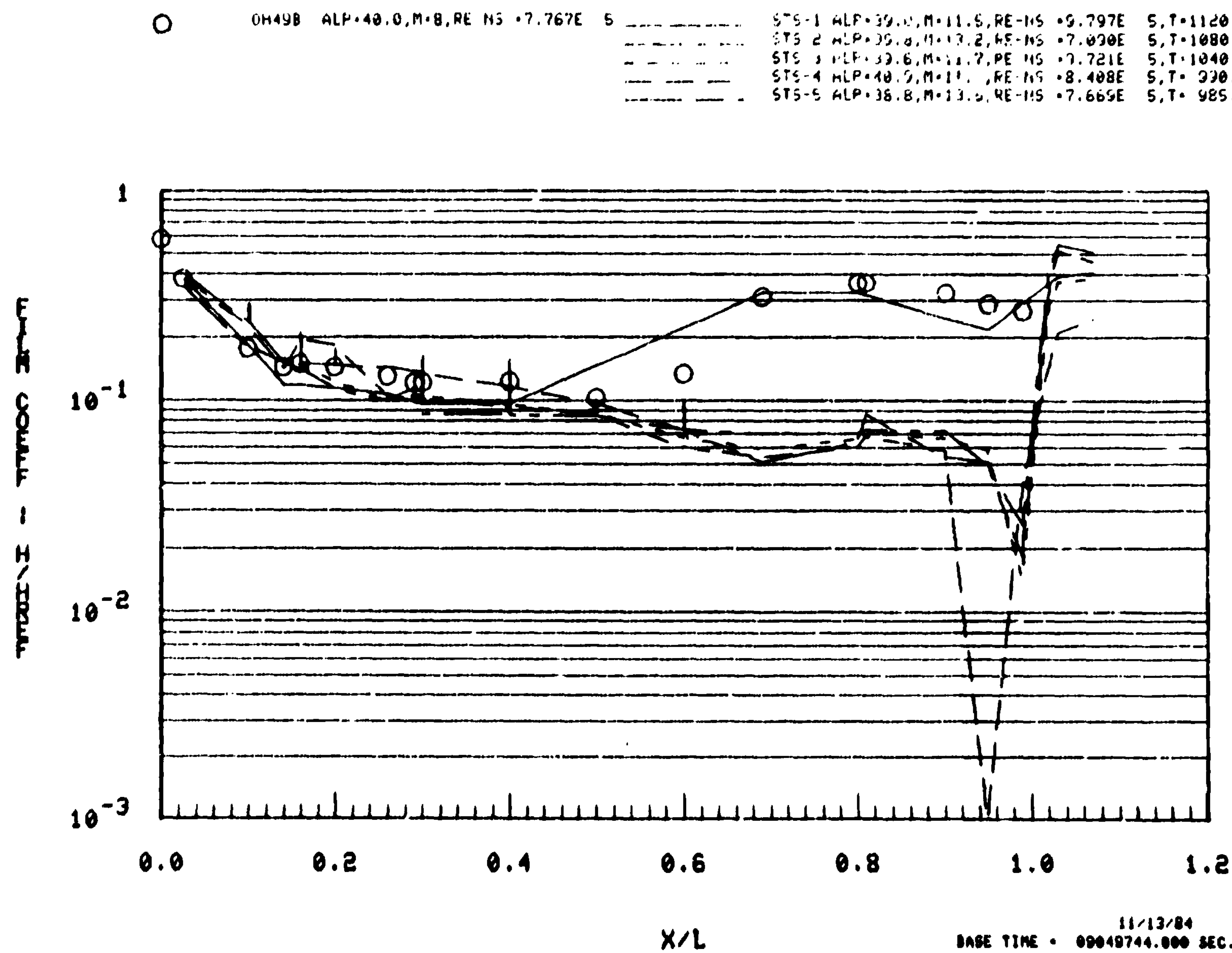

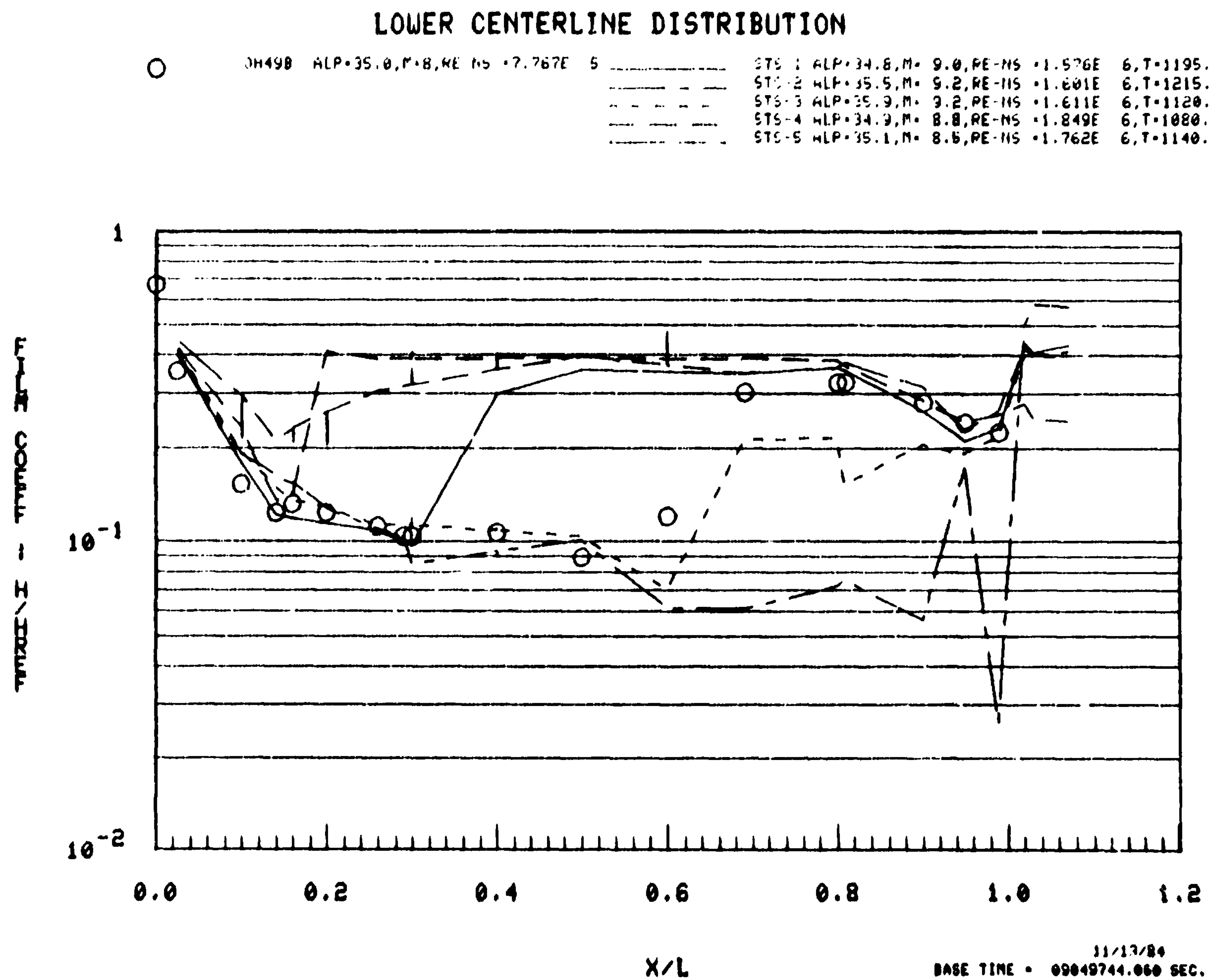
LOWER CENTERLINE DISTRIBUTION
OH49B ALP=35.0,M=8,RE NS =7.767E 5
STS 1 ALP=34.8,M= 9.0,RE-NS =1.576E 6,T=1195.
STS-2 ALP=35.5,M= 9.2,RE-NS =1.601E 6,T=1215.
STS-3 ALP=35.9,M= 9.2,RE-NS =1.611E 6,T=1120.
STS-4 ALP=34.9,M= 8.8,RE-NS =1.849E 6,T=1080.
STS-5 ALP=35.1,M= 8.6,RE-NS =1.762E 6,T=1140.
FILM COEFF : H/HREF
1
10^{-1}
10^{-2}
0.0
0.2
0.4
0.6
0.8
1.0
1.2
X/L
11/13/84
BASE TIME = 09049744.060 SEC.

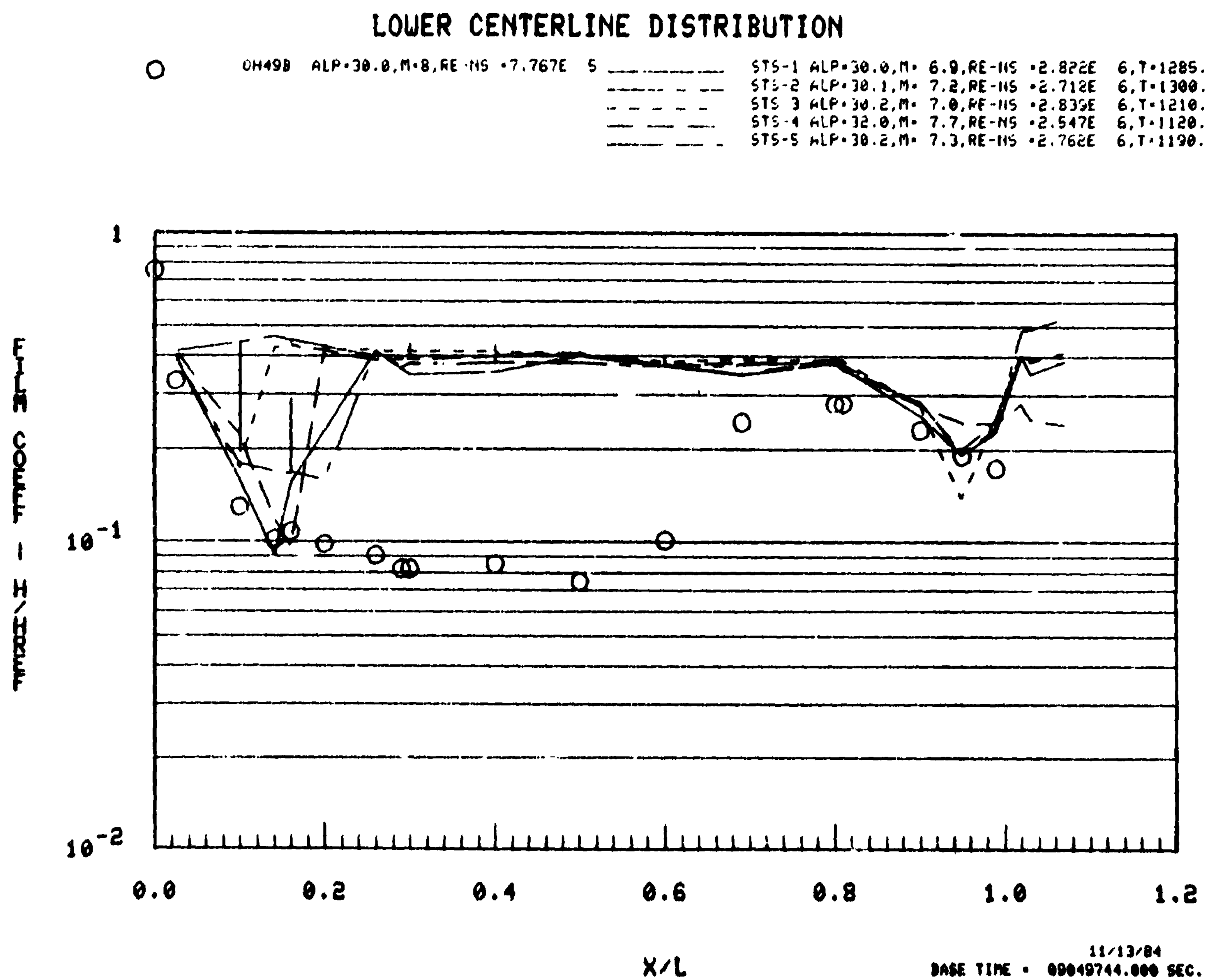
LOWER CENTERLINE DISTRIBUTION
OH49B ALP=30.0,M=8,RE-NS =7.767E 5
STS-1 ALP=30.0,M= 6.9,RE-NS =2.822E 6,T=1285.
STS-2 ALP=30.1,M= 7.2,RE-NS =2.712E 6,T=1300.
STS 3 ALP=30.2,M= 7.0,RE-NS =2.839E 6,T=1210.
STS-4 ALP=32.0,M= 7.7,RE-NS =2.547E 6,T=1120.
STS-5 ALP=30.2,M= 7.3,RE-NS =2.762E 6,T=1190.
1
10^{-1}
10^{-2}
FILM COEFF - H/HREF
0.0
0.2
0.4
0.6
0.8
1.0
1.2
X/L
11/13/84
BASE TIME = 09049744.000 SEC.

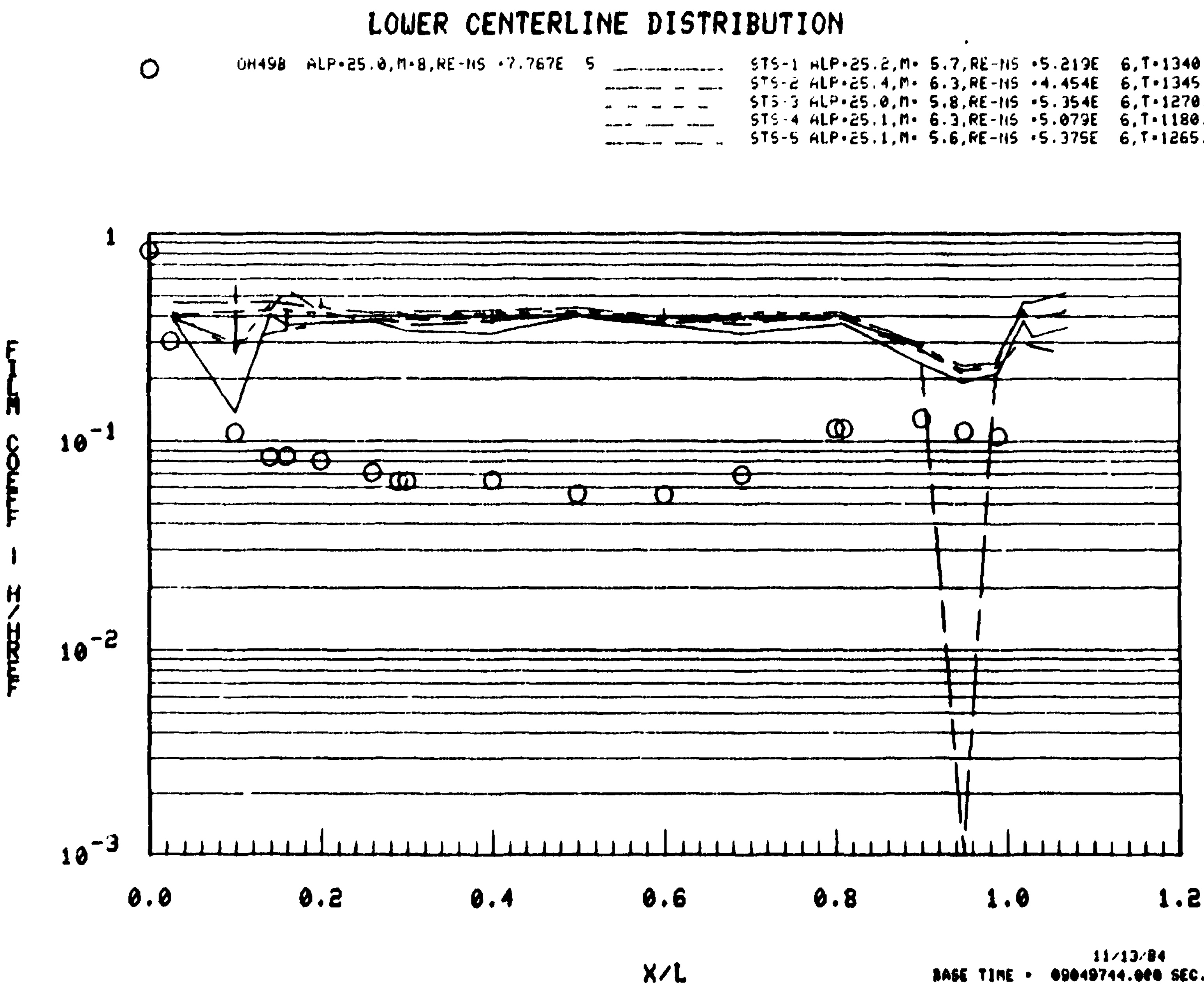
LOWER CENTERLINE DISTRIBUTION
OH49B ALP=25.0,M=8,RE-NS =7.767E 5
STS-1 ALP=25.2,M= 5.7,RE-NS =5.219E 6,T=1340.
STS-2 ALP=25.4,M= 6.3,RE-NS =4.454E 6,T=1345.
STS-3 ALP=25.0,M= 5.8,RE-NS =5.354E 6,T=1270.
STS-4 ALP=25.1,M= 6.3,RE-NS =5.079E 6,T=1180.
STS-5 ALP=25.1,M= 5.6,RE-NS =5.375E 6,T=1265.
FILM COEFF : H/HREF
1
10^-1
10^-2
10^-3
0.0
0.2
0.4
0.6
0.8
1.0
1.2
X/L
11/13/84
BASE TIME = 09049744.000 SEC.

LOWER CENTERLINE DISTRIBUTION

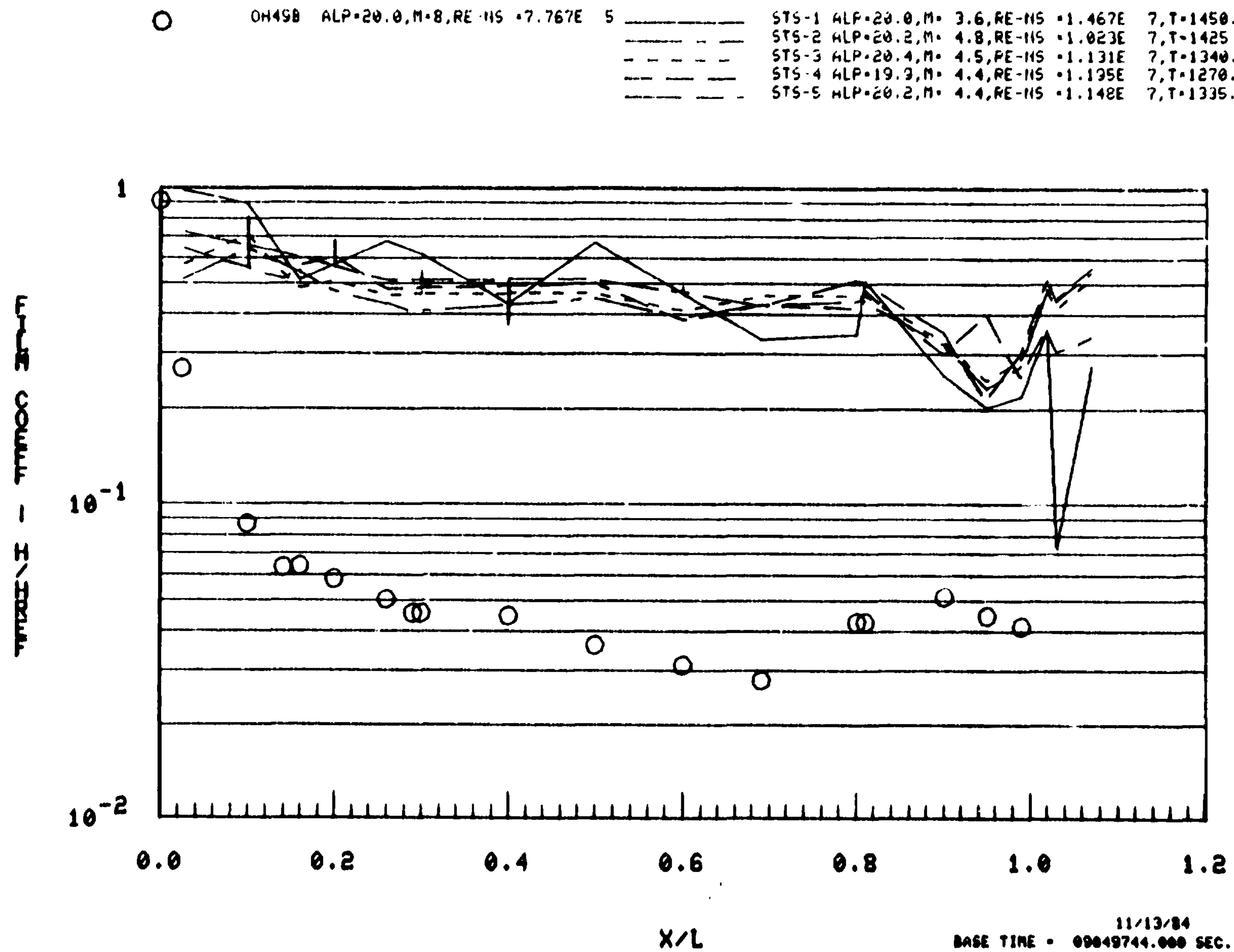

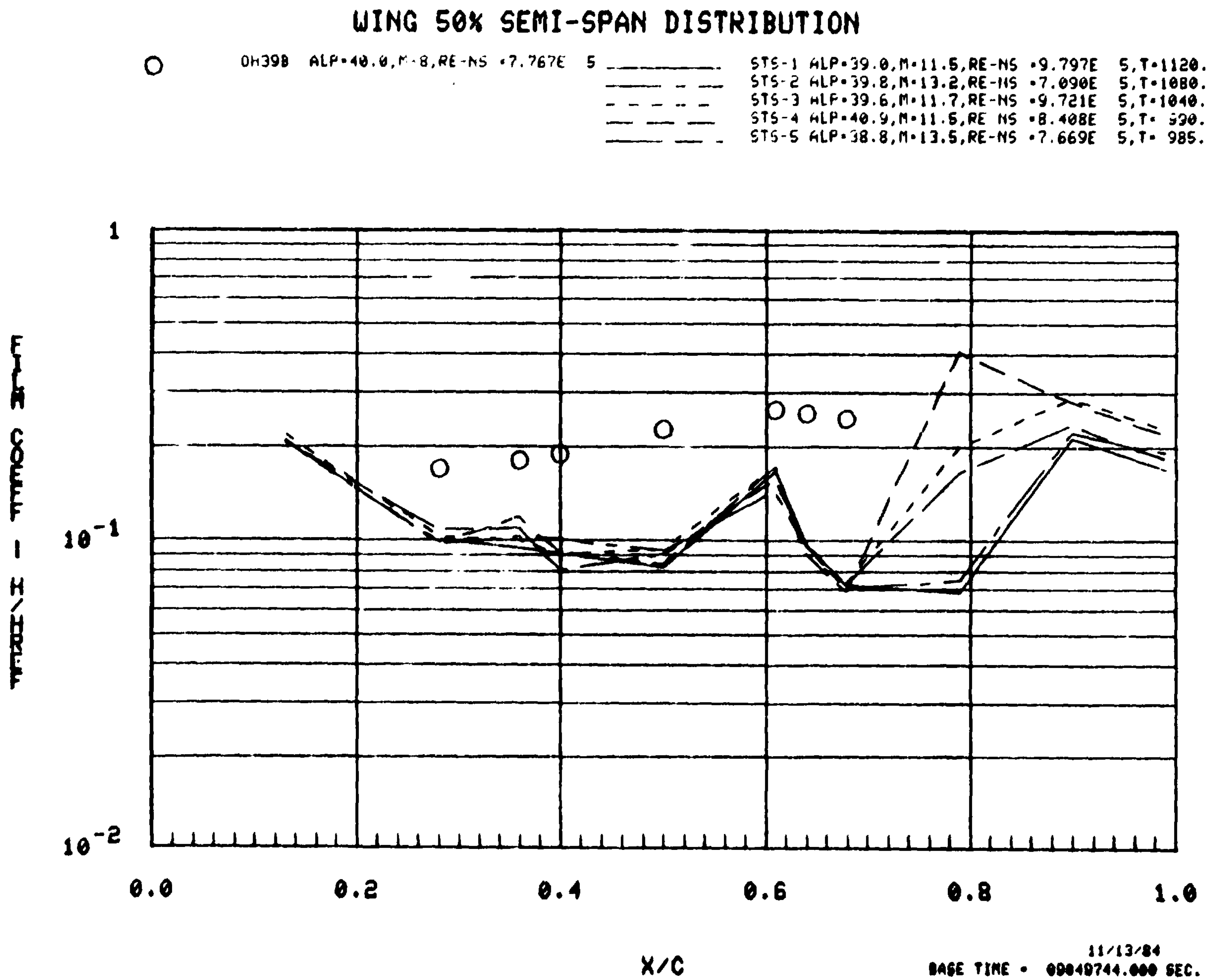
WING 50% SEMI-SPAN DISTRIBUTION
OH39B ALP=40.0,M=8,RE-NS =7.767E 5
STS-1 ALP=39.0,M=11.5,RE-NS =9.797E 5,T=1120.
STS-2 ALP=39.8,M=13.2,RE-NS =7.090E 5,T=1080.
STS-3 ALP=39.6,M=11.7,RE-NS =9.721E 5,T=1040.
STS-4 ALP=40.9,M=11.5,RE NS =8.408E 5,T= 990.
STS-5 ALP=38.8,M=13.5,RE-NS =7.669E 5,T= 985.
FILM COEFF - H/HREF
1
10^-1
10^-2
0.0
0.2
0.4
0.6
0.8
1.0
X/C
11/13/84
BASE TIME = 00040744.000 SEC.

WING 50% SEMI-SPAN DISTRIBUTION

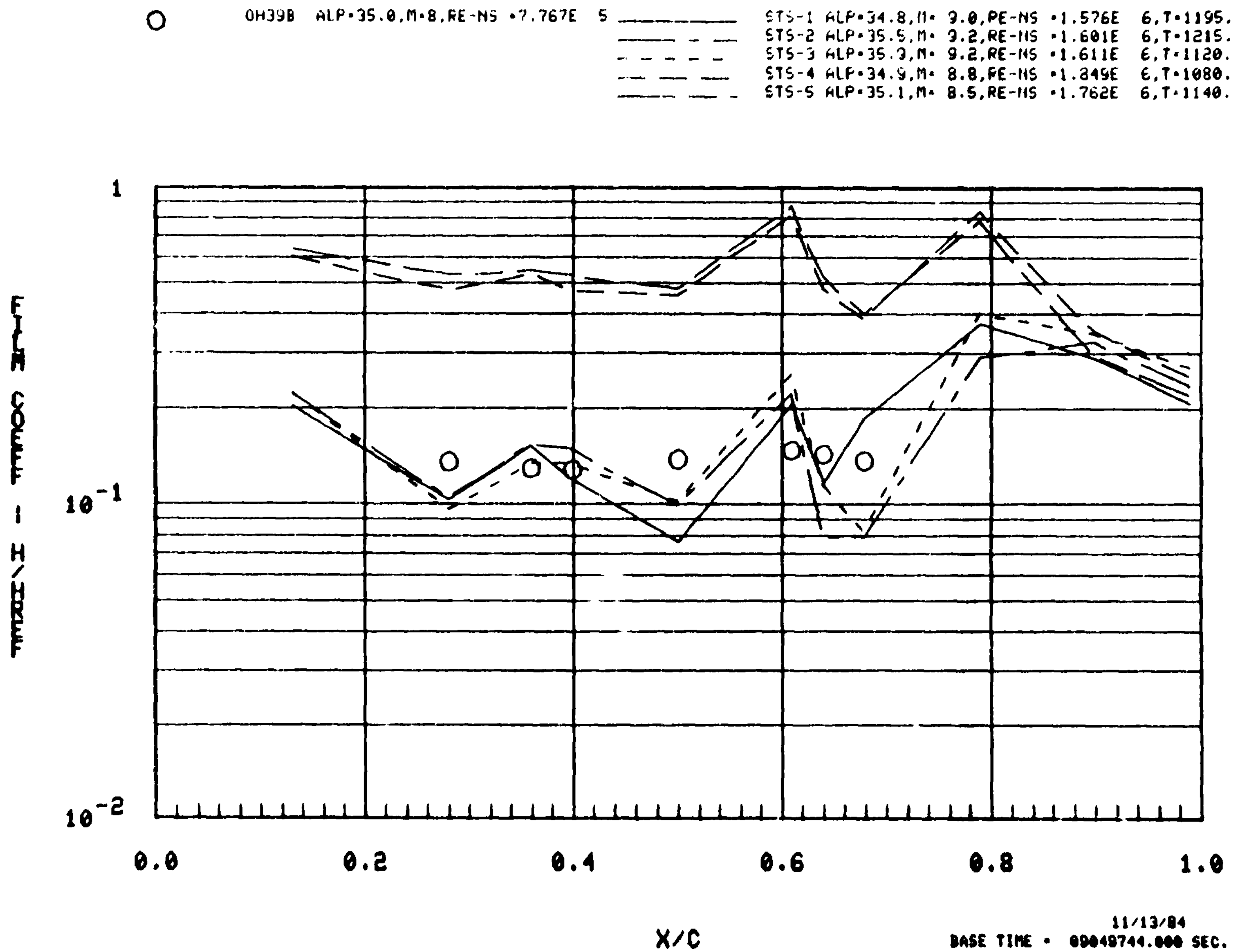

WING 50% SEMI-SPAN DISTRIBUTION

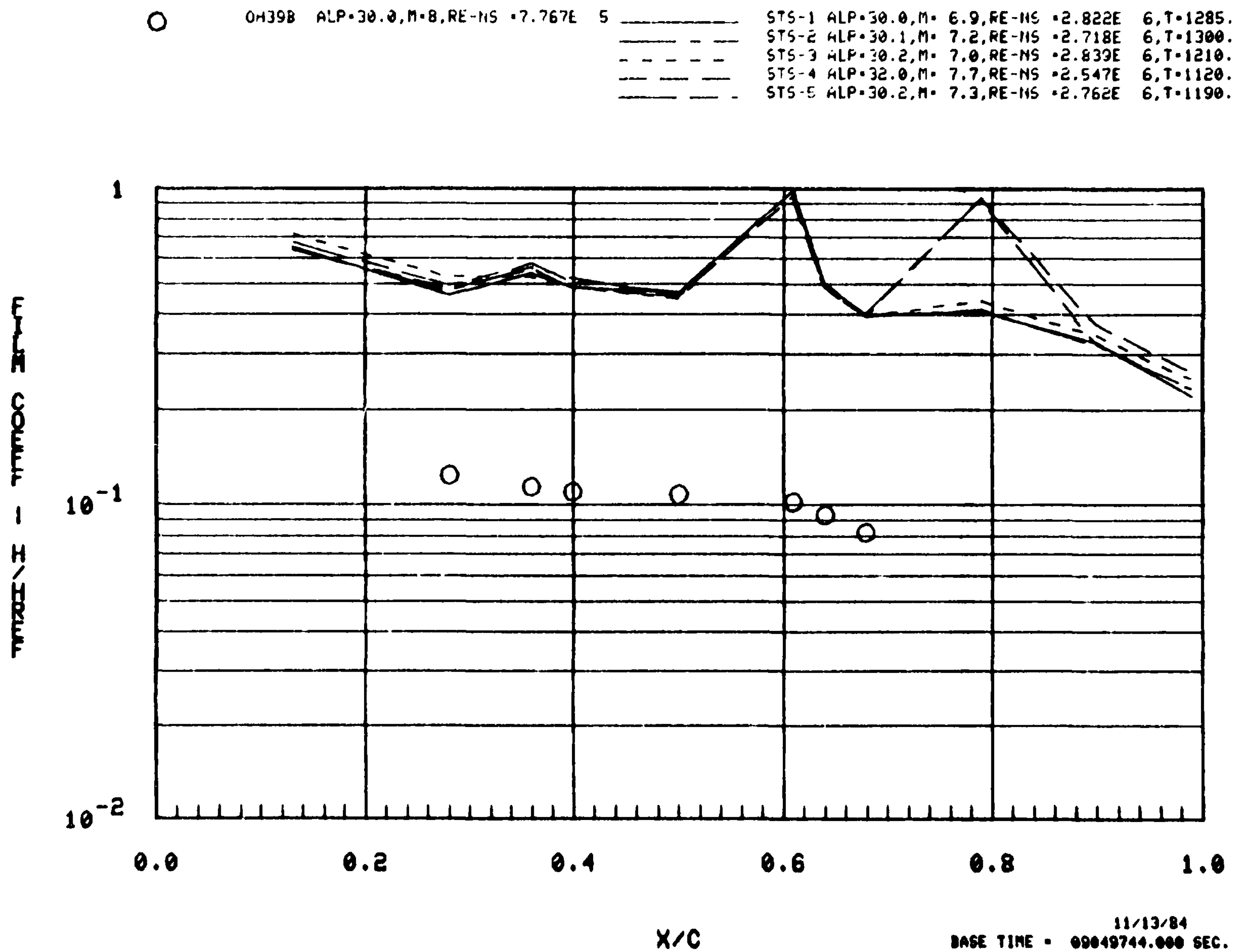

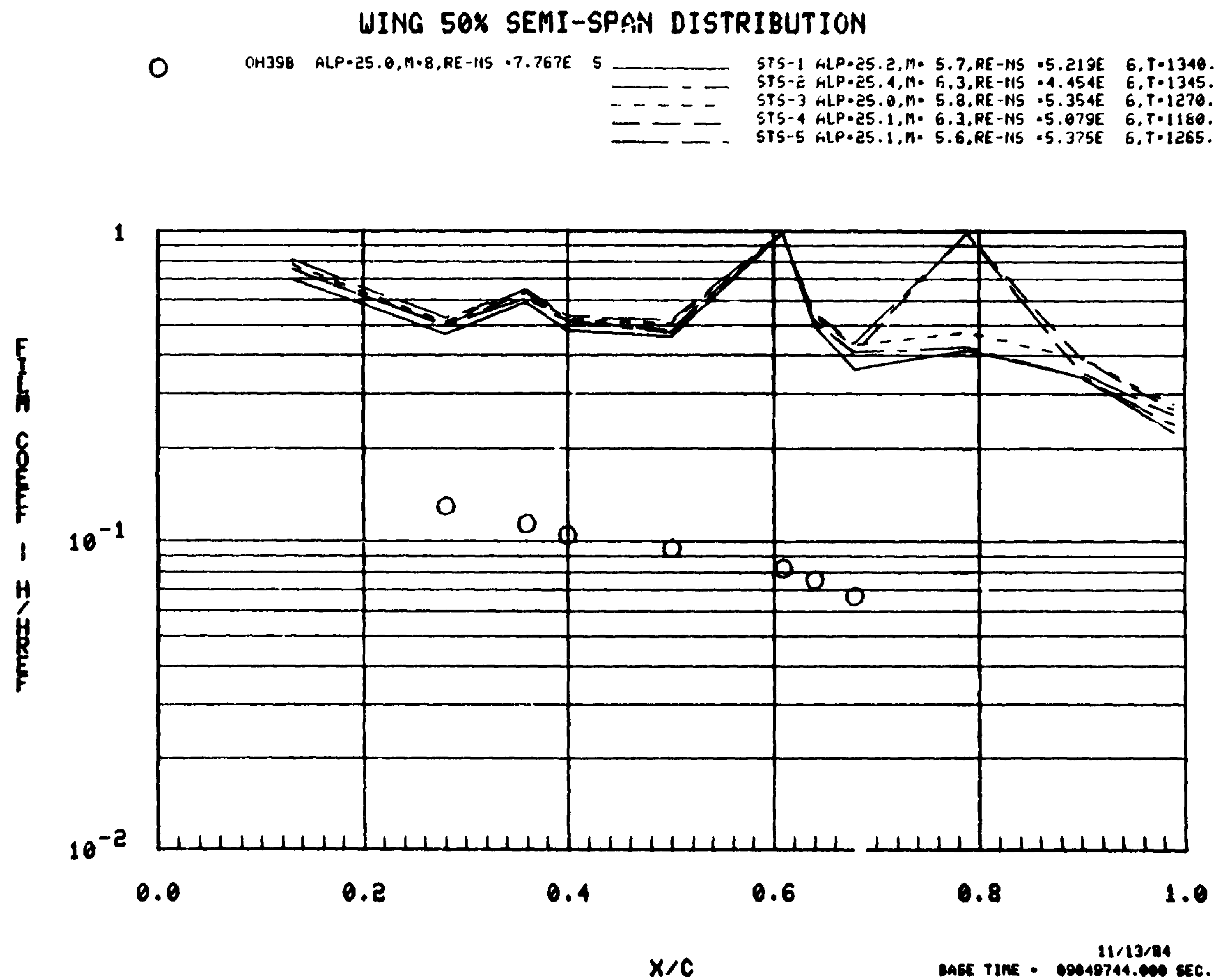

WING 50% SEMI-SPAN DISTRIBUTION
OH39B ALP=25.0,M=8,RE-NS =7.767E 5
STS-1 ALP=25.2,M= 5.7,RE-NS =5.219E 6,T=1340.
STS-2 ALP=25.4,M= 6.3,RE-NS =4.454E 6,T=1345.
STS-3 ALP=25.0,M= 5.8,RE-NS =5.354E 6,T=1270.
STS-4 ALP=25.1,M= 6.3,RE-NS =5.079E 6,T=1180.
STS-5 ALP=25.1,M= 5.6,RE-NS =5.375E 6,T=1265.
FILM COEFF - H/HREF
1
10^{-1}
10^{-2}
0.0
0.2
0.4
0.6
0.8
1.0
X/C
11/13/84
BASE TIME = 09049744.000 SEC.

WING 50% SEMI-SPAN DISTRIBUTION

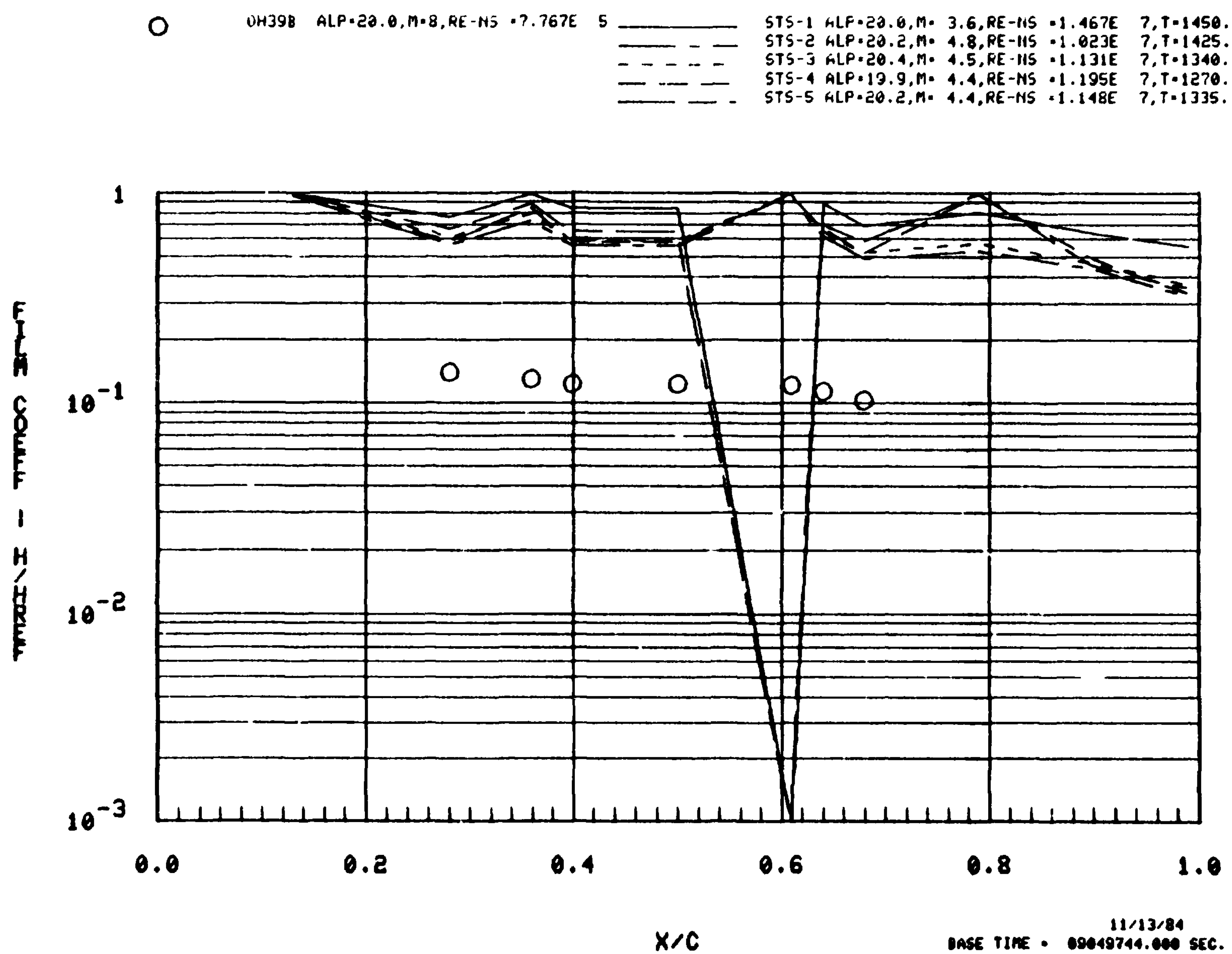

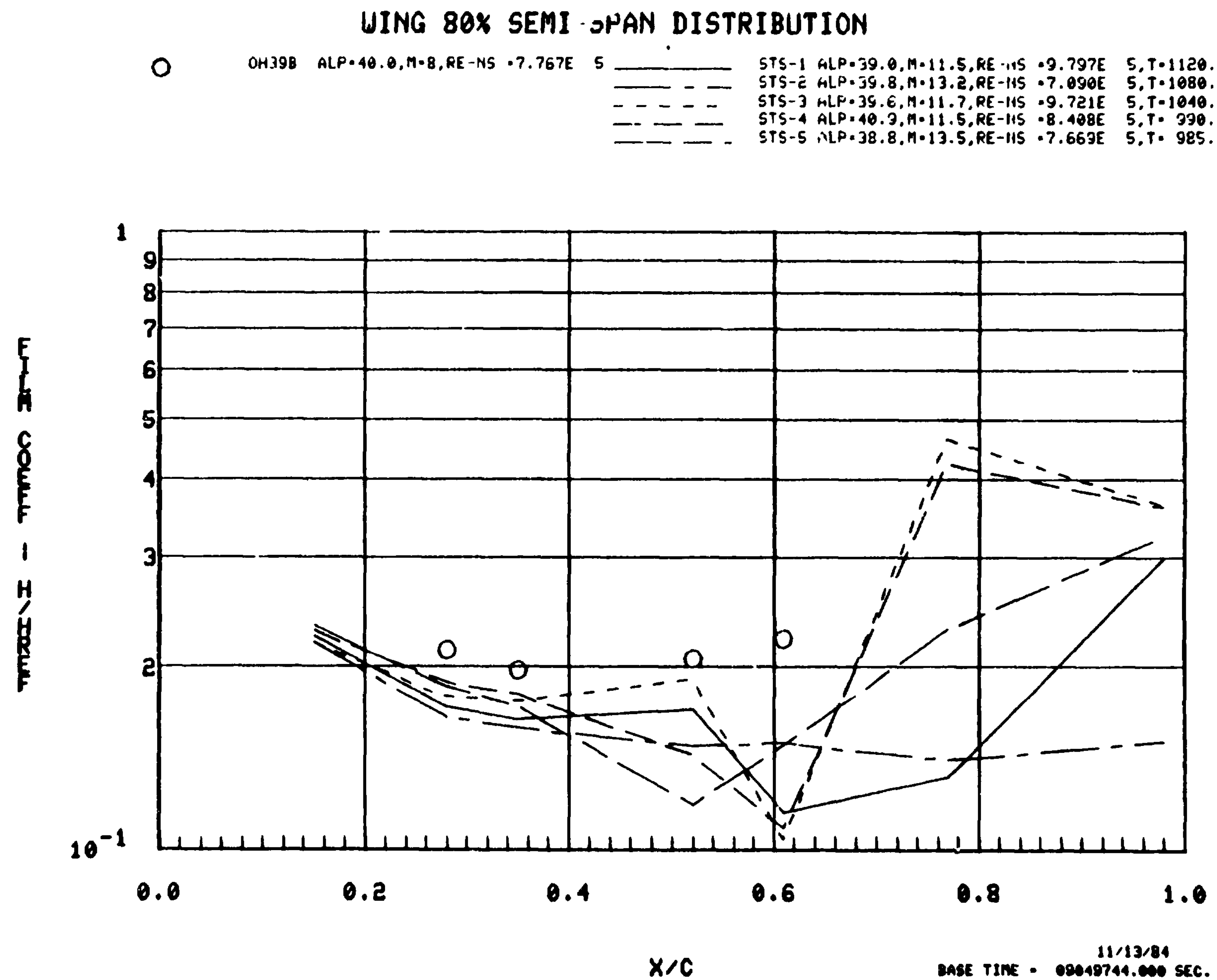

WING 80% SEMI-SPAN DISTRIBUTION
OH39B ALP=40.0,M=8,RE-NS =7.767E 5
STS-1 ALP=39.0,M=11.5,RE-NS =9.797E 5,T=1120.
STS-2 ALP=39.8,M=13.2,RE-NS =7.090E 5,T=1080.
STS-3 ALP=39.6,M=11.7,RE-NS =9.721E 5,T=1040.
STS-4 ALP=40.9,M=11.5,RE-NS =8.408E 5,T= 990.
STS-5 ALP=38.8,M=13.5,RE-NS =7.669E 5,T= 985.
FILM COEFF - H/HREF
X/C
11/13/84
BASE TIME = 09049744.000 SEC.

WING 80% SEMI-SPAN DISTRIBUTION

○ OH39B ALP=35.0,M=8,RE-NS =7.767E 5

STS-1 ALP=34.8,M= 9.0,RE-NS =1.576E 6,T=1195.
STS-2 ALP=35.5,M= 9.2,RE-NS =1.601E 6,T=1215.
STS-3 ALP=35.3,M= 9.2,RE-NS =1.611E 6,T=1120.
STS-4 ALP=34.9,M= 8.8,RE-NS =1.849E 6,T=1080.
STS-5 ALP=35.1,M= 8.5,RE-NS =1.762E 6,T=1140.

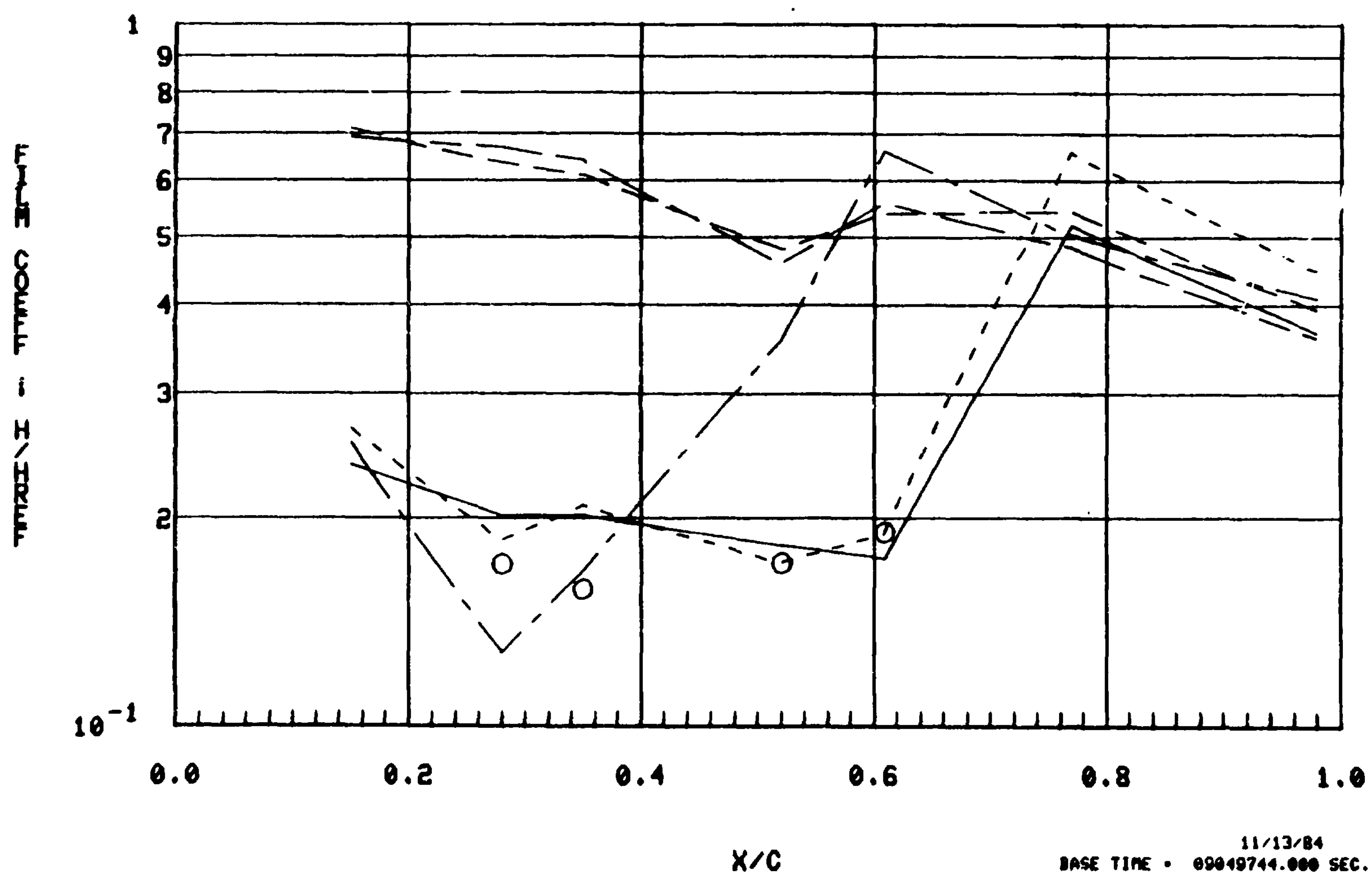

11/13/84
BASE TIME = 09049744.000 SEC.

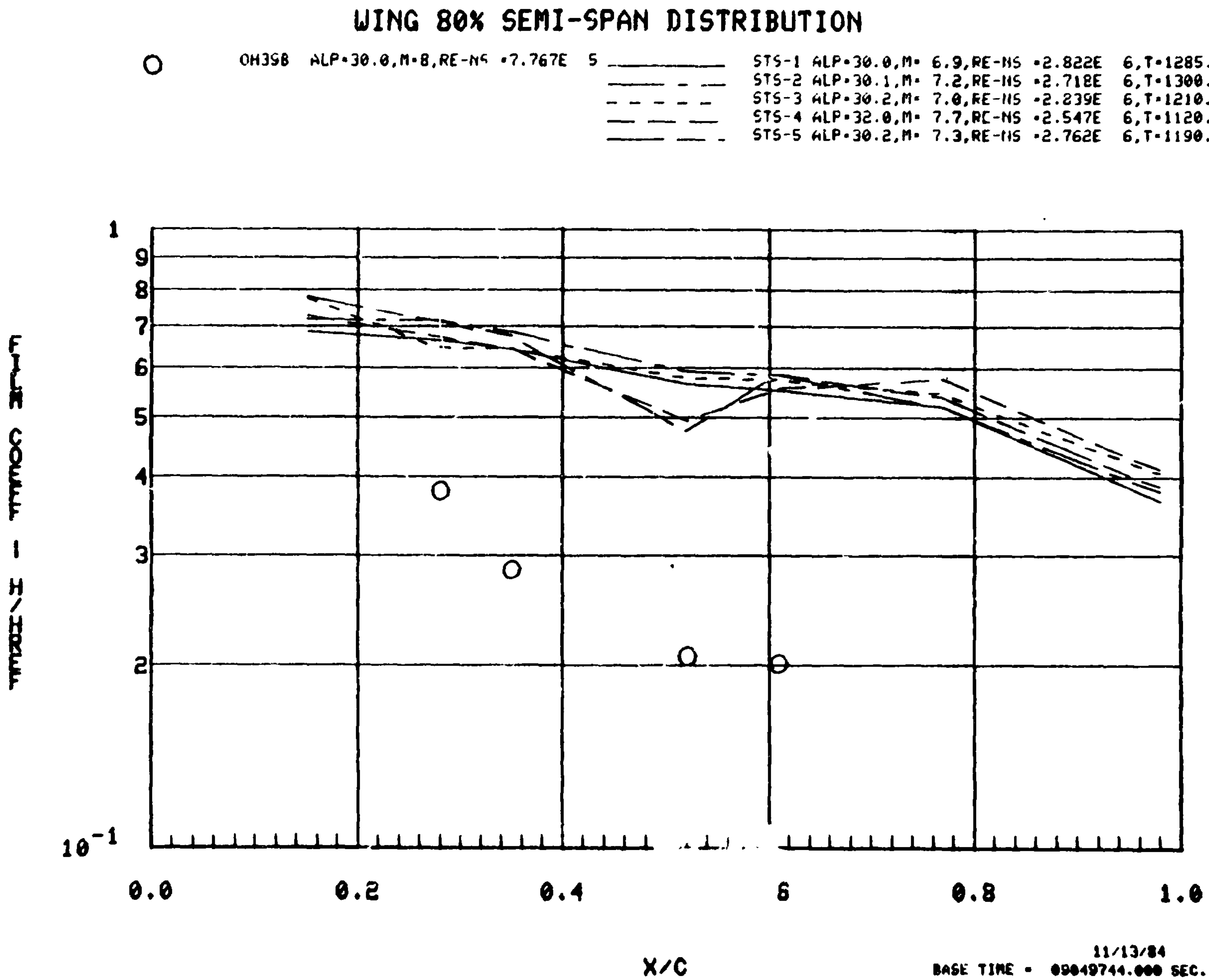
WING 80% SEMI-SPAN DISTRIBUTION
OH39B ALP=30.0,M=8,RE-NS =7.767E 5
STS-1 ALP=30.0,M= 6.9,RE-NS =2.822E 6,T=1285.
STS-2 ALP=30.1,M= 7.2,RE-NS =2.718E 6,T=1300.
STS-3 ALP=30.2,M= 7.0,RE-NS =2.239E 6,T=1210.
STS-4 ALP=32.0,M= 7.7,RE-NS =2.547E 6,T=1120.
STS-5 ALP=30.2,M= 7.3,RE-NS =2.762E 6,T=1190.
FILM COEFF - H/HREF
X/C
11/13/84
BASE TIME = 09049744.000 SEC.

WING 80% SEMI-SPAN DISTRIBUTION

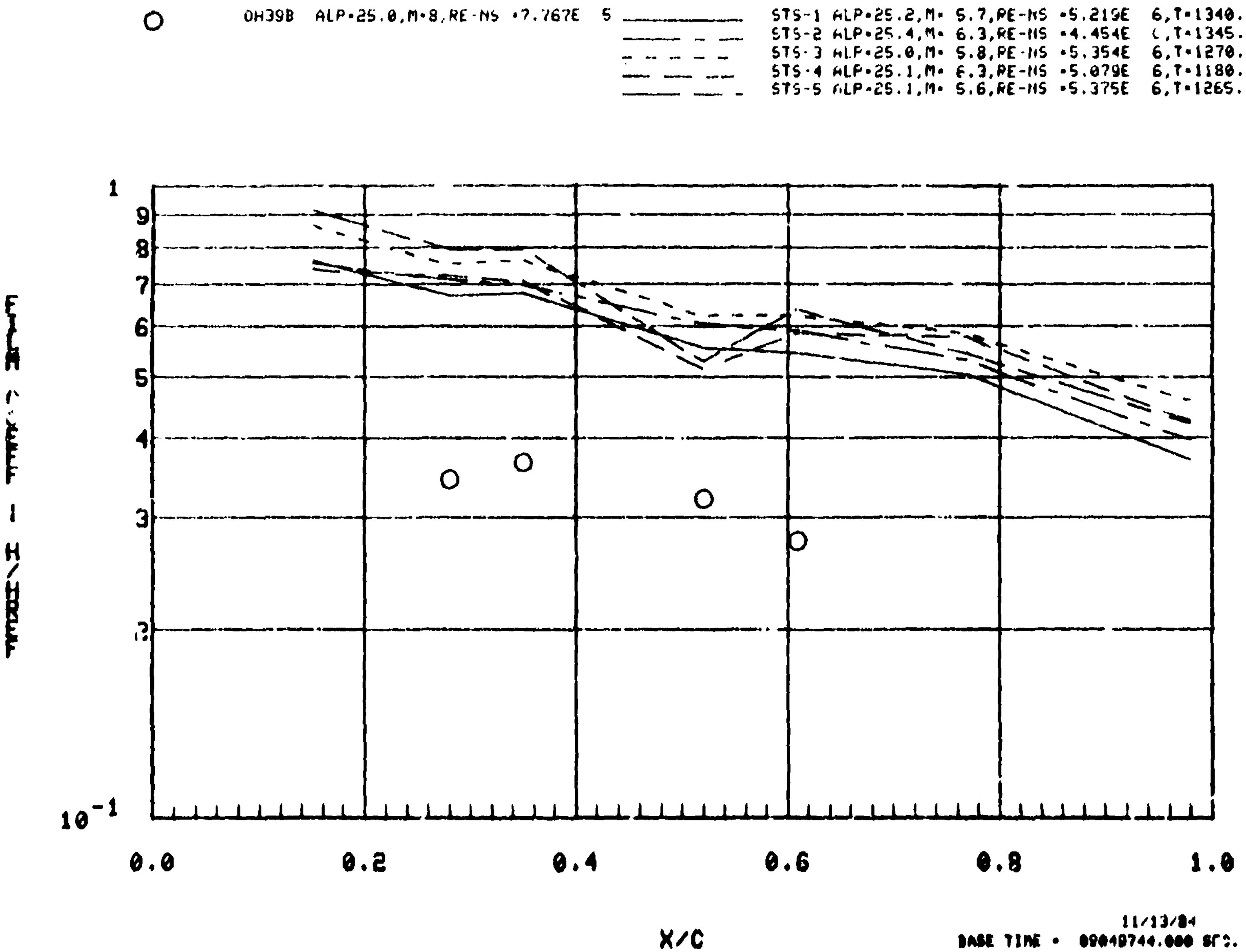

WING 80% SEMI-SPAN DISTRIBUTION

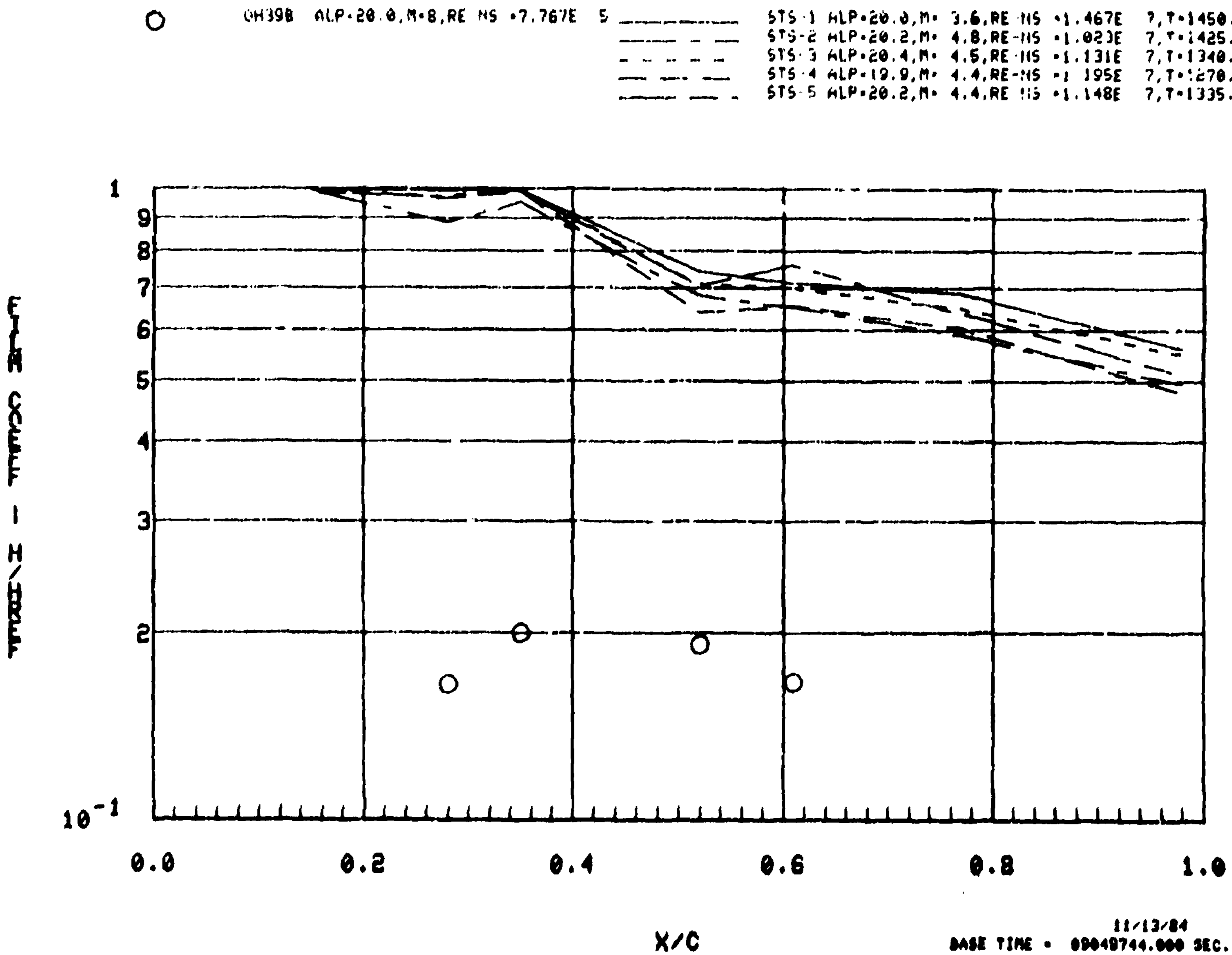

SIDE FUSELAGE (Z=400 TRACE) DISTRIBUTION

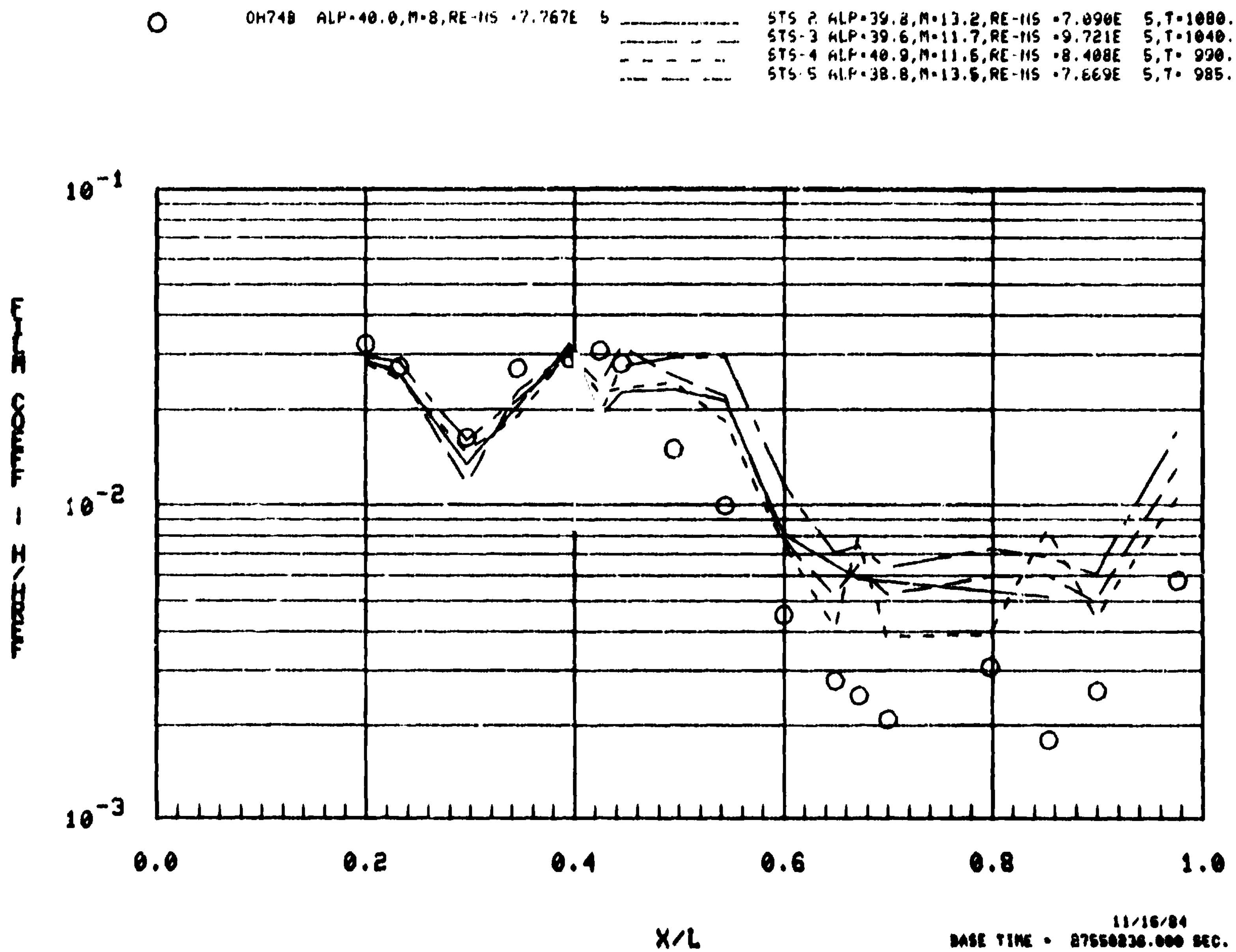

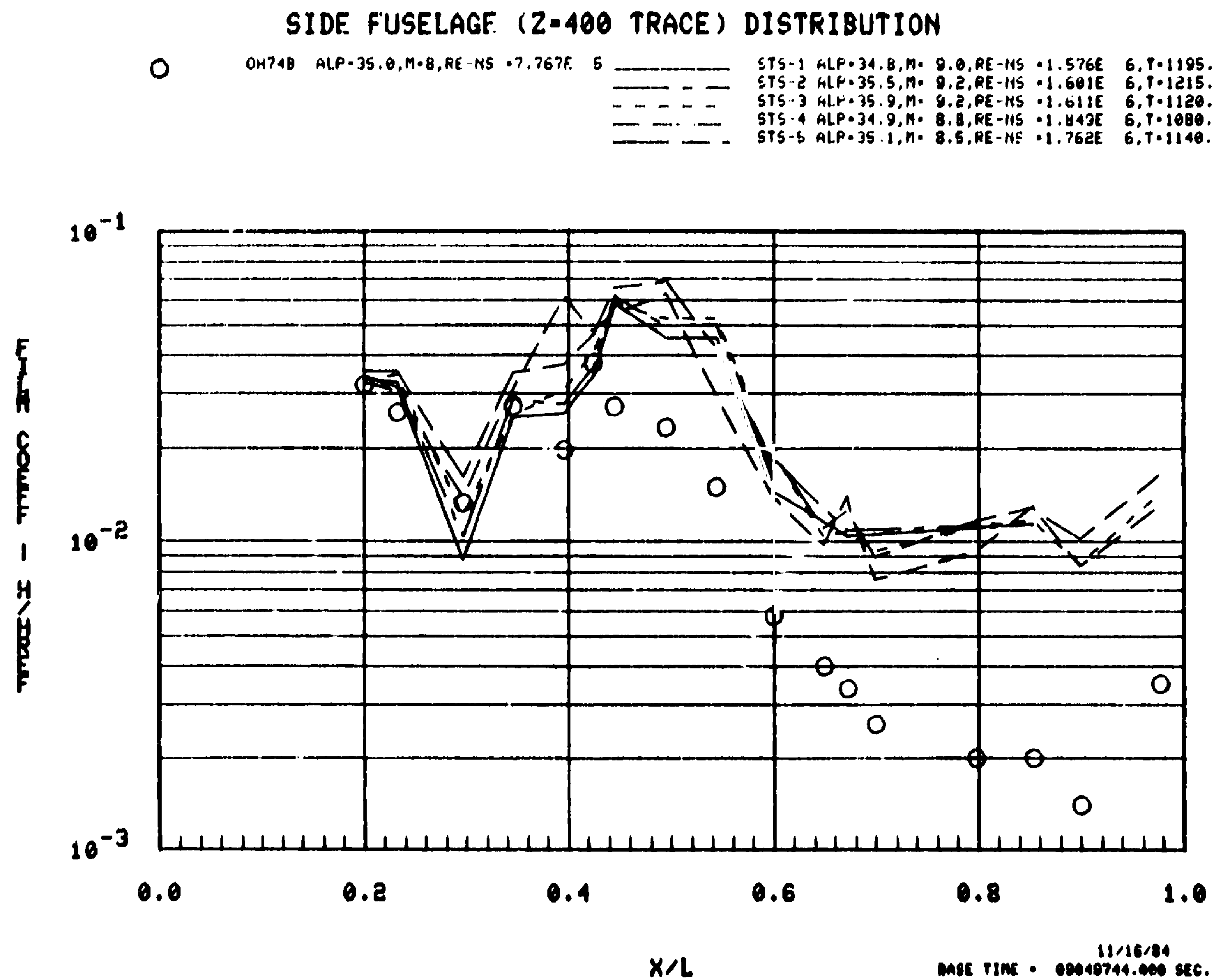
SIDE FUSELAGE (Z=400 TRACE) DISTRIBUTION
OH74B ALP=35.0,M=8,RE-NS =7.767E 5
STS-1 ALP=34.8,M= 9.0,RE-NS =1.576E 6,T=1195.
STS-2 ALP=35.5,M= 9.2,RE-NS =1.601E 6,T=1215.
STS-3 ALP=35.9,M= 9.2,RE-NS =1.611E 6,T=1120.
STS-4 ALP=34.9,M= 8.8,RE-NS =1.843E 6,T=1080.
STS-5 ALP=35.1,M= 8.6,RE-NS =1.762E 6,T=1140.
FILM COEFF - H/HREF
10^{-1}
10^{-2}
10^{-3}
0.0
0.2
0.4
0.6
0.8
1.0
X/L
11/16/84
BASE TIME = 09049744.000 SEC.

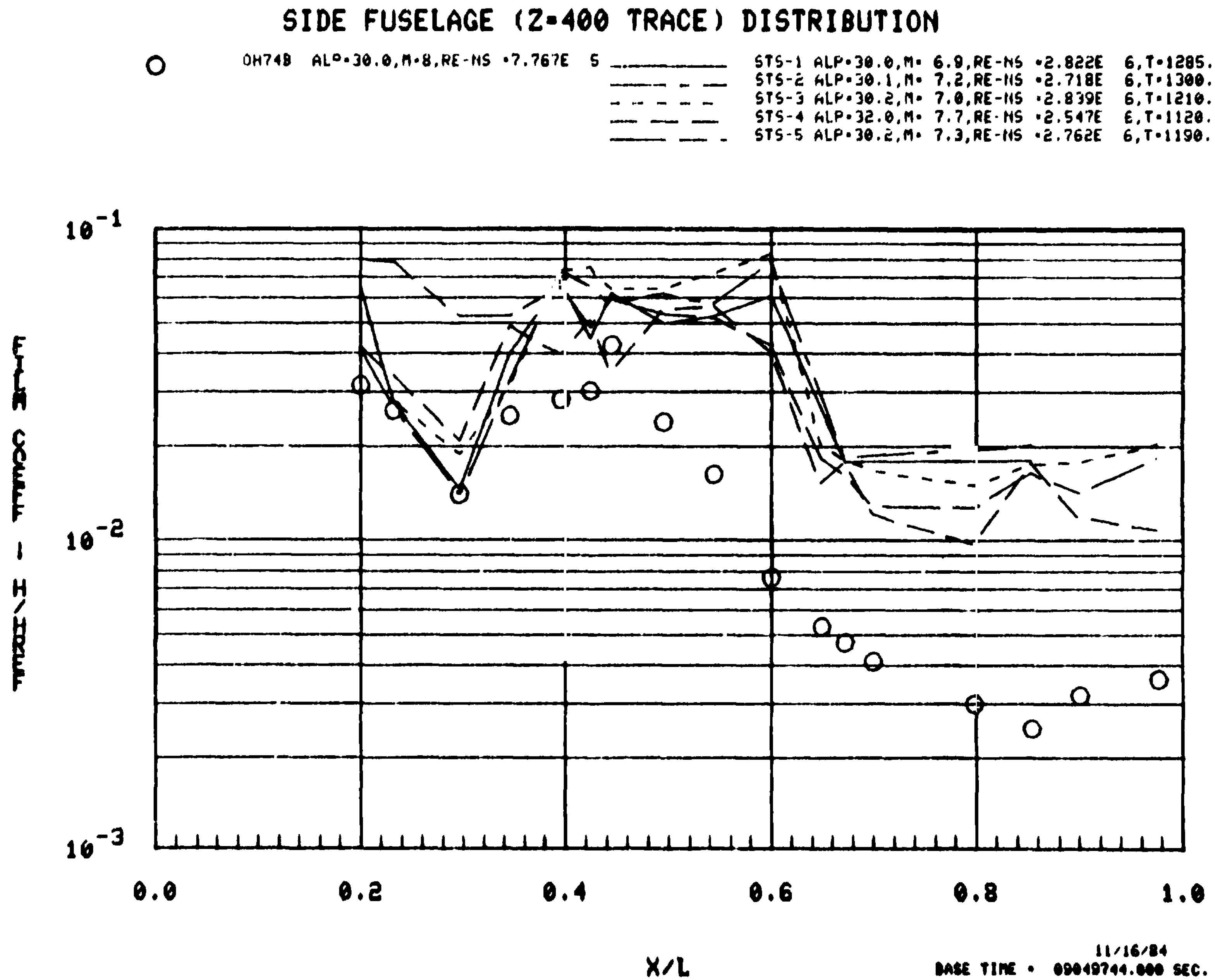

SIDE FUSELAGE (Z=400 TRACE) DISTRIBUTION
OH74B AL°=30.0,M=8,RE-NS =7.767E 5
STS-1 ALP=30.0,M= 6.9,RE-NS =2.822E 6,T=1285.
STS-2 ALP=30.1,M= 7.2,RE-NS =2.718E 6,T=1300.
STS-3 ALP=30.2,M= 7.0,RE-NS =2.839E 6,T=1210.
STS-4 ALP=32.0,M= 7.7,RE-NS =2.547E 6,T=1120.
STS-5 ALP=30.2,M= 7.3,RE-NS =2.762E 6,T=1190.
FILM COEFF - H/HREF
10^{-1}
10^{-2}
10^{-3}
0.0
0.2
0.4
0.6
0.8
1.0
X/L
11/16/84
BASE TIME = 09049744.000 SEC.

SIDE FUSELAGE (Z=400 TRACE) DISTRIBUTION

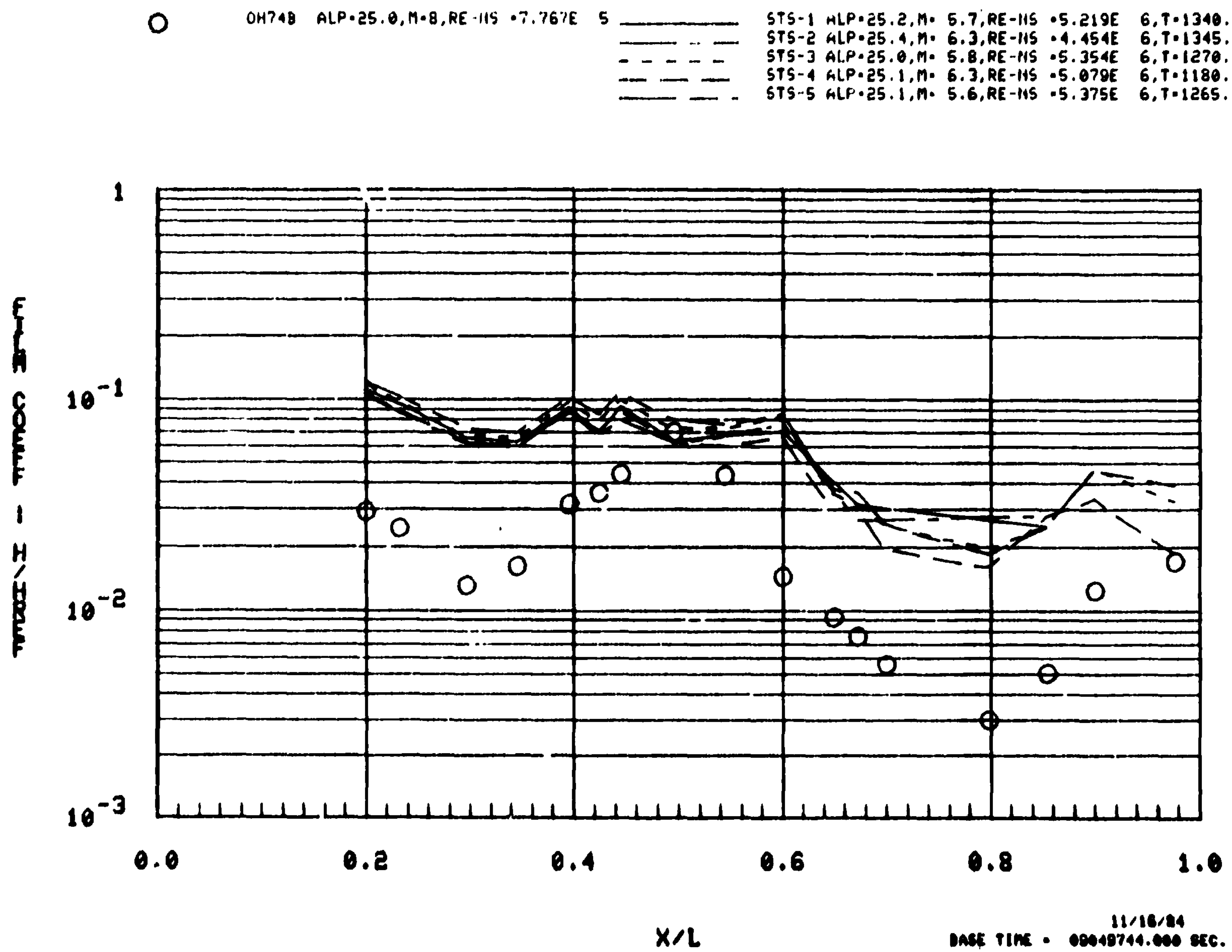

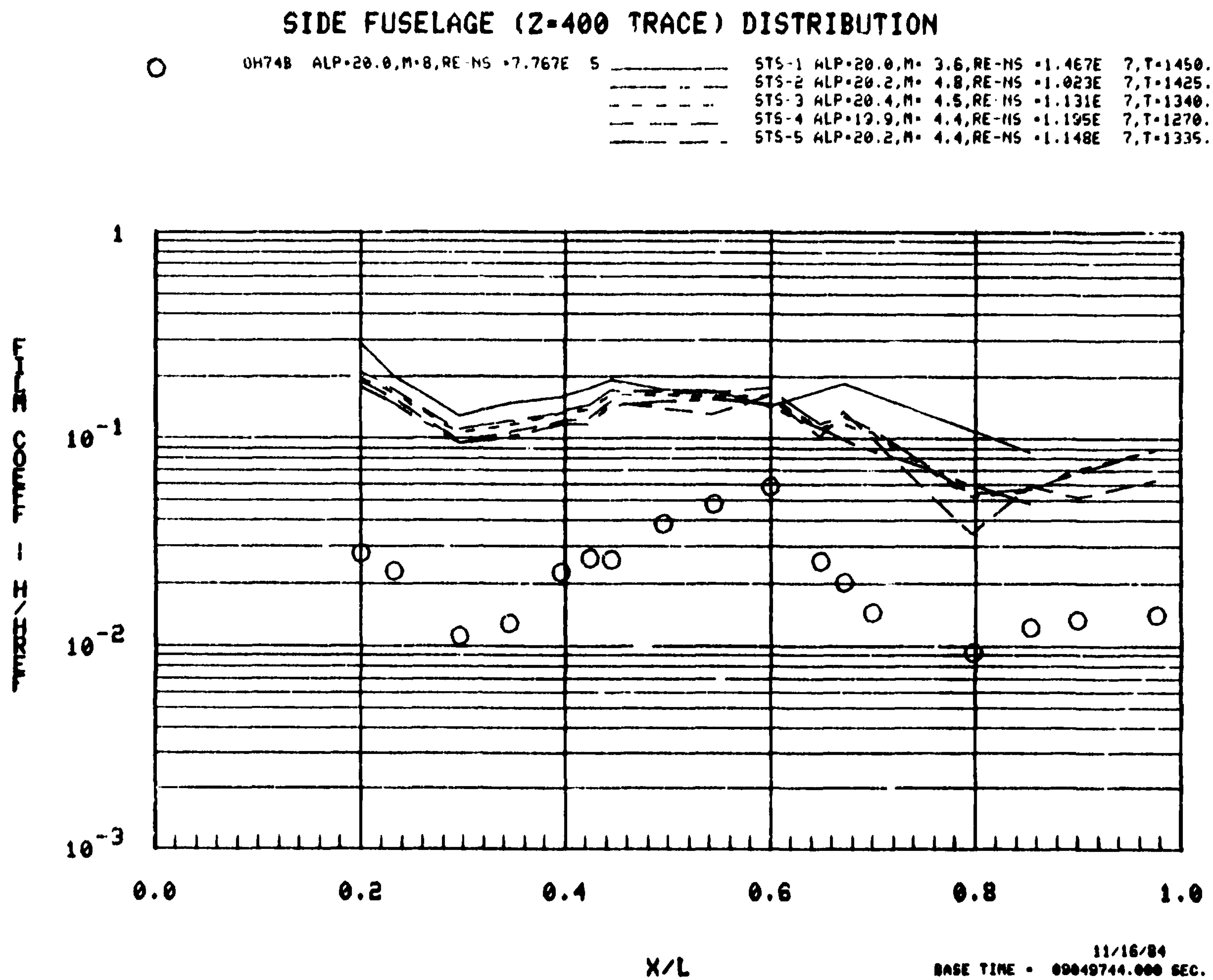

SIDE FUSELAGE (Z=400 TRACE) DISTRIBUTION
OH74B ALP=20.0,M=8,RE-NS =7.767E 5
STS-1 ALP=20.0,M= 3.6,RE-NS =1.467E 7,T=1450.
STS-2 ALP=20.2,M= 4.8,RE-NS =1.023E 7,T=1425.
STS-3 ALP=20.4,M= 4.5,RE-NS =1.131E 7,T=1340.
STS-4 ALP=19.9,M= 4.4,RE-NS =1.195E 7,T=1270.
STS-5 ALP=20.2,M= 4.4,RE-NS =1.148E 7,T=1335.
FILM COEFF - H/HREF
1
10^{-1}
10^{-2}
10^{-3}
0.0
0.2
0.4
0.6
0.8
1.0
X/L
11/16/84
BASE TIME = 09049744.000 SEC.

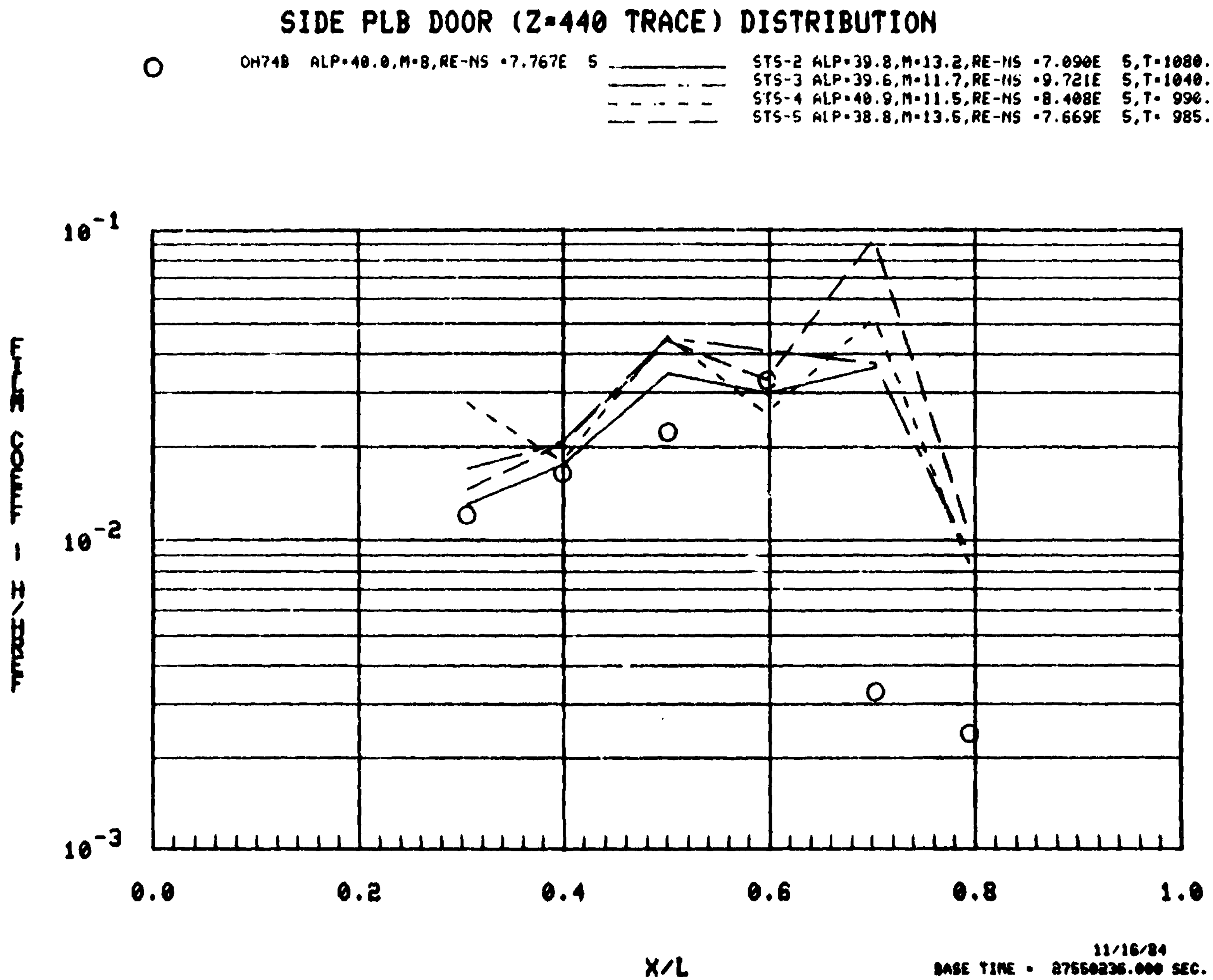

SIDE PLB DOOR (Z=440 TRACE) DISTRIBUTION
OH74B ALP=40.0,M=8,RE-NS =7.767E 5
STS-2 ALP=39.8,M=13.2,RE-NS =7.090E 5,T=1080.
STS-3 ALP=39.6,M=11.7,RE-NS =9.721E 5,T=1040.
STS-4 ALP=40.9,M=11.5,RE-NS =8.408E 5,T= 990.
STS-5 ALP=38.8,M=13.6,RE-NS =7.669E 5,T= 985.
FILM COEFF - H/HREF
10⁻¹
10⁻²
10⁻³
0.0
0.2
0.4
0.6
0.8
1.0
X/L
11/16/84
BASE TIME = 87550236.000 SEC.

SIDE PLB DOOR (Z-440 TRACE) DISTRIBUTION

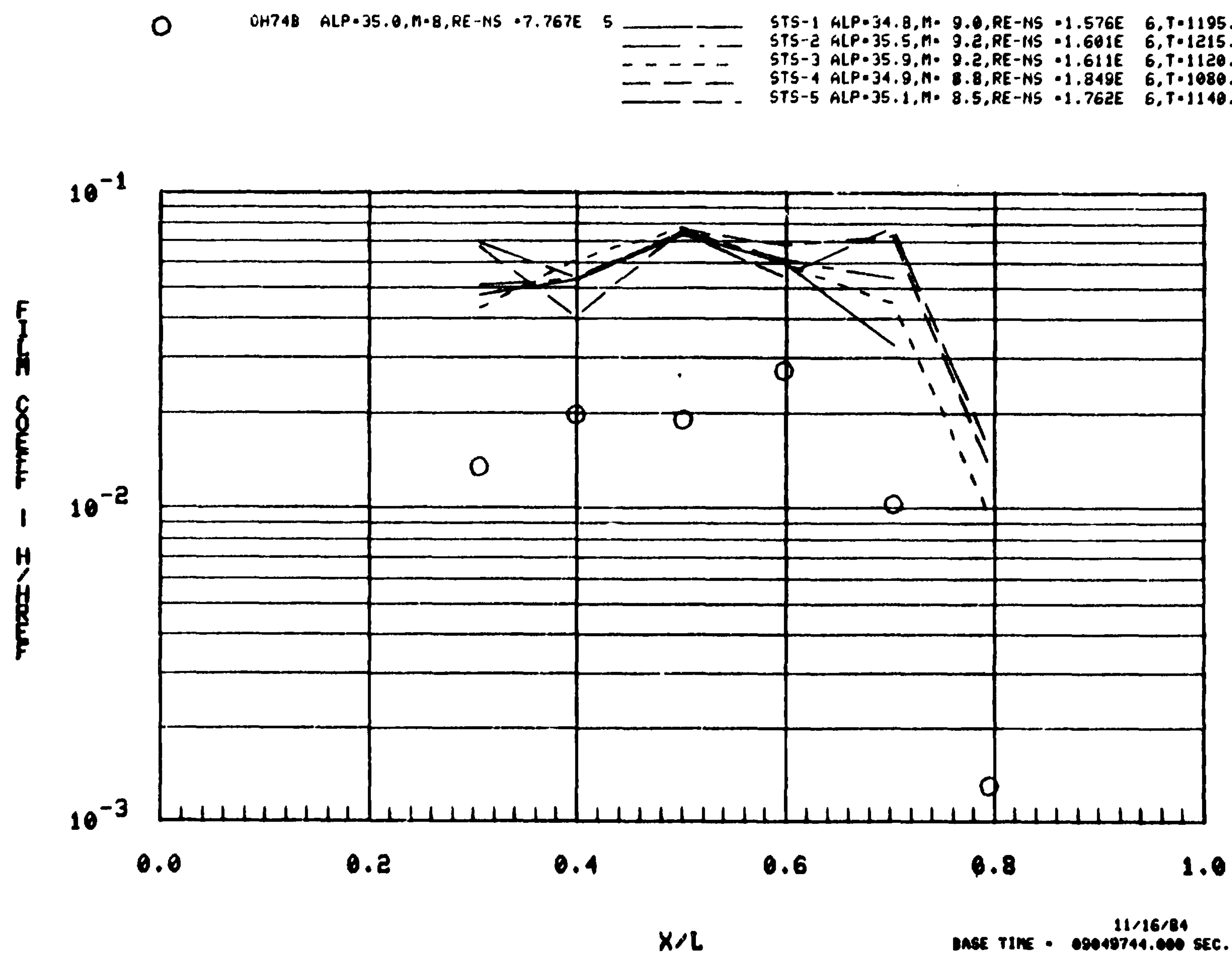

SIDE PLB DOOR (Z=440 TRACE) DISTRIBUTION

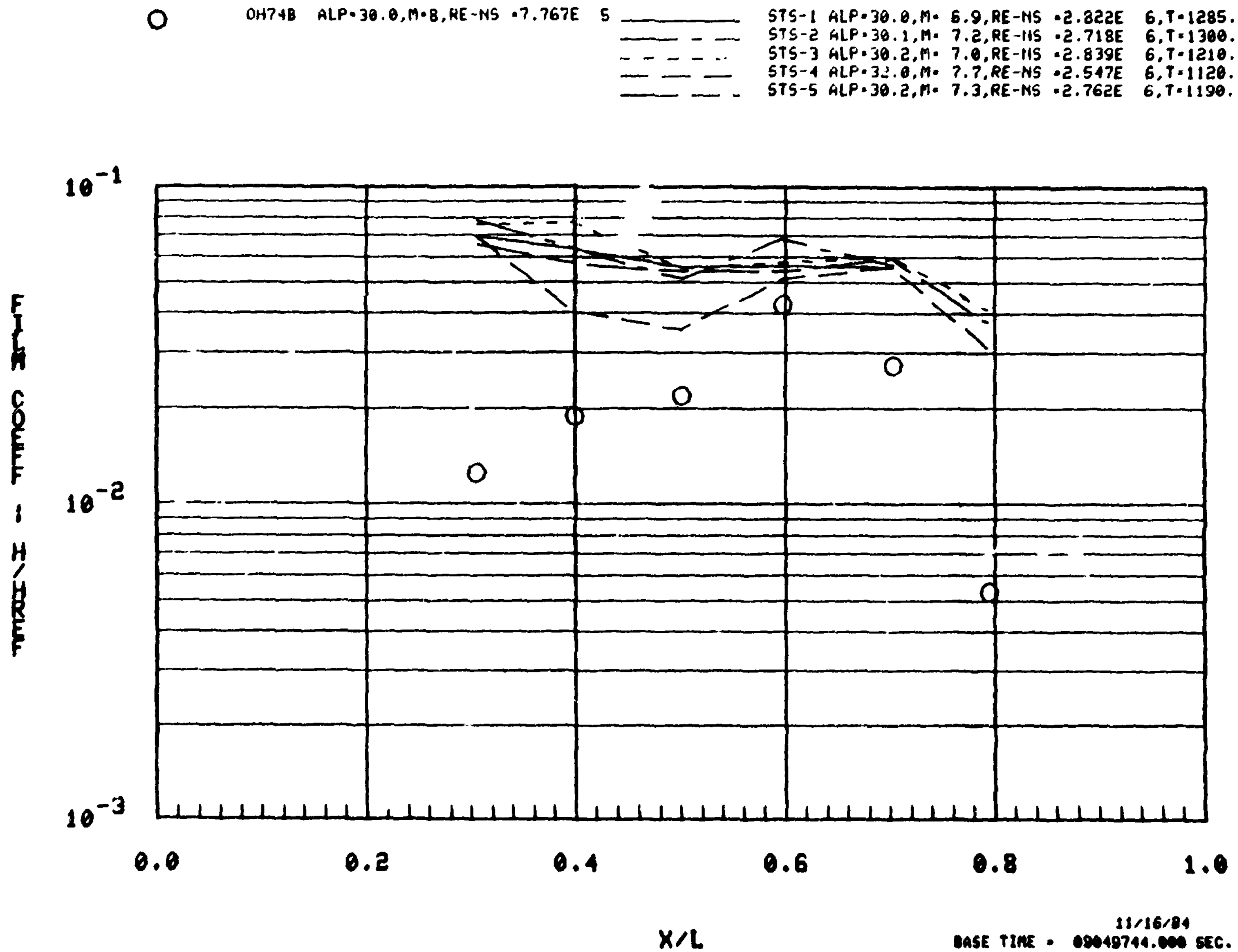

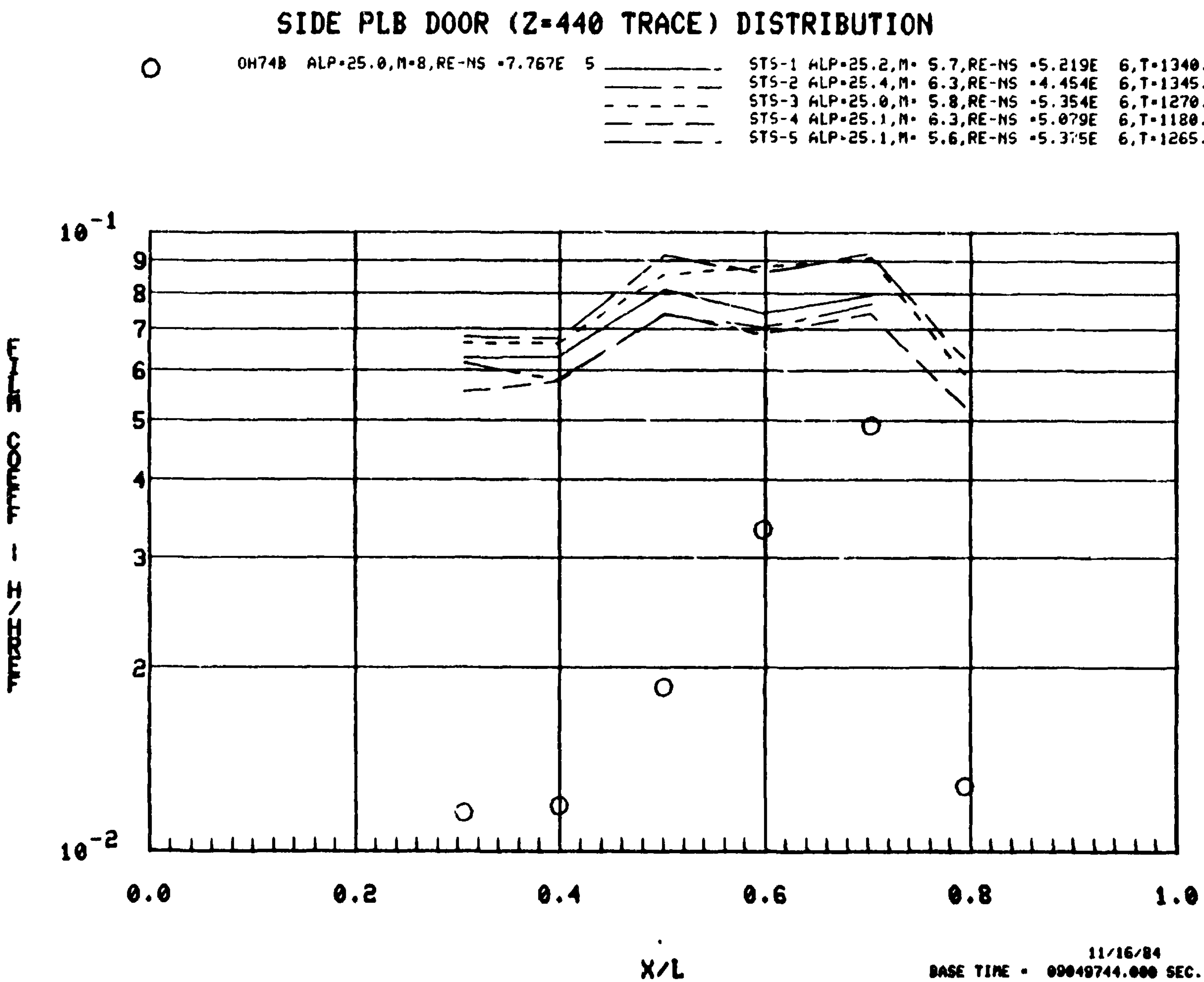

SIDE PLB DOOR (Z=440 TRACE) DISTRIBUTION
OH74B ALP=25.0,M=8,RE-NS =7.767E 5
STS-1 ALP=25.2,M= 5.7,RE-NS =5.219E 6,T=1340.
STS-2 ALP=25.4,M= 6.3,RE-NS =4.454E 6,T=1345.
STS-3 ALP=25.0,M= 5.8,RE-NS =5.354E 6,T=1270.
STS-4 ALP=25.1,M= 6.3,RE-NS =5.079E 6,T=1180.
STS-5 ALP=25.1,M= 5.6,RE-NS =5.375E 6,T=1265.
FILM COEFF - H/HREF
X/L
11/16/84
BASE TIME = 09049744.000 SEC.

SIDE PLB DOOR (Z=440 TRACE) DISTRIBUTION

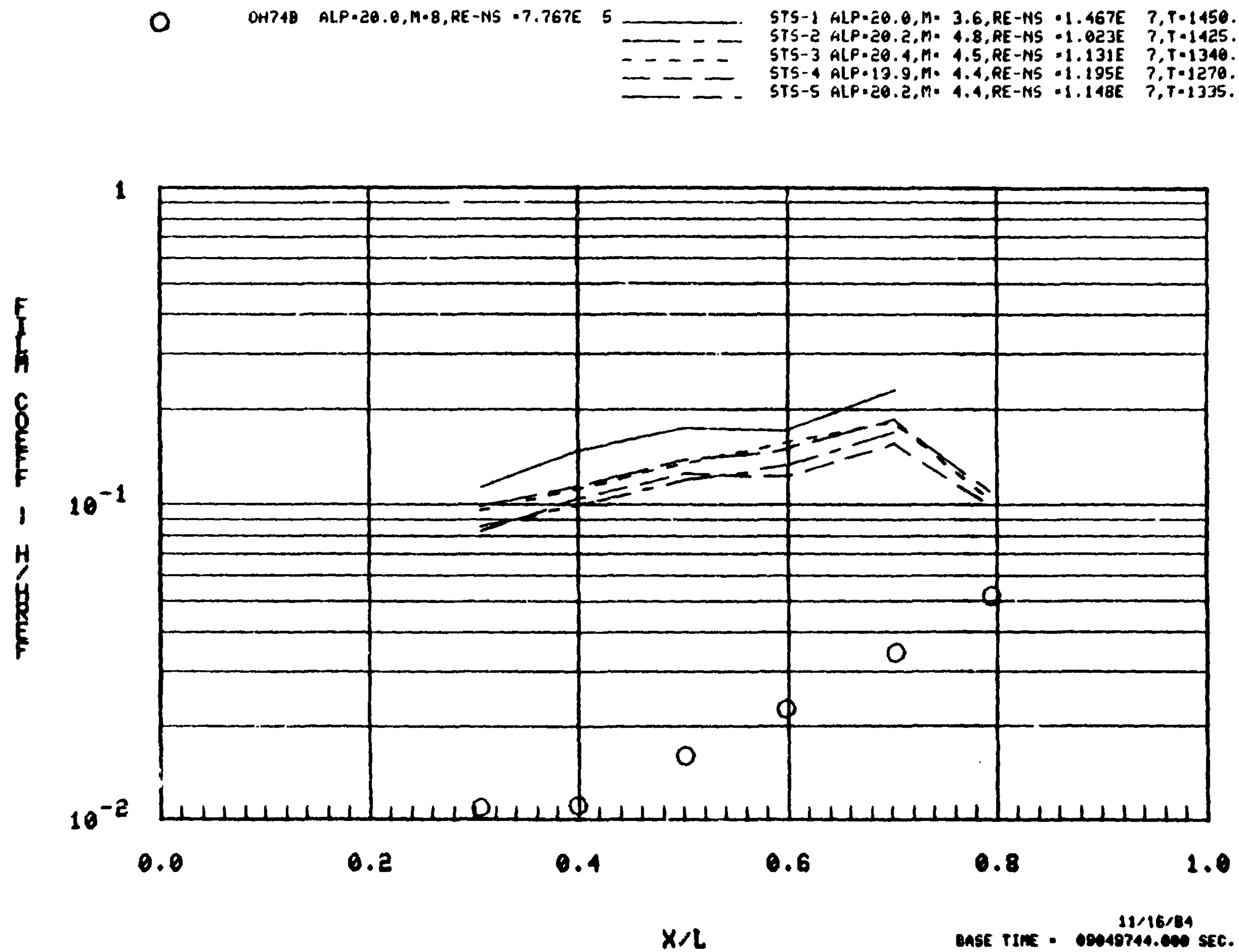

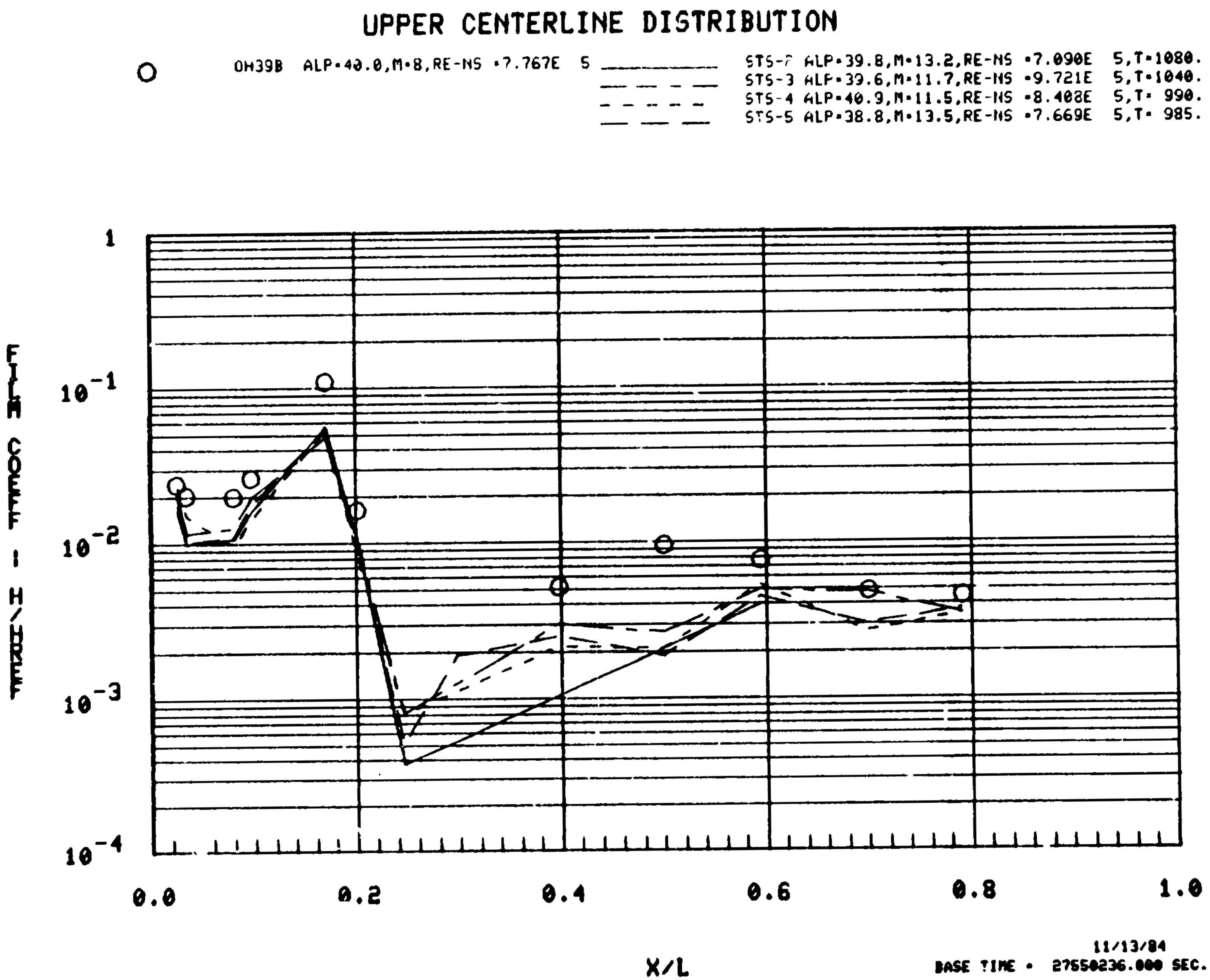

UPPER CENTERLINE DISTRIBUTION
OH39B ALP=40.0,M=8,RE-NS =7.767E 5
STS-2 ALP=39.8,M=13.2,RE-NS =7.090E 5,T=1080.
STS-3 ALP=39.6,M=11.7,RE-NS =9.721E 5,T=1040.
STS-4 ALP=40.9,M=11.5,RE-NS =8.408E 5,T= 990.
STS-5 ALP=38.8,M=13.5,RE-NS =7.669E 5,T= 985.
FILM COEFF : H/HREF
1
10-1
10-2
10-3
10-4
0.0
0.2
0.4
0.6
0.8
1.0
X/L
11/13/84
BASE TIME = 27550236.000 SEC.

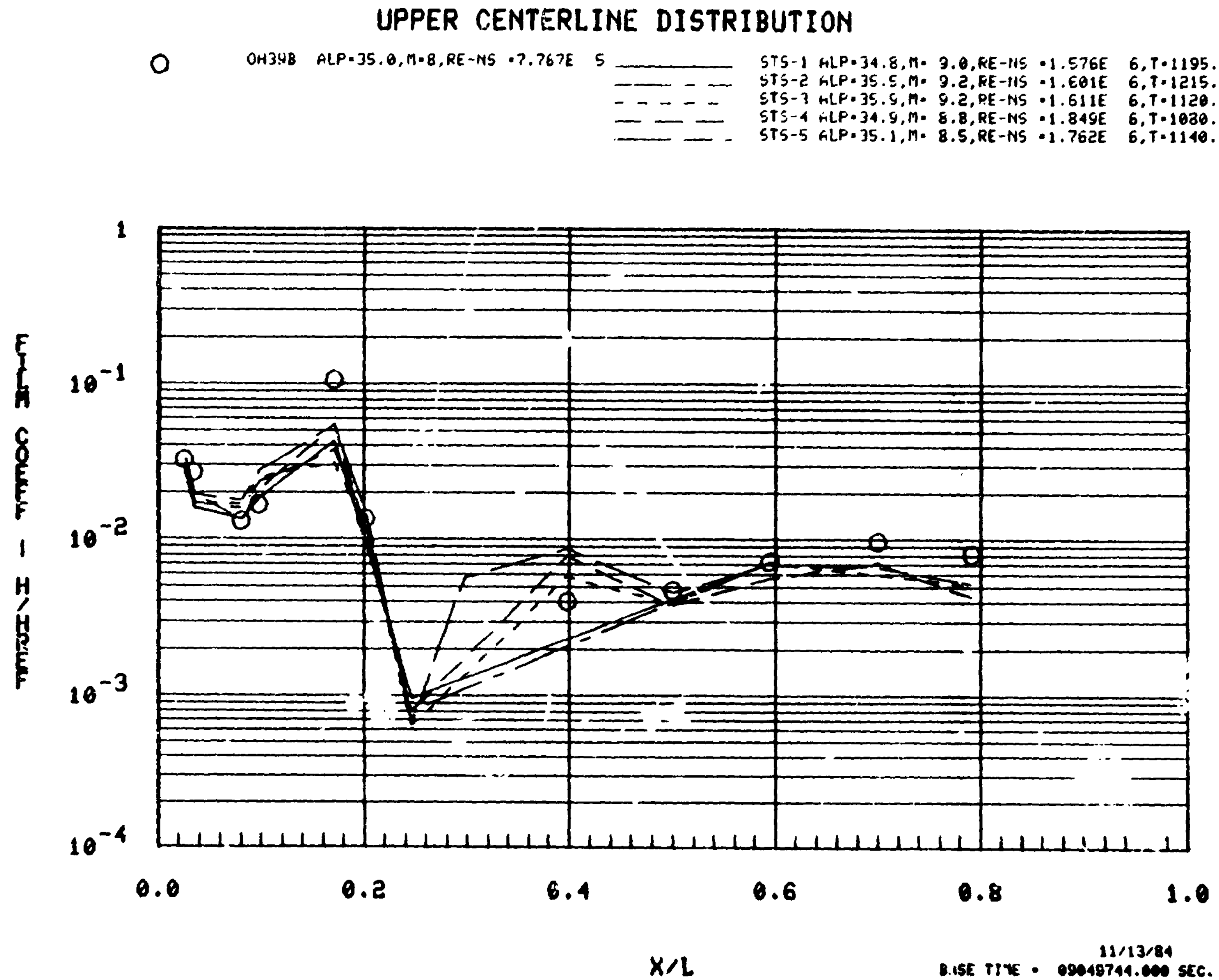
UPPER CENTERLINE DISTRIBUTION
OH39B ALP=35.0,M=8,RE-NS =7.767E 5
STS-1 ALP=34.8,M= 9.0,RE-NS =1.576E 6,T=1195.
STS-2 ALP=35.5,M= 9.2,RE-NS =1.601E 6,T=1215.
STS-3 ALP=35.5,M= 9.2,RE-NS =1.611E 6,T=1120.
STS-4 ALP=34.9,M= 8.8,RE-NS =1.849E 6,T=1080.
STS-5 ALP=35.1,M= 8.5,RE-NS =1.762E 6,T=1140.
FILM COEFF - H/HREF
1
10^-1
10^-2
10^-3
10^-4
0.0
0.2
0.4
0.6
0.8
1.0
X/L
11/13/84
BASE TIME = 09049744.000 SEC.

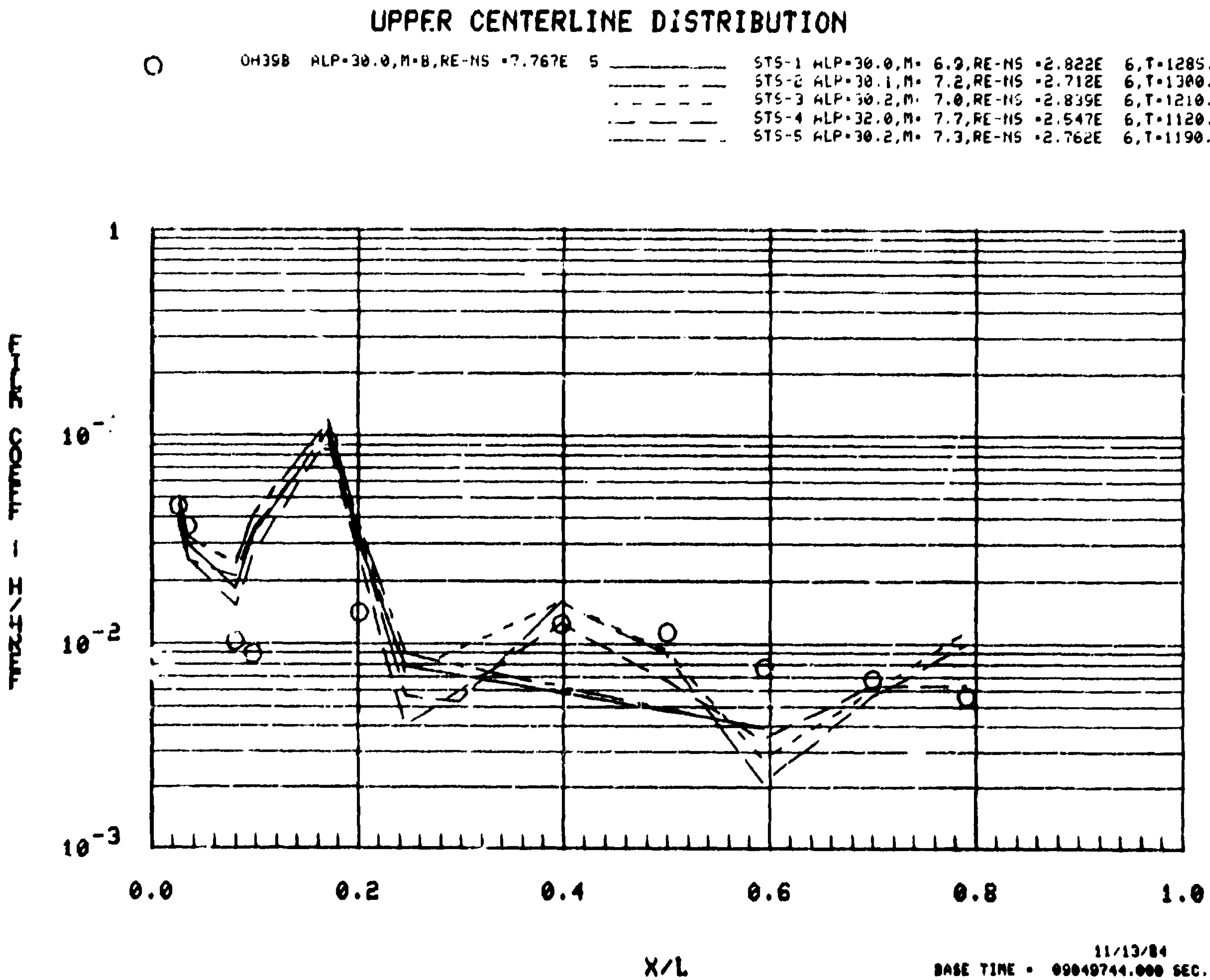

UPPER CENTERLINE DISTRIBUTION
OH39B ALP=30.0,M=8,RE-NS =7.767E 5
STS-1 ALP=30.0,M= 6.9,RE-NS =2.822E 6,T=1285.
STS-2 ALP=30.1,M= 7.2,RE-NS =2.712E 6,T=1300.
STS-3 ALP=30.2,M= 7.0,RE-NS =2.839E 6,T=1210.
STS-4 ALP=32.0,M= 7.7,RE-NS =2.547E 6,T=1120.
STS-5 ALP=30.2,M= 7.3,RE-NS =2.762E 6,T=1190.
FLT COEFF - H/HREF
X/L
11/13/84
BASE TIME = 09049744.000 SEC.

UPPER CENTERLINE DISTRIBUTION

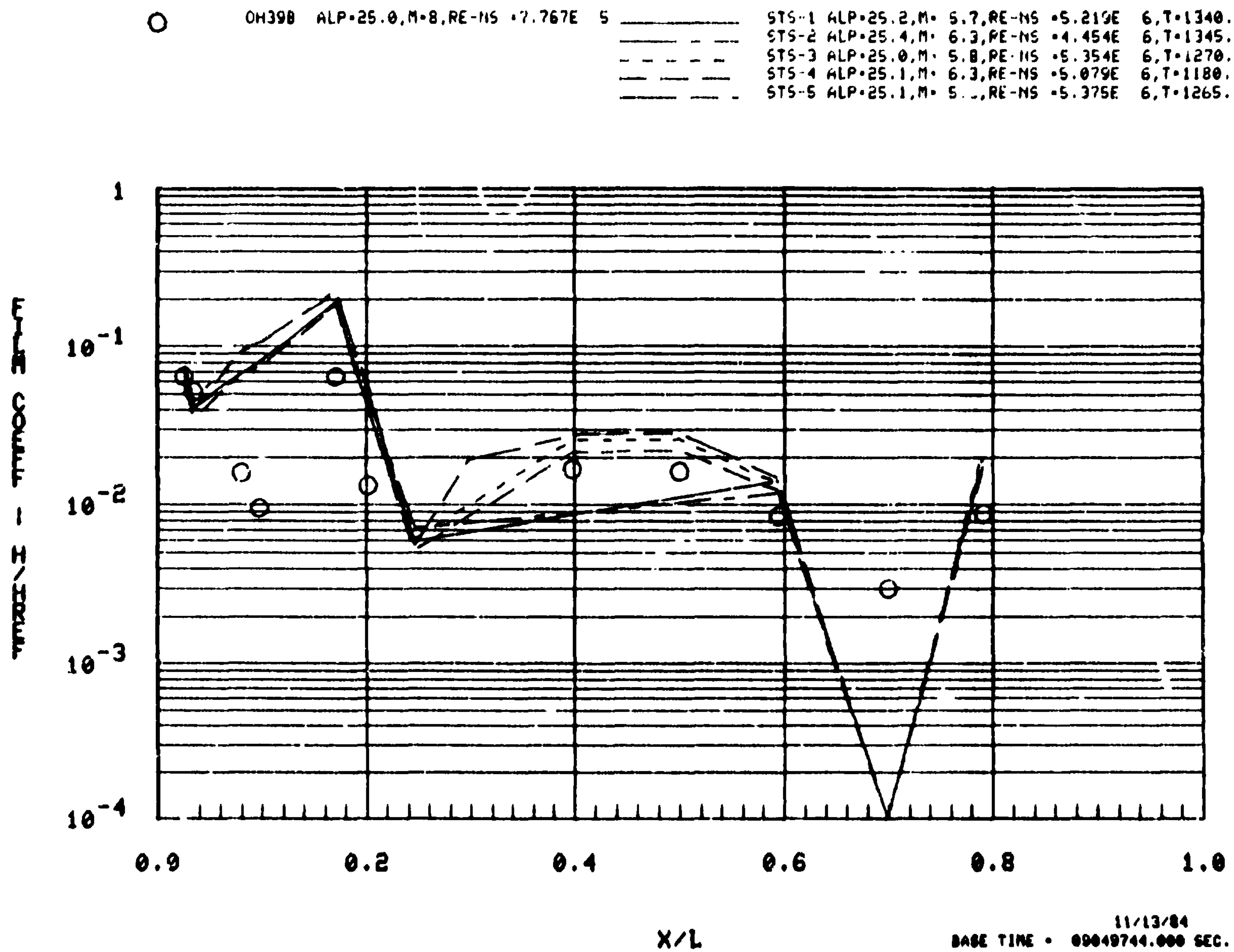

UPPER CENTERLINE DISTRIBUTION

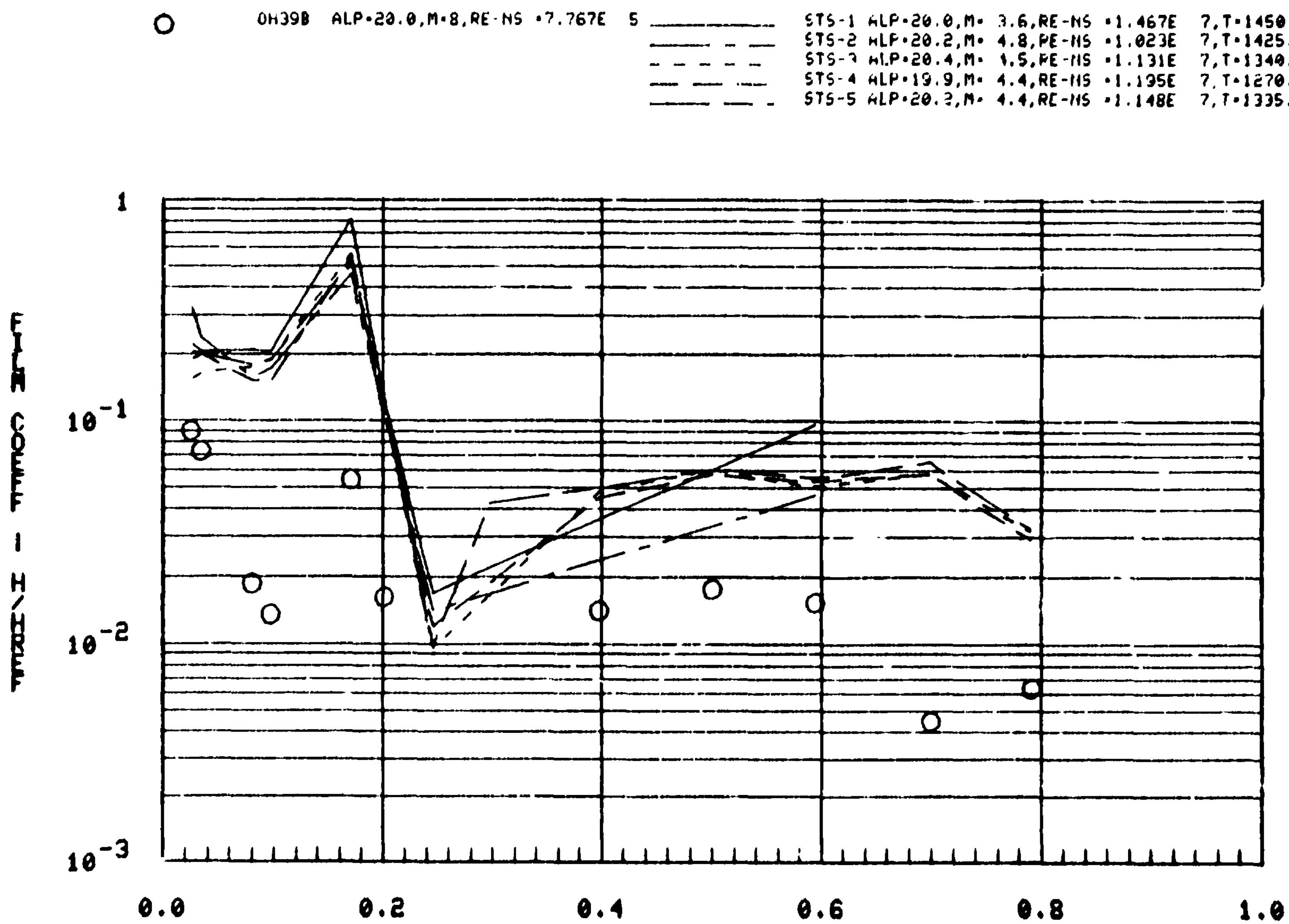

11/13/84
BASE TIME = 09049744.000 SEC.

OMS POD TRACE 3 DISTRIBUTION

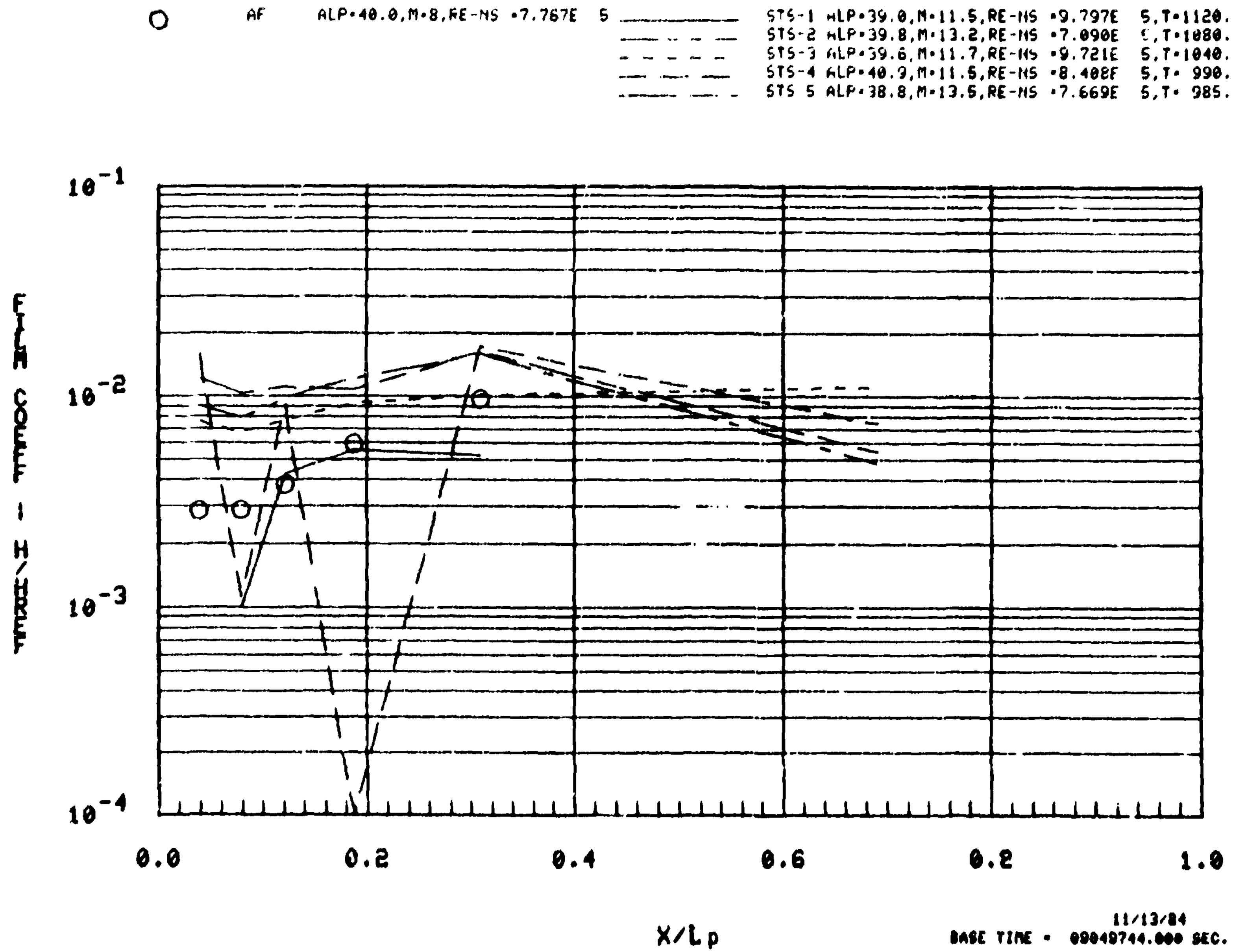

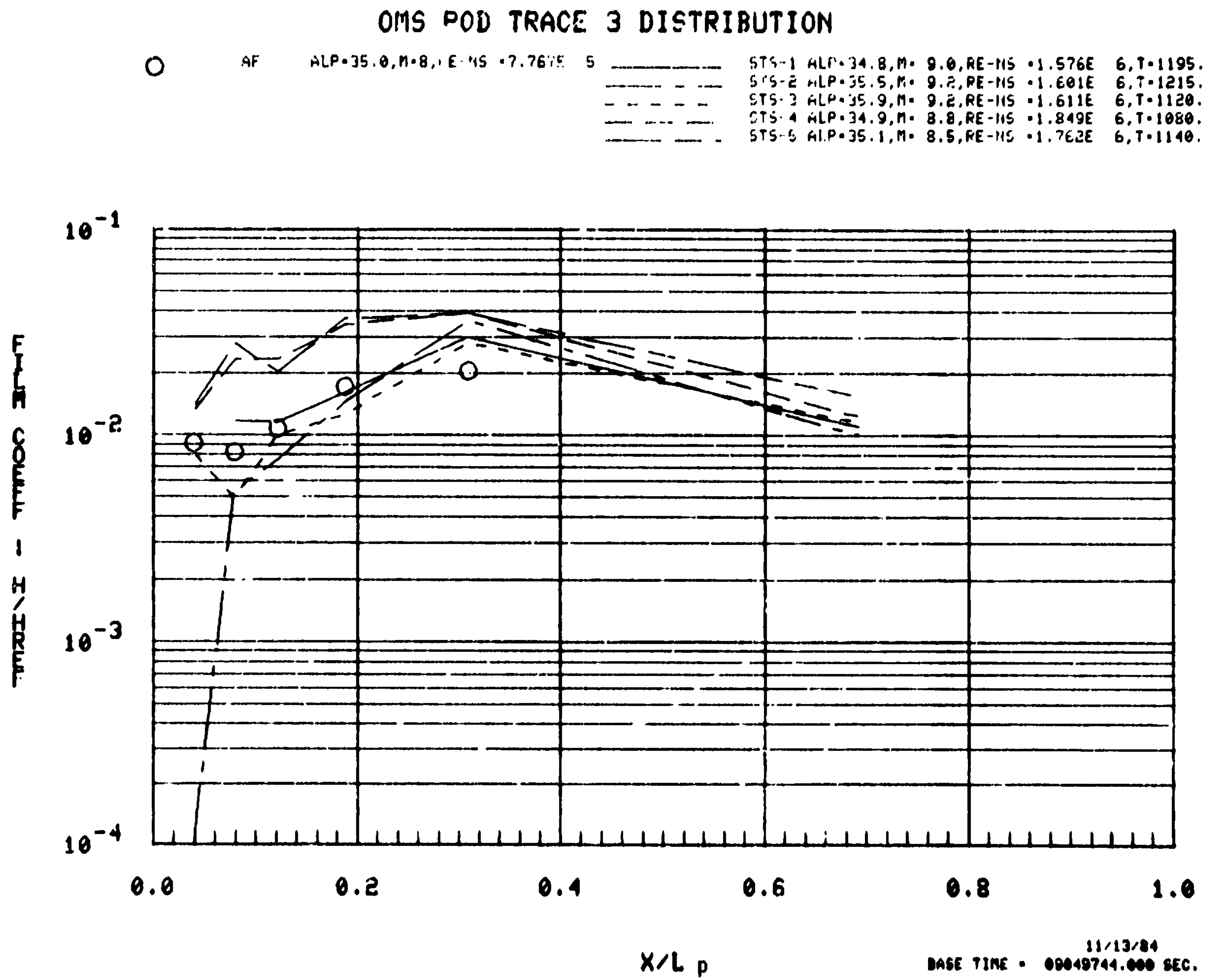

OMS POD TRACE 3 DISTRIBUTION
AF ALP=35.0,M=8,RE-NS =7.767E 5
STS-1 ALP=34.8,M= 9.0,RE-NS =1.576E 6,T=1195.
STS-2 ALP=35.5,M= 9.2,RE-NS =1.601E 6,T=1215.
STS-3 ALP=35.9,M= 9.2,RE-NS =1.611E 6,T=1120.
STS-4 ALP=34.9,M= 8.8,RE-NS =1.849E 6,T=1080.
STS-5 ALP=35.1,M= 8.5,RE-NS =1.762E 6,T=1140.
FILM COEFF : H/HREF
10^-1
10^-2
10^-3
10^-4
0.0
0.2
0.4
0.6
0.8
1.0
X/L p
11/13/84
BASE TIME = 09049744.000 SEC.

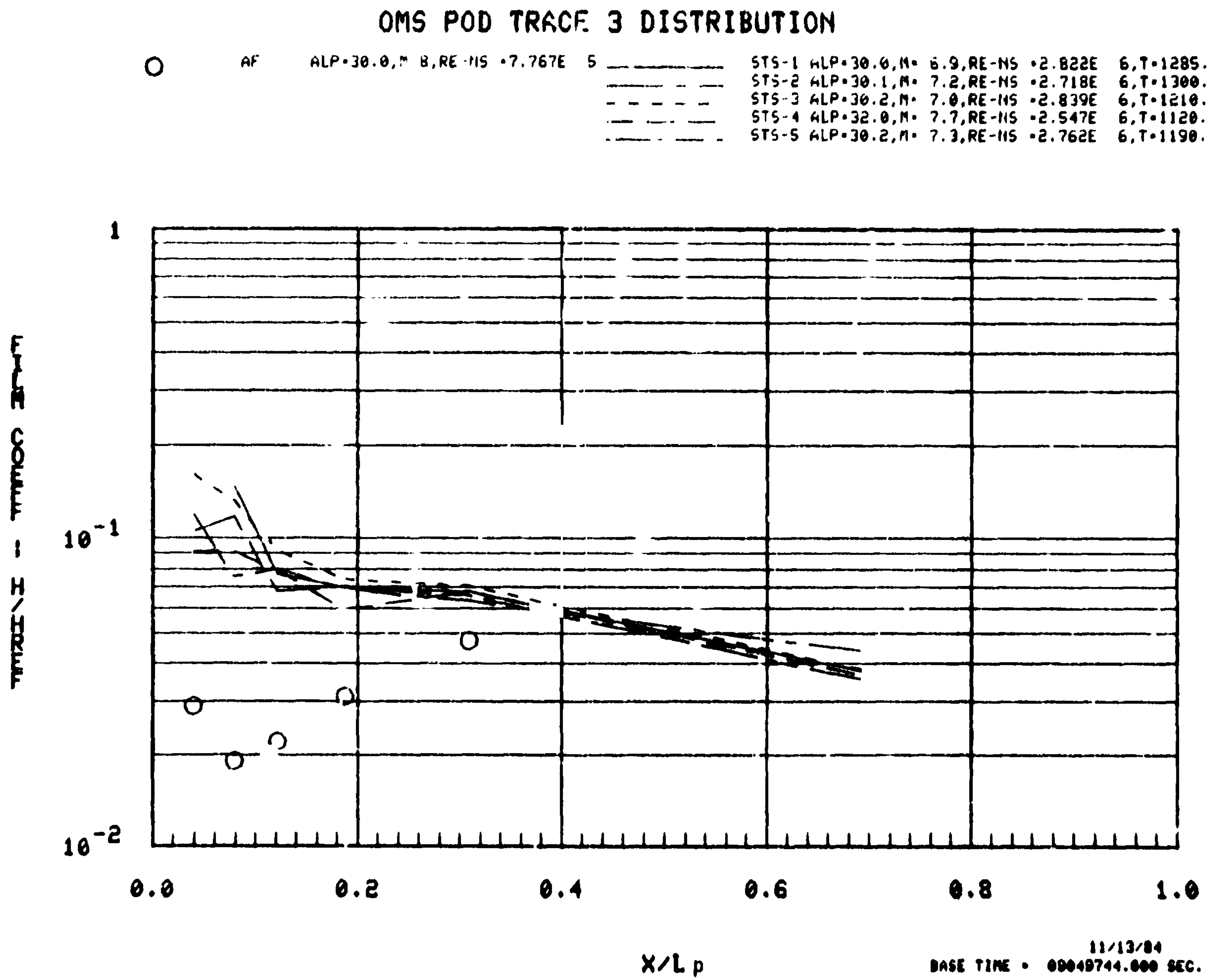

OMS POD TRACE 3 DISTRIBUTION
AF ALP=30.0,M 8,RE-NS =7.767E 5
STS-1 ALP=30.0,M= 6.9,RE-NS =2.822E 6,T=1285.
STS-2 ALP=30.1,M= 7.2,RE-NS =2.718E 6,T=1300.
STS-3 ALP=30.2,M= 7.0,RE-NS =2.839E 6,T=1210.
STS-4 ALP=32.0,M= 7.7,RE-NS =2.547E 6,T=1120.
STS-5 ALP=30.2,M= 7.3,RE-NS =2.762E 6,T=1190.
FILM COEFF : H/HREF
1
10^{-1}
10^{-2}
0.0
0.2
0.4
0.6
0.8
1.0
X/Lp
11/13/84
BASE TIME = 00049744.000 SEC.

OMS POD TRACE 3 DISTRIBUTION

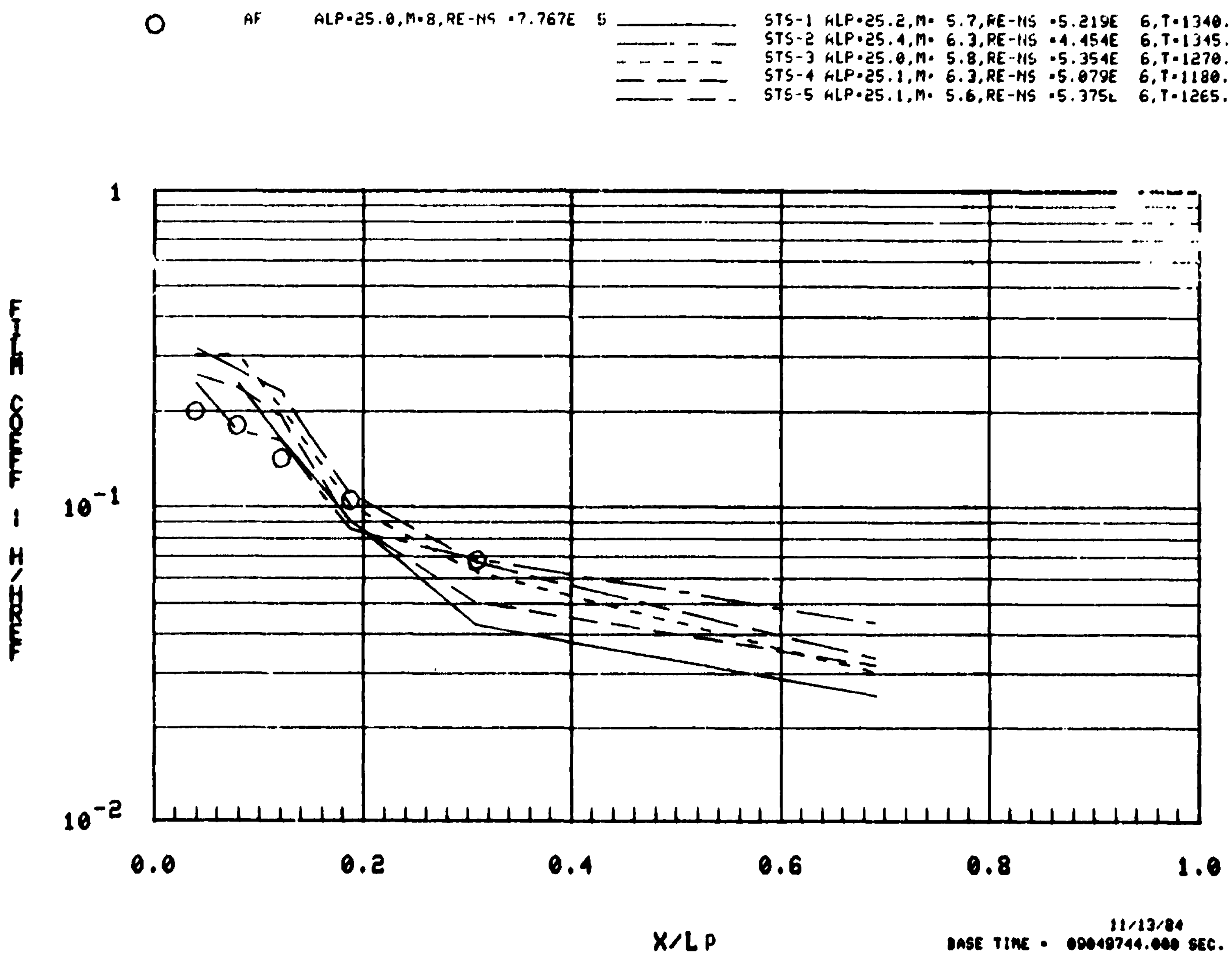

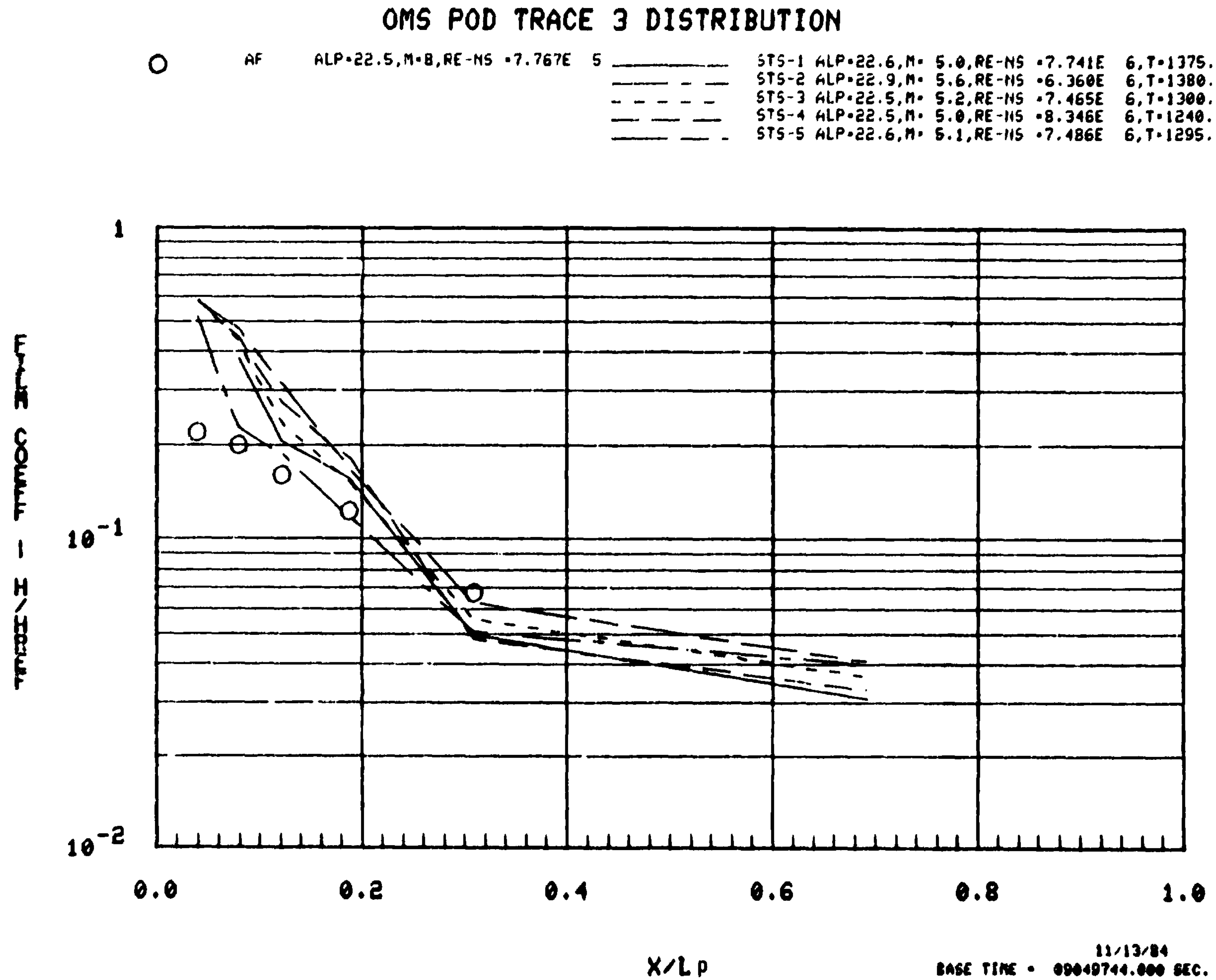
OMS POD TRACE 3 DISTRIBUTION
AF ALP=22.5,M=8,RE-NS =7.767E 5
STS-1 ALP=22.6,M= 5.0,RE-NS =7.741E 6,T=1375.
STS-2 ALP=22.9,M= 5.6,RE-NS =6.360E 6,T=1380.
STS-3 ALP=22.5,M= 5.2,RE-NS =7.465E 6,T=1300.
STS-4 ALP=22.5,M= 5.0,RE-NS =8.346E 6,T=1240.
STS-5 ALP=22.6,M= 5.1,RE-NS =7.486E 6,T=1295.
FILM COEFF , H/HREF
1
10^{-1}
10^{-2}
0.0
0.2
0.4
0.6
0.8
1.0
X/Lp
11/13/84
BASE TIME = 09040744.000 SEC.